frontiers | Research Topics

Insights in coronary artery disease 2022

Edited by
Turgay Celik

Published in
Frontiers in Cardiovascular Medicine

ISSN 1664-8714
ISBN 978-2-8325-3536-3
DOI 10.3389/978-2-8325-3536-3

About Frontiers

Frontiers is more than just an open access publisher of scholarly articles: it is a pioneering approach to the world of academia, radically improving the way scholarly research is managed. The grand vision of Frontiers is a world where all people have an equal opportunity to seek, share and generate knowledge. Frontiers provides immediate and permanent online open access to all its publications, but this alone is not enough to realize our grand goals.

Frontiers journal series

The Frontiers journal series is a multi-tier and interdisciplinary set of open-access, online journals, promising a paradigm shift from the current review, selection and dissemination processes in academic publishing. All Frontiers journals are driven by researchers for researchers; therefore, they constitute a service to the scholarly community. At the same time, the *Frontiers journal series* operates on a revolutionary invention, the tiered publishing system, initially addressing specific communities of scholars, and gradually climbing up to broader public understanding, thus serving the interests of the lay society, too.

Dedication to quality

Each Frontiers article is a landmark of the highest quality, thanks to genuinely collaborative interactions between authors and review editors, who include some of the world's best academicians. Research must be certified by peers before entering a stream of knowledge that may eventually reach the public - and shape society; therefore, Frontiers only applies the most rigorous and unbiased reviews. Frontiers revolutionizes research publishing by freely delivering the most outstanding research, evaluated with no bias from both the academic and social point of view. By applying the most advanced information technologies, Frontiers is catapulting scholarly publishing into a new generation.

What are Frontiers Research Topics?

Frontiers Research Topics are very popular trademarks of the *Frontiers journals series*: they are collections of at least ten articles, all centered on a particular subject. With their unique mix of varied contributions from Original Research to Review Articles, Frontiers Research Topics unify the most influential researchers, the latest key findings and historical advances in a hot research area.

Find out more on how to host your own Frontiers Research Topic or contribute to one as an author by contacting the Frontiers editorial office: frontiersin.org/about/contact

Insights in coronary artery disease: 2022

Topic editor
Turgay Celik — Wake Forest University, United States

Citation
Celik, T., ed. (2023). *Insights in coronary artery disease: 2022*. Lausanne: Frontiers Media SA. doi: 10.3389/978-2-8325-3536-3

Table of contents

frontiers | Frontiers in Cardiovascular Medicine

TYPE Editorial
PUBLISHED 07 September 2023
DOI 10.3389/fcvm.2023.1269388

OPEN ACCESS

EDITED AND REVIEWED BY
Tommaso Gori,
Johannes Gutenberg University Mainz,
Germany

*CORRESPONDENCE
Turgay Celik
tcelik@wakehealth.edu

RECEIVED 29 July 2023
ACCEPTED 24 August 2023
PUBLISHED 07 September 2023

CITATION
Celik T (2023) Editorial: Insights in coronary artery disease: 2022.
Front. Cardiovasc. Med. 10:1269388.
doi: 10.3389/fcvm.2023.1269388

Editorial: Insights in coronary artery disease: 2022

Turgay Celik*

Cardiovascular Section, Department of Internal Medicine, Wake Forest School of Medicine, Winston-Salem, NC, United States

KEYWORDS

coronary flow reserve, coronary arterial lesions, OCT, IVUS (intravascular ultrasound), coronary artery revascularization interventions

Editorial on the Research Topic
Insights in coronary artery disease: 2022

Atherosclerosis is a multifactorial disease that starts in childhood; inflammation plays a role at every step of atherogenesis, and risk factors further accelerate the underlying inflammatory process (1). Atherosclerotic disease affects the entire vessel and may cause difficulties in determining the significance of the lesion by angiography. Serial lesions can be a diagnostic challenge, as measuring the level of stenosis using invasive tests is affected by the complexity of factors (2). The combination of two lipid measures as the ratio of TG to HDL-C has been shown to be a reliable marker of endothelial damage and atherosclerosis caused by metabolic syndrome and insulin resistance. In this context, a high TG/HDL-C ratio, proposed as a marker of atherogenic dyslipidemia, has been associated with adverse long-term cardiovascular outcomes (3). TG/HDL-cholesterol ratio is seen as a new risk factor in a recent START study (De Luca et al.).

An acute coronary event due to a thrombosed lesion developing after mechanical rupture of an atheroma causes sudden death. Various morphology and tissue composition factors such as the cap thickness, lipid core stiffness, remodeling index, and blood pressure play a role in its mechanical stability. More recently, the presence of microcalcifications has also been shown to be an important factor. In a well-designed study, the authors showed that microcalcifications and cap thickness are the two most alarming biomechanical traits that govern the risk of mechanical rupture (Corti et al).

It is difficult to decide on coronary revascularization in patients with chest pain and moderate coronary artery stenosis. Therefore, functional evaluation is essential besides the anatomical evaluation of the presence of coronary artery. Fractional flow reserve (FFR) has been accepted as the gold standard for functionality in avoiding unnecessary interventions in the intermediate stenoses (Lee et al.). Computed tomography angiography (CTA) is used in a quick and easy way for coronary non-invasive evaluation. Intravascular ultrasound (IVUS) is used to show the morphological features of the lesion. Optical coherence tomography (OCT) has been observed to be more effective than IVUS in accurate anatomical assessment of coronary stenotic lesions with exceptionally high resolution during angiography (Lee et al.). In addition, computational fluid dynamics (CFD) have been applied to estimate computational FFR from coronary CTA- or OCT-based three-dimensional coronary model without using additional pressure guide wires or hyperemic agents.

Percutaneous coronary intervention (PCI) has a well-established role in revascularization for CAD. Despite the advances in PCI, the pathological changes that occur within the stent

still remain a mystery (Abouelnour and Gori). Today, we can evaluate the pathophysiological changes in the coronary vessels with different techniques. Many biomechanical factors, some preventable and some not, may cause restenosis after stent implantation. Intravascular imaging provides unique insights into the biological and mechanical issues that cause stent restenosis (Abouelnour and Gori).

Revascularization of chronic total occlusion (CTO) is considered a complex PCI and carries a higher risk of procedural failure, complications, and in-stent restenosis than other PCIs (4). CTO revascularization is among the most challenging procedures in interventional cardiology and no significant difference in mortality and morbidity was observed when compared with optimal medical treatment (Juricic et al.). Furthermore, comprehensive evaluation and advanced techniques are important to increase success rates and decrease complications. Intravascular examinations used during the procedure increase the success rate in this context. A recent study concluded that pre-stent IVUS assessment in CTO PCI provides important information on vessel morphology and size (Blessing et al.).

In addition to the pathophysiological evaluation before PCI, FFR is also a recommended method to increase the efficiency of revascularization (Leone et al.). A TARGET-FFR study found that FFR values of routine post-PCI physiology guidance can safely and effectively improve the final FFR values in a significant number of the worst-affected patients. FFR value ≥0.90 after PCI was shown to be associated with a reduced risk of adverse cardiovascular events (5).

In STEMI patients treated with PCI, the evaluation of coronary microcirculatory resistance index (IMR) may be a potential prognostic index in patients with multi-vessel disease (MVD) if it correlates significantly with differences in outcome and LV remodeling (6). In a recent study, Fineschi et al. (7) showed that impaired coronary microvascular function is commonly detected by IMR evaluation in the infarct territory and shows an early slow recovery over time after reperfusion. Besides, it was found that post-angioplasty IMR values were negatively correlated with LVEF only in patients with anterior MI.

The COMPARE II trial (7), a 5-year analysis comparing biodegradable polymer drug-eluting stents (BP-DES) with durable polymer DES (DP-DES) in the PCI population found similar early and late-term safety and efficacy results. However, BP-DES has been produced against persistent inflammation due to the presence of polymers, which are stated to be the most important cause of late stent thrombosis, and Lee and coworkers demonstrate that it reduces mortality due to late stent thrombosis compared with DP-DES (Lee et al.).

In conclusion, there have been important developments in the diagnosis, treatment, and follow-up of CAD. Although there are significant improvements, some essential problems remain unsolved in the management of patients with CAD.

Author contributions

TC: Writing – original draft.

Conflict of interest

The authors declare that the research was conducted in the absence of any commercial or financial relationships that could be construed as a potential conflict of interest.

The author(s) declared that they were an editorial board member of Frontiers, at the time of submission. This had no impact on the peer review process and the final decision.

Publisher's note

References

1. Balta S, Mikhailidis DP, Demirkol S, Ozturk C, Celik T, Iyisoy A. Endocan: a novel inflammatory indicator in cardiovascular disease? *Atherosclerosis*. (2015) 243 (1):339–43. doi: 10.1016/j.atherosclerosis.2015.09.030

2. Ilic I, Timcic S, Odanovic N, Otasevic P, Collet C. Serial stenosis assessment-can we rely on invasive coronary physiology. *Front Cardiovasc Med*. (2023) 10:1172906. doi: 10.3389/fcvm.2023.1172906

3. Bittner V, Johnson BD, Zineh I, Rogers WJ, Vido D, Marroquin OC, et al. The triglyceride/high-density lipoprotein cholesterol ratio predicts all-cause mortality in women with suspected myocardial ischemia. *Am Hear J*. (2009) 157(3):548–55. doi: 10.1016/j.ahj.2008.11.014

4. Galassi AR, Werner GS, Boukhris M, Azzalini L, Mashayekhi K, Carlino M, et al. Percutaneous recanalisation of chronic total occlusions: 2019 consensus document from the EuroCTO club. *EuroIntervention*. (2019) 15(2):198–208. doi: 10.4244/EIJ-D-18-00826

5. Collison D, Didagelos M, Aetesam-ur-Rahman M, Copt S, McDade R, McCartney P, et al. Post-stenting fractional flow reserve vs coronary angiography for optimization of percutaneous coronary intervention (TARGET-FFR). *Eur Hear J*. (2021) 42 (45):4656–68. doi: 10.1093/eurheartj/ehab449

6. Fineschi M, Verna E, Mezzapelle G, Bartolini D, Turiano G, Manari A, et al. A ssessing MICRO -vascular resistances via IMR to predict outcome in STEMI patients with multivessel disease undergoing primary PCI (AMICRO): rationale and design of a prospective multicenter clinical trial. *Am Hear J*. (2017) 187:37–44. doi: 10.1016/j.ahj.2017.02.019

7. Vlachojannis GJ, Smits PC, Hofma SH, Togni M, Vázquez N, Valdés M, et al. Biodegradable polymer biolimus-eluting stents versus durable polymer everolimus-eluting stents in patients with coronary artery disease: final 5-year report from the COMPARE II trial (abluminal biodegradable polymer biolimus-eluting stent versus durable P. *JACC Cardiovasc Interv*. (2017) 10(12):1215–21. doi: 10.1016/j.jcin.2017.02.029

frontiers | Frontiers in Cardiovascular Medicine

ORIGINAL RESEARCH
published: 13 April 2022
doi: 10.3389/fcvm.2022.874087

Clinical Impact and Prognostic Role of Triglyceride to High-Density Lipoprotein Cholesterol Ratio in Patients With Chronic Coronary Syndromes at Very High Risk: Insights From the START Study

Leonardo De Luca[1], Pier Luigi Temporelli[2], Furio Colivicchi[3], Lucio Gonzini[4], Maria Luisa Fasano[5], Massimo Pantaleoni[6], Gabriella Greco[7], Fabrizio Oliva[8], Domenico Gabrielli[1] and Michele Massimo Gulizia[9] on behalf of the START Investigators[†]*

[1] Department of Cardiosciences, Division of Cardiology, S. Camillo-Forlanini, Roma, Italy, [2] Division of Cardiology, Istituti Clinici Scientifici Maugeri, Istituto di Ricovero e Cura a Carattere Scientifico (IRCCS), Gattico-Veruno, Italy, [3] Division of Cardiology, S. Filippo Neri Hospital, Roma, Italy, [4] ANMCO Research Center, Firenze, Italy, [5] Division of Cardiology, Cardiac Rehabilitation Unit, S. Carlo Hospital, Potenza, Italy, [6] Division of Cardiology, Santa Maria Nuova Hospital, Reggio Emilia, Italy, [7] Division of Cardiology, Santo Spirito Hospital, Roma, Italy, [8] Cardiovascular Department, Division of Cardiology, "A. De Gasperis", ASST Grande Ospedale Metropolitano Niguarda, Milano, Italy, [9] Division of Cardiology, Garibaldi-Nesima Hospital, Catania, Italy

Background: Several studies have reported that the combination of high TG and low HDL-C, as simplified by the TG/HDL-C ratio, was a predictor of cardiovascular disease independent of LDL-C level. Nevertheless, poor data are available on the predictive role of TG/HDL-C ratio in very high risk (VHR) patients with chronic coronary syndromes (CCS).

Methods: Using the data from the STable Coronary Artery Diseases RegisTry (START) study, an Italian nationwide registry, we assessed the association between the TG/HDL-C ratio and baseline clinical characteristics, pharmacological treatment, and major adverse cardio-cerebrovascular events (MACCE) at 1 year in a large cohort of CCS patients at VHR.

Results: VHR patients with both TG and HDL-C levels available were grouped in tertiles of TG/HDL-C ratio: low (TG/HDL-C ratio <2, $n = 967$), middle (TG/HDL-C ratio 2–3.3, $n = 1{,}071$) and high (TG/HDL-C ratio >3.3, $n = 1{,}028$). At 1 year from enrolment, 232 (7.6%) patients presented a MACCE, with a higher incidence in the higher tertile, even though not statistically significant (6.0, 8.2, and 8.4% in the low, middle and high tertile, respectively; $p = 0.08$). At multivariable analysis, the TG/HDL-C ratio in tertiles did not result an independent predictor of the MACCE ($p = 0.29$) at 1-year follow-up (HR: 1.30; 95% CI: 0.93–1.82; $p = 0.12$ middle vs. lower tertile, and HR: 1.22; 95% CI: 0.87–1.72; $p = 0.25$ higher vs. lower).

Conclusions: In the present large, nationwide cohort of CCS patients at VHR a high TG/HD ratio did not emerge as independent predictor of MACCE at 1 year. Further studies with a longer follow-up are needed to better define the prognostic role of TG/HDL ratio in CCS.

Keywords: hypercholesterolemia, LDL-C, management, treatment, statin, chronic coronary syndrome

OPEN ACCESS

Edited by:
Carmine Pizzi,
Università di Bologna, Italy

Reviewed by:
Vojislav Giga,
University of Belgrade, Serbia
Giuseppe Ciliberti,
Azienda Ospedaliero Universitaria Ospedali Riuniti, Italy
Monica Verdoia,
University of Eastern Piedmont, Italy

****Correspondence:***
Leonardo De Luca
leo.deluca@libero.it;
ldeluca@scamilloforlanini.rm.it

*[†]See **Appendix** for a complete list of centers and investigators*

Specialty section:
This article was submitted to Coronary Artery Disease, a section of the journal Frontiers in Cardiovascular Medicine

Received: *11 February 2022*
Accepted: *25 March 2022*
Published: *13 April 2022*

Citation:
De Luca L, Temporelli PL, Colivicchi F, Gonzini L, Fasano ML, Pantaleoni M, Greco G, Oliva F, Gabrielli D and Gulizia MM (2022) Clinical Impact and Prognostic Role of Triglyceride to High-Density Lipoprotein Cholesterol Ratio in Patients With Chronic Coronary Syndromes at Very High Risk: Insights From the START Study. Front. Cardiovasc. Med. 9:874087. doi: 10.3389/fcvm.2022.874087

INTRODUCTION

Recent data suggested that concomitant high triglycerides (TG) and low high-density lipoprotein cholesterol (HDL-C) levels, as simplified by the TG/HDL-C ratio, characterize a specific cardio-metabolic profile known as atherogenic dyslipidemia, a predictor of coronary artery disease (CAD) development and elevated risk of cardiovascular adverse events, independent of low-density lipoprotein cholesterol (LDL-C) levels (1–4). The mechanisms by which a high TG/HDL-C ratio is associated with an increased cardiovascular risk seem to be related to metabolic syndrome, insulin resistance and consequent hyperinsulinemia, and to direct implications in endothelial damage and atherosclerosis (5, 6). The role of TG/HDL-C ratio for the long-term prediction of cardiovascular events has been reported in different clinical scenarios, such as diabetes mellitus (DM) (7), chronic kidney disease (CKD) (8), and acute coronary syndromes (ACS) (9).

Nevertheless, poor data are available on the predictive role of TG/HDL-C ratio in patients with established chronic coronary syndromes (CCS), particularly in those at very high risk (VHR). Therefore, using the data from the STable Coronary Artery Diseases RegisTry (START) study (10, 11), an Italian nationwide registry, we sought to assess the association between the TG/HDL-C ratio and baseline clinical characteristics, pharmacological treatment, and major adverse cardio-cerebrovascular events (MACCE) at 1 year in a large cohort of CCS patients at VHR.

METHODS

The design and main results of the START registry have been published previously (10). Briefly, the START was a prospective, observational, nationwide study aimed to evaluate the current presentation, management, treatment and quality of life of patients with CCS as seen by cardiologists in clinical practice in Italy, during a 3-month period (10). Enrolment was made at the end of outpatient or day-hospital visit or at hospital discharge. Data on baseline characteristics, including demographics, risk factors and medical history, were collected. Information on the use of diagnostic cardiac procedures, type and timing of revascularization therapy (if performed) and use of pharmacological or non-pharmacological therapies were recorded on an electronic case report form (CRF) at hospital discharge or the end of outpatient visit.

The Italian Association of Hospital Cardiologists (ANMCO) invited to participate all Italian cardiology wards, including university teaching hospitals, general and regional hospitals, and private clinics receiving patients with CCS. No specific protocols or recommendations for evaluation, management, and/or treatment have been put forth during this observational study (10).

All patients were informed of the nature and aims of the study and asked to sign an informed consent for the anonymous management of their individual data. Local Institutional Review Boards (IRB) approved the study protocol according to the current Italian rules.

One-hundred eighty-three cardiology centers included consecutive patients in the survey in different periods of 3 months between March 2016 and February 2017 (10).

All patients included into the analysis were evaluated for being at VHR according to the ESC/EAS clinical guidelines for the management of dyslipidemias [e.g., documented atherosclerotic cardiovascular disease including previous ACS, coronary revascularization, stable angina, stroke or transient ischemic attack, peripheral artery disease (PAD), DM with target organ damage or type 1 DM of long duration, severe CKD, a SCORE $\geq$10% for 10-year risk of fatal cardiovascular disease or familial hypercholesterolemia with atherosclerotic cardiovascular disease or another major risk factor] (12, 13).

Optimal medical therapy (OMT) has been defined as patients being prescribed aspirin or thienopyridine, β -blocker and a statin, at the maximum tolerated dosage (14). To be categorized as receiving OMT, individual patients must have been either prescribed or had reported contraindications to all medications in each category. Data on the use of angiotensin-converting enzyme inhibitors (ACE-I) or angiotensin II receptor blockers (ARB) were recorded and could be used to calculate their use among those patients in whom they were clinically indicated. Therefore, given that the guidelines for the management of CCS (14) recommend an ACE-I or ARB for some subgroups of patients, we also examined OMT including ACE-Is or ARBs, if indicated by an ejection fraction $\leq$40%, hypertension, DM or CKD (eligible patients).

In the present analysis, we considered the VHR patients with both TG and HDL- C available at enrollment.

Clinical Events and Follow-Up

Patients were followed up by visits or telephone interviews by investigators at 1 year from enrolment. Interviews included questions related to the occurrence of events, planned and unplanned hospitalizations and persistence to pharmacological therapies prescribed at enrolment.

The primary outcome of the present analysis was the time to the first occurrence of MACCE, a composite of all-cause mortality, hospitalization for MI, HF, stroke/TIA or myocardial revascularization at 1-year follow-up.

Statistical Analysis

The study cohort was stratified according the tertiles of TG/HDL-C ratio (<2; 2–3.3; >3). Categorical variables are presented as number and percentages and compared by the Chi-square test. Continuous variables are presented as mean and standard deviation (SD), except the TG levels, dosages of prescribed statins and time from revascularization to enrollment, which are reported as median and inter-quartile range (IQR) and were compared by the *t*-test or analysis of variance, if normally distributed, or by Mann-Withney *U*-test test or Kruskall-Wallis, if not.

A multivariable analysis (Cox regression) was performed in order to identify the independent predictors of MACCE at 1-year follow-up. We inserted in the model the TG/HDL-C ratio tertiles (low tertile as reference), and the following variables considered of clinical interest as covariates: age (continuous),

gender, prior ACS, prior revascularization, DM, hypertension, hypercholesterolemia, history of HF, PAD, history of major bleeding, CKD, the achievement of LDL-C target according to ESC/EAS guidelines (13), use of OMT at discharge. When more than two categories were present, dummy variables were introduced to define a reference group. Patients without a MACCE event was censored at their time of last observation. Kaplan–Meier curves were produced for the MACCE at 1- year follow-up and compared by log-rank test.

A $p < 0.05$ was considered statistically significant. All tests were 2-sided. Analyses were performed with SAS system software, version 9.4.

RESULTS

From the 5,070 consecutive patients with CCS enrolled in the registry, 4,751 (94.0%) were classified as VHR. Among this latter group of patients, 3,066 (64.5%) had both values of TG and HDL-C at baseline. Patients at VHR with both TG and HDL-C levels available were younger, less frequently females and more often active smokers, compared to VHR patients with TG and/or HDL-C not available, and that were also excluded from the analysis (**Supplementary Table 1**).

The TG/HDL ratios were normally distributed in the study population and the mean value was 3.10 ± 2.18 mg/dl. Patients at VHR with both TG and HDL-C levels available were grouped in tertiles of TG/HDL-C ratio: low (TG/HDL-C ratio <2, n = 967), middle (TG/HDL-C ratio 2–3.3, $n = 1{,}071$) and high (TG/HDL-C ratio >3.3, $n = 1{,}028$). Baseline characteristics of patients in the three groups are shown in **Table 1**. Although patients in the highest tertile, predominantly males, were significantly younger, they presented more often risk factors such as DM, smoking, hypertension, CKD and higher levels of glycaemia, serum uric acid, total and LDL cholesterol compared to patients in the other tertiles (**Table 1**). The median time between coronary revascularization and enrolment was 177 (IQR 35-1018) days.

At the time of enrollment, a statin was prescribed in 2,907 (94.8%) patients: 921 (95.2%) in the low, 1,015 (94.8%) in the middle and 971 (94–5%) in the high tertile of TG/HDL-C ratio ($p = 0.73$). Atorvastatin was the most prescribed statin compound (69.1%), followed by simvastatin (12.1%) and rosuvastatin (11.6%), without significative differences between the tertiles of TG/HDL-C ratio. The median dosages of statins prescribed in the 3 groups of patients are shown in **Supplementary Table 2**.

Omega-3 fatty acids were prescribed in 12.5, 11.6, and 22.5% in the low, middle and high tertile of TG/HDL-C ratio, respectively ($p < 0.0001$).

The association of statin and ezetimibe was prescribed in 11.9% and statin and omega-3 fatty acids in 12.2% of patients, with a significantly higher prevalence for the latter among those in the higher tertile of TG/HDL-C ratio, while other associations of cholesterol lowering agents were not frequently employed (**Figure 1**).

The other pharmacological therapies prescribed in the three groups are shown in **Figure 2**. A dual antiplatelet therapy, ACE-inhibitors or angiotensin II receptor blockers, beta-blockers, calcium channel antagonists, mineralocorticoid receptor antagonists and ranolazine were more frequently prescribed in patients in middle and high compared to low TG/HDL ratio tertiles.

Notably, an OMT was prescribed in 65.9, 71.4, and 75.6% in the low, middle and high tertile of TG/HDL-C ratio, respectively ($p < 0.0001$).

Clinical Events at 1 Year

Data on follow-up were available for 2,904 (95%) patients included in the analysis. The persistence to high dose statin at follow-up was 94.4, 94.2, and 95.6% in the low, middle and high tertile of TG/HDL-C ratio, respectively ($p = 0.41$).

At 1 year (median 369; IQR 362–378 days) from enrolment, MACCE was observed in 232 (7.9%) patients, and a higher incidence was observed in the higher tertile of TG/HDL ratio (6.0, 8.2, and 8.4% in the low, middle and high tertile, respectively), even though not statistically significant ($p = 0.08$). The single components of the MACCE respect to the 3 tertiles are reported in **Table 2**. The Kaplan-Meier curves of MACCE for the three tertiles are shown in **Figure 3**.

At multivariable analysis, the TG/HDL-C ratio in tertiles did not result an independent predictor of the MACCE ($p = 0.22$) at 1-year follow-up (HR: 1.30; 95% CI: 0.93–1.82; $p = 0.12$ middle vs lower tertile, and HR: 1.22; 95% CI: 0.87–1.72; $p = 0.25$ higher vs lower), while other variables such as history of HF (HR: 2.11; 95% CI: 1.54–2.88; $p < 0.0001$), CKD (HR 2.17; 95% CI: 1.56–3.02; $p < 0.0001$) and LDL-C target achievement (HR: 0.75; 95% CI: 0.55–1.01; $p = 0.04$) resulted as independent predictors of the MACCE.

DISCUSSION

In a large cohort of CCS patients at VHR enrolled in the START registry in Italy, we found that patients in the highest tertile of TG/HDL-C ratio were predominantly males and significantly younger, and presented more often risk factors such as DM, smoking, hypertension, CKD and higher levels of glycaemia, serum uric acid, total and LDL cholesterol compared to patients in the lower tertiles, i.e., low and middle. At 1 year from enrolment, the incidence of MACCE did not statistically differ between the 3 groups though it was higher in the high tertile compared to the low and middle one. At multivariable analysis, the TG/HDL-C ratio in tertiles did not emerge an independent predictor of the MACCE at 1-year follow-up.

Several studies have reported that the combination of high TG and low HDL-C level was a predictor of cardiovascular disease independent of LDL-C level (1–4, 15). Moreover, combining the two lipid measures into one as the ratio of TG to HDL-C has been proved to be a reliable indicator for metabolic syndrome, insulin resistance, with direct implications in endothelial damage and atherosclerosis (5, 6, 16, 17). Reference values for TG/HDL-C ratio and its association with cardiometabolic diseases in a mixed adult population were also recently identified (18).

In addition, an elevated TG/HDL-C ratio, which has been proposed as an easily obtainable marker of atherogenic dyslipidemia, has been associated with adverse long-term

TABLE 1 | Baseline clinical characteristics of VHR patients with TG and HDL-C available.

	Overall *n* = 3,066	Tertiles of TG/HDL-C ratio			*P*
		Low (<2) *n* = 967	Middle (2–3.3) *n* = 1071	High (>3.3) *n* = 1028	
Age (years), mean ± SD	67 ± 10	68 ± 10	68 ± 10	66 ± 10	<0.0001
Females, n (%)	555 (18.1)	214 (22.1)	183 (17.1)	158 (15.4)	0.0003
BMI (kg/m^2), mean ± SD	27.4 ± 4.0	26.3 ± 3.6	27.4 ± 3.9	28.4 ± 4.1	<0.0001
Risk factors and comorbidities, *n* (%)					
Active smokers	572 (18.7)	143 (14.8)	190 (17.7)	239 (23.3)	<0.0001
Hypercholesterolaemia	2,370 (77.3)	725 (75.0)	806 (75.3)	839 (81.6)	0.0003
Diabetes mellitus	1,025 (33.4)	247 (25.5)	342 (31.9)	436 (42.4)	<0.0001
Hypertension	2,430 (79.3)	736 (76.1)	844 (78.8)	850 (82.7)	0.001
Chronic renal dysfunction*	365 (11.9)	87 (9.0)	114 (10.6)	164 (16.0)	<0.0001
Peripheral artery disease	309 (10.1)	96 (9.9)	103 (9.6)	110 (10.7)	0.70
COPD	359 (11.7)	115 (11.9)	113 (10.6)	131 (12.7)	0.29
Malignancy	186 (6.1)	67 (6.9)	59 (5.5)	60 (5.8)	0.38
Cardiovascular history, *n* (%)					
Previous stroke/TIA	180 (5.9)	55 (5.7)	57 (5.3)	68 (6.6)	0.43
History of major bleeding	61 (2.0)	14 (1.5)	24 (2.2)	23 (2.2)	0.35
Atrial fibrillation	418 (13.6)	139 (14.4)	157 (14.7)	122 (11.9)	0.13
History of heart failure	415 (13.5)	117 (12.1)	138 (12.9)	160 (15.6)	0.06
Prior MI	2,190 (71.4)	698 (72.2)	774 (72.3)	718 (69.8)	0.39
Previous PCI/CABG	2,582 (84.2)	798 (82.5)	905 (84.5)	879 (85.5)	0.18
Haemodynamic parameters, mean ± SD; median (IQR)					
LVEF, % (*n* = 2,891)	50.0 ± 10.0	54.5 ± 9.8	54.0 ± 10.1	53.5 ± 9.9	0.10
SBP, mmHg	130 ± 16	130 ± 17	130 ± 16	130 ± 16	0.68
DBP, mmHg	76 ± 9	76 ± 9	76 ± 9	77 ± 9	0.03
HR, bpm	66 ± 11	65 ± 10	66 ± 12	67 ± 11	<0.0001
Hb, g/dL (*n* = 2,896)	13.6 ± 1.7	13.7 ± 1.6	13.6 ± 1.6	13.6 ± 1.8	0.87
Creatinine, mg/dL (*n* = 2,886)	1.1 ± 0.5	1.0 ± 0.4	1.0 ± 0.6	1.1 ± 0.6	<0,.0001
Total cholesterol, mg/dL (*n* = 3,033)	153.0 ± 38.4	150.4 ± 34.2	150.7 ± 37.4	158.0 ± 42.5	<0.0001
LDL cholesterol, mg/dL (*n* = 2,676)	86.0 ± 33.7	81.0 ± 30.2	86.0 ± 32.6	90.6 ± 37.1	<0.0001
LDL cholesterol ≤70 mg/dl, *n* (%)	901 (33.7)	316 (37.9)	310 (32.7)	275 (30.7)	0.005
LDL cholesterol ≤55 mg/dl, *n* (%)	395 (14.8)	141 (16.9)	128 (13.5)	126 (14.1)	0.10
LDL cholesterol ≤40 mg/dl, *n* (%)	107 (4.0)	33 (4.0)	40 (4.2)	34 (3.8)	0.89
HDL cholesterol, mg/dL	45.5 ± 13.6	56.6 ± 14.9	44.4 ± 8.9	36.3 ± 7.8	<0.0001
Triglycerides, mg/dL	112 (85-152)	76 (63-89)	110 (96-129)	170 (144-204)	<0.0001
Glycaemia, mg/dL (*n* = 2,742)	114.3 ± 36.0	109.3 ± 31.9	113.3 ± 35.4	120.3 ± 39.2	<0.0001
Uric acid, mg/dL (*n* = 1,968)	5.7 ± 1.7	5.4 ± 1.6	5.7 ± 1.6	6.1 ± 1.6	<0.0001

BMI, body mass index; CABG, coronary artery by-pass grafting; COPD, chronic obstructive pulmonary disease; DBP, diastolic blood pressure; Hb, hemoglobin; HDL, high density lipoprotein; HR, heart rate; LDL, low density lipoprotein; LVEF, left ventricular ejection fraction; MI, myocardial infarction; PCI, percutaneous coronary intervention; SBP, systolic blood pressure; TIA, transient ischemic attack.

**Dialysis, history of renal transplant or creatinine levels >1.5 mg/dL.*

cardiovascular outcomes and all-cause mortality in secondary prevention studies performed in gender-specific with suspected myocardial ischemia (4) or small country-specific (19) high-risk patients, as well as in patients presenting with ACS (9, 20). Poor data were available on the predictive role of TG/HDL-C ratio in patients with established CCS, particularly in those at VHR.

Recently, in a prospective, multicenter study enrolling 355 patients with stable angina at intermediate-low risk referred to coronary computed tomography angiography (CTA) and followed for 4.5 years, patients with a higher TG/HDL-C ratio presented a higher coronary atherosclerosis burden (21). In addition, both a higher TG/HDL-C ratio and the coronary CTA score were additional predictors of worse outcome, independently of other cardiovascular risk factors, the presence of obstructive CAD or ischemia (21). In contrast to these controlled studies, VHR CCS patients included in our registry were undertreated with statin therapies and were followed up for a short period of time. This may partly explain the lack of prognostic predictive value of the TG / HDL-C ratio observed in our analysis.

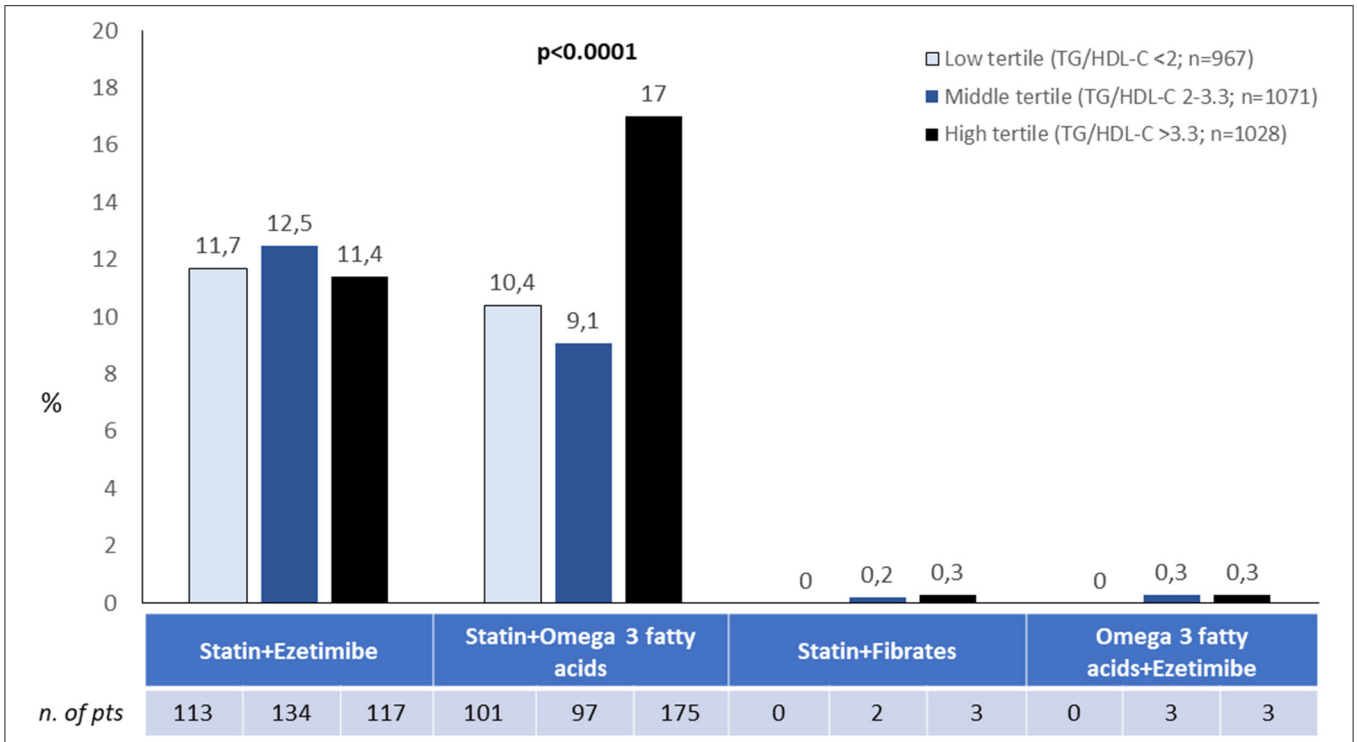

FIGURE 1 | Associations of lipid lowering strategies according to tertiles of TG/HDL ratio. Other possible combinations not shown were used in <0.5% of cases.

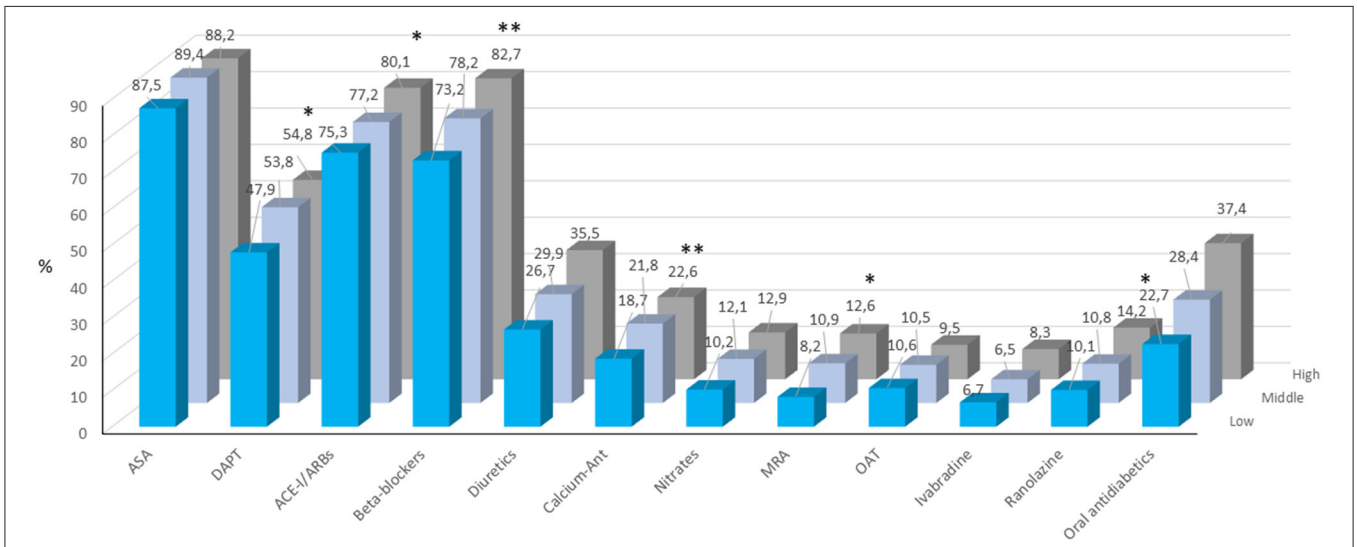

FIGURE 2 | Pharmacological treatment at enrolment in patients included the three TG/HDL-C tertiles. ACE-I, angiotensin converting enzyme inhibitors; ARB, angiotensin receptor blockers; ASA, acetylsalicylic acid; CCA, calcium channels antagonists; MRA, mineralocorticoid receptor antagonist; OAT, oral anticoagulant therapy. *$p < 0.05$; **$p < 0.0001$.

In fact, though the incidence of patients with MACCE was higher in the high tertile as compared to the low and middle one, a significative difference among the tertiles was not observed, and, at multivariable analysis, only history of HF and CKD resulted as independent predictors of the MACCE. However, it should be noted that a large majority of our study patients (71.1%) were receiving an OMT: 65.9%, 71.4 and 75.6% ($p < 0.0001$) in the low, middle and high tertile of TG/HDL-C ratio, respectively. Thus, the more widely represented OMT in the high tertile of TG/HDL-C ratio may partly account for the results.

TABLE 2 | Single components of MACCE at 1 year.

Events, *n* (%)	Overall *n* = 3,066	Tertiles of TG/HDL-C ratio			*p* value
		Low *n* = 967	Middle *n* = 1,071	High *n* = 1,028	
All-cause death	47 (1.5)	10 (1.0)	19 (1.8)	18 (1.8)	0.31
Myocardial Infarction	24 (0.8)	6 (0.6)	9 (0.8)	9 (0.9)	0.78
Heart Failure	48 (1.6)	11 (1.1)	23 (2.2)	14 (1.4)	0.15
Stroke	13 (0.4)	5 (0.5)	2 (0.2)	6 (0.6)	0.33
Myocardial revascularization	135 (4.4)	34 (3.5)	48 (4.5)	53 (5.2)	0.20

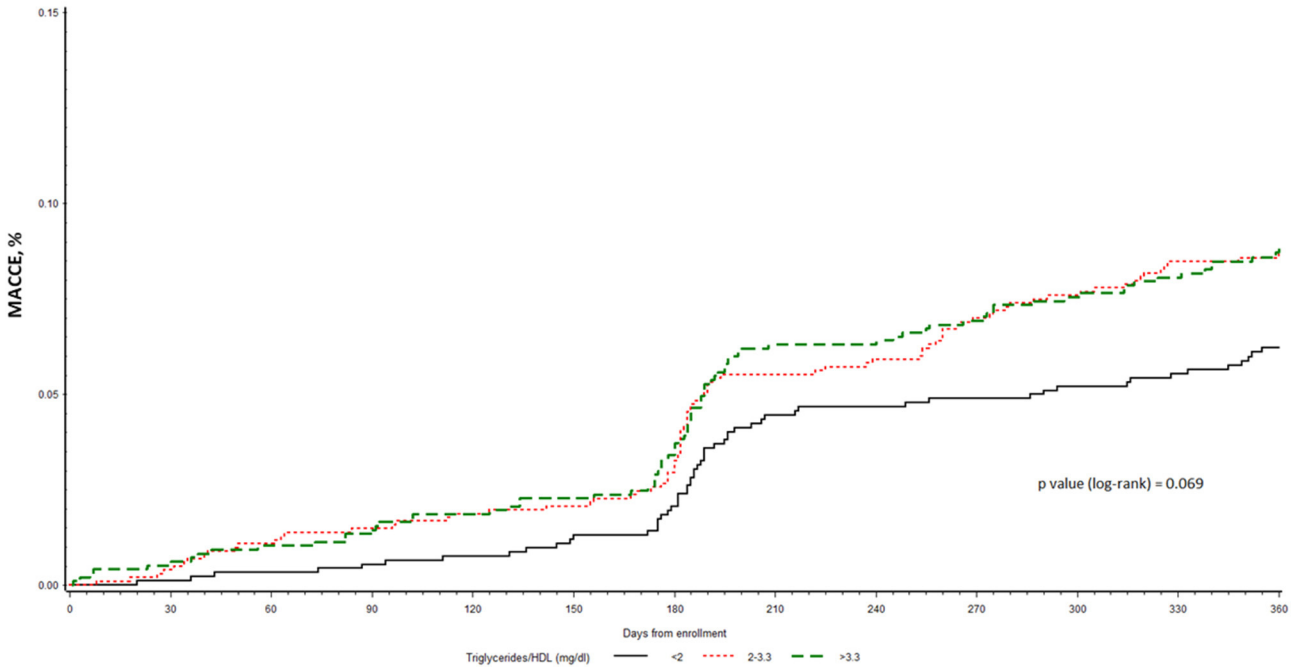

FIGURE 3 | Kaplan-Meier curves for time to MACCE among the three subgroups of CCS patients at VHR stratified by TG/HDL-C tertiles.

Moreover, the follow-up at 1 year was probably too short to observe a significant impact of TG/HDL-C ratio on clinical outcome. Indeed, even in a recent study in ACS patients with STEMI (9) a high TG/HDL-C ratio did not impact on 30-day and 1-year outcomes suggesting that a longer period is needed to reveal significant differences, as has been shown in other previous studies (15, 16, 19, 20).

Study Limitations

Our study must be evaluated in the light of some limitations. First, data reported in the present analysis are limited to the time of enrolment and we do not have data on long-term persistence to prescribed therapies, their changes and relative outcomes. Nevertheless, a clinical follow-up at 1 year from enrolment in the START study showed a persistence to OMT therapy higher than 90% (11). In addition, we considered values of TG and HDL-C at enrolment. Therefore, changes in statins regimen and dosing could have occurred later influencing the subsequent TG/HDL-C ratios. Finally, even if the participating centers were asked to include in the registry all consecutive patients with SCC, we were not able to verify the enrolment process, due to the absence of administrative auditing.

CONCLUSIONS

In the present large, nationwide cohort of consecutive CCS patients at VHR, a high TG/HD ratio did not emerge as independent predictor of cardio-cerebrovascular events at 1 year. Further larger studies with a longer follow-up period are needed to better define the clinical and prognostic role of TG/HDL ratio in CCS.

DATA AVAILABILITY STATEMENT

The raw data supporting the conclusions of this article will be made available by the authors, without undue reservation.

ETHICS STATEMENT

The studies involving human participants were reviewed and approved by San Camillo-Forlanini, Rome. The patients/participants provided their written informed consent to participate in this study.

AUTHOR CONTRIBUTIONS

LD and PT drafted the manuscript. LG analyzed the data. All other authors critically revised the article. All authors contributed to the article and approved the submitted version.

FUNDING

The sponsor of both studies was the Heart Care Foundation, a non-profit independent organization, which also owns the database. Database management, quality control of the data and data analyses were under the responsibility of the ANMCO Research Center Heart Care Foundation. The realization of this sub-analysis of the START study and the publication of its results was partially supported by an unrestricted grant by Menarini, Italy. No compensations were provided to participating sites, investigators, nor members of the Steering Committee. The Steering Committee had full access to all of the data and takes complete responsibility for the integrity of the data and the accuracy of the data analysis.

SUPPLEMENTARY MATERIAL

The Supplementary Material for this article can be found online at: https://www.frontiersin.org/articles/10.3389/fcvm.2022.874087/full#supplementary-material

REFERENCES

1. Carey VJ, Bishop L, Laranjo N, Harshfield BJ, Kwiat C, Sacks FM. Contribution of high plasma triglycerides and low high-density lipoprotein cholesterol to residual risk of coronary heart disease after establishment of low-density lipoprotein cholesterol control. *Am J Cardiol.* (2010) 106:757–63. doi: 10.1016/j.amjcard.2010.05.002
2. Jeppesen J, Hein HO, Suadicani P, Gyntelberg F. Low triglycerides-high high-density lipoprotein cholesterol and risk of ischemic heart disease. *Arch Intern Med.* (2001) 161:361–6. doi: 10.1001/archinte.161.3.361
3. Gaziano JM, Hennekens CH, O'Donnell CJ, Breslow JL, Buring JE. Fasting triglycerides, high-density lipoprotein, and risk of myocardial infarction. *Circulation.* (1997) 96:2520–5. doi: 10.1161/01.CIR.96.8.2520
4. Bittner V, Johnson BD, Zineh I, Rogers WJ, Vido D, Marroquin OC, et al. The TG/HDL cholesterol ratio predicts all cause mortality in women with suspected myocardial ischemia: a report from the women's ischemia syndrome evaluation (WISE). *Am Heart J.* (2009) 157:548–55. doi: 10.1016/j.ahj.2008.11.014
5. Murguía-Romero M, Jiménez-Flores JR, Sigrist-Flores SC, Espinoza-Camacho MA, Jiménez-Morales M, Piña E, et al. Plasma triglyceride/HDL-cholesterol ratio, insulin resistance, and cardiometabolic risk in young adults. *J Lipid Res.* (2013) 54:2795–9. doi: 10.1194/jlr.M040584
6. Armato J, Reaven G, Ruby R. Triglyceride/High-Density lipoprotein cholesterol concentration ratio identifies accentuated cardiometabolic risk. *Endocr Pract.* (2015) 21:495–500. doi: 10.4158/EP14479.OR
7. Boizel R, Benhamou PY, Lardy B, Laporte F, Foulon T, Halimi S. Ratio of triglycerides to HDL cholesterol is an indicator of LDL particle size in patients with type 2 diabetes and normal HDL cholesterol levels. *Diabetes Care.* (2000) 23:1679–85. doi: 10.2337/diacare.23.11.1679
8. Ho CI, Chen JY, Chen SY, Tsai YW, Weng YM, Tsao YC, et al. Relationship between TG/HDL-C ratio and metabolic syndrome risk factors with chronic kidney disease in healthy adult population. *Clinical Nutrition.* (2015) 34:874–80. doi: 10.1016/j.clnu.2014.09.007
9. Chen HC, Lee WC, Fang HY, Fang CY, Chen CJ, Yang CH, et al. Impact of high triglyceride/high-density lipoprotein cholesterol ratio (insulin resistance) in ST-segment elevation myocardial infarction. *Medicine.* (2020) 99:e22848. doi: 10.1097/MD.0000000000022848
10. De Luca L, Temporelli PL, Lucci D, Gonzini L, Riccio C, Colivicchi F, et al. START investigators. Current management and treatment of patients with stable coronary artery diseases presenting to cardiologists in different clinical contexts: a prospective, observational, nationwide study. *Eur J Prev Cardiol.* (2018) 25:43–53. doi: 10.1177/2047487317740663
11. De Luca L, Temporelli PL, Riccio C, Gonzini L, Marinacci L, Tartaglione SN, et al. START Investigators. Clinical outcomes, pharmacological treatment, and quality of life of patients with stable coronary artery diseases managed by cardiologists: 1-year results of the START study. *Eur Heart J Qual Care Clin Outcomes.* (2019) 5:334–42. doi: 10.1093/ehjqcco/qcz002
12. Mach F, Baigent C, Catapano AL, Koskinas KC, Casula M, Badimon L, et al. 2019 ESC/EAS Guidelines for the management of dyslipidaemias: lipid modification to reduce cardiovascular risk: The Task Force for the management of dyslipidaemias of the European Society of Cardiology (ESC) and European Atherosclerosis Society (EAS). *Eur Heart J.* (2020) 41:111–88. doi: 10.1093/eurheartj/ehz455
13. Catapano AL, Graham I, De Backer G, Wiklund O, Chapman MJ, Drexel H, et al.; ESC Scientific Document Group. 2016 ESC/EAS Guidelines for the Management of Dyslipidaemias. *Eur Heart J.* (2016) 37:2999–3058. doi: 10.1093/eurheartj/ehw272
14. Knuuti J, Wijns W, Saraste A, Capodanno D, Barbato E, Funck-Brentano C, et al.; ESC Scientific Document Group. 2019 ESC Guidelines for the diagnosis and management of chronic coronary syndromes: The Task Force for the diagnosis and management of chronic coronary syndromes of the European Society of Cardiology (ESC). *Eur Heart J.* (2020) 41:407–77. doi: 10.1093/eurheartj/ehz425
15. Andersson C, Lyass A, Vasan RS, Massaro JM, D'Agostino Sr RB, Robins SJ. Long-term risk of cardiovascular events across a spectrum of adverse major plasma lipid combinations in the Framingham Heart Study. *Am Heart J.* (2014) 168:878–83. doi: 10.1016/j.ahj.2014.08.007
16. Lee JS, Chang PY, Zhang Y, Kizer JR, Best LG, Howard BV. Triglyceride and HDL-C dyslipidemia and risks of coronary heart disease and ischemic stroke by glycemic dysregulation status: the Strong Heart Study. *Diabetes Care.* (2017) 40:529–37. doi: 10.2337/dc16-1958
17. Di Giorgi N, Michelucci E, Smit JM, Scholte AJHA, El Mahdiui M, Knuuti J, et al. A specific plasma lipid signature associated with high triglycerides and low HDL cholesterol identifies residual CAD risk in patients with chronic coronary syndrome. *Atherosclerosis.* (2021) 339:1–11. doi: 10.1016/j.atherosclerosis.2021.11.013
18. Lelis DF, Calzavara JVS, Santos RD, Sposito AC, Griep RH, Barreto SM, et al. Reference values for the triglyceride to high-density lipoprotein ratio and its association with cardiometabolic diseases in a mixed adult population: The ELSA-Brasil study. *J Clin Lipidol.* (2021) 15:699–711. doi: 10.1016/j.jacl.2021.07.005
19. Sultani R. Tong DC, Peverelle M, Lee YS, Baradi A, Wilson AM. Elevated triglycerides to high-density lipoprotein cholesterol (TG/HDL-C) ratio predicts long-term mortality in high-risk patients. *Heart Lung Circ.* (2020) 29:414–21. doi: 10.1016/j.hlc.2019.03.019

20. Wan K, Zhao J, Huang H, Zhang Q, Chen X, Zeng Z, et al. The association between trigyceride/high-density lipoprotein cholesterol ratio and all cause mortality in acute coronary syndrome after coronary revascularization. *PLoS ONE*. (2015) 10:e0123521. doi: 10.1371/journal.pone.0123521
21. Caselli C, De Caterina R, Smit JM, Campolo J, Mahdiui ME, Ragusa R, et al. EVINCI and SMARTool. Triglycerides and low HDL cholesterol predict coronary heart disease risk in patients with stable angina. *Sci Rep*. (2021) 11:20714. doi: 10.1038/s41598-021-00020-3

Conflict of Interest: The authors declare that the research was conducted in the absence of any commercial or financial relationships that could be construed as a potential conflict of interest.

Publisher's Note: All claims expressed in this article are solely those of the authors and do not necessarily represent those of their affiliated organizations, or those of the publisher, the editors and the reviewers. Any product that may be evaluated in this article, or claim that may be made by its manufacturer, is not guaranteed or endorsed by the publisher.

frontiers | Frontiers in Cardiovascular Medicine

ORIGINAL RESEARCH
published: 29 April 2022
doi: 10.3389/fcvm.2022.873114

Long-Term Clinical Outcomes Between Biodegradable and Durable Polymer Drug-Eluting Stents: A Nationwide Cohort Study

Seung-Jun Lee[1†], Dong-Woo Choi[2,3†], Yongsung Suh[4], Sung-Jin Hong[1], Chul-Min Ahn[1], Jung-Sun Kim[1], Byeong-Keuk Kim[1], Young-Guk Ko[1], Donghoon Choi[1], Eun-Cheol Park[2], Yangsoo Jang[1], Chung-Mo Nam[2] and Myeong-Ki Hong[1*]*

[1] Severance Cardiovascular Hospital, Yonsei University College of Medicine, Seoul, South Korea, [2] Department of Preventive Medicine, Yonsei University College of Medicine, Seoul, South Korea, [3] Cancer Big Data Center, National Cancer Control Institute, National Cancer Center, Goyang, South Korea, [4] Myongji Hospital, Hanyang University College of Medicine, Goyang, South Korea

OPEN ACCESS

Edited by:
Expedito Ribeiro,
University of São Paulo, Brazil

Reviewed by:
Sungsoo Cho,
Chung-Ang University, South Korea
Ji-Yong Jang,
National Health Insurance Service Ilsan Hospital, South Korea

***Correspondence:**
Myeong-Ki Hong
mkhong61@yuhs.ac
Chung-Mo Nam
cmnam@yuhs.ac

[†]These authors have contributed equally to this work and share first authorship

Specialty section:
This article was submitted to Coronary Artery Disease, a section of the journal Frontiers in Cardiovascular Medicine

Received: 10 February 2022
Accepted: 12 April 2022
Published: 29 April 2022

Citation:
Lee S-J, Choi D-W, Suh Y, Hong S-J, Ahn C-M, Kim J-S, Kim B-K, Ko Y-G, Choi D, Park E-C, Jang Y, Nam C-M and Hong M-K (2022) Long-Term Clinical Outcomes Between Biodegradable and Durable Polymer Drug-Eluting Stents: A Nationwide Cohort Study. Front. Cardiovasc. Med. 9:873114. doi: 10.3389/fcvm.2022.873114

Background: Despite the theoretical benefits of biodegradable polymer drug-eluting stents (BP-DES), clinical benefits of BP-DES over durable polymer DES (DP-DES) have not been clearly demonstrated. Using data from a large-volume nationwide cohort, we compared long-term clinical outcomes between BP-DES- and DP-DES-treated patients.

Methods: A retrospective cohort study that enrolled all patients who underwent percutaneous coronary intervention (PCI) with new-generation DES between 2010 and 2016 in Korea was conducted by using the National Health Insurance Service database. The outcomes of interest were all-cause death, cardiovascular death, and myocardial infarction (MI).

Results: A total of 127,731 patients treated with new-generation DES with thin struts (<90 μm) were enrolled for this analysis. After stabilized inverse probability of treatment weighting, the incidence of all-cause death was significantly lower in patients treated with BP-DES ($n = 19{,}521$) at 5 years after PCI (11.3 vs. 13.0% in those treated with DP-DES [$n = 108{,}067$], hazard ratio [HR] 0.92, 95% confidence interval [CI], 0.88–0.96, $p < 0.001$), while showing no statistically significant difference at 2 years after PCI (5.7 vs. 6.0%, respectively, HR 0.95, 95% CI, 0.89–1.01, $p = 0.238$). Similarly, use of BP-DES was associated with a lower incidence of cardiovascular death (7.4 vs. 9.6% in those treated with DP-DES, HR 0.82, 95% CI, 0.77–0.87, $p < 0.001$), and MI (7.4 vs. 8.7%, respectively, HR 0.90, 95% CI, 0.86–0.94, $p = 0.006$) at 5 years after PCI. There was no statistically significant difference of cardiovascular death (4.6 vs. 4.9%, respectively, HR 0.93, 95% CI, 0.85–1.01, $p = 0.120$) and MI (5.0 vs. 5.1%, respectively, HR 0.98, 95% CI, 0.92–1.05, $p = 0.461$) at 2 years after PCI.

Conclusions: Implantation of BP-DES was associated with a lower risk of all-cause death, cardiovascular death, and MI compared with DP-DES implantation. This difference was clearly apparent at 5 years after DES implantation.

Clinical Trial Registration: ClinicalTrial.gov, NCT04715594.

Keywords: coronary artery disease, drug-eluting stent, percutaneous coronary intervention, treatment outcome, stents

INTRODUCTION

Compared with first-generation drug-eluting stents (DES) that harbored the risk of stent thrombosis, new-generation DES with durable polymers (DP-DES) have successfully lowered the risk of stent thrombosis while maintaining the lower rate of in-stent restenosis, compared with bare-metal stents (1, 2). In addition, advances in stent manufacturing technology enabled the reduction of stent strut thickness while securing sufficient radial force, and the development of a biocompatible polymer that allows stable release of anti-proliferative drugs has significantly reduced the frequency of stent failure (3). Despite these advances in technology, very late stent thrombosis and neoatherosclerosis still contribute to late fatal clinical outcomes in some subjects who successfully underwent percutaneous coronary intervention (PCI) with new-generation DES (4). As a plausible explanation, persistence of polymer in the stent platform could continuously evoke chronic inflammation, delay endothelial healing, and accelerate neoatherosclerosis (4, 5). However, if the polymer disappears by gradual biodegradation within a certain period after PCI, additional polymer-related complications may not occur. Therefore, DESs with biodegradable polymers (BP-DES) have been developed and are currently being actively utilized in contemporary clinical practice (6). Despite the theoretical superiority of BP-DES over DP-DES, prior reports, including randomized trials that enabled the use of BP-DES in clinical practice, mostly failed to demonstrate the superiority of BP-DES compared with DP-DES in short-term periods (around 1-year follow-up) with a relatively insufficient number of study participants, considering the low rates of cardiac events after implantation of new-generation DES (7–10). To date, the clinical benefits of BP-DES over DP-DES are controversial (1, 7–11). In this regard, we sought to investigate the long-term clinical impact of BP-DES compared with DP-DES utilizing the large-volume nationwide cohort that covers the entire populations who received first- and new-generation DES implantation for coronary artery disease in Korea (CONNECT DES cohort registry).

MATERIALS AND METHODS

Study Design and Data

This study was a retrospective analysis of the national health claims database established by the National Health Insurance Service (NHIS) of Korea. This database contains claimed medical cost, detailed information of prescribed drugs including the number of pills and drug dosage, and medical history presented as International Classification of Diseases, Tenth Revision (ICD-10) codes. Most of the Korean population (97.1%) are forced to subscribe to the NHIS, which is a sole insurer managed by the Korean government. Given that NHIS also covers information for the remaining population (2.9%) categorized as medical aid subjects, this cohort is considered to represent the entire Korean population (12). We were also provided with the death certificates with ICD-10 codes from the National Institute of Statistics of Korea. This study was approved by the Institutional Review Board of our institute. Informed consent was waived because personal information was masked after cohort generation according to strict confidentiality guidelines of the Korean Health Insurance Review and Assessment Service. This study is registered at ClinicalTrial.gov (NCT04715594).

Study Population and Covariates

Among about 51.5 million inhabitants included in the Korean NHIS database, we recruited 273,670 patients (≥20 years old) who were treated with DES between January 2005 and December 2016 in Korea (CONNECT DES cohort registry). First-generation DES implantation was more frequently performed between 2005 and 2009. New-generation DESs were more frequently implanted between 2010 and 2016. According to the stringent policy of the NHIS database to protect personal information, type of polymer, generation of DES, strut thickness and type of eluted drugs were only provided without the DES product names. **Figure 1** shows the study flow. DES implantation was performed in 273,670 patients between 2005 and 2016. Among 273,670 patients, 95,878 patients were excluded from this study: patients who were implanted with first-generation DES ($n = 69,316$); those who had a prior history of PCI or coronary artery bypass surgery ($n = 5,517$) because clinical events during follow-up cannot be discriminated whether those were caused by a prior PCI (coronary artery bypass surgery) or index PCI; those who died within 7 days after index PCI ($n = 4,823$) because these early death might be not due to different DESs but to clinical characteristic of the patients; those with four or more stents implanted ($n = 936$); those who were implanted with both types of DES ($n = 9,751$); and those with missing medical information ($n = 5,535$). Therefore, 177,792 patients who were treated with new-generation DES remained. Among these patients, those implanted with new-generation DES with thick struts (≥90 μm thickness) ($n = 41,550$) or struts not commonly used worldwide ($n = 8,511$) were further excluded. Consequently, the remaining 127,731 patients who were treated with new-generation DES with thin struts (BP-DES, 19,683 patients and DP-DES, 108,048 patients) were finally included in the analysis of this study (**Figure 1**). The list of included or excluded new-generation DES are presented in **Supplementary Table 1**.

Study Procedures and Outcomes

We utilized the ICD-10 codes, fee-for-service, and prescribed drug codes that were claimed during the study period provided by NHIS database, and death-certificates provided by the National Statistical Office. The NHIS database was reviewed and evaluated for the appropriateness of medication prescriptions across the country, which enabled accurate monitoring of drug compliance and prescription status (13, 14). The clinical outcomes of interest were all-cause death, cardiovascular death, and myocardial infarction (MI). Cardiovascular death was ascertained from the National Statistical Office of Korea, which provided the death certificates with an accuracy of 92% for specific cause of death

Abbreviations: CI, confidence interval; DES, drug-eluting stent; BP-DES, DES with biodegradable polymers; DP-DES, DES with durable polymers; HR, hazard ratio; IPTW, inversed probability of treatment weighting; MI, myocardial infarction; HIS, National Health Insurance Service; PCI, percutaneous coronary intervention; SMD, standardized mean difference.

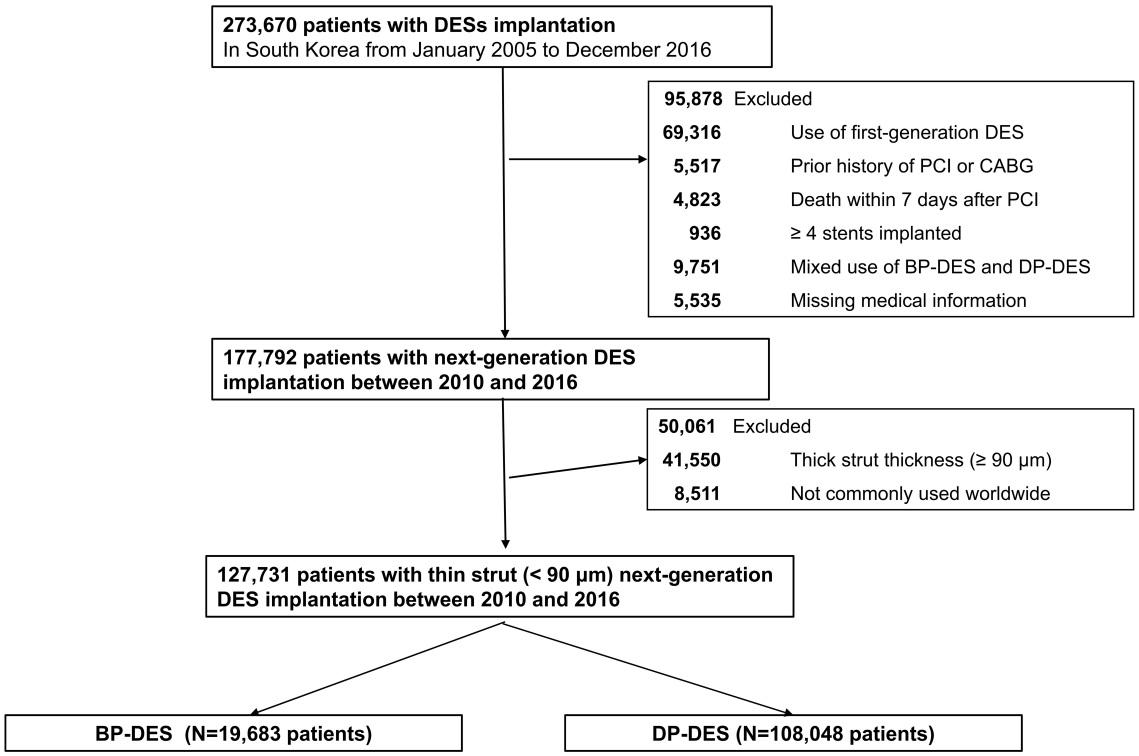

FIGURE 1 | A flowchart of study population. DES, drug-eluting stent; BP-DES, biodegradable polymer drug-eluting stent; CABG, coronary artery bypass graft; DP-DES, durable polymer drug-eluting stent; PCI, percutaneous coronary intervention.

(12, 15). Cardiovascular death was identified by a death certificate with at least one cardiovascular-related diagnosis (acute MI, stroke, heart failure or sudden cardiac death) (16). MI was defined by the ICD-10 codes corresponding to acute MI (14), and satisfying one or more of the following conditions: (1) concurrent presence of claims for coronary angiography, (2) admission *via* emergency department, or (3) performance of cardiac biomarker testing more than 4 times. Additionally, we included baseline comorbidities and drug prescription status before PCI for the propensity score calculation, and inverse probability treatment of weighting (IPTW) was used to account for differences in baseline characteristics, medical history and confounding bias (13, 16). Details regarding covariates included in the propensity score calculation are described in **Supplementary Table 2**.

Sensitivity Analysis

In order to assess the consistency of our analyses, we performed subgroup analyses for all-cause death, cardiovascular death, or MI stratified by age, sex, hypertension, diabetes mellitus, presentation as acute MI, chronic kidney disease with severe renal impairment, and prior cerebrovascular accidents.

Statistical Analysis

Continuous variables are reported as mean and standard deviation, while dichotomous variables are presented as frequencies and their percentages. To minimize the effect of confounding bias, we calculated the inverse probability of treatment weights (IPTW) by the propensity score, which was calculated by logistic regression with covariates including age, sex, history of comorbidities and medications, and year of PCI (**Supplementary Table 2**). We also stabilized the weights by multiplying IPTW by the marginal probability of receiving treatment. The effect size difference between the two groups for all comorbidities and medications was calculated using the standardized mean difference (SMD) and Kernel density plots. SMD values above 0.2 were regarded as potential imbalance between the two groups. Cumulative incidence curves and the rate of the clinical outcomes of interest during follow-up were plotted using the Kaplan–Meier method. The adjusted hazard ratio (HR) for each clinical outcome of interest was calculated using a Cox proportional hazard regression model. Cause-specific hazard model was used to consider death as a competing risk when comparing the incidences of cardiovascular death or MI. The variables that were not balanced between the groups after IPTW-adjustment such as "year of PCI" and "duration of DAPT" were incorporated as covariates for multivariable regression analyses. A two-sided p-values of <0.05 were considered significant. Statistical analyses were conducted using SAS version 9.4 (SAS Institute, Cary, NC, USA) and R version 3.6 (The R Foundation, www.R-project.org).

RESULTS

Baseline clinical characteristics and medical history of the whole cohort population before and after stabilized IPTW are

TABLE 1 | Baseline characteristics and medications at discharge after index PCI.

	Before stabilized IPTW (*N* = 127,731)			After stabilized IPTW (*N* = 127,588)		
	BP-DES (*N* = 19,683)	**DP-DES (*N* = 108,048)**	**SMD**	**BP-DES (*N* = 19,521)**	**DP-DES (*N* = 108,067)**	**SMD**
Age, years	64.8 ± 11.7	64.7 ± 11.5	0.013	64.6 ± 11.6	64.7 ± 11.5	0.005
Women	5,405 (27.5)	31,494 (29.1)	0.037	5,590 (28.6)	31,211 (28.9)	0.005
Comorbidity						
Hypertension	12,301 (62.5)	70,798 (65.5)	0.063	12,750 (65.3)	70,265 (65.0)	0.006
Dyslipidemia	8,573 (43.6)	42,647 (39.5)	0.083	7,852 (40.2)	43,375 (40.1)	0.002
Diabetes mellitus	6,902 (35.1)	37,518 (34.7)	0.007	6,855 (35.1)	37,532 (34.7)	0.008
Chronic kidney disease with severe renal impairment*	1,334 (6.8)	6,861 (6.3)	0.017	1,218 (6.2)	6,924 (6.4)	0.007
Heart failure	2,680 (13.6)	14,960 (13.8)	0.007	2,666 (13.7)	14,925 (13.8)	0.004
Chronic liver disease	1,820 (9.2)	10,340 (9.6)	0.011	1,835 (9.4)	10,284 (9.5)	0.004
Chronic pulmonary disease	1,292 (6.6)	7,823 (7.2)	0.027	1,358 (7.0)	7,707 (7.1)	0.007
Peripheral arterial occlusive disease	731 (3.7)	4,028 (3.7)	0.001	734 (3.8)	4,020 (3.7)	0.002
Atrial fibrillation or flutter	734 (3.7)	3,802 (3.5)	0.011	708 (3.6)	3,835 (3.5)	0.004
Prior malignancy	1,052 (5.3)	4,895 (4.5)	0.038	917 (4.7)	5,028 (4.7)	0.002
Prior stroke or TIA	1,761 (8.9)	10,636 (9.8)	0.031	1,840 (9.4)	10,481 (9.7)	0.009
Prior ICH	114 (0.6)	550 (0.5)	0.010	92 (0.5)	557 (0.5)	0.006
Presentation as AMI	3,719 (18.9)	19,037 (17.6)	0.033	3,514 (18.0)	19,343 (17.9)	0.011
Thyroid disorder	530 (2.7)	2,923 (2.7)	0.001	551 (2.8)	2,924 (2.7)	0.007
Osteoporosis	1,296 (6.6)	7,574 (7.0)	0.017	1,364 (7.0)	7,492 (6.9)	0.002
Medication prior to PCI						
Anticoagulant	763 (3.9)	3,590 (3.3)	0.030	693 (3.5)	3,680 (3.4)	0.008
Anti-platelet agent	9,311 (47.3)	54,635 (50.6)	0.065	9,721 (49.8)	54,102 (50.1)	0.020
BP-lowering agents†	12,625 (64.1)	69,117 (64.0)	0.004	12,510 (64.1)	69,118 (64.0)	0.002
β-Blockers	13,559 (68.9)	78,945 (73.1)	0.092	14,148 (72.5)	78,217 (72.4)	0.002
RAAS blockade	12,414 (63.1)	72,293 (66.9)	0.081	12,619 (64.6)	71,577 (66.2)	0.013
Statin	18,681 (94.9)	102,711 (95.1)	0.007	18,584 (95.2)	102,664 (95.0)	0.007
Duration of DAPT after PCI						
<12 months	6,349 (32.1)	26,904 (24.9)	0.175	5,845 (30.5)	27,827 (25.7)	0.104
≥12 months	13,334 (67.9)	81, 144 (75.1)		13,676 (69.5)	80,240 (74.3)	
Year of PCI						
2010	145 (0.7)	14,861 (13.8)	1.178	212 (1.1)	14,702 (13.6)	1.190
2011	171 (0.9)	11,721 (10.8)		252 (1.3)	11,630 (10.8)	
2012	220 (1.1)	10,054 (9.3)		291 (1.5)	9,962 (9.2)	
2013	417 (2.1)	9,339 (8.6)		404 (2.1)	9,306 (8.6)	
2014	2,557 (13.0)	18,583 (17.2)		2,041 (10.5)	18,553 (17.2)	
2015	4,332 (22.0)	22,011 (20.4)		3,815 (19.5)	22,193 (20.5)	
2016	11,841 (60.2)	21,479 (19.9)		12,506 (64.1)	21,721 (20.1)	

*Values are the mean ± standard deviation or n (%). AMI, acute myocardial infarction; BP-DES, biodegradable polymer drug-eluting stent; BP, blood pressure; DP-DES, durable polymer drug-eluting stent; ICH, intracranial hemorrhage; IPTW, inverse probability of treatment weighting; PCI, percutaneous coronary intervention; RAAS, renin-angiotensin-aldosterone-system; SMD, standardized mean difference; TIA, transient ischemic attack; DAPT, dual antiplatelet therapy. *Chronic kidney disease with advanced stage requiring intensive medical therapy and financial assistance from health insurance. † Alpha receptor antagonists, calcium-channel blocker or diuretics.*

presented in **Table 1**. After stabilized IPTW, there was no evidence of inequality in the baseline clinical characteristics and medications between the two groups (all SMD < 0.1, **Supplementary Figures 1**, **2**), except for the duration of dual antiplatelet therapy (DAPT) and year of index PCI. The incidence and relative hazards for the clinical outcomes of interest between the two groups after stabilized IPTW are presented in **Table 2**. At 5 years after index PCI, the incidence of all-cause death was significantly lower in patients treated with BP-DES (11.3 vs. 13.0% in those treated with DP-DES, HR 0.92, 95% CI, 0.88–0.96, $p < 0.001$; **Figure 2A**), while showing no statistically significant difference at 2 years after PCI (5.7 vs. 6.0%, respectively, HR 0.95, 95% CI, 0.89–1.01, $p = 0.238$). Statistical significance of reduced all-cause death was achieved in the BP-DES group at 3 years after index PCI (7.7 vs. 8.4% in DP-DES group, HR 0.93, 95% CI, 0.87–0.99, $p = 0.015$). Similarly, use of BP-DES was associated with a lower incidence of cardiovascular death (7.4 vs. 9.6% in those treated with DP-DES, HR 0.82, 95%

TABLE 2 | Risk of clinical outcome between biodegradable and durable polymer DES after stabilized inverse probability of treatment weighting.

	Follow-up time	BP-DES (*N* = 19,521)	DP-DES (*N* = 108,067)	R0isk difference (95% CI)*	Hazard ratio (95% CI)†	*P*-value
All-cause death	1 year	644 (3.3%)	3,795 (3.5%)	−0.2 (−0.5 to 0.1)	0.94 (0.86 to 1.02)	0.322
	2 year	1,113 (5.7%)	6,484 (6.0%)	−0.3 (−0.7 to 0.1)	0.95 (0.89 to 1.01)	0.238
	3 year	1,496 (7.7%)	9,040 (8.4%)	−0.7 (−1.1 to −0.3)	0.93 (0.87 to 0.99)	0.015
	4 year	1,989 (10.2%)	11,810 (10.9%)	−0.7 (−1.2 to −0.2)	0.92 (0.87 to 0.97)	<0.001
	5 year	2,211 (11.3%)	14,092 (13.0%)	−1.7 (−2.2 to −1.2)	0.92 (0.88 to 0.96)	<0.001
Cardiovascular death	1 year	547 (2.8%)	3,242 (3.0%)	−0.2 (−0.5 to 0.1)	0.93 (0.85 to 1.02)	0.137
	2 year	898 (4.6%)	5,295 (4.9%)	−0.3 (−0.6 to 0.0)	0.93 (0.85 to 1.01)	0.120
	3 year	1,146 (5.9%)	7,262 (6.7%)	−0.8 (−1.2 to −0.4)	0.87 (0.82 to 0.93)	<0.001
	4 year	1,357 (7.0%)	9,045 (8.4%)	−1.4 (−1.9 to −0.9)	0.83 (0.78 to 0.88)	<0.001
	5 year	1,450 (7.4%)	10,414 (9.6%)	−2.2 (−2.7 to −1.7)	0.82 (0.77 to 0.87)	<0.001
Myocardial infarction	1 year	599 (3.1%)	3,476 (3.2%)	−0.1 (−0.4 to 0.1)	0.96 (0.88 to 1.05)	0.783
	2 year	967 (5.0%)	5,479 (5.1%)	−0.1 (−0.4 to 0.2)	0.98 (0.92 to 1.05)	0.461
	3 year	1,179 (6.0%)	7,012 (6.5%)	−0.4 (−0.8 to 0.0)	0.94 (0.88 to 1.00)	0.394
	4 year	1,378 (7.1%)	8,405 (7.8%)	−0.7 (−1.1 to −0.3)	0.92 (0.87 to 0.97)	0.037
	5 year	1,447 (7.4%)	9,435 (8.7%)	−1.3 (−1.7 to −0.9)	0.90 (0.86 to 0.94)	0.006

*BP-DES, biodegradable polymer drug-eluting stents; DP-DES, durable polymer drug-eluting stent; CI, confidence interval. Number in parentheses represent the percentage. *Risk difference (95% CI) were calculated by Poisson regression with identity link. † Hazard ratios (95% CI) were calculated by Cox proportional hazard model.*

CI, 0.77–0.87, $p < 0.001$; **Figure 2B**), and MI (7.4 vs. 8.7% in those treated with DP-DES, HR 0.90, 95% CI, 0.86–0.94, $p = 0.006$; **Figure 2C**) at 5 years after index PCI, while showing no statistically significant difference at 2 years after index PCI (4.6 vs. 4.9%, respectively, HR 0.93, 95% CI, 0.85–1.01, $p = 0.120$ for cardiovascular death; 5.0 vs. 5.1%, respectively, HR 0.98, 95% CI, 0.92–1.05, $p = 0.461$ for MI). The incidence and relative hazards for the outcomes of interest between the two groups before stabilized IPTW are presented in **Supplementary Table 3**. In a landmark analysis between 2 and 5 years after index PCI, the use of BP-DES was distinctly associated with reduced occurrence of all-cause death (5.9 vs. 7.4% in patients treated with DP-DES, HR 0.91, 95% CI, 0.86–0.96, $p < 0.001$; **Figure 2D**), cardiovascular death (3.1 vs. 4.9%, respectively, HR 0.73, 95% CI, 0.67–0.80, $p < 0.001$; **Figure 2E**) and MI (2.7 vs. 3.9%, respectively, HR 0.79, 95% CI, 0.72–0.87, $p < 0.001$; **Figure 2F**) (**Supplementary Table 4**). Multivariable regression analysis also revealed consistent favorable impact of BP-DES compared with DP-DES on all-cause or cardiovascular death at 5-years after PCI (**Supplementary Tables 5**, **6**). A subgroup analysis showed that BP-DES had a consistent beneficial effect on the 5-year incidence of all-cause death (**Figure 3**), cardiovascular death (**Figure 4**), or MI (**Supplementary Figure 3**) across subgroups.

DISCUSSION

To the best of our knowledge, the results of our analyses were derived from a nationwide cohort with the largest study population ever published. Of note, a major strength of our study was inclusion of all patients treated with thin-strut DESs that are commonly used world-wide in daily clinical practice. Therefore, very-high-risk patients who were usually excluded in prior randomized studies were entirely included in this study. In addition, there was completeness in monitoring for demographic characteristics, comorbidities, medication history, occurrence of clinical events requiring hospitalization, and prescription status of essential cardiac medications such as anti-platelet agents during 5-year follow-up after index PCI. Through analysis of the death certificates provided by the National Statistical Office, we could discriminate cardiovascular death from all-cause death. Therefore, we could investigate the impact of remnant polymer in new-generation DES on cardiovascular death. The principal findings of our study are as follows: (1) In the early term period, the rates for the clinical outcomes of interest were not significantly different between BP- and DP-DES-treated patients; however, (2) the cumulative incidence of clinical events was gradually different between the two groups as time passed after index PCI. Favorable results for the clinical outcomes of interest were distinctly apparent at 5 years after index PCI in BP-DES-treated patients.

It has been suggested that anti-proliferative drugs *per se* and their polymer carriers in the coronary arterial bed continuously evoke chronic vascular inflammation (4, 5) that leads to delayed vascular healing and incomplete endothelial strut coverage and potentially contributes to clinical presentation of very late stent thrombosis and MI (17). Autopsy studies elucidated a more robust extra-cellular matrix deposition in the re-stenotic lesions of implanted DP-DES compared with bare-metal stents (18), which are considered to play a crucial role in the development of neoatherosclerosis and consequent stent failure (4).

Prior randomized clinical trials and meta-analyses comparing BP- and DP-DES have demonstrated confounding results (6–9, 11). The BIOFLOW V randomized trial showed a significant clinical benefit of biodegradable polymer sirolimus-eluting stents ($n = 884$ patients) over the durable polymer everolimus-eluting stents ($n = 450$ patients) by reducing 1-year incidence rate of target-lesion failure (11). However, the Bio-RESORT

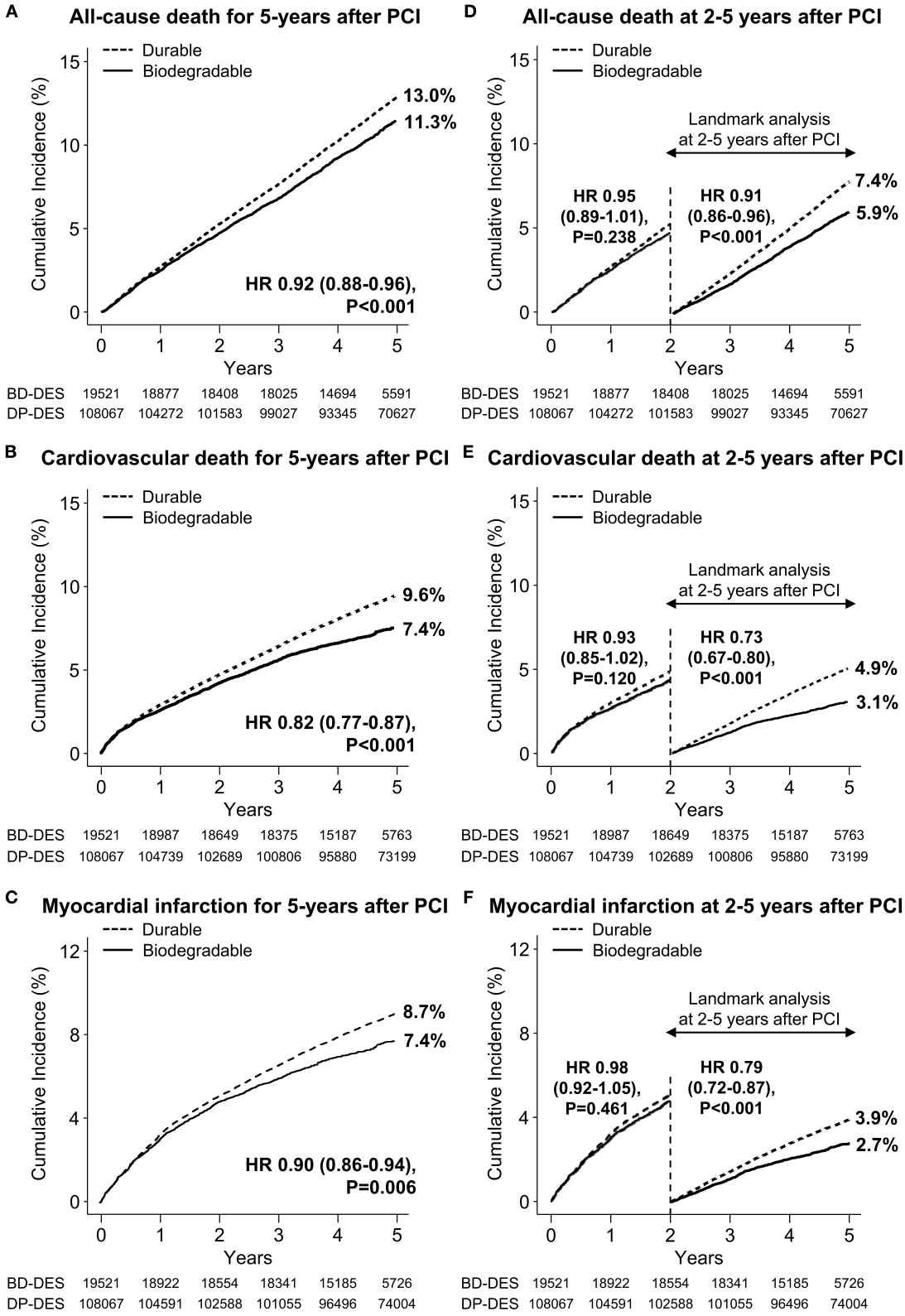

FIGURE 2 | Time-to-event curves for the clinical outcome of interest and landmark analysis between 2 and 5 years after PCI. The cumulative incidence of **(A)** all-cause death, **(B)** cardiovascular death, and **(C)** myocardial infarction for 5 years after new-generation drug-eluting stent implantation. Landmark analyses between 2 and 5 years after index percutaneous coronary intervention for the cumulative incidence of **(D)** all-cause death, **(E)** cardiovascular death, and **(F)** myocardial infarction are presented. BP-DES, biodegradable polymer drug-eluting stent; DES, drug-eluting stent; DP-DES, durable polymer drug-eluting stent; HR, hazard ratio.

Covariates	Biodegradable		Durable		Hazard ratio (95% CI)	P for interaction
	Patient N	5-year mortality	Patient N	5-year mortality		
Age						
< 65 years	9558	372 (3.9)	51976	2314 (4.5)	0.91 (0.81-1.01)	0.67
≥ 65 years	9963	1839 (18.5)	56091	11778 (21.0)	0.93 (0.84-1.02)	
Sex						
Female	5590	794 (14.2)	31211	4790 (15.3)	0.96 (0.89-1.03)	0.19
Male	13931	1417 (10.2)	76856	9302 (12.1)	0.89 (0.85-0.94)	
Hypertension						
No	6770	634 (9.4)	37802	4027 (10.7)	0.93 (0.85-1.00)	0.72
Yes	12751	1577 (12.4)	70265	10065 (14.3)	0.91 (0.86-0.96)	
Diabetes mellitus						
No	12666	1082 (8.5)	70535	7011 (9.9)	0.91 (0.85-0.97)	0.87
Yes	6855	1129 (16.5)	37532	7081 (18.9)	0.93 (0.87-0.99)	
Presentation as Acute MI						
No	16007	1759 (11.0)	88724	11218 (12.6)	0.92 (0.88-0.96)	0.94
Yes	3514	452 (12.9)	19343	2874 (14.9)	0.92 (0.83-1.01)	
Chronic kidney disease with severe renal impairment						
No	18303	1783 (9.7)	101143	11530 (11.4)	0.90 (0.86-0.94)	0.09
Yes	1218	428 (35.1)	6924	2562 (37.0)	0.98 (0.89-1.08)	
Prior CVA						
No	17681	1846 (10.4)	97586	11653 (11.9)	0.92 (0.88-0.97)	0.76
Yes	1840	365 (19.8)	10481	2439 (23.3)	0.91 (0.81-1.00)	

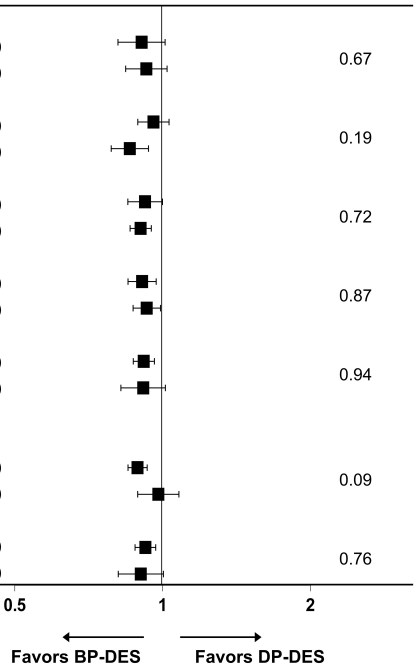

FIGURE 3 | Subgroup analyses for all-cause death. Numbers and percentages show the number of patients at risk, those who died with any cause of death, and the all-cause mortality rate at 5 years after drug-eluting stent implantation. CI, confidence interval; CVA, cerebrovascular accidents; BP-DES, biodegradable polymer drug-eluting stent; DP-DES, durable polymer drug-eluting stent; MI, myocardial infarction.

Covariates	Biodegradable		Durable		Hazard ratio (95% CI)	P for interaction
	Patient N	5-year mortality	Patient N	5-year mortality		
Age						
< 65 years	9558	235 (2.5)	51976	1640 (3.2)	0.83 (0.72 to 0.95)	0.91
≥ 65 years	9963	1215 (12.2)	56091	8774 (15.6)	0.82 (0.77 to 0.87)	
Sex						
Female	5590	536 (9.6)	31211	3626 (11.6)	0.86 (0.78-0.94)	0.29
Male	13931	914 (6.6)	76856	6788 (8.8)	0.81 (0.75-0.86)	
Hypertension						
No	6770	403 (6.0)	37802	2886 (7.6)	0.83 (0.74-0.92)	0.94
Yes	12751	1047 (8.2)	70265	7528 (10.7)	0.82 (0.77-0.88)	
Diabetes mellitus						
No	12666	713 (5.6)	70535	5185 (7.4)	0.83 (0.76-0.89)	0.88
Yes	6855	737 (10.8)	37532	5229 (13.9)	0.82 (0.76-0.88)	
Presentation as Acute MI						
No	16007	1151 (7.2)	88724	8218 (9.3)	0.82 (0.77-0.87)	0.93
Yes	3514	299 (9.0)	19343	2196 (11.4)	0.82 (0.73-0.91)	
Chronic kidney disease with severe renal impairment						
No	18303	1173 (6.4)	101143	8523 (8.4)	0.81 (0.76-0.86)	0.41
Yes	1218	277 (22.8)	6924	1891 (27.3)	0.86 (0.76-0.97)	
Prior CVA						
No	17681	1197 (6.8)	97586	8530 (8.7)	0.83 (0.78-0.88)	0.45
Yes	1840	253 (13.8)	10481	1884 (18.0)	0.79 (0.69-0.90)	

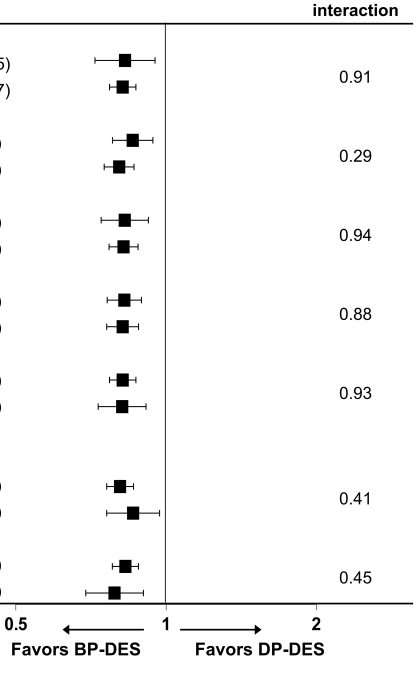

FIGURE 4 | Subgroup analyses for cardiovascular death. Numbers and percentages show the number of patients at risk, those who died with cardiovascular disease, and the cardiovascular mortality rate at 5 years after drug-eluting stent implantation. CI, confidence interval; CVA, cerebrovascular accidents; BP-DES, biodegradable polymer drug-eluting stent; DP-DES, durable polymer drug-eluting stent; MI, myocardial infarction.

randomized trial showed no statistically significant difference of primary endpoint at 12 months between biodegradable polymer everolimus-eluting (n = 1,172 patients) and sirolimus-eluting stents (n = 1,173 patients) vs. durable polymer zotarolimus-eluting stents (n = 1,169) (9). A meta-analysis that included 19,886 patients derived from 16 randomized clinical trials found no statistically distinct benefit of BP-DES over DP-DES during a mean follow-up duration of 26 months (6). It might be inappropriate to prove the clinical benefits of BP-DES over DP-DES within 12 months after index PCI. Because DAPT for about 12 months was usually recommended in most studies, the complications or clinical presentations caused by persistent polymer in DP-DES might be masked by DAPT.

Neoatherosclerosis is one of the main mechanisms of very late stent thrombosis after DES implantation (19). Persistence of polymer of DP-DES in the coronary vascular bed may also provoke chronic inflammation characterized by infiltration of inflammatory cells such as macrophage or lymphocytes, playing a central role in the progression of neoatherosclerosis (4). And, the development of neoatherosclerosis is a time-dependent phenomenon; the frequency of neoatherosclerosis increases with the stent age. Our prior intracoronary optical coherence tomography study showed that neoatherosclerosis was observed in 45.7% of patients between 3 and 5 years, 61.5% between 5 and 7 years and 73.9% more than 7 years after DES implantation (20). Therefore, neoatherosclerosis observed at the very late period was significantly associated with very late stent thrombosis. Furthermore, since the polymer degradation are generally known to take about 6–24 months (21, 22), it could be difficult to detect a statistical difference in clinical outcomes according to the polymer properties in early period. These prior findings may provide a plausible explanation for the beneficial effects of BP-DES that appear after a certain period of time post-new generation DES implantation. Indeed, in a prior large nationwide cohort that compared the effect of BP- and DP-DES in real-world practice (total 57,487 patients; BP-DES-treated patients, 10,032 and DP-DES-treated patients, 47,455), there was no significant difference in the occurrence of all-cause mortality or myocardial infarction for 2 years after index PCI (10). Similarly, our analysis also revealed no statistically significant difference in the occurrence of the outcomes of interest at 2 years after new-generation DES implantation; however, significant differences were gradually observed at 3 years post-DES implantation, favoring BP-DES. Based on our prior optical coherence tomography analysis and this newly acquired nationwide claims data analysis, we may postulate that the adverse effects of permanent remnant polymer in the coronary artery start to appear at about 3 years post-PCI and become distinct at about 5 years post-PCI. In addition, the increase in risk of cardiovascular events due to permanent remnant polymer is statistically clear, but the degree is somewhat modest, so it may be necessary to analyze a very large number of patients in order to identify statistically clear differences. The BIOSCIENCE randomized trial reported that 5-year risk of target lesion failure was similar between biodegradable polymer sirolimus-eluting stent (n = 1,063 patients) vs. durable polymer everolimus-eluting stent (n = 1,056 patients) (23). The ISAR-TEST 4 randomized trial recently reported that the 10-year incidence of major adverse cardiac events was not statistically different between biodegradable polymer sirolimus-eluting stents (n = 1,299 patients) vs. durable polymer everolimus-eluting stents (n = 652 patients) (24). These studies did not show a clinical benefit of BP-DES over DP-DES at 5- or 10-year follow-up (23, 24). The main reason for failure to demonstrate the theoretical benefits of BP-DES over DP-DES in these clinical studies might be inappropriately small number of study populations. With the number of all-cause deaths during 5-year follow-up and a total sample size of 127,731, our study had about 82.1% power to detect an HR of 0.80 in the comparison of the BP-DES group with the DP-DES group at a two-tailed alpha level of 5.0%. Further, because in contrast to usual design of randomized controlled trials, we did not exclude the very high-risk patients, the incorporation of very high-risk patients could have attributed to demonstrating a clinical benefit of BP-DES that become distinct over time.

LIMITATIONS

This study has several limitations. First, the findings from this observational study cannot be applied to establish causal relationships and persistent residual confounding factors should be considered in the interpretation of our results, although we tried to minimize the bias through IPTW. Furthermore, as the NHIS database does not contain laboratory parameters or clinical information except for the diagnostic codes, unmeasured variables could have affected the results of our analyses. Second, because this database does not include angiographic or procedural information, including the extent and complexity of coronary artery disease, the impact of high-risk procedural characteristics was not fully considered in the interpretation of our analyses. Furthermore, since the result of electrocardiography was not available in this database, the impact of clinical presentation such as ST-elevation MI or non-ST elevation MI was not considered in statistical analyses. Third, to protect patients' personal information and avoid unnecessary conflict with the device manufacturer, the NHIS database provides information of DESs after sufficient encryption work, which includes DES generation, polymer degradability, and strut thickness. Finally, the temporal difference between the groups still remained even after IPTW-adjustment. Thus, care should be taken in interpretation of our result, although we adjusted the temporal difference in all regression analyses. Therefore, further analyses such as impact of the eluted drug or stent material was not performed, which should be carried out through following research.

CONCLUSIONS

In this nationwide cohort of all patients treated with new-generation DES in Korea, BP-DES implantation was associated with a lower risk of all-cause death, cardiovascular death or MI. This difference appeared around 3 years after DES implantation and became more distinct with time.

DATA AVAILABILITY STATEMENT

The data analyzed in this study is subject to the following licenses/restrictions: the datasets generated for the analyses are not publicly available because of strict government restrictions. Requests to access these datasets should be directed to M-KH, mkhong61@yuhs.ac.

ETHICS STATEMENT

The studies involving human participants were reviewed and approved by Severance Hospital Institutional Review Board. The Ethics Committee waived the requirement of written informed consent for participation.

AUTHOR CONTRIBUTIONS

S-JL, D-WC, C-MN, and M-KH contributed to the conception and design and verified the data and conducted all analyses. S-JL and M-KH wrote the study protocol. D-WC and C-MN performed the programming to extract the data from the NHIS database. M-KH had full access to all the data in the study and take responsibility for the integrity of the data and the accuracy of the data analysis. YS, S-JH, C-MA, J-SK, B-KK, Y-GK, DC, E-CP, and YJ provided a critical review of manuscript. All authors read and approved on the final publication.

FUNDING

This work was supported by the Cardiovascular Research Center, Seoul, South Korea.

SUPPLEMENTARY MATERIAL

The Supplementary Material for this article can be found online at: https://www.frontiersin.org/articles/10.3389/fcvm.2022.873114/full#supplementary-material

REFERENCES

1. Bangalore S, Toklu B, Patel N, Feit F, Stone GW. Newer-generation ultrathin strut drug-eluting stents versus older second-generation thicker strut drug-eluting stents for coronary artery disease. *Circulation.* (2018) 138:2216–26. doi: 10.1161/CIRCULATIONAHA.118.034456
2. Byrne RA, Stone GW, Ormiston J, Kastrati A. Coronary balloon angioplasty, stents, and scaffolds. *Lancet.* (2017) 390:781–92. doi: 10.1016/S0140-6736(17)31927-X
3. Palmerini T, Benedetto U, Biondi-Zoccai G, Della Riva D, Bacchi-Reggiani L, Smits PC, et al. Long-term safety of drug-eluting and bare-metal stents: Evidence from a comprehensive network meta-analysis. *J Am Coll Cardiol.* (2015) 65:2496–507. doi: 10.1016/j.jacc.2015.04.017
4. Otsuka F, Byrne RA, Yahagi K, Mori H, Ladich E, Fowler DR, et al. Neoatherosclerosis: Overview of histopathologic findings and implications for intravascular imaging assessment. *Eur Heart J.* (2015) 36:2147–59. doi: 10.1093/eurheartj/ehv205
5. Guagliumi G, Shimamura K, Sirbu V, Garbo R, Boccuzzi G, Vassileva A, et al. Temporal course of vascular healing and neoatherosclerosis after implantation of durable- or biodegradable-polymer drug-eluting stents. *Eur Heart J.* (2018) 39:2448–56. doi: 10.1093/eurheartj/ehy273
6. El-Hayek G, Bangalore S, Casso Dominguez A, Devireddy C, Jaber W, Kumar G, et al. Meta-analysis of randomized clinical trials comparing biodegradable polymer drug-eluting stent to second-generation durable polymer drug-eluting stents. *JACC Cardiovasc Interv.* (2017) 10:462–73. doi: 10.1016/j.jcin.2016.12.002
7. Raungaard B, Jensen LO, Tilsted HH, Christiansen EH, Maeng M, Terkelsen CJ, et al. Zotarolimus-eluting durable-polymer-coated stent versus a biolimus-eluting biodegradable-polymer-coated stent in unselected patients undergoing percutaneous coronary intervention (SORT OUT VI): a randomised non-inferiority trial. *Lancet.* (2015) 385:1527–35. doi: 10.1016/S0140-6736(14)61794-3
8. Smits PC, Hofma S, Togni M, Vazquez N, Valdes M, Voudris V, et al. Abluminal biodegradable polymer biolimus-eluting stent versus durable polymer everolimus-eluting stent (COMPARE II): a randomised, controlled, non-inferiority trial. *Lancet.* (2013) 381:651–60. doi: 10.1016/S0140-6736(12)61852-2
9. von Birgelen C, Kok MM, van der Heijden LC, Danse PW, Schotborgh CE, Scholte M, et al. Very thin strut biodegradable polymer everolimus-eluting and sirolimus-eluting stents versus durable polymer zotarolimus-eluting stents in allcomers with coronary artery disease (BIO-RESORT): a three-arm, randomised, non-inferiority trial. *Lancet.* (2016) 388:2607–17. doi: 10.1016/S0140-6736(16)31920-1
10. Buccheri S, James S, Lindholm D, Frobert O, Olivecrona GK, Persson J, et al. Clinical and angiographic outcomes of bioabsorbable vs. permanent polymer drug-eluting stents in Sweden: a report from the Swedish Coronary and Angioplasty Registry (SCAAR). *Eur Heart J.* (2019) 40:2607–15. doi: 10.1093/eurheartj/ehz244
11. Kandzari DE, Mauri L, Koolen JJ, Massaro JM, Doros G, Garcia-Garcia HM, et al. Ultrathin, bioresorbable polymer sirolimus-eluting stents versus thin, durable polymer everolimus-eluting stents in patients undergoing coronary revascularisation (BIOFLOW V): a randomised trial. *Lancet.* (2017) 390:1843–52. doi: 10.1016/S0140-6736(17)32249-3
12. Choi EK. Cardiovascular research using the Korean national health information database. *Korean Circ J.* (2020) 50:754–72. doi: 10.4070/kcj.2020.0171
13. Kim J, Kang D, Park H, Kang M, Park TK, Lee JM, et al. Long-term beta-blocker therapy and clinical outcomes after acute myocardial infarction in patients without heart failure: nationwide cohort study. *Eur Heart J.* (2020) 41:3521–9. doi: 10.1093/eurheartj/ehaa376
14. Kang DO, An H, Park GU, Yum Y, Park EJ, Park Y, et al. Cardiovascular and bleeding risks associated with nonsteroidal anti-inflammatory drugs after myocardial infarction. *J Am Coll Cardiol.* (2020) 76:518–29. doi: 10.1016/j.jacc.2020.06.017
15. Won TY, Kang BS, Im TH, Choi HJ. The study of accuracy of death statistics. *Korean J Emerg Med.* (2007) 18:256–62.
16. You SC, Rho Y, Bikdeli B, Kim J, Siapos A, Weaver J, et al. Association of ticagrelor vs clopidogrel with net adverse clinical events in patients with acute coronary syndrome undergoing percutaneous coronary intervention. *JAMA.* (2020) 324:1640–50. doi: 10.1001/jama.2020.16167
17. Joner M, Finn AV, Farb A, Mont EK, Kolodgie FD, Ladich E, et al. Pathology of drug-eluting stents in humans: delayed healing and late thrombotic risk. *J Am Coll Cardiol.* (2006) 48:193–202. doi: 10.1016/j.jacc.2006.03.042
18. Nakano M, Otsuka F, Yahagi K, Sakakura K, Kutys R, Ladich ER, et al. Human autopsy study of drug-eluting stents restenosis: histomorphological predictors and neointimal characteristics. *Eur Heart J.* (2013) 34:3304–13. doi: 10.1093/eurheartj/eht241
19. Taniwaki M, Radu MD, Zaugg S, Amabile N, Garcia-Garcia HM, Yamaji K, et al. Mechanisms of very late drug-eluting stent thrombosis assessed by optical coherence tomography. *Circulation.* (2016) 133:650–60. doi: 10.1161/CIRCULATIONAHA.115.019071
20. Lee SY, Hur SH, Lee SG, Kim SW, Shin DH, Kim JS, et al. Optical coherence tomographic observation of in-stent neoatherosclerosis in lesions

with more than 50% neointimal area stenosis after second-generation drug-eluting stent implantation. *Circ Cardiovasc Interv*. (2015) 8:e001878. doi: 10.1161/CIRCINTERVENTIONS.114.001878

21. Garg S, Bourantas C, Serruys PW. New concepts in the design of drug-eluting coronary stents. *Nat Rev Cardiol*. (2013) 10:248–60. doi: 10.1038/nrcardio.2013.13
22. Pilgrim T, Piccolo R, Heg D, Roffi M, Tuller D, Muller O, et al. Ultrathin strut biodegradable polymer sirolimus-eluting stent versus durable polymer everolimus-eluting stent for percutaneous coronary revascularisation (BIOSCIENCE): a randomised, single-blind, non-inferiority trial. *Lancet*. (2014) 384:2111–22. doi: 10.1016/S0140-6736(14)61038-2
23. Pilgrim T, Piccolo R, Heg D, Roffi M, Tuller D, Muller O, et al. Ultrathin-strut, biodegradable-polymer, sirolimus-eluting stents versus thin-strut, durable-polymer, everolimus-eluting stents for percutaneous coronary revascularisation: 5-year outcomes of the BIOSCIENCE randomised trial. *Lancet*. (2018). 392:737–46. doi: 10.1016/S0140-6736(18)31715-X
24. Kufner S, Joner M, Thannheimer A, Hoppmann P, Ibrahim T, Mayer K, et al. Ten-year clinical outcomes from a trial of three limus-eluting stents with different polymer coatings in patients with coronary artery disease. *Circulation*. (2019) 139:325–33. doi: 10.1161/CIRCULATIONAHA.118.038065

Conflict of Interest: The authors declare that the research was conducted in the absence of any commercial or financial relationships that could be construed as a potential conflict of interest.

Publisher's Note: All claims expressed in this article are solely those of the authors and do not necessarily represent those of their affiliated organizations, or those of the publisher, the editors and the reviewers. Any product that may be evaluated in this article, or claim that may be made by its manufacturer, is not guaranteed or endorsed by the publisher.

frontiers | Frontiers in Cardiovascular Medicine

MINI REVIEW
published: 23 May 2022
doi: 10.3389/fcvm.2022.882330

Primary Aldosteronism and Ischemic Heart Disease

Shivaraj Patil[1]*, *Chaitanya Rojulpote*[2] and *Aman Amanullah*[1]

[1] Department of Cardiology, Einstein Medical Center, Philadelphia, PA, United States, [2] Department of Medicine, The Wright Center for Graduate Medical Education, Scranton, PA, United States

Cardiovascular disease, in particular ischemic heart disease is a major cause of morbidity and mortality worldwide. Primary aldosteronism is the leading cause of secondary hypertension, yet commonly under diagnosed, and represents a major preventable risk factor. In contrast to historical teaching, recent studies have shown that excess aldosterone production is associated with increased burden of ischemic heart disease disproportionate to the effects caused by hypertension alone. Aldosterone through its genomic and non-genomic actions exerts various detrimental cardiovascular changes contributing to this elevated risk. Recognition of primary hyperaldosteronism and understanding the distinctive pathophysiology of ischemic heart disease in primary aldosteronism is crucial to develop strategies to improve outcomes.

Keywords: primary hyperaldosteronism (PA), ischemic heart disease, atherosclerosis, secondary hypertension, coronary artery disease

OPEN ACCESS

Edited by:
Carmine Pizzi,
Università di Bologna, Italy

Reviewed by:
Valentina Vicennati,
University of Bologna, Italy
Guido Di Dalmazi,
University of Bologna, Italy

***Correspondence:**
Shivaraj Patil
patilshi@einstein.edu

Specialty section:
This article was submitted to Coronary Artery Disease, a section of the journal Frontiers in Cardiovascular Medicine

Received: *23 February 2022*
Accepted: *14 April 2022*
Published: *23 May 2022*

Citation:
Patil S, Rojulpote C and Amanullah A (2022) Primary Aldosteronism and Ischemic Heart Disease. Front. Cardiovasc. Med. 9:882330. doi: 10.3389/fcvm.2022.882330

INTRODUCTION

Cardiovascular diseases (CVDs), consisting of ischemic heart disease, heart failure, peripheral arterial disease, and several other cardiac and vascular conditions, constitute the leading cause of global mortality and are a major contributor to reduced quality of life (1). Amongst CVDs, ischemic heart disease (IHD) is the main global cause of death, accounting for more than 9 million deaths in 2016 according to the World Health Organization (WHO) estimates. Although IHD rates are decreasing globally, risk factor prevalence is rising (2). Hypertension is a major modifiable risk factor for ischemic heart disease with nearly 1.39 billion adults affected worldwide in 2010 (3). It is estimated that risk of a fatal coronary event doubles with an increase in systolic blood pressure of 20 mm Hg or each 10-mm Hg increase in diastolic blood pressure (4). Aldosterone, a steroid hormone secreted by the adrenal gland, is an important regulator of blood pressure and primary hypersecretion of this hormone leads to dysregulation of homeostatic control mechanisms. Moreover, normotensive individuals with higher plasma aldosterone levels within physiological range are at an increased risk of subsequent rise in blood pressure and development of incident hypertension (5). The effect of excess production of aldosterone has traditionally been conceptualized as a result of its action on renal collecting duct principal cells, via mineralocorticoid receptors (MR), to induce sodium and water reabsorption and potassium excretion clinically culminating in hypertension associated with low or low-normal serum potassium levels. Historically, primary aldosteronism was considered an uncommon disease, however, with advances in diagnostic technology, primary aldosteronism (PA) is now identified as the most common endocrinological cause of secondary hypertension, with aldosterone producing adenoma (APA) and bilateral adrenal hyperplasia (BAH, idiopathic hyperaldosteronism) accounting for vast majority of cases (6). Recent evidence has linked primary aldosteronism with increased cardiovascular morbidity and mortality, out of proportion to the

adverse effects caused solely by elevated blood pressure, underscoring its pleiotropic effect and multifaceted role in cardiovascular pathophysiology (7–9). In this review, we aim to focus on the prevalence and pathophysiologic mechanisms of IHD in primary aldosteronism.

PREVALENCE OF ISCHEMIC HEART DISEASE IN PRIMARY ALDOSTERONISM

The true prevalence of PA is underestimated, with current studies reporting a prevalence of 3–13% in primary care setting and up to 30% in referral centers (6). The prevalence of IHD and MI in patients with primary aldosteronism is variable depending on the study design and diagnostic criteria ranging from 1.7 to 20% and 0.9 to 4.4%, respectively. The pooled prevalence of IHD and MI in PA were estimated to be 3.4 and 1.7% respectively (**Table 1**). Various epidemiological studies clearly demonstrate that individuals with primary aldosteronism experience higher burden of IHD compared to individuals with essential hypertension with comparable demographic and cardiovascular risk factor profile (8, 10, 11). Individuals with PA presenting with unilateral subtype, or plasma aldosterone concentration $\geq$125 pg/ml are at a greater risk of CVD (10). It has also been observed that hypokalemic variant of primary aldosteronism is associated with excessive burden of ischemic heart disease compared to normokalaemia variant, possibly due to effects of higher concentration of aldosterone exposure (12). Additionally, patients with primary hyperaldosteronism are more likely to have experienced an ischemic cardiovascular complication (non-fatal myocardial infarction or angina) at the time of diagnosis of PA than otherwise similar patients with essential hypertension (11). These data should draw the clinician's attention to broaden the scope to suspect PA, especially when severity of IHD or CVD morbidity is considered out of proportion to that effectuated by essential hypertension.

PATHOPHYSIOLOGY OF ISCHEMIC HEART DISEASE IN PRIMARY ALDOSTERONISM

IHD occurs due to an imbalance between myocardial blood supply and myocardial demand, either at rest or exertion. Atherosclerosis is the major pathophysiological process involved in development of IHD. IHD can be silent, termed as silent myocardial ischemia, or manifest clinically either as acute coronary syndrome, secondary to plaque rupture and coronary thrombosis, or as stable angina, due to fixed narrowing of the coronary arteries from plaque buildup in the vessel wall and luminal narrowing. Conventional risk factors for IHD include increased age, hypertension, diabetes mellitus, smoking, hyperlipidemia, and family history of IHD. Excess aldosterone not only adversely affects the vasculature and cardiac muscle, but also influences cardiovascular risk factors *via* various biochemical pathways, uniquely contributing to the development of IHD (**Figure 1**).

Effect of Hyperaldosteronism on Blood Pressure and Left Ventricle

It is well known that elevated aldosterone levels raise blood pressure via its genomic action mediated through mineralocorticoid receptor (MR) to absorb sodium and water in the renal collecting ducts causing volume expansion. Additionally, hyperaldosteronism increases blood pressure

TABLE 1 | Prevalence of ischemic heart disease in primary aldosteronism.

Study	Age (years)	Gender (men %)	SBP (mmHg)	DBP (mmHg)	IHD (%)	MI (%)
Ohno et al. (10) (Japan) (*N* = 2,582)	53.2 ± 11.3	47.1	141.4 ± 18.2	86.5 ± 12.8	2.1	0.9
Mulatero et al. (49) (Italy) (*N* = 270)	44 ± 8.5	59.6	155 ± 21	96 ± 12	2.6	4.0
Savard et al. (11) (France) (*N* = 459)	51.1 ± 10.2	67	151 ± 24.4	87.7 ± 13.1	5.7	4.4
Reincke et al. (50) (Germany) (*N* = 300)	50.0	61	168 ± 25	99 ± 16	4	-
Milliez et al. (51) (France) (*N* = 124)	52 ± 10	67	176 ± 23	107 ± 14	-	4
Choi et al. (52) (South Korea) (*N* = 85)	46.1 ± 10.3	43.5	173.8 ± 33.6	106.1 ± 19.2	20	-
Nishimura et al. (53) (Japan) (*N* = 58)	45 ± 9	53.4	166 ± 30	96.5 ± 18	1.7	-
Catena et al. (8) (Italy) (*N* = 54)	53 ± 12	70.4	167 ± 16	103 ± 9	20	-
Pooled prevalence IHD/MI (*N* = 3,808/3,435)					3.4	1.7

SBP, systolic blood pressure; DBP, diastolic blood pressure; IHD, ischemic heart disease; MI, myocardial infarction.

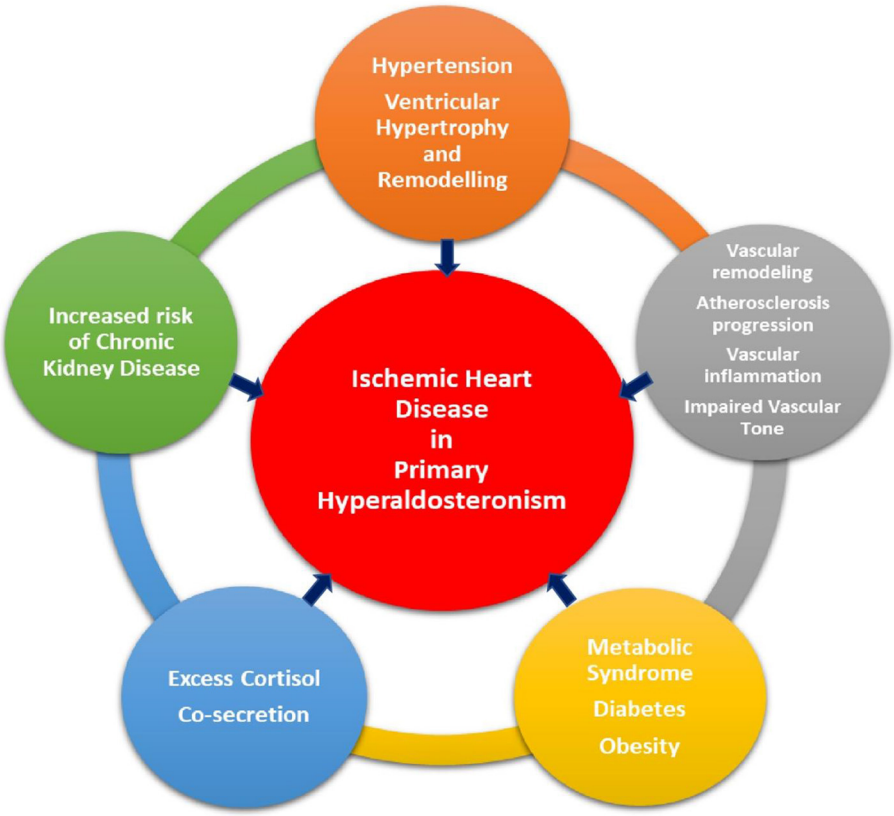

FIGURE 1 | Pathways through which primary aldosteronism plays a role in the development of ischemic heart disease.

mediated *via* its harmful effect on vascular remodeling. Hypertension due to PA is often undiagnosed and chronic exposure to elevated blood pressure, results in compensatory left ventricular (LV) hypertrophy. In addition, long term exposure of cardiac myocyte to elevated aldosterone levels leads to myocyte hypertrophy by increasing myocardial expression of cardiotrophin-1 (CT-1), a cytokine that induces expression of myosin light chain and skeletal α-actin and enhances myosin light chain phosphorylation (13). In addition, exposure to aldosterone causes increased mRNA levels of α- and β-myosin heavy chain via activation of mineralocorticoid receptors (MRs), extracellular signal-regulated kinase (ERK), c-Jun N-terminal kinase and protein kinase C-α (14). Remodeling of left ventricle in PA not only occurs via cardiac myocyte hypertrophy but also simultaneously via cardiac fibrosis through chronic inflammation, and dysregulation of extra cellular matrix metabolism (15). This results in stiffening of the LV with subsequent elevation in LV end-diastolic pressure (LVEDP). High LVEDP compromises diastolic coronary blood flow (CBF) by decreasing the coronary perfusion pressure (CPP) leading to decreased myocardial oxygen supply (16, 17). A combination of increased LV mass and diminished diastolic CBF causes supply-demand mismatch resulting in myocardial ischemia.

Effect of Hyperaldosteronism on Vasculature

Elevated serum aldosterone levels in PA patients lead to detrimental effects on the endothelium via genomic and nongenomic mechanisms via mineralocorticoid receptor-dependent and independent manners. Excess generation of reactive oxygen species (ROS) via increased NADPH oxidase production, decreased endothelial expression of G6PD, and mitochondrial ROS generation in the electron transport chain and release result in oxidative stress and amplify vascular inflammation. These processes are thought to be mediated via MR-independent (via extracellular-signal-regulated kinase (ERK) 1/2, c-Jun N-terminal kinase (JNK) and GPER pathways) and MR-dependent pathways. Aldosterone also increases the expressions of adhesion molecules, namely ICAM1 and VCAM-1, and inflammatory markers, such as COX-2 and MCP-1 in the endothelium, which induces monocytes and macrophage infiltration. The infiltrated monocyte-derived macrophages which are rich in NADPH oxidase further augment the generation of ROS and worsen vascular inflammation. The infiltrated macrophages ingest oxidized low-density lipoproteins and become foam cells, which potentiate the formation of atherosclerotic plaque. Aldosterone promotes inflammatory

plaque formation via placental growth factor (PlGF) which binds to VEGF type 1 receptors on endothelial and inflammatory cells, and further promotes vascular smooth cell proliferation and monocyte chemotaxis, which are fundamental processes of atherosclerosis. Aldosterone also increases the formation of vasoconstrictors and decreases production and bioavailability of nitric oxide causing impairment of vascular relaxation. Aldosterone via MR-dependent pathways in the endothelium and vascular smooth muscle cells induces vascular fibrosis contributing to vascular stiffness and remodeling (18, 19).

Effect of Hyperaldosteronism on Obesity, Diabetes, and Metabolic Syndrome

Diabetes is a well-established risk factor for IHD and is considered a coronary artery disease equivalent (20). PA is linked to increased risk of diabetes and metabolic syndrome. Clustering of hypertension, abdominal obesity, dyslipidemia and impaired glucose metabolism, is more commonly encountered in PA patients than individuals with essential hypertension (21, 22). Hyperaldosteronism is thought to cause increase in fat mass through mineralocorticoid receptor activation in adipocytes, which in turn induce excess aldosterone production through the actions of adipocytokines (CTRP1, leptin, and resistin) and activation of the sympathetic nervous system, which turns on the renin-angiotensin-aldosterone system, thereby creating a vicious cycle (23, 24). Deranged glucose metabolism occurs through aldosterone mediated impaired insulin sensitivity in skeletal muscle and adipose tissue *via* the MR receptor, and impaired insulin secretion, albeit the underlying mechanisms leading to decreased insulin secretion are poorly understood (25). In addition, blockade of MR has shown to improve coronary flow reserve on cardiac PET scan among individuals with type 2 diabetes without clinical evidence of ischemic heart disease, suggesting that excess MR activation in diabetes contributes to coronary microvascular dysfunction (26).

Effect of Hyperaldosteronism on Kidneys

Primary aldosteronism causes renal dysfunction, independent of blood pressure, by inducing renal fibrosis, vascular remodeling, and podocyte injury *via* MR stimulation from excess aldosterone production (27). Chronic kidney disease is an independent risk factor for development of ischemic heart disease (28). Renal dysfunction increases oxidative stress, imparts endothelial dysfunction, and promotes systemic inflammation which accelerates atherosclerosis.

ROLE OF HYPERCORTISOLISM IN PRIMARY HYPERALDOSTERONISM

Individuals with PA frequently have excess cortisol co-secretion, which can further worsen cardio-metabolic risk through their synergistic effects (29, 30). Cortisol is normally converted to an inactive metabolite, cortisone, by the action of 11β-hydroxysteroid dehydrogenase type 2(11β-HSD2). However, in hypercortisolism the activity of this enzyme is decreased, albeit due to unclear reasons (31). Loss of 11β-HSD2 has been shown to promote atherogenesis *via* activation of MR stimulating pro-inflammatory processes in the endothelium of knock-out murine models (32). Likewise, individuals with hypercortisolism demonstrate an increased burden of coronary calcification and noncalcified coronary plaque. Additionally, hypercortisolism promotes a prothrombotic state (33). This phenotype of PA and glucocorticoid co-secretion underscores the importance of additional screening for hypercortisolism due to therapeutic and prognostic implications (34).

ROLE OF ALDOSTERONE EXCESS POST-ACUTE MYOCARDIAL INFARCTION

After acute myocardial infarction (MI) circulating levels of serum aldosterone are elevated as a consequence of neurohormonal activation (35). Hyperaldosteronism after acute MI effectuates a myriad of maladaptive changes in the post-MI heart which increase morbidity and mortality (36, 37). Post-MI hyperaldosteronism contributes to ventricular remodeling that involves both infarcted and non-infarcted zones, which at a cellular level occurs through myocyte apoptosis, myocyte hypertrophy, macrophage/monocyte infiltration, and collagen deposition *via* fibroblast activation and proliferation. Excess aldosterone also induces endothelial dysfunction by reducing nitric oxide generation and increasing formation of reactive oxygen species (38). Moreover, elevated aldosterone leads to electrical remodeling, lengthened action potential duration, increase in Ca^{2+} current (I_{Ca}) and a decrease in K^+ transient outward current (I_{to}), even before morphological remodeling occurs, creating a pro-arrhythmogenic milieu (39).

The Eplerenone Post-Acute Myocardial Infarction Heart Failure Efficacy and Survival Study (EPHESUS) showed beneficial effect of MR antagonists when utilized in the early post-MI period, namely by decreasing the incidence of sudden cardiac death and heart failure hospitalizations (40). Current guidelines recommend treatment with MR antagonists in patients with acute MI with ejection fraction <40% and clinical heart failure or diabetes (41, 42). Given the unfavorable effects of hyperaldosteronism in the post-MI setting, and the positive impact of aldosterone antagonists among patients with post MI systolic heart failure, the role aldosterone antagonists in improving outcomes in post-MI patients without systolic heart failure has garnered incredible clinical interest. A recent pilot study showed MR antagonists when initiated prior to reperfusion in STEMI patients resulted in improvement in ventricular remodeling at the end of 3 months, however, no impact on reducing MI size was seen (43). Despite abundant preclinical and mechanistic data supporting the concept, no clinically meaningful benefit, i.e., reduction in overall or cardiovascular mortality, ventricular arrhythmia, or rehospitalization, with use of MR antagonists in early post-MI patients without evidence of heart failure has been demonstrated in major prospective randomized clinical trials (44, 45). This underscores the need for more adequately powered prospective randomized trials evaluating the safety and efficacy of MRA administration in early post-MI patients without evidence of HF.

EFFECT OF PRIMARY ALDOSTERONISM TREATMENT ON ISCHEMIC HEART DISEASE

If diagnosed, patients with PA can be offered targeted treatment, either in the form of unilateral adrenalectomy for APA, or mineralocorticoid receptor antagonists, typically used for BAH, and sometimes for APA who are unable or unwilling to undergo adrenalectomy. Despite the presence of increased cardiovascular morbidity in PA patients at the time of diagnosis, administration of appropriate treatment results in improved cardiovascular outcome, when the effects of excess aldosterone are permanently removed. Younger age and shorter duration of hypertension independently predict beneficial cardiovascular outcomes, underscoring the importance of a timely correction of this disorder (8). Surgical adrenalectomy appears to be superior in mitigating adverse cardiovascular events compared to medical therapy in unilateral PA (46). PA patients on MR antagonist therapy with unsuppressed plasma renin activity (PRA) $\geq$ 1 ng/ml/h, a marker of effective MR blockade, seem to have comparable cardiovascular outcomes to those with essential hypertension. In contrast, patients with suppressed PRA $<$ 1 ng/ml/h experience poorer cardiovascular outcomes despite similar blood pressure control (47). Future prospective studies are necessary to determine treatment approaches in patients with PA to optimize cardiovascular outcomes. Given the reversal of this increased cardiovascular risk through therapy, a robust effort to diagnose and effectively treat PA, undoubtedly reduces health costs and improves quality of life (48).

CONCLUSION

Primary aldosteronism is common, with true prevalence expected to be higher than current estimates. Furthermore, it carries a significantly worse cardiovascular prognosis compared to individuals with essential hypertension. Early detection of this entity could not only improve outcomes for patients but also potentially be cost saving for the healthcare system.

AUTHOR CONTRIBUTIONS

SP and CR made substantial contribution to the article design and conception of the work, contributed to the acquisition of data, and drafting and editing of the manuscript. AA and SP made critical revisions. All authors read and approved the final manuscript.

FUNDING

This work was funded by Einstein Medical Center, Philadelphia.

REFERENCES

1. Mensah GA, Roth GA, Fuster V. The global burden of cardiovascular diseases and risk factors: 2020 and beyond. *J Am Coll Cardiol.* (2019) 74:2529-32. doi: 10.1016/j.jacc.2019.10.009
2. Nowbar AN, Gitto M, Howard JP, Francis DP, Al-Lamee R. Mortality from ischemic heart disease. *Circ Cardiovasc Qual Outcomes.* (2019) 12:e005375. doi: 10.1161/CIRCOUTCOMES.118.005375
3. Mills KT, Bundy JD, Kelly TN, Reed JE, Kearney PM, Reynolds K, et al. Global disparities of hypertension prevalence and control: a systematic analysis of population-based studies from 90 countries. *Circulation.* (2016) 134:441-50. doi: 10.1161/CIRCULATIONAHA.115.018912
4. Rosendorff C, Lackland DT, Allison M, Aronow WS, Black HR, Blumenthal RS, et al. Treatment of hypertension in patients with coronary artery disease: a scientific statement from the American Heart Association, American College of Cardiology, and American Society of Hypertension. *Circulation.* (2015) 131:e435-70. doi: 10.1161/CIR.0000000000000207
5. Vasan R. Evans C, Larson Mg et al. Serum aldosterone and the insidence of hypertension in nonhypertensive persons. *N Engl Med.* (2004) 351:33-42. doi: 10.1056/NEJMoa033263
6. Libianto R, Fuller PJ, Young MJ, Yang J. Primary aldosteronism is a public health issue: challenges and opportunities. *J Hum Hypertens.* (2020) 34:478-86. doi: 10.1038/s41371-020-0336-2
7. Xanthakis V, Vasan RS. Aldosterone and the risk of hypertension. *Curr Hypertens Rep.* (2013) 15:102-7. doi: 10.1007/s11906-013-0330-y
8. Catena C, Colussi G, Nadalini E, Chiuch A, Baroselli S, Lapenna R, et al. Cardiovascular outcomes in patients with primary aldosteronism after treatment. *Arch Int Med.* (2008) 168:80-5. doi: 10.1001/archinternmed.2007.33
9. Wu X, Yu J, Tian H. Cardiovascular risk in primary aldosteronism: a systematic review and meta-analysis. *Medicine.* (2019) 98:e15985. doi: 10.1097/MD.0000000000015985
10. Ohno Y, Sone M, Inagaki N, Yamasaki T, Ogawa O, Takeda Y, et al. Prevalence of cardiovascular disease and its risk factors in primary aldosteronism: a multicenter study in Japan. *Hypertension.* (2018) 71:530-7. doi: 10.1161/HYPERTENSIONAHA.117.10263
11. Savard S, Amar L, Plouin P-F, Steichen O. Cardiovascular complications associated with primary aldosteronism: a controlled cross-sectional study. *Hypertension.* (2013) 62:331-6. doi: 10.1161/HYPERTENSIONAHA.113.01060
12. Born-Frontsberg E, Reincke M, Rump L, Hahner S, Diederich S, Lorenz R, et al. Participants of the German conn's registry. cardiovascular and cerebrovascular comorbidities of hypokalemic and normokalemic primary aldosteronism: results of the German Conn's Registry. *J Clin Endocrinol Metab.* (2009) 94:1125-30. doi: 10.1210/jc.2008-2116
13. López-Andrés N, Martin-Fernandez B, Rossignol P, Zannad F, Lahera V, Fortuno MA, et al. A role for cardiotrophin-1 in myocardial remodeling induced by aldosterone. *Am J Physiol Heart Circul Physiol.* (2011) 301:H2372-82. doi: 10.1152/ajpheart.00283.2011
14. Okoshi M, Yan X, Okoshi K, Nakayama M, Schuldt A. O´ Connell Td, et al. Aldosterone directly stimulates cardiac myocyte hypertrophy. *J Card Fail.* (2004) 10:511-8. doi: 10.1016/j.cardfail.2004.03.002
15. Tsai C-H, Pan C-T, Chang Y-Y, Chen Z-W, Wu V-C, Hung C-S, et al. Left ventricular remodeling and dysfunction in primary aldosteronism. *J Hum Hypertens.* (2021) 35:131-47. doi: 10.1038/s41371-020-00426-y
16. Nguyen T, Do H, Pham T, Vu LT, Zuin M, Rigatelli G. Left ventricular dysfunction causing ischemia in patients with patent coronary arteries. *Perfusion.* (2018) 33:115-22. doi: 10.1177/0267659117727826
17. Lorell BH, Carabello BA. Left ventricular hypertrophy: pathogenesis, detection, and prognosis. *Circulation.* (2000) 102:470-9. doi: 10.1161/01.CIR.102.4.470
18. Chen Z-W, Tsai C-H, Pan C-T, Chou C-H, Liao C-W, Hung C-S, et al. Endothelial dysfunction in primary aldosteronism. *Int J Mol Sci.* (2019) 20:5214. doi: 10.3390/ijms20205214

19. Chrissobolis S. Vascular consequences of aldosterone excess and mineralocorticoid receptor antagonism. *Curr Hypertens Rev.* (2017) 13:46-56. doi: 10.2174/1573402113666170228151402
20. Hajar R. Diabetes as "coronary artery disease risk equivalent": a historical perspective. *Heart Views.* (2017) 18:34. doi: 10.4103/HEARTVIEWS.HEARTVIEWS_37_17
21. Monticone S, D'Ascenzo F, Moretti C, Williams TA, Veglio F, Gaita F, et al. Cardiovascular events and target organ damage in primary aldosteronism compared with essential hypertension: a systematic review and meta-analysis. *Lancet Diabetes Endocrinol.* (2018) 6:41-50. doi: 10.1016/S2213-8587(17)30319-4
22. Fallo F, Veglio F, Bertello C, Sonino N, Della Mea P, Ermani M, et al. Prevalence and characteristics of the metabolic syndrome in primary aldosteronism. *J Clin Endocrinol Metab.* (2006) 91:454-9. doi: 10.1210/jc.2005-1733
23. Urbanet R, Nguyen Dinh Cat A, Feraco A, Venteclef N, El Mogrhabi S, Sierra-Ramos C, et al. Adipocyte mineralocorticoid receptor activation leads to metabolic syndrome and induction of prostaglandin D2 synthase. *Hypertension.* (2015) 66:149-57. doi: 10.1161/HYPERTENSIONAHA.114.04981
24. Ohno Y, Sone M, Inagaki N, Yamasaki T, Ogawa O, Takeda Y, et al. Obesity as a key factor underlying idiopathic hyperaldosteronism. *J Clin Endocrinol Metab.* (2018) 103:4456-64. doi: 10.1210/jc.2018-00866
25. Luther JM. Effects of aldosterone on insulin sensitivity and secretion. *Steroids.* (2014) 91:54-60. doi: 10.1016/j.steroids.2014.08.016
26. Garg R, Rao AD, Baimas-George M, Hurwitz S, Foster C, Shah RV, et al. Mineralocorticoid receptor blockade improves coronary microvascular function in individuals with type 2 diabetes. *Diabetes.* (2015) 64:236-42. doi: 10.2337/db14-0670
27. Hundemer GL, Curhan GC, Yozamp N, Wang M, Vaidya A. Renal outcomes in medically and surgically treated primary aldosteronism. *Hypertension.* (2018) 72:658-66. doi: 10.1161/HYPERTENSIONAHA.118.11568
28. Sarnak M. American Heart Association Councils on kidney in cardiovascular disease, high blood pressure research, clinical cardiology, and epidemiology and prevention. Kidney disease as a risk factor for development of cardiovascular disease: a statement from the American Heart Association Councils on Kidney in Cardiovascular Disease, High Blood Pressure Research, Clinical Cardiology, and Epidemiology and Prevention. *Hypertension.* (2003) 42:1050-65. doi: 10.1161/01.HYP.0000102971.85504.7c
29. Gerards J, Heinrich DA, Adolf C, Meisinger C, Rathmann W, Sturm L, et al. Impaired glucose metabolism in primary aldosteronism is associated with cortisol cosecretion. *J Clin Endocrinol Metab.* (2019) 104:3192-202. doi: 10.1210/jc.2019-00299
30. Adolf C, Köhler A, Franke A, Lang K, Riester A, Löw A, et al. Cortisol excess in patients with primary aldosteronism impacts left ventricular hypertrophy. *J Clin Endocrinol Metab.* (2018) 103:4543-52. doi: 10.1210/jc.2018-00617
31. Stewart PM, Walker BR, Holder G, O'Halloran D, Shackleton C. 11 Beta-hydroxysteroid dehydrogenase activity in cushing's syndrome: explaining the mineralocorticoid excess state of the ectopic adrenocorticotropin syndrome. *J Clin Endocrinol Metabol.* (1995) 80:3617-20. doi: 10.1210/jcem.80.12.8530609
32. Deuchar GA, McLean D, Hadoke PW, Brownstein DG, Webb DJ, Mullins JJ, et al. 11β-hydroxysteroid dehydrogenase type 2 deficiency accelerates atherogenesis and causes proinflammatory changes in the endothelium in Apoe–/– mice. *Endocrinology.* (2011) 152:236-46. doi: 10.1210/en.2010-0925
33. Neary NM, Booker OJ, Abel BS, Matta JR, Muldoon N, Sinaii N, et al. Hypercortisolism is associated with increased coronary arterial atherosclerosis: analysis of noninvasive coronary angiography using multidetector computerized tomography. *J Clin Endocrinol Metab.* (2013) 98:2045-52. doi: 10.1210/jc.2012-3754
34. Peng K-Y, Liao H-W, Chan C-K, Lin W-C, Yang S-Y, Tsai Y-C, et al. Presence of subclinical hypercortisolism in clinical aldosterone-producing adenomas predicts lower clinical success. *Hypertension.* (2020) 76:1537-44. doi: 10.1161/HYPERTENSIONAHA.120.15328
35. Udell JA, Morrow DA, Braunwald E, Swedberg K, Bode C, Rifai N, et al. Inhibition of the renin-angiotensin system reduces the rise in serum aldosterone in acute coronary syndrome patients with preserved left ventricular function: observations from the avant garde-timi 43 trial. *Clin Chem.* (2013) 59:959-67. doi: 10.1373/clinchem.2012.199729
36. Mignano A, Pitruzzella V, Arnone G, Arnone MT, Rotolo A, Assennato P, et al. Prognostic role of aldosterone in patients with acute coronary syndrome: short and medium term follow-up. *J Cardiovasc Med.* (2014) 15:27-32. doi: 10.2459/JCM.0b013e328364129c
37. Beygui F, Collet J-P, Benoliel J-J, Vignolles N, Dumaine R, Barthélémy O, et al. High plasma aldosterone levels on admission are associated with death in patients presenting with acute st-elevation myocardial infarction. *Circulation.* (2006) 114:2604-10. doi: 10.1161/CIRCULATIONAHA.106.634626
38. Cohn JN, Colucci W. Cardiovascular effects of aldosterone and post–acute myocardial infarction pathophysiology. *Am J Cardiol.* (2006) 97:4-12. doi: 10.1016/j.amjcard.2006.03.004
39. Perrier E, Kerfant B-G, Lalevee N, Bideaux P, Rossier MF, Richard S, et al. Mineralocorticoid receptor antagonism prevents the electrical remodeling that precedes cellular hypertrophy after myocardial infarction. *Circulation.* (2004) 110:776-83. doi: 10.1161/01.CIR.0000138973.55605.38
40. Pitt B. Eplerenone post-acute myocardial infarction heart failure efficacy and survival study investigators: eplerenone, a selective aldosterone blocker, in patients with left ventricular dysfunction after myocardial infarction. *N Engl J Med.* (2003) 348:1309-21. doi: 10.1056/NEJMoa030207
41. Amsterdam EA, Wenger NK, Brindis RG, Casey Jr DE, Ganiats TG, Holmes Jr DR, et al. 2014 Aha/Acc guideline for the management of patients with non–st-elevation acute coronary syndromes: executive summary: a report of the American College of Cardiology/American Heart Association Task Force on practice guidelines. *Circulation.* (2014) 130:2354-94. doi: 10.1161/CIR.0000000000000133
42. O'gara PT, Kushner FG, Ascheim DD, Casey DE, Chung MK, De Lemos JA, et al. 2013 Accf/Aha Guideline for the Management of St-elevation myocardial infarction: a report of the American College of Cardiology Foundation/American Heart Association Task Force on Practice Guidelines. *J Am Coll Cardiol.* (2013) 61:e78-140. doi: 10.1161/CIR.0b013e3182742c84
43. Bulluck H, Fröhlich GM, Nicholas JM, Mohdnazri S, Gamma R, Davies J, et al. Mineralocorticoid receptor antagonist pre-treatment and early post-treatment to minimize reperfusion injury after st-elevation myocardial infarction: the minimize stemi trial. *Am Heart J.* (2019) 211:60-7. doi: 10.1016/j.ahj.2019.02.005
44. Beygui F, Cayla G, Roule V, Roubille F, Delarche N, Silvain J, et al. Early aldosterone blockade in acute myocardial infarction: the albatross randomized clinical trial. *J Am Coll Cardiol.* (2016) 67:1917-27. doi: 10.1016/j.jacc.2016.02.033
45. Montalescot G, Pitt B, Lopez de Sa E, Hamm CW, Flather M, Verheugt F, et al. Early eplerenone treatment in patients with acute st-elevation myocardial infarction without heart failure: the randomized double-blind reminder study. *Eur Heart J.* (2014) 35:2295-302. doi: 10.1093/eurheartj/ehu164
46. Huang W-C, Chen Y-Y, Lin Y-H, Chueh JS. Composite cardiovascular outcomes in patients with primary aldosteronism undergoing medical versus surgical treatment: a meta-analysis. *Front Endocrinol.* (2021) 12:644260. doi: 10.3389/fendo.2021.644260
47. Hundemer GL, Curhan GC, Yozamp N, Wang M, Vaidya A. Cardiometabolic outcomes and mortality in medically treated primary aldosteronism: a retrospective cohort study. *Lancet Diabetes Endocrinol.* (2018) 6:51-9. doi: 10.1016/S2213-8587(17)30367-4
48. Lubitz CC, Economopoulos KP, Sy S, Johanson C, Kunzel HE, Reincke M, et al. Cost-effectiveness of screening for primary aldosteronism and subtype diagnosis in the resistant hypertensive patients. *Circulation.* (2015) 8:621-30. doi: 10.1161/CIRCOUTCOMES.115.002002
49. Mulatero P, Monticone S, Bertello C, Viola A, Tizzani D, Iannaccone A, et al. Long-term cardio-and cerebrovascular events in patients with primary aldosteronism. *J Clin Endocrinol Metab.* (2013) 98:4826-33. doi: 10.1210/jc.2013-2805
50. Reincke M, Fischer E, Gerum S, Merkle K, Schulz S, Pallauf A, et al. Observational study mortality in treated primary aldosteronism: the German Conn's Registry. *Hypertension.* (2012) 60:618-24. doi: 10.1161/HYPERTENSIONAHA.112.197111
51. Milliez P, Girerd X, Plouin P-F, Blacher J, Safar ME, Mourad J-J. Evidence for an increased rate of cardiovascular events in patients

with primary aldosteronism. *J Am Coll Cardiol.* (2005) 45:1243-8. doi: 10.1016/j.jacc.2005.01.015
52. Kim SH, Ahn JH, Hong HC, Choi HY, Kim YJ, Kim NH, et al. Changes in the clinical manifestations of primary aldosteronism. *Korean J Int Med.* (2014) 29:217. doi: 10.3904/kjim.2014.29.2.217
53. Nishimura M, Uzu T, Fujii T, Kuroda S, Nakamura S, Inenaga T, et al. Cardiovascular complications in patients with primary aldosteronism. *Am J Kidney Dis.* (1999) 33:261-6. doi: 10.1016/S0272-6386(99)70298-2

Conflict of Interest: The authors declare that the research was conducted in the absence of any commercial or financial relationships that could be construed as a potential conflict of interest.

Publisher's Note: All claims expressed in this article are solely those of the authors and do not necessarily represent those of their affiliated organizations, or those of the publisher, the editors and the reviewers. Any product that may be evaluated in this article, or claim that may be made by its manufacturer, is not guaranteed or endorsed by the publisher.

frontiers | Frontiers in Cardiovascular Medicine

ORIGINAL RESEARCH
published: 26 May 2022
doi: 10.3389/fcvm.2022.867723

Pre-infarction Angina: Time Interval to Onset of Myocardial Infarction and Comorbidity Predictors

Yohei Sotomi[1] Yasunori Ueda[2], Shungo Hikoso[1], Katsuki Okada[1,3], Tomoharu Dohi[1], Hirota Kida[1], Bolrathanak Oeun[1], Akihiro Sunaga[1], Taiki Sato[1], Tetsuhisa Kitamura[4], Hiroya Mizuno[1], Daisaku Nakatani[1], Yasuhiko Sakata[5], Hiroshi Sato[6], Masatsugu Hori[7], Issei Komuro[8] and Yasushi Sakata[1] on behalf of the Osaka Acute Coronary Insufficiency Study (OACIS)*

[1] Department of Cardiovascular Medicine, Osaka University Graduate School of Medicine, Osaka, Japan, [2] Cardiovascular Division, National Hospital Organization Osaka National Hospital, Osaka, Japan, [3] Department of Transformative System for Medical Information, Osaka University Graduate School of Medicine, Osaka, Japan, [4] Division of Environmental Medicine and Population Sciences, Department of Social and Environmental Medicine, Graduate School of Medicine, Osaka University, Osaka, Japan, [5] Department of Clinical Medicine and Development and Department of Cardiovascular Medicine, National Cerebral and Cardiovascular Center, Suita, Japan, [6] School of Human Welfare Studies Health Care Center and Clinic, Kwansei Gakuin University, Hyogo, Japan, [7] Osaka International Cancer Institute, Osaka, Japan, [8] Department of Cardiovascular Medicine, University of Tokyo Graduate School of Medicine, Tokyo, Japan

OPEN ACCESS

Edited by:
Shun Kohsaka,
Keio University, Japan

Reviewed by:
Kentaro Jujo,
Tokyo Women's Medical University, Japan
Erhan Tenekecioglu,
University of Health Sciences, Turkey

***Correspondence:**
Shungo Hikoso
hikoso@cardiology.med.osaka-u.ac.jp

Specialty section:
This article was submitted to Coronary Artery Disease, a section of the journal Frontiers in Cardiovascular Medicine

Received: 01 February 2022
Accepted: 06 May 2022
Published: 26 May 2022

Citation:
Sotomi Y, Ueda Y, Hikoso S, Okada K, Dohi T, Kida H, Oeun B, Sunaga A, Sato T, Kitamura T, Mizuno H, Nakatani D, Sakata Y, Sato H, Hori M, Komuro I and Sakata Y (2022) Pre-infarction Angina: Time Interval to Onset of Myocardial Infarction and Comorbidity Predictors. Front. Cardiovasc. Med. 9:867723. doi: 10.3389/fcvm.2022.867723

Aims: As part of efforts to identify candidates for patient education aimed at decreasing mortality from acute myocardial infarction, we investigated the prevalence of pre-infarction angina and its predictors among comorbidities in patients who were hospitalized with acute myocardial infarction (MI).

Methods: We conducted a prospective multicenter observational registry of MI patients from 1998 to 2014 (N = 12,093). The present study investigated the prevalence of pre-infarction angina and its predictors among comorbidities with a logistic regression model. Pre-infarction angina was defined as chest pain/oppression observed within 1 month before the onset of MI but which lasted <30 min.

Results: After excluding 976 (8.1%) patients with missing data on pre-infarction angina, 11,117 patients [66.4 ± 12.0 years, 9,096 (75.2%) male] were analyzed. Of these, 5,428 patients (48.8%) experienced pre-infarction angina before the onset of MI, while 5,689 (51.2%) experienced sudden onset of acute MI. Most patients experienced the first episode of angina >6 h before the onset of MI, while 15% did so ≤6 h before. Patients with hypertension, diabetes, dyslipidemia, or a family history of MI had a higher probability of pre-infarction angina than those without. Elderly patients and those with a history of cerebrovascular disease were less likely to experience pre-infarction angina.

Conclusions: Almost half of MI patients in our registry experienced pre-infarction angina before MI onset. Patients with hypertension, diabetes, dyslipidemia, or a family history of MI had a higher probability of experiencing pre-infarction angina than those without.

Keywords: acute myocardial infarction, pre-infarction angina, prevention, public education, real-world

INTRODUCTION

The in-hospital mortality rate of patients with acute myocardial infarction (MI) has improved to <10% due to advanced treatment after hospital admission, including primary percutaneous coronary intervention (1–3). Nevertheless, many cardiac arrests and deaths occur out-of-hospital, and acute MI remains a life-threatening condition worldwide (4). Once a person suffers acute MI, the overall mortality rate is 30%−40%, and the out-of-hospital mortality rate is 25%−30% (5). Indeed, as many as 77% of overall deaths from coronary heart disease occur out of hospital (1). Some MI patients who die before reaching a hospital likely experience prodrome before the onset of MI. Appropriate medical contact in this pre-infarction angina phase may prevent the onset of MI and save lives (5). However, this requires that patients be able to recognize their symptoms as pre-infarction angina, which in turn highlights the importance of public education in encouraging timely medical consultation. Nevertheless, which MI patients are more likely to experience pre-infarction angina remains unclear.

Many public campaigns to prevent disease are underway, including "Know Diabetes by Heart" by the American Heart Association and American Diabetes Association and the "STOP MI Campaign" by the Japanese Circulation Society. The scope and reach of these campaigns will be expanded by the upcoming internet of things (IoT) technology (6, 7). Examples include the possibility of detecting ischemia using smart devices (8). For MI, such campaigns will best be targeted at populations with a higher probability of pre-infarction angina. However, it is still unknown which comorbidities are likely to accompany pre-infarction angina in these patients.

Here, to identify suitable candidates for public education, we investigated the prevalence of pre-infarction angina and its predictors among comorbidities.

METHODS

Study Population

We used the Osaka Acute Coronary Insufficiency Study (OACIS) database ($N = 12{,}093$) to investigate (1) the prevalence of pre-infarction angina, (2) time to onset of MI, and (3) associations between patients' comorbidities and pre-infarction angina. The OACIS was a prospective, multicenter observational study designed to collect and analyze demographic, procedural, and outcome data in patients with acute MI at 25 collaborating hospitals with cardiac emergency units. Patients were enrolled from 1998 to 2014 and followed until 2019. Written informed consent was obtained from each patient (9, 10). A diagnosis of acute MI was made if the patient fulfilled at least two of the following three criteria: (1) history of central chest pressure, pain, or tightness lasting ≥30 min, (2) typical ECG changes (ie, ST-segment elevation ≥0.1 mV in one standard limb lead or two precordial leads, ST-segment depression ≥0.1 mV in two leads, abnormal Q waves, or T-wave inversion in two leads), and (3) a rise in serum creatinine phosphokinase concentration to more than twice the normal laboratory value (11, 12). All 25 collaborating hospitals were encouraged to enroll consecutive patients with acute MI.

For the present study, we prospectively collected OACIS data obtained by research cardiologists and trained research nurses using a specific reporting form. The OACIS study (and any subanalyses) are registered with the UMIN-CTR (University Hospital Medical Information Network Clinical Trials Registry) in Japan (ID: UMIN000004575). The study protocol complied with the Helsinki Declaration. The study was approved by the ethics committee of Osaka University Hospital (approval number: 14360).

Definition of Pre-infarction Angina and Onset of MI

Pre-infarction angina was defined as chest pain/oppression within 1 month before the onset of MI which lasted <30 min. Only typical chest pain was considered as pre-infarction angina; atypical symptoms such as shortness of breath, diaphoresis, fatigue, or pain at a site other than the chest were neither considered as pre-infarction angina nor recorded in this study. The presence and characteristics of typical chest pain were actively enquired about during registration. Onset of MI was defined as the start of chest pain which lasted ≥30 min. Time interval from the first episode of pre-infarction angina to the onset of MI was prospectively collected.

Statistical Analysis

Eligible patients were stratified by the presence or absence of pre-infarction angina. Categorical variables are expressed as counts (percentages) and compared with the Chi-squared test or Fisher exact test. Continuous variables are expressed as median (interquartile range) and compared using the Mann–Whitney *U*-test. Data are presented by listwise deletion. Serial change in the prevalence of pre-infarction angina from 1998 to 2014 was evaluated with the Cochran-Armitage trend test. We used a logistic regression model to investigate the relationship between patient comorbidities and pre-infarction angina. The following factors were selected based on clinician consensus and included in the model: age, sex, hypertension, smoking, prior MI, family history of MI, cerebrovascular disease, cancer, arteriosclerosis obliterans (ASO), hemoglobin per 1 g/dl, creatinine per 0.1 mg/dl, low density lipoprotein cholesterol (LDL-C) per 10 mg/dl, and HbA1c per 1.0%. Because the exclusion of cases with missing data could have caused bias in this analysis and loss of power in detecting statistical differences, missing data were imputed by random forest imputation using the "missForest" package prior to the logistic regression analysis. All statistical analyses were performed with R software (version 4.0.5; R Foundation for Statistical Computing, Vienna, Austria).

RESULTS

Study Subjects

After excluding 976 patients (8.1%) with missing data on pre-infarction angina, 11,117 patients [66.4 ± 12.0 years, 9,096 (75.2%) male] were analyzed (**Figure 1**). Baseline characteristics of patients excluded vs. included in the present analysis are

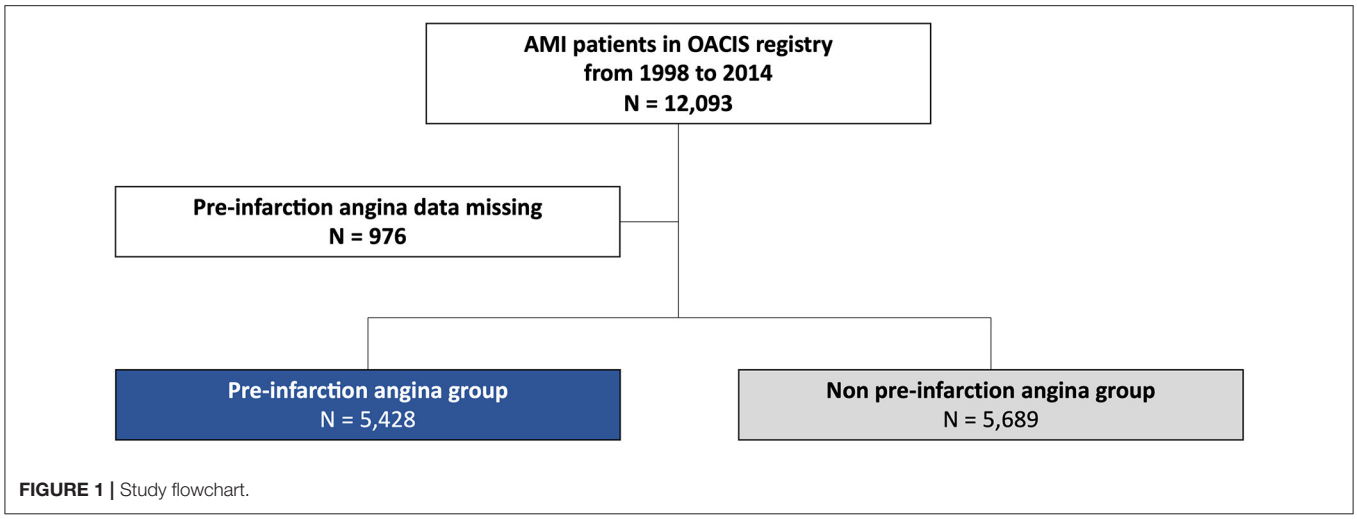

FIGURE 1 | Study flowchart.

tabulated in **Supplemental Table 1**. Patients excluded from the analysis were older, less likely to be male, and showed a higher prevalence of diabetes mellitus, hypertension, and chronic kidney disease and a lower prevalence of dyslipidemia and smoking than those analyzed. Of the 11,117 patients analyzed, 5,428 patients (48.8%) experienced pre-infarction angina before the onset of MI, while 5,689 patients (51.2%) experienced sudden onset of acute MI. Baseline demographics of patients with and without pre-infarction angina are tabulated in **Table 1**. Patients with pre-infarction angina showed a higher prevalence of dyslipidemia, more frequently had a family history of MI, and less frequently had a history of cerebrovascular disease than those without. Peak CK level was significantly lower in patients with pre-infarction angina than in those without (13).

Prevalence of Pre-infarction Angina

Serial change in the prevalence of pre-infarction angina is illustrated in **Figure 2**. During the study period from 1998 to 2014, prevalence gradually decreased (P for trend < 0.001). Crude rates of pre-infarction angina in specific patient subgroups stratified by sex are tabulated in **Table 2**. The prevalence in male patients in their 50s, for example, was 52.2%. In both sexes, patients in their 80s had a lower prevalence of pre-infarction angina than younger patients. Patients with dyslipidemia showed a higher prevalence of pre-infarction angina than those without in both sexes, whereas patients with a history of cerebrovascular disease showed a lower prevalence than those without.

Time from the first episode of pre-infarction angina to the onset of MI is summarized in **Figure 3**. Time to MI onset was >6 h for most patients, vs. ≤ 6 h for 15%.

Predictors of Pre-infarction Angina

Patients with hypertension, diabetes, dyslipidemia, or a family history of MI had a higher probability of experiencing pre-infarction angina than those without (**Figure 4**). Elderly patients and those with a history of cerebrovascular disease were less likely to experience pre-infarction angina.

DISCUSSION

In this study, we used data from a large-scale prospective observational registry to investigate the prevalence of pre-infarction angina and its related comorbidities. Approximately half of the MI patients in the registry experienced pre-infarction angina before the onset of MI. In most patients, the time from the onset of angina to that of MI was >6 h, but was ≤ 6 h in 15%. Patients with hypertension, diabetes, dyslipidemia, or a family history of MI had a higher probability of pre-infarction angina than those without. Further, elderly patients and those with a history of cerebrovascular disease were less likely to experience pre-infarction angina.

Prevalence of Pre-infarction Angina and Time Interval to the Onset of MI

Although a number of studies have reported the prevalence of pre-infarction angina, most had relatively small cohorts and a retrospective design (4, 14–18). Results varied from approximately 30%−55%, presumably because of different definitions of pre-infarction angina. Our present analysis provides the first prospective evidence for pre-infarction angina rates, as collected in the largest cohort with a pre-defined definition under current practice standards. Approximately half of the MI patients experienced pre-infarction angina within 1 month before the onset of MI. Of note, this study investigated the prevalence of pre-infarction angina in patients who were admitted to hospital for acute MI. This is not strictly the same as the true prevalence of pre-infarction angina for all MI patients. As presented in **Figure 2**, prevalence in our cohort over time gradually but significantly decreased (P for trend <0.001). This implies that recent patients with pre-infarction angina were treated at the unstable angina stage more frequently than before, assuming that the true prevalence of pre-infarction

TABLE 1 | Baseline characteristics.

	Pre-infarction angina (+)	Pre-infarction angina (–)	*P*-Value	Missing (%)
Patients, *n*	5,428	5,689		
Age, years	66.00 [57.00, 74.00]	67.00 [59.00, 75.00]	<0.001	0
Male sex	4,126 (76.0)	4,316 (75.9)	0.886	0
Body mass index	23.53 [21.51, 25.78]	23.42 [21.30, 25.65]	0.001	6.4
Diabetes mellitus	1,843 (34.7)	1,812 (32.9)	0.043	3.3
Hypertension	3,242 (61.5)	3,315 (60.2)	0.166	3.7
Dyslipidemia	2,393 (46.0)	2,309 (42.5)	<0.001	5.1
Smoking	3,415 (64.1)	3,510 (63.7)	0.648	3.3
Chronic kidney disease	384 (7.3)	404 (7.4)	0.921	3.6
Prior myocardial infarction	613 (11.6)	652 (11.7)	0.902	2.8
Family history of MI	526 (14.0)	441 (11.3)	0.001	31.1
Cerebrovascular disease	418 (7.9)	569 (10.4)	<0.001	3.6
Cancer	276 (5.2)	346 (6.3)	0.020	3.6
ASO	127 (2.4)	147 (2.7)	0.415	3.6
Hemoglobin, g/dl	14.10 [12.50, 15.30]	13.80 [12.30, 15.10]	<0.001	52.0
Creatinine, mg/dl	0.83 [0.70, 1.06]	0.90 [0.70, 1.11]	<0.001	30.4
Low density lipoprotein cholesterol, mg/dl	124.00 [100.75, 148.10]	118.00 [94.00, 142.25]	<0.001	63.9
HbA1c, %	5.60 [5.20, 6.60]	5.50 [5.10, 6.40]	<0.001	27.2
ST-elevation myocardial infarction	4,450 (83.5)	4,847 (86.7)	<0.001	1.8
Culprit vessel				
Right coronary artery	1,633 (32.4)	1,987 (38.7)	<0.001	8.9
Left anterior descending artery	2,564 (50.8)	2,299 (44.8)	<0.001	8.9
Left circumflex artery	843 (16.7)	765 (14.9)	0.015	8.9
Left main trunk	135 (2.7)	132 (2.6)	0.798	8.9
Peak CK, IU/L	1,801.00 [828.00, 3,512.50]	2,093.00 [994.25, 4,024.00]	<0.001	6.0
Peak CK-MB, IU/L	163.00 [72.00, 315.00]	181.00 [85.17, 356.00]	<0.001	14.0

Data are expressed as median [interquartile range] or number (percentage).
ASO, arteriosclerosis obliterans; CK, creatine kinase; CK-MB, creatine kinase myocardial band; MI, myocardial infarction.

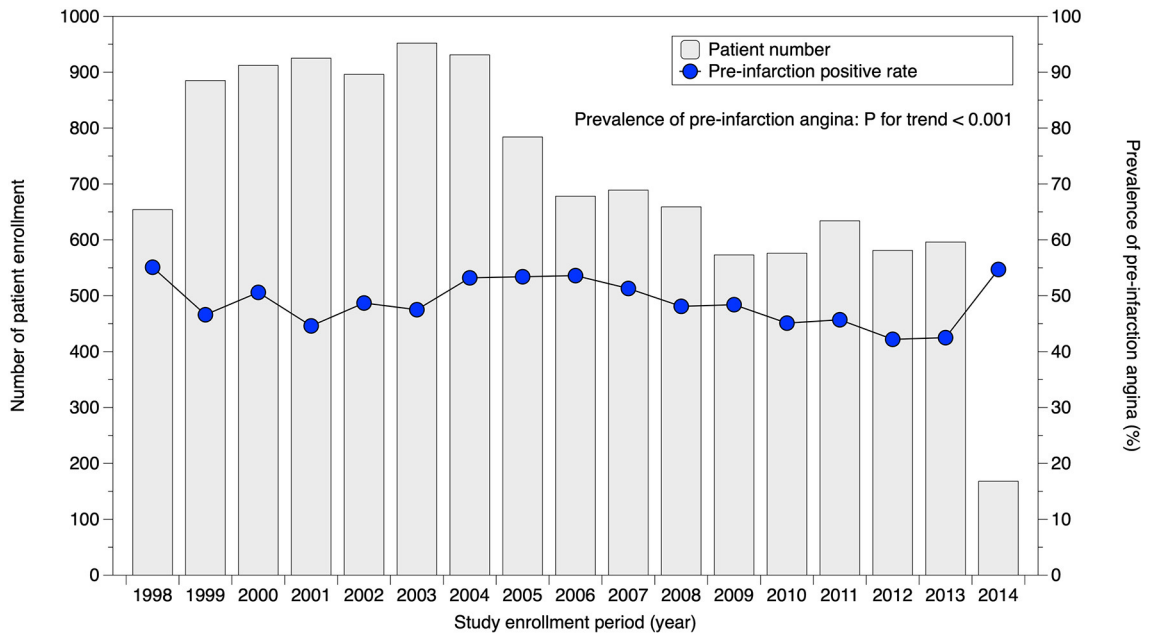

FIGURE 2 | Serial change in prevalence of pre-infarction angina. Prevalence of pre-infarction angina slightly but significantly decreased over time (*P* for trend < 0.001).

TABLE 2 | Crude rates of pre-infarction angina.

	Male *N* = 8,442	Female *N* = 2,674
Overall	4,126/8,442 (48.9)	1,302/2,674 (48.7)
Age		
20s–40s	473/921 (51.4)	40/82 (48.8)
50s	1,038/1,989 (52.2)	114/210 (54.3)
60s	1,326/2,744 (48.3)	372/687 (54.1)
70s	993/2,073 (47.9)	470/925 (50.8)
80s-	295/713 (41.4)	306/770 (39.7)
P-value*	<0.001	<0.001
Hypertension (–)	1,630/3,404 (47.9)	400/820 (48.8)
Hypertension (+)	2,372/4,782 (49.6)	870/1,774 (49.0)
P-value†	0.131	0.935
Diabetes mellitus (–)	2,653/5,461 (48.6)	810/1,701 (47.6)
Diabetes mellitus (+)	1,378/2,756 (50.0)	465/899 (51.7)
P-value†	0.233	0.051
Dyslipidemia (–)	2,178/4,577 (47.6)	629/1,360 (46.2)
Dyslipidemia (+)	1,778/3,509 (50.7)	615/1,192 (51.6)
P-value†	0.006	0.008
Smoking (–)	996/2,039 (48.8)	915/1,874 (48.8)
Smoking (+)	3,055/6,209 (49.2)	360/715 (50.3)
P-Value†	0.800	0.516
Family history of MI (–)	2,493/5,152 (48.4)	750/1,542 (48.6)
Family history of MI (+)	412/755 (54.6)	114/212 (53.8)
P-Value†	0.002	0.184
Cerebrovascular disease (–)	3,688/7,466 (49.4)	1,163/2,307 (50.4)
Cerebrovascular disease (+)	314/706 (44.5)	104/281 (37.0)
P-Value†	0.014	<0.001

Data are presented as number (percentage).

**P value indicates comparison in different ages. Multiple pairwise comparison with the Bonferroni correction (P-values <0.005 were considered statistically significant) showed that (1) in male patients, those in their 80s had a significantly lower prevalence of pre-infarction angina than those in their 20–40s and 50s; (2) in female patients, those in their 80s had a lower prevalence of pre-infarction angina than those in their 50s, 60s, and 70s. The other comparisons were not statistically significant.*

† P value indicates comparison between patients with and without the comorbidity.

MI, myocardial infarction.

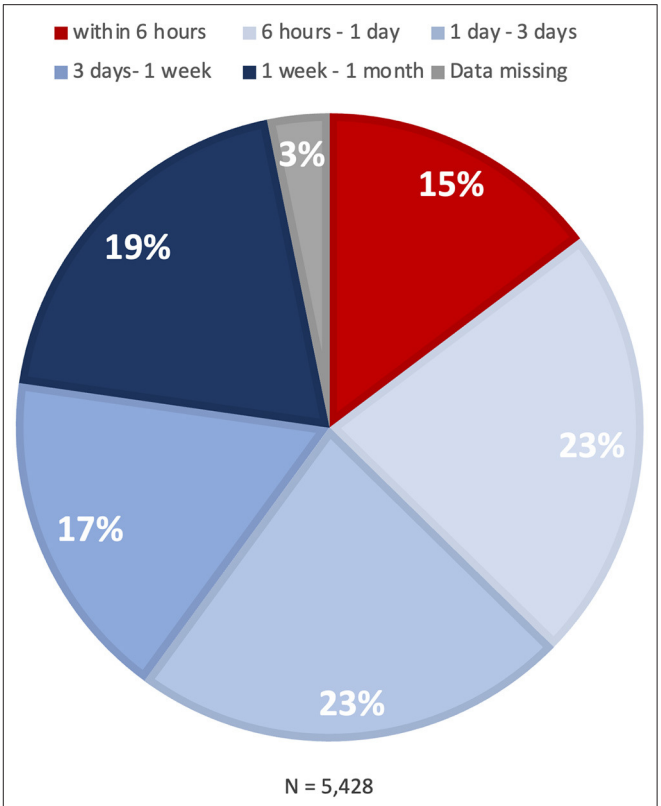

FIGURE 3 | Time to onset of myocardial infarction. A pie chart indicates the distribution of time from the onset of pre-infarction angina to the onset of myocardial infarction.

angina did not change over time. Nevertheless, the decrease was markedly limited, and improvement with public education appears likely.

Although time interval from pre-infarction angina to MI onset has been reported, the study was conducted about five decades ago (18). Among 99 patients who experienced chest pain before MI, six patients (6%) experienced warning symptoms within 24 h of major infarction, while the majority (94%) did so 1 day or more before. Our study (N = 11,117) showed that approximately 60% of patients with pre-infarction angina have sufficient time to see a doctor before MI onset (>24 h). For the remaining 40%, in contrast, MI occurred within 24 h after the onset of pre-infarction angina. Of note, 15 percent of the MI patients had ≤6 h from pre-infarction angina to onset, which would favor the earliest possible medical contact. It is likely that the different proportions between the present and previous finding are attributable to different definitions of pre-infarction angina.

Possible Mechanisms of Pre-infarction Angina and Its Predictors

The pathology of MI is likely related to the presence or absence of pre-infarction angina, although in the present series we do not have data on the pathology of MI in individual cases. The presence of pre-infarction angina may imply that the coronary artery was gradually occluded, whereas its absence might suggest that the coronary artery was suddenly occluded. In patients with pre-infarction angina, MI is likely to develop from severe coronary stenosis *via* unstable angina or mild stenosis due to rupture of vulnerable plaque with gradual thrombus formation. A pathological study indicated that coronary occlusion is often preceded by a variable period of plaque instability and thrombus formation, initiated days or weeks before total occlusion (19). In patients without pre-infarction angina, MI is likely to develop from mild stenosis with vulnerable plaque and its rupture or erosion and subsequent sudden thrombus formation. A pathology study showed that fresh thrombus (<1 day) was present in approximately half (49%) of MI patients (19). This is closely similar to the proportion with pre-infarction angina in the current study. Gradual occlusion may cause "pre-conditioning" for ischemia, which may in turn explain the lower peak cardiac

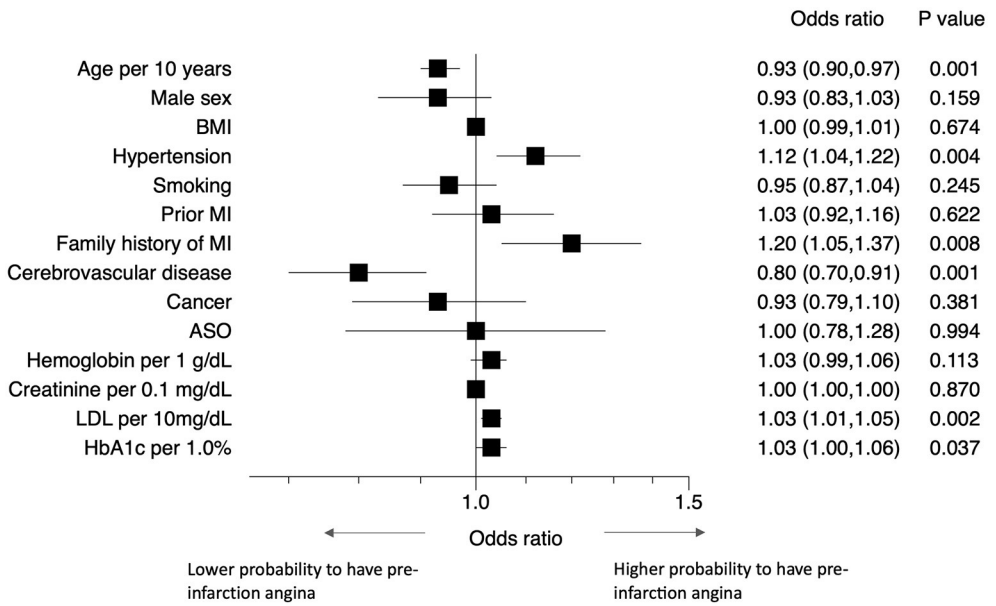

FIGURE 4 | Predictors of pre-infarction angina. Forest plots showing the odds ratios of having pre-infarction angina with various comorbidities. ASO, arteriosclerosis obliterans; BMI, body mass index; LDL-C, low density lipoprotein cholesterol; MI, myocardial infarction.

enzyme levels in patients with pre-infarction angina than in those without.

Patients with a family history of MI, hypertension, dyslipidemia, or diabetes had a higher probability of pre-infarction angina than those without. A family history of MI probably indicates that the patients become well-informed on the disease and its symptoms. Hypertension and dyslipidemia are both common risk factors of atherosclerosis. We speculate that these factors inhibit sudden massive thrombus formation. However, the precise mechanism is still unknown and remains to be investigated in future studies. Our finding for diabetes is particularly notable, because it appears to contradict previous findings: these indicated that patients with diabetes mellitus may not report classic ischemic chest pain but may instead present with dyspnea, nausea, fatigue, cough, or other non-specific symptoms due to diabetes-associated cardiovascular autonomic neuropathy (20–22). In contrast, our study showed that diabetes mellitus was a predictor of pre-infarction angina. When we divided patients into those with and without diabetes, diabetic patients more frequently experienced pre-infarction angina (typical chest pain) than non-diabetic patients [50.4 vs. 48.3%, $P = 0.043$]. A number of reasons for this difference can be considered, including differences in race, medical system, and patient education level, as well as the up-to-datedness of treatment for diabetes and lower prevalence of diabetic neuropathy (23) than previously thought (20, 21). Selection bias might also play a role—our assessment was limited to MI patients admitted to hospital, and did not include patients who died out of hospital. This finding should be confirmed in a large-scale study.

We also found that elderly patients and those with a history of cerebrovascular disease were less likely to experience pre-infarction angina. Both of these risk factors may be associated with sensory and motor disorders—this may in turn lead to an increased anginal threshold and lower burden of daily activity, and consequently to the absence of typical angina.

Clinical Implications and Future Perspectives

Hypertension, diabetes, dyslipidemia, and a family history of MI are all well-known risk factors of coronary artery disease. Nevertheless, our study did show the additional clinical importance of these comorbidities. Patients with them had a higher probability of pre-infarction angina, which can act as a warning of MI before its onset. This point is the novelty of the present findings. Accordingly, patients should be educated to easily recognize pre-infarction angina themselves, as a warning of MI. Atypical symptoms might be difficult to interpret for patients and even physicians. In our study, half of the MI patients experienced "typical" anginal symptoms, which are easy to interpret and therefore a useful aid to prompt diagnosis. Physicians should never dismiss the chance of prompt diagnosis of angina and prevention of MI (18). Rapid action by physicians and patients in the pre-infarction angina phase can prevent the onset of MI in at least half of MI patients. Public education efforts such as the Japanese Circulation Society's "STOP MI Campaign" are helpful, and indeed likely even more efficient in reducing the mortality of MI than in-hospital treatment, given that approximately half of out-of-hospital deaths might be avoided (5). Mortality of MI in Japan decreased after the launch of the STOP MI Campaign in 2014 from 31.1% (2014) to 24.8%

(2020), albeit that the reason for this decrease is multifactorial (24, 25).

Social media and smart devices may have major potential in this field (6–8). A public campaign through social media was shown to be effective in reducing COVID-19 infection in the United States (7). In the field of ischemic heart disease, public education through a short message service significantly shortened the onset-to-door time of MI patients (6). As for smart devices, the Apple watch can detect atrial fibrillation and provide patients with an alert (26, 27). We have also noted the increased use of this technology in our clinical practice, with more and more patients presenting at our outpatient clinic with an Apple watch showing an electrocardiogram of atrial fibrillation. In ischemic heart disease also, the possibility of detecting ischemia was recently reported (8). Although the clinical use of this technology in ischemic heart disease has yet to be validated, we consider that it is only a matter of time before it is incorporated into daily clinical practice. Automatic detection of pre-infarction angina and an alert by a smart device may prevent the onset of MI. Public education in combination with advanced smart technology and recent IoT infrastructure must surely be effective. Our present study suggests that patient subpopulations with hypertension, diabetes, dyslipidemia, or a family history of MI are suitable candidates for public education. Such a targeted public campaign in combination with smart devices and social media might show a synergistic effect. This research finding should be implemented in designing future prospective large-scale studies with the upcoming IoT technology.

Study Limitations

Several limitations of our study should be acknowledged. First, angina as a symptom is subjective, although the definition was pre-defined and the data were prospectively collected. Second, the current population was limited to patients who were admitted to a hospital due to myocardial infarction, and the present findings might not therefore be directly applicable to patients who were not admitted to hospitals, namely out-of-hospital deaths. Third, patients excluded from the present analysis [$N =$ 976 (8.1%)] showed significantly different baseline characteristics to those who were analyzed, resulting in a degree of selection bias. Lastly, the generalizability of the findings to other regions and ethnicities is limited by racial differences, differing healthcare systems, etc. in Japan compared with other countries.

In conclusion, we found that half of the MI patients in our registry experienced pre-infarction angina before the onset of MI. Most patients with pre-infarction angina had sufficient time ($>$6 h) to go to the hospital before MI onset. However, 15% had only $\leq$6 h, which would favor early medical contact. Patients with hypertension, diabetes, dyslipidemia, or a family history of MI had a higher probability of having pre-infarction angina than those without. This study suggested the need to reappraise these common coronary risk factors. Prompt medical consultation may enable treatment at the pre-infarction angina stage, and thereby be preventive for MI. This patient sub-population may represent a good target for public education. Future prospective large-scale studies with upcoming IoT technology are warranted.

DATA AVAILABILITY STATEMENT

Our study data will not be made available to other researchers for purposes of reproducing the results because of Institutional Review Board restrictions.

ETHICS STATEMENT

The studies involving human participants were reviewed and approved by Osaka University Hospital. The patients/participants provided their written informed consent to participate in this study.

AUTHOR CONTRIBUTIONS

YSo, YU, and SH: concept and design, data analysis and statistical analysis, and manuscript draft. All authors: critical revision, editing, and approval of the final manuscript. All authors contributed to the article and approved the submitted version.

FUNDING

This work was supported by Grants-in-Aid for University and Society Collaboration (#19590816, #19390215, and #25461055) from the Japanese Ministry of Education, Culture, Sports, Science and Technology, Tokyo, Japan.

ACKNOWLEDGMENTS

We thank Nagisa Yoshioka, Satomi Kishimoto, Kyoko Tatsumi, Noriko Murakami, Mariko Kishida, Rie Nagai, Sugako Mitsuoka, and all of the OACIS research coordinators and nurses for their excellent assistance with data collection.

SUPPLEMENTARY MATERIAL

The Supplementary Material for this article can be found online at: https://www.frontiersin.org/articles/10.3389/fcvm.2022.867723/full#supplementary-material

REFERENCES

1. Virani SS, Alonso A, Benjamin EJ, Bittencourt MS, Callaway CW, Carson AP, et al. Heart disease and stroke statistics-2020 update: a report from the American Heart Association. *Circulation.* (2020) 141:e139–596. doi: 10.1161/CIR.0000000000000746

2. O'Gara PT, Kushner FG, Ascheim DD, Casey DE Jr., Chung MK, de Lemos JA, et al. 2013 Accf/aha guideline for the management of St-elevation myocardial infarction: a report of the American College of Cardiology Foundation/American Heart Association Task Force on Practice Guidelines. *Circulation.* (2013) 127:e362–425. doi: 10.1161/CIR.0b013e318274 2cf6

3. Takagi K, Tanaka A, Yoshioka N, Morita Y, Yoshida R, Kanzaki Y, et al. In-hospital mortality among consecutive patients with st-elevation myocardial infarction in modern primary percutaneous intervention era ∼ insights from 15-year data of single-center hospital-based registry. *PLoS ONE.* (2021) 16:e0252503. doi: 10.1371/journal.pone.0252503
4. Dudas K, Lappas G, Stewart S, Rosengren A. Trends in out-of-hospital deaths due to coronary heart disease in Sweden (1991 to 2006). *Circulation.* (2011) 123:46–52. doi: 10.1161/CIRCULATIONAHA.110.964999
5. Ueda Y, Tahara Y, Itoh T, Tsujita K, Sakuma M, Amano T, et al. New strategy to prevent acute myocardial infarction by public education- a position statement of the committee on public education about emergency medical care of the Japanese Circulation Society. *Circ J.* (2021) 85:319–22. doi: 10.1253/circj.CJ-20-1308
6. Saberi F, Adib-Hajbaghery M, Zohrehie J. The effects of public education through short message service on the time from symptom onset to hospital arrival in patients with myocardial infarction: a field trial. *ARYA Atheroscler.* (2017) 13:97–102.
7. Breza E, Stanford FC, Alsan M, Alsan B, Banerjee A, Chandrasekhar AG, et al. Effects of a large-scale social media advertising campaign on holiday travel and Covid-19 infections: a cluster randomized controlled trial. *Nat Med.* (2021) 27:1622–8. doi: 10.1038/s41591-021-01487-3
8. Drexler M, Elsner C, Gabelmann V, Gori T, Munzel T. Apple watch detecting coronary ischaemia during chest pain episodes or an apple a day may keep myocardial infarction away. *Eur Heart J.* (2020) 41:2224. doi: 10.1093/eurheartj/ehaa290
9. Sotomi Y, Ueda Y, Hikoso S, Nakatani D, Suna S, Dohi T, et al. Manual thrombus aspiration and its procedural stroke risk in myocardial infarction. *J Am Heart Assoc.* (2021) 10:e022258. doi: 10.1161/JAHA.121.022258
10. Sotomi Y, Hikoso S, Nakatani D, Dohi T, Mizuno H, Okada K, et al. Practical assessment of the tradeoff between fatal bleeding and coronary thrombotic risks using the academic research consortium for high bleeding risk criteria. *J Atheroscler Thromb.* (2021) 28. doi: 10.5551/jat.62999
11. Nakatani D, Sakata Y, Suna S, Usami M, Matsumoto S, Shimizu M, et al. Incidence, predictors, and subsequent mortality risk of recurrent myocardial infarction in patients following discharge for acute myocardial infarction. *Circ J.* (2013) 77:439–46. doi: 10.1253/circj.CJ-11-1059
12. Masuda M, Nakatani D, Hikoso S, Suna S, Usami M, Matsumoto S, et al. Clinical impact of ventricular tachycardia and/or fibrillation during the acute phase of acute myocardial infarction on in-hospital and 5-year mortality rates in the percutaneous coronary intervention era. *Circ J.* (2016) 80:1539–47. doi: 10.1253/circj.CJ-16-0183
13. Reiter R, Henry TD, Traverse JH. Preinfarction angina reduces infarct size in St-elevation myocardial infarction treated with percutaneous coronary intervention. *Circ Cardiovasc Interv.* (2013) 6:52–8. doi: 10.1161/CIRCINTERVENTIONS.112.973164
14. Fujita M, Sasayama S, Araie E, Ohno A, Yamanishi K, Hirai T. Significance of pre-infarction angina for occurrence of post-infarction angina. *Eur Heart J.* (1988) 9:159–64. doi: 10.1093/oxfordjournals.eurheartj.a062469
15. Lorgis L, Gudjoncik A, Richard C, Mock L, Buffet P, Brunel P, et al. Pre-infarction angina and outcomes in non-St-segment elevation myocardial infarction: data from the rico survey. *PLoS ONE.* (2012) 7:e48513. doi: 10.1371/journal.pone.0048513
16. Brand FN, Larson M, Friedman LM, Kannel WB, Castelli WP. Epidemiologic assessment of angina before and after myocardial infarction: the framingham study. *Am Heart J.* (1996) 132:174–8. doi: 10.1016/S0002-8703(96)90406-8
17. McSweeney JC, Cody M, O'Sullivan P, Elberson K, Moser DK, Garvin BJ. Women's early warning symptoms of acute myocardial infarction. *Circulation.* (2003) 108:2619–23. doi: 10.1161/01.CIR.0000097116.29625.7C
18. Stowers M, Short D. Warning symptoms before major myocardial infarction. *Br Heart J.* (1970) 32:833–8. doi: 10.1136/hrt.32.6.833
19. Rittersma SZ, van der Wal AC, Koch KT, Piek JJ, Henriques JP, Mulder KJ, et al. Plaque instability frequently occurs days or weeks before occlusive coronary thrombosis: a pathological thrombectomy study in primary percutaneous coronary intervention. *Circulation.* (2005) 111:1160–5. doi: 10.1161/01.CIR.0000157141.00778.AC
20. Faerman I, Faccio E, Milei J, Nunez R, Jadzinsky M, Fox D, et al. Autonomic neuropathy and painless myocardial infarction in diabetic patients. Histologic evidence of their relationship. *Diabetes.* (1977) 26:1147–58. doi: 10.2337/diabetes.26.12.1147
21. Nakagawa S, Mitamura H, Kimura M. [Characteristics of acute myocardial infarction, preinfarct angina and postinfarct angina in patients with diabetes mellitus]. *J Cardiol.* (1992) 22:11–20.
22. Junghans C, Sekhri N, Zaman MJ, Hemingway H, Feder GS, Timmis A. Atypical chest pain in diabetic patients with suspected stable angina: impact on diagnosis and coronary outcomes. *Eur Heart J Qual Care Clin Outcomes.* (2015) 1:37–43. doi: 10.1093/ehjqcco/qcv003
23. Ebata-Kogure N, Nozawa K, Murakami A, Toyoda T, Haga Y, Fujii K. Clinical and economic burdens experienced by patients with painful diabetic peripheral neuropathy: an observational study using a Japanese Claims Database. *PLoS ONE.* (2017) 12:e0187250. doi: 10.1371/journal.pone.0187250
24. *Vital Statistics 2020: Ministry of Health, Labour and Welfare, Japan*. Available online at: https://wwwmhlwgojp/toukei/saikin/hw/jinkou/geppo/nengai20/dl/h6pdf (accessed January 2022).
25. *Vital Statistics 2014: Ministry of Health, Labour and Welfare, Japan*. Available online at: https://wwwmhlwgojp/toukei/saikin/hw/jinkou/kakutei14/dl/11_h7pdf (accessed January 2022).
26. Perez MV, Mahaffey KW, Hedlin H, Rumsfeld JS, Garcia A, Ferris T, et al. Large-scale assessment of a smartwatch to identify atrial fibrillation. *N Engl J Med.* (2019) 381:1909–17. doi: 10.1056/NEJMoa1901183
27. Seshadri DR, Bittel B, Browsky D, Houghtaling P, Drummond CK, Desai MY, et al. Accuracy of apple watch for detection of atrial fibrillation. *Circulation.* (2020) 141:702–3. doi: 10.1161/CIRCULATIONAHA.119.044126

Conflict of Interest: YSo received research grants from Abbott Medical Japan, and speaker honoraria from Abbott Medical Japan, Boston Scientific Japan, TERUMO, Japan Lifeline, Biosensors, and Medtronic, and is an endowed chair funded by TOA EIYO. YU received research grants from Abbott Medical Japan and Medtronic, and lecture fees from NIPRO. HM is an endowed chair funded by TERUMO, Asahi Intecc, NIPRO, and Shimadzu Corporation, and received personal fees from Medtronic Japan, Japan Lifeline, and Abbott Medical Japan. YasushiS received grants from Abbott Medical Japan and Biotronik.

The remaining authors declare that the research was conducted in the absence of any commercial or financial relationships that could be construed as a potential conflict of interest.

frontiers | Frontiers in Cardiovascular Medicine

ORIGINAL RESEARCH
published: 13 June 2022
doi: 10.3389/fcvm.2022.925414

Computational Fractional Flow Reserve From Coronary Computed Tomography Angiography—Optical Coherence Tomography Fusion Images in Assessing Functionally Significant Coronary Stenosis

Yong-Joon Lee[1†], Young Woo Kim[2†], Jinyong Ha[3†], Minug Kim[3], Giulio Guagliumi[4], Juan F. Granada[5], Seul-Gee Lee[6], Jung-Jae Lee[6], Yun-Kyeong Cho[7], Hyuck Jun Yoon[7], Jung Hee Lee[8], Ung Kim[8], Ji-Yong Jang[9], Seung-Jin Oh[9], Seung-Jun Lee[1], Sung-Jin Hong[1], Chul-Min Ahn[1], Byeong-Keuk Kim[1], Hyuk-Jae Chang[1], Young-Guk Ko[1], Donghoon Choi[1], Myeong-Ki Hong[1], Yangsoo Jang[10], Joon Sang Lee[2] and Jung-Sun Kim[1]**

[1] Division of Cardiology, Severance Cardiovascular Hospital, Yonsei University College of Medicine, Seoul, South Korea, [2] Department of Mechanical Engineering, Yonsei University, Seoul, South Korea, [3] Department of Electrical Engineering, Sejong University, Seoul, South Korea, [4] Department of Cardiovascular, Ospedale Papa Giovanni XXIII, Bergamo, Italy, [5] Cardiovascular Research Foundation, Columbia University Medical Center, New York, NY, United States, [6] Yonsei Cardiovascular Research Institute, Yonsei University College of Medicine, Seoul, South Korea, [7] Department of Cardiology, Keimyung University Dongsan Hospital, Daegu, South Korea, [8] Division of Cardiology, Yeungnam University Medical Center, Yeungnam University College of Medicine, Daegu, South Korea, [9] National Health Insurance Service Ilsan Hospital, Goyang, South Korea, [10] Division of Cardiology, CHA Bundang Medical Center, CHA University College of Medicine, Seongnam, South Korea

Background: Coronary computed tomography angiography (CTA) and optical coherence tomography (OCT) provide additional functional information beyond the anatomy by applying computational fluid dynamics (CFD). This study sought to evaluate a novel approach for estimating computational fractional flow reserve (FFR) from coronary CTA-OCT fusion images.

Methods: Among patients who underwent coronary CTA, 148 patients who underwent both pressure wire-based FFR measurement and OCT during angiography to evaluate intermediate stenosis in the left anterior descending artery were included from the prospective registry. Coronary CTA-OCT fusion images were created, and CFD was applied to estimate computational FFR. Based on pressure wire-based FFR as a reference, the diagnostic performance of Fusion-FFR was compared with that of CT-FFR and OCT-FFR.

Results: Fusion-FFR was strongly correlated with FFR (r = 0.836, P < 0.001). Correlation between FFR and Fusion-FFR was stronger than that between FFR and CT-FFR (r = 0.682, P < 0.001; z statistic, 5.42, P < 0.001) and between FFR

OPEN ACCESS

Edited by:
Matteo Tebaldi,
Azienda Ospedaliero Universitaria—Cardiology Unit, Italy

Reviewed by:
Roberto Scarsini,
Integrated University Hospital Verona, Italy
Rajiv Rampat,
William Harvey Hospital, United Kingdom

***Correspondence:**
Joon Sang Lee
joonlee@younsei.ac.kr
Jung-Sun Kim
kjs1218@yuhs.ac

[†] These authors have contributed equally to this work and share first authorship

Specialty section:
This article was submitted to Coronary Artery Disease, a section of the journal Frontiers in Cardiovascular Medicine

Received: 21 April 2022
Accepted: 25 May 2022
Published: 13 June 2022

Citation:
Lee Y-J, Kim YW, Ha J, Kim M, Guagliumi G, Granada JF, Lee S-G, Lee J-J, Cho Y-K, Yoon HJ, Lee JH, Kim U, Jang J-Y, Oh S-J, Lee S-J, Hong S-J, Ahn C-M, Kim B-K, Chang H-J, Ko Y-G, Choi D, Hong M-K, Jang Y, Lee JS and Kim J-S (2022) Computational Fractional Flow Reserve From Coronary Computed Tomography Angiography—Optical Coherence Tomography Fusion Images in Assessing Functionally Significant Coronary Stenosis. Front. Cardiovasc. Med. 9:925414. doi: 10.3389/fcvm.2022.925414

and OCT-FFR (r = 0.705, $P < 0.001$; z statistic, 4.38, $P < 0.001$). Area under the receiver operating characteristics curve to assess functionally significant stenosis was higher for Fusion-FFR than for CT-FFR (0.90 vs. 0.83, P = 0.024) and OCT-FFR (0.90 vs. 0.83, P = 0.043). Fusion-FFR exhibited 84.5% accuracy, 84.6% sensitivity, 84.3% specificity, 80.9% positive predictive value, and 87.5% negative predictive value. Especially accuracy, specificity, and positive predictive value were superior for Fusion-FFR than for CT-FFR (73.0%, P = 0.007; 61.4%, $P < 0.001$; 64.0%, $P < 0.001$) and OCT-FFR (75.7%, P = 0.021; 73.5%, P = 0.020; 69.9%, P = 0.012).

Conclusion: CFD-based computational FFR from coronary CTA-OCT fusion images provided more accurate functional information than coronary CTA or OCT alone.

Clinical Trial Registration: [www.ClinicalTrials.gov], identifier [NCT03298282].

Keywords: fractional flow reserve (FFR), coronary computed tomography angiography (coronary CTA), optical coherence tomography (OCT), fusion image, computational fluid dynamics (CFD)

INTRODUCTION

Deciding whether to recommend coronary revascularization to patients with chest pain and intermediate stenosis on coronary angiography is challenging (1, 2). Therefore, in addition to the anatomical assessment of coronary stenosis, functional assessment is essential to evaluate the presence of myocardial ischemia, particularly in the setting of intermediate stenosis (1–5). Pressure wire-based fractional flow reserve (FFR) has been considered the gold standard for functional assessment of intermediate stenosis; it helps reduce unnecessary revascularization procedures (6, 7). Coronary computed tomography angiography (CTA) is a widely used non-invasive method for visualizing the coronary artery, and intravascular optical coherence tomography (OCT) has been used for accurate anatomical assessment of coronary stenotic lesions during angiography with exceptional higher resolution than intravascular ultrasound (8–10). In addition, computational fluid dynamics (CFD) has been applied to estimate computational FFR from coronary CTA- or OCT-based three-dimensional coronary model without using additional pressure guide wires or hyperemic agents (11–14). However, no studies have heretofore evaluated the usefulness of fusion images generated from both coronary CTA and OCT in clinical practice. Since many patients undergo coronary CTA to evaluate suspected coronary artery disease before being referred for angiography, it is hypothesized that if not only OCT but also coronary CTA images are available, the coronary CTA-OCT fusion images can be created and can provide more reliable information about coronary stenosis by combining delicate vessel curvature found in coronary CTA images with accurate lumen contour found in OCT images (8, 9, 15). Thus, this study aimed to present a novel approach for estimating CFD-based computational FFR from coronary CTA-OCT fusion images (Fusion-FFR). Pressure wire-based FFR was used as a reference to assess the diagnostic performance of Fusion-FFR as well as FFR derived from coronary CTA or OCT alone (CT-FFR or OCT-FFR) in patients with intermediate coronary stenosis.

MATERIALS AND METHODS

Subjects and Study Design

The Integrated Coronary Multicenter Imaging Registry is a collaboration between four institutions in South Korea, created to evaluate the clinical impact of anatomical information from coronary CTA and OCT, as well as the functional information from FFR in patients with intermediate coronary stenosis with clinical follow-up (ClinicalTrials.gov, Identifier: NCT03298282). This study complied with the principles of the Declaration of Helsinki, and the Institutional Review Board at each participating center approved this study protocol. Written informed consent was obtained from all patients. Briefly, among patients who underwent coronary CTA for chest pain before being referred for coronary angiography, a total of 180 patients who had undergone both pressure wire-based FFR measurement and OCT examination during angiography to evaluate intermediate stenosis (40–70%) in any coronary artery were enrolled between November 2017 and June 2019 (the detailed inclusion and exclusion criteria are presented in **Supplementary Table 1**). Of these, 32 patients were excluded due to no intermediate stenosis of the left anterior descending artery (LAD) (n = 18), poor image quality of coronary CTA or OCT (n = 9), and incomplete OCT coverage (n = 5). Consequently, a total of 148 patients with intermediate stenosis on LAD were included in this study, and pressure wire-based FFR was used as a reference to assess the diagnostic performance of CFD- based computational FFRs (**Supplementary Figure 1**). The primary outcome was the correlation between pressure wire-based FFR and computational FFRs. The secondary outcome was the diagnostic performance of computational FFRs in assessing functionally significant stenosis. The correlation and diagnostic performance of Fusion-FFR were compared to those of CT-FFR and OCT-FFR.

Image Acquisition, Analysis, and Fractional Flow Reserve Measurement

All subjects underwent coronary CTA before coronary angiography. Coronary CTA performance and acquisition

of CTA images (64— or higher detector row scanners with prospective or retrospective electrocardiographic gating) were in accordance with the Society of Cardiovascular Computed Tomography guidelines (16). OCT imaging of the target lesion was performed using a frequency-domain OCT system (C7-XR OCT imaging system, LightLab Imaging Inc., St. Jude Medical, MN, United States). Cross-sectional OCT images were generated at a rotational speed of 100 frames/s. The fiber probe was withdrawn at 20 mm/s within the stationary imaging sheath.

All quantitative coronary angiography (QCA) and OCT analyses were performed at an independent core laboratory of Cardiovascular Research Center (Seoul, South Korea), and coronary CTA analysis was performed at Yonsei University CONNECT-AI Research Center (Seoul, South Korea) by experienced analysts who were blinded to the patient and procedure data. QCA analysis was performed using an off-line quantitative coronary angiographic system (CAAS, Pie Medical Instruments, Maastricht, Netherlands). Using the guiding catheter for magnification calibration, minimal lumen diameter was measured from diastolic frames in a single, matched view, showing the smallest lumen diameter. Coronary CTA analysis was performed using semi-automated image analysis software (QAngio CT RE, Medis Medical Imaging Systems, Leiden, Netherlands). Coronary CTA stenosis was evaluated by determining lumen diameter stenosis in each coronary segment $\geq$ 2 mm in diameter, using an 18-segment coronary model (12, 17). OCT analysis was performed using certified software (QIvus, Medis Medical Imaging Systems, Leiden, Netherlands). The reference lumen area was the region within the same segment as the lesion with the largest lumen. These reference area was proximal or distal to the stenotic area (usually within 10 mm of the stenosis, without major intervening branches). The minimal lumen area was identified at the segment with the smallest lumen area. Area stenosis was calculated as follows: [(mean reference lumen area - minimal lumen area) $\div$ mean reference lumen area] $\times$ 100%. OCT-based plaque characteristics were also assessed; they are defined in **Supplementary Table 2**.

FFR was measured using a 0.014-inch pressure guidewire (St. Jude Medical, MN, United States). After equalizing process, the pressure guidewire was positioned distal to the target lesion. Hyperemia was induced by intravenous adenosine administered at 140 μg/kg/min *via* an antecubital vein. FFR was calculated as follows: mean hyperemic distal coronary pressure/mean aortic pressure. When FFR was $\leq$ 0.80, the stenotic lesion was considered functionally significant.

Three-Dimensional Coronary Model Reconstruction and Image Fusion With Coronary Computed Tomography Angiography and Optical Coherence Tomography

Coronary CTA lumen contours at 0.25 mm intervals were manually extracted by experienced experts at the core laboratory. When coronary CTA lumen contours with side branches were extracted, the information regarding the direction of the side branches was also included. To create an OCT-derived three-dimensional coronary model for blood flow simulation, OCT lumen contours at 0.2 mm intervals were extracted using fully automated software (MATLAB, MathWorks, MA, United States), using the spatial continuity of the arterial walls in the transverse cross-sectional plane (18). A simple three-dimensional model was generated by eliminating side branches at bifurcations of the target lesions; thus, overall lumen contours were extracted by estimating the mother vessel lumen. The extracted lumen contour data were then used to create a three-dimensional model using semi-automated software designed in-house (Unity, Unity Technologies, CA, United States).

The entire image fusion process was performed as follows. Bifurcation directions of the coronary CTA and OCT lumens were identified as references. Coronary CTA lumens were then exchanged with the corresponding OCT lumens, while circumferential angulation and correction of the longitudinal location of the OCT lumens were applied to match the bifurcation direction of the target coronary CTA lumens. Since the lumen intervals differed for coronary CTA and OCT, OCT lumens were interpolated to obtain the same interval as the CTA lumens. Finally, the sizes of the remaining coronary CTA lumens were manually adjusted using the corresponding fusion model as a reference, and the fusion lumen data points were connected by ray casting to generate a meticulous three-dimensional coronary model.

Computational Fluid Dynamics-Based Computational Fractional Flow Reserve Estimation

CFD-based blood flow simulation of reconstructed three-dimensional models was performed using the lattice Boltzmann method, which has been widely used for biofluidics; it uses lattice grids instead of complicated meshes for complex three-dimensional models (19, 20). Blood was modeled as an incompressible non-Newtonian fluid with a density of 1,060 kg/m^3 based on the Carreau–Yasuda model (21). The inlet flow was designated as a steady flow condition based on the patient's mean blood pressure assessed during coronary angiography. For the outlet boundary condition, a resistance model was used to reflect the circulatory resistance (22). Moreover, a no-slip boundary condition was used to calculate the interaction between the vessel wall and blood flow. Detailed equations and numerical methods used for estimating CFD-based computational FFR have been described previously (20). For each patient, Fusion-FFR, CT-FFR, and OCT-FFR were estimated. In addition, vorticity, helicity, and wall shear stress were also estimated and compared to support our hypothesis regarding the impact of vessel curvature of coronary CTA toward fusion images (23, 24).

Statistical Analyses

Continuous variables were reported as means $\pm$ standard deviations or medians (interquartile ranges), and categorical variables were reported as numbers (percentages). Continuous

variables were compared using Student's *t*-test or Mann-Whitney test, as appropriate. Pearson correlation coefficient was calculated to evaluate the relationships between pressure wire-based FFR and computational FFRs (Fusion-FFR, CT-FFR, and OCT-FFR). The Bland–Altman analysis was also performed. Receiver operating characteristics (ROC) curve analysis was performed to evaluate the diagnostic performance of the computational FFRs in assessing functionally significant stenosis. The comparison between correlation coefficients was performed using Steiger's *Z*-test, and the comparison between ROC curves was performed using DeLong's test. The diagnostic accuracy, sensitivity, specificity, positive predictive value, and negative predictive values were also calculated as simple proportions with 95% confidence intervals (CIs), and the comparisons of these parameters were performed using R packages (R foundations for Statistical Computing, Vienna, Austria), including DTComPair. Other statistical analyses were performed using IBM SPSS, version 25.0 (IBM Corp., Armonk, NY, United States), and MedCalc, version 18.2.1 (MedCalc Software, Ostend, Belgium). All tests were two-sided, and a P-value < 0.05 was considered statistically significant.

RESULTS

Baseline Characteristics and Computational Fractional Flow Reserve Estimation

The baseline clinical characteristics, coronary angiographic, coronary CTA, and OCT findings are presented in **Tables 1**, **2**. The median time between coronary CTA and coronary angiography with OCT evaluation was 11 days (interquartile range: 4–18 days). Among 148 patients, 109 patients (73.6%) were male, and 44 patients (29.7%) presented with acute coronary syndrome. The LAD was considered as culprit vessel causing acute coronary syndrome in 21 patients (14.2%). There were bifurcation lesions with the side branch of $\geq$ 2.5 mm in diameter in 39 patients (26.4%). There were no complications during any of the procedures. The median pressure wire-based FFR at maximal hyperemia was 0.82 (interquartile range, 0.74–0.87). Functionally significant stenosis was observed in 65 patients (43.9%). The median CT-FFR was 0.78 (interquartile range, 0.72–0.84), OCT-FFR was 0.80 (interquartile range, 0.75–0.86), and Fusion-FFR was 0.81 (interquartile range, 0.74–0.85). A representative example of the three-dimensional coronary model reconstruction as well as the coronary CTA-OCT image fusion is presented in **Figure 1**. The three-dimensional model reconstruction for coronary CTA and OCT was completed within approximately 3 min. The entire image fusion with corresponding three-dimensional model reconstruction processes was completed within approximately 3 min, and estimation of Fusion-FFR using CFD was completed within approximately 15 min for each patient.

TABLE 1 | Baseline clinical characteristics.

Variables	Total (n = 148)
Age (years)	63.4 ± 8.8
Male	109 (73.6)
Body mass index (kg/m^2)	25.0 ± 2.9
Acute coronary syndrome	44 (29.7)
Hypertension	83 (56.1)
Diabetes mellitus	46 (31.1)
Dyslipidemia	72 (48.6)
Current smoker	33 (22.3)
Previous percutaneous coronary intervention	7 (4.7)

Data are presented as the mean ± standard deviation (SD) or number (%).

Correlation and Diagnostic Performance of Computational Fractional Flow Reserves

Fusion-FFR was strongly correlated with FFR (correlation coefficient, $r = 0.836$, $P < 0.001$; mean difference, 0.00 ± 0.06)

TABLE 2 | Lesion characteristics.

Variables	Total (n = 148)
Coronary angiography analysis	
Reference vessel diameter (mm)	3.0 ± 0.5
Minimal lumen diameter (mm)	1.4 ± 0.5
Diameter stenosis (%)	53.9 ± 16.9
Lesion length (mm)	21.8 ± 9.8
Bifurcation lesions	39 (26.4)
Pressure wire-based FFR measurement	
FFR	0.82 (0.74–0.87)
FFR ≤ 0.8	65 (43.9)
Coronary computed tomography angiography analysis	
CTA stenosis (%)	61.1 ± 19.3
CTA stenosis ≥ 50%	107 (72.3)
Agatston score	283.7 ± 434.6
Agatston score ≥ 300	42 (28.4)
Optical coherence tomography analysis	
Proximal reference segment lumen area (mm^2)	7.2 ± 2.6
Distal reference segment lumen area (mm^2)	6.5 ± 3.1
Minimal lumen area of target lesion (mm^2)	2.3 ± 1.2
Area stenosis (%)	84.3 ± 6.8
Plaque morphology	
Fibrous	28 (18.9)
Fibrocalcific	88 (59.5)
Lipid	64 (43.2)
Intimal vasculature	62 (41.9)
Cholesterol crystal	66 (44.6)
Calcific nodule	16 (10.8)
CFD-based computational FFR estimation	
Fusion-FFR	0.81 (0.74–0.85)
Fusion-FFR ≤ 0.8	68 (45.9)
CT-FFR	0.78 (0.72–0.84)
CT-FFR ≤ 0.8	89 (60.1)
OCT-FFR	0.80 (0.75–0.86)
OCT-FFR ≤ 0.8	73 (49.3)

Data are presented as the mean ± SD, number (%), or median (interquartile range). CFD, computational fluid dynamics; CTA, computed tomography angiography; CT-FFR, computational FFR from coronary CTA; FFR, fractional flow reserve; Fusion-FFR, computational FFR from coronary CTA-OCT fusion images; OCT, optical coherence tomography; OCT-FFR, computational FFR from OCT.

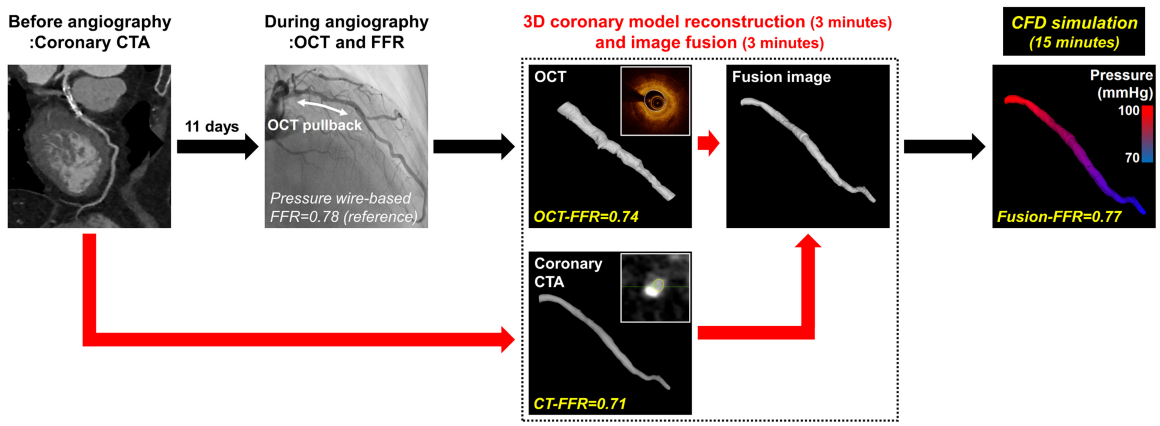

FIGURE 1 | Overview of estimating CFD-based computational FFR from coronary CTA-OCT fusion images in patients with intermediate coronary stenosis. The current study evaluated a novel approach to estimate CFD-based computational FFR from coronary CTA-OCT fusion images in patients with intermediate coronary stenosis in the left anterior descending artery. CFD, computational fluid dynamics; CTA, computed tomography angiography; CT-FFR, computational FFR from coronary CTA; FFR, fractional flow reserve; Fusion-FFR, computational FFR from coronary CTA-OCT fusion images; OCT, optical coherence tomography; OCT-FFR, computational FFR from OCT.

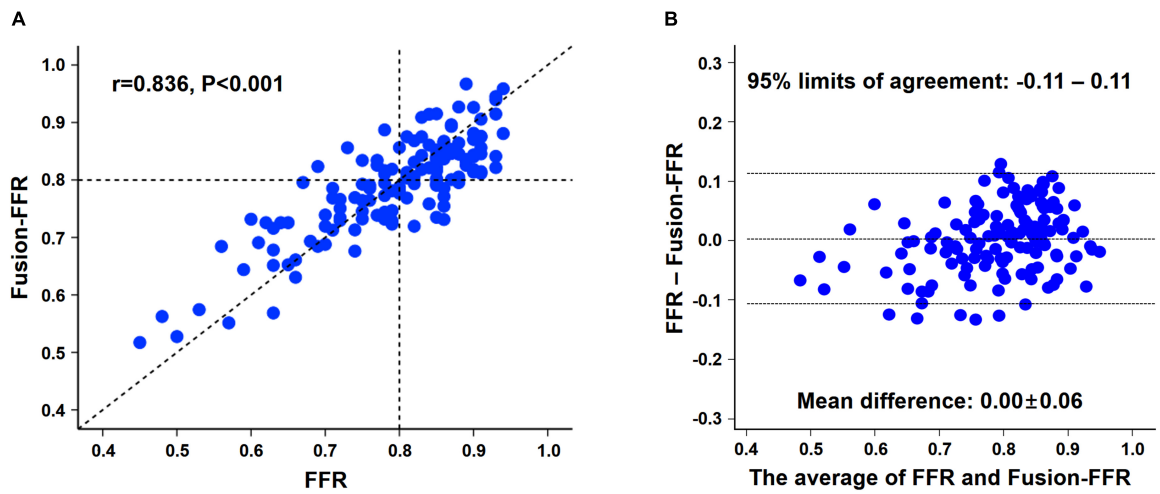

FIGURE 2 | Relationship between pressure wire-based FFR and Fusion-FFR. Correlation **(A)** and agreement **(B)** between pressure wire-based FFR and Fusion-FFR. FFR, fractional flow reserve; Fusion-FFR, computational FFR from coronary CTA-OCT fusion images.

(**Figures 2A,B**). Although CT-FFR was well correlated with FFR (r = 0.682, P < 0.001; mean difference, 0.02 ± 0.08), the correlation between FFR and Fusion-FFR was stronger (z statistic, 5.42, P < 0.001) (**Figure 3A** and **Supplementary Figure 2A**). Similarly, although OCT-FFR was well correlated with FFR (r = 0.705, P < 0.001; mean difference, 0.00 ± 0.07), the correlation between FFR and Fusion-FFR was stronger (z statistic, 4.38, P < 0.001) (**Figure 3B** and **Supplementary Figure 2B**). The correlation between FFR and CT-FFR was not different from that between FFR and OCT-FFR (z statistic, 0.58, P = 0.562). Anatomic variables were weakly correlated with FFR (percentage area stenosis on OCT: r = −0.451; percentage coronary CTA stenosis: r = −0.300).

The area under the ROC curve in assessing functionally significant stenosis is presented in **Figure 4**. The area was higher for Fusion-FFR than for CT-FFR (0.90 [95% CI: 0.84–0.94] vs. 0.83 [95% CI: 0.76–0.89], P = 0.024) and OCT-FFR (0.90 [95% CI: 0.84–0.94] vs. 0.83 [95% CI: 0.76–0.89], P = 0.043). The area was not different between CT-FFR and OCT-FFR (P = 0.947). The area was also higher for Fusion-FFR than for anatomic variables (percentage area stenosis on OCT: 0.78 [95% CI: 0.71–0.85]; percentage coronary CTA stenosis: 0.70 [95% CI: 0.62–0.77]). The diagnostic performance of computational FFRs in assessing functionally significant stenosis is presented in **Table 3**. Fusion-FFR exhibited 84.5% accuracy, 84.6% sensitivity, 84.3% specificity, 80.9% positive predictive value, and 87.5% negative predictive value. The diagnostic performance, especially accuracy, specificity, and positive predictive value were superior for Fusion-FFR, compared to those of CT-FFR (73.0%, P = 0.007; 61.4%,

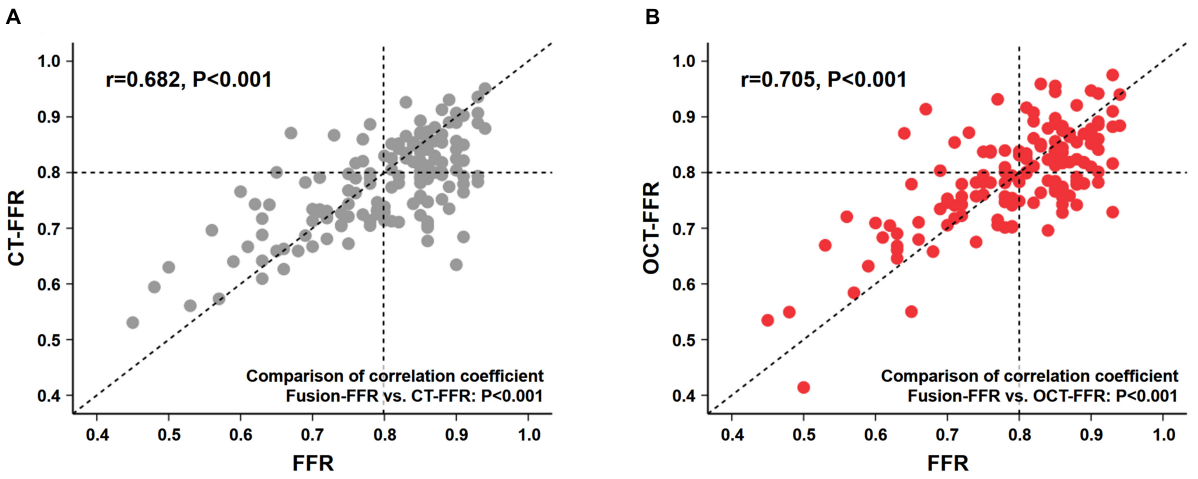

FIGURE 3 | Correlation between pressure wire-based FFR and CFD-based computational FFR from coronary CTA or OCT images. Correlation between pressure wire-based FFR and CT-FFR **(A)**, and between FFR and OCT-FFR **(B)**. CFD, computational fluid dynamics; CTA, computed tomography angiography; CT-FFR, computational FFR from coronary CTA; FFR, fractional flow reserve; OCT, optical coherence tomography; OCT-FFR, computational FFR from OCT.

$P < 0.001$; 64.0%, $P < 0.001$) and OCT-FFR (75.7%, $P = 0.021$; 73.5%, $P = 0.020$; 69.9%, $P = 0.012$). The diagnostic performance was not different between CT-FFR and OCT-FFR, except for specificity which was superior for OCT-FFR ($P = 0.041$).

DISCUSSION

Main Findings

This study presented a novel approach for estimating CFD-based computational FFR in patients with intermediate stenosis in the LAD, which was derived from coronary CTA-OCT fusion images. The main findings were as follows: (1) Fusion-FFR was strongly correlated with pressure wire-based FFR; although CT-FFR and OCT-FFR were also well correlated with FFR, Fusion-FFR was more strongly correlated; (2) area under the ROC curve in assessing functionally significant stenosis was higher for Fusion-FFR than for CT-FFR and OCT-FFR; and (3) the diagnostic performance, especially accuracy, specificity, and positive predictive value of Fusion-FFR were superior to those of CT-FFR and OCT-FFR.

Clinical Implications of Computational Fractional Flow Reserve From Fusion Images

Deciding whether to proceed with coronary revascularization is difficult, and simple angiographic assessment of luminal narrowing has led to a misdiagnosis rate as high as 40% (1, 2, 25). Therefore, functional assessment of coronary stenosis by FFR measurement is important to make appropriate decisions regarding coronary revascularization, especially in patients with intermediate stenosis (1–7). Although coronary CTA and OCT were originally developed for anatomical evaluation of coronary vessels and plaques, recent techniques have applied CFD to estimate computational FFR from three-dimensional coronary models derived from these images and demonstrated favorable results (11–14). In addition, current advances in image reconstruction techniques have also enabled more precise

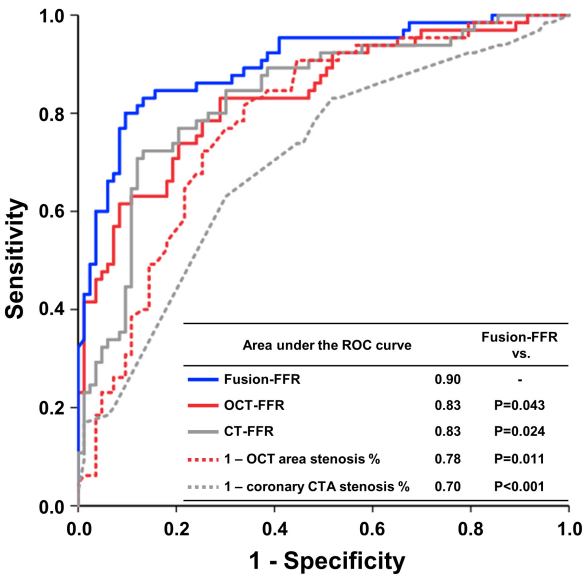

FIGURE 4 | Receiver operating characteristics curves in assessing functionally significant stenosis for CFD-based computational FFRs and anatomic variables. Receiver operating characteristics (ROC) curves with area under the curve to assess functionally significant stenosis for Fusion-FFR, OCT-FFR, CT-FFR, percentage area stenosis on OCT, and percentage coronary CTA stenosis. CFD, computational fluid dynamics; CTA, computed tomography angiography; CT-FFR, computational FFR from coronary CTA; FFR, fractional flow reserve; Fusion-FFR, computational FFR from coronary CTA-OCT fusion images; OCT, optical coherence tomography; OCT-FFR, computational FFR from OCT.

TABLE 3 | Diagnostic performance of CFD-based computational FFRs in assessing functionally significant stenosis.

	Fusion-FFR	CT-FFR	OCT-FFR	*p*-value	
				Fusion-FFR vs. CT-FFR	Fusion-FFR vs. OCT-FFR
Accuracy	84.5 (77.0–89.9)	73.0 (65.2–78.3)	75.7 (67.5–82.3)	0.007	0.021
Sensitivity	84.6 (75.8–93.4)	87.7 (78.9–93.8)	78.5 (68.5–88.5)	0.527	0.248
Specificity	84.3 (76.5–92.2)	61.4 (54.6–66.2)	73.5 (64.0–83.0)	<0.001	0.020
Positive predictive value	80.9 (71.5–90.2)	64.0 (57.6–68.5)	69.9 (59.3–80.4)	<0.001	0.012
Negative predictive value	87.5 (80.3–94.7)	86.4 (76.7–93.2)	81.3 (72.5–90.2)	0.799	0.120

Values are presented as % (95% confidence interval).
CFD, computational fluid dynamics; CTA, computed tomography angiography; CT-FFR, computational FFR from coronary CTA; FFR, fractional flow reserve; Fusion-FFR, computational FFR from coronary CTA-OCT fusion images; OCT, optical coherence tomography; OCT-FFR, computational FFR from OCT.

three-dimensional model reconstruction *via* the fusion of images from different imaging tools (26). Coronary CTA allows detailed visualization of vessel curvature but has the disadvantage of low resolution; in contrast, OCT produces exceptionally high-resolution images but does not allow sufficient visualization of vessel curvature (8–10). Therefore, fusing images from both methods is expected to provide more reliable information about the coronary stenotic lesions by combining detailed vessel curvature data from coronary CTA with accurate lumen contour data from OCT. Since the excellent resolution of OCT is widely known, we estimated several CFD-based flow characteristics to support our hypothesis regarding the contribution of vessel curvature of coronary CTA toward fusion images (10, 13). Coronary CTA and fusion images showed higher vorticity, helicity, and wall shear stress than those of OCT with insufficient visualization of vessel curvatures (**Supplementary Figure 3**). To the best of our knowledge, this is the first study to investigate CFD-based computational FFR using coronary CTA-OCT fusion images in patients with intermediate stenosis, and our technique has shown promising results. Fusion-FFR was strongly correlated with pressure wire-based FFR, had a high area under the ROC curve in assessing functionally significant stenosis, and exhibited good diagnostic performance.

Fusion-Fractional Flow Reserve vs. Coherence Tomography-Fractional Flow Reserve and Optical Coherence Tomography-Fractional Flow Reserve

According to the DISCOVER-FLOW (Diagnosis of Ischemia-Causing Stenoses Obtained *Via* Non-invasive Fractional Flow Reserve) study, CT-FFR and pressure wire-based FFR were well correlated (r = 0.717, $P < 0.001$), and the area under the ROC curve for detecting ischemia was higher for CT-FFR than for coronary CTA stenosis (0.90 vs. 0.75, P = 0.001) (11). Superior diagnostic performance of CT-FFR vs. coronary CTA stenosis was also reported in the NXT (Analysis of Coronary Blood Flow Using CT Angiography: Next Steps) trial with a higher area under the ROC curve for detecting ischemia (0.90 vs. 0.81, $P < 0.001$) (12). However, use of CT-FFR is limited by the low resolution of coronary CTA images (13, 27). In contrast, OCT provides high-resolution images, thereby supplying more precise information regarding coronary arteries and atherosclerotic plaques (10). In their first study estimating OCT-FFR using CFD, Ha et al. found that OCT-FFR and pressure wire-based FFR were well correlated (r = 0.72, $P < 0.001$), and the area under the ROC curve for detecting ischemia was high (0.93) (13). Similarly, Yu et al. also reported that OCT-FFR and pressure wire-based FFR were well correlated (r = 0.70, $P < 0.001$), and the area under the ROC curve for detecting ischemia was higher for OCT-FFR than for area stenosis on OCT (0.93 vs. 0.80, P = 0.002) (14).

Although previous approaches for estimating computational FFR from coronary CTA or OCT were innovative, they used only a single tool. Currently, OCT is widely used to visualize the microstructures of coronary stenotic lesions and plaques, and many patients undergo coronary CTA to assess suspected coronary artery disease before being referred for angiography (9, 10, 15). Thus, we hypothesized that if we encounter intermediate stenosis during angiography, which needs further anatomical or functional assessment, OCT can provide not only precise anatomical information based on high resolutions but also functional information based on CFD (OCT-FFR) without using additional guide wires or hyperemic agents. In addition, if the patients have already undergone coronary CTA for evaluation of chest pain before angiography, we might be able to fuse the coronary CTA and OCT images to obtain more reliable, functional information regarding coronary stenosis (Fusion-FFR). In this study, although computational FFR estimated from the single modality of coronary CTA or OCT was well correlated with FFR, Fusion-FFR showed a stronger correlation with FFR and exhibited a significantly higher area under the ROC curve in assessing functionally significant stenosis. Likewise, the diagnostic performance, especially accuracy, specificity, and positive predictive value of Fusion-FFR, were superior to those of CT-FFR and OCT-FFR. Our findings regarding the benefits of fusing images from different imaging tools are reflective of improved lumen size determination and hemodynamic assessment using a three-dimensional fusion model of three-dimensional QCA and OCT, compared with three-dimensional QCA alone (26). Thus, our findings suggest that computational FFR from fusion images of two different imaging tools, coronary CTA and OCT, may be more valuable than computational FFR based on a single tool in the setting of intermediate coronary stenosis, especially for excluding functionally non-significant stenosis and consequently for reducing unnecessary revascularization procedures.

Further Applications of Coronary Optical Coherence Tomography—Optical Coherence Tomography Fusion Images

To overcome the limitations of CFD, previous studies have demonstrated the possibility of on-site application of CT-FFR based on machine learning with the advantage of high processing speed. However, its performance was limited by the image quality or calcium burden (28, 29). In this regard, in patients with both coronary CTA and OCT images, machine learning may be applied to coronary CTA-OCT fusion images, which contain data not only from coronary CTA but also from OCT with high-resolution images, to overcome the limitations of machine learning-based CT-FFR and enhance the on-site application of Fusion-FFR technique in real-world clinical practice. In addition, recent studies have shown that machine learning algorithms can accurately detect anatomical features on OCT, such as thin-cap fibroatheroma, as well as identify relevant anatomical features on coronary CTA, which are associated with present and future ischemic events (30, 31). Efficiency and cost savings are improved in clinical practice by making full use of available diagnostic modalities. Thus, future studies based on machine learning to explore the effect of anatomical and functional information from coronary CTA-OCT fusion images to identify current myocardial ischemia and predict future cardiovascular events are expected.

Study Limitations

This study has some limitations. First, as a retrospective analysis of a prospectively enrolled registry, it has the inherent limitations of the current study design. Furthermore, although statistical significance was found for superior diagnostic performance of Fusion-FFR vs. CT-FFR and OCT-FFR, the study population was relatively small. Second, we assessed FFR alone in LAD lesions to reduce possible confounding factors. Besides, we chose this artery due to its clinical importance, and the correlation between anatomical and functional indices is better for the LAD than for other coronary arteries (13, 32). Third, we removed the side branches while reconstructing the three-dimensional coronary model to simplify the process for CFD. Although this study focused on combining detailed vessel curvature from coronary CTA with accurate lumen contour from OCT and demonstrated promising results, the effects of side branches on computational FFR require further investigation. Fourth, in total, 14 patients (7.8%) were excluded due to poor quality of coronary images or incomplete OCT coverage. Fifth, the cut-off value $\leq$ 0.80 was used not only for pressure wire-based FFR but also computational FFRs in non-hyperemic condition to define functionally significant stenosis. Sixth, microvascular resistance was not assessed in this study, therefore, the effect of microvascular dysfunction on functional assessment of coronary stenosis could not be evaluated. Nevertheless, the current study results are innovative and warrant further larger population-based prospective studies, including all coronary vessels and side branches, to assess the real-world clinical applicability of the Fusion-FFR technique in patients with both coronary CTA and OCT images. In addition, machine learning may be applied to coronary CTA-OCT fusion images to enhance the on-site application of Fusion-FFR technique during the angiographic procedure.

CONCLUSION

A novel approach of estimating computational FFR from coronary CTA-OCT fusion images provided more accurate functional information than FFR computed from coronary CTA or OCT alone.

DATA AVAILABILITY STATEMENT

The original contributions presented in this study are included in the article/**Supplementary Material**, further inquiries can be directed to the corresponding authors.

ETHICS STATEMENT

The studies involving human participants were reviewed and approved by the Institutional Review Board of Severance Cardiovascular Hospital, Keimyung University Dongsan Hospital, Yeungnam University Medical Center, and National Health Insurance Service Ilsan Hospital. The patients/participants provided their written informed consent to participate in this study.

AUTHOR CONTRIBUTIONS

Y-JL, YK, and JH did the data analyses and wrote the original draft. All authors interpreted the results, contributed to the critical revising of the manuscript, and approved the final version of the manuscript for submission.

FUNDING

This work was supported by the Technology Innovation Program (20010978: Development of the drug eluting bioresorbable coronary vascular stent having 100μm thick struts) funded by the Ministry of Trade, Industry and Energy (Sejong-city, South Korea), the Bio and Medical Technology Development Program (2017M3A9E9073370 and 2017M3A9E9073585) of the National Research Foundation funded by the Ministry of Science and ICT (Sejong City, South Korea), the Cardiovascular Research Center (Seoul, South Korea), and funded by research grants from Chong Kun Dang (Seoul, South Korea).

SUPPLEMENTARY MATERIAL

The Supplementary Material for this article can be found online at: https://www.frontiersin.org/articles/10.3389/fcvm.2022.925414/full#supplementary-material

REFERENCES

1. Pijls NH, De Bruyne B, Peels K, Van Der Voort PH, Bonnier HJ, Bartunek JKJJ, et al. Measurement of fractional flow reserve to assess the functional severity of coronary-artery stenoses. *N Engl J Med.* (1996) 334:1703–8. doi: 10.1056/nejm199606273342604
2. Kern MJ, Samady H. Current concepts of integrated coronary physiology in the catheterization laboratory. *J Am Coll Cardiol.* (2010) 55:173–85. doi: 10.1016/j.jacc.2009.06.062
3. Fihn SD, Gardin JM, Abrams J, Berra K, Blankenship JC, Dallas AP, et al. 2012 ACCF/AHA/ACP/AATS/PCNA/SCAI/STS guideline for the diagnosis and management of patients with stable ischemic heart disease: a report of the American College of Cardiology Foundation/American Heart Association task force on practice guidelines, and the American College of Physicians, American Association for Thoracic Surgery, Preventive Cardiovascular Nurses Association, Society for Cardiovascular Angiography and Interventions, and Society of Thoracic Surgeons. *Circulation.* (2012) 126:e354–471. doi: 10.1161/CIR.0b013e318277d6a0
4. Neumann FJ, Sousa-Uva M, Ahlsson A, Alfonso F, Banning AP, Benedetto U, et al. 2018 ESC/EACTS Guidelines on myocardial revascularization. *Eur Heart J.* (2019) 40:87–165. doi: 10.1093/eurheartj/ehy394
5. Knuuti J, Wijns W, Saraste A, Capodanno D, Barbato E, Funck-Brentano C, et al. 2019 ESC Guidelines for the diagnosis and management of chronic coronary syndromes. *Eur Heart J.* (2020) 41:407–77. doi: 10.1093/eurheartj/ehz425
6. Pijls NH, van Schaardenburgh P, Manoharan G, Boersma E, Bech JW, van't Veer M, et al. Percutaneous coronary intervention of functionally nonsignificant stenosis: 5-year follow-up of the DEFER Study. *J Am Coll Cardiol.* (2007) 49:2105–11. doi: 10.1016/j.jacc.2007.01.087
7. Tonino PA, De Bruyne B, Pijls NH, Siebert U, Ikeno F, van' t Veer M, et al. Fractional flow reserve versus angiography for guiding percutaneous coronary intervention. *N Engl J Med.* (2009) 360:213–24. doi: 10.1056/NEJMoa0807611
8. Min JK, Shaw LJ, Berman DS. The present state of coronary computed tomography angiography a process in evolution. *J Am Coll Cardiol.* (2010) 55:957–65. doi: 10.1016/j.jacc.2009.08.087
9. Mintz GS. Clinical utility of intravascular imaging and physiology in coronary artery disease. *J Am Coll Cardiol.* (2014) 64:207–22. doi: 10.1016/j.jacc.2014.01.015
10. Sinclair H, Bourantas C, Bagnall A, Mintz GS, Kunadian V. OCT for the identification of vulnerable plaque in acute coronary syndrome. *J Am Coll Cardiol Img.* (2015) 8:198–209. doi: 10.1016/j.jcmg.2014.12.005
11. Koo BK, Erglis A, Doh JH, Daniels DV, Jegere S, Kim HS, et al. Diagnosis of ischemia-causing coronary stenoses by noninvasive fractional flow reserve computed from coronary computed tomographic angiograms. Results from the prospective multicenter DISCOVER-FLOW (Diagnosis of Ischemia-Causing Stenoses Obtained Via Noninvasive Fractional Flow Reserve) study. *J Am Coll Cardiol.* (2011) 58:1989–97. doi: 10.1016/j.jacc.2011.06.066
12. Norgaard BL, Leipsic J, Gaur S, Seneviratne S, Ko BS, Ito H, et al. Diagnostic performance of noninvasive fractional flow reserve derived from coronary computed tomography angiography in suspected coronary artery disease: the NXT trial (Analysis of coronary blood flow using CT angiography: next steps). *J Am Coll Cardiol.* (2014) 63:1145–55. doi: 10.1016/j.jacc.2013.11.043
13. Ha J, Kim JS, Lim J, Kim G, Lee S, Lee JS, et al. Assessing computational fractional flow reserve from optical coherence tomography in patients with intermediate coronary stenosis in the left anterior descending artery. *Circ Cardiovasc Interv.* (2016) 9:e003613. doi: 10.1161/circinterventions.116.003613
14. Yu W, Huang J, Jia D, Chen S, Raffel OC, Ding D, et al. Diagnostic accuracy of intracoronary optical coherence tomography-derived fractional flow reserve for assessment of coronary stenosis severity. *EuroIntervention.* (2019) 15:189–97. doi: 10.4244/eij-d-19-00182
15. Yonetsu T, Jang IK. Advances in intravascular imaging: new insights into the vulnerable plaque from imaging studies. *Korean Circ J.* (2018) 48:1–15. doi: 10.4070/kcj.2017.0182
16. Abbara S, Blanke P, Maroules CD, Cheezum M, Choi AD, Han BK, et al. SCCT guidelines for the performance and acquisition of coronary computed tomographic angiography: a report of the society of Cardiovascular Computed Tomography Guidelines Committee: endorsed by the North American Society for Cardiovascular Imaging (NASCI). *J Cardiovasc Comput Tomogr.* (2016) 10:435–49. doi: 10.1016/j.jcct.2016.10.002
17. Leipsic J, Abbara S, Achenbach S, Cury R, Earls JP, Mancini GJ, et al. SCCT guidelines for the interpretation and reporting of coronary CT angiography: a report of the Society of Cardiovascular Computed Tomography Guidelines Committee. *J Cardiovasc Comput Tomogr.* (2014) 8:342–58. doi: 10.1016/j.jcct.2014.07.003
18. Akbar A, Khwaja TS, Javaid A, Kim JS, Ha J. Automated accurate lumen segmentation using L-mode interpolation for three-dimensional intravascular optical coherence tomography. *Biomed Opt Express.* (2019) 10:5325–36. doi: 10.1364/boe.10.005325
19. Kang DY, Ahn JM, Kim YW, Moon JY, Lee JS, Koo BK, et al. Impact of coronary lesion geometry on fractional flow reserve: data from interventional cardiology research in-cooperation society-fractional flow reserve and intravascular ultrasound registry. *Circ Cardiovasc Imaging.* (2018) 11:e007087. doi: 10.1161/circimaging.117.007087
20. Kim YW, Yu H-J, Kim J-S, Ha J, Choi J, Lee JS. Coronary artery decision algorithm trained by two-step machine learning algorithm. *RSC Adv.* (2020) 10:4014–22. doi: 10.1039/C9RA08999C
21. Boyd J, Buick JM, Green S. Analysis of the Casson and Carreau-Yasuda non-Newtonian blood models in steady and oscillatory flows using the lattice Boltzmann method. *Phys Fluids.* (2007) 19:093103. doi: 10.1063/1.2772250
22. Madhavan S, Kemmerling EMC. The effect of inlet and outlet boundary conditions in image-based CFD modeling of aortic flow. *BioMed Eng Online.* (2018) 17:1–20. doi: 10.1186/s12938-018-0497-1
23. Schäfer M, Barker AJ, Kheyfets V, Stenmark KR, Crapo J, Yeager ME, et al. Helicity and vorticity of pulmonary arterial flow in patients with pulmonary hypertension: quantitative analysis of flow formations. *J Am Heart Assoc.* (2017) 6:e007010. doi: 10.1161/jaha.117.007010
24. Gijsen F, Katagiri Y, Barlis P, Bourantas C, Collet C, Coskun U, et al. Expert recommendations on the assessment of wall shear stress in human coronary arteries: existing methodologies, technical considerations, and clinical applications. *Eur Heart J.* (2019) 40:3421–33. doi: 10.1093/eurheartj/ehz551
25. Park SJ, Kang SJ, Ahn JM, Shim EB, Kim YT, Yun SC, et al. Visual-functional mismatch between coronary angiography and fractional flow reserve. *J Am Coll Cardiol Intv.* (2012) 5:1029–36. doi: 10.1016/j.jcin.2012.07.007
26. Kweon J, Kang SJ, Kim YH, Lee JG, Han S, Ha H, et al. Impact of coronary lumen reconstruction on the estimation of endothelial shear stress: in vivo comparison of three-dimensional quantitative coronary angiography and three-dimensional fusion combining optical coherent tomography. *Eur Heart J Cardiovasc Imaging.* (2018) 19:1134–41. doi: 10.1093/ehjci/jex222
27. Taylor CA, Fonte TA, Min JK. Computational fluid dynamics applied to cardiac computed tomography for noninvasive quantification of fractional flow reserve: scientific basis. *J Am Coll Cardiol.* (2013) 61:2233–41. doi: 10.1016/j.jacc.2012.11.083
28. Coenen A, Kim YH, Kruk M, Tesche C, De Geer J, Kurata A, et al. Diagnostic accuracy of a machine-learning approach to coronary computed tomographic angiography-based fractional flow reserve: result from the MACHINE consortium. *Circ Cardiovasc Imaging.* (2018) 11:e007217. doi: 10.1161/circimaging.117.007217
29. Tesche C, Otani K, De Cecco CN, Coenen A, De Geer J, Kruk M, et al. Influence of coronary calcium on diagnostic performance of machine learning CT-FFR: results from MACHINE registry. *J Am Coll Cardiol Img.* (2020) 13:760–70. doi: 10.1016/j.jcmg.2019.06.027
30. Min HS, Yoo JH, Kang SJ, Lee JG, Cho H, Lee PH, et al. Detection of optical coherence tomography-defined thin-cap fibroatheroma in the coronary artery using deep learning. *EuroIntervention.* (2020) 16:404–12. doi: 10.4244/eij-d-1x00487
31. Yang S, Koo BK, Hoshino M, Lee JM, Murai T, Park J, et al. CT Angiographic and plaque predictors of functionally significant coronary disease and

outcome using machine learning. *J Am Coll Cardiol Img.* (2020) 14:629–41. doi: 10.1016/j.jcmg.2020.08.025

32. Kang SJ, Lee JY, Ahn JM, Mintz GS, Kim WJ, Park DW, et al. Validation of intravascular ultrasound-derived parameters with fractional flow reserve for assessment of coronary stenosis severity. *Circ Cardiovasc Interv.* (2011) 4:65–71. doi: 10.1161/circinterventions.110.959148

Conflict of Interest: GG was a consultant in St. Jude Medical and has received institutional research grants.

The remaining authors declare that the research was conducted in the absence of any commercial or financial relationships that could be construed as a potential conflict of interest.

Publisher's Note: All claims expressed in this article are solely those of the authors and do not necessarily represent those of their affiliated organizations, or those of the publisher, the editors and the reviewers. Any product that may be evaluated in this article, or claim that may be made by its manufacturer, is not guaranteed or endorsed by the publisher.

frontiers | Frontiers in Cardiovascular Medicine

TYPE Review
PUBLISHED 29 July 2022
DOI 10.3389/fcvm.2022.916616

OPEN ACCESS

EDITED BY
Tommaso Gori,
Johannes Gutenberg University
Mainz, Germany

REVIEWED BY
Christoph Gräni,
Universitätsspital Bern, Switzerland
Silvana Molossi,
Baylor College of Medicine,
United States

*CORRESPONDENCE
Nino Cocco
ninococco@gmail.com

SPECIALTY SECTION
This article was submitted to
Coronary Artery Disease,
a section of the journal
Frontiers in Cardiovascular Medicine

RECEIVED 09 April 2022
ACCEPTED 01 June 2022
PUBLISHED 29 July 2022

CITATION
Cocco N, Madonna R, Cammalleri V, Cocco G, De Stefano D, Ricciardi D, Grigioni F and Ussia GP (2022) Percutaneous treatment of a CTO in an anomalous right coronary artery: A rupture paved the way for new insights.
Front. Cardiovasc. Med. 9:916616.
doi: 10.3389/fcvm.2022.916616

Percutaneous treatment of a CTO in an anomalous right coronary artery: A rupture paved the way for new insights

Nino Cocco[1]*, Rosalinda Madonna[2], Valeria Cammalleri[1], Giulio Cocco[3], Domenico De Stefano[1], Danilo Ricciardi[1], Francesco Grigioni[1] and Gian Paolo Ussia[1]

[1]Department of Cardiovascular Sciences, Campus Bio-Medico University of Rome, Rome, Italy, [2]Cardiology Division, Department of Surgical, Medical, Molecular Pathology and Critical Care, University of Pisa, Azienda Ospedaliero Universitaria Pisana Ospedale di Cisanello, Pisa, Italy, [3]Unit of Ultrasound in Internal Medicine, Department of Medicine and Aging Sciences, University of Chieti G D'Annunzio, Chieti, Italy

An anomalous aortic origin of a coronary artery (AAOCA) from the opposite sinus, with an interarterial course, has been associated with an increased risk of myocardial ischemia and sudden death. As the exact pathophysiology of AAOCA is not well understood, the clinical management is also not well defined. With increased use of non-invasive imaging, the diagnosis of AAOCA is increasing and the association of anomalous origin and atherosclerotic disease is becoming a more important topic. We report a rare case of AAOCA chronic total occlusion (CTO). A 40-year-old Caucasian man was referred for invasive coronary angiography (ICA) due to typical chest pain and positive myocardial scintigraphy. ICA demonstrated CTO of an anomalous right coronary artery (ARCA) originating from the left side of the ascending aorta with an interarterial course. There was no lesion in the left coronary artery. During the procedure, unexpected rupture of the coronary artery occurred after dilatation with a small balloon at low pressure. The complication in this case was handled with good procedural final result but was an occasion for a food for thought. Coronary artery perforations are rare but life-threatening procedural complications that are usually caused by predisposing anatomical and procedural factors. We issue a warning on the risk of complications during complex percutaneous coronary intervention of these arteries, and we reconsidered the pathophysiology of the anomaly in a way that could change the approach to the disease. Based on this complication, we hypothesized that the wall of the artery could be fragile due to histopathological alterations, which could have a role in the pathophysiology of coronary malignancy. Future autopsy studies should be focused on the analysis of the arterial wall of the patient affected by sudden death with this anomaly.

KEYWORDS

anomalous right coronary artery, sudden death, anomalous aortic origin of a coronary artery, chronic total occlusion, percutaneous coronary intervention, PCI complication

Introduction

An anomalous aortic origin of a coronary artery (AAOCA) from the opposite sinus, with an interarterial course between the pulmonary artery and aorta, has been associated with an increased risk of myocardial ischemia and sudden cardiac death (SCD) (1–4). The degree of risk (5, 6) and the pathophysiology of myocardial ischemia (7, 8) are debatable. Guidelines are limited and recommendations are mainly based on expert opinions (9, 10). Moreover, with increased use of non-invasive imaging to evaluate coronary artery disease, an increase in the absolute numbers of AAOCA is expected, with a concomitant increase in the prevalence of coronary artery disease. The management of patients affected by anomalous origin and atherosclerotic disease is becoming a more important topic in the field of coronary artery disease (11). We report a rare case of an anomalous right coronary artery (ARCA) originating from the left side of the ascending aorta with symptomatic chronic total occlusion (CTO). An unexpected complication led us to reconsider the pathophysiological basis of ARCA and to suspect histological involvement of the arterial wall.

The goals of this paper are three-fold: (1) to attempt an estimation of SCD specific for right AAOCA (ARCA) based on extrapolations of incidence numbers of SCD in the population and report the prevalence of right AAOCA, (2) to review the presumed pathophysiology of SCD in ARCA and present new insights, and (3) to issue a warning on the risk of complications during percutaneous coronary intervention (PCI) for ARCA CTO.

Case description

A 40-year-old Caucasian man, without any remarkable risk factors, was hospitalized for investigation and treatment of a several-month-history of class II angina. Myocardial scintigraphy, three weeks prior, showed moderate reversible perfusion defects involving the inferoposterior wall area. The patient was previously healthy and participated in non-competitive soccer. A 12-lead electrocardiogram and baseline echocardiography showed no abnormal wall motion and well-functioning valves. A baseline angiogram was performed from the right radial artery. The left coronary artery, originating from the left sinus, did not exhibit significant stenosis. There was Rentrop III collaterality towards the right coronary artery (RCA). The RCA, originating high and anteriorly over the left sinus, showed CTO in the middle tract (Figure 1). A Jr4 guide-catheter was chosen and a 1,5 × 8 mm anchoring balloon was placed in the conus artery. The occlusion was smoothly crossed with a tapered polymeric guidewire supported by a 1.8 Fr microcatheter. The attempt to bring the microcatheter beyond the occlusion failed because of the friction encountered, so we performed a predilatation with 1.5 × 12 mm compliant balloon. Good anterograde flow was restored (Figure 2). A second dilatation with a 2 × 15 mm balloon at 10 atm was performed to better prepare the lesion. A few seconds after this dilatation, the patient experienced chest pain. Angiography revealed a type II Ellis perforation in the midline and an extensive type D dissection distally to the ostium (Figure 3; Supplementary Video 1). A 3 × 26 mm zotarolimus eluting stent was implanted with long inflation (5 min). After deployment, the effusion disappeared. Four additional stents were implanted to cover

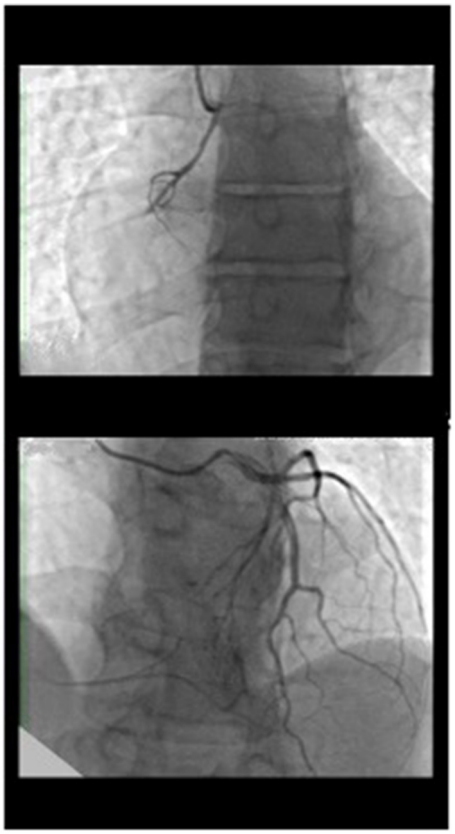

FIGURE 1
Coronary angiography of the left system showed left coronary artery normally positioned without atherosclerotic disease with rentrop III heterocoronary collateral circulation toward the right coronary artery, which has an anomalous origin on the left side of the ascending aorta and chronic occlusion in the proximal atrioventricular tract.

Abbreviations: AAOCA, Anomalous aortic origin of a coronary artery; ALCA, Anomalous left coronary artery; ARCA, Anomalous right coronary artery; CTO, Chronic total occlusion; ICA, Invasive coronary angiography; PCI, Percutaneous coronary intervention; RCA, Right coronary artery; SD, Sudden death; SCD, Sudden cardiac death.

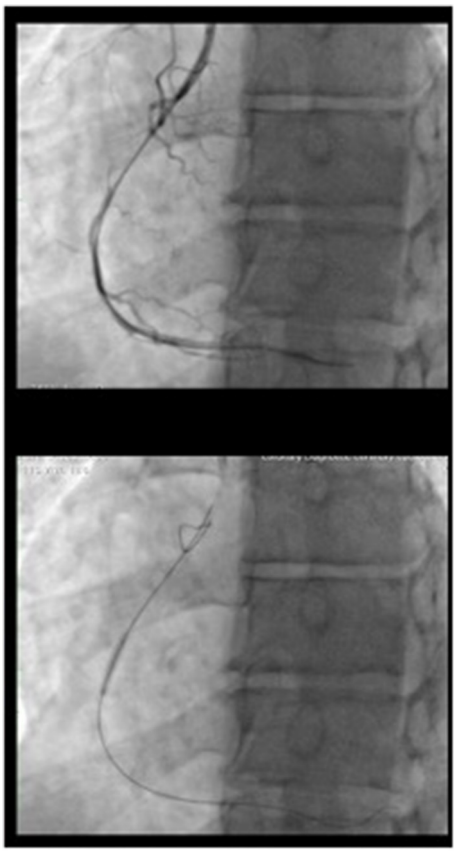

FIGURE 2
CTO treatment procedure: The occlusion was crossed with a tapered polymeric guidewire supported by microcatheter. The flow was restored after a dilatation of the occlusion with 1.5 x 12 balloon. Than a dilatation with a 2 x 15 balloon at 10 atm was performed.

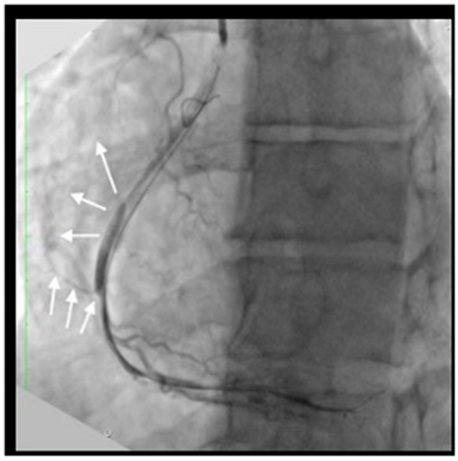

FIGURE 3
Procedural complication: The angiography after CTO dilatation with compliant 2 x 15 mm balloon at 10 atm showed coronary Ellis II perforation (white arrow) and diffuse type D dissection.

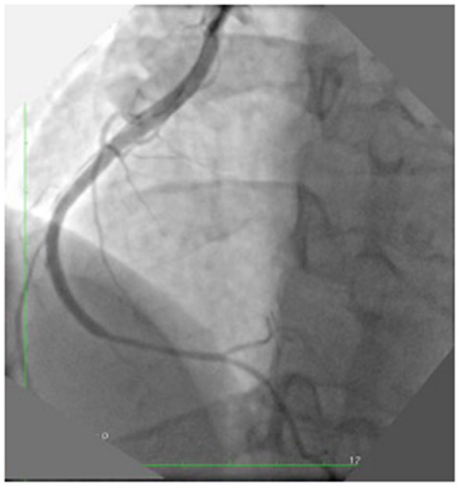

FIGURE 4
Post PCI final result: A first stent was implanted in the ruptured tract with long inflation (5 min). After the deployment the effusion disappeared. Four additional stents were implanted to cover the dissection. The final angiography showed a good result.

the dissection. The final angiography showed a good result (Figure 4; Supplementary Video 2). Echocardiography showed negligible pericardial effusion. The patient was clinically stable and asymptomatic. Troponin levels remained stable on two occasions. A coronary computed tomography scan (CTA) confirmed the anomalous antero-left high origin of the RCA 17 mm from the sinotubular junction, and showed the angled ostium and interarterial course, about 2 cm between the aorta and pulmonary trunk (Figure 5), with modest effusion (10 mm) on CTA.

Discussion

Prevalence of ARCA and risk of sudden death

Coronary artery anomalies have been reported as the second most frequent cause of SCD in young athletes, accounting for 12% of deaths (12, 13). Coronary artery anomalies arising from the pulmonary artery or the wrong sinus with an interarterial course between the pulmonary artery and aorta, referred to as AAOCA, are more often related to sudden death (SD) (14, 15). The most common subtype is an ARCA arising from the left side (prevalence 0.23%), followed by an anomalous left coronary artery (ALCA) arising from the right side (prevalence 0.03%) (1, 16). ALCA from the pulmonary artery is extremely rare (11, 15). Although evidence demonstrates that interarterial ALCA and ARCA are associated

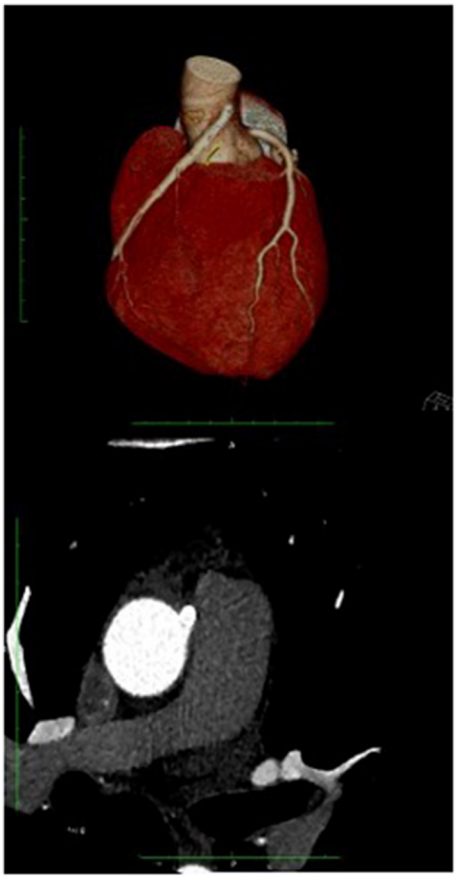

FIGURE 5
Coronary TC: The coronary TC confirmed the anomalous origin from opposite site of ascending aorta 17 mm from the sinotubular junction, with interarterial course. Modest effusion (10 mm).

with an increased risk of SCD, their absolute risk in the general population is unknown. Thus, controversy remains regarding the optimal approach to risk stratify and manage these patients. With increased use of non-invasive imaging, the prevalence is increasing (1, 16) and could become a serious public health hazard.

The first data on the rates of SCD in AAOCA came almost exclusively from autopsy series, which reported high, yet discrepant, mortality rates between studies (0-50% for ARCA and 30-100% for ALCA) (1, 4, 12). In the first series, 50% of SD cases had anomalous coronary arteries (30% right and 80% left) (1, 4, 12). From this data, the estimated risk of SCD in AAOCA was very high (50% for ALCA and 25% for ARCA) (17, 18) and many authors agreed that surgical correction should have been the first line of therapy in these patients (19–22). However, this autopsy statistic report has been proven wrong. It reported on the chance of a person who dies suddenly having an anomalous coronary artery, not the risk of SD from an anomalous coronary artery, only reflecting the prevalence of AAOCA in those who died. Subsequent studies indicated that the risk of SD was far lower, but discrepancy in the data remains. The rate of death from AAOCA has been reported as being between 0.07 and 0.61 per 100,000 person years (5, 12, 16, 20, 22). From this data, it was determined that the cumulative risk of death over a 20-year period from the age of 15–34 years in patients with AAOCA was 6.3% for ALCA and 0.2% for ARCA (23). Assuming the prevalence of AAOCA is 0.1-0.2% (24–27), the risk of death for AAOCA is 0.12–0.15% (1:860–1:652), involving above all young people engaged in frequent vigorous exercise and patients with ALCA (5, 28). A more recent review of a database of 5,100 cases of SCD referred to a specialist cardiac pathology center between January 1994 and March 2017, and identified a subgroup of 30 cases (0.6%) with AAOCA (15). The number of SCD from ARCA and ALCA were compared, and, although ALCA is considered more malignant, the SCD numbers for ARCA were slightly higher (11 patients, 37% vs. 10 patients 37%, respectively). ALCA from the pulmonary artery occurred in seven cases (23%). Exercise-induced SCD was associated more frequently with ALCA than ARCA, where death occurred often at rest or during sleep. The mean age was much higher, compared to previous studies (28+/−17 years); there were patients in the fifth and sixth decades of life, most with ARCA.

The risk of SCD in patients with AAOCA are inconclusive due to the conflicting results. We believe this discrepancy could have stemmed from the fact that ARCA and ALCA have different clinical features and the identification of a unique risk of AAOCA (29) could have been the original reason for the conflicting results in the literature. SCD was more likely to occur in ALCA than ARCA; in fact, SCD in young, trained patients are mainly caused by ALCA. But, when we consider the populations of each age group, the number of SCD cases were equivalent or even greater for ARCA (15), since ARCA was more prevalent (0.23 vs. 0.03%) (6, 11, 30). In patients of older age, death often occurs at rest or during sleep (15). Thus, ARCA is not a minor disease but a different disease, most likely with a different pathophysiological pathway as well. The risk of SD in a patient with ARCA has not been properly analyzed. We attempted to estimate the risk of SD based on the data from previous studies.

The age-adjusted national incidence of SCD is 60 per 100,000 (95% confidence interval; 54–66 per 100,000) (31, 32) and 0.6% thereof are caused by AAOCA (15), translating to an incidence of 3,6 per 1,000,000 per year. ARCA are found in 36% of SCD caused by AAOCA (15), translating to an incidence of 1,3 per 1,000,000 per year. Since the prevalence of ARCA is 0.23%, we can derive that 1,3 per 2300 persons a year with ARCA experience SCD. Therefore, the incidence of SD in a patient with ARCA is about 1:1800. This is the first attempt to estimate the incidence of SCD in a patient specifically affected by ARCA.

TABLE 1 ARCA CTO procedures reported in the literature.

Cases	Age/sex	Technique used	Origin of the RCA	Site of occlusion	Complications
Kaneda et al. (45)	66 y/M	Antegrade	Left sinus	Proximal atrioventricular tract	None
Fang et al. (47)	74 y/M	Antegrade	High anterior	Proximal atrioventricular tract	Cusp dissection
Abdou and Wu (27)	58 y/M	Antegrade	Left sinus	Proximal atrioventricular tract	Aorto-coronary dissection
Porwal et al. (44)	71 y/F	Antegrade	Left sinus	Proximal atrioventricular tract	None
Senguttuvan et al. (43)	49 y/M	Antegrade	Left sinus	Proximal atrioventricular tract	None
Gasparini et al. (46)	65 y/M	Retrograde	Left sinus	Proximal atrioventricular tract	None
Yamada et al. (42)	43 y/M	Retrograde	Left sinus	Ostial	None
Young et al. (48)	68 y/M	Antegrade	Left sinus	Proximal atrioventricular tract	None
Patra et al. (26)	58 y/M	Antegrade	Left sinus	Proximal atrioventricular tract	None
Our case	40 y/M	Antegrade	High anterior left aorta	Proximal atrioventricular tract	Dissection and perforation

Anomalous origin of a coronary artery from the opposite sinus pathophysiology: The enigma of the true denominator

Assuming the pathophysiological understanding of the disease is key to predict the risk of SCD in AAOCA; several studies have attempted to isolate a key primary factor, but no single anatomical component of the coronary artery has been isolated. Several studies have been done to find a true "denominator" causing ischemia and SCD. Several putative mechanisms have been proposed to account for the association between SCD and an anomalous origin of a coronary artery from the opposite sinus. The downstream event is presumed to be ischemia (8, 33–37). Historically, the interarterial course was thought to be the crucial abnormality, assuming a scissor-like mechanism created by the close proximity of the aorta and pulmonary artery, especially during exertion (1, 2, 8). However, the pulmonary artery is unlikely to exert sufficient pressure to occlude a coronary artery in the absence of pulmonary hypertension. Therefore, the interarterial course may act only as a surrogate for other anatomical high-risk features, including a slit-like ostium, acute take off angle, and proximal narrowing (also referred to as hypoplasia) with an elliptical vessel shape and intramural course. The anatomical high-risk feature of a slit-like ostium at the ectopic origin is defined as a $\geq$50% reduction in the minimal lumen diameter compared to the normal distal reference diameter (34). Thus, the deformed coronary ostium with a decreased cross-sectional area acts as an ostial stenosis. Due to the slit-like ostium opening, during exercise and systolic expansion of the aortic root, the orifice can collapse in a valve-like manner (34, 35). An acute take-off angle (less than 45°) is defined as an axial course of the proximal segment tangential to the great vessel circumference. Kinking of an anomalous coronary artery during exercise was proposed as a contributing ischemia-inducing mechanism (8, 34). The intramural course length is considered the most relevant feature in terms of hemodynamic repercussion (6, 35–37). The intramural coronary artery is slit-like and is characterized by thin inner and outer aortic wall layers and lateral luminal compression that undergoes phasic increases with each systole (38). This anatomical feature is considered by many authors as being related to SCD, especially if associated with the other features mentioned above (37). Unfortunately, in clinical practice, none of these have been shown to be useful in the prognostic assessment of SD and there are no prognostically distinguishing pathological features that could be prospectively defined (7–10). Finally, another theory postulates that compression and kinking of the anomalous artery could cause intimal damage and a propensity to spasm and ischemia (39, 40), which was described more than 20 years ago, but considered implausible by the majority (8, 41).

We describe a rare case of anterograde CTO of the RCA with anomalous origin from the opposite side of the ascending aorta. Data regarding complex PCI, especially for CTO, in this setting are very limited (24, 26, 27, 42–48). The procedure was unexpectedly complicated by perforation and extensive type D dissection after predilatation with a small balloon at low pressure. Coronary perforation is a rare, but life-threatening, complication. It is usually due to high pressure balloon dilatation or the use of an oversized balloon in the context of predisposing factors such as tortuosity, calcification, old age, CTO, or small vessel caliber (24). The myocardial bridge is also an important predisposing factor (25). A 2 mm diameter balloon inflated at 10 atm in a 3.5 mm diameter artery causing perforation is almost inexplicable, even in a CTO procedure. The rupture could be explained by structural fragility of the artery. An anomalous course with acute angulation may favor the complication but there could also be a histopathological explanation. In the myocardial bridge, for example, the anomalous course of the artery is associated with intimal and endothelial differences in the tunneled artery that predispose to a greater risk of rupture during PCI. The intimal layer is thinner, and the endothelial

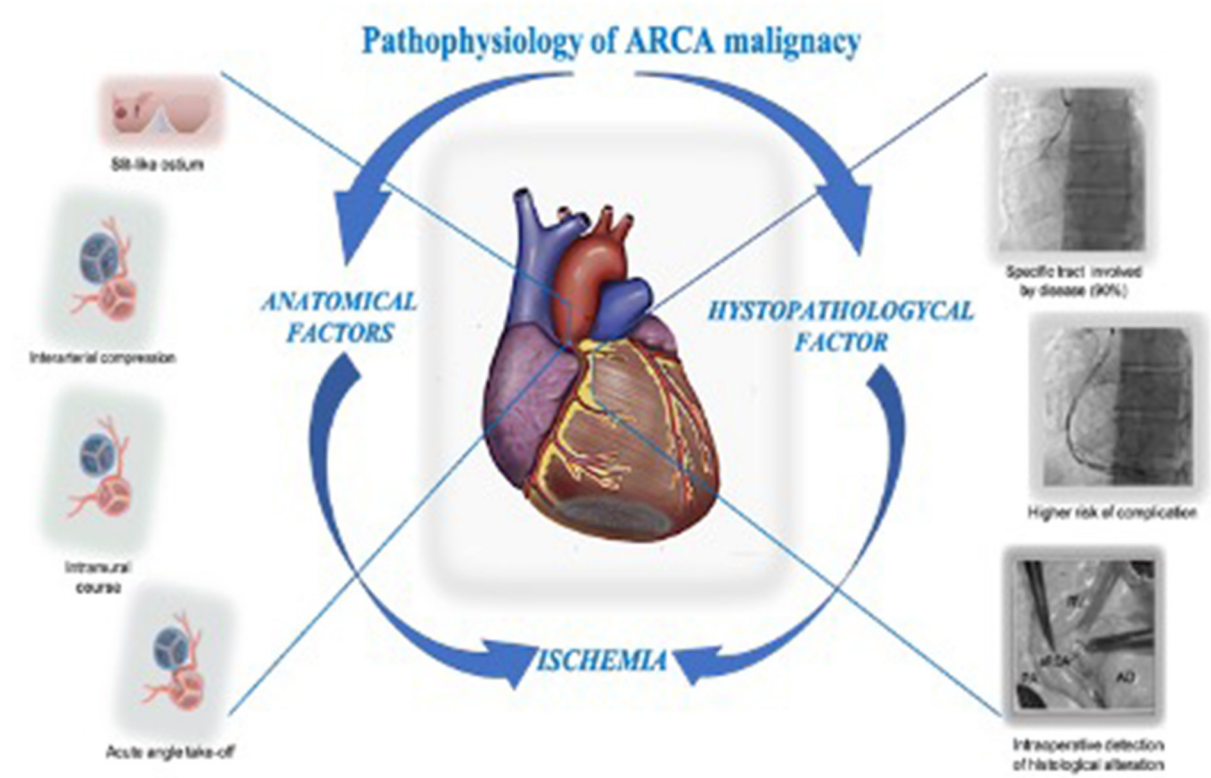

FIGURE 6
ARCA presumed ischemia pathophysiology: The downstream event in the pathophysiology of ARCA malignancy in the contest of SCD is presumed to be ischemic. The anatomical feature like the interarterial passage causing compression in a scissor-like mechanism, the slit-like ostium acting as an ostial stenosis, the acute take-off angle causing kinking, and the intramural course causing compression, are historically considered involved in the pathogenesis of ischemia. Unfortunately, in clinical practice none of these have been shown to be useful in the prognostic assessment of SD. The higher incidence of procedural complications in the context of ARCA CTO treatment, the presence of a specific tract of the artery involved by the disease (90% of the case reported in literature), and the intraoperative detection of histological alteration of the anomalous artery wall in a patient who suffered from a SCA call us to reconsider the histopathological alteration in the pathogenesis of ischemia and ARCA malignancy. ARCA, anomalous right anomalous coronary originating from the left side; CTO, chronic total occlusion; SCD, sudden cardiac death.

cells are spindle shaped. This alteration and compression carry a major risk for perforation (25). Bunji et al. (39) hypothesized that the RCA located between the aorta and the pulmonary artery is prone to compression or kinking phenomena, resulting in intimal disruption and subsequent predisposition to vasospasm that correlates with ischemia and SCD. The histopathological alteration causing wall fragility could also be an explanation for the complication in our case.

PCI in an anomalous coronary artery is difficult, particularly with CTO, due to technical complexities, from engaging the coronary ostium to delivery of hardware through the vessel. Only a few cases have been reported in the literature (24, 26, 27, 42–48) (Table 1).

Nine cases of ARCA CTO have been reported in the literature. Three major complications, two of which were not related to catheter manipulation, were mentioned. A case of aorto-coronary dissection due to balloon dilatation and rupture was described by Abdou and Wu (27). In this case, the type D dissection started from the proximal ARCA and extended retrograde, involving the aorta. Estimation of the risk of complication is not the purpose of this paper, considering the small number of patients, but this trend is unusual. Furthermore, analysis of the cases showed a common tract of occlusion in most cases. Nine out of ten cases involved the proximal atrioventricular part of the artery, in the area between the cone branch and the first branch for the acute margin (27, 42–48). Due to the difference in anatomy of the anomalous artery, we divided it into four segments. We considered the proximal segment to be the tract from the origin to the origin of the conus or sinoatrial branches, the proximal atrioventricular segment the tract from the conus branch to halfway to the acute margin, the middle segment the tract from this halfway point to the acute margin, and a distal segment from the acute margin to the base of the heart at the junction of the atrial and ventricular

septum. Analyzing the non-CTO PCI cases in the literature, we confirmed that the tract of disease in ARCA was almost always the proximal atrioventricular segment. A review of 18 cases with imaging showed that 16 had proximal atrioventricular segment involvement (49–62), five of six had SCA- STEMI (58–62), and 11 of 12 had chronic critical stenosis (49–58). Furthermore, Bruls et al. (63) described a case of resuscitated SD in a 37-year-old man with ARCA in whom they performed coronary artery bypass grafting. After surgical examination of the artery, several initial branches in its first segment (infundibular branch or the sinus nodal artery) and a fibrously thickened wall were noted. These data suggest that histological alteration may play an important role in ARCA malignancy (Figure 6).

There is no greater tragedy in medicine than SD in an apparently healthy person. AAOCA is the second leading cause of SCD in athletes, and with increased use of non-invasive imaging, the prevalence is expected to increase. The interarterial course is believed to be the factor of malignancy in this context and a lot of effort has been made to find a true denominator in understanding the pathophysiological pathway. After almost 50 years, none of the suspected anatomical factors have been shown to be useful in the prognostic assessment of SD and there are no prognostically distinguishing pathological features that could be prospectively defined. Therefore, the clinical management is still not defined. The strategy of the common pathway causing malignancy has failed, thus, the interarterial course may act only as a surrogate. ARCA and ALCA have very different clinical features. ALCA is rare but more malignant and, among AAOCA patients, causes most SD cases in young patients. ARCA is relatively common and less malignant, but when populations of each age group are evaluated, the number of SCDs it causes are equal, or even greater than ALCA. These patients are older, and deaths often occur at rest. Therefore, ARCA is not a minor disease, but a different disease. Based on this assumption, the pathophysiological basis of malignancy could also be different. In our case, an unexpected complication led to reconsideration of a possible parietal structural involvement in ARCA malignancy. The theory of histological alteration of the arterial wall playing a role in the pathophysiology of ARCA malignancy is plausible based on three observations: (1) the higher incidence of coronary periprocedural major dissection; (2) the evidence of a specific tract of the artery being affected by disease (90% of the cases reported), which may render it particularly prone to stress, torsion, or kinking, and thus more prone to histological alteration; and (3) the intraoperative detection of wall alteration of the anomalous artery that was demonstrated during surgical examination of the first tract of ARCA in a 36-year-old patient.

The istologyical alteration causing spasm and ischemia, suspected by some authors but considered implausible by the community, especially after studies performed with intracoronary acetylcholine, would seem to disprove this hypothesis. We hypothesized that this alteration could involve ARCA in specific segments and that spasm may not be the only factor for ischemia. This alteration could render arteries more prone to compression, kinking, atherosclerosis, or thrombus. We also hypothesized that each patient may have a different involvement and that the few patients with more important histological distortion could be those at most risk. The histological pattern of the anomalous arterial wall was never evaluated.

In conclusion, 50 years since the identification of the relationship between SCD and AAOCA, the risk of SCD in a carrier patient has still not been defined and the pathophysiological causes of the disease are unclear. For the first time in the literature, we issue a warning on the risk of complications during percutaneous treatment of a CTO in an anomalous right coronary artery and we reconsidered the pathophysiological basis of the anomaly in a way that could change the approach to the disease.

Author contributions

All authors listed have made a substantial, direct, and intellectual contribution to the work and approved it for publication.

Conflict of interest

The authors declare that the research was conducted in the absence of any commercial or financial relationships that could be construed as a potential conflict of interest.

Publisher's note

Supplementary material

The Supplementary Material for this article can be found online at: https://www.frontiersin.org/articles/10.3389/fcvm.2022.916616/full#supplementary-material

References

1. Cheitlin MD, De Castro CM, McAllister HA. Sudden death as a complication of anomalous left coronary origin from the anterior sinus of valsalva, A not-so-minor congenital anomaly. *Circulation.* (1974) 50:780–7. doi: 10.1161/01.CIR.50.4.780

2. Roberts WC, Siegel RJ, Zipes DP. Origin of the right coronary artery from the left sinus of valsalva and its functional consequences: analysis of 10 necropsy patients. *Am J Cardiol.* (1982) 49:863–8. doi: 10.1016/0002-9149(82)91970-1

3. Kragel AH, Roberts WC. Anomalous origin of either the right or left main coronary artery from the aorta with subsequent coursing between aorta and pulmonary trunk: analysis of 32 necropsy cases. *Am J Cardiol.* (1988) 62:771–7. doi: 10.1016/0002-9149(88)91220-9

4. Frescura C, Basso C, Thiene G, Corrado D, Pennelli T, Angelini A, et al. Anomalous origin of coronary arteries and risk of sudden death: a study based on autopsy population of congenital heart disease. *Hum Pathol.* (1998) 29:689–95. doi: 10.1016/S0046-8177(98)90277-5

5. Peñalver JM, Mosca RS, Weitz D, Phoon CK. Anomalous aortic origin of coronary arteries from the opposite sinus: a critical appraisal of risk. *BMC Cardiovasc Disord.* (2012) 12:83. doi: 10.1186/1471-2261-12-83

6. Cheezum MK, Liberthson RR, Shah NR, Villines TC, O'Gara PT, Landzberg MJ, et al. Anomalous aortic origin of a coronary artery from the inappropriate sinus of valsalva. *J Am Coll Cardiol.* (2017) 69:1592–608. doi: 10.1016/j.jacc.2017.01.031

7. Taylor AJ, Byers JP, Cheitlin MD, Virmani R. Anomalous right or left coronary artery from the contralateral coronary sinus: "high-risk" abnormalities in the initial coronary artery course and heterogeneous clinical outcomes. *Am Heart J.* (1997) 133:428–35. doi: 10.1016/S0002-8703(97)70184-4

8. Bigler MR, Ashraf A, Seiler C, Praz F, Ueki Y, Windecker S, et al. Hemodynamic relevance of anomalous coronary arteries originating from the opposite sinus of Valsalva-in search of the evidence. *Front CardioVasc Med.* (2020) 7:591326. doi: 10.3389/fcvm.2020.591326

9. Baumgartner H, De Backer J. The ESC clinical practice guidelines for the management of adult Congenital Heart Disease 2020. *Eur Heart J.* (2020) 41:4153–4. doi: 10.1093/eurheartj/ehaa701

10. Stout KK, Daniels CJ, Aboulhosn JA, Bozkurt B, Broberg CS, Colman JM, et al. AHA/ACC Guideline for the Management of Adults With Congenital Heart Disease: Executive Summary: a report of the american college of cardiology/american heart association task force on clinical practice guidelines. *J Am Coll.* (2018). doi: 10.1016/j.jacc.2018.08.1028

11. Cheezum MK, Ghoshhajra B, Bittencourt MS, Hulten EA, Bhatt A, Mousavi N, et al. Anomalous origin of the coronary artery arising from the opposite sinus: prevalence and outcomes in patients undergoing coronary CTA. *Eur Heart J Cardiovasc Imaging.* (2017) 18:224–35. doi: 10.1093/ehjci/jev323

12. Maron BJ, Shirani J, Poliac LC, Mathenge R, Roberts WC, Mueller FO. Sudden death in young competitive athletes. Clinical, demographic, and pathological profiles. *JAMA.* (1996) 276:199–204. doi: 10.1001/jama.1996.03540030033028

13. Maron BJ, Doerer JJ, Haas TS, Tierney DM, Mueller FO. Sudden deaths in young competitive athletes: analysis of 1866 deaths in the United States, 1980–2006. *Circulation.* (2009) 119:1085–92. doi: 10.1161/CIRCULATIONAHA.108.804617

14. Hill SF, Sheppard MN, A. silent cause of sudden cardiac death especially in sport: congenital coronary artery anomalies. *Br J Sports Med.* (2014) 48:1151–6. doi: 10.1136/bjsports-2013-092195

15. Finocchiaro G, Behr ER, Tanzarella G, Papadakis M, Malhotra A, Dhutia H, et al. Anomalous coronary artery origin and sudden cardiac death: clinical and pathological insights from a national pathology registry. *JACC Clin Electrophysiol.* (2019) 5:516–22. doi: 10.1016/j.jacep.2018.11.015

16. Corrado D, Basso C, Pavei A, Michieli P, Schiavon M, Thiene G. Trends in sudden cardiovascular death in young competitive athletes after implementation of a preparticipation screening program. *JAMA.* (2006) 296:1593–601. doi: 10.1001/jama.296.13.1593

17. Liberthson RR, Dinsmore RE, Fallon JT. Aberrant coronary artery origin from the aorta. Report of 18 patients, review of literature and delineation of natural history and management. *Circulation.* (1979) 59:748–54. doi: 10.1161/01.CIR.59.4.748

18. Jaggers J, Lodge AJ. Surgical therapy for anomalous aortic origin of the coronary arteries. *Semin Thorac Cardiovasc Surg Pediatr Card Surg Annu.* (2005) 8:122–7. doi: 10.1053/j.pcsu.2005.01.004

19. Erez E, Tam VK, Doublin NA, Stakes J. Anomalous coronary artery with aortic origin and course between the great arteries: improved diagnosis, anatomic findings, and surgical treatment. *Ann Thorac Surg.* (2006) 82:973–7. doi: 10.1016/j.athoracsur.2006.04.089

20. Eckart RE, Scoville SL, Campbell CL, Shry EA, Stajduhar KC, Potter RN, et al. Sudden death in young adults: a 25-year review of autopsies in military recruits. *Ann Intern Med.* (2004) 141:829–34. doi: 10.7326/0003-4819-141-11-200412070-00005

21. Gulati R, Reddy VM, Culbertson C. Helton G, Suleman S, Reinhartz O, et al. Surgical management of coronary artery arising from the wrong coronary sinus, using standard and novel approaches. *J Thorac Cardiovasc Surg.* (2007) 134:1171–8. doi: 10.1016/j.jtcvs.2007.02.051

22. Vouhé PR. Anomalous aortic origin of a coronary artery is always a surgical disease. *Semin Thorac Cardiovasc Surg Pediatr Card Surg Annu.* (2016) 19:25–9. doi: 10.1053/j.pcsu.2015.12.007

23. Brothers J, Carter C, McBride M, Spray T, Paridon S. Anomalous left coronary artery origin from the opposite sinus of valsalva: evidence of intermittent ischemia. *J Thorac Cardiovasc Surg.* (2010) 140:e27–9. doi: 10.1016/j.jtcvs.2009.06.029

24. Patel VG, Brayton KM, Tamayo A, Mogabgab O, Michael TT, Lo N, et al. Angiographic success and procedural complications in patients undergoing percutaneous coronary chronic total occlusion interventions: a weighted meta-analysis of 18,061 patients from 65 studies. *JACC Cardiovasc Intv.* (2013) 6:128–36. doi: 10.1016/j.jcin.2012.10.011

25. Pourhoseini S, Bakhtiari M, Babaee A, Ostovan MA, Eftekhar-Vaghefi SH, Ostovan N, et al. Increased risk of coronary perforation during percutaneous intervention of myocardial bridge: what histopathology says. *J Cardiovasc Thorac Res.* (2017) 9:108–12. doi: 10.15171/jcvtr.2017.18

26. Patra S, Halder A, Chakraborty R, Dey S. Percutaneous coronary intervention in chronic total occlusion of anomalous right coronary artery: an onerous journey. *Am J Cardiovasc Dis.* (2021) 11:624—7.

27. Abdou SM, Wu C-J. Treatment of aortocoronary dissection complicating anomalous origin right coronary artery and chronic total intervention with intravascular ultrasound guided stenting. *Catheter Cardiovasc Interv.* (2011) 78:914–9. doi: 10.1002/ccd.23021

28. Mirchandani S, Phoon CK. Management of anomalous coronary arteries from the contralateral sinus. *Int J Cardiol.* (2005) 102:383–9. doi: 10.1016/j.ijcard.2004.10.010

29. Gentile F, Castiglione V, De Caterina R. Coronary artery anomalies. *Circulation.* (2021) 144:983–96. doi: 10.1161/CIRCULATIONAHA.121.055347

30. Davis JA, Cecchin F, Jones TK, Portman MA. Major coronary artery anomalies in a pediatric population: incidence and clinical importance. *J Am Coll Cardiol.* (2001) 37:593–7. doi: 10.1016/S0735-1097(00)01136-0

31. Stecker EC, Reinier K, Marijon E, Narayanan K, Teodorescu C, Uy-Evanado A, et al. Public health burden of sudden cardiac death in the United States. *Circ Arrhythm Electrophysiol.* (2014) 7:212–7. doi: 10.1161/CIRCEP.113.001034

32. Kuriachan VP, Sumner GL, Mitchell LB. Sudden cardiac death. *Curr Probl Cardiol.* (2015) 40:133–200. doi: 10.1016/j.cpcardiol.2015.01.002

33. Maron BJ. Triggers for sudden cardiac death in the athlete. *Cardiol Clin.* (1996) 14:195–210. doi: 10.1016/S0733-8651(05)70273-3

34. Virmani R, Chun PK, Goldstein RE, Robinowitz M, McAllister HA. Acute takeoffs of the coronary arteries along the aortic wall and congenital coronary ostial valve-like ridges: association with sudden death. *J Am Coll Cardiol.* (1984) 3:766–71. doi: 10.1016/S0735-1097(84)80253-3

35. Angelini P, Walmsley R, Cheong BY, Ott DA. Left main coronary artery originating from the proper sinus but with acute angulation and an intramural course, leading to critical stenosis. *Tex Heart Inst J.* (2010) 3 7:221–5.

36. Kaushal S, Backer CL, Popescu AR, Walker BL, Russell HM, Koenig PR, et al. Intramural coronary length correlates with symptoms in patients with anomalous aortic origin of the coronary artery. *Ann Thorac Surg.* (2011) 92:986–91. doi: 10.1016/j.athoracsur.2011.04.112

37. Jegatheeswaran A, Devlin PJ, Mccrindle BW, Williams WG, Jacobs ML, Blackstone EH, et al. Features associated with myocardial ischemia in anomalous aortic origin of a coronary artery: a congenital heart surgeons' society study. *J Thorac Cardiovasc Surg.* (2019) 158:822–834.e3. doi: 10.1016/j.jtcvs.2019.02.122

38. Angelini P. Coronary artery anomalies – current clinical issues, definitions, classification, incidence, clinical relevance, and treatment guidelines. *Tex Heart Inst J.* (2002) 29:271–8.

39. Bunji K. kanaya H, Ikeda M, Uno Y, Fujita S, Kato F, et al. Acute inferior myocardial infarction and coronary spasm in a patient with an anomalous origin

of the right coronary artery from the left sinus of Valsalva. *Jpn Circ J.* (2000) 64:641–3. doi: 10.1253/jcj.64.641

40. Maddoux GL, Goss JE, Ramo BW, Raff GL, Heuser RR, Shadoff N, et al. Angina and vasospasm at rest in a patient with an anomalous left coronary system het. *Cardiovasc Diagn.* (1989) 16:95–8. doi: 10.1002/ccd.1810160205

41. Grani C, Kaufmann PA, Windecker S, Buechel RR. Diagnosis and management of anomalous coronary arteries with a malignant course. *Inter Cardiol.* (2019) 14:83–8. doi: 10.15420/icr.2019.1.1

42. Yamada R, Hirohata A, Kume T, Neishi Y, Uemura S. Retrograde coronary intervention for chronic total occlusion of RCA ostium with anomalous origin: a case report. *J Cardiol Cases.* (2019) 19:182–5. doi: 10.1016/j.jccase.2019.01.003

43. Senguttuvan NB, Sharma SK, Kini A. Percutaneous intervention of chronic total occlusion of anomalous right coronary artery originating from left sinus - use of mother and child technique using guideliner. *Indian Heart J.* (2015) 67 Suppl 3:S41–2. doi: 10.1016/j.ihj.2015.10.300

44. Porwal SC, Vishwanath H, Tasgaonkar R, Sitapara T, Thakkar A. Percutaneous coronary intervention in chronic total occlusion of anomalous right coronary artery. *Int J Clin Med.* (2014) 05:567–71. doi: 10.4236/ijcm.2014.510078

45. Kaneda H, Takahashi S, Saito S. Successful coronary intervention for chronic total occlusion in an anomalous right coronary artery using the retrograde approach via a collateral vessel. *J Invasive Cardiol.* (2007) 19:E1–4.

46. Gasparini G, Oreglia J, Reimers B. Successful retrograde recanalization of a very rare anomalous origin right coronary artery chronic total occlusion. *J Cardiovasc Dis Diagn.* (2017) 5:10.00263–1000264

47. Fang HY, Wu CC, Wu CJ. Successful transradial antegrade coronary intervention of a rare right coronary artery high anterior downward takeoff anomalous chronic total occlusion by double anchoring technique and retrograde guidance. *Int Heart J.* (2009) 50:531–8) 29:271–8. doi: 10.1536/ihj.50.531

48. Young L, Harb SC, Puri R, Khatri J. Percutaneous coronary intervention of an anomalous coronary chronic total occlusion: the added value of three-dimensional printing. *Catheter Cardiovasc Interv.* (2020) 96:330–5. doi: 10.1002/ccd.28625

49. Bigler MR, Huber AT, Räber L, Gräni C. A case report of a symptomatic right anomalous coronary artery with concomitant atherosclerotic disease: the benefit of a sequential comprehensive non-invasive and invasive diagnostic approach. *European Heart. Case Rep.* (2021) 5:ytab081. doi: 10.1093/ehjcr/ytab081

50. Musial B, Schob A, De Marchena E, Kessler KM. Percutaneous transluminal coronary angioplasty of anomalous right coronary artery. *Cathet Cardiovasc Diagn.* (1991) 22:39–41. doi: 10.1002/ccd.1810220109

51. Charney R, Spindola-Franco Serge C, Grose R. Coronary angioplasty of anomalous Righ coronary arteries. *Cathet Cardiovasc Diagn.* (1993) 29:23–235. doi: 10.1002/ccd.1810290312

52. Çalişkan M, Çiftçi Z, Güllü H, Alpaslan M. Anomalous right coronary artery from the left sinus of valsalva presenting a challenge for percutaneous coronary intervention Türk Kardiyol Dern Arş - Arch Turk. *Soc Cardiol.* (2009) 37:44–7.

53. Cohen MG, Tolleson TR, Peter RH, Harrison JK, Sketch MH. Successful percutaneous coronary intervention with stent implantation in anomalous right coronary arteries arising from the left sinus of Valsalva: A report of two cases. *Catheter Cardiovasc Interv.* (2002) 55:105–8. doi: 10.1002/ccd.10062

54. Sun D, Bogart D. A technique to perform PCI and stenting in an anomalous RCA from the left sinus of Valsalva. *Case Rep Cardiol.* (2012) 2012:article ID 801423. doi: 10.1155/2012/801423

55. Yumoto K, Aoki H, Shirai Y, Shinoda Y, Kato K. Successful coronary stenting in anomalous right coronary artery by using an inner catheter with mother and child technique under multislice CT guidance. *Cardiovasc Interv Ther.* (2013) 28:106–10. doi: 10.1007/s12928-012-0124-1

56. Uthayakumaran K, Subban V, Lakshmanan A, Pakshirajan B, Solirajaram R, Krishnamoorthy J, et al. Coronary intervention in anomalous origin of the right coronary artery (ARCA) from the left sinus of Valsalva (LSOV): a single center experience. *Indian Heart J.* (2014) 430e:434 doi: 10.1016/j.ihj.2014.05.029

57. Suryanarayana P, Lee JZ, Abidov A, Lotun K. Anomalous right coronary artery: case series and review of literature. *Cardiovasc Revasc Med.* (2015) 16:362–6. doi: 10.1016/j.carrev.2015.03.006

58. Chakraborty B, Chan CNS, Tan AF. Percutaneous transluminal coronary angioplasty of an anomalous right coronary artery arising from a separate ostium in the left sinus of valsalva a case report. *Angiology.* (1995) 46:629–32 doi: 10.1177/000331979504600711

59. Conde-Vela CS, Sabate M, Jime'Nez P, Quevedo, Herna R, Ndez-Antoli'N. Primary percutaneous coronary intervention of an anomalous right coronary artery originating from the left sinus of valsalva acute. *Cardiac Care J.* (2006) 8:229–32. doi: 10.1080/17482940600973018

60. Matchison JC, Shavelle DM. Primary percutaneous coronary intervention of an anomalous right coronary artery arising from the left coronary cusp using an undersized Judkins catheter: A case report. *Int J Angiol.* (2007) 16:33–5. doi: 10.1055/s-0031-1278243

61. Azzarelli S, Amico F, Giacoppo M, Argentino V, Di Mario C, Fiscella A. Primary coronary angioplasty in a patient with anomalous origin of the right coronary artery from the left sinus of Valsalva. *J Cardiovasc Med (Hagerstown).* (2007) 8:943–5. doi: 10.2459/JCM.0b013e328012b0e7

62. Aznaouridis K, Alahmar A. Transradial primary angioplasty of anomalous right coronary artery from the left sinus of valsalva. *Indian Heart J.* (2017) 69:411–3. doi: 10.1016/j.ihj.2017.05.001

63. Bruls S, Durieux R, Gach O, Lancellotti P, Defraigne JO. Sudden cardiac death revealed by an anomalous origin of the right coronary artery from the left sinus of Valsalva. *Ann Thorac Surg.* (2020) 110:e315–764. doi: 10.1016/j.athoracsur.2020.02.034

frontiers | Frontiers in Cardiovascular Medicine

TYPE Original Research
PUBLISHED 03 August 2022
DOI 10.3389/fcvm.2022.922366

OPEN ACCESS

EDITED BY
Sabato Sorrentino,
University of Magna Graecia, Italy

REVIEWED BY
Marisa Avvedimento,
University of Naples Federico II, Italy
Michele Cacia,
Humanitas Research Hospital, Italy

*CORRESPONDENCE
Recha Blessing
recha.blessing@unimedizin-mainz.de
Zisis Dimitriadis
dimitriadiszisis@gmail.com

SPECIALTY SECTION
This article was submitted to Coronary Artery Disease, a section of the journal Frontiers in Cardiovascular Medicine

RECEIVED 17 April 2022
ACCEPTED 11 July 2022
PUBLISHED 03 August 2022

CITATION
Blessing R, Buono A, Ahoopai M, Geyer M, Knorr M, Brandt M, Steven S, Drosos I, Muenzel T, Wenzel P, Gori T and Dimitriadis Z (2022) Use of intravascular ultrasound for optimal vessel sizing in chronic total occlusion percutaneous coronary intervention. *Front. Cardiovasc. Med.* 9:922366. doi: 10.3389/fcvm.2022.922366

Use of intravascular ultrasound for optimal vessel sizing in chronic total occlusion percutaneous coronary intervention

Recha Blessing[1]*, Andrea Buono[2], Majid Ahoopai[1], Martin Geyer[1], Maike Knorr[1], Moritz Brandt[1,3], Sebastian Steven[1,3,4], Ioannis Drosos[5], Thomas Muenzel[1,4], Philip Wenzel[1,3,4], Tommaso Gori[1,4] and Zisis Dimitriadis[5]*

[1]University Medical Center Mainz, Center of Cardiology, Johannes Gutenberg University, Mainz, Germany, [2]Interventional Cardiology Unit, Fondazione Poliambulanza, Brescia, Italy, [3]Center for Thrombosis and Hemostasis, Johannes Gutenberg University, Mainz, Germany, [4]German Center for Cardiovascular Research (DZHK), Mainz Partner Site Rhine-Main, Mainz, Germany, [5]Division of Cardiology, Department of Medicine III, University Hospital Frankfurt, Goethe University Frankfurt am Main, Frankfurt, Germany

Aim: The aim of this study is to provide evidence on how use of standardized intravascular ultrasound (IVUS) use impacts stent size choice in the setting of chronic total occlusion (CTO) percutaneous coronary intervention (PCI) compared to visual estimation.

Methods and results: Data of 82 consecutive patients who had successfully undergone IVUS-guided revascularization of CTO at the University Medical Center Mainz were analyzed. Angiography-based stent size prediction for the proximal and distal vessels was compared to the implanted stent diameter after IVUS assessment. Angiography-based stent size prediction for the proximal vessel was 3.09 ± 0.41, whereas IVUS use demonstrated larger vessel diameter, resulting in larger implanted stent diameter (3.24 ± 0.45, $p < 0.001$). Proximal vessel stent size prediction was underestimated in the majority of patients by angiographic estimation. Angiography-based stent size prediction for the distal vessel was 2.79 ± 0.38, whereas IVUS use demonstrated larger vessel diameter, resulting in larger implanted stent diameter (2.92 ± 0.39, $p < 0.001$).

Conclusion: Pre-stent IVUS assessment in CTO PCI provides important information on vessel morphology and size. Angiography-based stent size prediction for the proximal and distal vessels was frequently underestimated, IVUS use demonstrated larger vessel diameter, resulting in significantly larger implanted stent diameter.

KEYWORDS

intravascular ultrasound (IVUS), percutaneous coronary intervention (PCI), CTO percutaneous coronary intervention, coronary artery disease, complex PCI

Introduction

Revascularization of a chronic total occlusion (CTO) of a coronary artery considered as a complex percutaneous coronary intervention (PCI), with higher rates of procedural failure (1), complications (2, 3), and in-stent restenosis than less complex PCIs (4, 5). Advances in catheter techniques, materials, and treatment algorithms have increased the success rate of CTO PCI.

In addition to these technical advances, intracoronary imaging, particularly intravascular ultrasound (IVUS), has been proposed as a tool to optimize CTO recanalization procedures (1, 6, 7).

Currently, the use of IVUS is recommended for positioning and crossing of the guidewire with the Global Chronic Total Occlusion Crossing Algorithm (e.g., for penetrating of the cap, confirming true lumen positioning after antegrade dissection and re-entry, ADR, and controlled antegrade and retrograde tracking, CART) and increases the safety and efficiency of CTO PCIs (6–10).

Besides information for wire placement, IVUS also provides information about lesion length, morphology, and vessel diameter (11), allowing for optimization of stent selection, expansion, and apposition (12–14). The correct choice of stent length and diameter is a mandatory step to avoid strut malapposition due to undersizing and incomplete coverage of the lesion. In fact, in the CTO scenario, correct stent choice by visual/angiographic assessment is challenging even for experienced operators, as the distal vessel is often narrow, diffusely diseased, and degenerated because of chronic hypoperfusion (15–17). Therefore CTO PCIs result in high occurrence of stent-vessel mismatch due to difficult visual estimation of vessel size in the CTO context.

The aim of this study was to investigate the difference between angiography- and IVUS-assessed vessel diameter in patients undergoing CTO PCI and to show that IVUS assessment is a mandatory step not only for guidewire positioning and post-stent control but also delivers important information before stent implantation.

Materials and methods

Study design and study population

The study was prospectively conducted from July 2019 to July 2021. Data from 82 consecutive patients (≥18 years) who had successfully undergone IVUS-guided revascularization of CTO at the University Medical Center Mainz were analyzed. CTO was defined as a lesion with 100% stenosis and Thrombolysis In Myocardial Infarction (TIMI) flow grade 0 that exists for more than 3 months. The duration of occlusion was determined either based on the clinical record of previous coronary angiograms or clinical (onset of symptoms) or angiographic probability (e.g., collateralization). In-stent CTOs were considered as an exclusion criterion.

Coronary angiography and subsequent PCI were performed by an experienced operator in the CTO field and intracoronary imaging. The CTO hybrid algorithm (18, 19) was used in all the cases, starting with antegrade approaches and, in case of failure, escalation in retrograde approach. IVUS studies were performed using a commercially available system (PHILIPS Volcano; Cambridge, MA, United States).

Once the coronary wire crossed the CTO body and reached the distal true lumen, by protocol, the entire diseased vessel was be predilatated with a 2-mm noncompliant (NC) balloon in order to allow perfusion and vessel diameter assessment. All estimations were conducted by the same 4 experienced interventional cardiologists who assessed all the 82 lesions.

The CTO operator (who performed the procedure) and the three experienced interventional cardiologists were asked to choose the size of the stent(s) on the basis of visual proximal and distal vessel diameter estimation. Predicted proximal and distal vessel diameters have been intended as the reference vessel diameters situated, respectively 5 mm proximally and distally to the CTO caps. Thereafter, IVUS assessment of the vessel was performed: distal and proximal vessel diameters (defined as mean diameter, an average of of minimal and maximal diameters) were calculated. External elastic lamina (EEL) to external elastic lamina was meassured by IVUS to assess the vessel diameter (**Figure 1**).

The size of the stents was selected on the basis of the mean diameter (with a 1:1 or near 1:1 ratio). If one stent was sufficient to treat the entire lesion, stent size was selected according the mean distal vessel diameter, and the proximal vessel diameter was used to determine the balloon diameter for proximal optimization. In cases with a relevant difference between distal and proximal mean diameters (>1 mm), an extra stent in the proximal part with a more suitable diameter was implanted in order to avoid stent fracture after a POT.

After stent implantation, post-dilatation was routinely performed with NC balloons in order to achieve a 1:1 ratio between stent and vessel diameter in all the treated segments. IVUS assessment was conducted on all the patients to determine stent length and achieve complete coverage of the lesion.

Second-generation drug-eluting stents were implanted in all the patients. Recommendations regarding antiplatelet regime after intervention were carried out in adherence to the guidelines (20). A follow-up with outpatient visit and surveillance angiography was performed after 6 months.

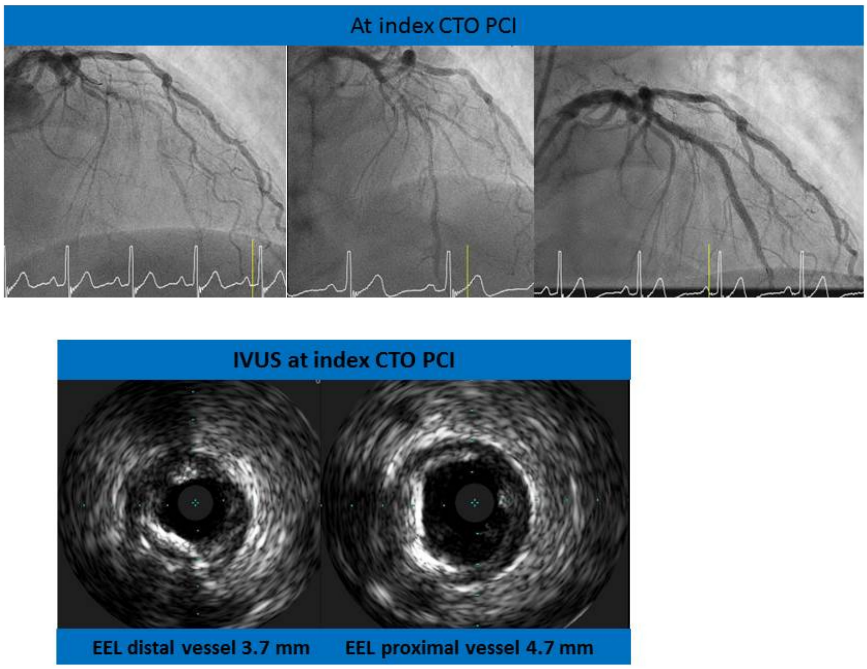

FIGURE 1
Revascularization of the left anterior descending artery (LAD). Examples of intravascular ultrasound (IVUS) assessment of the chronic total occlusion (CTO) vessel: distal and proximal vessel diameters.

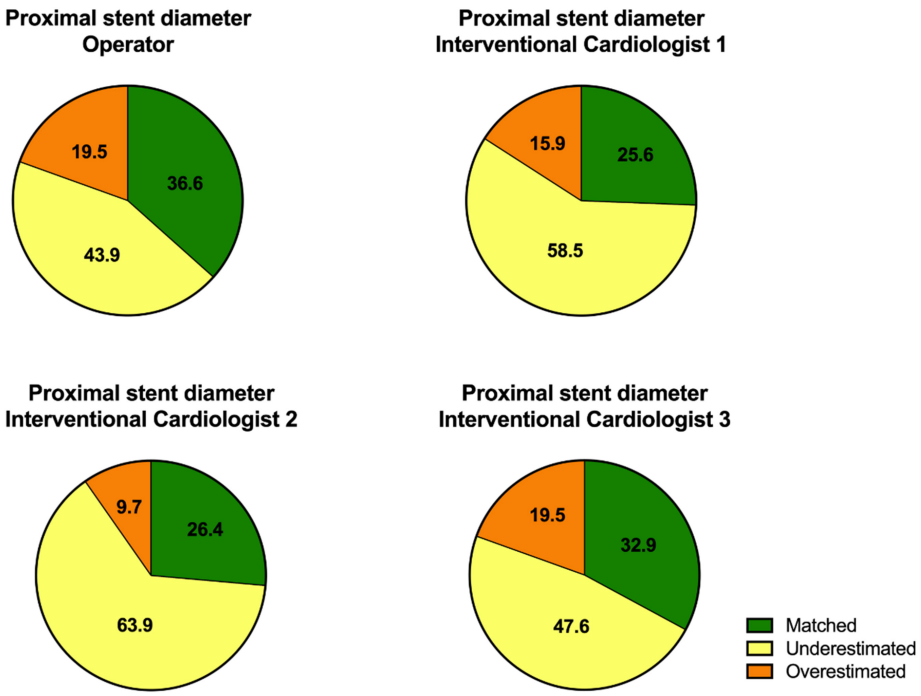

FIGURE 2
The diagrams show the values of the proximal stent diameter estimated by the operator who performed the CTO PCI and the three additional interventional cardiologists.

TABLE 1 Proximal stent parameters [estimation, intravascular ultrasound (IVUS), and implantation].

IVUS guided PCI ($n = 82$)

	Estimated proximal stent diameter	Implanted proximal stent diameter	*p*-value
Operator 1	3.09 ± 0.41 mm	3.24 ± 0.45 mm	**0.001**
Interventionalcardiologist 1	2.94 ± 0.45 mm		**<0.001**
Interventionalcardiologist 2	2,89 ± 0.29 mm		**<0.001**
Interventionalcardiologist 3	3.08 ± 0.54 mm		**0.004**
IVUS value	3.87 ± 0.64 mm		

Values are mean ± SD.

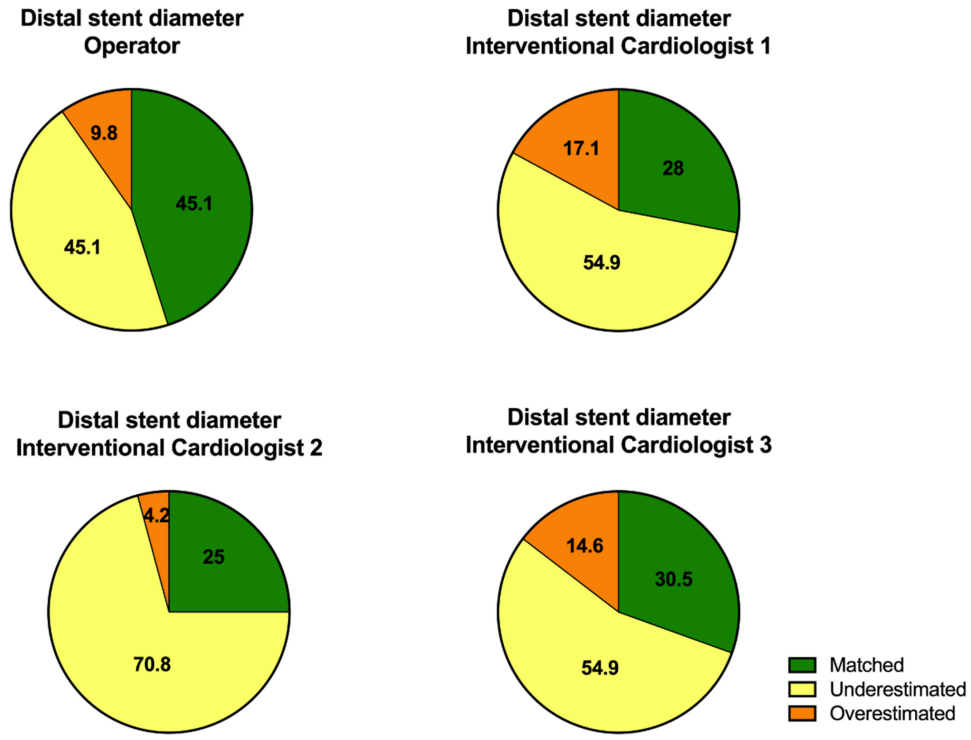

FIGURE 3
The diagrams show the values of the distal stent diameter estimated by the operator who performed the CTO PCI and the three additional interventional cardiologists.

The study conformed to the Declaration of Helsinki and was approved by the local ethics committee. All the participants provided written informed consent.

Statistical analysis

Normal distribution was tested by QQ-plot analysis and the Kolmogorov–Smirnov test. Continuous normally distributed data were presented as mean and standard deviation, and differences were tested by the Student's *t*-test; Non-normally distributed variables were presented as median and minimum and maximum values, and group comparisons were performed by the Mann-Whitney U test. Categorical data were presented as absolute and relative frequencies, and comparisons between groups were performed by chi -square test. Differences were considered statistically significant if $p < 0.05$.

The statistical analyses were performed using SPSS (version 23; IBM SPSS Statistics).

Results

Eighty-two patients with successful IVUS-guided CTO PCI were prospectively included in the study. Clinical follow-up (outpatient visit and surveillance coronary angiography) was

TABLE 2 Distal stent parameters (estimation, IVUS, and implantation).

IVUS guided PCI ($n = 82$)

	Estimated distal stent diameter	Implanted distal stent diameter	*p*-value
Operator 1	2.79 ± 0.38 mm	2.92 ± 0.39 mm	**<0.001**
Interventionalcardiologist 1	2.77 ± 0.39 mm		**<0.001**
Intervetnionalcardiologist 2	2.61 ± 0.26 mm		**<0.001**
Intervetnionalcardiologist 3	2,70 ± 0.49 mm		**<0.001**
IVUS value	3.15 ± 0.49 mm		

Values are mean ± SD.

available for 72 (87.8%) of the patients. The mean follow-up period was 210 ± 20 days.

Stent parameters

The average number of implanted stents was 2 ± 0.8. The estimated proximal and distal stent diameters of the operator were analyzed, and we found the following results for the proximal part of the lesion: angiography-based stent size prediction for the proximal vessel was 3.09 ± 0.41 mm, whereas IVUS use demonstrated larger vessel diameter, resulting in significantly larger implanted stent diameter (3.24 ± 0.45 mm, $p < 0.001$).

The analysis of the estimated proximal stent diameter by the other interventional cardiologists (interventional cardiologists 1, 2, and 3) also showed that proximal stent diameter was underestimated in majority of the patients by angiography. The results of the proximal stent parameters are shown in **Figure 2** and **Table 1**.

The analysis of the distal part of the lesion showed the following results: angiography-based stent size prediction for the distal vessel was 2.79 ± 0.38 mm, whereas IVUS use demonstrated larger vessel diameter, resulting in significantly larger implanted stent diameter (2.92 ± 0.39 mm, $p < 0.001$).

The analysis of the estimated distal stent diameter by the other interventional cardiologists (interventional cardiologists 1, 2, and 3) also showed that distal stent diameter was underestimated in majority of the patients by angiography.

The results of the distal stent parameters are presented in **Figure 3** and **Table 2**.

Clinical and angiographic outcomes

After discharge, none of the patients suffered from a cardiac event (cardiac death, nonfatal myocardial infarction, and stent thrombosis) within 6 months of the follow-up period. We observed 2 (2.77%) re-occlusions and 6 (8.33%) target lesion revascularizations on the 6-month surveillance coronary angiography. None of the patients developed acute renal failure after the CTO PCI. The comparison of GRF values before and 1 day after the CTO PCI showed no difference [81 (10–117) vs. 80.5 (14–120), p.15]. Clinical and angiographic parameters at baseline are shown in **Table 3**. **Table 4** summarizes the clinical and angiographic outcomes at follow-up.

Discussion

The main findings of our study are the following: first, values of the proximal and distal vessel diameters were estimated commonly smaller by visual assessment than by IVUS, which led to change in implanted stent diameter. Second, IVUS assessment was associated with good outcomes in the angiographic and clinical follow-up. Third, we found IVUS assessment to be safe and feasible in CTO PCI with low rate of complications.

Intravascular ultrasound-guided PCI is the most effective method to perform an optimal PCI with low rates of target lesion revascularization, target vessel revascularization, and major adverse cardiac events, but in the clinical routine, it is frequently underused. A meta-analysis published in 2016 showed that IVUS guided PCI reduces major adverse cardiac events (all-cause and cardiovascular deaths, myocardial infarction, target lesion revascularization, and target vessel revascularization) and stent thrombosis compared to angiography-guided PCI in complex lesions (21). To date, there are only a few studies investigating the effects and benefits of IVUS-guided CTO PCI.

Compared to the IVUS assessed diameter, the vessel diameter assessed by angiography was frequently underestimated in our collective. Estimation of vessel diameter by angiography is often complicated by significant calcification and tortuosity of the diffusely diseased and narrowed CTO vessel. In contrast, by IVUS, EEL to EEL is measured to assess vessel diameter, and this method is less affected by these factors. Another challenge of angiographic assessment was found by Allahwala et al. They showed in a collective of 174 patients that the distal vessel size was increased by 31.1% after successful CTO recanalization (17).

Kalogeropoulos et al. demonstrated in an observational study that after IVUS assessment of the lesion significantly longer stents and larger stent diameter were implanted in CTO

TABLE 3 Clinical and angiographic parameters at baseline.

	IVUS guided (n = 82)
Demographics characteristics	
Age, yrs	62.13 ± 11.20
Male	69 (84.1)
BMI kg/m^2	27.40 (21.64–43.03)
Diabetes mellitus	16 (19.5)
Hypertension	70 (85.4)
Hyperlipidemia	77 (93.9)
Current smoking	21 (25.6)
Ex-smoker	24 (29.9)
Multivessel CAD	69 (84.1)
GFR (ml/min)	81 (10–117)
LVEF (%)	55 (15–66)
LVEF ≤ 40%	10 (12.3)
Previous stroke	5 (6.1)
PAD	11 (13.4)
Previous CABG	7 (8.5)
Previous MI	25 (30.5)
Previous PCI	59 (72)
Procedural characteristics	
CTO vessel	
RCA	41 (50.0)
LAD	19 (23.3)
LCX	22 (26.8)
J-CTO Score	1.78 ± 0.73
Antegrade access	79 (96.3)
Number of stents ≤ 3	3 (3.7)
Total stent length >20 mm	57 (69.5)
Fluoroscopic time (min)	25.65 (10.62–55.48)
Contrast (ml)	208 (48–450)
Complications at baseline	
Bleeding	0
Ventricular fibrillation	0
complication of access side	0
Stroke	0
Cardiac death	0
Acutekidneyfailure	0

Values are n (%), median (minimum-maximum), or mean ± SD.
yrs, years; BMI, body mass index; CAD, coronary artery disease; GFR, glomerular filtration rate; LVEF, left ventricular ejection fraction; PAD, peripheral artery disease; CABG, coronary artery bypass graft; MI, myocardial infarction; PCI, percutaneous coronary intervention; RCA, right coronary artery; LAD, left anterior descending coronary artery; and LCX, left circumflex coronary artery.

PCI. In the clinical follow-up, there was no difference in the rate of clinical events (all-cause death, cardiac death, myocardial infarction, and target vessel revascularization) (22). Based on these data, IVUS offers the possibility for accurate measurement of vessel diameter and lesion length and enables optimal stent choice in the CTO PCI setting. An optimal stent choice (good stent apposition and complete lesion coverage) reduces the rate

TABLE 4 Clinical and angiographic outcomes at follow-up.

Angiographic outcome	IVUS guided (n = 72)
Re-occlusion	2 (2.77)
TLR	6 (8.33)
Acute MI	0
Major bleeding	0

Values are n(%).
TLR, target lesión revascularization; and MI, myocardial infarction.

of restenosis and adverse clinical events (all-cause death, cardiac death, and myocardial infarction) after PCI (12, 23, 24).

In our collective, we found a significant difference between estimated and implanted stent diameters after IVUS use, which underscores the difficulty of assessment of stent diameter by angiography and the benefit of pre-stent IVUS use. Both proximal and distal stent diameters were underestimated.

Our collective showed a low restenosis rate in the follow-up, and this is most likely explained by the optimized choice of stent diameter by IVUS guidance.

Our study has several limitations. First, the sample size is limited and is not adequately powered to address the clinical endpoints. For this purpose, our analysis should be intended as hypothesis generating, and further prospective studies with larger cohorts are needed to investigate the benefit of pre-stent IVUS assessment in CTO PCI. Second, the IVUS technique was mandatorily used to choose the stent diameter, but we did not recommend by protocol a post-stent IVUS assessment. Moreover, information concerning the pre-recanalization status of the distal target vessel has not been routinely collected: the presence of CTOs with well-developed collateral could have mitigated IVUS usefulness in stent size choice, since angiographic estimation seems easier if the distal vessel is not diseased. Lastly, the follow-up was short, and this could explain the low number of major clinical events.

Conclusion

Intravascular ultrasound is an important tool to achieve a procedural and short-term efficacy in the CTO scenario.

Based only on angiographic appearance, proximal and distal reference vessel diameters were often underestimated when compared to intravascular ultrasound assessment. This aspect has led to change in stent selection, with a low rate of TLR at 6-month follow-up.

Data availability statement

The raw data supporting the conclusions of this article will be made available by the authors, without undue reservation.

Ethics statement

The studies involving human participants were reviewed and approved by the Ethics Committee of Rhineland Palatinate. The patients/participants provided their written informed consent to participate in this study.

Author contributions

ZD, AB, and TG: conceptualization and supervision. ZD and AB: methodology. RB: software, formal analysis, data curation, writing (original draft preparation), and visualization. ZD, TG, AB, and RB: validation and investigation. TM: resources and project administration. MA, MG, MB, SS, MK, and ID: writing (review and editing). All authors have read and agreed to the published version of the manuscript.

Conflict of interest

The authors declare that the research was conducted in the absence of any commercial or financial relationships that could be construed as a potential conflict of interest.

Publisher's note

References

1. Galassi AR, Werner GS, Boukhris M, Azzalini L, Mashayekhi K, Carlino M, et al. Percutaneous recanalisation of chronic total occlusions: 2019 consensus document from the EuroCTO Club. *EuroIntervention.* (2019) 15:198–208. doi: 10.4244/EIJ-D-18-00826

2. Azzalini L, Carlino M, Bellini B, Marini C, Pazzanese V, Toscano E, et al. Long-term outcomes of chronic total occlusion recanalization versus percutaneous coronary intervention for complex non-occlusive coronary artery disease. *Am J Cardiol.* (2020) 125:182–8. doi: 10.1016/j.amjcard.2019.10.034

3. Hirai T, Nicholson WJ, Sapontis J, Salisbury AC, Marso SP, Lombardi W, et al. A detailed analysis of perforations during chronic total occlusion angioplasty. *JACC Cardiovasc Interv.* (2019) 12:1902–12. doi: 10.1016/j.jcin.2019.05.024

4. Kang J, Cho Y-S, Kim S-W, Park JJ, Yoon YE, Oh I-Y, et al. Intravascular ultrasound and angiographic predictors of in-stent restenosis of chronic total occlusion lesions. *PLoS One.* (2015) 10:e0140421. doi: 10.1016/j.jacc.2012.10.036

5. Valenti R, Vergara R, Migliorini A, Parodi G, Carrabba N, Cerisano G, et al. Predictors of reocclusion after successful drug-eluting stent-supported percutaneous coronary intervention of chronic total occlusion. *J Am Coll Cardiol.* (2013) 61:545–50. doi: 10.1016/j.jacc.2012.10.036

6. Dash D, Li L. Intravascular ultrasound guided percutaneous coronary intervention for chronic total occlusion. *Curr Cardiol Rev.* (2015) 11:323–317. doi: 10.2174/1573403X11666150909105827

7. Galassi AR, Sumitsuji S, Boukhris M, Brilakis ES, Di Mario C, Garbo R, et al. Utility of intravascular ultrasound in percutaneous revascularization of chronic total occlusions: an overview. *JACC Cardiovasc Interv.* (2016) 9:1979–91. doi: 10.1016/j.jcin.2016.06.057

8. Finn MT, Doshi D, Cleman J, Song L, Maehara A, Hatem R, et al. Intravascular ultrasound analysis of intraplaque versus subintimal tracking in percutaneous intervention for coronary chronic total occlusions: one year outcomes. *Catheter Cardiovasc Interv.* (2019) 93:1048–56. doi: 10.1002/ccd.27958

9. Harding SA, Wu EB, Lo S, Lim ST, Ge L, Chen J-Y, et al. A new algorithm for crossing chronic total occlusions from the Asia Pacific chronic total occlusion club. *JACC Cardiovasc Interv.* (2017) 10:2135–43. doi: 10.1016/j.jcin.2017.06.071

10. Wu EB, Brilakis ES, Mashayekhi K, Tsuchikane E, Alaswad K, Araya M, et al. Global chronic total occlusion crossing algorithm: JACC state-of-the-art review. *J Am Coll Cardiol.* (2021) 78:840–53.

11. Malaiapan Y, Leung M, White AJ. The role of intravascular ultrasound in percutaneous coronary intervention of complex coronary lesions. *Cardiovasc Diagn Ther.* (2020) 10:1371–88. doi: 10.21037/cdt-20-189

12. Tian N-L, Gami S-K, Ye F, Zhang J-J, Liu Z-Z, Lin S, et al. Angiographic and clinical comparisons of intravascular ultrasound- versus angiography-guided drug-eluting stent implantation for patients with chronic total occlusion lesions: two-year results from a randomised AIR-CTO study. *EuroIntervention.* (2015) 10:1409–17. doi: 10.4244/EIJV10I12A245

13. Hong S-J, Kim B-K, Shin D-H, Kim J-S, Hong M-K, Gwon H-C, et al. Usefulness of intravascular ultrasound guidance in percutaneous coronary intervention with second-generation drug-eluting stents for chronic total occlusions (from the Multicenter Korean-Chronic Total Occlusion Registry). *Am J Cardiol.* (2014) 114:534–40. doi: 10.1016/j.amjcard.2014.05.027

14. Kim B-K, Shin D-H, Hong M-K, Park HS, Rha S-W, Mintz GS, et al. Clinical impact of intravascular ultrasound-guided chronic total occlusion intervention with zotarolimus-eluting versus biolimus-eluting stent implantation: randomized study. *Circ Cardiovasc Interv.* (2015) 8:e002592. doi: 10.1161/CIRCINTERVENTIONS.115.002592

15. Mohandes M, Vinhas H, Fernández F, Moreno C, Torres M, Guarinos J. When intravascular ultrasound becomes indispensable in percutaneous coronary intervention of a chronic total occlusion. *Cardiovasc Revasc Med.* (2018) 19(3 Pt A):292–7. doi: 10.1016/j.carrev.2017.10.004

16. Allahwala UK, Brilakis ES, Byrne J, Davies JE, Ward MR, Weaver JC, et al. Applicability and interpretation of coronary physiology in the setting of a chronic total occlusion. *Circ Cardiovasc Interv.* (2019) 12:e007813. doi: 10.1161/CIRCINTERVENTIONS.119.007813

17. Allahwala UK, Ward MR, Bhindi R. Change in the distal vessel luminal diameter following chronic total occlusion revascularization. *Cardiovasc Interv Ther.* (2018) 33:345–9. doi: 10.1007/s12928-017-0491-8

18. Brilakis ES, Mashayekhi K, Tsuchikane E, Abi Rafeh N, Alaswad K, Araya M, et al. Guiding principles for chronic total occlusion percutaneous coronary intervention. *Circulation.* (2019) 140:420–33.

19. Brilakis ES, Grantham JA, Rinfret S, Wyman RM, Burke MN, Karmpaliotis D, et al. A percutaneous treatment algorithm for crossing coronary chronic total occlusions. *JACC Cardiovasc Interv.* (2012) 5:367–79. doi: 10.1016/j.jcin.2012.02.006

20. Neumann FJ, Sousa-Uva M, Ahlsson A, Alfonso F, Banning AP, Benedetto U, et al. 2018 ESC/EACTS Guidelines onmyocardial revascularization. *Kardiol Pol.* (2018) 76:1585–664. doi: 10.5603/KP.2018.0228

21. Bavishi C, Sardar P, Chatterjee S, Khan AR, Shah A, Ather S, et al. Intravascular ultrasound-guided vs. angiography-guided drug-eluting stent implantation in complex coronary lesions: meta-analysis of randomized trials. *Am Heart J.* (2017) 185:26–34. doi: 10.1016/j.ahj.2016.10.008

22. Kalogeropoulos AS, Alsanjari O, Davies JR, Keeble TR, Tang KH, Konstantinou K, et al. Impact of intravascular ultrasound on chronic total occlusion percutaneous revascularization. *Cardiovasc Revasc Med.* (2021) 33:32–40. doi: 10.1016/j.carrev.2021.01.008

23. Darmoch F, Alraies MC, Al-Khadra Y, Moussa Pacha H, Pinto DS, Osborn EA. Intravascular ultrasound imaging-guided versus coronary angiography-guided percutaneous coronary intervention: a systematic review and meta-analysis. *J Am Heart Assoc.* (2020) 9:e013678. doi: 10.1161/JAHA.119.013678

24. Kwon O, Lee PH, Lee S-W, Brilakis ES, Lee J-Y, Yoon Y-H, et al. Clinical outcomes of post-stent intravascular ultrasound examination for chronic total occlusion intervention with drug-eluting stents. *EuroIntervention.* (2021) 17:e639–46. doi: 10.4244/EIJ-D-20-00941

frontiers | Frontiers in Cardiovascular Medicine

TYPE Review
PUBLISHED 09 August 2022
DOI 10.3389/fcvm.2022.843734

OPEN ACCESS

EDITED BY
William Kongto Hau,
The Chinese University of Hong Kong, Hong Kong SAR, China

REVIEWED BY
Dario Buccheri,
Ospedale Sant Antonio, Italy
Daniele Giacoppo,
Mater Private Hospital, Ireland
Rajiv Rampat,
William Harvey Hospital, United Kingdom

*CORRESPONDENCE
Tommaso Gori
tommaso.gori@unimedizin-mainz.de

SPECIALTY SECTION
This article was submitted to Coronary Artery Disease, a section of the journal Frontiers in Cardiovascular Medicine

RECEIVED 26 December 2021
ACCEPTED 21 July 2022
PUBLISHED 09 August 2022

CITATION
Abouelnour A and Gori T (2022) Intravascular imaging in coronary stent restenosis: Prevention, characterization, and management. *Front. Cardiovasc. Med.* 9:843734. doi: 10.3389/fcvm.2022.843734

Intravascular imaging in coronary stent restenosis: Prevention, characterization, and management

Amr Abouelnour[1,2] and Tommaso Gori[1]*

[1]Zentrum für Kardiologie, Kardiologie I, Deutsches Zentrum für Herz und Kreislauf Forschung, University Medical Center Mainz, Mainz, Germany, [2]Department of Cardiovascular Medicine, Cardiovascular Institute, Assiut University, Assiut, Egypt

Despite the introduction of drug-eluting stents to combat the neointimal hyperplasia that occurred after BMS implantation, in-stent restenosis is still encountered in a significant number of patients, particularly as increasingly complex lesions are tackled by percutaneous coronary intervention. Many biological and mechanical factors interplay to produce restenosis, some of which are avoidable. Intravascular imaging provided unique insights into various forms of stent-related mechanical issues that contribute to this phenomenon. From a practical perspective, intravascular imaging can therefore help to optimize the stenting procedure to avert these issues. Moreover, once the problem of restenosis eventuates, imaging can guide the management by tackling the underlying identified mechanism. Finally, it can be used to evaluate the re-intervention results. Nevertheless, with the emergence of different treatment options, more evidence is needed to define patient/lesion-specific characteristics that may help to tailor treatment selection in a way that improves clinical outcomes.

KEYWORDS

coronary, in-stent restenosis, intravascular imaging, intravascular ultrasound, optical coherence tomography, characteristics, management, prevention

Introduction

In spite of all the technological evolution of percutaneous coronary intervention (PCI) (**Figure 1**), in-stent restenosis (ISR) remains the commonest failure mechanism post-PCI, occurring in 3 to 20% of patients depending on patient's and lesion characteristics and stent type (1). In the drug-eluting-stent (DES) era, the rate of ISR has decreased, but the absolute numbers actually increase due to the progression of PCI as a tool to treat increasingly complex coronary artery disease.

The traditional anatomic substrate of ISR is neointimal hyperplasia, resulting primarily from vascular smooth muscle cell proliferation. This classically occurred after bare metal-stent (BMS) implantation peaking early between 6 and 12 months. However, DES-ISR can peak years after implantation, the so-called "late catch-up" phenomenon

(2). This is probably due to delayed healing and persistent inflammation, with the more frequent appearance of "neoatherosclerosis."

Because various biological and mechanical mechanisms can contribute to DES ISR, e.g., drug resistance, hypersensitivity to the drug or polymer, etc. (3), the management of such challenging problem requires the identification of any underlying mechanical problems that can be rectified. Intravascular imaging with intravascular ultrasound (IVUS) or optical coherence tomography (OCT) allows this systematic investigation, to tailor interventions and tackle the underlying mechanism and to optimize the results of any necessary repeated interventions. In addition, intravascular imaging can call attention to potential new device-related issues. However, further evidence is still needed to prove that intravascular imaging-guided management of ISR improves clinical outcomes and/or prevents recurrences in this setting. From another standpoint, intravascular imaging has helped to clarify the relationship of certain lesion characteristics to the risk of ISR. For instance, IVUS has shown that although a well-developed collateral circulation (collateral flow index $\geq$0.25) is associated with more severe stenoses at baseline, it does not predict an increased risk of ISR (4).

Angiographic ISR is usually defined arbitrarily in binary terms as diameter stenosis of >50% in-stent or at its edges (5-mm segments adjacent to the stent) on coronary angiography (5). This provides simplicity but is also rooted in the physiologic significance of such degree of narrowing and has been shown to offer the best balance of sensitivity and specificity, compared to other more accurate but less accessible cutoffs, in terms of predicting clinically driven target lesion revascularization (TLR) (6, 7). However, because this is a 2-dimensional assessment, it is contingent on obtaining the worst-stenosis projection. Besides, it relies on the visual estimation of the operator that has to judge the ISR using the body of the stent, with a small margin of proximal and distal vessel. Even with the introduction of computer-assisted quantitative angiography, as a more objective clinical tool, limitations exist pertaining to the technology, technique, and analysis (8). Percentage diameter stenosis at follow-up coronary angiography and late luminal loss are also well-studied continuous-scale parameters used to describe the degree of restenosis (9). Late loss, as a measure of absolute renarrowing [= minimum lumen diameter (MLD) immediately post-procedure − MLD at follow-up], was shown to be a generalizable and powerful endpoint across both BMS and DES, as well as across different stented vessel sizes. However, since the site of the MLD at implantation and that of MLD at follow-up do not need to be exactly the same, this measure does not reflect absolute neointimal proliferation. Percent diameter stenosis [= (1 − (MLD/reference vessel diameter)) × 100], albeit another good measure to follow-up a given patient, is dependent on the reference vessel size, complicating its use as a comparator (10). In contrast, intravascular imaging allows a 3-dimensional cross-sectional assessment of the artery, permitting a direct visualization and quantification of the stent area, neointimal area, and luminal area (11), where restenosis is usually defined as a cross-sectional area re-narrowing >75% of the reference vessel segment (12). In addition, timely online quantitation is available rather than visual estimation. Earlier studies validated IVUS for *de novo* coronary lesions against stress myocardial perfusion single-photon emission computed tomography, as well as invasive coronary flow reserve, proposing criteria such as an IVUS minimum lumen area (MLA) <4.0 mm^2 or corrected percent area stenosis $\geq$75% as the indicators of functional significance (13, 14). However, with the consolidation of myocardial fractional flow reserve (FFR) and other invasive physiological indices such as the instantaneous wave-free ratio (iFR) as the contemporary gold standard to assess the significance of coronary stenotic lesions, it became clear that many factors including ethnicity, vessel size, lesion location, the type of imaging used, etc., preclude the adoption of a universal cutoff by intracoronary imaging to intervene, and that intracoronary imaging can more readily provide thresholds for safe deferral of intervention (15).

The challenge of defining clinically relevant restenosis is compounded by the reality that the mere anatomic detection of a restenosis by angiography and intravascular imaging, especially if moderate, does not automatically signify a "clinical" or "functional" restenosis that can produce symptoms or objective evidence of ischemia. This uncoupling of anatomic and clinical restenosis might be attributed to the effect of other geometric aspects of the lesion (including its length) on flow, the status of endothelial function, collateral circulation, and the size of the subtended myocardial bed (9). Therefore, surrogate clinical endpoints such as TLR emerged, to capture a

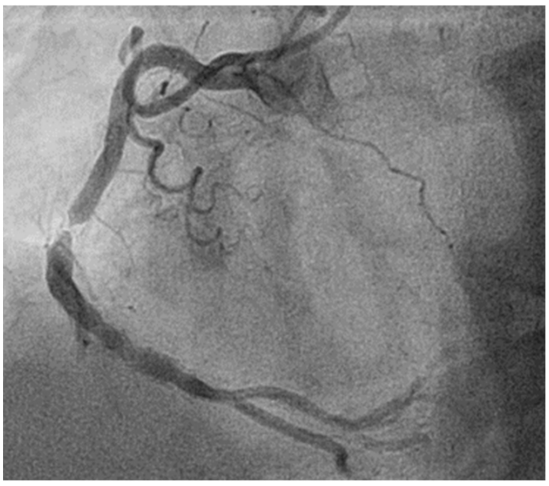

FIGURE 1
Angiographic appearance of an in-stent restenosis in segment 2 of the right coronary.

specific treatment's ability to maintain long-term patency at the particular intervention site. The academic research consortium (ARC) criteria for TLR thus emphasize the clinical context in addition to anatomic luminal measurements, in the form of recurrent symptoms, objective signs of ischemia by non-invasive testing, or abnormal results of any invasive functional diagnostic test, unless the diameter stenosis is ≥70% (16, 17). Of note, this ARC consensus highlights the fact that early TLR events (<30 days after stenting) are unlikely to be due to ISR but are most likely a result of subacute stent thrombosis.

Intravascular imaging can guide the management of ISR through multiple stages. On the one hand, it can help to optimize the stenting procedure by predicting and avoiding ISR. On the other hand, once the ISR problem has set in, such modalities can help to identify the underlying mechanism. Finally, imaging can evaluate ISR treatment results.

Prevention of restenosis

Intravascular ultrasound-guided BMS implantation was shown to modestly reduce restenosis and the need for repeat revascularization (18–20). However, the impact of IVUS-guided DES implantation on target vessel revascularization (TVR) was more controversial (21, 22). More recent studies and meta-analyses show that IVUS-guided PCI is associated with a significantly lower risk of TLR in all generations of DES, both in stable angina and in acute coronary syndromes (ACSs) (23–27). In complex PCI, earlier studies showed no impact of IVUS guidance on TLR (28), but later ones (or subgroup analyses thereof) confirmed that IVUS use reduces the risk of ischemia-driven TLR (29–32) and that such benefit is sustained on the longer term (33, 34).

Similarly, OCT guidance seemed to lower the 1-year risk of a composite that included TLR, only on unadjusted analyses (35). From another angle, when nearly 1,000 lesions in the same study were retrospectively analyzed, suboptimal stent deployment defined according to the presence of at least one of specific quantitative OCT criteria was associated with an increased risk of major adverse cardiac events (MACEs) including TLR. These criteria included in-stent MLA <4.5 mm^2, distal dissection >200 μm, and distal or proximal reference lumen area (at stent edges) <4.5 mm^2 in the presence of significant plaque (36). In another large observational study, where almost 90 thousand patients were analyzed (OCT used in over 1,100 patients, IVUS used in almost 11 thousand patients, and angiography alone used in slightly over 75 thousand patients), OCT-guided procedures were associated with a reduction in the prespecified primary endpoint of all-cause mortality at a median of nearly 5 years, but the study did not provide information about TLR on the long term, because the prespecified secondary composite endpoint was restricted to in-hospital events (37). From another perspective, OCT-guided PCI in patients with non-ST segment elevation ACS was shown to modestly improve the post-procedural fractional flow reserve (FFR), mostly by the optimization of stent expansion, when compared to fluoroscopy-guided PCI. In this study, post-PCI OCT revealed stent underexpansion in 42% of patients (38).

Interestingly, a prospective multicenter 1:1 randomized study has directly compared OCT to IVUS in patients undergoing PCI with a second-generation DES. The study successfully demonstrated that OCT-guided PCI was non-inferior to IVUS-guided PCI, regarding both angiographic in-stent and in-segment stenosis at 8 months, as well as ischemia-driven TLR at 12 months (39). Likewise, a meta-analysis incorporating that study among others, encompassing over 17 thousand patients, showed no difference in comparative efficacy between IVUS and OCT in terms of TLR, although OCT did not significantly lower the risk of TLR compared to angiography guidance (27).

This review provides an overview on the various forms of mechanical stent-related problems that can be detected by intravascular imaging and have been linked with varying degrees to ISR. **Table 1** summarizes the relative strengths of IVUS and OCT for the detection of each of these problems.

Stent underexpansion

The most frequent technically preventable mechanism of ISR in the DES era is stent underexpansion (40), often

TABLE 1 Relative strengths of IVUS and OCT for the detection of various underlying mechanisms of ISR.

Application/finding	Angiography	IVUS	OCT
Stent sizing	+	++	+
EEL/vessel wall visualization	–	++	+
Calcium pre-PCI	+ if severe	+ arc	+ arc and thickness/area
Peri-stent calcium	–	–	+
Acute stent malapposition	+	++	+++
Geographic miss	–	+	+
Edge dissection	+	++	+++
In-stent tissue prolapse	–	+	++
Stent fracture	+ (Stent-boost++)	+	++ (3D +++)
Longitudinal stent deformation	+	++	+++
Non-uniform strut distribution	–	+	+
Neointimal characterization	–	+	++
Multiple layers of stent	+	++	+++

+, feasible; ++, good; +++, very good.

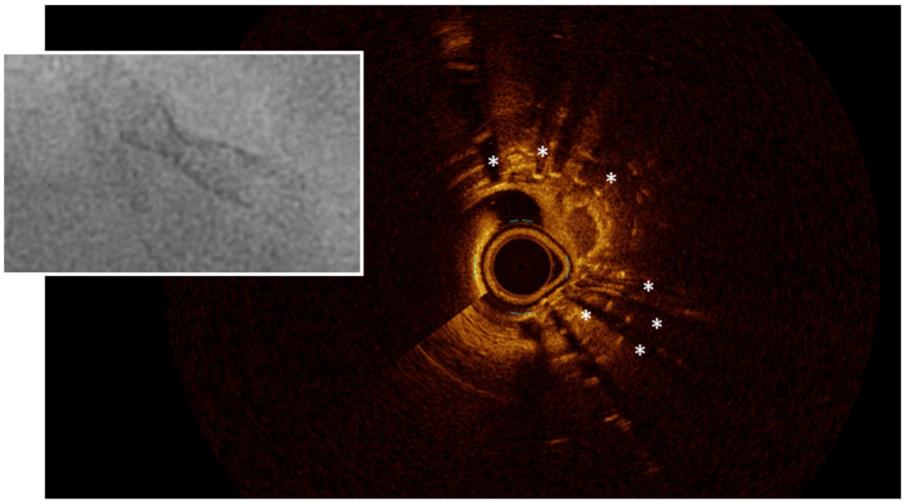

FIGURE 2
Stent underexpansion. OCT image of an incomplete expansion of a stent resulting in restenosis despite moderate neointima proliferation. The asterisks (*) mark stent struts. The small picture demonstrates the incomplete apposition at angiography.

unrecognized at angiography (**Figure 2**). Post-PCI minimum stent area (MSA) is consistently the strongest predictor of ISR. In an early study of almost 500 lesions in 425 patients who underwent successful IVUS-guided stenting, based on the empiric criteria, an intrastent minimal lumen cross-sectional area ≥55% of the average reference vessel was the only criterion that was associated with a higher probability of freedom from ISR, independently from vessel size (41). However, more recent accumulating evidence suggested that the absolute stent expansion (MSA as an absolute measure) matters more than the relative expansion (MSA compared to a predefined reference area) in predicting the stent patency in the long term. In a study of over 1,500 patients [nearly 1,100 with paclitaxel-eluting stents (PESs), and nearly 500 with BMS], post-PCI MSA was the independent predictor of subsequent ISR at 9 months, with an optimal threshold of 5.7 mm^2 for PES (42). Similarly, for sirolimus-eluting stents (SESs), post-procedural final MSA by IVUS was one of the only two independent predictors of angiographic restenosis; the other predictor being the stent length. In that study, the final MSA cutoff that best predicted ISR was 5.5 mm^2 (43). Similar data have been shown for the second-generation DES, where a study of almost 1,000 lesions identified the post-stenting MSA as the only independent predictor of angiographic ISR in zotarolimus-eluting stents (ZESs) and in everolimus-eluting stents (EESs). The best MSA cutoff value was 5.5 mm^2 for the prediction of SES restenosis, 5.3 mm^2 for ZES ISR, and 5.4 mm^2 for EES (44). Most recently, this was challenged by an IVUS substudy of the ADAPT-DES registry (Assessment of Dual Antiplatelet Therapy with Drug-Eluting Stents), where ten different stent expansion indices were compared for their association with a primary endpoint of lesion-specific 2-year clinically driven TLR or definite stent thrombosis. Interestingly, only MSA/vessel area at the MSA site (best cutoff was 38.9%) was independently associated with the study endpoint, after adjusting for morphologic and procedural parameters. In other words, stent/vessel area at the MSA site was superior to absolute MSA (and other expansion indices) in predicting the study endpoint, driven mainly by the difference in TLR rather than stent thrombosis (45).

Whereas the studies mentioned above investigated non-left main lesions, Kang et al. showed that for unprotected left main (LM) stenting, ISR was more frequent in lesions with underexpansion of at least one segment, with a significantly lower event-free survival rate than in lesions with no underexpansion. The MSA cutoffs that best predicted ISR on a segmental basis were 5.0 mm^2 for ostial left circumflex (LCX), 6.3 mm^2 for ostial left anterior descending (LAD), 7.2 mm^2 for the polygon of confluence (POC), and 8.2 mm^2 for the LM above the POC (46).

Likewise, in chronic total occlusions (CTO) that are successfully recanalized, IVUS has shown that a smaller MSA is a major predictor of angiographic ISR (47). Additionally, similar to patients with stable coronary artery disease, a smaller MSA after primary PCI was shown to be an independent predictor of angiographic restenosis (48).

Concurring with the intravascular ultrasound (IVUS) findings, post-stenting optical coherence tomography (OCT) has shown that a small MSA (defined as <5.0 mm^2 for DES) is an independent predictor of 1-year device-oriented clinical endpoints (49). It is important to note, however, that these thresholds do not define optimal stenting, such that a larger MSA is still associated with less ISR, until an MSA of about 8 mm^2, where a plateau is reached (50).

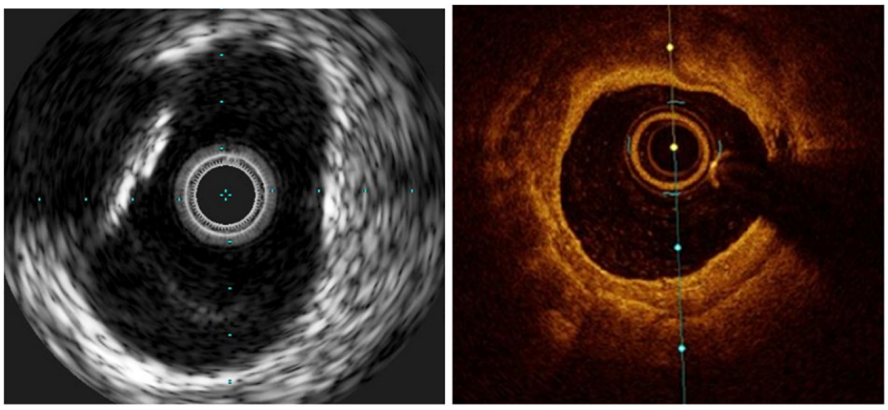

FIGURE 3
Calcific lesions at intravascular ultrasound **(Left)** and optical coherence tomography **(Right)**. The limitation of IVUS in this case is that the lesion projects a shadow that does not allow measuring its depth.

Interestingly, when compared to phantom models, OCT was more accurate and reproducible in the assessment of coronary luminal dimensions than IVUS which overestimated those dimensions and was less reproducible (51). Earlier studies, however, suggested that OCT guidance would yield smaller stent expansion and more residual reference segment stenosis than IVUS guidance, because of the greater ability of IVUS to visualize the vessel border compared to OCT, both before and after intervention. This would potentially lead to more stent restenosis (52). Nevertheless, when OCT-guided stenting was compared to IVUS-guided stenting in the ILUMIEN (optical coherence tomography compared with intravascular ultrasound and with angiography to guide coronary stent implantation) II study, both approaches resulted in a comparable degree of stent expansion, defined as MSA divided by the mean of the proximal and distal reference lumen areas (53).

Regarding the relative stent expansion, the EAPCI consensus views a cutoff of >80% for the MSA relative to average (proximal and distal) reference lumen area, as a reasonable and realistic target to employ in clinical practice, taking into consideration that more stringent targets such as >90% were frequently not achieved in the respective clinical trials (54).

Stent underexpansion could be due to stent underdeployment (the use of low deployment pressures), stent undersizing, or heavily calcified lesions that preclude adequate stent expansion despite high deployment and/or post-dilation pressures. It is important therefore to recognize target lesion calcium, so as to consider pre-stenting calcium modification techniques, e.g., rotational, or orbital atherectomy, cutting, or scoring balloons. Intravascular imaging is more sensitive for calcium detection than angiography. In a study of 1,155 native vessel target lesions in stable patients, IVUS detected calcium in 73% whereas angiography detected calcium in only 40% (55). This is in line with the results of other studies, which showed a good sensitivity and specificity of IVUS to detect intralesional calcium compared to pathology. In one study that examined the ability of IVUS to accurately depict circumferential calcified lesions on autopsy arterial segments, IVUS had a sensitivity of 89% and a specificity of 97% (56). In another study of 50 coronary vessel segments, IVUS was compared to corresponding histologic sections and had an overall sensitivity of 90% and a specificity of 100% for the detection of dense, coherent calcium, even though it had a much lower sensitivity (64%) for visualizing microcalcification (57).

While it is difficult to evaluate calcium thickness or area with IVUS because its surface reflects ultrasound waves almost entirely, OCT can penetrate through calcium, so that its thickness and area can be evaluated (**Figure 3**). This was shown to be relevant, although to a lesser degree than the arc of calcium, so that it affects the minimal stent diameter achieved (58). In another study, a thinner calcium thickness after rotational atherectomy (optimal threshold was 0.67 mm) predicted the formation of cracks after balloon angioplasty which in turn permitted a larger lumen gain and a greater stent cross-sectional area (59). An OCT-based calcium scoring system has been proposed, whereby a maximum angle of calcium >180°, together with a maximal thickness >0.5 mm, and length >5 mm, predicted stent underexpansion (based on the smallest stent area divided by the average of proximal and distal reference luminal areas) with a slightly better ability than the angiographic detection of severe calcium (60). On the other hand, it has been demonstrated that the detection of calcium fractures by OCT (**Figure 4**) confirms adequate modification of heavily calcified culprit lesions before stenting and resulted in a greater MSA, and stent expansion immediately post-PCI, as well as smaller percent diameter stenosis, less frequent binary restenosis, and less ischemic-driven TLR, at 10-month follow-up (61).

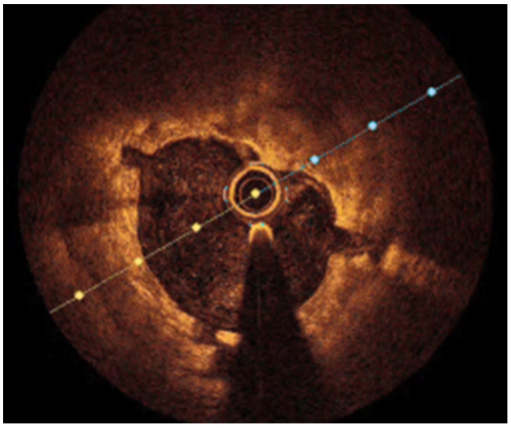

FIGURE 4
Cracks in the subintimal calcium after coronary lithotripsy.

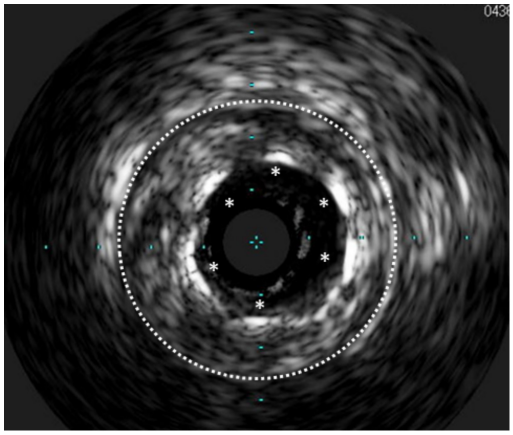

FIGURE 5
Stent undersizing demonstrated at IVUS. The white dotted line marks the lamina externa, where the stent struts (*) should lie.

Stent undersizing

There is no clear-cut evidence to support routine use of intracoronary imaging for stent sizing. However, there is some evidence to support intracoronary imaging guidance in long lesions and CTOs (62–64), although the greater CTO success achieved in the imaging-guided group in terms of, e.g., a greater MSA (at least in part due to bigger implanted stent diameters), did not always translate into better clinical outcomes, with the exception of less stent thrombosis and less TLR in longer lesions (65, 66). In addition, the EAPCI expert consensus recommends its use in LM lesions, patients with ACS, or other complex lesion morphologies (67). Nevertheless, there seems to be less benefit in simple lesions or patients with stable clinical presentation (54, 68).

Imaging-guided stent sizing is based on either the external elastic lamina (EEL) diameters of the distal reference, usually rounded down by ≥0.5 mm or alternatively, reference lumen diameters can be used, rounded up by 0.5 mm. Particularly in smaller or very calcific arteries, or in the setting of diffusely diseased vessels (including chronic total occlusions) or acute coronary syndromes, imaging-guided sizing is often larger than the angiographic reference diameters.

For its superior capacity to distinguish the EEL, IVUS is considered to be the gold standard method for guiding stent sizing (**Figure 5**). Because of the limited tissue penetration of OCT (1–2 mm) compared to IVUS (5–6 mm), it is often not able to visualize the EEL at the lesion site. The introduction of artificial intelligence-based methods in the latest iteration of the OCT software by the company Abbott vascular, however, significantly streamlines these processes (**Figure 6**). Therefore, an algorithm was proposed by the ILUMIEN III and IV studies (54, 69), where the EEL diameter was used if the EEL circumference was visible for ≥180°. In such case, the proximal

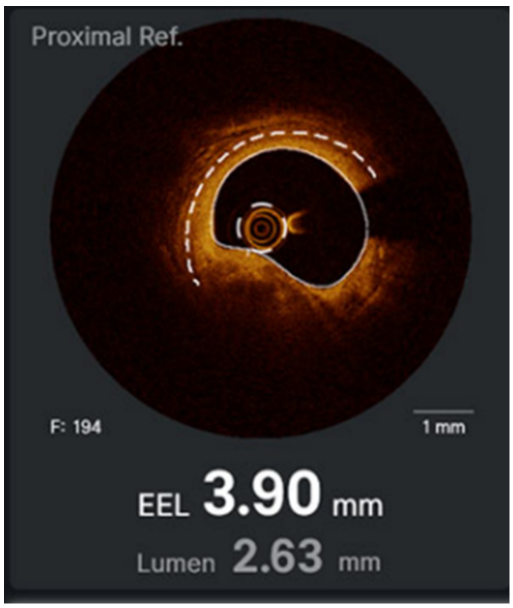

FIGURE 6
Artificial intelligence-driven stent/vessel sizing.

and distal reference mean EEL diameters were measured, and the smaller of these diameters rounded down to the nearest 0.25 mm was used. In case the EEL cannot be seen ≥180°, the stent diameter was determined as 100% of the lumen diameter. Compared to the respective reference, a final lumen area ≥90% was considered acceptable. Using this algorithm, OCT-guided PCI was non-inferior to operator-directed IVUS guidance in terms of the post-PCI MSA, with no difference in procedural MACE up to 1 year (54, 68). Because ILUMIEN III was underpowered to detect differences in clinical outcomes,

another adequately powered ongoing trial, ILUMIEN IV trial (NCT03507777), is geared to rigorously test this aspect (69).

From a practical perspective, the EAPCI consensus on the clinical use of intracoronary imaging highlights the distal lumen reference-based sizing as a safe and straightforward approach, which can be followed by an optimization of the mid and proximal stent segments. The mean distal lumen diameter with up rounding of the stent diameter by 0–0.25 mm may be used, or alternatively, the mean EEL (if adequately visualized) with down rounding to the nearest 0.25 mm stent size can be used (67).

Geographic miss

Longitudinal geographic miss (GM) refers to an injured or diseased vessel segment not covered by the stent. Both IVUS and OCT provide valuable information to determine an appropriate (relatively plaque-free) landing zone for stent implantation, to avoid GM and have adequate lesion coverage.

In a study of over 1,500 patients with SES implanted, GM had a four-fold increase in the incidence of edge restenosis, with a significantly higher rate of TVR at 1 year, after adjusting for clinical and anatomic factors (70). In another smaller retrospective study of 167 SES, a larger reference percentage of plaque area at baseline IVUS was among the factors associated with edge restenosis (71). Similarly, residual edge plaque burden was the only independent predictor of angiographic stent edge restenosis at 9 months after PES implantation (72). Another IVUS study of newer generation DESs in almost 1,000 lesions concluded that edge restenosis was predicted by post-stenting reference segment plaque burden and reference segment MLA. The predictive cutoff of the reference plaque burden was 54.5% overall (56.3% for endeavor ZES, 57.3% for resolute ZES, and 54.2% for EES) (73).

Comparable results were obtained by OCT in a retrospective study of 319 patients with EES implantation. The independent predictors of binary angiographic stent edge restenosis at 9 to 12 months were lipidic plaque in the stent edge segment (optimal cutoff was an arc ≥185) and MLA (optimal cutoff was 4.1 mm^2) (74).

Interestingly, in a prospective single-center randomized study of 200 patients, comparing OCT-guided PCI with vs. without co-registration, there was no significant difference in GM, even though co-registration enabled more precise stent location. There was also a trend for less severe edge dissection with co-registration, which did not reach statistical significance (75).

Edge dissection

Optical coherence tomography has a greater sensitivity to detect post-procedural stent edge dissections than IVUS

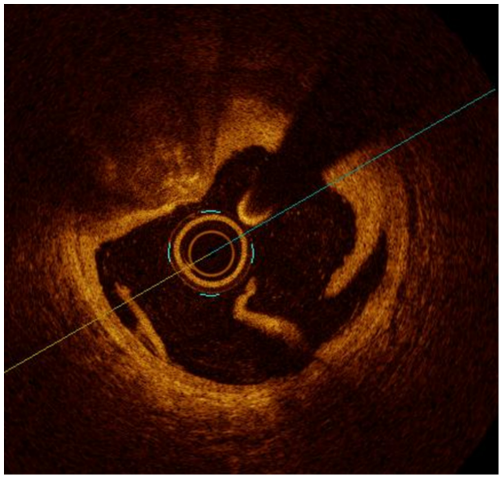

FIGURE 7
Edge dissection.

(**Figure 7**), attributable to its greater resolution. This is confirmed, for example, by data from ILUMIEN III, where untreated edge dissections as detected by OCT were more frequently present after IVUS-guided and angiography-guided PCI than after OCT-guided PCI. Not only untreated major dissections (≥60° in circumference and/or ≥3 mm in length) and medial dissections were more common after IVUS-guided PCI than after OCT-guided PCI, but indeed, OCT detected nearly 25% of total dissections and 15% of major dissections that were overlooked by IVUS (54). This agrees with the data from other smaller-scale studies (51). However, these findings had no impact on stent-oriented outcomes (68).

On the other hand, although it has previously been shown in a porcine model that the degree of arterial injury is strongly correlated with the magnitude of restenotic response (76), and one group has shown that IVUS-detected edge dissections were related to more restenosis with subsequent TLR (77), Radu et al. demonstrated, however, that non-flow limiting edge dissections identified by OCT at baseline completely healed on serial follow-up at 1 year, except for the longest flaps (2.81 and 2.42 mm), which were only partially healed. In all cases, however, this did not produce restenosis as assessed by OCT at 1-year follow-up, nor did it result in MACE within that year. Moreover, the two cases with persistent/partially healed dissections had no MACE up to 3 years of follow-up (78). This aligns with a multitude of other studies that employed angiographic (71, 73, 74, 79), IVUS (80), and OCT follow-up (81–84). Similarly, in a study of over 1,000 stents implanted to treat 900 lesions (including both BMS and DES), stent edge dissection detected by OCT had no impact on device-oriented clinical endpoints at 1 year of follow-up (49).

Of note, other groups related certain OCT-derived characteristics of the edge dissection to MACE, e.g., dissection flap thickness ≥200 μm (85), or 310 μm (86), or dissection

length >3.55 mm (87), but none of these groups demonstrated an association specifically with edge restenosis.

In-stent tissue protrusion/prolapse

Optical coherence tomography seems to be more sensitive than IVUS for intrastent tissue protrusion detection (51) (**Figure 8**). However, the impact of tissue protrusion/prolapse (TP) on restenosis and TLR is controversial, with several studies failing to establish a significant relationship

An early study of 407 native coronary lesions, where post-intervention IVUS was done, failed to show an association of minor plaque prolapse (detected in nearly quarter of the lesions) and 6-month angiographic restenosis (88). In another serial IVUS study of 205 lesions in patients with diabetes, plaque prolapse was not associated with increased neointimal proliferation or angiographic restenosis (89).

From the OCT perspective, irregular in-stent TP independently predicted 1-year device-oriented clinical endpoints, primarily driven by TLR that was not for stent thrombosis. This is probably because irregular tissue protrusion represents a moderate to severe vessel injury with a high likelihood of medial disruption and lipid core penetration resulting in restenosis (49). However, in another serial OCT and IVUS study, although the lumen area in lesions with TP significantly decreased due to neointimal proliferation at follow-up (with greater late lumen area loss in IVUS-detected than in OCT-only-detected TP), no impact on clinically relevant restenosis was demonstrated (81).

Interestingly, in a prespecified substudy of the ADAPT-DES, TP detected by IVUS was associated with less clinically driven TLR at 2 years, in part because of greater stent expansion in these lesions which was presumably among the causes of TP, and because greater stent expansion counterbalanced the impact of TP to maintain a good acute result in terms of luminal dimensions (90).

Acute stent malapposition

Optical coherence tomography has a greater ability to detect acute stent malapposition (ASM) than IVUS (**Figure 9**). For instance, when the same lesions were evaluated post-PCI with frequency-domain OCT and IVUS, incomplete stent apposition was detected in more lesions by OCT than by IVUS (39 vs. 14%) (51). Similarly, in the ILUMIEN III trial, OCT was significantly more sensitive than IVUS at detecting malapposition. Moreover, OCT procedural guidance led to fewer malappositions than did IVUS guidance (54).

The clinical outcome of ASM yet is uncertain, i.e., no clear connection exists between ASM (in the absence of underexpansion) and subsequent TLR. This is probably because ASM may subsequently resolve. In a serial OCT study of 66 stents (including EES, ZES, and BMS), 71.5% of the ASM segments were completely integrated into the vessel wall at 6-month follow-up. The maximum ASM distance per strut (or ASM volume) was the only predictor for the percentage of malapposed struts at follow-up, so that a maximum ASM distance <270 μm was grossly covered and spontaneously reapposed in 100% of cases at follow-up, whereas distances ≥850 μm resulted in persistent ASM and delayed coverage in 100% of cases (91). The same concept was demonstrated in another serial OCT study of 77 patients, which showed spontaneous resolution of ASM at 8- to 12-month follow-up,

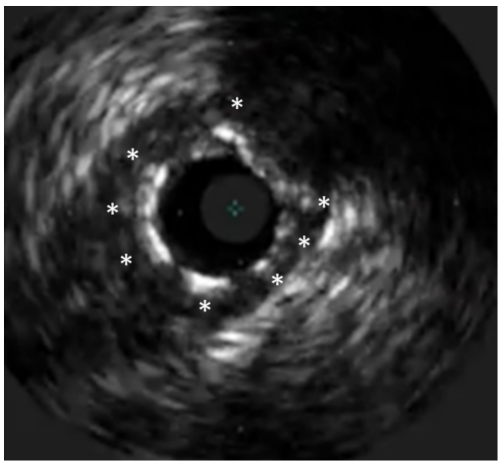

FIGURE 8
Tissue prolapse after PCI of a chronic total occlusion. The stent struts are marked with *, at 1 o'clock a prolapse of a calcific plaque can be seen.

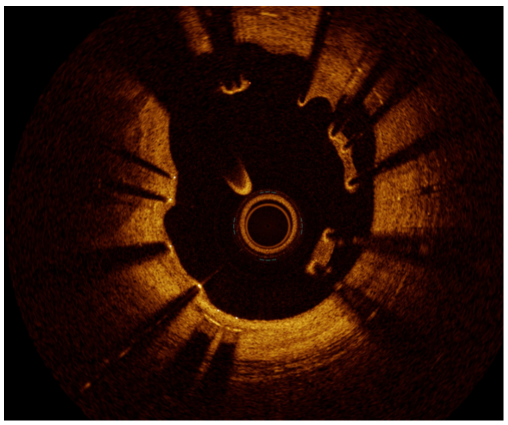

FIGURE 9
Malapposition. Although not being a direct cause of restenosis, the flow disturbance caused by the malapposed struts may cause neointima proliferation distal to the site.

which occurred to a greater extent in EES than in SES. The best cutoff of the ASM acute distance for predicting late persistent malapposition at follow-up was > 355 μm for EES and > 285 μm for SES (92). A third OCT study with a longer follow-up of 2 years has shown a very close cutoff endoluminal distance for the resolution of ASM in cobalt chromium EES of 359 μ m (93).

Consequently, in one study, for example, of over 350 lesions, where patients received post-stenting OCT, ASM was observed in 62% of lesions, and yet, there was no difference in clinical events including TLR between patients with and without stent malapposition (94). In another retrospective analysis of post-procedural OCT findings in 864 patients, variable grades of ASM were detected in 72.3% of stents, but had no relation to ISR, nor to TLR (95). Similarly, in acute coronary syndrome patients, post-procedural OCT-detected ASM was not associated with device-oriented events including TLR (96). On the other hand, in an integrated analysis of IVUS substudies of multiple trials, where 1,580 patients were evaluated (with either PES or BMS implanted), stent malapposition had no impact on the rates of restenosis nor MACE including TLR at 9 months (97). Furthermore, in the IVUS substudy of ADAPT-DES trial, ASM did not influence clinically driven TLR at 2-year follow-up (98).

Stent fracture

A stent fracture undermines the scaffolding at its site as well as the local drug delivery in the case of a DES. This is coupled with mechanical irritation of the vessel by the fractured struts. Moreover, evidence has been shown by IVUS for recoil of the edges of the struts just proximal and distal to the fracture site (99). Therefore, stent fractures associate with higher rates of ISR and TLR (100–102). Intravascular imaging can help to identify the cases of stent fracture overlooked on angiography, in the context of ISR (103, 104), particularly with overlapping of the proximal and distal fragments (99). Sometimes, stent fracture is followed by longitudinal overlapping that shows up as a single arc of double layers of stent struts in the same circumference on consecutive frames in the middle of a single stent (99). Three-dimensional OCT provides further help in challenging cases such as single strut fractures (105, 106). Nevertheless, stent-boost technology and multidetector computed tomography can frequently make the diagnosis obviating the need for dedicated intracoronary imaging (107, 108).

In a recent case series, our group reported that fracture, classified in four different patterns, typically results in a focal ISR at the fracture point (**Figure 10**) (109). In that study, we proposed an OCT-based classification in different patterns of increased severity (from single stacked struts to rupture and gap), and indeed, more complex fracture patterns were more common in the presence of device failure than in incidentally discovered fractures. In the same study, we also reported an association of stent fractures with stent eccentricity and asymmetry, which theoretically are among aspects that intracoronary imaging can help to optimize. Once a fracture is diagnosed, it is yet to be investigated in further studies how such imaging-based classification scheme would inform the management.

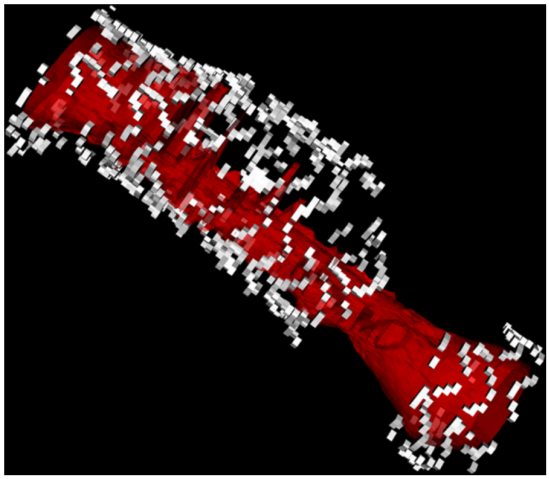

FIGURE 10
3D reconstruction of a stent fracture and gap associated with ISR (the lumen is depicted in red).

Longitudinal stent deformation

It is uncertain whether longitudinal stent deformation (LSD) relates to outcome including ISR. In a pooled analysis of patients treated with ZES and EES, rates of target lesion failure were numerically but not significantly higher in lesions with quantitative coronary angiography (QCA)-based LSD (110). However, in another study of EES-treated lesions, it was shown that LSD with resulting overlap leads to an excessive neointimal hyperplasia (NIH), ISR, and TLR (99). The mechanism is unclear but is probably non-uniform drug distribution.

Non-uniform strut distribution

Takebayashi et al. have demonstrated in patients with SES implanted stents, that non-uniform strut distribution represented by a larger maximum interstrut angle on IVUS analysis independently predicted NIH formation and subsequent restenosis (111).

Characterization of restenosis

Mehran et al. originally proposed an angiographic classification for ISR (classes I to IV) that predicted more

TLR with increasing ISR class (112). Although the classification was based on the geographic position of ISR on angiography in relation to the previously implanted stent, its accuracy was verified in the same study by IVUS. Despite that, the classification has several limitations; for instance, it was developed in the BMS era just as DES was dawning. Consequently, in RIBS-II trial, for example, which compared SES with balloon angioplasty as a treatment for ISR, the Mehran classification was unable to predict late loss in the SES group (113). On the other hand, such classification does not really address the possible underlying causes for ISR, nor does it describe the nature of the restenotic tissue itself. As a result, it would not be able to prescribe management pathways given the plethora of newly developed interventional tools available to tackle ISR.

Intracoronary imaging has greater sensitivity to detect and characterize ISR (114). In an IVUS study that investigated the patterns of ISR among different stent generations, BMS restenosis presented later with more NIH compared to DES (including both first- and second-generation DES). Additionally, the total stent length was longer in DES ISR, and the stent cross-sectional area at the site of the minimal luminal area (MLA) was smaller, compared to BMS ISR. Regarding the underlying mechanism, stent fracture was seen only in DES, but stent malapposition was seen equally across all stent generations (115). In a prospective multicenter registry conducted in Nordic and Baltic countries, IVUS showed that stent underexpansion was more common in DES ISR than in BMS ISR, and that DES more frequently had focal ISR compared to BMS, with less intimal hyperplasia (116).

Because of a higher resolution, OCT has permitted more detailed characterization of the underlying etiology of ISR. Furthermore, it highlighted the morphologic difference between DES-ISR and BMS-ISR (117). In other words, OCT allowed better characterization of the neointimal tissue type, including identification of in-stent neoatherosclerosis, which could potentially guide therapy. In BMS-ISR, the typical pattern is a homogeneous high-signal tissue band, which is a characteristic of neointimal hyperplasia, with high smooth muscle cell content (**Figure 11**). In contrast, DES-ISR is typically characterized by attenuated, layered, heterogeneous tissue, which may represent proteoglycan-rich neointimal tissue, or neoatherosclerotic plaque (**Figure 12**) (118). Regions of the so-called peri-strut low-intensity (PSLIA) have been associated with accelerated restenosis due to inflammation, proteoglycan accumulation, and edema (**Figure 13**). Therefore, whereas neointimal formation peaks at about 6 months after BMS implantation, neointimal formation after DES implantation is a dynamic process that could creep out to even 5 years (118). In-stent neoatherosclerosis can also cause DES failure, through intimal rupture and thrombus formation, which usually presents with an ACS rather than stable angina (26). Of note, some studies suggest that stent age (i.e., longer implant duration) rather than stent type is the strongest and most consistent predictor of neoatherosclerosis (119).

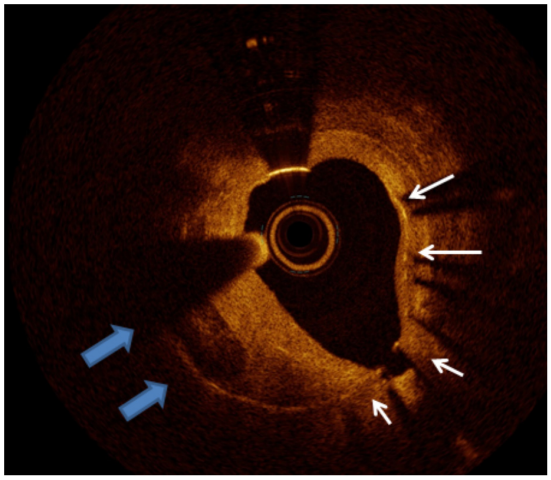

FIGURE 11
Calcific neointima. The white arrows mark the stent struts, the left quadrant arc occupied by neointima presenting calcific neoatherosclerosis. The remaining homogeneous neointima is compatible with fibrous tissue.

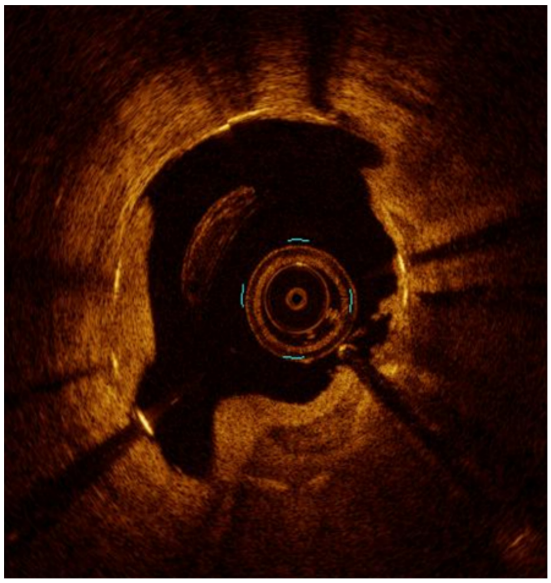

FIGURE 12
Neoatherosclerosis.

Similar findings have been elicited by integrated backscatter (IB) ultrasound which revealed more low-IB tissue in the neointima of late restenosis (detected at ≥13 months after stent implantation) than in that of early restenosis, suggesting neoatherosclerosis as one of the mechanisms of late ISR (120). Furthermore, in patients with DES ISR, it seems that the underlying mechanism can impact the restenotic tissue

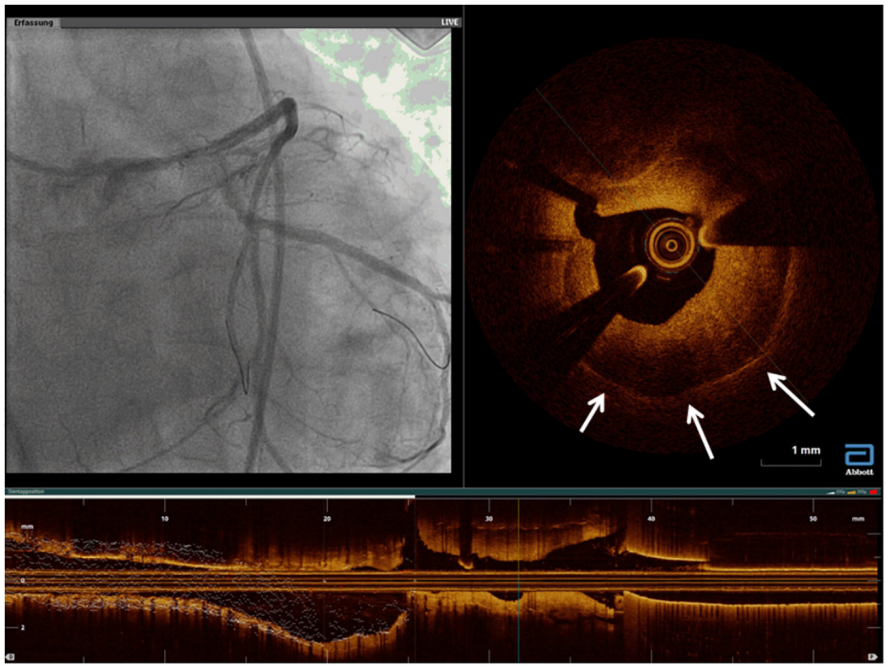

FIGURE 13
A case of rapidly growing in-stent restenosis of the left main (3 months from previous angiography). The white arrows mark areas of peri-strut low-intensity compatible with inflammatory processes and with a rapid progression of disease.

composition, e.g., stent fracture has been shown by IB-IVUS to be associated with larger lipid volume within the neointima, indicating a contribution to the development of neoatherosclerosis (121).

A classification of ISR has been proposed based on the qualitative OCT assessment of a small mixed sample of BMS and different generations of DES, where restenotic tissue was described as "layered," "homogeneous," or "heterogeneous." These patterns were not validated against histologic data, and no insights were provided as to the clinical and prognostic value (122). Recently, Yamamoto et al. proposed a novel classification of ISR after DES implantation, based on OCT imaging, that should be more accommodating of the different ISR tissues encountered. In total, six patterns were proposed (**Supplementary Figure 1**): Type I is a "homogeneous high-intensity tissue" pattern, representing neointimal tissue composed of smooth muscle cells in a proteoglycan and collagen-rich matrix; type II is a "heterogeneous tissue with signal attenuation" pattern and was the most frequent pattern reported, suggestive of delayed arterial healing and/or the presence of an organized thrombus; type III is a "speckled heterogeneous tissue" pattern, indicating organized thrombus and fibrinoids with smooth muscle cells poorly and focally distributed, probably an early phase of type II; type IV is a "heterogeneous tissue containing poorly delineated region with invisible struts," comprising atheromatous tissue, including large fibroatheroma or a large amount of foam cell accumulation within the neointima; type V is a "heterogeneous tissue containing sharply delineated low-intensity region," representing dense calcified plates; and type VI is a "bright protruding tissue with an irregular surface," representing calcified nodules. Because this classification has the potential to differentiate lipidic atherosclerotic neointima and calcified neointima from other neointimal tissue, it may help in guiding the treatment strategy. Although in high-lipid-content neoatherosclerosis, minimal lesion preparation would be preferable to reduce no-reflow and periprocedural infarction, in calcified neointima aggressive preparation is necessary to permit adequate stent expansion (123). Importantly, Imanaka et al. validated OCT patterns of neointimal tissue following DES implantation against histopathology and showed that the heterogeneous pattern with invisible strut on OCT identifies the presence of lipid atherosclerotic tissue within neointima (124). Systematic prospective studies are emerging to define the clinical implication of these morphological patterns on prognosis and management.

Another group used OCT gray-scale signal intensity to provide a quantitative neointimal analysis and expectedly found significantly different values among the different neointimal prototypes (homogeneous, non-homogeneous, and neoatherosclerosis), although different patterns coexisted in a significant proportion of ISR lesions. However, no correlation to the gold standard of histology was offered, nor is the impact on clinical and angiographic outcomes clear (125).

Evaluating restenosis by intravascular imaging vs. non-invasive imaging

Non-invasive imaging in the setting of ISR was primarily investigated as a method of surveillance/screening in lesions with a reported relatively high rate of ISR, e.g., LM PCI, to avoid resubjecting the patient to invasive coronary angiography for that purpose.

Van Mieghem et al. showed in a population undergoing LM stenting that multisclice computed tomography (CT) by a 16-slice scanner had good agreement for measuring the mean stent cross-sectional area but did not report the Bland-Altman results for the MLA (126). With the introduction of 64-slice multidetector CT (MDCT), Andreini et al. examined the agreement between luminal area measurements on CT to those on IVUS in a group of 24 patients. MDCT systematically underestimated the MLA compared to IVUS, with wide limits of agreement (127). Later, Veselka et al. have demonstrated that dual-source computed tomography (by measuring the MLA) can exclude in-segment restenosis after LM bifurcation stenting with a negative predictive value (NPV) of 97%, using IVUS-measured MLA as the gold standard (128).

Another very appealing application is the possibility of using CT to efficiently diagnose stent fracture, which as described is one of the underlying mechanisms for ISR (107, 108, 129, 130).

On the other hand, Kang et al. compared angiographic and IVUS assessment of ISR severity (LM and multivessel ISR were not included) to single-photon emission computed tomography (SPECT) as a measure of functional significance of the lesion. The overall diagnostic accuracy of IVUS-derived parameters to predict a positive SPECT was only 70% similar to that of angiography in the same study (an MLA cutoff $\leq$2.1 mm^2, which performed best among other parameters, had a positive predictive value (PPV) of only 62%, and a NPV of only 77%) (131). This can be attributed on the one hand to the inherent limitations of SPECT, e.g., artifacts, spatial resolution, the confounding effect of microcirculation, etc., with the potential of false positives and negatives, and on the other hand, to the multitude of factors that influence the IVUS assessment, e.g., the need for different cutoff MLA values for different lesion locations, varying vessel diameters, and different ethnicities or body habitus (15).

Management of restenosis

The initial step in ISR management is identifying the underlying cause which in turn dictates the treatment strategy (**Figure 14**). Intracoronary imaging can help to differentiate between a mechanical cause and a biological cause and discriminate between various mechanical causes. That said, clinical evidence supporting a clear advantage for routine intravascular imaging in ISR is still lacking. In other words, there is a lack of evidence on the use of individualized therapeutic strategies to target specific underlying ISR substrates detected by intravascular imaging, and whether this individualized approach improves clinical outcomes. Therefore, the 2018 ESC guidelines on myocardial revascularization give a class IIa C recommendation for the performance of IVUS and/or OCT to detect stent-related mechanical problems leading to restenosis (132). The use of intracoronary imaging is also recommended by a recent expert consensus of the EAPCI on the management of myocardial revascularization failure (133). Along the same lines, the 2021 ACC/AHA/SCAI guideline for coronary artery revascularization provides a class 2a C-LD recommendation for the use of IVUS or OCT to determine the mechanism of stent failure (134). Early on it seemed as if the only independent predictor of late clinical outcome after re-intervention for ISR was the final MLA obtained, regardless of the means used to achieve it (135). An optimal treatment algorithm is discussed in detail in two recent excellent reviews by Waksman et al. (114, 136). The algorithm overall is in line with the corroborating evidence available in different situations as presented below.

From a practical standpoint, in cases of stent undersizing or underexpansion (Waksman type I A), identifying the tissue composition can guide optimal device choice. Soft tissue will probably respond to treatment with high-pressure balloon inflation, whereas calcific lesions might require other devices including rotational atherectomy, intravascular lithotripsy (IVL), or excimer laser coronary angioplasty (ECLA). Similar calcium modification prior to DES would be needed in the case of calcific neoatherosclerosis (Waksman type II C) (136).

In retrospect, peri-stent calcium-related stent underexpansion can be detected by both IVUS and OCT, but OCT can better evaluate the thickness of calcium. It is often the result of the underutilization of calcium modification tools before stenting such as rotational or orbital atherectomy, or ECLA. Possible management options for this problem include rotational atherectomy, ECLA, and most recently IVL.

The off-label use of rotational atherectomy "stent-ablation" was reported in a small-sized retrospective non-randomized study to achieve a lower but acceptable rate of procedural success, and a similar rate of procedural complications compared to excimer laser with contrast media injection (if certain intraprocedural precautions are observed to avoid dissections and burr entrapment) (137). In another observational single-center study of 11 patients, stent-ablation had a high rate of procedural success (all but one patient), with MACE occurring in only one patient at a median follow-up of 26 months (138). In this situation, rotational atherectomy is capable of ablating metallic stent struts, but it is the fragmentation of any underlying calcific or fibrotic tissue surrounding the unexpanded stent that is thought to facilitate the following expansion of the stent (137). A third

Waksman In-Stent Restenosis Classification

Type	Definition		Therapeutic Guidance
I	Mechanical	Stent underexpansion (Type I A)	High pressure balloon, ELCA, or IVL. Underexpansion must be treated prior to further stent implantation
		Stent fracture (Type I B)	DES
II	Biologic	Neointimal hyperplasia (Type II A)	Balloon, DCB, DES, or VBT
		Neoatherosclerosis, non-calcified (Type II B)	DCB, or DES
		Neoatherosclerosis, calcified (Type II C)	Scoring balloon, ELCA, OA or RA prior to DES
III	Mixed pattern: Combined mechanical and biologic etiology		High-pressure NC balloon with DCB, DES, or VBT
IV	Chronic total occlusion		DCB or DES; VBT for multiple layers, CABG as needed
V	>2 layers of stent		Balloon, DCB, VBT, or CABG

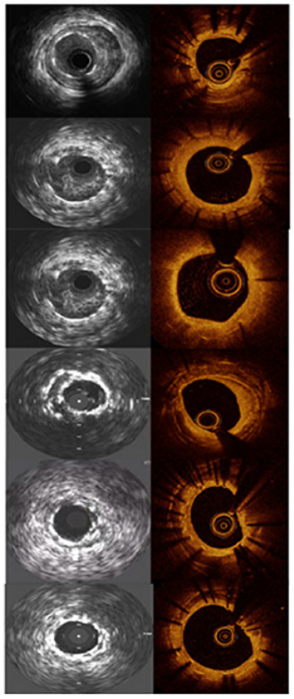

FIGURE 14
Imaging-guided treatment of ISR. ELCA, excimer laser coronary atherectomy; IVL, intravascular lithotripsy; DES, drug-eluting stent; DCB, drug-coated balloon; VBT, vascular brachytherapy; OA, orbital atherectomy; RA, rotational atherectomy; NC, non-compliant; CABG, coronary artery bypass graft. Reproduced with permission from Shlofmitz et al. (136).

group studied 12 patients in a prospective registry. Despite excellent procedural results, MACE occurred in 50% of patients at 6-month follow-up, which could be attributed at least in part to the modest outcomes and the higher intrinsic risk of such patients. Consequently, the authors emphasized the importance of ample lesion preparation upfront, to limit such bailout situations (139).

Several authors reported individual case reports of using ECLA to expand an undilatable stent, but the ELLEMENT registry was the first large prospective, multicenter observational registry (n = 28) to evaluate contrast-enhanced laser therapy to modify stented plaques resistant to high-pressure balloon expansion. Procedural success was achieved in 27 patients (96.4%), with MACE occurring only in two patients at 6-month follow-up (one death and one TLR) (140).

Recently, studies reported that OCT-diagnosed calcium can be effectively treated with IVL to induce calcium fracture and thus achieve larger final MLA and MSA independently of the eccentricity of the lesion (141–144). In the disrupt CAD III OCT substudy, the mechanism of calcium modification appeared to be circumferential and longitudinal calcium fractures (identified in almost 70% of the lesions), but the subsequent stent expansion and MSA were similar regardless of calcium fracture identification by OCT (144). The use of this device in ISR has been reported by several groups but is currently off-label (145–149). For instance, in a recent retrospective single-center analysis of six patients (two with calcium-mediated stent underexpansion, two with calcified neointima, and two with both), IVL with subsequent high-pressure balloon dilation (followed by DES implantation or drug-coated balloon (DCB) deployment) was feasible and safe and had promising short- and mid-term results in almost all patients (angiographic success was not achieved in one patient with residual stenosis >20%, but similar to others, no intraprocedural complications occurred) (150). Similarly, in a case series of 13 patients who had stent underexpansion even with the use of appropriately sized dedicated very high-pressure/cutting balloons (≥30 atm), IVL successfully allowed MSA gain in all cases, with no in-hospital or 30-day MACE (151). IVL balloon sizing was guided by intravascular imaging.

In a recent retrospective study of 50 patients who underwent IVL, 13 patients had ISR as the target lesion. Angiographic success occurred in 100% and none experienced death, MACE, or major bleeding at 30 days (152). Most recently, a prospective multicenter observational study of IVL in calcified coronary lesions included ISR with stent underexpansion in almost 30%

(n = 40) of the enrolled procedures. The primary endpoint of final procedural success was achieved in 97.5% of the ISR subgroup, with failure in only one patient (2.5%). Genuine MACE occurred in only two patients (one cardiac death due to procedure-related perforation, and another due to acute in-stent thrombosis), none of them in the ISR subgroup. Notably, rotablation was adjunctively used in 13.4% of the overall study population before IVL, and in 2.2% following IVL, suggesting that it could be complementary to IVL in particular situations to facilitate IVL balloon delivery or in case IVL was unable to adequately modify the lesion (153).

In cases where IVL is performed soon after the stenting procedure (within 6–12 months, if re-endothelialization is not yet complete), the impact on the integrity of the DES polymers is currently unknown and warrants evaluation (151, 154). Recently, Mousa and coworkers demonstrated in a case series of five patients with acute stent underexpansion in heavily calcified lesions, that angiographic success could be achieved in all cases, with no procedure-related MACE in the mid-term (follow-up ranged from 6 months to 24 months) (155). However, such theoretical risk of polymer damage might not be that relevant in the context of ISR, because by that time, most second-generation DES is fully re-endothelialized (156, 157).

In addition to peri-stent calcium with an underexpanded stent, calcified in-stent neoatherosclerosis can produce ISR (Waksman type II C). Reported cases show promising results with the use of IVL (complemented by rotational atherectomy in some instances) for managing such patients and illustrate the role of OCT in making the appropriate diagnosis and confirming an adequate result of IVL (158–160).

The other scenario is a well-expanded stent with excessive NIH (Waksman type II A), which is probably best treated with cutting or scoring balloons followed by DCB, an additional DES with an alternative drug (heterostenting), or vascular brachytherapy (VBT) (114).

Overall, DES and more recently DCB seem to be the most effective treatment approaches for ISR, backed by the results of several meta-analyses (161–164), with a recent collaborative meta-analysis pointing to a higher risk of TLR associated with paclitaxel-coated balloon (PCB) compared with DES, in the subgroup of patients with DES-ISR (165). It is worth noting that the enrolled trials in these meta-analyses included patients with both restenosed BMS and DES.

Tada et al. managed to show in a retrospective study that morphological assessment of the ISR tissue by OCT can guide the selection of the appropriate treatment strategy. This group compared different treatment strategies based on the OCT restenosis tissue characterization, in terms of mid-term ISR recurrence (re-ISR = binary restenosis on angiography) and TLR. The study population comprised a majority of patients with DES-ISR and a minority with BMS-ISR, and three strategies were compared: plain old balloon angioplasty (POBA) only, with high-pressure or scoring balloon inflated to almost rated burst pressure, POBA followed by PCB, or POBA followed by DES implantation and post-dilation. Importantly, PCB and DES performed equally across all tissue morphologies. Furthermore, in patients with homogeneous or high backscatter tissue pattern, PCI with POBA only was an independent predictor of re-ISR, which was attributed to the high proliferative activity of vascular smooth muscle cells in this lesion subset. Similarly, PCB and DES had lower ISR rates compared to POBA only, in patients with a layered neointima, but with no difference in TLR rates. Notably, such lesions include a certain amount of vascular smooth muscle cells in their adluminal layer. Contrarily, in patients with a heterogeneous or low backscatter neointima, there was no difference between the three treatment approaches, mostly due to the speculated excessive inflammation and hypersensitivity to drugs and/or polymers in this lesion pattern, where the use of a DES or PCB might aggravate inflammation (166). It is reasonable to infer that non-calcified neoatherosclerosis (Waksman type II B) can be approached in a similar manner (136).

Recently, the results of a pooled analysis of the OCT substudies of the RIBS IV and V prospective randomized clinical trials (patients with DES-ISR and BMS-ISR, respectively) have shown concurring results. The presence of neoatherosclerosis at the time of the index ISR procedure (detected by OCT) did not influence acute and long-term re-PCI outcomes (including angiographic and OCT outcomes at 6–9 months, and clinical outcomes at 3 years of follow-up). Moreover, these substudies suggested that both PCB and EES are effective and safe treatment options for ISR with neoatherosclerosis, although the limited sample size did not allow for more definitive conclusions as to the differential response to the chosen treatment (167).

When PCB was compared to EES, in the treatment of BMS ISR in 55 patients, OCT showed a better healing response in terms of stent strut coverage with PCB than EES, with no difference in the mean NIH area nor the luminal areas between the two treatments. Subsequently, there was no difference in the TLR rates either (168). Interestingly, Pleva et al. reported a significantly lower 12-month late luminal loss with PCB than with EES, when used to treat BMS restenosis, but with no difference in MACE (162). In contrast, the RIBS V trial has showed a lower rate of TLR at 3-year follow-up (with no difference in stent thrombosis rates) (169) with the use of EES than with PCB.

Bioresorbable vascular scaffolds (BVSs) emerged as another treatment option in ISR, where OCT proved to be helpful in optimizing implantation (170). However, late angiographic and clinical results were shown to be inferior to second generation DES (171–173).

In the very challenging subset of resistant/recurrent ISR, intracoronary imaging can be very helpful in delineating the number of stent layers at the lesion site, in addition to assessing the expansion of each stent layer. In the case of multiple layers of ISR, VBT is mostly the treatment of choice, as

further stent layers are to be avoided (114, 174, 175). DCB is another option to avoid multiple metallic layers. However, it was shown recently to be less effective for ISR lesions with three or more previously implanted stent layers, with significantly higher rates of the primary endpoint of MACE (mainly driven by TLR) and the secondary endpoint of TLR, both >40% at 1 year (176). Waksman et al. in their algorithm adopt the same approach that in the presence of >2 layers of stent (Waksman type V), an additional layer of stent should better be avoided (136). In cases where DES implantation is used to treat ISR, it has been illustrated by IVUS that stent underexpansion is a significant cause of recurrence, which highlights the importance of intravascular imaging to ensure adequate stent expansion (177).

In keeping with this, Yin et al. explored in a retrospective observational study the ISR characteristics by OCT that lead to repeat DES stenting underexpansion. The study included restenotic BMS, as well as first- and second-generation DES. Old stent underexpansion (MSA <4.5 mm^2 and expansion <70%), multiple layers of old stent, significant neointimal, or peri-stent calcium (maximum calcium angle >180° and/or maximum calcium thickness >0.5 mm) were all independently associated with new stent underexpansion, which in turn had a higher rate of myocardial infarction and TLR at 2 years (178). Therefore, in cases with significant calcium, disruption by ELCA or IVL should be considered to facilitate full expansion of the new stent, akin to *de novo* stenting.

Another subset for recurrent ISR is stent fracture (Waksman type I B), where repeat stenting with an EES or ZES was non-different from the use of DCB, in terms of 12-month binary re-restenosis and repeat TLR, which were unfortunately high in both groups (179). In contrast, another prospective large-scale study that assigned treatment for stent fracture-related ISR, depending on the fracture angiographic subtype (180) (repeat DES for type I/II, and balloon angioplasty for type III/IV), had lower repeat ISR and repeat TLR rates, which were not different from those in the non-fracture comparator group (102). In either study, intravascular imaging did not inform the choice of treatment, and therefore, its added value in that respect remains unexplored.

Knowledge gaps

Definitions of ISR based on intracoronary imaging need to be further validated in terms of clinical outcomes, to replace the angiographic restenosis that is as yet too often used as a study endpoint.

The most effective protocol (and tool) for imaging-guided stent implantation has to be determined, to avert the key mechanical problem of stent underexpansion but also to best recognize other predictors of stent failure. For instance, different intravascular imaging-based stent sizing approaches were proposed, including more conservative vs. more aggressive approaches, for selection of the appropriate stent diameter, but they have not been compared head-to-head, in terms of feasibility and clinical outcomes including ISR and clinically driven TLR.

Once the ISR has set in, there is a lack of evidence as to whether an individualized/tailored ISR management approach based on the underlying substrate/mechanism detected by intravascular imaging has an impact on clinical outcomes. In other words, treatment recommendations are largely based on the observational data and expert consensus rather than randomized controlled trials. Therefore, the added value of the systematic use of intracoronary imaging in guiding re-interventions is still unsettled. The results of the ongoing ILUMIEN IV trial (NCT03507777) and IMPROVE trial (NCT04221815) will help to better define the role of OCT and IVUS, respectively, in this regard (69, 181). An ideal treatment-oriented imaging-based classification would in particular enable the identification of lesions in which DCB angioplasty can provide sufficiently good outcomes without the need for additional stent implantation.

Newer technologies such as high-definition ultrasound warrant further head-to-head comparisons with established technologies such as OCT, in terms of PCI guidance, and impact on clinical outcomes.

Future directions

The cost-effectiveness of IVUS, particularly in patients at a greater risk of restenosis, has been shown (182). However, similar studies are needed for OCT to overcome the financial barrier in countries where the additional cost is prohibitive because of inadequate reimbursement. This will promote wider adoption and integration into routine practice.

Refinements in technology, such as lower-profile and more deliverable imaging catheters, faster pullbacks, higher resolution, and fully automated software to support online assessment, are expected to make the imaging technology more user-friendly and more widely adopted.

A recently developed 60-MHz high-definition IVUS (HD-IVUS) system tends to combine the advantages of IVUS and OCT, in the sense that it offers superior axial resolution compared to contemporary 40–45 MHz IVUS transducers (<40 vs. ~100 μm), faster catheter pullback speeds (10 vs. 0.5 mm/s), and more temporal resolution (60 vs. 30 frames/second) and yet maintains the advantage of greater imaging penetration relative to OCT, with visualization of the vessel wall (EEL) (183). Although data are still preliminary and derived from small-sized studies, each of HD-IVUS and OCT seems to maintain some of its original strengths. For example, in a prospective study of 29 lesions in 29 patients, HD-IVUS had an excellent concordance

with OCT on luminal area measurements, both pre- and post-intervention. However, before intervention, HD-IVUS offered better visualization of the EEL. Moreover, after intervention, OCT more frequently identified TP, stent-edge dissection, and ASM. It is still unclear whether this additional morphological information provided by OCT compared to HD-IVUS has clinical implications (184).

Another interesting development is the ultrafast single cardiac cycle OCT system developed by Kim et al. with a pullback speed of 100 mm/s, with the prospective ECG triggering technology, which enabled imaging of long coronary segments of a swine *in vivo* within one cardiac cycle, with minimal cardiac motion artifact. This technology has yet to be translated to clinical use (185).

In an attempt to obtain more physiologic insight by IVUS after stenting, it has been retrospectively shown that the difference in intraluminal intensity of blood speckle on IB-IVUS between the ostium of the target vessel and the distal reference of the implanted stent may predict TVR, based on its relationship to post-procedural FFR (186). This approach needs to be prospectively tested.

Author contributions

AA wrote the first draft of the manuscript. TG provided figures and supervision. Both authors are responsible for further revisions. Both authors contributed to the article and approved the submitted version.

Conflict of interest

The authors declare that the research was conducted in the absence of any commercial or financial relationships that could be construed as a potential conflict of interest.

Publisher's note

Supplementary material

The Supplementary Material for this article can be found online at: https://www.frontiersin.org/articles/10.3389/fcvm.2022.843734/full#supplementary-material

References

1. Dangas GD, Claessen BE, Caixeta A, Sanidas EA, Mintz GS, Mehran R. In-stent restenosis in the drug-eluting stent era. *J Am Coll Cardiol.* (2010) 56:1897–907.

2. Park DW, Hong MK, Mintz GS, Lee CW, Song JM, Han KH, et al. Two-year follow-up of the quantitative angiographic and volumetric intravascular ultrasound analysis after nonpolymeric paclitaxel-eluting stent implantation: Late "catch-up" phenomenon from ASPECT Study. *J Am Coll Cardiol.* (2006) 48:2432–9. doi: 10.1016/j.jacc.2006.08.033

3. Buccheri D, Piraino D, Andolina G, Cortese B. Understanding and managing in-stent restenosis: A review of clinical data, from pathogenesis to treatment. *J Thorac Dis.* (2016) 8:E1150–62.

4. Perera D, Postema P, Rashid R, Patel S, Blows L, Marber M, et al. Does a well developed collateral circulation predispose to restenosis after percutaneous coronary intervention? An intravascular ultrasound study. *Heart.* (2006) 92:763–7. doi: 10.1136/hrt.2005.067322

5. Roubin GS, King SB III, Douglas JS Jr. Restenosis after percutaneous transluminal coronary angioplasty: The Emory University Hospital experience. *Am J Cardiol.* (1987) 60:39B–43B.

6. Gould KL, Lipscomb K, Hamilton GW. Physiologic basis for assessing critical coronary stenosis. Instantaneous flow response and regional distribution during coronary hyperemia as measures of coronary flow reserve. *Am J Cardiol.* (1974) 33:87–94. doi: 10.1016/0002-9149(74)90743-7

7. Cutlip DE, Chauhan MS, Baim DS, Ho KK, Popma JJ, Carrozza JP, et al. Clinical restenosis after coronary stenting: Perspectives from multicenter clinical trials. *J Am Coll Cardiol.* (2002) 40:2082–9.

8. Rosenschein U, Topol EJ. Uncoupling clinical outcomes and coronary angiography: A review and perspective of recent trials in coronary artery disease. *Am Heart J.* (1996) 132:910–20. doi: 10.1016/s0002-8703(96)90335-x

9. Kuntz RE, Baim DS. Defining coronary restenosis. Newer clinical and angiographic paradigms. *Circulation.* (1993) 88:1310–23. doi: 10.1161/01.cir.88.3.1310

10. Mauri L, Orav EJ, Kuntz RE. Late loss in lumen diameter and binary restenosis for drug-eluting stent comparison. *Circulation.* (2005) 111:3435–42.

11. Garcia-Garcia HM, Shen Z, Piazza N. Study of restenosis in drug eluting stents: New insights from greyscale intravascular ultrasound and virtual histology. *EuroIntervention.* (2009) 5:D84–92.

12. Byrne RA, Joner M, Alfonso F, Kastrati A. Treatment of in-stent restenosis. In: Bhatt DL editor. *Cardiovascular intervention: A companion to Braunwald's heart disease.* (Amsterdam: Elsevier) (2016). p. 209–22.

13. Nishioka T, Amanullah AM, Luo H, Berglund H, Kim CJ, Nagai T, et al. Clinical validation of intravascular ultrasound imaging for assessment of coronary stenosis severity: Comparison with stress myocardial perfusion imaging. *J Am Coll Cardiol.* (1999) 33:1870–8.

14. Abizaid A, Mintz GS, Pichard AD, Kent KM, Satler LF, Walsh CL, et al. Clinical, intravascular ultrasound, and quantitative angiographic determinants of the coronary flow reserve before and after percutaneous transluminal coronary angioplasty. *Am J Cardiol.* (1998) 82:423–8.

15. Nogic J, Prosser H, O'Brien J, Thakur U, Soon K, Proimos G, et al. The assessment of intermediate coronary lesions using intracoronary imaging. *Cardiovasc Diagn Ther.* (2020) 10:1445–60.

16. Cutlip DE, Windecker S, Mehran R, Boam A, Cohen DJ, van Es GA, et al. Clinical end points in coronary stent trials: A case for standardized definitions. *Circulation.* (2007) 115:2344–51. doi: 10.1161/CIRCULATIONAHA.106.685313

17. Garcia-Garcia HM, McFadden EP, Farb A, Mehran R, Stone GW, Spertus J, et al. Standardized end point definitions for coronary intervention trials:

The academic research consortium-2 consensus document. *Circulation.* (2018) 137:2635–50.

18. Oemrawsingh PV, Mintz GS, Schalij MJ, Zwinderman AH, Jukema JW, van der Wall EE, et al. Intravascular ultrasound guidance improves angiographic and clinical outcome of stent implantation for long coronary artery stenoses: Final results of a randomized comparison with angiographic guidance (TULIP Study). *Circulation.* (2003) 107:62–7. doi: 10.1161/01.cir.0000043240.87526.3f

19. Fitzgerald PJ, Oshima A, Hayase M, Metz JA, Bailey SR, Baim DS, et al. Final results of the can routine ultrasound influence stent expansion (CRUISE) study. *Circulation.* (2000) 102:523–30. doi: 10.1161/01.cir.102.5.523

20. Parise H, Maehara A, Stone GW, Leon MB, Mintz GS. Meta-analysis of randomized studies comparing intravascular ultrasound versus angiographic guidance of percutaneous coronary intervention in pre-drug-eluting stent era. *Am J Cardiol.* (2011) 107:374–82. doi: 10.1016/j.amjcard.2010.09.030

21. Hur SH, Kang SJ, Kim YH, Ahn JM, Park DW, Lee SW, et al. Impact of intravascular ultrasound-guided percutaneous coronary intervention on long-term clinical outcomes in a real world population. *Catheter Cardiovasc Interv.* (2013) 81:407–16. doi: 10.1002/ccd.23279

22. Zhang Y, Farooq V, Garcia-Garcia HM, Bourantas CV, Tian N, Dong S, et al. Comparison of intravascular ultrasound versus angiography-guided drug-eluting stent implantation: A meta-analysis of one randomised trial and ten observational studies involving 19,619 patients. *EuroIntervention.* (2012) 8:855–65.

23. Ahn JM, Kang SJ, Yoon SH, Park HW, Kang SM, Lee JY, et al. Meta-analysis of outcomes after intravascular ultrasound-guided versus angiography-guided drug-eluting stent implantation in 26,503 patients enrolled in three randomized trials and 14 observational studies. *Am J Cardiol.* (2014) 113:1338–47. doi: 10.1016/j.amjcard.2013.12.043

24. Jang JS, Song YJ, Kang W, Jin HY, Seo JS, Yang TH, et al. Intravascular ultrasound-guided implantation of drug-eluting stents to improve outcome: A meta-analysis. *JACC Cardiovasc Interv.* (2014) 7:233–43.

25. Maehara A, Mintz GS, Witzenbichler B, Weisz G, Neumann FJ, Rinaldi MJ, et al. Relationship between intravascular ultrasound guidance and clinical outcomes after drug-eluting stents. *Circ Cardiovasc Interv.* (2018) 11:e006243.

26. Kang SJ, Mintz GS, Akasaka T, Park DW, Lee JY, Kim WJ, et al. Optical coherence tomographic analysis of in-stent neoatherosclerosis after drug-eluting stent implantation. *Circulation.* (2011) 123:2954–63.

27. Buccheri S, Franchina G, Romano S, Puglisi S, Venuti G, D'Arrigo P, et al. Clinical outcomes following intravascular imaging-guided versus coronary angiography-guided percutaneous coronary intervention with stent implantation: A systematic review and bayesian network meta-analysis of 31 studies and 17,882 patients. *JACC Cardiovasc Interv.* (2017) 10:2488–98. doi: 10.1016/j.jcin.2017.08.051

28. Chieffo A, Latib A, Caussin C, Presbitero P, Galli S, Menozzi A, et al. A prospective, randomized trial of intravascular-ultrasound guided compared to angiography guided stent implantation in complex coronary lesions: The AVIO trial. *Am Heart J.* (2013) 165:65–72. doi: 10.1016/j.ahj.2012.09.017

29. Choi KH, Song YB, Lee JM, Lee SY, Park TK, Yang JH, et al. Impact of intravascular ultrasound-guided percutaneous coronary intervention on long-term clinical outcomes in patients undergoing complex procedures. *JACC Cardiovasc Interv.* (2019) 12:607–20.

30. Witzenbichler B, Maehara A, Weisz G, Neumann FJ, Rinaldi MJ, Metzger DC, et al. Relationship between intravascular ultrasound guidance and clinical outcomes after drug-eluting stents: The assessment of dual antiplatelet therapy with drug-eluting stents (ADAPT-DES) study. *Circulation.* (2014) 129:463–70.

31. Hong SJ, Kim BK, Shin DH, Nam CM, Kim JS, Ko YG, et al. Effect of intravascular ultrasound-guided vs angiography-guided everolimus-eluting stent implantation: The IVUS-XPL randomized clinical trial. *JAMA.* (2015) 314:2155–63.

32. Zhang J, Gao X, Kan J, Ge Z, Han L, Lu S, et al. Intravascular ultrasound versus angiography-guided drug-eluting stent implantation: The ULTIMATE trial. *J Am Coll Cardiol.* (2018) 72:3126–37.

33. Hong SJ, Mintz GS, Ahn CM, Kim JS, Kim BK, Ko YG, et al. Effect of intravascular ultrasound-guided drug-eluting stent implantation: 5-year follow-up of the IVUS-XPL randomized trial. *JACC Cardiovasc Interv.* (2020) 13:62–71. doi: 10.1016/j.jcin.2019.09.033

34. Gao XF, Ge Z, Kong XQ, Kan J, Han L, Lu S, et al. 3-year outcomes of the ultimate Trial comparing intravascular ultrasound versus angiography-guided drug-eluting stent implantation. *JACC Cardiovasc Interv.* (2021) 14:247–57.

35. Prati F, Di Vito L, Biondi-Zoccai G, Occhipinti M, La Manna A, Tamburino C, et al. Angiography alone versus angiography plus optical coherence tomography to guide decision-making during percutaneous coronary intervention: The Centro per la lotta contro l'infarto-optimisation of percutaneous coronary intervention (CLI-OPCI) study. *EuroIntervention.* (2012) 8:823–9. doi: 10.4244/EIJV8I7A125

36. Prati F, Romagnoli E, Burzotta F, Limbruno U, Gatto L, La Manna A, et al. Clinical impact of OCT findings during PCI: The CLI-OPCI II study. *JACC Cardiovasc Imaging.* (2015) 8:1297–305. doi: 10.1016/j.jcmg.2015.08.013

37. Jones DA, Rathod KS, Koganti S, Hamshere S, Astroulakis Z, Lim P, et al. Angiography alone versus angiography plus optical coherence tomography to guide percutaneous coronary intervention: Outcomes from the Pan-London PCI Cohort. *JACC Cardiovasc Interv.* (2018) 11:1313–21. doi: 10.1016/j.jcin.2018.01.274

38. Meneveau N, Souteyrand G, Motreff P, Caussin C, Amabile N, Ohlmann P, et al. Optical coherence tomography to optimize results of percutaneous coronary intervention in patients with non-st-elevation acute coronary syndrome: Results of the multicenter, randomized doctors study (does optical coherence tomography optimize results of stenting). *Circulation.* (2016) 134:906–17.

39. Kubo T, Shinke T, Okamura T, Hibi K, Nakazawa G, Morino Y, et al. Optical frequency domain imaging vs. intravascular ultrasound in percutaneous coronary intervention (OPINION trial): One-year angiographic and clinical results. *Eur Heart J.* (2017) 38:3139–47. doi: 10.1093/eurheartj/ehx351

40. Mintz GS. Features and parameters of drug-eluting stent deployment discoverable by intravascular ultrasound. *Am J Cardiol.* (2007) 100:26M–35M. doi: 10.1016/j.amjcard.2007.08.019

41. Moussa I, Moses J, Di Mario C, Albiero R, De Gregorio J, Adamian M, et al. Does the specific intravascular ultrasound criterion used to optimize stent expansion have an impact on the probability of stent restenosis? *Am J Cardiol.* (1999) 83:1012–7. doi: 10.1016/s0002-9149(99)00006-5

42. Doi H, Maehara A, Mintz GS, Yu A, Wang H, Mandinov L, et al. Impact of post-intervention minimal stent area on 9-month follow-up patency of paclitaxel-eluting stents: An integrated intravascular ultrasound analysis from the TAXUS IV, V, and VI and TAXUS ATLAS workhorse, long lesion, and direct stent trials. *JACC Cardiovasc Interv.* (2009) 2:1269–75. doi: 10.1016/j.jcin.2009.10.005

43. Hong MK, Mintz GS, Lee CW, Park DW, Choi BR, Park KH, et al. Intravascular ultrasound predictors of angiographic restenosis after sirolimus-eluting stent implantation. *Eur Heart J.* (2006) 27:1305–10.

44. Song HG, Kang SJ, Ahn JM, Kim WJ, Lee JY, Park DW, et al. Intravascular ultrasound assessment of optimal stent area to prevent in-stent restenosis after zotarolimus-, everolimus-, and sirolimus-eluting stent implantation. *Catheter Cardiovasc Interv.* (2014) 83:873–8. doi: 10.1002/ccd.24560

45. Fujimura T, Matsumura M, Witzenbichler B, Metzger DC, Rinaldi MJ, Duffy PL, et al. Stent expansion indexes to predict clinical outcomes: An IVUS substudy from ADAPT-DES. *JACC Cardiovasc Interv.* (2021) 14:1639–50. doi: 10.1016/j.jcin.2021.05.019

46. Kang SJ, Ahn JM, Song H, Kim WJ, Lee JY, Park DW, et al. Comprehensive intravascular ultrasound assessment of stent area and its impact on restenosis and adverse cardiac events in 403 patients with unprotected left main disease. *Circ Cardiovasc Interv.* (2011) 4:562–9. doi: 10.1161/CIRCINTERVENTIONS.111.964643

47. Werner GS, Gastmann O, Ferrari M, Scholz KH, Schunemann S, Figulla HR. Determinants of stent restenosis in chronic coronary occlusions assessed by intracoronary ultrasound. *Am J Cardiol.* (1999) 83:1164–9.

48. Choi SY, Maehara A, Cristea E, Witzenbichler B, Guagliumi G, Brodie B, et al. Usefulness of minimum stent cross sectional area as a predictor of angiographic restenosis after primary percutaneous coronary intervention in acute myocardial infarction (from the HORIZONS-AMI Trial IVUS substudy). *Am J Cardiol.* (2012) 109:455–60. doi: 10.1016/j.amjcard.2011.10.005

49. Soeda T, Uemura S, Park SJ, Jang Y, Lee S, Cho JM, et al. Incidence and Clinical significance of poststent optical coherence tomography findings: One-year follow-up study from a multicenter registry. *Circulation.* (2015) 132:1020–9. doi: 10.1161/CIRCULATIONAHA.114.014704

50. Maehara A, Matsumura M, Ali ZA, Mintz GS, Stone GWIVUS-. Guided versus OCT-guided coronary stent implantation: A critical appraisal. *JACC Cardiovasc Imaging.* (2017) 10:1487–503. doi: 10.1016/j.jcmg.2017.09.008

51. Kubo T, Akasaka T, Shite J, Suzuki T, Uemura S, Yu B, et al. OCT compared with IVUS in a coronary lesion assessment: The OPUS-CLASS study. *JACC Cardiovasc Imaging.* (2013) 6:1095–104. doi: 10.1016/j.jcmg.2013.04.014

52. Habara M, Nasu K, Terashima M, Kaneda H, Yokota D, Ko E, et al. Impact of frequency-domain optical coherence tomography guidance for optimal coronary stent implantation in comparison with intravascular ultrasound guidance. *Circ Cardiovasc Interv.* (2012) 5:193–201.

53. Maehara A, Ben-Yehuda O, Ali Z, Wijns W, Bezerra HG, Shite J, et al. Comparison of stent expansion guided by optical coherence tomography versus intravascular ultrasound: The ILUMIEN II study (observational study of optical coherence tomography [OCT] in patients undergoing fractional flow reserve [FFR] and percutaneous coronary intervention). *JACC Cardiovasc Interv.* (2015) 8:1704–14. doi: 10.1016/j.jcin.2015.07.024

54. Ali ZA, Maehara A, Genereux P, Shlofmitz RA, Fabbiocchi F, Nazif TM, et al. Optical coherence tomography compared with intravascular ultrasound and with angiography to guide coronary stent implantation (ILUMIEN III: OPTIMIZE PCI): A randomised controlled trial. *Lancet.* (2016) 388:2618–28.

55. Mintz GS, Popma JJ, Pichard AD, Kent KM, Satler LF, Chuang YC, et al. Patterns of calcification in coronary artery disease. A statistical analysis of intravascular ultrasound and coronary angiography in 1155 lesions. *Circulation.* (1995) 91:1959–65. doi: 10.1161/01.cir.91.7.1959

56. Kostamaa H, Donovan J, Kasaoka S, Tobis J, Fitzpatrick L. Calcified plaque cross-sectional area in human arteries: Correlation between intravascular ultrasound and undecalcified histology. *Am Heart J.* (1999) 137:482–8. doi: 10.1016/s0002-8703(99)70496-5

57. Friedrich GJ, Moes NY, Muhlberger VA, Gabl C, Mikuz G, Hausmann D, et al. Detection of intralesional calcium by intracoronary ultrasound depends on the histologic pattern. *Am Heart J.* (1994) 128:435–41. doi: 10.1016/0002-8703(94)90614-9

58. Kobayashi Y, Okura H, Kume T, Yamada R, Kobayashi Y, Fukuhara K, et al. Impact of target lesion coronary calcification on stent expansion. *Circ J.* (2014) 78:2209–14.

59. Maejima N, Hibi K, Saka K, Akiyama E, Konishi M, Endo M, et al. Relationship between thickness of calcium on optical coherence tomography and crack formation after balloon dilatation in calcified plaque requiring rotational atherectomy. *Circ J.* (2016) 80:1413–9. doi: 10.1253/circj.CJ-15-1059

60. Fujino A, Mintz GS, Matsumura M, Lee T, Kim SY, Hoshino M, et al. A new optical coherence tomography-based calcium scoring system to predict stent underexpansion. *EuroIntervention.* (2018) 13:e2182–9. doi: 10.4244/EIJ-D-17-00962

61. Kubo T, Shimamura K, Ino Y, Yamaguchi T, Matsuo Y, Shiono Y, et al. Superficial calcium fracture after PCI as assessed by OCT. *JACC Cardiovasc Imaging.* (2015) 8:1228–9. doi: 10.1016/j.jcmg.2014.11.012

62. Park H, Ahn JM, Kang DY, Lee JB, Park S, Ko E, et al. Optimal stenting technique for complex coronary lesions: Intracoronary imaging-guided pre-dilation, stent sizing, and post-dilation. *JACC Cardiovasc Interv.* (2020) 13:1403–13. doi: 10.1016/j.jcin.2020.03.023

63. Kim BK, Shin DH, Hong MK, Park HS, Rha SW, Mintz GS, et al. Clinical impact of intravascular ultrasound-guided chronic total occlusion intervention with zotarolimus-eluting versus biolimus-eluting stent implantation: Randomized study. *Circ Cardiovasc Interv.* (2015) 8:e002592. doi: 10.1161/CIRCINTERVENTIONS.115.002592

64. Shlofmitz E, Torguson R, Zhang C, Craig PE, Mintz GS, Khalid N, et al. Impact of intravascular ultrasound on outcomes following percutaneous coronary intervention in complex lesions (iOPEN complex). *Am Heart J.* (2020) 221:74–83. doi: 10.1016/j.ahj.2019.12.008

65. Tian NL, Gami SK, Ye F, Zhang JJ, Liu ZZ, Lin S, et al. Angiographic and clinical comparisons of intravascular ultrasound- versus angiography-guided drug-eluting stent implantation for patients with chronic total occlusion lesions: Two-year results from a randomised AIR-CTO study. *EuroIntervention.* (2015) 10:1409–17. doi: 10.4244/EIJV10I12A245

66. Hong SJ, Kim BK, Shin DH, Kim JS, Hong MK, Gwon HC, et al. Usefulness of intravascular ultrasound guidance in percutaneous coronary intervention with second-generation drug-eluting stents for chronic total occlusions (from the multicenter Korean-chronic total occlusion registry). *Am J Cardiol.* (2014) 114:534–40. doi: 10.1016/j.amjcard.2014.05.027

67. Raber L, Mintz GS, Koskinas KC, Johnson TW, Holm NR, Onuma Y, et al. Clinical use of intracoronary imaging. Part 1: Guidance and optimization of coronary interventions. An expert consensus document of the European association of percutaneous cardiovascular interventions. *Eur Heart J.* (2018) 39:3281–300.

68. Ali ZA, Karimi Galougahi K, Maehara A, Shlofmitz RA, Fabbiocchi F, Guagliumi G, et al. Outcomes of optical coherence tomography compared with intravascular ultrasound and with angiography to guide coronary stent implantation: One-year results from the ILUMIEN III: OPTIMIZE PCI trial. *EuroIntervention.* (2021) 16:1085–91. doi: 10.4244/EIJ-D-20-00498

69. Ali Z, Landmesser U, Karimi Galougahi K, Maehara A, Matsumura M, Shlofmitz RA, et al. Optical coherence tomography-guided coronary stent implantation compared to angiography: A multicentre randomised trial in PCI – design and rationale of ILUMIEN IV: OPTIMAL PCI. *EuroIntervention.* (2021) 16:1092–9. doi: 10.4244/EIJ-D-20-00501

70. Costa MA, Angiolillo DJ, Tannenbaum M, Driesman M, Chu A, Patterson J, et al. Impact of stent deployment procedural factors on long-term effectiveness and safety of sirolimus-eluting stents (final results of the multicenter prospective STLLR trial). *Am J Cardiol.* (2008) 101:1704–11. doi: 10.1016/j.amjcard.2008.02.053

71. Sakurai R, Ako J, Morino Y, Sonoda S, Kaneda H, Terashima M, et al. Predictors of edge stenosis following sirolimus-eluting stent deployment (a quantitative intravascular ultrasound analysis from the SIRIUS trial). *Am J Cardiol.* (2005) 96:1251–3. doi: 10.1016/j.amjcard.2005.06.066

72. Liu J, Maehara A, Mintz GS, Weissman NJ, Yu A, Wang H, et al. An integrated TAXUS IV, V, and VI intravascular ultrasound analysis of the predictors of edge restenosis after bare metal or paclitaxel-eluting stents. *Am J Cardiol.* (2009) 103:501–6.

73. Kang SJ, Cho YR, Park GM, Ahn JM, Kim WJ, Lee JY, et al. Intravascular ultrasound predictors for edge restenosis after newer generation drug-eluting stent implantation. *Am J Cardiol.* (2013) 111:1408–14. doi: 10.1016/j.amjcard.2013.01.288

74. Ino Y, Kubo T, Matsuo Y, Yamaguchi T, Shiono Y, Shimamura K, et al. Optical coherence tomography predictors for edge restenosis after everolimus-eluting stent implantation. *Circ Cardiovasc Interv.* (2016) 9:e004231. doi: 10.1161/CIRCINTERVENTIONS.116.004231

75. Koyama K. A prospective, single-center, ramdomized study to assess whether co-registration of OCT and angiography can reduce geographic miss. (2016). TCTMD; October. doi: 10.1002/ccd.27854

76. Schwartz RS, Huber KC, Murphy JG, Edwards WD, Camrud AR, Vlietstra RE, et al. Restenosis and the proportional neointimal response to coronary artery injury: Results in a porcine model. *J Am Coll Cardiol.* (1992) 19:267–74. doi: 10.1016/0735-1097(92)90476-4

77. Kobayashi N, Mintz GS, Witzenbichler B, Metzger DC, Rinaldi MJ, Duffy PL, et al. Prevalence, features, and prognostic importance of edge dissection after drug-eluting stent implantation: An ADAPT-DES intravascular ultrasound substudy. *Circ Cardiovasc Interv.* (2016) 9:e003553. doi: 10.1161/CIRCINTERVENTIONS.115.003553

78. Radu MD, Raber L, Heo J, Gogas BD, Jorgensen E, Kelbaek H, et al. Natural history of optical coherence tomography-detected non-flow-limiting edge dissections following drug-eluting stent implantation. *EuroIntervention.* (2014) 9:1085–94. doi: 10.4244/EIJV9I9A183

79. Hong MK, Park SW, Lee NH, Nah DY, Lee CW, Kang DH, et al. Long-term outcomes of minor dissection at the edge of stents detected with intravascular ultrasound. *Am J Cardiol.* (2000) 86:791–5,A9. doi: 10.1016/s0002-9149(00)01085-7

80. Sheris SJ, Canos MR, Weissman NJ. Natural history of intravascular ultrasound-detected edge dissections from coronary stent deployment. *Am Heart J.* (2000) 139:59–63. doi: 10.1016/s0002-8703(00)90309-0

81. Kume T, Okura H, Miyamoto Y, Yamada R, Saito K, Tamada T, et al. Natural history of stent edge dissection, tissue protrusion and incomplete stent apposition detectable only on optical coherence tomography after stent implantation - preliminary observation. *Circ J.* (2012) 76:698–703. doi: 10.1253/circj.cj-11-0845

82. Chamie D, Bezerra HG, Attizzani GF, Yamamoto H, Kanaya T, Stefano GT, et al. Incidence, predictors, morphological characteristics, and clinical outcomes of stent edge dissections detected by optical coherence tomography. *JACC Cardiovasc Interv.* (2013) 6:800–13. doi: 10.1016/j.jcin.2013.03.019

83. De Cock D, Bennett J, Ughi GJ, Dubois C, Sinnaeve P, Dhooge J, et al. Healing course of acute vessel wall injury after drug-eluting stent implantation assessed by optical coherence tomography. *Eur Heart J Cardiovasc Imaging.* (2014) 15:800–9.

84. Kawamori H, Shite J, Shinke T, Otake H, Matsumoto D, Nakagawa M, et al. Natural consequence of post-intervention stent malapposition, thrombus, tissue prolapse, and dissection assessed by optical coherence tomography at mid-term follow-up. *Eur Heart J Cardiovasc Imaging.* (2013) 14:865–75. doi: 10.1093/ehjci/jes299

85. Prati F, Romagnoli E, La Manna A, Burzotta F, Gatto L, Marco V, et al. Long-term consequences of optical coherence tomography findings during percutaneous coronary intervention: The centro per la lotta contro l'infarto – Optimization of percutaneous coronary intervention (CLI-OPCI) LATE study. *EuroIntervention.* (2018) 14:e443–51. doi: 10.4244/EIJ-D-17-01111

86. Bouki KP, Sakkali E, Toutouzas K, Vlad D, Barmperis D, Phychari S, et al. Impact of coronary artery stent edge dissections on long-term clinical outcome in patients with acute coronary syndrome: An optical coherence tomography study. *Catheter Cardiovasc Interv.* (2015) 86:237–46. doi: 10.1002/ccd.25855

87. van Zandvoort LJC, Tomaniak M, Tovar Forero MN, Masdjedi K, Visseren L, Witberg K, et al. Predictors for clinical outcome of untreated stent edge dissections as detected by optical coherence tomography. *Circ Cardiovasc Interv.* (2020) 13:e008685.

88. Hong MK, Park SW, Lee CW, Kang DH, Song JK, Kim JJ, et al. Long-term outcomes of minor plaque prolapsed within stents documented with intravascular ultrasound. *Catheter Cardiovasc Interv.* (2000) 51:22–6. doi: 10.1002/1522-726x(200009)51:1<22::aid-ccd6>3.0.co;2-i

89. Futamatsu H, Sabate M, Angiolillo DJ, Jimenez-Quevedo P, Corros C, Morikawa-Futamatsu K, et al. Characterization of plaque prolapse after drug-eluting stent implantation in diabetic patients: A three-dimensional volumetric

intravascular ultrasound outcome study. *J Am Coll Cardiol.* (2006) 48:1139–45. doi: 10.1016/j.jacc.2006.05.050

90. Qiu F, Mintz GS, Witzenbichler B, Metzger DC, Rinaldi MJ, Duffy PL, et al. Prevalence and clinical impact of tissue protrusion after stent implantation: An ADAPT-DES intravascular ultrasound substudy. *JACC Cardiovasc Interv.* (2016) 9:1499–507. doi: 10.1016/j.jcin.2016.05.043

91. Gutierrez-Chico JL, Wykrzykowska J, Nuesch E, van Geuns RJ, Koch KT, Koolen JJ, et al. Vascular tissue reaction to acute malapposition in human coronary arteries: Sequential assessment with optical coherence tomography. *Circ Cardiovasc Interv.* (2012) 5:S1–8. doi: 10.1161/CIRCINTERVENTIONS.111.965301

92. Shimamura K, Kubo T, Akasaka T, Kozuma K, Kimura K, Kawamura M, et al. Outcomes of everolimus-eluting stent incomplete stent apposition: A serial optical coherence tomography analysis. *Eur Heart J Cardiovasc Imaging.* (2015) 16:23–8.

93. Sotomi Y, Onuma Y, Dijkstra J, Miyazaki Y, Kozuma K, Tanabe K, et al. Fate of post-procedural malapposition of everolimus-eluting polymeric bioresorbable scaffold and everolimus-eluting cobalt chromium metallic stent in human coronary arteries: Sequential assessment with optical coherence tomography in ABSORB Japan trial. *Eur Heart J Cardiovasc Imaging.* (2018) 19:59–66. doi: 10.1093/ehjci/jew329

94. Im E, Kim BK, Ko YG, Shin DH, Kim JS, Choi D, et al. Incidences, predictors, and clinical outcomes of acute and late stent malapposition detected by optical coherence tomography after drug-eluting stent implantation. *Circ Cardiovasc Interv.* (2014) 7:88–96. doi: 10.1161/CIRCINTERVENTIONS.113.000797

95. Romagnoli E, Gatto L, La Manna A, Burzotta F, Taglieri N, Saia F, et al. Role of residual acute stent malapposition in percutaneous coronary interventions. *Catheter Cardiovasc Interv.* (2017) 90:566–75.

96. Prati F, Romagnoli E, Gatto L, La Manna A, Burzotta F, Limbruno U, et al. Clinical impact of suboptimal stenting and residual intrastent plaque/thrombus protrusion in patients with acute coronary syndrome: The CLI-OPCI ACS substudy (centro per la lotta contro l'infarto-optimization of percutaneous coronary intervention in acute coronary syndrome). *Circ Cardiovasc Interv.* (2016) 9:e003726. doi: 10.1161/CIRCINTERVENTIONS.115.003726

97. Steinberg DH, Mintz GS, Mandinov L, Yu A, Ellis SG, Grube E, et al. Long-term impact of routinely detected early and late incomplete stent apposition: An integrated intravascular ultrasound analysis of the TAXUS IV, V, and VI and TAXUS ATLAS workhorse, long lesion, and direct stent studies. *JACC Cardiovasc Interv.* (2010) 3:486–94. doi: 10.1016/j.jcin.2010.03.007

98. Wang B, Mintz GS, Witzenbichler B, Souza CF, Metzger DC, Rinaldi MJ, et al. Predictors and long-term clinical impact of acute stent malapposition: An assessment of dual antiplatelet therapy with drug-eluting stents (ADAPT-DES) intravascular ultrasound substudy. *J Am Heart Assoc.* (2016) 5:e004438. doi: 10.1161/JAHA.116.004438

99. Inaba S, Mintz GS, Yun KH, Yakushiji T, Shimizu T, Kang SJ, et al. Mechanical complications of everolimus-eluting stents associated with adverse events: An intravascular ultrasound study. *EuroIntervention.* (2014) 9:1301–8. doi: 10.4244/EIJV9I11A220

100. Chakravarty T, White AJ, Buch M, Naik H, Doctor N, Schapira J, et al. Meta-analysis of incidence, clinical characteristics and implications of stent fracture. *Am J Cardiol.* (2010) 106:1075–80. doi: 10.1016/j.amjcard.2010.06.010

101. Kuramitsu S, Iwabuchi M, Haraguchi T, Domei T, Nagae A, Hyodo M, et al. Incidence and clinical impact of stent fracture after everolimus-eluting stent implantation. *Circ Cardiovasc Interv.* (2012) 5:663–71.

102. Kan J, Ge Z, Zhang JJ, Liu ZZ, Tian NL, Ye F, et al. Incidence and clinical outcomes of stent fractures on the basis of 6,555 patients and 16,482 drug-eluting stents from 4 centers. *JACC Cardiovasc Interv.* (2016) 9:1115–23. doi: 10.1016/j.jcin.2016.02.025

103. Lee S-H, Park J-S, Shin D-G, Kim Y-J, Hong G-R, Kim W, et al. Frequency of stent fracture as a cause of coronary restenosis after sirolimus-eluting stent implantation. *Am J Card.* (2007) 100:627–30.

104. Yamada KP, Koizumi T, Yamaguchi H, Kaneda H, Bonneau HN, Honda Y, et al. Serial angiographic and intravascular ultrasound analysis of late stent strut fracture of sirolimus-eluting stents in native coronary arteries. *Int J Cardiol.* (2008) 130:255–9. doi: 10.1016/j.ijcard.2007.08.082

105. Okamura T, Matsuzaki M. Sirolimus-eluting stent fracture detection by three-dimensional optical coherence tomography. *Catheter Cardiovasc Interv.* (2012) 79:628–32. doi: 10.1002/ccd.23268

106. Hiltrop N, De Cock D, Ferdinande B, Adriaenssens T. Detailed in vivo visualization of stent fracture causing focal restenosis using 3D reconstruction software for high-resolution optical coherence tomography images. *Eur Heart J Cardiovasc Imaging.* (2014) 15:714. doi: 10.1093/ehjci/jet273

107. Acar RD, Bulut M, Akcakoyun M. Are we aware of stent fracture? *Herz.* (2015) 40:417–22.

108. Alexopoulos D, Xanthopoulou I. Coronary stent fracture: how frequent it is? Does it matter? *Hellenic J Cardiol.* (2011) 52:1–5.

109. Schochlow K, Weissner M, Blachutzik F, Boeder NF, Trobs M, Lorenz L, et al. Coronary stent strut fractures: Classification, prevalence and clinical associations. *J Clin Med.* (2021) 10:1765. doi: 10.3390/jcm10081765

110. Rhee TM, Park KW, Lee JM, Lee MS, Jeon KH, Kang HJ, et al. Predictors and long-term clinical outcome of longitudinal stent deformation: Insights from pooled analysis of korean multicenter drug-eluting stent cohort. *Circ Cardiovasc Interv.* (2017) 10:e005518. doi: 10.1161/CIRCINTERVENTIONS.117.005518

111. Takebayashi H, Mintz GS, Carlier SG, Kobayashi Y, Fujii K, Yasuda T, et al. Nonuniform strut distribution correlates with more neointimal hyperplasia after sirolimus-eluting stent implantation. *Circulation.* (2004) 110:3430–4. doi: 10.1161/01.CIR.0000148371.53174.05

112. Mehran R, Dangas G, Abizaid AS, Mintz GS, Lansky AJ, Satler LF, et al. Angiographic patterns of in-stent restenosis: Classification and implications for long-term outcome. *Circulation.* (1999) 100:1872–8. doi: 10.1161/01.cir.100.18.1872

113. Alfonso F, Perez-Vizcayno MJ, Hernandez R, Bethencourt A, Marti V, Lopez-Minguez JR, et al. A randomized comparison of sirolimus-eluting stent with balloon angioplasty in patients with in-stent restenosis: Results of the restenosis intrastent: Balloon angioplasty versus elective sirolimus-eluting stenting (RIBS-II) trial. *J Am Coll Cardiol.* (2006) 47:2152–60. doi: 10.1016/j.jacc.2005.10.078

114. Shlofmitz E, Iantorno M, Waksman R. Restenosis of drug-eluting stents: A new classification system based on disease mechanism to guide treatment and state-of-the-art review. *Circ Cardiovasc Interv.* (2019) 12:e007023.

115. Goto K, Zhao Z, Matsumura M, Dohi T, Kobayashi N, Kirtane AJ, et al. Mechanisms and patterns of intravascular ultrasound in-stent restenosis among bare metal stents and first- and second-generation drug-eluting stents. *Am J Cardiol.* (2015) 116:1351–7.

116. Jensen LO, Vikman S, Antonsen L, Kosonen P, Niemela M, Christiansen EH, et al. Intravascular ultrasound assessment of minimum lumen area and intimal hyperplasia in in-stent restenosis after drug-eluting or bare-metal stent implantation. The Nordic Intravascular Ultrasound Study (NIVUS). *Cardiovasc Revasc Med.* (2017) 18:577–82.

117. Her AY, Shin ES. Current management of in-stent restenosis. *Korean Circ J.* (2018) 48:337–49.

118. Byrne RA, Joner M, Tada T, Kastrati A. Restenosis in bare metal and drug-eluting stents: Distinct mechanistic insights from histopathology and optical intravascular imaging. *Minerva Cardioangiol.* (2012) 60:473–89.

119. Song L, Mintz GS, Yin D, Yamamoto MH, Chin CY, Matsumura M, et al. Neoatherosclerosis assessed with optical coherence tomography in restenotic bare metal and first- and second-generation drug-eluting stents. *Int J Cardiovasc Imaging.* (2017) 33:1115–24. doi: 10.1007/s10554-017-1106-2

120. Ando H, Suzuki A, Sakurai S, Kumagai S, Kurita A, Waseda K, et al. Tissue characteristics of neointima in late restenosis: Integrated backscatter intravascular ultrasound analysis for in-stent restenosis. *Heart Vessels.* (2017) 32:531–8. doi: 10.1007/s00380-016-0903-1

121. Uchida Y, Ichimiya S, Ishii H, Oishi H, Aoki T, Miki Y, et al. Impact of coronary stent fracture on restenotic neointimal tissue characterization after drug-eluting stent implantation. *Int Heart J.* (2017) 58:861–7. doi: 10.1536/ihj.16-571

122. Gonzalo N, Serruys PW, Okamura T, van Beusekom HM, Garcia-Garcia HM, van Soest G, et al. Optical coherence tomography patterns of stent restenosis. *Am Heart J.* (2009) 158:284–93.

123. Yamamoto W, Fujii K, Otsuji S, Takiuchi S, Kakishita M, Ibuki M, et al. Optical coherence tomography characteristics of in-stent restenosis after drug-eluting stent implantation: A novel classification and its clinical significance. *Heart Vessels.* (2020) 35:38–45. doi: 10.1007/s00380-019-01461-7

124. Imanaka T, Fujii K, Hao H, Shibuya M, Saita T, Kawakami R, et al. Ex vivo assessment of neointimal characteristics after drug-eluting stent implantation: Optical coherence tomography and histopathology validation study. *Int J Cardiol.* (2016) 221:1043–7. doi: 10.1016/j.ijcard.2016.07.110

125. Xhepa E, Byrne RA, Rivero F, Rroku A, Cuesta J, Ndrepepa G, et al. Qualitative and quantitative neointimal characterization by optical coherence tomography in patients presenting with in-stent restenosis. *Clin Res Cardiol.* (2019) 108:1059–68. doi: 10.1007/s00392-019-01439-5

126. Van Mieghem CA, Cademartiri F, Mollet NR, Malagutti P, Valgimigli M, Meijboom WB, et al. Multislice spiral computed tomography for the evaluation of stent patency after left main coronary artery stenting: A comparison with conventional coronary angiography and intravascular ultrasound. *Circulation.* (2006) 114:645–53. doi: 10.1161/CIRCULATIONAHA.105.608950

127. Andreini D, Pontone G, Bartorelli AL, Trabattoni D, Mushtaq S, Bertella E, et al. Comparison of feasibility and diagnostic accuracy of 64-slice multidetector computed tomographic coronary angiography versus invasive coronary angiography versus intravascular ultrasound for evaluation of in-stent restenosis. *Am J Cardiol.* (2009) 103:1349–58. doi: 10.1016/j.amjcard.2009.01.343

128. Veselka J, Cadova P, Adla T, Zemanek D. Dual-source computed tomography angiography and intravascular ultrasound assessment of restenosis in patients after coronary stenting for bifurcation left main stenosis: A pilot study. *Arch Med Sci.* (2012) 8:455–61. doi: 10.5114/aoms.2012.29220

129. Pang JH, Kim D, Beohar N, Meyers SN, Lloyd-Jones D, Yaghmai V. Detection of stent fractures: A comparison of 64-slice CT, conventional cine-angiography, and intravascular ultrasonography. *Acad Radiol.* (2009) 16:412–7. doi: 10.1016/j.acra.2008.10.010

130. Li P, Gai L. Coronary stent fracture detected by multidetector computed tomography. *Int J Cardiovasc Imaging.* (2010) 26:729–30.

131. Kang SJ, Cho YR, Park GM, Ahn JM, Han SB, Lee JY, et al. Predictors for functionally significant in-stent restenosis: An integrated analysis using coronary angiography, IVUS, and myocardial perfusion imaging. *JACC Cardiovasc Imaging.* (2013) 6:1183–90. doi: 10.1016/j.jcmg.2013.09.006

132. Neumann FJ, Sousa-Uva M, Ahlsson A, Alfonso F, Banning AP, Benedetto U, et al. [2018 ESC/EACTS guidelines on myocardial revascularization. The Task Force on myocardial revascularization of the European society of cardiology (ESC) and EUROPEAN (EACTS)]. *G Ital Cardiol (Rome)* (2019) 20:1S–61S.

133. Stefanini GG, Alfonso F, Barbato E, Byrne RA, Capodanno D, Colleran R, et al. Management of myocardial revascularisation failure: An expert consensus document of the EAPCI. *EuroIntervention.* (2020) 16:e875–90. doi: 10.4244/EIJ-D-20-00487

134. Lawton JS, Tamis-Holland JE, Bangalore S, Bates ER, Beckie TM, Bischoff JM, et al. 2021 ACC/AHA/SCAI guideline for coronary artery revascularization: A report of the American college of cardiology/American heart association joint committee on clinical practice Guidelines. *Circulation* (2021):145:e4–17.

135. Schiele F, Meneveau N, Seronde MF, Deforet MF, Gupta S, Bassand JP. Predictors of event-free survival after repeat intracoronary procedure for in-stent restenosis; Study with angiographic and intravascular ultrasound imaging. *Eur Heart J.* (2000) 21:754–62. doi: 10.1053/euhj.1999.1906

136. Shlofmitz E, Case BC, Chen Y, Chezar-Azerrad C, Hashim H, Garcia-Garcia HM, et al. Waksman in-stent restenosis classification: A mechanism-based approach to the treatment of restenosis. *Cardiovasc Revasc Med.* (2021) 33:62–7. doi: 10.1016/j.carrev.2021.06.004

137. Ferri LA, Jabbour RJ, Giannini F, Benincasa S, Ancona M, Regazzoli D, et al. Safety and efficacy of rotational atherectomy for the treatment of undilatable underexpanded stents implanted in calcific lesions. *Catheter Cardiovasc Interv.* (2017) 90:E19–24. doi: 10.1002/ccd.26836

138. Hernandez-Enriquez M, Campelo-Parada F, Lhermusier T, Bouisset F, Roncalli J, Elbaz M, et al. Long-term outcomes of rotational atherectomy of underexpanded stents. A single center experience. *J Interv Cardiol.* (2018) 31:465–70. doi: 10.1111/joic.12491

139. Edes IF, Ruzsa Z, Szabo G, Lux A, Geller L, Molnar L, et al. Rotational atherectomy of undilatable coronary stents: Stentablation, a clinical perspective and recommendation. *EuroIntervention.* (2016) 12:e632–5. doi: 10.4244/EIJV12I5A103

140. Latib A, Takagi K, Chizzola G, Tobis J, Ambrosini V, Niccoli G, et al. Excimer laser lesion modification to expand non-dilatable stents: The ELLEMENT registry. *Cardiovasc Revasc Med.* (2014) 15:8–12. doi: 10.1016/j.carrev.2013.10.005

141. Blachutzik F, Honton B, Escaned J, Hill JM, Werner N, Banning AP, et al. Safety and effectiveness of coronary intravascular lithotripsy in eccentric calcified coronary lesions: A patient-level pooled analysis from the Disrupt CAD I and CAD II Studies. *Clin Res Cardiol.* (2021) 110:228–36. doi: 10.1007/s00392-020-01737-3

142. Mattesini A, Nardi G, Martellini A, Sorini Dini C, Hamiti B, Stolcova M, et al. Intravascular imaging to guide lithotripsy in concentric and eccentric calcific coronary lesions. *Cardiovasc Revasc Med.* (2020) 21:1099–105. doi: 10.1016/j.carrev.2020.04.016

143. Alfonso F, Bastante T, Antuna P, de la Cuerda F, Cuesta J, Garcia-Guimaraes M, et al. Coronary lithoplasty for the treatment of undilatable calcified de novo and in-stent restenosis lesions. *JACC Cardiovasc Interv.* (2019) 12:497–9.

144. Hill JM, Kereiakes DJ, Shlofmitz RA, Klein AJ, Riley RF, Price MJ, et al. Intravascular lithotripsy for treatment of severely calcified coronary artery disease. *J Am Coll Cardiol.* (2020) 76:2635–46.

145. Szolc P, Guzik B, Wiewiorka L, Niewiara L, Kleczynski P, Legutko J. Intravascular lithotripsy for the treatment of a heavily calcified recurrent in-stent restenosis in patient with chronic coronary syndrome. *Kardiol Pol.* (2021) 79:1159–60. doi: 10.33963/KP.a2021.0079

146. Ali ZA, McEntegart M, Hill JM, Spratt JC. Intravascular lithotripsy for treatment of stent underexpansion secondary to severe coronary calcification. *Eur Heart J.* (2020) 41:485–6.

147. Kalogeropoulos AS, Karamasis GV, Pavlidis AN, Papadothomakos N, Sakadakis E, Vardas P, et al. Combined shockwave intravascular lithotripsy and ultrahigh-pressure balloon dilatation for the treatment of stent underexpansion secondary to severe coronary calcification. *Kardiol Pol.* (2021) 79:205–6. doi: 10.33963/KP.15753

148. Tovar Forero MN, Van Mieghem NM, Daemen J. Stent underexpansion due to heavy coronary calcification resistant to rotational atherectomy: A case for coronary lithoplasty? *Catheter Cardiovasc Interv.* (2020) 96:598–600. doi: 10.1002/ccd.28641

149. Tovar Forero MN, Wilschut J, Van Mieghem NM, Daemen J. Coronary lithoplasty: A novel treatment for stent underexpansion. *Eur Heart J.* (2019) 40:221. doi: 10.1093/eurheartj/ehy593

150. Brunner FJ, Becher PM, Waldeyer C, Zengin-Sahm E, Schnabel RB, Clemmensen P, et al. Intravascular lithotripsy for the treatment of calcium-mediated coronary in-stent restenoses. *J Invasive Cardiol.* (2021) 33:E25–31.

151. Yeoh J, Cottens D, Cosgrove C, Mallek K, Strange J, Anderson R, et al. Management of stent underexpansion using intravascular lithotripsy-defining the utility of a novel device. *Catheter Cardiovasc Interv.* (2021) 97:22–9. doi: 10.1002/ccd.28715

152. Wiens EJ, Sklar JC, Wei YH, Aleem Q, Minhas K. Real-world outcomes in treatment of highly calcified coronary lesions with intravascular shockwave lithotripsy. *Indian Heart J.* (2021) 73:653–5. doi: 10.1016/j.ihj.2021.09.002

153. El Jattari H, Holvoet W, De Roeck F, Cottens D, Ungureanu C, Bennett J, et al. Intracoronary lithotripsy in calcified coronary lesions: A multicenter observational study. *J Invasive Cardiol.* (2022) 34:E24–31.

154. Nikolakopoulos I, Vemmou E, Xenogiannis I, Brilakis ES. Combined use of intravascular lithotripsy and brachytherapy: A new approach for the treatment of recurrent coronary in-stent restenosis. *Catheter Cardiovasc Interv.* (2021) 97:1402–6. doi: 10.1002/ccd.29332

155. Mousa MAA, Bingen BO, Amri IA, Digiacomo S, Karalis I, Jukema JW, et al. Bail-out intravascular lithotripsy for the treatment of acutely underexpanded stents in heavily calcified coronary lesions: A case series. *Cardiovasc Revasc Med.* (2022) 40:189–94. doi: 10.1016/j.carrev.2021.12.002

156. Otsuka F, Vorpahl M, Nakano M, Foerst J, Newell JB, Sakakura K, et al. Pathology of second-generation everolimus-eluting stents versus first-generation sirolimus– and paclitaxel-eluting stents in humans. *Circulation.* (2014) 129:211–23.

157. Inoue T, Shite J, Yoon J, Shinke T, Otake H, Sawada T, et al. Optical coherence evaluation of everolimus-eluting stents 8 months after implantation. *Heart.* (2011) 97:1379–84.

158. Chen G, Zrenner B, Pyxaras SA. Combined rotational atherectomy and intravascular lithotripsy for the treatment of severely calcified in-stent neoatherosclerosis: A mini-review. *Cardiovasc Revasc Med.* (2019) 20:819–21. doi: 10.1016/j.carrev.2018.10.007

159. Chan KH, Sia JE, Tan HC. Intravascular lithotripsy for the treatment of severe calcific neointimal hyperplasia in a bare metal stent 17 years after implantation. *Coron Artery Dis.* (2021) 32:172–4. doi: 10.1097/MCA.0000000000000905

160. Salazar C, Escaned J, Tirado G, Gonzalo N. Intravascular lithotripsy for recurrent restenosis caused by severe calcific neoatherosclerosis. *EuroIntervention.* (2020) 16:e351–2. doi: 10.4244/EIJ-D-19-00268

161. Giacoppo D, Gargiulo G, Aruta P, Capranzano P, Tamburino C, Capodanno D. Treatment strategies for coronary in-stent restenosis: Systematic review and hierarchical Bayesian network meta-analysis of 24 randomised trials and 4880 patients. *BMJ.* (2015) 351:h5392. doi: 10.1136/bmj.h5392

162. Pleva L, Kukla P, Kusnierova P, Zapletalova J, Hlinomaz O. Comparison of the efficacy of paclitaxel-eluting balloon catheters and everolimus-eluting stents in the treatment of coronary in-stent restenosis: The treatment of in-stent restenosis study. *Circ Cardiovasc Interv.* (2016) 9:e003316.

163. Siontis GC, Stefanini GG, Mavridis D, Siontis KC, Alfonso F, Perez-Vizcayno MJ, et al. Percutaneous coronary interventional strategies for treatment of in-stent restenosis: A network meta-analysis. *Lancet.* (2015) 386:655–64.

164. Lee JM, Park J, Kang J, Jeon KH, Jung JH, Lee SE, et al. Comparison among drug-eluting balloon, drug-eluting stent, and plain balloon angioplasty for the treatment of in-stent restenosis: A network meta-analysis of 11 randomized, controlled trials. *JACC Cardiovasc Interv.* (2015) 8:382–94. doi: 10.1016/j.jcin.2014.09.023

165. Giacoppo D, Alfonso F, Xu B, Claessen B, Adriaenssens T, Jensen C, et al. Paclitaxel-coated balloon angioplasty vs. drug-eluting stenting for the treatment of coronary in-stent restenosis: A comprehensive, collaborative, individual patient

data meta-analysis of 10 randomized clinical trials (DAEDALUS study). *Eur Heart J.* (2020) 41:3715–28.

166. Tada T, Kadota K, Hosogi S, Miyake K, Ohya M, Amano H, et al. Association between tissue characteristics assessed with optical coherence tomography and mid-term results after percutaneous coronary intervention for in-stent restenosis lesions: A comparison between balloon angioplasty, paclitaxel-coated balloon dilatation, and drug-eluting stent implantation. *Eur Heart J Cardiovasc Imaging.* (2015) 16:1101–11. doi: 10.1093/ehjci/jev031

167. Gonzalo N, Salazar CH, Perez-Vizcayno MJ, Gomez-Polo JC, Jimenez-Quevedo P, Jimenez-Valero S, et al. Influence of neoatherosclerosis on prognosis and treatment response in patients with in-stent restenosis. *Rev Esp Cardiol (Engl Ed).* (2021) 74:427–35. doi: 10.1016/j.rec.2020.03.005

168. Adriaenssens T, Dens J, Ughi G, Bennett J, Dubois C, Sinnaeve P, et al. Optical coherence tomography study of healing characteristics of paclitaxel-eluting balloons vs. everolimus-eluting stents for in-stent restenosis: The SEDUCE (safety and efficacy of a drug eluting balloon in coronary artery restenosis) randomised clinical trial. *EuroIntervention.* (2014) 10:439–48. doi: 10.4244/EIJV10I4A77

169. Alfonso F, Perez-Vizcayno MJ, Garcia Del Blanco B, Otaegui I, Masotti M, Zueco J, et al. Long-term results of everolimus-eluting stents versus drug-eluting balloons in patients with bare-metal in-stent restenosis: 3-year follow-up of the RIBS v clinical trial. *JACC Cardiovasc Interv.* (2016) 9:1246–55. doi: 10.1016/j.jcin.2016.03.037

170. Rivero F, Bastante T, Cuesta J, Benedicto A, Restrepo JA, Alfonso F. Treatment of in-stent restenosis with bioresorbable vascular scaffolds: Optical coherence tomography insights. *Can J Cardiol.* (2015) 31:255–9.

171. Alfonso F, Cuesta J, Perez-Vizcayno MJ, Garcia Del Blanco B, Rumoroso JR, Bosa F, et al. Bioresorbable vascular scaffolds for patients with in-stent restenosis: The RIBS VI study. *JACC Cardiovasc Interv.* (2017) 10:1841–51.

172. Picard F, Avram R, Marquis-Gravel G, Tadros VX, Ly HQ, de Hemptinne Q, et al. Bioresorbable vascular scaffold to treat in-stent restenosis: Single-center experience. *J Interv Cardiol.* (2017) 30:558–63.

173. Moscarella E, Tanaka A, Ielasi A, Cortese B, Coscarelli S, De Angelis MC, et al. Bioresorbable vascular scaffold versus everolimus-eluting stents or drug eluting balloon for the treatment of coronary in-stent restenosis: 1-year follow-up of a propensity score matching comparison (the BIORESOLVE-ISR Study). *Catheter Cardiovasc Interv.* (2018) 92:668–77.

174. Negi SI, Torguson R, Gai J, Kiramijyan S, Koifman E, Chan R, et al. Intracoronary brachytherapy for recurrent drug-eluting stent failure. *JACC Cardiovasc Interv.* (2016) 9:1259–65.

175. Varghese MJ, Bhatheja S, Baber U, Kezbor S, Chincholi A, Chamaria S, et al. Intravascular brachytherapy for the management of repeated multimetal-layered drug-eluting coronary stent restenosis. *Circ Cardiovasc Interv.* (2018) 11:e006832. doi: 10.1161/CIRCINTERVENTIONS.118.006832

176. Yabushita H, Kawamoto H, Fujino Y, Tahara S, Horikoshi T, Tada M, et al. Clinical outcomes of drug-eluting balloon for in-stent restenosis based on the number of metallic layers. *Circ Cardiovasc Interv.* (2018) 11:e005935. doi: 10.1161/CIRCINTERVENTIONS.117.005935

177. Fujii K, Mintz GS, Kobayashi Y, Carlier SG, Takebayashi H, Yasuda T, et al. Contribution of stent underexpansion to recurrence after sirolimus-eluting stent implantation for in-stent restenosis. *Circulation.* (2004) 109:1085–8. doi: 10.1161/01.CIR.0000121327.67756.19

178. Yin D, Mintz GS, Song L, Chen Z, Lee T, Kirtane AJ, et al. In-stent restenosis characteristics and repeat stenting underexpansion: Insights from optical coherence tomography. *EuroIntervention.* (2020) 16:e335–43. doi: 10.4244/EIJ-D-18-01191

179. Sakamoto Y, Yamawaki M, Araki M, Kobayashi N, Mori S, Tsutsumi M, et al. Comparison of 12-month angiographic outcomes between repeat drug-eluting stent implantation and drug-coated balloon treatment for restenotic lesion caused by stent fracture. *Heart Vessels.* (2019) 34:1589–94. doi: 10.1007/s00380-019-01398-x

180. Popma JJ, Tiroch K, Almonacid A, Cohen S, Kandzari DE, Leon MB. A qualitative and quantitative angiographic analysis of stent fracture late following sirolimus-eluting stent implantation. *Am J Cardiol.* (2009) 103:923–9. doi: 10.1016/j.amjcard.2008.12.022

181. Shlofmitz E, Torguson R, Mintz GS, Zhang C, Sharp A, Hodgson JM, et al. The IMPact on revascularization outcomes of intravascular ultrasound-guided treatment of complex lesions and economic impact (IMPROVE) trial: Study design and rationale. *Am Heart J.* (2020) 228:65–71. doi: 10.1016/j.ahj.2020.08.002

182. Alberti A, Giudice P, Gelera A, Stefanini L, Priest V, Simmonds M, et al. Understanding the economic impact of intravascular ultrasound (IVUS). *Eur J Health Econ.* (2016) 17:185–93.

183. Waters KR, Bautista R, Zelenka R, Masters D, Reynolds JS, Nelson S, et al. Development of a high-definition intravascular ultrasound imaging system and catheter. In: *Proceedings of the 2011 IEEE International Ultrasonics Symposium; 2011 18-21 Oct*, Orlando, FL: IEEE. (2011).

184. Garcia-Guimaraes M, Antuna P, De la Cuerda F, Maruri-Sanchez R, Cuesta J, Bastante T, et al. High-definition IVUS versus OCT to assess coronary artery disease and results of stent implantation. *JACC Cardiovasc Imaging.* (2020) 13:519–21. doi: 10.1016/j.jcmg.2019.08.019

185. Kim TS, Park H-S, Jang S-J, Song JW, Cho HS, Kim S, et al. Single cardiac cycle three-dimensional intracoronary optical coherence tomography. *Biomed Opt Express.* (2016) 7:4847–58.

186. Saito Y, Kitahara H, Okuya Y, Nakayama T, Fujimoto Y, Kobayashi Y. Novel predictor of target vessel revascularization after coronary stent implantation: Intraluminal intensity of blood speckle on intravascular ultrasound. *Catheter Cardiovasc Interv.* (2019) 93:604–10. doi: 10.1002/ccd.27859

frontiers | Frontiers in Cardiovascular Medicine

TYPE Original Research
PUBLISHED 18 August 2022
DOI 10.3389/fcvm.2022.983003

OPEN ACCESS

EDITED BY
Simone Biscaglia,
University Hospital of Ferrara, Italy

REVIEWED BY
Gabriele Pesarini,
Integrated University Hospital Verona, Italy
Luigi Di Serafino,
Federico II University Hospital, Italy

*CORRESPONDENCE
Antonio Maria Leone
antoniomarialeone@policlinicogemelli.it;
antoniomarialeone@gmail.com

SPECIALTY SECTION
This article was submitted to Coronary Artery Disease, a section of the journal Frontiers in Cardiovascular Medicine

RECEIVED 30 June 2022
ACCEPTED 25 July 2022
PUBLISHED 18 August 2022

CITATION
Leone AM, Migliaro S, Zimbardo G, Cialdella P, Basile E, Galante D, Di Giusto F, Anastasia G, Vicere A, Petrolati E, Di Stefano A, Campaniello G, D'Amario D, Vergallo R, Montone RA, Buffon A, Romagnoli E, Aurigemma C, Burzotta F, Trani C and Crea F (2022) Safety and effectiveness of post percutaneous coronary intervention physiological assessment: Retrospective data from the post-revascularization optimization and physiological evaluation of intermediate lesions using fractional flow reserve registry. *Front. Cardiovasc. Med.* 9:983003. doi: 10.3389/fcvm.2022.983003

Safety and effectiveness of post percutaneous coronary intervention physiological assessment: Retrospective data from the post-revascularization optimization and physiological evaluation of intermediate lesions using fractional flow reserve registry

Antonio Maria Leone[1]*, Stefano Migliaro[2], Giuseppe Zimbardo[3], Pio Cialdella[3], Eloisa Basile[2], Domenico Galante[2], Federico Di Giusto[2], Gianluca Anastasia[2], Andrea Vicere[2], Edoardo Petrolati[2], Antonio Di Stefano[2], Giorgia Campaniello[2], Domenico D'Amario[1], Rocco Vergallo[1], Rocco Antonio Montone[1], Antonino Buffon[1,2], Enrico Romagnoli[1], Cristina Aurigemma[1], Francesco Burzotta[1,2], Carlo Trani[1,2] and Filippo Crea[1,2]

[1]Dipartimento di Scienze Cardiovascolari, Fondazione Policlinico Universitario Agostino Gemelli (IRCCS), Rome, Italy, [2]Dipartimento di Scienze Cardiovascolari, Università Cattolica del Sacro Cuore, Rome, Italy, [3]Policlinico Casilino, Rome, Italy

Background: While the importance of invasive physiological assessment (IPA) to choose coronary lesions to be treated is ascertained, its role after PCI is less established. We evaluated feasibility and efficacy of Physiology-guided PCI in the everyday practice in a retrospective registry performed in a single high-volume and "physiology-believer" center.

Materials and methods: The PROPHET-FFR study (NCT05056662) patients undergoing an IPA in 2015–2020 were retrospectively enrolled in three groups: Control group comprising patients for whom PCI was deferred based on a IPA; Angiography-Guided PCI group comprising patients undergoing PCI based on an IPA but without a post-PCI IPA; Physiology-guided PCI group comprising patients undergoing PCI based on an IPA and an IPA after PCI, followed by a physiology-guided optimization, if indicated. Optimal result was defined by an FFR value $\geq$ 0.90.

10.3389/fcvm.2022.983003

Results: A total of 1,322 patients with 1,591 lesions were available for the analysis. 893 patients (67.5%) in Control Group, 249 patients (18.8%) in Angiography-guided PCI Group and 180 patients (13.6%) in Physiology-guided PCI group. In 89 patients a suboptimal functional result was achieved that was optimized in 22 cases leading to a "Final FFR" value of 0.90 ± 0.04 in Angiography-Guided PCI group. Procedural time, costs, and rate of complications were similar. At follow up the rate of MACEs for the Physiology-guided PCI group was similar to the Control Group (7.2% vs. 8.2%, $p = 0.765$) and significantly lower than the Angiography-guided PCI Group (14.9%, $p < 0.001$), mainly driven by a reduction in TVRs.

Conclusion: "Physiology-guided PCI" is a feasible strategy with a favorable impact on mid-term prognosis. Prospective studies using a standardized IPA are warrant to confirm these data.

KEYWORDS

FFR, PCI, physiology-guided optimization, post-PCI evaluation, function based management CCS (chronic coronary syndrome)

Background

While the importance of invasive physiological assessment (IPA) to choose coronary lesions to be treated is ascertained, its role in evaluating the immediate result of PCI and its optimization is much less established (1, 2). Nevertheless, the unmet need for a help in assessing result of revascularization is evident when considering that one in four patients after an angiographically successful PCI still experiences recurrent angina, persistence of documented ischemia or MACEs within 2 years (3–6). Given the excellent performance of invasive physiological assessment evaluation for diagnostic purposes, it seems intuitive to utilize this approach also to assess PCI result. Yet, the association between post-PCI fractional flow reserve (FFR) results and risk of subsequent events is still debated (7).

The aim of this study was to evaluate the use of physiology-guided PCI in terms of prevalence, feasibility, and performance on in-hospital and mid-term outcomes in contemporary interventional procedures from the Cath Lab performing the largest number of IPAs in Italy.[1]

Abbreviations: CCS, chronic coronary syndrome; CD, cardiac death; cFFR, contrast-FFR; dPR, diastolic resting pressure ratio; FFR, Fractional Flow Reserve; iFR, instantaneous wave free ratio; IPA, invasive physiological assessment; LAD, left anterior descending; LVEF, Left Ventricle Ejection Fraction; MACE, Major Adverse Cardiovascular Events; MI, myocardial infarction; NHPR, non-hyperemic pressure ratio; NSTEACS, non-ST segment elevation acute coronary syndromes; PCI, Percutaneous Coronary Intervention; RFR, resting full-cycle ratio; STEMI, ST segment elevation myocardial infarction; TVR, Target Vessel Revascularization.

1 https://gise.it/statisticheNazionali

Materials and methods

Study design and population

The Post-Revascularization Optimization and Physiological Evaluation of intermediate Lesions using FFR (PROPHET-FFR) is a single center ambispective study held at Policlinico Universitario A. Gemelli IRCCS in Rome evaluating the feasibility and the technical and clinical efficacy of Physiology-guided PCI. All patients able to give a valid informed consent and undergoing an IPA at the Fondazione Policlinico Universitario A. Gemelli IRCCS in Rome (Italy) are enrolled and included in one of the following three groups as described in **Figure 1**:

1. Group 1 comprising patients for whom PCI is deferred based on an IPA [FFR > 0.80 and/or non-hyperaemic pressure ratio (NHPR) > 0.89 and/or contrast FFR (cFFR) > 0.87) (Control Group).
2. Group 2 comprising patients who undergo PCI based on an IPA but without any subsequent IPA after PCI (Angiography-Guided PCI).
3. Group 3 comprising patients who undergo PCI based on an IPA and with a subsequent IPA after PCI (Physiology-guided PCI) followed by a physiology-guided optimization, if indicated.

Considering the ambispective nature of the study, the PROPHET-FFR study is divided in a first retrospective phase followed by a second prospective phase. In the former, the operators were free to decide the strategy. The latter is currently ongoing and the operators are

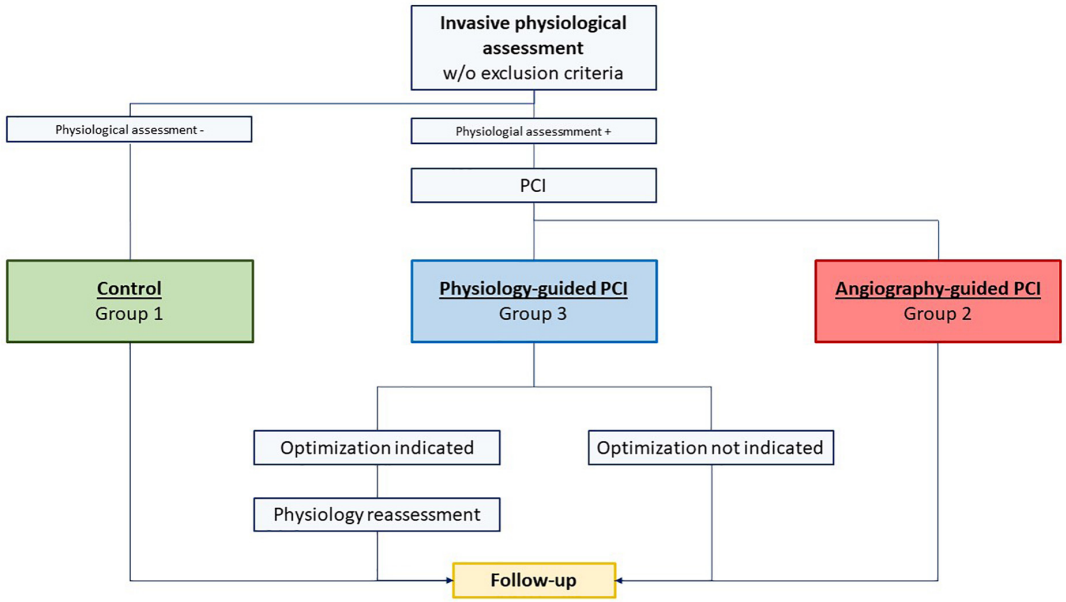

FIGURE 1
Study flow chart: group 1 comprised patients for whom percutaneous coronary intervention (PCI) was deferred based on an invasive physiological assessment [Fractional flow reserve (FFR) > 0.80 and/or non-hyperemic pressure ratio (NHPR) > 0.89 and/or contrast FFR (cFFR) > 0.87] (Control Group); group 2 comprised patients who underwent PCI based on an invasive physiological assessment but without any subsequent invasive physiological assessment after PCI (Angiography-Guided PCI); group 3 comprised patients who underwent PCI based on an invasive physiological assessment and with a subsequent invasive physiological assessment after PCI (Physiology-guided PCI) followed by a physiology-guided optimization, if indicated.

again free to decide the strategy but in case of choice of Physiology-guided PCI they are recommended to adhere to the flow chart described in our recent review paper (8). We report here the results of the retrospective phase.

All patients with acute and chronic coronary syndromes referred to our center from January 2015 to June 2020 for physiological assessment of an angiographically intermediate coronary stenosis, not presenting any of the exclusion criteria below reported were retrospectively enrolled. For ST segment elevation myocardial infarction (STEMI) non-culprit lesions only were enrolled. Exclusion criteria were the following: history of severe poorly uncontrolled pulmonary disease, hemodynamic instability during the diagnostic or therapeutic procedure, need of mechanical circulatory or ventilatory support, life expectancy < 1-year, indication to surgical revascularization, major procedural complications during percutaneous revascularization making post-PCI functional evaluation unsafe or impossible (cardiac arrest needing cardiopulmonary resuscitation, major bleeding, large iatrogenic coronary dissection, coronary embolization in a main vessel, suspected stroke, coronary no-reflow).

The protocol was approved by the Ethics Committee of the Fondazione Policlinico Universitario A. Gemelli IRCCS of Rome and is registered in Clinicaltrials.gov (NCT05056662).

Study protocol

After coronary angiography, baseline IPA was performed in every patient. Because of the observational nature of the study, the choice about the index to adopt [either NHPRs including instantaneous wave free ratio (iFR), resting full-cycle ratio (RFR), and diastolic resting pressure ratio (dPR)], conventional FFR or contrast-FFR (cFFR) and its interpretation were left to operators' discretion. Physiological assessments were performed using Pressure Wire Certus and Pressure Wire X by Abbott Vascular Inc., Verrata Plus by Philips Inc., and Navvus catheter by Acist Inc.

For FFR assessment, hyperemia was obtained using adenosine, administered either by intra-venous (9) or intra-coronary route (10). The operators were encouraged to place the wire as distal as possible in the vessel and decided about indication and modality of revascularization according to the physiological results. We excluded only those patients treated with PCI despite the evidence of non-ischemic values for all indexes.

At the end of PCI operators were free to choose if and how to repeat IPA and to decide about the opportunity and modality of performing an additional optimization with an optional final physiological assessment. Similarly, the choice of performing a pullback maneuver prior and after PCI was left to operator's discretion.

"Post-PCI" IPA was defined as the assessment performed once the operator considered the revascularization completed based on the angiographic assessment. "Post-optimization" IPA was considered the assessment made after any further action taken to improve the physiological result. Consequently, "Final results" comprised both "Post PCI results," for those cases not further optimized and "Post optimization results" in case of optimization and retesting.

Data collection, follow-up, and study endpoints

All baseline demographic, clinical, and procedural data were retrieved from the patient database of Fondazione Policlinico Universitario A. Gemelli IRCCS, Rome. Clinical follow-up was performed by telephone interviews and out-patient visits performed according to a pre-specified set of questions by a group of physicians unaware of the details of the procedure and consequently of the grouping. Clinical data were integrated with hospital records in case of need. Follow up was censored at 3 years from index procedure. Events were adjudicated by two independent operators (SM and PC) and a random cluster review, blinded to group affiliation, was periodically performed by the Principal Investigator (AL).

Primary endpoint of the study was the first occurrence of a major adverse cardiovascular event (MACE) defined as the composite of cardiac death (CD), spontaneous myocardial infarction (MI), and target vessel revascularization (TVR). CD was defined according to Academic Research Consortium-2 indication (11), MI was defined according to ESC 4th definition of Myocardial Infarction (12), TVR was defined as the clinically driven revascularization of the target vessel. Secondary endpoints were the single components of MACE as well as the rate of unplanned hospitalizations leading to coronary angiography.

In addition, procedural and in-hospital outcome was also investigated by analyzing radioscopic time, amount of contrast medium, post-procedural release of markers of myonecrosis, rate of peri-procedural myocardial injury and of type 4a MI and global costs associated with the different strategies according to our previously published paper (13).

Study groups and statistical analysis

The study flow chart is presented in **Figure 1**. As previously mentioned, patients were divided into three groups: Group 1 (Control Group), Group 2 (Angiography-guided PCI), and Group 3 (Physiology-guided PCI). Comparisons were made among the three groups.

Categorical variables were reported as frequencies and percentages while continuous variables were reported as means with standard deviation or median with interquartile range according to normality. Differences among categorical variables were assessed using Pearson χ^2 test while differences among continuous variables were calculated using the independent ANOVA test. Differences among medians were compared by Mann–Whitney test. *Post hoc* analysis with Bonferroni's correction was used to identify pairwise differences. Survival was analyzed by Kaplan Meier method with stratified log-rank test to show the incidence of clinical endpoints and to check for intergroup differences and with Cox proportional hazard ratio method to identify the impact in time of clinical variables of interest. ROC curve analysis was run to identify the best cut-off value of final FFR to predict the outcomes. All tests were 2-tailed, and a $P < 0.05$ was considered statistically significant. Statistical analyses were performed using SPSS statistics for Windows, version 24.0 (SPSS, Chicago, IL, IBM Inc., United States) and GraphPad 9.0 (GraphPad Software, San Diego, CA, United States).

Results

Baseline characteristics

A total of 1,556 patients were screened for enrolment: 54 patients denied informed consent, 47 were managed at variance with the initial IPA, and 133 were lost to follow up. Consequently, a total of 1,322 patients with 1,591 lesions were available for the analysis. Among these, 893 patients (67.5%) with 1,137 lesions (71.4%) were included in Group 1 (Control Group), 249 patients (18.8%) with 265 lesions (16.6%) in Group 2 (Angiography-guided PCI), and 180 patients (13.6%) with 189 lesions (11.8%) in Group 3 (Physiology-guided PCI). In three cases a loss of connection or a damage of the pressure wire was observed and in two cases the operator chose to abandon rewiring of the stented segment after a gentle attempt. In all cases the operator had the opportunity to open a new device for the physiological assessment or to use a more aggressive approach but chose to avoid it based on the good angiographic result. These cases were included in Group 2.

Baseline clinical characteristics of the groups are reported in **Tables 1**, **2**.

Mean age was 69.1 ± 10.4 years. Overall, most of patients were male (72.3%) but males were slightly less represented in Group 1 vs. the others [617 (69.1%) vs. 193 (77.5%) vs. 146 (81.5%), $p < 0.001$]. Interestingly, diabetic patients were significantly more prevalent in group 3 vs. the others [69 (38.3%) vs. 234 (26.5%) and 70 (28.1%), $p = 0.006$)]. Mean left ventricular ejection fraction was 57.2% ± 8.9% while 58 patients (4.3%) only

10.3389/fcvm.2022.983003

TABLE 1 Clinical characteristics of the patients' groups.

Patients (n = 1,322)	Group 1 (n = 893)	Group 2 (n = 249)	Group 3 (n = 180)	P-value (global)
Age (years)	69.2 ± 10.6	69.1 ± 9.7	68.1 ± 10.0	0.480
BMI	26.7 ± 4.4	26.1 ± 3.7	27.5 ± 5.0	0.108
Male gender	617 (69.1)	193 (77.5)	146 (81.5)	0.001
Hypertension	742 (83.6)	214 (85.9)	146 (81.6)	0.465
EF	57.1 ± 8.9	57.4 ± 8.7	57.3 ± 9.1	0.908
Ejection fraction < 40%	39 (4.4)	12 (4.8)	7 (3.9)	0.897
Dyslipidemia	558 (62.8)	164 (66.1)	113 (62.8)	0.623
Statin	512 (61.1)	158 (66.1)	105 (66.0)	0.239
Diabetes	234 (26.5)	70 (28.1)	69 (38.3)	0.006
Smoke	402 (46.2)	123 (50.6)	82 (49.1)	0.428
Beta blockers	590 (66)	168 (67.4)	111 (61.6)	0.539
ACE-I	579 (68.1)	179 (71.8)	109 (60.5)	0.201
CCB	146 (16.3)	43 (17.2)	25 (13.8)	0.833
DIURETICS	159 (17.8)	59 (22.4)	24 (13.3)	0.107
CKD	67 (7.5)	22 (8.8)	18 (10)	0.650
MDRD female	76.7 ± 29.3	72.6 ± 31.6	84.5 ± 36.6	0.474
MDRD male	79.4 ± 28.5	84.2 ± 22.6	81.6 ± 23.1	0.411
Family history	244 (27.3)	61 (24.5)	48 (26.6)	0.626
Previous MI	198 (22.2)	66 (26.5)	40 (22.2)	0.344
Previous PCI	319 (35.7)	92 (36.9)	56 (31.1)	0.769
Previous CABG	27 (3.0)	8 (3.2)	6 (3.3)	0.970
Clinical presentation				< 0.001
CCS	669 (74.9)	161 (64.7)	139 (77.2)	
NSTEACS	158 (17.7)	77 (30.9)	33 (18.3)	
STEACS	66 (7.4)	11 (4.4)	8 (4.4)	
Multivessel disease				< 0.001
2VD	88 (9.8)	75 (30.1)	50 (27.7)	
3VD	27 (3.0)	22 (8.8)	15 (8.3)	
PCI on other vessel	207 (23.2)	74 (29.7)	56 (31.1)	0.020
LAD involvement	638 (71.40)	218 (87.5)	147 (81.6)	< 0.001

had a left ventricular ejection fraction < 40% with a similar distribution among groups. Admission diagnosis was chronic coronary syndrome (CCS) in 73.3% of cases, non-ST segment elevation acute coronary syndromes (NSTEACS) in 20.2% and ST segment elevation myocardial infarction (STEMI) in 6.4%. In Group 2 a higher prevalence of NSTEACS at the cost of less CCS presentations was observed [NSTEACS: 158 (17.7%) vs. 77 (30.9%) vs. 33 (18.3%), $p < 0.001$; CCS 669 (74.9%) vs. 161 (64.7%) vs. 139 (77.2%), $p < 0.001$)]. More than one third of the patients experienced a previous PCI while almost one in four patients had a previous myocardial infarction with no difference among groups. The majority of the lesions were located in the left anterior descending (LAD) artery, but non-LAD lesions were more frequent in Group 1 which also had a lower incidence of multivessel disease.

Final diagnostic decision was driven by conventional FFR in 1,193 (74.9%) lesions, by cFFR alone in 280 (17.5%) lesions and by NHPRs in 104 (RFR/iFR 62 + Pd/Pa 42) (6.5%) lesions.

As expected, mean baseline FFR was significantly higher in Group 1 (0.88 ± 0.04) in comparison to both other groups that, conversely, did not differ from each other (0.76 ± 0.03 vs. 0.76 ± 0.04).

"Post-PCI" invasive physiological assessment

From the 180 patients of Group 3, "Post-PCI" IPA was performed by conventional FFR in 114 (60.3%) cases, by cFFR in 62 (32.8%), and by NHPRs in 13 (7 iFR/RFR + 6 Pd/Pa) (6.8%) cases. The mean "post PCI" FFR was 0.89 ± 0.05 with an average increase after PCI (and before any optimization) of 19 ± 8.5% (**Figure 2A**). In 58 (30.6%) lesions post-PCI FFR value was < 0.90 while only in 4 (2.1%) cases was < 0.80. In those patients in which a non-FFR based approach was

10.3389/fcvm.2022.983003

TABLE 2 Procedural characteristics of the lesions' groups.

Lesions (n = 1,591)	Group 1 (n = 1,137)	Group 2 (n = 265)	Group 3 (n = 189)	p-value (global)	p-value (3 vs. 2)
In stent lesion	51 (4.5)	12 (4.5)	15 (7.9)	0.120	
Lesion site				< 0.001	
LAD	743 (65.3)	227 (83.7)	160 (84.6)		
Cx	228 (20.1)	13 (4.9)	11 (5.8)		
RCA	166 (14.6)	25 (9.4)	18 (9.5)		
Hyperemia induction				0.985	
Adenosine ic	248 (24.2)	56 (24.1)	37 (23.6)		
Adenosine iv	777 (75.8)	176 (75.9)	120 (76.4)		
Angiographic lesion severity	53.4 ± 9.1	62.1 ± 9.9	64.4 ± 11.5	0.462	
Stent length		33.4 ± 17.6	34.7 ± 17.0		0.472
Number of stent, median (IQR)		1 (1–2)	1 (1–2)		0.354
Number stent, average		1.3 ± 0.60	1.27 ± 0.64		0.241
Stent diameter, mm		3.0 ± 0.42	2.95 ± 0.34		0.203
Optimization by post-dilation, n (%)			10 (5.3)		
Optimization with a new stent, n (%)			12 (6.3)		
Physiological parameters					
Baseline Pd/Pa	0.95 ± 0.03	0.89 ± 0.05	0.89 ± 0.05	< 0.001	1
Baseline FFR	0.88 ± 0.04	0.76 ± 0.03	0.76 ± 0.03	< 0.001	0.082
Baseline IFR	0.92 ± 0.05	0.82 ± 0.08	0.87 ± 0.03	< 0.001	1.0
Baseline cFFR	0.91 ± 0.06	0.81 ± 0.03	0.80 ± 0.05	< 0.001	1.0
Post-PCI Pd/Pa			0.94 ± 0.03		
Post-PCI FFR			0.89 ± 0.05		
Post-PCI IFR			0.92 ± 0.03		
Post-PCI cFFR			0.89 ± 0.04		
Post-optimization Pd/Pa			0.94 ± 0.02		
Post-optimization cFFR			0.91 ± 0.03		
Post-optimization FFR			0.92 ± 0.05		
Final FFR			0.90 ± 0.04		
Final cFFR			0.90 ± 0.03		

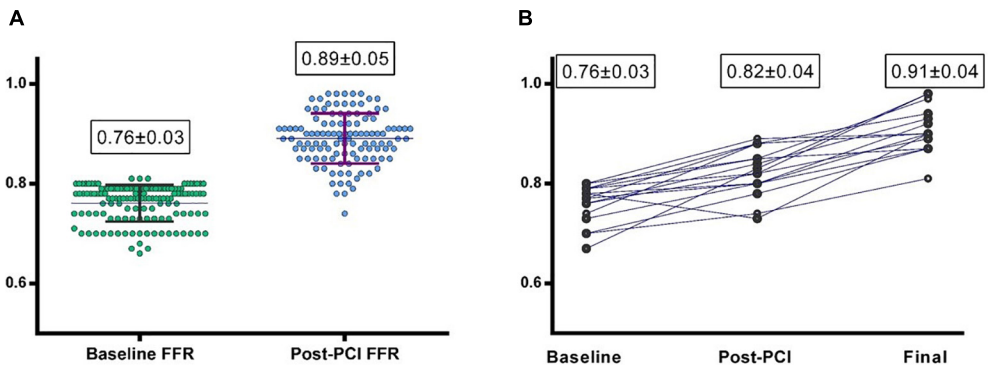

FIGURE 2
(A) Baseline and post-PCI fractional flow reserve (FFR) values in group 3 (Physiology-guided PCI). **(B)** Baseline, post PCI and final FFR values in the 22 patients undergoing "Physiology-guided Optimization."

10.3389/fcvm.2022.983003

TABLE 3 In-hospital outcomes.

Patients (n = 1,322)	Group 1 (n = 893)	Group 2 (n = 249)	Group 3 (n = 180)	p-value	p-value (3 vs. 2)	p-value (3 vs. 1)	p-value (2 vs. 1)
Fluoroscopy time (min)	12.7 ± 9.5	19.8 ± 12.2	21.6 ± 8.9	< 0.001	0.558	< 0.001	< 0.001
Total contrast dose (ml)	163.0 ± 69.0	236.3 ± 116.6	278.7 ± 168.4	< 0.001	0.011	< 0.001	< 0.001
Post-procedural troponin (ng/L)	2.32 ± 5.8	1.82 ± 6.74	2.74 ± 7.24	0.109	1.0	0.272	1.0
Post-procedural creatinine (mg/dl)	1.22 ± 1.20	1.16 ± 0.93	1.19 ± 1.01	0.887	1.0	1.0	1.0
Post-procedural CK-MB (ng/L)	1.4 ± 4.7	4.9 ± 5.5	4.3 ± 4.7	0.375	1.0	0.091	0.087
Procedural cost (euros)	1900 ± 1856	3329 ± 2325	3152 ± 1814	< 0.001	1.0	< 0.001	< 0.001
Total days of hospital stay	6.5 ± 5.9	8.5 ± 6.4	6.0 ± 4.3	< 0.001	< 0.001	< 0.001	1.0
Myocardial injury		43 (17.2)	25 (13.8)		0.141		
Periprocedural MI		5 (2.0)	4 (2.2)		1.0		

TABLE 4 Intravascular imaging use.

Lesions (n = 1,591)	Group 1 (n = 1,137)	Group 2 (n = 265)	Group 3 (n = 189)	P-value (global)	P-value (3 vs. 2)	P-value (3 vs. 1)	P-value (2 vs. 1)
Use of intravascular imaging (%)	3 (0.3)	14 (5.3)	8 (4.2)	< 0.001	1.0	< 0.001	< 0.001

used, 28 (14.8%) lesions showed a cFFR < 0.90, 1 (0.5%) a iFR/RFR < 0.90 and 2 (1%) Pd/Pa < 0.92.

A total of 22 (11.6%) lesions underwent physiology-guided optimization; in 12 of these cases the optimization was driven by a post-PCI FFR value < 0.90 and in 8 of these cases by cFFR < 0.90. Optimization consisted of post-dilation of the previously implanted stent with a larger balloon in 10 cases and of the implantation of another stent proximally or distally in 4 and 6 cases, respectively.

"Post-optimization" result was reassessed by FFR in nine of these cases, by cFFR in 10 cases, while the remaining were retested by NHPRs; of these optimized lesions, only two were left with an FFR post-optimization < 0.90 and only three cases ended with cFFR < 0.90.

The mean "Post-optimization" FFR value was 0.92 ± 0.05 with an FFR improvement from baseline of 18% ± 7.4%. This led to a mean overall "Final FFR" value of 0.90 ± 0.04 for Group 3 (Figure 2B; Table 2) that was even significantly higher than FFR in Group 1 (p < 0.001).

Procedural and in-hospital outcomes

Procedural and in-hospital outcomes are presented in Table 3. Procedural time was higher in Group 2 and 3 (19.8 ± 12.2 and 21.6 ± 8.9 min) than in Group 1 (12.7 ± 9.5, p < 0.001) but without a significant difference among them (p = 0.56). Physiology-guided PCI required a higher amount of contrast medium compared to Angiography-guided PCI and Control Group (278.7 ± 168.4 ml vs. 163.0 ± 69.0 and 236.3 ± 116.6, p < 0.001) while no difference in post-procedural creatinine and post-procedural release of myocardial damage markers was observed. While Physiology-guided PCI did not increase the overall costs compared to Angio-guided PCI (3152 ± 1814 vs. 3329 ± 2325 euros, p = 1), it was associated to a reduced length of stay (6.0 ± 4.3 vs. 8.5 ± 6.4 days, p < 0.001). No significant difference was seen for the number, total length and mean diameter of implanted stents between Groups 2 and 3 (Table 2) as well for the use of intravascular imaging (Table 4).

Rate of in-hospital MACE was low and not significantly different between Group 2 and 3 as well the incidence of periprocedural myocardial injury or type 4a MI (Table 3).

Clinical follow-up

The median length of follow up (FU) for the overall population was 21 months (IQR 14–32). A total of 124 (9.3%) MACEs were observed at 36 months including 33 (2.4%) MI, 84

(6.3%) TVR, and 24 (1.8%) CD. The rate of MACE was higher in Group 2 (14.9%) compared both to Group 1 and 3 (8.2% and 7.2%, $p < 0.001$ and $p = 0.004$) while it was not significantly different between Group 1 vs. 3 ($p = 0.765$). The difference in the primary endpoint was mainly driven by the rate of TVRs that were not significantly different comparing Group 3 to Group 1 (5.0% vs. 5.3%) but significantly higher in Group 2 (11.2%) compared to both Group 1 and 3 ($p < 0.001$ **Figure 3**; **Table 5**). Considering the possible interference of clinical presentation on subsequent outcomes, given the higher baseline risk profile of unstable patients, we reiterated survival analysis on patients with chronic coronary syndromes only; results consistently showed a lower incidence of MACE in Physiology-guided PCI, driven by a reduction in TVR (**Figure 4**; **Table 6**).

No significant difference was observed in the incidence of MI and CD. Cardiac hospitalizations were significantly higher in Group 2 and 3 compared to Group 1 ($p < 0.001$) without significant differences between Group 2 and 3 ($p = 0.26$). These results were confirmed at lesion-level analysis. Specifically, the difference in TVR between Group 2 and 3 was statistically significant (10.9% vs. 4.8%, $p = 0.004$).

Cox regression analysis confirmed the significant difference in MACE rate among the groups even after adjustment for potential confounders (age, gender, hypertension, diabetes, chronic kidney disease, previous MI, previous PCI, clinical presentation, LVEF, and multivessel disease) with strategy of revascularization and previous MI being the only factors influencing the outcomes (**Table 7**).

Yet, ROC curve analysis (**Figure 5**) for cases of Physiology-guided PCI in which FFR was the main technique for guiding PCI, showed a modest capacity to predict event free survival with an AUC of 59%; the best cutoff for MACE free survival still appeared to be 0.90 (sensitivity 43%, specificity 75%).

Discussion

Despite physiological assessment after PCI seems a reasonable strategy to have an immediate measure of the efficacy of revascularization, its use in clinical practice still remains limited. In the present study we present the result of a real-world application of this approach in patients who underwent a physiological assessment of intermediate coronary stenosis.

The main results are the following:

(1) Post PCI IPA is performed in a minority of patients while a persistently suboptimal result is rather frequent in spite of an acceptable angiographic result.

(2) A "Physiology-guided PCI" is a feasible and safe approach to check the immediate result of revascularization.

(3) Physiology-guided PCI was associated to a better outcome as compared to Angiography-guided PCI.

Despite being strongly recommended by current guidelines on revascularization, IPA is underutilized in clinical practice (14). In addition, when ischemic lesions are recognized and treated by PCI, the operators repeat IPA after PCI only in a minority of cases. Our retrospective study confirms these findings, showing that the majority of patients are still treated by an Angiography-guided PCI even after a significant result at IPA. This is quite surprising because physiological reassessment at this stage is obviously costless and associated with a limited increase in procedural time. However, when an IPA is performed after PCI, a suboptimal result is quite frequent despite an angiographically satisfying result (15), including lesions still below the "ischemic" threshold (16, 17). In our study we confirm these findings but, unlike other studies enrolling a wide spectrum of different lesions and patients with an indication to PCI, we focused on intermediate coronary artery stenosis that are the main field of application of IPA and for which a class IA was assigned by ESC Guidelines on myocardial revascularization. In our cohort about 50% of all lesions exhibited a post-PCI suboptimal physiological result (FFR < 0.90), although rarely 0.80. These suboptimal results can be further ameliorated by additional interventions, such as stent post-dilation or stenting proximally or distally to the already implanted stent.

The main novelty of the present study is the evidence of a potential beneficial effect of a Physiology-guided PCI over a standard Angiography-guided approach. Indeed, we found that Physiology-guided PCI resulted in a similar final FFR value and in a comparable rate of MACE in comparison to control patients in whom PCI was deferred based on the IPA of intermediate lesions. Moreover, the rate of MACE was significantly lower than that observed in Angiography-guided PCI in the absence of a relevant increase of procedural complexity and of in-hospital events, mainly driven by a reduction in the rate of TVR. Length of stay of group 2 appeared to be slightly longer but this observation may be mostly attributable to the higher prevalence of ACS patients in this group.

Recently, the TARGET-FFR (18) trial demonstrated that a physiology-guided strategy was associated with a lower rate of suboptimal results in comparison to a standard angiographic approach. However, this appeared to have a marginal effect on clinical events. Notably, despite a suboptimal result occurring in less than 50% of cases, in only two thirds of these lesions investigators were able to identify a substrate for further optimization. This means that not only a suboptimal result is frequent but that it is often hardly amenable for improvement because of the presence of diffuse disease or other technical reasons. In our cohort, only 22% of all post-PCI evaluations were followed by any optimization; this could be due not only to the overall quite high post-PCI results but mostly to the lack of a shared and definite cut-off to consider and

10.3389/fcvm.2022.983003

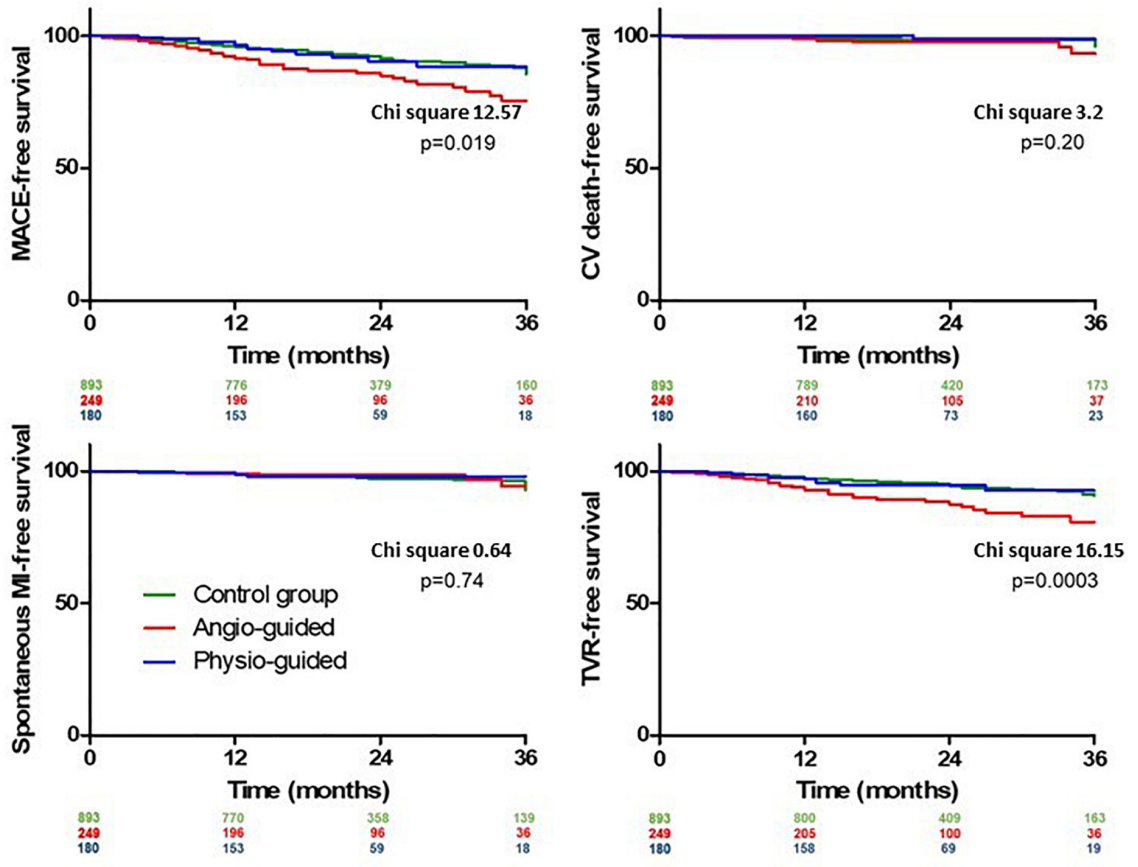

FIGURE 3
Kaplan Meier curves for out-of-hospital outcomes comparing group 1 (Control Group), group 2 [Angiography-Guided percutaneous coronary intervention (PCI)] and group 3 (Physiology-guided PCI).

TABLE 5 Out-of-hospital outcomes.

Patients (n = 1,322)	Group 1 (n = 893)	Group 2 (n = 249)	Group 3 (n = 180)	P-value (global)	P-value (3 vs. 2)	P-value (3 vs. 1)	P-value (2 vs. 1)
Follow-up, (months)	25.4 ± 16.2	23.9 ± 15.6	22.0 ± 13.3	0.024	0.650	0.028	0.599
MACE (%)	74 (8.2)	37 (14.9)	13 (7.2)	0.004	0.015	0.765	0.003
Myocardial infarctions	25 (2.8)	5 (2.0)	3 (1.7)	0.580	1.000	0.606	0.655
Cardiac deaths	16 (1.8)	7 (2.8)	1 (0.6)	0.224	0.147	0.334	0.311
TVR	47 (5.3)	28 (11.2)	9 (5.0)	0.002	0.024	1	0.001
cardiac hospitalizations	164 (18.4)	80 (32.1)	48 (26.7)	< 0.001	0.241	0.018	< 0.001
All-cause death	33 (3.7)	19 (7.6)	4 (2.2)	0.048	0.048	0.620	0.030

optimal. Actually, we confirmed that 0.90 is the cutoff with the higher predictive value but this result was achieved with a very modest sensitivity.

In our study, the inclusion of only intermediate coronary stenosis with an indication to diagnostic IPA has played a role in reducing the prevalence of suboptimal and ischemic result after PCI. In this setting, however, it is even more remarkable the reduction in TVR in comparison to the standard angiography-based approach. In addition, it is interesting to note that this comes not only without a significant increase in the complexity of the procedure, as clearly demonstrated by a similar fluoroscopy time but even without a significant increase in the rate in-hospital events, in the length of stay and in total costs, possibly due to the surrogate use of the

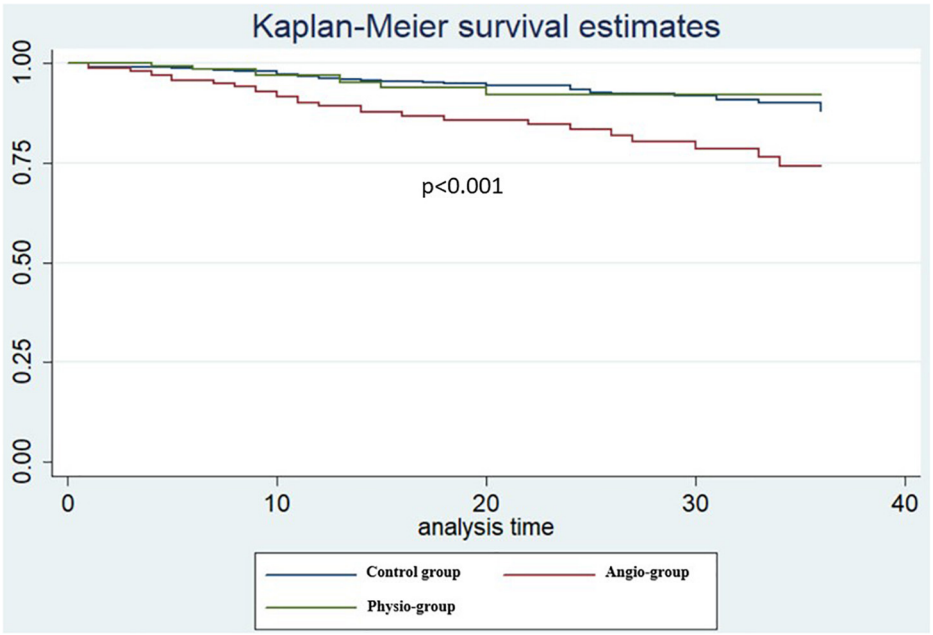

FIGURE 4
Kaplan Meier curves patients with chronic coronary syndromes only at pairwise log rank comparison [Physiology-guided percutaneous coronary intervention (PCI) vs. Angiography-guided PCI p = 0.007, Physiology-guided PCI vs. Control Group p = 0.89].

TABLE 6 Out of hospital outcomes for patients with chronic coronary syndromes.

CCS patients (n = 969)	Group 1 (n = 669)	Group 2 (n = 161)	Group 3 (n = 139)	P-value (global)	P-value (3 vs. 2)	P-value (3 vs. 1)	P-value (2 vs. 1)
Follow-up, (months)	21.9 ± 9.8	20.5 ± 10.8	19.5 ± 9.5	0.013	0.363	0.006	0.100
MACE (%)	46 (6.9)	27 (16.8)	8 (5.8)	< 0.001	0.002	1.000	0.000
Myocardial infarction	13 (1.9)	3 (1.9)	2 (1.4)	0.923	1.000	1.000	1.000
Cardiac death	12 (1.8)	6 (3.7)	0 (0.0)	0.057	0.051	0.462	0.308
Target vessel revascularization	29 (4.3)	21 (13)	7 (5.0)	< 0.001	0.009	1	< 0.001
Cardiac hospitalizations	111 (16.6)	56 (34.8)	33 (23.7)	< 0.001	0.052	0.166	< 0.001

pressure wire instead of the expensive intracoronary imaging for PCI guidance and optimization. However, this strategy should be implemented using a quite rigorous algorithm aimed at identifying not only the presence of any suboptimal result, but also if this is due to a diffuse disease or to a geographically missed focal lesion located distally or proximally to the stented segment. In an effort to standardize this evaluation, several groups, including ours (9), have suggested a systematic approach to correctly diagnose and treat a suboptimal functional result.

The first step in any systematic post-PCI IPA is to define what "a suboptimal result" means. During the years, several cut-off values for post-PCI FFR have been proposed although most of the data bulks around 0.89 and 0.91 (19), with recent evidence hinting at the possibility of different cutoff for different vessels (20). In line with previous data, our study suggests that the best cut-off value is above 0.9, but this threshold has, however, a modest ability of predicting MACE occurrence at follow-up.

Accordingly, a large meta-analysis of 105 studies confirmed the relation among FFR below 0.9 and the risk of MACE or TVR and the recent FFR-SEARCH study which showed that patients with post-PCI FFR < 0.9 had 6.2% incidence of TVR at 48 months vs. 3.9% for FFR above 0.9 (18, 21).

Once a "suboptimal functional result" is observed, choosing how to manage the lesion is a complex task; indeed, a suboptimal post-PCI FFR could recognize a wide range of causes from stent under-expansion, to edge dissection, missed stenosis, diffuse atherosclerotic disease etc. One of the limitations of the postprocedural IPA of coronary circulation is its limited ability

10.3389/fcvm.2022.983003

TABLE 7 Cox regression analysis for major adverse cardiovascular events (MACE).

	Hazard ratio	95% confidence interval	*p*
Age	1.008	0.990–1.027	0.373
Male gender	0.838	0.569–1.234	0.371
Hypertension	1.267	0.741–2.168	0.387
Diabetes	1.379	0.945–2.014	0.096
Chronic kidney disease	0.714	0.331–1.540	0.390
Previous MI	1.625	1.056–2.500	0.027
Previous PCI	1.166	0.773–1.758	0.464
Clinical presentation			
NSTEMI vs. CCS	1.392	0.681–2.846	0.364
STEMI vs. CCS	1.341	0.889–2.022	0.162
Ejection fraction < 40%	1.855	0.899–3.825	0.094
Multivessel disease	1.414	0.926–2.160	0.109
Revascularization strategy without post-PCI functional assessment	1.893	1.002–3.575	0.049

Coordinates of the Curve

Test Result Variable(s): FINAL FFR

Positive if Greater Than or Equal To[a]	Sensitivity	1 - Specificity
,0000	1,000	1,000
,7900	,990	1,000
,8050	,980	1,000
,8150	,971	1,000
,8250	,931	1,000
,8350	,922	,750
,8450	,902	,750
,8550	,814	,750
,8650	,784	,750
,8750	,696	,500
,8850	,618	,500
,8950	,569	,500
,9050	,431	,250
,9150	,343	,250
,9250	,284	,250
,9350	,265	,250
,9450	,216	,125
,9550	,167	,125
,9650	,127	,000
,9750	,078	,000
1,0000	,000	,000

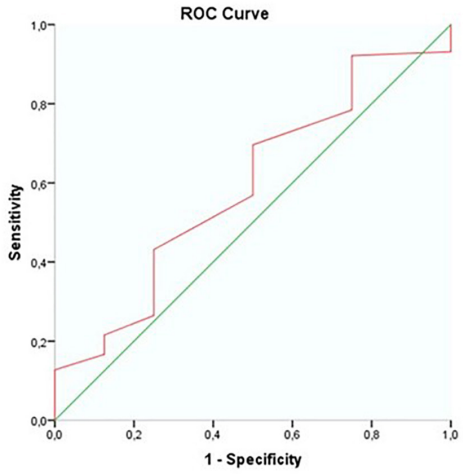

FIGURE 5
ROC curves for the ability of final fractional flow reserve (FFR) value to predict major adverse cardiovascular events (MACE)-free survival.

to identify the causes of a suboptimal result. In this regard, a pressure pullback maneuver can help in the identification of the causes of a suboptimal result limiting intracoronary imaging to doubtful cases (8).

Limitations

As any other observational study, the PROPHET-FFR study suffers from some limitations. First of all, it is a single center study with a retrospective design. This is clearly demonstrated by the fact that of over 1,300 patients, only 180 received post-PCI physiology and of those, only 12% (22°pts) received post-PCI optimization. However, this design is intentional in the present phase to take a snapshot of the preference of the operators in a center with a large experience in coronary physiology without forcing them to follow a specific algorithm. For example, in the present study the pressure pullback maneuver was not systematically performed, neither in the pre-PCI assessment, when new indexes, such as the pullback pressure gradient (PPG) proposed by Collet et al. (21) could help in planning the procedure, nor in the post-PCI phase. This is a limitation of the study which will be amended in the ongoing prospective phase in which we will test a standardized approach to a fully "Physiology-guided PCI" and compare the outcome results with those obtained in the retrospective phase

(8). We believe that the use of this approach could improve clinical outcomes by reducing the number of those lesions with a suboptimal functional result not further optimized that represent, in our study as in other similar studies (16–18), the most important limitation.

Conclusion

In conclusion, our observational study suggests that "Physiology-guided PCI" in intermediate coronary stenosis is a feasible strategy, associated with a significant cost sparing and more importantly with potential favorable impact on mid-term prognosis. The lack of a strong cutoff and the need for a systematic approach to localize and manage the suboptimal results make imperative the completion of prospective studies using a standardized physiological approach.

Data availability statement

The raw data supporting the conclusions of this article will be made available by the authors, without undue reservation.

Ethics statement

The studies involving human participants were reviewed and approved by Comitato Etico del Policlinico Gemelli di Roma. The patients/participants provided their written informed consent to participate in this study.

Author contributions

AL: conception and design, analysis and interpretation of data, drafting, and revising critically the manuscript for important intellectual content. SM: analysis of data and drafting of the manuscript. GZ, PC, EB, DG, FD, GA, AV, EP, AD, GC, DD'A, RV, RM, AB, ER, and CA: collection, analysis, and interpretation of data. FB, CT, and FC: important intellectual contribution. All authors contributed to the article and approved the submitted version.

Funding

The authors thank the Italian Ministry of Health for the funding within the "Ricerca corrente 2021" project.

Conflict of interest

FB and CT disclose having been involved in advisory board meetings or having received speaker's fees from Abbott, Abiomed, Medtronic, and Biotronic. CA has been involved in advisory board activities by Abbott, Abiomed, Medtronic, and Biotronic.

The remaining authors declare that the research was conducted in the absence of any commercial or financial relationships that could be construed as a potential conflict of interest.

Publisher's note

All claims expressed in this article are solely those of the authors and do not necessarily represent those of their affiliated organizations, or those of the publisher, the editors and the reviewers. Any product that may be evaluated in this article, or claim that may be made by its manufacturer, is not guaranteed or endorsed by the publisher.

References

1. Neumann FJ, Sechtem U, Banning AP, et al. 2019 ESC Guidelines for the diagnosis and management of chronic coronary syndromes. *Eur Heart J.* (2020) 41:407–77. doi: 10.1093/eurheartj/ehz425

2. Neumann FJ, Sousa-Uva M, Ahlsson A, Alfonso F, Banning AP, Benedetto U, et al. 2018 ESC/EACTS Guidelines on myocardial revascularization. *Eur Heart J.* (2019) 40:87–165. doi: 10.1093/eurheartj/ehy394

3. Liu PY, Lin WY, Lin LF, Lin CS, Lin WS, Cheng SM, et al. Chest pain with normal thallium-201 myocardial perfusion image – is it really normal? *Acta Cardiol Sin.* (2016) 32:328. doi: 10.6515/ACS20150517A

4. Valgimigli M, Tebaldi M, Borghesi M, Vranckx P, Campo G, Tumscitz C, et al. Two-year outcomes after first- or second-generation drug-eluting or bare-metal stent implantation in all-comer patients undergoing percutaneous coronary intervention: a pre-specified analysis from the PRODIGY study (PROlonging Dual Antiplatelet Treatment After Grading stent-induced Intimal hyperplasia studY). *JACC Cardiovasc Intervent.* (2014) 7:20–8. doi: 10.1016/J.JCIN.2013.09.008

5. Cohen DJ, Van Hout B, Serruys PW, Mohr FW, Macaya C, den Heijer P, et al. Quality of life after PCI with drug-eluting stents or coronary-artery bypass surgery. *N Engl J Med.* (2011) 364:1016–26. doi: 10.1056/NEJMOA1001508

6. Stone GW, Ellis SG, Gori T, Metzger DC, Stein B, Erickson M, et al. Blinded outcomes and angina assessment of coronary bioresorbable scaffolds: 30-day and 1-year results from the ABSORB IV randomised trial. *Lancet.* (2018) 392:1530–40. doi: 10.1016/S0140-6736(18)32283-9

7. Ding D, Huang J, Westra J, Cohen DJ, Chen Y, Andersen BK, et al. Immediate post-procedural functional assessment of percutaneous coronary intervention: current evidence and future directions. *Eur Heart J.* (2021) 42:2695–707. doi: 10.1093/EURHEARTJ/EHAB186

8. Zimbardo G, Cialdella P, Di Giusto F, Migliaro S, Anastasia G, Petrolati E, et al. Physiological assessment after percutaneous coronary intervention: the hard truth. *Panminerva Med.* (2021) 2021:9. doi: 10.23736/S0031-0808.21.04363-9

9. Bedogni F, Indolfi C, Ribichini F, Verna E, Leone AM, Polimeni A, et al. Position paper on the theoretical basis, practical application and health economic evaluation of the functional assessment of coronary lesions endorsed by the Italian Society of Invasive Cardiology (SICI-GISE)]. *G Ital Cardiol.* (2015) 16:116–28. doi: 10.1714/1798.19590

10. Leone AM, Porto I, De Caterina AR, Basile E, Aurelio A, Gardi A, et al. Maximal hyperemia in the assessment of fractional flow reserve: intracoronary adenosine versus intracoronary sodium nitroprusside versus intravenous adenosine: the NASCI (Nitroprussiato versus Adenosina nelle Stenosi Coronariche Intermedie) study. *JACC Cardiovasc Intervent.* (2012) 5:402–8. doi: 10.1016/j.jcin.2011.12.014

11. Garcia-Garcia HM, McFadden EP, Farb A, Mehran R, Stone GW, Spertus J, et al. Standardized end point definitions for coronary intervention trials: the academic research consortium-2 consensus document. *Circulation.* (2018) 137:2635–50. doi: 10.1161/CIRCULATIONAHA.117.029289

12. Thygesen K, Alpert JS, Jaffe AS, Chaitman BR, Bax JJ, Morrow DA, et al. Fourth universal definition of myocardial infarction (2018). *Circulation.* (2018) 138:e618–51. doi: 10.1161/CIR.0000000000000617

13. Burzotta F, Leone AM, Aurigemma C, Zambrano A, Zimbardo G, Arioti M, et al. Fractional flow reserve or optical coherence tomography to guide management of angiographically 11 coronary stenosis: a single-center trial. *JACC Cardiovasc Intervent.* (2020) 13:49–58. doi: 10.1016/J.JCIN.2019.09.034

14. Tebaldi M, Biscaglia S, Fineschi M, Musumeci G, Marchese A, Leone AM, et al. Evolving routine standards in invasive hemodynamic assessment of coronary stenosis: the nationwide Italian SICI-GISE cross-sectional ERIS study. *JACC Cardiovasc Intervent.* (2018) 11:1482–91. doi: 10.1016/J.JCIN.2018.04.037

15. Diletti R, Masdjedi K, Daemen J, van Zandvoort LJC, Neleman T, Wilschut J, et al. Impact of poststenting fractional flow reserve on long-term clinical outcomes: the FFR-SEARCH study. *Circ Cardiovasc Intervent.* (2021) 14:9681. doi: 10.1161/CIRCINTERVENTIONS.120.009681

16. Uretsky BF, Agarwal SK, Vallurupalli S, Al-Hawwas M, Hasan R, Miller K, et al. Prospective evaluation of the strategy of functionally optimized coronary intervention. *J Am Heart Associat.* (2020) 9:15073. doi: 10.1161/JAHA.119.015073

17. Agarwal SK, Kasula S, Hacioglu Y, Ahmed Z, Uretsky BF, Hakeem A. Utilizing post-intervention fractional flow reserve to optimize acute results and the relationship to long-term outcomes. *JACC Cardiovasc Intervent.* (2016) 9:1022–31. doi: 10.1016/J.JCIN.2016.01.046

18. Collison D, Didagelos M, Aetesam-Ur-Rahman M, Copt S, McDade R, McCartney P, et al. Post-stenting fractional flow reserve vs coronary angiography for optimization of percutaneous coronary intervention (TARGET-FFR). *Eur Heart J.* (2021) 42:4656–68. doi: 10.1093/EURHEARTJ/EHAB449

19. Hwang D, Lee JM, Lee HJ, Kim SH, Nam CW, Hahn JY, et al. Influence of target vessel on prognostic relevance of fractional flow reserve after coronary stenting. *Eurointervention.* (2019) 15:457–64. doi: 10.4244/EIJ-D-18-00913

20. Rimac G, Fearon WF, De Bruyne B, Ikeno F, Matsuo H, Piroth Z, et al. Clinical value of post-percutaneous coronary intervention fractional flow reserve value: a systematic review and meta-analysis. *Am Heart J.* (2017) 183:1–9. doi: 10.1016/J.AHJ.2016.10.005

21. Collet C, Sonck J, Vandeloo B, Mizukami T, Roosens B, Lochy S, et al. Measurement of hyperemic pullback pressure gradients to characterize patterns of coronary atherosclerosis. *J Am Coll Cardiol.* (2019) 74:1772–84. doi: 10.1016/J.JACC.2019.07.072

frontiers | Frontiers in Cardiovascular Medicine

TYPE Systematic Review
PUBLISHED 20 September 2022
DOI 10.3389/fcvm.2022.946027

OPEN ACCESS

EDITED BY
Massimo Iacoviello,
University of Foggia, Italy

REVIEWED BY
Satoru Mitomo,
New Tokyo Hospital, Japan
Vincenzo De Marzo,
Università degli Studi di Genova, Italy

*CORRESPONDENCE
Jaffer Shah
jaffer.shah@kateb.edu.af

SPECIALTY SECTION
This article was submitted to Coronary Artery Disease, a section of the journal Frontiers in Cardiovascular Medicine

RECEIVED 17 May 2022
ACCEPTED 16 August 2022
PUBLISHED 20 September 2022

CITATION
Abusnina W, Mostafa MR, Al-Abdouh A, Radaideh Q, Ismayl M, Alam M, Shah J, Yousfi NE, Paul TK, Ben-Dor I and Dahal K (2022) Outcomes of atherectomy in treating severely calcified coronary lesions in patients with reduced left ventricular ejection fraction: A systematic review and meta-analysis. *Front. Cardiovasc. Med.* 9:946027. doi: 10.3389/fcvm.2022.946027

Outcomes of atherectomy in treating severely calcified coronary lesions in patients with reduced left ventricular ejection fraction: A systematic review and meta-analysis

Waiel Abusnina[1], Mostafa Reda Mostafa[2], Ahmad Al-Abdouh[3], Qais Radaideh[1], Mahmoud Ismayl[1], Mahboob Alam[4], Jaffer Shah[5]*, Noraldeen El Yousfi[6], Timir K. Paul[7], Itsik Ben-Dor[8] and Khagendra Dahal[1]

[1]Department of Cardiology, Creighton University School of Medicine, Omaha, NE, United States, [2]Department of Medicine, Rochester Regional/Unity Hospital, Rochester, NY, United States, [3]Department of Medicine, University of Kentucky, Lexington, KY, United States, [4]Section of Cardiology, Department of Medicine, Baylor College of Medicine, Houston, TX, United States, [5]Medical Research Center, Kateb University, Kabul, Afghanistan, [6]Tripoli Medical Center, Tripoli, Libya, [7]Department of Medical Education, University of Tennessee at Nashville, Nashville, TN, United States, [8]Section of Interventional Cardiology, MedStar Washington Hospital Center, Washington, DC, United States

Background: Severely calcified coronary lesions with reduced left ventricular (LV) function result in worse outcomes. Atherectomy is used in treating such lesions when technically feasible. However, there is limited data examining the safety and efficacy of atherectomy without hemodynamic support in treating severely calcified coronary lesions in patients with reduced left ventricular ejection fraction (LVEF).

Objective: To evaluate the clinical outcomes of atherectomy in patient with reduced LVEF.

Methods: We searched PubMed, Cochrane CENTRAL Register and ClinicalTrials.gov (inception through July 21, 2021) for studies evaluating the outcomes of atherectomy in patients with severe LV dysfunction. We used random-effect model to calculate risk ratio (RR) with 95% confidence interval (CI). The endpoints were in-hospital and long term all-cause mortality, cardiac death, myocardial infarction (MI), and target vessel revascularization (TVR).

Results: A total of 7 studies consisting of 2,238 unique patients were included in the analysis. The median follow-up duration was 22.4 months. The risk of in-hospital all-cause mortality using atherectomy in patients with severely reduced LVEF compared to the patients with moderate reduced or preserved LVEF was [2.4vs.0.5%; RR:5.28; 95%CI 1.65–16.84; $P = 0.005$], the risk of long term all-cause mortality was [21 vs. 8.8%; RR of 2.84; 95% CI 1.16–6.95; $P = 0.02$]. In-hospital TVR risk was 2.0 vs. 0.6% (RR: 4.15; 95% CI 4.15–15.67;

$P = 0.04$) and long-term TVR was [6.0 vs. 9.9%; RR of 0.75; 95% CI 0.39–1.42; $P = 0.37$]. In-hospital MI was [7.1 vs. 5.4%; RR 1.63; 95% CI 0.91–2.93; $P = 0.10$], long-term MI was [7.5 vs. 5.7; RR 1.74; 95%CI 0.95–3.18; $P = 0.07$).

Conclusion: Our meta-analysis suggested that the patients with severely reduced LVEF when using atherectomy devices experienced higher risk of clinical outcomes in the terms of all-cause mortality and cardiac mortality. As we know that the patients with severely reduced LVEF are inherently at increased risk of adverse clinical outcomes, this information should be considered hypothesis generating and utilized while discussing the risks and benefits of atherectomy in such high risk patients. Future studies should focus on the comparison of outcomes of different atherectomy devices in such patients. Adjusting for the inherent mortality risk posed by left ventricular dysfunction may be a strategy while designing a study.

KEYWORDS

reduced ejection fraction, left ventricular dysfunction, severe coronary calcification, atherectomy, percutaneous coronary intervention

Introduction

Severely calcified coronary lesions exist in up to 20% of patients undergoing percutaneous coronary intervention (PCI) (1). Performing PCI to severely calcified coronary artery lesions is technically challenging because of the difficulty of balloon or stent delivery and optimal stent apposition and expansion, which may lead to underexpansion with increased risk of stent thrombosis and restenosis (2). Atherectomy is one of the effective ways to treat severely calcified coronary lesions that can modify calcified plaques to facilitate balloon or stent delivery and optimize stent expansion (3, 4). The 2011 American College of Cardiology Foundation/American Heart Association/Society for Cardiovascular Angiography and Interventions PCI guidelines gave Class IIa (level of evidence C) recommendation for rotablator for the treatment of heavily calcified plaques that cannot be crossed by a balloon catheter or adequately dilated before stenting (5).

Patients with severe coronary artery calcifications and severely reduced left ventricular ejection fraction (LVEF) have worse prognosis than those with normal LVEF, and pose technical challenges in standard PCI techniques (6). Although coronary artery bypass grafting (CABG) has been recommended for patients with left ventricular (LV) systolic dysfunction as a first line revascularization strategy (6), due to the technological advances and improvements in intervention techniques, high-risk PCI using atherectomy is an alternative to high-risk CABG (7–9). As there are a few reports that have focused on the clinical outcomes of atherectomy in patients with severe LV dysfunction, we aimed to perform a systematic review and meta-analysis of available literature in this regard.

Abbreviations: PCI, Percutaneous coronary intervention; LVEF, Left ventricular ejection fraction; CAC,Coronary artery calcification; CABG, Coronary artery bypass grafting.

Methods

Data source and search strategy

A meta-analysis was performed according to the Preferred Reporting Items for Systematic Reviews an Meta-Analyses (PRISMA) 2009 guidelines (10). Two reviewers (WA and MA) independently identified the relevant studies by an electronic search of the PubMed, EMBASE, Cochrane Central Register of Controlled Trials, and ClinicalTrials.gov databases (from inception to July 2021) (Supplementary Table 1). References of the retrieved studies were also screened further for relevant studies. The following search terms and key words were used: "atherectomy" OR "orbital atherectomy" OR "rotational atherectomy" AND "reduced ejection fraction" OR "heart failure with reduced ejection fraction" OR "left ventricular dysfunction" AND "severely calcified coronary lesions" and "coronary artery disease." There was no language, publication date or publication status restrictions imposed.

Study selection

Two investigators (WA and MA) independently assessed the eligibility of studies on the basis of titles, abstracts, and full-text reports. Discrepancies in study selection were discussed and resolved with the third investigator (KD). Eligible studies had to

TABLE 1 Study characteristics included in the meta-analysis.

Study	Type	Total	Type of Atherectomy	# of arms	Severely reduced EF	Moderate reduced EF	normal EF	Follow up
Lee et al. (8)	prospective	437	orbital	three groups	26–40%	41–50%	> 50%	In-hospital/12 months
Shlofmitz et al. (15)	retrospective	438	orbital	two groups	≤40	>40	30 days	
Watanabe et al., (11)	retrospective	270	rotational	two groups	≤35%	>35%		in–hospital/30 days
Whiteside et al., (12)	retrospective	131	rotational	three groups	≤30 %	30–50%	>50%	in-hospital
Mankerious et al. (13)	retrospective	644	rotational	three groups	≤35%	36–54%	≥55%	in-hospital/5 years
Zhang et al. (3)	retrospective	140	rotational	three groups	≤35%	36–50%	>50%	in-hospital/24 months
Yoshida et al. (14)	retrospective	178	rotational	three groups	≤35%	36–50%	>50%	in-hospital/12 months

EF, ejection fraction.

satisfy the following prespecified criteria: (a) Studies evaluating the use of atherectomy for coronary lesions in patients with left ventricular dysfunction (b) availability of clinical outcome data. The exclusion criteria were lack of any clinical outcome data and duplicated publications. Our study population included patients with severely reduced LVEF, moderate LVEF and preserved LVEF. We compared patients with severely reduced LVEF as one groups to the combined (moderate and preserved LVEF) as one group. Severely reduced LVEF and moderate LVEF were attributed according to the definition used in each study as shown in (Table 1).

Data extraction and quality assessment

Two investigators (WA and QA) independently extracted data (baseline characteristics, definition of outcomes and number of events) using a standardized data abstraction form. The same investigators independently and systematically assessed the studies' methodological quality using the Newcastle Ottawa Scale (Supplementary Table 2), disagreements were resolved by a third author (KD). We assessed for publication bias using the funnel plots for the outcomes (Supplementary Figure 1).

Outcome measures

The endpoints were in-hospital and long term all-cause mortality, cardiac death, myocardial infarction (MI), and target vessel revascularization (TVR). Procedural outcomes were also analyzed including slow or no reflow, perforation and dissection. Endpoints were attributed according to the definition used in each study. Definition of MI in each included study were reported in the Supplementary Table 3.

Statistical analysis

For categorical outcomes, the risk ratios (RRs) with 95% confidence intervals (CI) were calculated and study -specific RR were combined with the DerSimonian and Laird random effects model with the estimate of heterogeneity using the Mantel–Haenszel model. We used I^2 statistic to measure heterogeneity among the trials; a value of 0% indicates no observed heterogeneity, and values of 25, 50, and 75% define low, moderate, and high heterogeneity, respectively. The presence of publication bias for each outcome was investigated by visual estimation of funnel plots when data was available for at least three studies. Results were reported according to the Preferred Reporting Items for Systematic Reviews and Meta-Analyses Protocol (PRISMA-P) 2015 statement. Analyses were performed using Review Manager (RevMan) Version 5.3 (The Nordic Cochrane Center, The Cochrane Collaboration, Copenhagen, Denmark).

Results

Search results

Figure 1 displays the PRISMA diagram for study search and selection. A total of seven studies (six retrospective and one prospective studies) including 2, 238 patients, 270 with severely reduced LVEF, and 1,968 patients with moderately reduced or preserved LVEF were included in the meta-analysis. The median follow-up duration for long term outcome was 22.4 months. The characteristics of the included studies and the patients' demographics are presented in Tables 1, 2, respectively.

Clinical outcomes

In-hospital and long term outcomes (all-cause mortality, cardiac death, MI and TVR) were reported in all the studies. In-hospital all-cause mortality and TVR were significantly higher

10.3389/fcvm.2022.946027

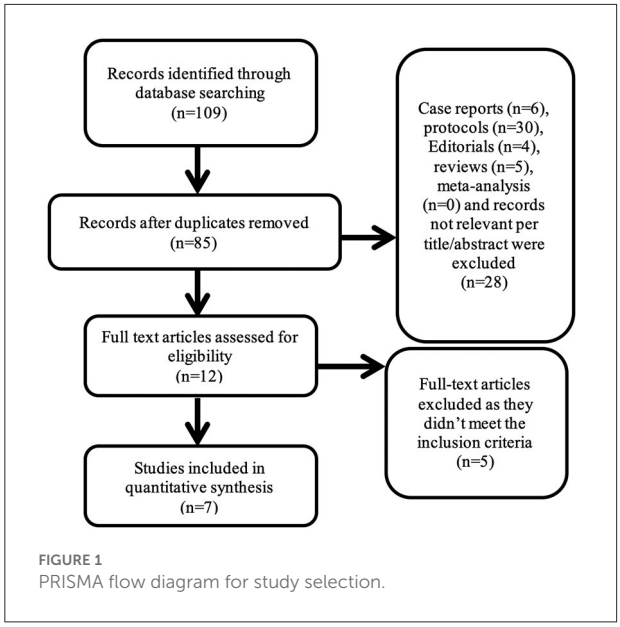

FIGURE 1
PRISMA flow diagram for study selection.

in patients with severely reduced LVEF as compared to patients with moderate and preserved LVEF who had atherectomy (RR: 5.28; 95% CI 1.65–16.84; $P = 0.005$; $I^2 = 0\%$; Figure 2A) and (RR: 4.15; 95% CI 4.15–15.67; $P = 0.04$; $I^2 = 0\%$; Figure 2D), respectively. There was no significant difference between the two groups in in-hospital cardiac death (RR of 3.71; 95% CI 0.55–24.87; $P = 0.18$; $I^2 = 0\%$; Figure 2B) and MI (RR of 1.63; 95% CI 0.91–2.93; $P = 0.10$; $I^2 = 0\%$; Figure 2C). Patients with severely reduced LVEF had higher rate of long term all-cause mortality (RR of 2.84; 95% CI 1.16–6.95; $P = 0.02$; $I^2 = 53\%$; Figure 3A) and long-term cardiac death (RR of 4.27; 95% CI 1.68–10.83; $P = 0.002$; $I^2 = 24\%$; Figure 3B) compared with moderate and preserved LVEF. There was no difference between the two groups in term of long-term MI (RR of 1.74; 95% CI 0.95–3.18; $P = 0.07$; $I^2 = 28\%$; Figure 3C) and long-term TVR (RR of 0.75; 95% CI 0.39–1.42; $P = 0.37$; $I^2 = 18\%$; Figure 3D).

Procedural complications

Procedural complications including slow flow or no reflow, coronary perforation, and coronary dissection were analyzed (Figure 4). Slow or no reflow was significantly higher in patients with severely reduced LVEF (RR: 4.19; 95% CI 2.03–8.65; $P = 0.0001$; $I^2 = 44\%$; Figure 4A). Atherectomy in patients with severely reduced LVEF is associated with higher coronary perforation (RR: 2.11; 95% CI 1.00–4.45; $P = 0.05$; $I^2 = 0\%$; Figure 4B). There was no difference between the two groups in peri-procedural dissection (RR: 2.05; 95% CI 0.84–4.98; $P = 0.11$; $I^2 = 26\%$; Figure 4C).

TABLE 2 Baseline characteristics of the all the included studies.

Study	Lee AI 2017			Shlofmitz et al. (15)		Watanabe et al. (11)		Whiteside et al. (12)			Mankerious et al. (13)			Zhang et al. (3)			Yoshida et al.[3] (14)		
	EF (26-40%)	EF 41-50%	EF > 50%	EF ≤ 40	EF > 40	EF ≤ 35%	EF > 35%	EF ≤ 30	EF 30-50	EF > 50	EF ≤ 35%	EF 36-54	EF ≥ 55	EF ≤ 35%	EF (36-50%)	EF>50%	EF ≤ 35%	EF 36-50%	EF ≥ 50
Number of participants	33	90	314	69	369	33	237	18	42	71	82	170	392	10	11	119	25	44	109
Age, mean (years)	71.3 ± 1.9	71.7 ± 1.1	71.3 ± 0.5	73.8 ± 12.3	73.6 ± 9.5	69.7± 7	70.8 ± 8.8	69.6 ± 11.7	66.6 ± 11.2	67.9 ± 8.9	72.5 ± 8.7	72.9 ± 8.3	71.9 ± 8.4	76 ± 9.3	75.9 ± 9.2	69.9 ± 9.1	72.2 ± 8.8	76.8 ± 8.6	73.9 ± 8.2
Men	84.8%	75.6%	59.9%	71%	67.5%	76%	75.9%	77.8%	76.2%	60.6%	78%	75.3%	73.5%	40%	45.5%	60.5%	60%	77.3%	59.6%
Diabetes mellitus	42.4%	46.7%	33.1%	50.7%	39.8%	55%	51.3%	61.1%	54.8%	53.5%	32.1%	37.6%	34.1%	70%	54.5%	49.6%	52%	50%	62.4%
Previous Myocardial infarction	53.1%	37.5%	15.4%	31.9%	12.7%	91%	28.7%	72.2%	38.1%	15.5%	N/A	N/A	N/A	40%	36.4%	15.1%	20%	38.6%	16.5%
Hypertension	90.9%	91.1%	91.7%	82.6%	86.7%	88%	88.9%	100%	95.2%	85.9%	90.1%	94.7%	89.5%	100%	63.6%	75.6%	28%	43%	64%
Chronic kidney disease	N/A	N/A	N/A	36.8%	15.8%	90%	54.9%	n/a	N/A	N/A	32.2%	24.4%	11%	n/a	n/a	n/a	72% %	45.5%	47.7%
Smoker	75.8%	74.4%	62.7%	11.6%	3.0%	58%	63.9%	n/a	N/A	N/A	33.3%	27.6	32.6%	n/a	n/a	n/a	60%%	75.1%	50.2%
Imepla	N/A	N/A	N/A	9 (13%)	0	N/A	N/A	N/A	N/A	N/A	1 (1.2%)	0	0	N/A	N/A	N/A	N/A	N/A	N/A
IABP	N/A	N/A	N/A	6 (8.7%)	6 (1.6)	5 (15%)	5 (2.1%)	2 (11.1%)	1 (2.4%)	0	4 (4.9%)	1 (0.6%)	1 (0.3%)	N/A	N/A	N/A	7 (24.1%)	2 (4.4%)	13 (11%)
ECMO	N/A	N/A	N/A	1 (1.4%)	0	N/A	N/A	N/A	N/A	N/A	N/A	N/A	N/A	N/A	N/A	N/A	N/A	N/A	N/A

EF, ejection fraction; N/A, not available.

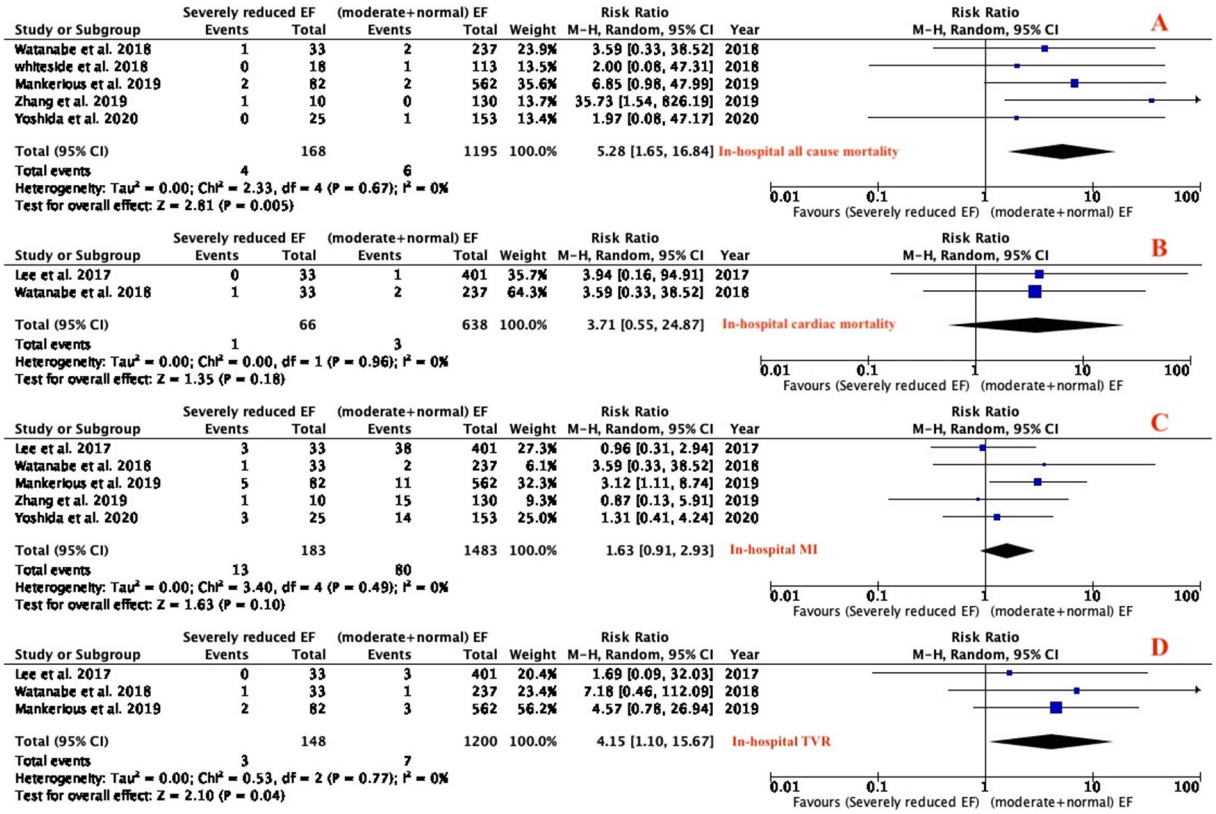

FIGURE 2
Forest plot of in-hospital outcomes (all-cause mortality, cardiac mortality, MI, TVR). (MI, myocardial infarction; TVR, target vessel revascularization).

Heterogenicity, publication bias and asymmetry

With respect to clinical outcomes, there was no heterogeneity for in-hospital all-cause mortality ($P = 0.005$, $I^2 = 0\%$), cardiac mortality ($P = 0.18$, $I^2 = 0\%$), MI ($P < 0.10$, $I^2 = 0\%$) and TVR ($p < 0.04$, $I^2 = 0\%$). Heterogenicity was low for long term cardiac mortality ($P < 0.002$, $I^2 = 24\%$), MI ($P < 0.07$, $I^2 = 28\%$), and TVR ($P < 0.37$, $I^2 = 18\%$). There was moderate heterogeneity for long term all-cause mortality ($P = 0.02$, $I^2 = 53\%$). Overall, heterogenicity was low and there was no evidence of publication bias on visual inspection of funnel plots for the clinical outcomes (Supplemental Figure 1).

Discussion

The current meta-analysis evaluated in-hospital and long-term outcomes of patients with severely calcified coronary lesions who underwent PCI with atherectomy. We divided the patients in two groups depending on their LV dysfunction and compared their clinical risks. The main findings of the analysis were (1) Treating severely calcified coronary artery disease with atherectomy in patients with severely reduced LVEF had significant higher in-hospital and long term all-cause mortality risks compared to the patients with moderate or preserved LVEF, (2) There was no significant difference in in-hospital cardiac mortality between the two groups while long term cardiac mortality was significantly higher in patients with severe coronary artery calcification (CAC) and severely reduced LVEF who underwent atherectomy, (3) The risk of in-hospital MI was higher in patients with severely reduced LVEF while no difference in long term MI compared to those patients with moderately reduced or preserved LVEF. (4) There was increased risk of no reflow/slow flow but similar risk of coronary perforation and dissection between two groups.

Severe CAC makes PCI challenging and difficult to achieve optimal results. Despite advances in interventional equipment and techniques, the outcome in patients with severe CAC remains worse than those with non-calcified coronary stenosis (16, 17). Generally, PCI in patients with LVEF <35% is associated with higher in-hospital mortality rates (18) and

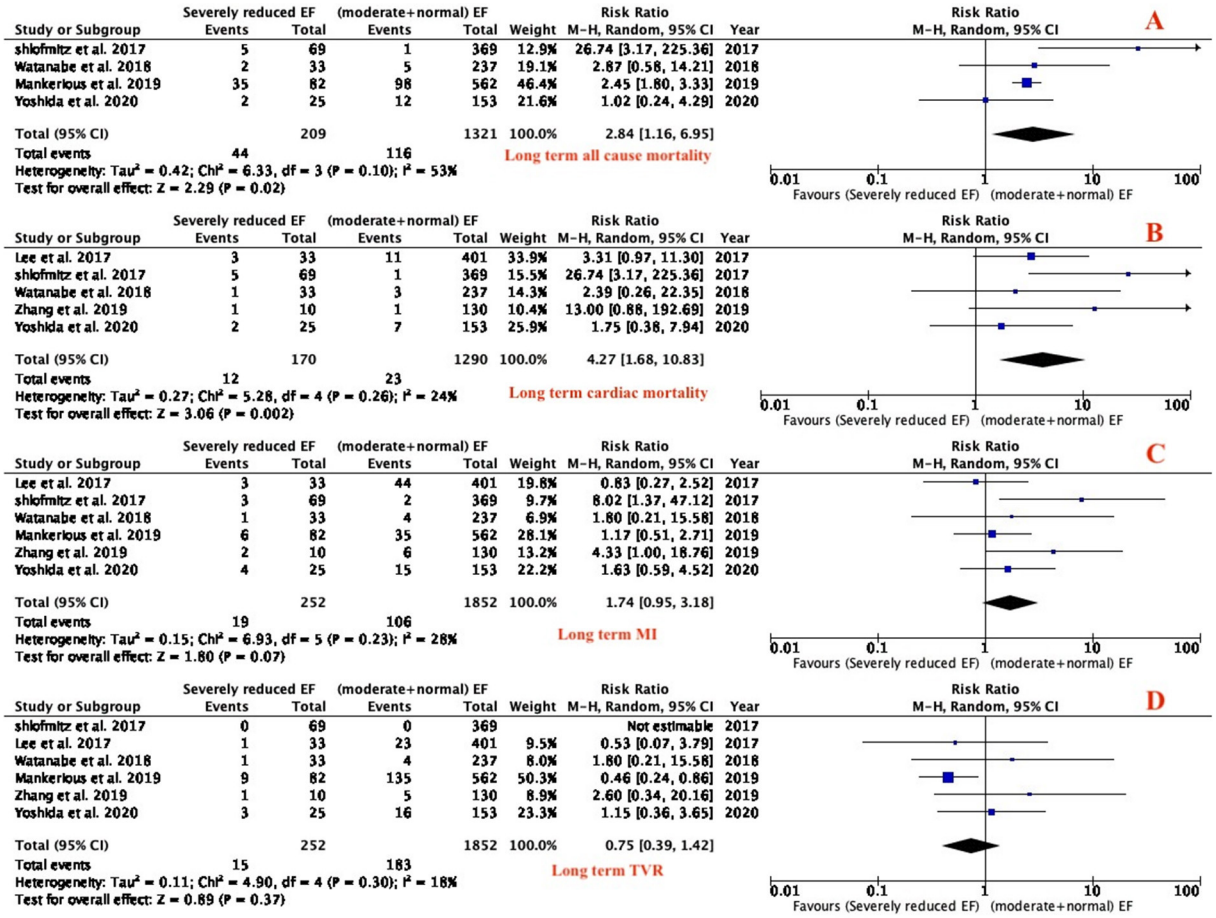

FIGURE 3
Forest plot of long term outcomes (all-cause mortality, cardiac mortality, MI, TVR). (MI, myocardial infarction; TVR, target vessel revascularization).

is considered as a high-risk PCI (5, 6). Patients with severe CAC and left ventricular systolic dysfunction undergoing PCI has worse prognosis and increased risk of adverse events after PCI, including death (19–21). Left ventricular systolic dysfunction was also reported to be an independent predictor of poor clinical outcomes in patients undergoing rotational atherectomy (22). The atherectomy technique has been widely critiqued for its association with high complication rates, and is still performed in patients with high pre-procedural risk, like patients with severely LVEF, which can further increase the risk(23). Pivotal Trial to Evaluate the Safety and Efficacy of the Diamondback 360°® Orbital Atherectomy System in Treating De Novo, Severely Calcified Coronary Lesions (ORBIT II) showed that preparation of severely calcified plaque with the Orbital Atherectomy System not only helped facilitate stent delivery, but had lower rates of in-hospital Q-wave MI (0.7%), cardiac death (0.2%), and TVR(0.7%).(24) In addition, the rate of 1-year cardiac death in ORBIT II study increased as LVEF decreased. However, a study by Jujo et al. (25) suggested that using rational atherectomy in treating treat severely calcified coronary artery stenoses as therapeutic strategy, is associated with increased rates of PCI success and improved long-term CV mortality.

There are several explanations for the increased mortality among severely reduced LVEF patients with atherectomy. First, there is inherently increased mortality associated with low LVEF compared to normal EF patients (26) Second, the use of atherectomy can increase the risk of the mechanical and thermal injury and distal micro embolization causing no-reflow or slow flow, which may carry a more deleterious effect among low LVEF than preserved LVEF patients (27) with the resulting microvascular dysfunction leading to worse outcomes. An analysis from National Cardiovascular Data Registry CathPCI Registry showed increase in the temporal use of coronary atherectomy, either orbital or rotational, with a temporal decline in MI (odds ratio 0.97 [95%CI 0.96–0.98], $P<0.001$) (4). On

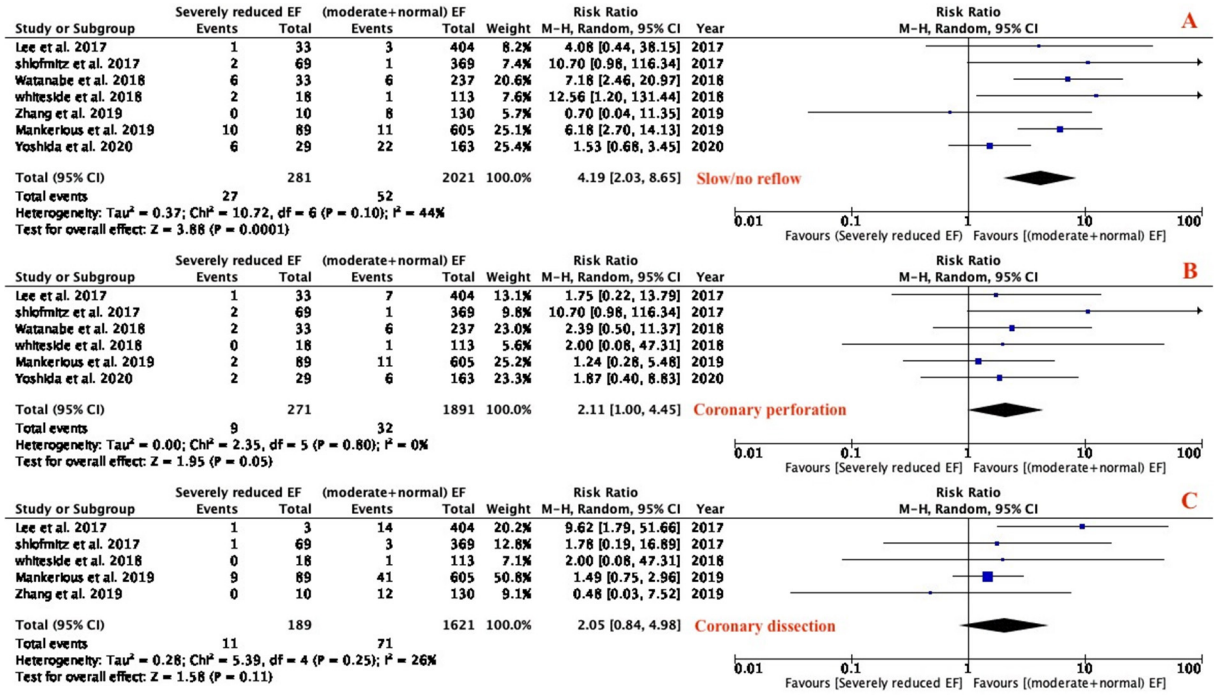

FIGURE 4
Forest plot of procedural outcomes (slow/no reflow, coronary perforation, dissection).

the other hand, McEntegart et al. (28) reported that rotational atherectomy was associated with a type 4A MI rate of 24% as detected by cardiac magnetic resonance imaging. Our study demonstrated non-significant difference in both in-hospital MI [(RR of 1.63; 95% CI 0.91–2.93; $P = 0.10$) and long-term MI (RR of 1.74; 95% CI 0.95–3.18; $P = 0.07$] in patients with severely reduced LVEF compared to the other group. However, Atherectomy has been tested in several high risk population and showed comparable adverse cardiac events in patients with acute coronary syndrome and in patients with calcified lesions ≥25 mm of length (29, 30). While atherectomy in reduced EF was independently linked to worse cardiac events including death and MI (22, 31), PROTECT II (32) has shown that the use of mechanical support device during atherectomy was associated with poor MACE in reduced EF groups which denotes that the utility of mechanical support devices would be an independent predictor of worse outcomes in such a compromised subset of population.

Our meta-analysis demonstrates higher rates of in-hospital TVR in the groups with severely reduced LVEF while the long term TVR rates were not different between the two groups. One study showed that TVR rates at 5 years were not affected by LVEF (13). In ORBIT II, the rate of 1-year TVR was comparable across the LVEF groups (24). The lack of difference in TVR rates at follow up between the compared groups might be explained by the late catch-up phenomena, and the likelihood of microembolization having more deleterious effect in patients with depressed LVEF. It was also reported that in severely calcified lesions that necessitated rotational atherectomy, thin-strut drug eluting stent resulted in lower rates of TVR compared to thick-strut drug eluting stent (33).

Limitations

The main limitation of this meta-analysis is that the cohort of patients with severely reduced LVEF are inherently high risk population with worse outcomes due to underlying cardiac pathology independently from the atherectomy use. Another major limitation of our study is the relatively small sample size, which may limit the generalization of the results. However, we need to understand that it may not be feasible to generate a large sample of patients in such cohorts. Also, our study has other several limitations including the use of different atherectomy devices, with different size and number of burr. Moreover, severely reduced LVEF was defined differently in the included studies. In addition, the studies were non-randomized, which can have inherent selection bias. Other main limitation is that the outcomes were not adjusted for different variables. Despite all these limitations, we believe that the current review adds to the understanding of clinical outcomes in patients with reduced LVEF with severely calcified lesions with the use of atherectomy.

Conclusion

Our meta-analysis suggested that the patients with severely reduced LVEF when using atherectomy devices experienced higher risk of clinical outcomes in the terms of all-cause mortality and cardiac mortality. As we know that the patients with severely reduced LVEF are inherently at increased risk of adverse clinical outcomes, this information should be considered hypothesis generating and utilized while discussing the risks and benefits of atherectomy in such high risk patients. Future studies should focus on the comparison of outcomes of different atherectomy devices in such patients. Adjusting for the inherent mortality risk posed by left ventricular dysfunction may be a strategy while designing a study.

Data availability statement

The original contributions presented in the study are included in the article/Supplementary material, further inquiries can be directed to the corresponding author/s.

Author contributions

WA, MRM, KD, and AA-A commenced the idea of this research. WA, MRM, AA-A, QR, MI, MA, JS, and NE drafted this manuscript. WA and MRM collected the data of this research. WA, MRM, and AA-A analyzed these data. TP, IB-D, KD, WA, and MRM critically reviewed this manuscript. All authors designed this research and approved the final manuscript. WA and KD supervised this research. All authors contributed to the article and approved the submitted version.

Conflict of interest

The authors declare that the research was conducted in the absence of any commercial or financial relationships that could be construed as a potential conflict of interest.

Publisher's note

Supplementary material

The Supplementary Material for this article can be found online at: https://www.frontiersin.org/articles/10.3389/fcvm.2022.946027/full#supplementary-material

SUPPLEMENTAL FIGURE 1
Funnel plot of the in-hospital and long term outcomes. MI, myocardial infarction; TVR, target vessel revascularization.

SUPPLEMENTAL TABLE 1
Search Strategy.

SUPPLEMENTAL TABLE 2
Risk of bias assessment.

SUPPLEMENTAL TABLE 3
Summarizing the definition of in-hospital myocardial infarction in each included study.

References

1. Wong SC. Role of mechanical coronary atherectomy in the treatment of severely calcified lesions. *Circ Cardiovasc Interv.* (2020) 13:e008789. doi: 10.1161/CIRCINTERVENTIONS.119.008789

2. Lee MS, Shah N. The impact and pathophysiologic consequences of coronary artery calcium deposition in percutaneous coronary interventions. *J Invasive Cardiol.* (2016) 28:160–7.

3. Zhang HP, Zhao Y, Ai H, Li H, Tang GD, Zheng NX, et al. Outcomes of coronary rotational atherectomy in patients with reduced left ventricular ejection fraction. *J Int Med Res.* (2020) 48:030006051989514. doi: 10.1177/0300060519895144

4. Beohar N, Kaltenbach LA, Wojdyla D, Pineda AM, Rao SV, Stone GW, et al. Trends in usage and clinical outcomes of coronary atherectomy. *Circ Cardiovasc Interv.* (2020) 13:e008239. doi: 10.1161/CIRCINTERVENTIONS.119.008239

5. Levine GN, Bates ER, Blankenship JC, Bailey SR, Bittl JA, Cercek B, et al. 2011 ACCF/AHA/SCAI guideline for percutaneous coronary intervention. *Circulation.* (2011) 124:2574–609. doi: 10.1161/CIR.0b013e31823a5596

6. Neill WWO, Kleiman NS, Moses J, Henriques JPS, Dixon S, Massaro J, et al. A prospective, randomized clinical trial of hemodynamic support with impella 2.5 vs. intra-aortic balloon pump in patients undergoing high-risk percutaneous. *Circulation.* (2012) 126:1717–27. doi: 10.1161/CIRCULATIONAHA.112.098194

7. Patterson T, Perera D, Redwood SR. Intra-aortic balloon pump for high-risk percutaneous coronary intervention. *Circ Cardiovasc Interv.* (2014) 7:712–20. doi: 10.1161/CIRCINTERVENTIONS.114.001258

8. Lee M, Généreux P, Shlofmitz R, Phillipson D, Anose BM, Martinsen BJ, et al. Orbital atherectomy for treating de novo, severely calcified coronary lesions: 3-year results of the pivotal ORBIT II trial. *Cardiovasc Revascularization Med.* (2017) 18:261–4. doi: 10.1016/j.carrev.2017.01.011

9. Boden WE, O'Rourke RA, Teo KK, Hartigan PM, Maron DJ, Kostuk WJ, et al. Optimal medical therapy with or without PCI for stable coronary disease. *N Engl J Med.* (2007) 356:1503–16. doi: 10.1056/NEJMoa070829

10. Liberati A, Altman DG, Tetzlaff J, Mulrow C, Gotzsche PC, Ioannidis JPA, et al. The PRISMA statement for reporting systematic reviews and meta-analyses of studies that evaluate healthcare interventions: explanation and elaboration. *BMJ.* (2009) 339:b2700–b2700. doi: 10.1136/bmj.b2700

11. Watanabe Y, Naganuma T, Kawamoto H, Ishiguro H, Nakamura S. In-hospital outcomes after rotational atherectomy in patients with low ejection fraction. *Scand Cardiovasc J.* (2018) 52:177–82. doi: 10.1080/14017431.2018.1455988

12. Whiteside HL, Ratanapo S, Nagabandi A, Kapoor D. Outcomes of rotational atherectomy in patients with severe left ventricular dysfunction without hemodynamic support. *Cardiovasc Revasc Med.* (2018) 19:660–5. doi: 10.1016/j.carrev.2018.02.008

13. Mankerious N, Hemetsberger R, Toelg R, Abdel-Wahab M, Richardt G, Allali A. Acute and long-term outcomes of patients with impaired left ventricular systolic function undergoing rotational atherectomy: a single-center observational retrospective study. *Cardiol Ther.* (2019) 8:267–81. doi: 10.1007/s40119-019-0143-4

14. Yoshida R, Ishii H, Morishima I, Tanaka A, Takagi K, Yoshioka N, et al. Rotational atherectomy for severely calcified lesions in patients with left ventricular systolic dysfunction: one-year outcomes from asingle-center registry analysis. *Cardiovasc Revasc Med.* (2020) 21:1220–7. doi: 10.1016/j.carrev.2020.03.033

15. Shlofmitz E, Meraj P, Jauhar R, Sethi SS, Shlofmitz RA, Lee MS. Safety of orbital atherectomy in patients with left ventricular systolic dysfunction. *J Interv Cardiol.* (2017) 30:415–20. doi: 10.1111/joic.12405

16. Pyxaras SA, Mangiacapra F, Wijns W, Di Serafino L, De Vroey F, Toth G, et al. ACEF and clinical SYNTAX score in the risk stratification of patients with heavily calcified coronary stenosis undergoing rotational atherectomy with stent implantation. *Catheter Cardiovasc Interv.* (2014) 83:1067–73. doi: 10.1002/ccd.25360

17. Bourantas C V, Zhang Y-J, Garg S, Iqbal J, Valgimigli M, Windecker S, et al. Prognostic implications of coronary calcification in patients with obstructive coronary artery disease treated by percutaneous coronary intervention: a patient-level pooled analysis of 7 contemporary stent trials. *Heart.* (2014) 100:1158–64. doi: 10.1136/heartjnl-2013-305180

18. Wallace TW, Berger JS, Wang A, Velazquez EJ, Brown DL. Impact of left ventricular dysfunction on hospital mortality among patients undergoing elective percutaneous coronary intervention. *Am J Cardiol.* (2009) 103:355–60. doi: 10.1016/j.amjcard.2008.09.088

19. Kaneko H, Yajima J, Oikawa Y, Tanaka S, Fukamachi D, Suzuki S, et al. Impact of aging on the clinical outcomes of Japanese patients with coronary artery disease after percutaneous coronary intervention. *Heart Vessels.* (2014) 29:156–64. doi: 10.1007/s00380-013-0339-9

20. Mamas MA, Anderson SG, O'Kane PD, Keavney B, Nolan J, Oldroyd KG, et al. Impact of left ventricular function in relation to procedural outcomes following percutaneous coronary intervention: insights from the British Cardiovascular Intervention Society. *Eur Heart J.* (2014) 35:3004–12. doi: 10.1093/eurheartj/ehu303

21. Keelan PC, Johnston JM, Koru-Sengul T, Detre KM, Williams DO, Slater J, et al. Comparison of In-Hospital and One-Year outcomes in patients with left ventricular ejection fractions $\leq$4, 41 to 49, and $\geq$50% having percutaneous coronary revascularization. *Am J Cardiol.* (2003) 91:1168–72. doi: 10.1016/S0002-9149(03)00261-3

22. Édes IF, Ruzsa Z, Szabó G, Nardai S, Becker D, Benke K, et al. Clinical predictors of mortality following rotational atherectomy and stent implantation in high-risk patients: a single center experience. *Catheter Cardiovasc Interv.* (2015) 86:634–41. doi: 10.1002/ccd.25945

23. Cockburn J, Hildick-Smith D, Cotton J, Doshi S, Hanratty C, Ludman P, et al. Contemporary clinical outcomes of patients treated with or without rotational coronary atherectomy — An analysis of the UK central cardiac audit database. *Int J Cardiol.* (2014) 170:381–7. doi: 10.1016/j.ijcard.2013.11.018

24. Chambers JW, Feldman RL, Himmelstein SI, Bhatheja R, Villa AE, Strickman NE, et al. Pivotal trial to evaluate the safety and efficacy of the orbital atherectomy system in treating De Novo, Severely Calcified Coronary Lesions (ORBIT II). *JACC Cardiovasc Interv.* (2014) 7:510–8. doi: 10.1016/j.jcin.2014.01.158

25. Jujo K, Otsuki H, Tanaka K, Fukushima N, Okai I, Nakashima M, et al. Long-term cardiovascular prognosis after rotational atherectomy in hemodialysis patients: data from the J2T multicenter registry. *Int J Cardiol.* (2019) 285:14–20. doi: 10.1016/j.ijcard.2019.03.022

26. Pocock SJ, Wang D, Pfeffer MA, Yusuf S, McMurray JJV, Swedberg KB, et al. Predictors of mortality and morbidity in patients with chronic heart failure. *Eur Heart J.* (2006) 27:65–75. doi: 10.1093/eurheartj/ehi555

27. MacIsaac AI, Bass TA, Buchbinder M, Cowley MJ, Leon MB, Warth DC, et al. High speed rotational atherectomy: outcome in calcified and noncalcified coronary artery lesions. *J Am Coll Cardiol.* (1995) 26:731–6. doi: 10.1016/0735-1097(95)00206-J

28. McEntegart M, Corcoran D, Carrick D, Clerfond G, Sidik N, Collison D, et al. Incidence of procedural myocardial infarction and cardiac magnetic resonance imaging-detected myocardial injury following percutaneous coronary intervention with rotational atherectomy. *EuroIntervention.* (2018) 14:819–23. doi: 10.4244/EIJ-D-17-01077

29. Iannaccone M, Barbero U. D'ascenzo F, Latib A, Pennacchi M, Rossi ML, et al. Rotational atherectomy in very long lesions: results for the ROTATE registry. *Catheter Cardiovasc Interv.* (2016) 88:E164–72. doi: 10.1002/ccd.26548

30. Iannaccone M, Piazza F, Boccuzzi G, D'Ascenzo F, Latib A, Pennacchi M, et al. ROTational AThErectomy in acute coronary syndrome: early and midterm outcomes from a multicentre registry. *EuroIntervention.* (2016) 12:1457–64. doi: 10.4244/EIJ-D-15-00485

31. Abdel-Wahab M, Baev R, Dieker P, Kassner G, Khattab AA, Toelg R, et al. Long-term clinical outcome of rotational atherectomy followed by drug-eluting stent implantation in complex calcified coronary lesions. *Catheter Cardiovasc Interv.* (2013) 81:285–91. doi: 10.1002/ccd.24367

32. Cohen MG, Ghatak A, Kleiman NS, Naidu SS, Massaro JM, Kirtane AJ, et al. Optimizing rotational atherectomy in high-risk percutaneous coronary interventions: insights from the PROTECT II study. *Catheter Cardiovasc Interv.* (2014) 83:1057–64. doi: 10.1002/ccd.25277

33. Lee Y, Tanaka A, Mori N, Yoshimura T, Nakamura D, et al. Thin-strut drug-eluting stents are more favorable for severe calcified lesions after rotational atherectomy than thick-strut drug-eluting stents. *J Invasive Cardiol.* (2014) 26:41–5.

frontiers | Frontiers in Cardiovascular Medicine

TYPE Original Research
PUBLISHED 28 September 2022
DOI 10.3389/fcvm.2022.970415

OPEN ACCESS

EDITED BY
Istvan Szokodi,
University of Pécs, Hungary

REVIEWED BY
Claudia Penna,
University of Turin, Italy
Timothy P. Fitzgibbons,
University of Massachusetts Medical School, United States

*CORRESPONDENCE
Michael Koeppen
michael.koeppen@med.uni-tuebingen.de

†These authors have contributed equally to this work

SPECIALTY SECTION
This article was submitted to Coronary Artery Disease, a section of the journal Frontiers in Cardiovascular Medicine

RECEIVED 15 June 2022
ACCEPTED 22 August 2022
PUBLISHED 28 September 2022

CITATION
Heck-Swain KL, Li J, Ruan W, Yuan X, Wang Y, Koeppen M and Eltzschig HK (2022) Myeloid hypoxia-inducible factor HIF1A provides cardio-protection during ischemia and reperfusion *via* induction of netrin-1. *Front. Cardiovasc. Med.* 9:970415. doi: 10.3389/fcvm.2022.970415

Myeloid hypoxia-inducible factor HIF1A provides cardio-protection during ischemia and reperfusion *via* induction of netrin-1

Ka Lin Heck-Swain[1†], Jiwen Li[2,3†], Wei Ruan[2,4†], Xiaoyi Yuan[2], Yanyu Wang[2], Michael Koeppen[1*†] and Holger K. Eltzschig[2†]

[1]Department of Anesthesiology and Intensive Care Medicine, Tübingen University Hospital, Eberhard Karls University of Tübingen, Tübingen, Germany, [2]Department of Anesthesiology, McGovern Medical School, The University of Texas Health Science Center at Houston, Houston, TX, United States, [3]Department of Cardiac Surgery, Sir Run Run Shaw Hospital, School of Medicine, Zhejiang University, Hangzhou, China, [4]Department of Anesthesiology, Second Xiangya Hospital, Central South University, Changsha, China

The transcription factor hypoxia-inducible factor HIF1A induces cardioprotection from ischemia and reperfusion injury. Here, we investigate tissue-specific pathways that are critical for HIF1A-elicited tissue protection. Initial studies showed that mice with induced global Hif1a deletion (*Hif1a*$^{loxP/loxP}$ UbiquitinCre+) have exaggerated myocardial injury during *in situ* ischemia and reperfusion. Surprisingly, this phenotype was mirrored only in mice with myeloid-specific *Hif1a* deletion (*Hif1a*$^{loxP/loxP}$ LysM Cre+). In contrast, mice with myocardial specific (*Hif1a*$^{loxP/loxP}$ Myosin Cre+), or vascular *Hif1a* deletion (*Hif1a*$^{loxP/loxP}$ VEcadherin Cre+) experienced similar levels of injury as controls. Subsequent studies using adoptive transfer of *Hif1a*-deficient polymorphonuclear neutrophils (PMNs) prior to myocardial injury demonstrated increased reperfusion injury. On the contrary, the adoptive transfer of PMNs treated *ex vivo* with the hypoxia inducible factor (HIF) stabilizer dimethyloxalylglycine (DMOG) was associated with attenuated myocardial injury. Furthermore, DMOG-mediated cardioprotection was abolished in *Hif1a*$^{loxP/loxP}$ LysM Cre+ mice, but not in *Hif2a*$^{loxP/loxP}$ LysM Cre+ mice. Finally, studies of PMN-dependent HIF1A target genes implicated the neuronal guidance molecule netrin-1 in mediating the cardioprotective effects of myeloid HIF1A. Taken together, the present studies identified a functional role for myeloid-expressed HIF1A in providing cardioprotection during ischemia and reperfusion injury, which is mediated, at least in part, by the induction of the netrin-1 neuronal guidance molecule in neutrophils.

KEYWORDS

hypoxia, myocardial infarction, polymorphonuclear neutrophil (PMN), reperfusion, heart, hypoxia inducible factor (HIF)

Introduction

Myocardial infarction remains one of the leading causes of death worldwide. Most commonly, it is an aftereffect of a coronary artery occlusion leading to myocardial ischemia (1). As a consequence of ischemia, myocardial tissue develops profound hypoxia (2), leading to tissue necrosis if blood flow is not restored in time. During myocardial ischemia, tissue hypoxia becomes a strong transcriptional stimulus that activates a coordinated transcriptional program that promotes increased resistance to ischemia and reperfusion injury (3, 4). A central role in the coordination of this adaptive response is mediated by the stabilization of the hypoxia-inducible transcription factor HIF1A (5).

Under normoxic conditions, HIF1A is constantly degraded through the proteasomal pathway due to hydroxylation by prolylhydroxylases (PHDs), causing subsequent binding of the von Hippel Lindau gene product, which targets HIF1A for degradation (6, 7). However, when oxygen levels drop, PHDs become inactivated and HIF1A is rapidly stabilized, translocates to the nucleus, and binds to the promoter region of hypoxia inducible factor (HIF) target genes to induce their transcription (2, 3). HIF1A is known to regulate a wide array of genes. For example, gene expression profiles in endothelial cells exposed to normoxia or hypoxia indicate that more than 600 target genes are regulated by HIF1A, including gene repression or induction (8). In cardiomyocytes, HIF1A increases the expression of glycolytic pathway enzymes, thereby enhancing their capacity to generate ATP under anaerobic conditions and promoting their ability to cope with ischemic tissue injury (9). In myeloid cells, HIF1A transcriptional activity can regulate cell functions or drive the release of cardioprotective HIF1A target genes (10–12), which can significantly influence inflammatory processes (13). For example, stabilization of HIF1A in hypoxia increases the life span of usually short-lived polymorphonuclear neutrophils (PMN) (14). Furthermore, stabilization of HIF1A increases the motility of myeloid cells toward a chemotactic gradient, bringing them to the site of injury (15, 16).

Based on studies implicating HIF1A stabilization in tissue adaptation and protection during hypoxia or inflammation (3, 17, 18), research efforts were initiated to use this pathway as a therapeutic target. Several pharmaceutical companies have been successful in finding small molecule inhibitors for PHDs that can be used as HIF activators. In fact, several recent phase-3 clinical trials successfully tested the PHD inhibitors roxadustat or vadadustat for the treatment of renal anemia (19–22). Furthermore, experimental studies provide evidence that PHD inhibitors induce cardioprotection from ischemia and reperfusion injury (5, 23). Together, these studies highlight that the HIF1A pathway could be utilized as a therapeutic target for myocardial ischemia and reperfusion injury.

Cardioprotection by HIF1A is supported by several previous studies (24–26). However, the cellular source of HIF-mediated cardioprotection remains unknown. HIF1A is ubiquitously expressed, including cells involved in myocardial ischemia and reperfusion injury, such as cardiomyocytes, vascular endothelial cells, and myeloid cells (23, 27). To uncover the individual contributions of different cellular compartments during HIF1A-dependent cardioprotection, we used transgenic mice with a *Hif1a* gene flanked by a LoxP site. When breeding these mice with tissue-specific expression of Cre recombinase, we stepwise deleted *Hif1a* from different cellular compartments. Surprisingly, we found that the predominant source of HIF1A-mediated cardioprotection involves myeloid cells and uncovered a novel contribution of PMN.

Materials and methods

Mice

All animal procedures were performed in an accredited facility of the American Association for Laboratory Animal Care and approved by the University of Colorado Denver and the Institutional Animal Care and Use Committee of the University of Texas Health Science Center at Houston (UTHealth). For all studies, we used mice with an age of 8–16 weeks. C57BL/6J mice were purchased from The Jackson Laboratory (Bar Harbor, ME, United States). *Hif1a*$^{loxP/loxP}$ (B6.129-*Hif1a*^{TM3Rsjo}/J) (28), *Hif2a*$^{loxP/loxP}$ (Epas1tm1Mcs/J) (23), *Ntn1*$^{loxP/loxP}$ (B6.129(SJL)-Ntn1tm1.1Tek/J) (12). These animals were crossed with the following mouse lines, that express Cre-recombinase under the control of a tissue-specific promoter: tamoxifen-inducible Ubiquitin Cre+ (B6.Cg-Ndor1Tg (UBC-cre/ERT2) 1Ejb/J) (29), LysM Cre+ (B6.129P2-Lyz2TM 1 (cre)Ifo /J) (30), VE-cadherin-Cre+ (B6.Cg-Tg(Cdh5-cre)7Mlia/J) (31, 32), and tamoxifen inducible Myosin-Cre+ (B6.FVB(129)-A1cfTg). For studies using Myosin-Cre+ or Ubiquitin Cre+ mice, mice received tamoxifen dissolved in peanut oil for 5 days (1 mg/day i.p.), followed by a resting period of 7 days prior to experimentation. Mice were genotyped by GeneTyper (New York, NY, United States) or in house according to the recommended protocol.

Human neutrophil isolation and cell culture

From healthy subjects, human blood was collected in tubes containing anticoagulant citrate (S-monovette #04.1902,

Sarstedt, Nümbrecht, Germany). Neutrophils were isolated using a Percoll-based protocol. Briefly, whole blood was applied to the discontinuous Percoll gradient containing equal vols of 63 and 72% Percoll solution and centrifuged at 400 ($\times$ *g*) for 30 min without brake. A mixture of neutrophils and red blood cells was collected at the Percoll gradient interface, in which the latter were subsequently removed by isotonic lysis (NH_4Cl solution). Neutrophils were then pelleted and washed with HBSS(-). Neutrophil purity/viability was assessed by loading a small aliquot into a particle count and size analyzer (Coulter, Backman Coulter) following the manufacturer's instructions. In total, 1–2 $\times$ 10^6 PMN per ml of blood were typically isolated with >95% purity and viability. After isolation, neutrophils were rested 30 min before experiments. Cells were cultured 2.5 $\times$ 10^6 cells/ml in RPMI 1640 with 10% FCS at 37°C in 21% O_2 (0 h timepoint) or 2% O_2 (hypoxia timepoints).

Murine model for myocardial ischemia

A detailed procedure of *in situ* myocardial ischemia and reperfusion injury has previously been described (23, 33–35). In summary, we exposed mice to 60 min of myocardial ischemia followed by 2 h of reperfusion, followed by an analysis of the size of the infarct and a measurement of cardiac troponin I (cTnI) in serum. Dimethyloxalylglycine (DMOG) was administered to mice 4 h before ischemia started (1 mg/mouse, dissolved in normal saline, intraperitoneal). Successful occlusion of LCA occlusion was confirmed by a color change in LCA-supplied cardiac tissue. After 60 min of ischemia, the weights were removed to allow reperfusion of the tissue. During ischemia, we administered normal saline at a constant rate of 0.1 ml/h. At the beginning of reperfusion, we increased the infusion rate to 0.6 mL/h.

Infarct staining

The detailed procedure to measure the percentage of infarcted area relative to the area undergoing ischemia (area at risk) using a counterstain technique was previously described (23, 33). At the end of the experiment, the circulation was flushed with 5 ml of normal saline and LCA was permanently occluded. After injection of Evan's blue dye (600 µl, 1%), the heart was excised by the heart basis and kept at −20°C for 15 min. The hearts were then cut and incubated with 1% triphenyltetrazolium chloride (TTC) for 10 min at 37°C before fixation in 4% neutral buffer formalin. To prevent bleaching of the dye, photographs of the heart slices were taken the day after the experiments. For this, tissue slices were placed between glass slides and pictures were taken using a Nikon D5300 camera at 32× magnification. The AAR and infarct size were measured by ImageJ software (National Institutes of Health, United States; Version 1.51k). If an air bubble was accidentally injected into the cardiac circulation during Evan's blue injection, resulting in incomplete delimitation of AAR, the sample was excluded.

Cardiac troponin I enzyme-linked immunosorbent assay

As an additional line of evidence for myocardial injury, cTnI was measured by enzyme-linked immunosorbent assay (ELISA), as described (36) using the cTnI ELISA Kit (Life Diagnostic, #CTNI-1-HS).

Neutrophil depletion and adoptive transfer

Untouched PMNs were isolated from bone marrow in donor mice of the indicated genotype (aged 6–8 weeks) using the EasySep mouse neutrophil enrichment kit (Stemcell Technologies Inc.). In a subset of the experiment PMN from C57/J animals, 1 mM DMOG (Sigma-Aldrich, #D3695) or vehicle solution was incubated for 60 min. Then 1 $\times$ 10^6 cells were injected into neutrophil-depleted mice through an arterial catheter over a 10-min period 60 min prior to myocardial ischemia. The detailed procedure for neutrophil depletion *in vivo* was previously described (37) using Ly6G-specific mAb 1A8 antibody (BioXCell).

Immunoblotting experiments

To study the expression of Netrin-1, immunoblotting methods were conducted. At the end of each timepoint, neutrophils in the medium were collected and centrifuged at 500 ($\times$ *g*) for 5 min to collect cells. Cells were immediately lysed in IP lysis buffer (Pierce #87788, ThermoFisher) on ice for 30 min and then centrifuged at 12,000 ($\times$ g) for 10 min. The protein concentration of the lysates was measured by the BCA Assay (#23225, ThermoFisher) then incubated in Laemmli sample buffer containing 2-mercaptoethanol at 95°C for 5 min. Lysate proteins (40 µg) were separated on 7.5% SDS polyacrylamide gels by SDS-PAGE and then transferred to PVDF membranes using a Bio-Rad Mini Trans-Blot cell. Netrin-1 (LSBio, LS-C743016) and β-actin (Santa Cruz, sc-130656), used as loading control, were detected using specific primary antibodies. The membranes were subsequently incubated with a secondary antibody coupled to HRP conjugate (Invitrogen #65-6120). The

membranes were incubated with ECL reagents (Clarity Max, Bio-Rad, and Immunocruz, Santa Cruz, respectively) and the chemiluminescent signal detected by the Fusion Imaging System (Vilber Lourmat). Protein expression was quantified by densitometry using ImageJ (National Institutes of Health, United States; Version 1.51k) and normalized to the expression of β -actin.

Statistical analysis

The N numbers were predetermined by power analysis to detect a mean difference of 20% with 8% standard deviation (SD). Outliers were detected by the Grubb test and removed from the data. All data approximately followed the normal distribution and were plotted as mean ± SD. The experimental data were analyzed by the unpaired two-sided student *t*-test or ANOVA with Tukey test for multiple comparison. A *p*-value less than 0.05 was considered statistically significant. Statistical analyzes were performed using Prism (version 9.1.2, GraphPad Software Inc.).

Results

Global-induced deletion of Hif1A is associated with increased myocardial ischemia and reperfusion injury

Previous studies have implicated HIF1A in cardioprotection from ischemia and reperfusion injury (5, 23, 38). For example, mice with Hif1a heterozygote deletion are not protected by ischemic preconditioning (39). Similarly, pharmacologic stabilizers of HIF, such as DMOG, provide robust cardioprotection during ischemia and reperfusion (5). However, the fact that mice with Hif1a homozygous deletion die during embryogenesis (40) has made it difficult to provide direct genetic evidence for *Hif1a* during cardioprotection. Thus, we generated mice with induced global deletion of *Hif1a* after tamoxifen treatment by crossing $Hif1a^{loxP/loxP}$ mice with Ubiquitin Cre+ mice to generate $Hif1a^{loxP/loxP}$ Ubiquitin Cre+ mice (41). To achieve global-induced *Hif1a* deletion, mice were treated daily with tamoxifen for 5 days (1 mg i.p./day) and recovered for 7 days before myocardial ischemia and reperfusion injury, using a previously described *in situ* model (**Figure 1A**) (34). Western blot analysis for Hif1a showed the expression of the Hif1a protein in response to Hif1a stabilizer treatment (DMOG, 1 mg i.p.) in Ubiquitin Cre+ mice. On the contrary, the Hif1a protein did not accumulate in cardiac tissue in $Hif1a^{loxP/loxP}$ Ubiquitin Cre+ mice after DMOG treatment (**Figure 1B**), suggesting a successful deletion of Hif1a in these animals.

To assess the functional consequences of global-induced deletion of Hif1a in myocardial ischemia and reperfusion injury, we exposed $Hif1a^{loxP/loxP}$ Ubiquitin Cre+ mice to *in situ* myocardial ischemia and reperfusion after treatment and recovery with tamoxifen (**Figure 1A**) and evaluated myocardial injury by infarct sizes and serum troponin levels. These studies demonstrated significantly larger myocardial infarct sizes after 60 min of ischemia and 2 h of reperfusion in $Hif1a^{loxP/loxP}$ Ubiquitin-Cre+ mice compared to littermate control Ubiquitin Cre+ mice after tamoxifen treatment (**Figures 1C,D**). Similarly, $Hif1a^{loxP/loxP}$ Ubiquitin Cre+ mice experienced significantly elevated of the cardiac injury marker troponin I (**Figure 1E**). Together, these studies demonstrate that Hif1a induced deletion is associated with dramatic increases in myocardial injury after ischemia and reperfusion, and confirm previous studies implicating HIF1A in cardioprotection (5, 38).

Tissue-specific *Hif1a deletion* reveals a selective role for myeloid-derived Hif1A in mediating cardioprotection during ischemia and reperfusion

Based on the above studies showing that global-induced deletion of Hif1A has deleterious effects during *in situ* myocardial ischemia and reperfusion injury, we next pursued studies to identify tissue-specific contributions of *Hif1a* in cardioprotection. To do this, we generated mice with *Hif1a* deletion in different tissue compartments, including cardiomyocytes ($Hif1a^{loxP/loxP}$ Myosin Cre+ mice) (23), vascular endothelial cells ($Hif1a^{loxP/loxP}$ VEcadherin Cre+ mice) (27) or myeloid cells ($Hif1a^{loxP/loxP}$ LysM Cre+ mice) (42). We subjected these mouse lines with Cre+ control mice of the same sex, weight, and age to 60 min of myocardial ischemia and 120 min of reperfusion and measured myocardial injury by assessing the size area of the infarct and serum troponin levels, as previously (12, 23, 35, 43). Consistent with previous studies (23), we found that $Hif1a^{loxP/loxP}$ Myosin Cre+ mice had similar infarct sizes and troponin I levels compared to Myosin Cre+ controls (**Figures 2A–C**). Similarly, deletion of Hif1a in vascular endothelia ($Hif1a^{loxP/loxP}$ VEcadherin Cre+ mice) did not alter the susceptibility to myocardial injury (**Figures 2D–F**). Surprisingly, we found the predominant phenotype in mice with Hif1a deletion in the myeloid compartment. Indeed, $Hif1a^{loxP/loxP}$ LysM Cre+ mice had dramatic increases in myocardial infarct sizes, and increased troponin I leakage into the plasma, as compared to LysM Cre+ control animals (**Figures 2G–I**). Together, these studies provide novel evidence that mice with myeloid-specific *Hif1a* deletion experience increased susceptibility to myocardial

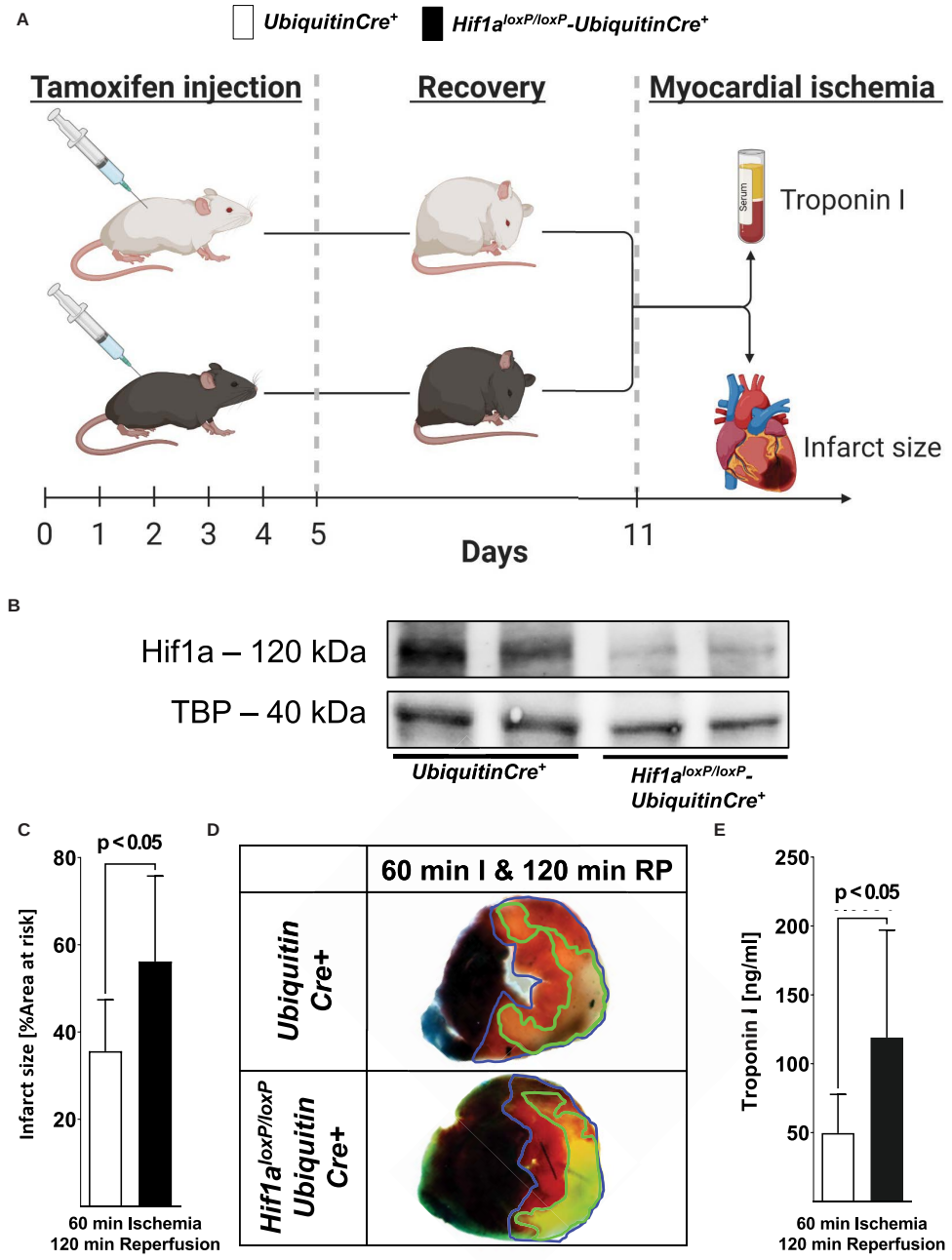

FIGURE 1

Functional consequences of the induced global deletion of *Hif1a* during myocardial ischemia and reperfusion injury. **(A)** Experimental approach to study global induced Hif1a-deficiency. *Hif1a*$^{loxP/loxP}$ mice were crossed with Cre-recombinase expressing mice under the control of a ubiquitin promoter (UbiquitinCre+); these mice express cre-recombinase under the control of a tamoxifen inducer. Control animals with sex and weight matched (UbiquitinCre+) or *Hif1a*$^{loxP/loxP}$ UbiquitinCre+ mice received a daily dose of 1 mg i.p. tamoxifen 5 consecutive days to induce Cre recombinase activity. After 7 days, the animals underwent experimental protocols (60 min of *in situ* myocardial ischemia followed by 120 min of reperfusion), followed by serum collection to determine the concentrations of troponin I and TCC staining for infarct sizes. **(B)** Hif1A immunoblot performed on protein isolated from myocardial tissue after treatment with the pharmacological HIF activator dimethyloxalylglycine (1 mg DMOG i.p.) 4 h before tissue collection from UbiquitinCre+ or *Hif1a*$^{loxP/loxP}$ UbiquitinCre+. A representative image of three individual experiments is presented. **(C)** The infarct sizes of UbiquitinCre+ or *Hif1a*$^{loxP/loxP}$ UbiquitinCre+ mice are displayed as a percentage of the area at risk after 60 min of ischemia, followed by 120 min of reperfusion (UbiquitinCre+ $n = 7$; *Hif1a*$^{loxP/loxP}$ UbiquitinCre+ $n = 5$, per group mean ± SD; statistical analysis by two-sided, unpaired Student's *t*-test; mice were matched by age, sex, and weight). **(D)** Representative infarct staining of UbiquitinCre+ or *Hif1a*$^{loxP/loxP}$ UbiquitinCre+ mice (60 min of ischemia and 120 min of reperfusion). **(E)** Troponin serum levels after 60 min of ischemia, followed by 120 min of reperfusion in UbiquitinCre+ or *Hif1a*$^{loxP/loxP}$ UbiquitinCre+ mice (UbiquitinCre+ $n = 12$; *Hif1a*$^{loxP/loxP}$ UbiquitinCre+ $n = 8$ presented as mean ± SD; compared by Student's *t*-test).

ischemia and reperfusion injury, essentially resembling the findings in mice with induced global deletion of Hif1A (**Figures 1C–E**).

Transfer of *Hif1a*-deficient polymorphonuclear neutrophils is associated with more severe myocardial ischemia and reperfusion injury

The above studies indicate myeloid-dependent HIF1A in cardio-protection from ischemia and reperfusion injury. As next step, we pursued studies to further characterize specific cellular populations that are critical in this response. Due to the fact that PMNs are the predominant bone marrow-derived inflammatory cells in the post-ischemic myocardium (36), we next performed studies to address PMN-dependent HIF1A. For this purpose, we performed an adoptive transfer as described previously (43). In short, C57BL6J animals received 250 μg of 1A8 Ly6G-antibody 24 h prior to experimentation to deplete PMNs. On the day of the experiment, we isolated a pure population of mature PMNs from *Hif1a*$^{loxP/loxP}$ LysM Cre+ or matched wild-type control mice and infused *via* an intravascular catheter into PMN-depleted animals followed by 60 min of myocardial ischemia followed by 2 h of reperfusion (**Figure 3A**). In line with a functional role of HIF1A expressed in PMNs, we found that reconstitution with *Hif1a*-deficient PMNs was associated with dramatically increased infarcts sizes, when compared to mice reconstituted with control PMNs (**Figures 3B,C**), resembling myocardial injury phenotypes in *Hif1a*$^{loxP/loxP}$ LysM Cre+ mice. Together, these results indicate that PMN-dependent Hif1a deficiency is associated with elevated myocardial ischemia and reperfusion injury and implicates PMN-dependent HIF1A in cardioprotection.

Pharmacologic stabilization of hypoxia inducible factor in isolated polymorphonuclear neutrophils prior to myocardial injury confers cardioprotection

Based on the above studies showing that reconstitution with Hif1A-deficient PMNs prior to myocardial injury is associated with more severe myocardial infarction after ischemia and reperfusion, we next pursued opposite studies using PMNs treated *ex vivo* with a pharmacologic HIF activator. For this purpose, we used the HIF stabilizer DMOG. Previous studies from our laboratory had shown that systemic treatment with DMOG provides cardioprotection *via* stabilization of HIF1A (5, 23, 38). Similar to the experimental approach above, we first pursued PMN depletion prior to the experimentation by injecting mice with 250 μg of 1A8 Ly6G-antibody 24 h prior to myocardial ischemia and reperfusion. We isolated PMNs from C57BL6J mice and subsequently exposed PMNs for 60 min to vehicle or 1 mM DMOG (44). After the incubation period, we performed an adoptive transfer into PMN-depleted mice followed by 60 min of *in situ* ischemia and 120 min of reperfusion (**Figure 4A**). Mice that had received PMNs pre-treated with DMOG had significantly attenuated myocardial injury as compared to vehicle controls (**Figures 4B,C**). Taken together, these studies highlight that adoptive transfer of *ex vivo* DMOG treated PMNs before myocardial ischemia and reperfusion is associated with attenuated reperfusion injury and suggests a functional role of PMN-dependent HIF in cardioprotection.

Selective role of myeloid HIF1A deficiency in mediating the cardioprotective effects of prolylhydroxylase-inhibitor treatment dimethyloxalylglycine

Previous studies have implicated both isoforms of HIFA (HIF1A or HIF2A) in cardio-protection from ischemia and reperfusion injury, including protective effects mediated by treatment with HIF stabilizers such as DMOG (5, 23, 35). To gain insight into the relative contributions of myeloid-expressed *Hif1a* or *Hif2a* in mediating DMOG elicited cardioprotection, we compared *Hif1a*$^{loxP/loxP}$ LysM Cre+ or *Hif2a*$^{loxP/loxP}$ LysM Cre+ on their capacity for infarct size reduction provided by pre-treatment with DMOG. In these studies, *Hif1a*$^{loxP/loxP}$ LysM Cre+, or *Hif2a*$^{loxP/loxP}$ LysM Cre+ were pre-treated with 1 mg DMOG i.p. or vehicle control 4 h before myocardial ischemia. Subsequently, animals were exposed to 60 min of myocardial ischemia and 120 min of reperfusion. In line with a functional role of myeloid-expressed Hif1a in mediating DMOG-protection we found that *Hif2a*$^{loxP/loxP}$ LysM Cre+ mice are responsive to DMOG pre-treatment with reduced ischemia and reperfusion injury compared to vehicle, as demonstrated in myocardial infarct sizes and troponin I-leakage (**Figures 5A–C**). In contrast, we found that *Hif1a*$^{loxP/loxP}$ LysM Cre+ failed to respond to pre-treatment with DMOG. Myocardial infarct size of *Hif1a*$^{loxP/loxP}$ LysM Cre+ pre-treated with DMOG were similar to that of *Hif1a*$^{loxP/loxP}$ LysM Cre+ pretreated with vehicle control (**Figures 5D–F**). Taken together, these results indicate that myeloid HIF1A as opposed to myeloid HIF2A is required for the cardio-protection provided by PHD inhibitors. In conjunction with our studies showing attenuated infarct sizes after *ex vivo* treatment with HIF stabilizer, these findings provide additional data implicating PMN-dependent HIF1A in cardio-protection from ischemia and reperfusion injury.

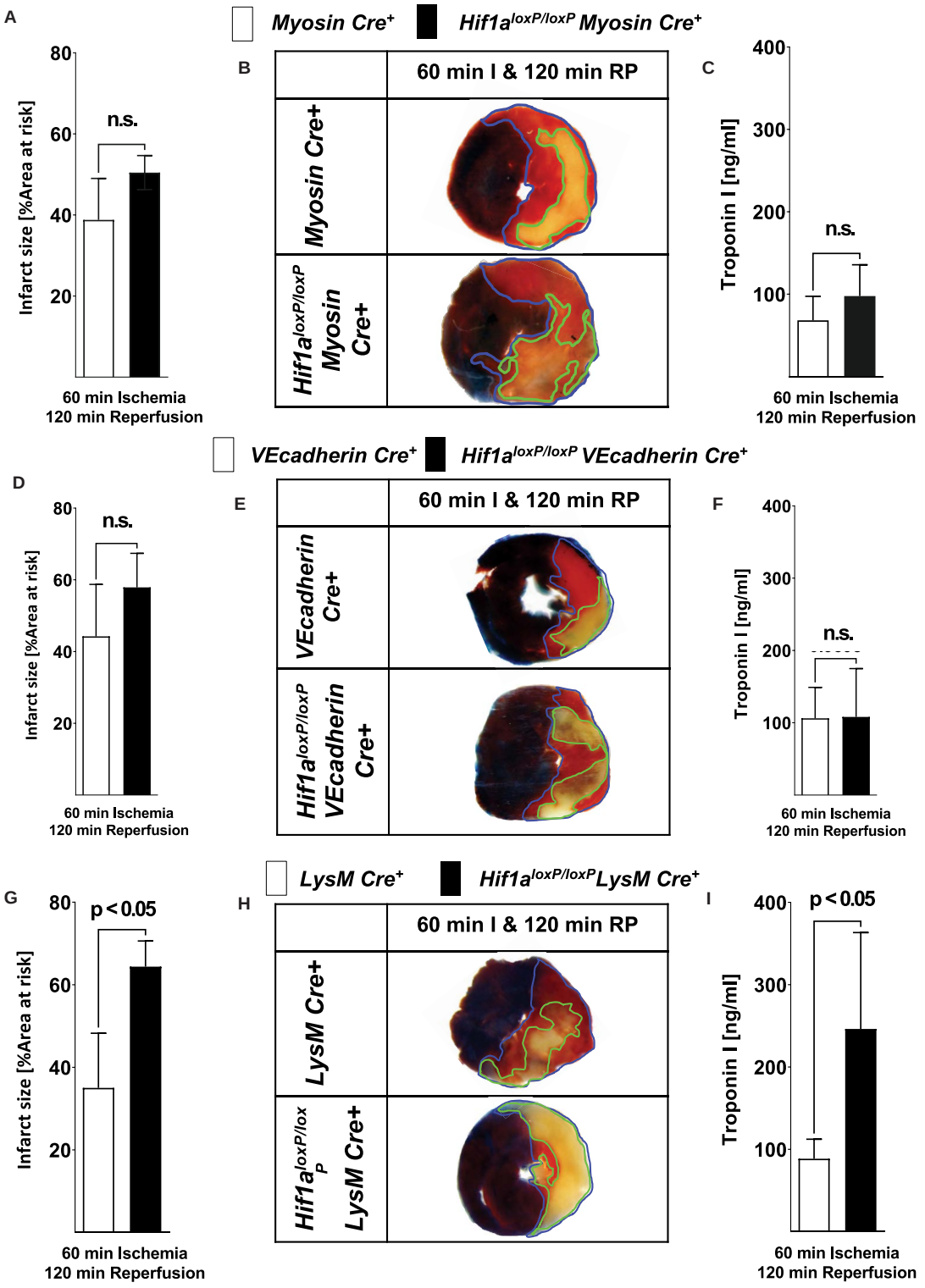

FIGURE 2

Myocardial ischemia and reperfusion injury in mice with tissue-specific Hif1a deletion in cardiac myocytes, vascular endothelia, or myeloid inflammatory cells. **(A–I)** *Hif1a*$^{loxP/loxP}$ were crossed with mice expressing Cre-recombinase under the control of heavy chain myosin promoter including a tamoxifen inducer (*Hif1a*$^{loxP/loxP}$ Myosin Cre+ mice) (23), vascular endothelial cadherin (*Hif1a*$^{loxP/loxP}$ VEcadherin Cre+ mice) (27). (*Hif1a*$^{loxP/loxP}$ VEcadherin Cre+) or lysozyme 2 (*Hif1a*$^{loxP/loxP}$ LysM Cre+ mice) (42) to generate tissue-specific HIF1A-deficient animals. Mice underwent 60 min of myocardial ischemia, followed by 120 min of reperfusion. Myocardial injury was determined by area at risk and troponin I serum concentration in *Hif1a*$^{loxP/loxP}$ Myosin Cre+ mice and age, sex, and weighed Myosin Cre+ mice who were matched received 1 mg of i.p. tamoxifen per day for 5 days followed by 7 days of recovery prior to experimentation. Infarct sizes ± SD in Myosin Cre+ or *Hif1a*$^{loxP/loxP}$

(Continued)

FIGURE 2 (Continued)
Myosin Cre+ presented as a percentage to the area-at-risk after 60 min of ischemia, followed by 120 min of reperfusion (Myosin Cre+ $n = 6$; $Hif1a^{loxP/loxP}$ Myosin Cre+ $n = 4$). **(B)** Representative infarct staining of Myosin Cre+ or $Hif1a^{loxP/loxP}$ Myosin Cre+ (60 min of ischemia and 120 min reperfusion). **(C)** Serum levels of troponin after 60 min ischemia, followed by 120 min of reperfusion in Myosin Cre+ or $Hif1a^{loxP/loxP}$ Myosin Cre+ (Myosin Cre+ $n = 5$; $Hif1a^{loxP/loxP}$ Myosin Cre+ $n = 5$). **(D)** Infarct sizes ± SD in VEcadherin Cre+ or $Hif1a^{loxP/loxP}$ VEcadherin Cre+ presented as percentage to the area-at-risk after 60 min of ischemia, followed by 120 min of reperfusion (VEcadherin Cre+ $n = 7$; $Hif1a^{loxP/loxP}$ VEcadherin Cre+ $n = 7$). **(E)** Representative infarct staining from VEcadherin Cre+ or $Hif1a^{loxP/loxP}$ VEcadherin Cre+ (60 min of ischemia and 120 min reperfusion). **(F)** Serum levels of Troponin after 60 min ischemia, followed by 120 min of reperfusion in VEcadherin Cre+ or $Hif1a^{loxP/loxP}$ VEcadherin Cre+ (VEcadherin Cre+ $n = 4$; $Hif1a^{loxP/loxP}$ VEcadherin Cre+ $n = 6$). **(G)** Infarct sizes ± SD in LysM Cre+ or $Hif1a^{loxP/loxP}$ LysM Cre+ presented as percentage to the area-at-risk after 60 min of ischemia, followed by 120 min of reperfusion (LysM Cre+ $n = 8$; $Hif1a^{loxP/loxP}$ LysM Cre+ $n = 4$). **(H)** Representative infarct staining of LysM Cre+ or $Hif1a^{loxP/loxP}$ LysM Cre+ (60 min of ischemia and 120 min reperfusion). **(I)** Troponin serum levels after 60 min ischemia, followed by 120 min of reperfusion in LysM Cre+ or $Hif1a^{loxP/loxP}$ LysM Cre+ (LysM Cre+ $n = 4$; $Hif1a^{loxP/loxP}$ LysM Cre+ $n = 3$); (all values represent mean ± SD; statistical significance assessed by two-sided, unpaired Student's *t*-test).

Identification of neuronal guidance molecule netrin-1 as polymorphonuclear neutrophil-dependent Hif1A target critical for hypoxia inducible factor-dependent cardioprotection

Based on the above studies demonstrating functional roles of neutrophil-dependent HIF1A in cardioprotection from ischemia and reperfusion, we subsequently pursued studies to identify a transcriptional target in PMNs that would account for these observations. Recent studies from our laboratory had shown that PMN-derived netrin-1 functions to attenuate *in situ* myocardial ischemia and reperfusion injury. Netrin-1 was originally described as a neuronal guidance molecule important in brain development (45). However, more recent studies implicate netrin in orchestrating inflammatory events, including myocardial inflammation (46). Moreover, other studies had implicated HIF1A in the transcriptional regulation of netrin-1 during hypoxia, and identified netrin-1 as a classic HIF-target gene (42, 47). To examine a functional role of hypoxia-signaling in inducing PMN-dependent netrin-1, we first examined expression of netrin-1 during condition of ambient hypoxia. For this purpose, we freshly isolated human PMNs from peripheral blood and submitted the cells to 0, 2, and 4 h of ambient hypoxia (2% oxygen) and probed the cell lysates for netrin-1 expression by Western blot. Consistent with previous studies showing induction of netrin-1 expression during hypoxia (47), we found a very robust induction of PMN-dependent netrin-1 during ambient hypoxia (**Figures 6A,B**). Recent studies from our laboratory demonstrated the mice with deletion of myeloid-expressed netrin-1 ($Ntn1^{loxP/loxP}$ LysM Cre+ mice) experience increased myocardial infarct sizes and show that elevated levels of netrin-1 during myocardial infarction predominantly stems from PMNs (12). To further establish a link between the HIF-pathway and myeloid-dependent netrin-1 during cardioprotection, we next pursued studies with the pharmacologic HIF stabilizer DMOG. Here, we hypothesized that if myeloid-dependent HIF functions through induction of netrin-1 to provide cardioprotection, the cardioprotective effects of DMOG would be abolished in $Ntn1^{loxP/loxP}$ LysM Cre+ mice. To address this hypothesis, we treated $Ntn1^{loxP/loxP}$ LysM Cre+ mice with DMOG (1 mg i.p. 4 h prior to myocardial ischemia) or vehicle control, a treatment protocol that we had previously shown to be effective in reducing myocardial infarct sizes (5, 23). Consistent with a functional role of PMN-dependent netrin-1 in mediating DMOG-dependent cardioprotection, we found that the previously shown reduction of myocardial infarct sizes associated with DMOG treatment (**Figures 5A–C**) (5, 23) were completely abolished in $Ntn1^{loxP/loxP}$ LysM Cre+ mice (**Figures 6C–E**). Together with recent studies from our laboratory showing that $Ntn1^{loxP/loxP}$ LysM Cre+ mice experience increased infarct sizes (12), these findings implicate HIF-dependent induction of netrin-1 in the cardioprotection provided by myeloid-expressed HIF1A during ischemia and reperfusion injury of the heart.

Discussion

Hypoxia-inducible factors such as HIF1A have been implicated in tissue adaption during limited oxygen availability, inflammation, or ischemia and reperfusion injury (48). While previous studies have directly implicated HIF1a in limiting myocardial infarct sizes during ischemia and reperfusion injury (5, 38, 39, 49, 50), the relative contributions of HIF1A expressed in different cell types in the heart remain elusive. To investigate tissue-specific functions of HIF1A in cardioprotection from *in situ* ischemia and reperfusion injury, we took a stepwise approach. In initial studies, we used a genetic approach, where Hif1A deletion was induced in the adult mouse, thereby circumventing embryonic lethality of homozygote Hif1a deletion (40). These studies revealed dramatic increase of myocardial infarct sizes in mice with induced global Hif1A deletion ($Hif1a^{loxP/loxP}$ UbiquitinCre+ mice) as compared to Cre+ controls. As second step, we pursued studies of myocardial ischemia and reperfusion injury in mice with genetic deletion of *Hif1a* in different tissue compartments,

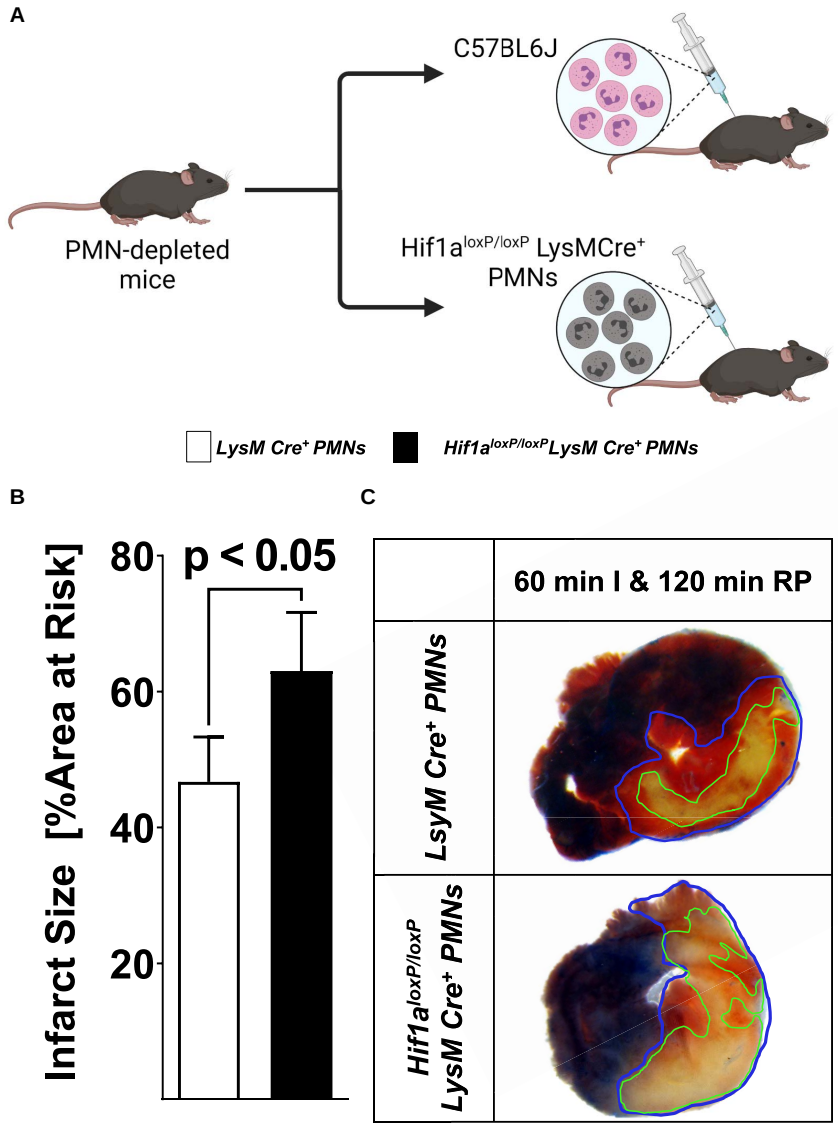

FIGURE 3
Effects of adoptive transfer of polymorphonuclear neutrophils (PMN) from *Hif1a*$^{loxP/loxP}$ LysM Cre+ to wild-type mice during myocardial ischemia and reperfusion injury. **(A)** Schematic of adoptive transfer model. PMNs deficient in C57BL6J or Hif1a-deficient PMNs (*Hif1a*$^{loxP/loxP}$ LysM Cre+) were isolated by negative selection and transferred to PMN-depleted C57BL6 animals (1A8 Ly6G specific antibody 24 h prior to experiment). The animals were then subjected to 60 min of ischemia, followed by 120 min of reperfusion with assessment of myocardial injury. **(B)** Infarct sizes ± SD in mice receiving PMN from C57BL6J or *Hif1a*$^{loxP/loxP}$ LysM Cre+ mice presented as a percentage of the area at risk after 60 min of ischemia, followed by 120 min of reperfusion (LysM Cre+ PMNs n = 4; *Hif1a*$^{loxP/loxP}$ LysM Cre+ n = 4; all values represented as mean ± SD; statistical significance evaluated by two-sided, unpaired Student's t-test). **(C)** Representative infarct staining of neutrophil-depleted mice receiving PMNs from LysM Cre+ or *Hif1a*$^{loxP/loxP}$ LysM Cre+ mice.

including cardiomyocytes (*Hif1a*$^{loxP/loxP}$ Myosin Cre+ mice), vascular endothelial cells (*Hif1a*$^{loxP/loxP}$ VEcadherin Cre+ mice) or in myeloid inflammatory cells (*Hif1a*$^{loxP/loxP}$ LysM Cre+ mice). To our surprise, only mice with deletion of *Hif1a* in myeloid inflammatory cells resembled the previous findings we had established in mice with induced global deletion of Hif1A, thereby indirectly implicating myeloid-dependent *Hif1a* in cardio-protection from ischemia and reperfusion. Due to the critical functions and high presence of PMNs during myocardial reperfusion injury (51), we studied mice with reconstitution of wild-type or *Hif1a*-deficient neutrophils following antibody-mediate PMN depletion (52). While mice with *Hif1a*-deficient PMNs experience increased myocardial injury, mice with reconstitution of wild-type PMN that received *ex vivo* treatment with HIF stabilizer DMOG were protected. Finally, studies that focused on transcriptional targets of

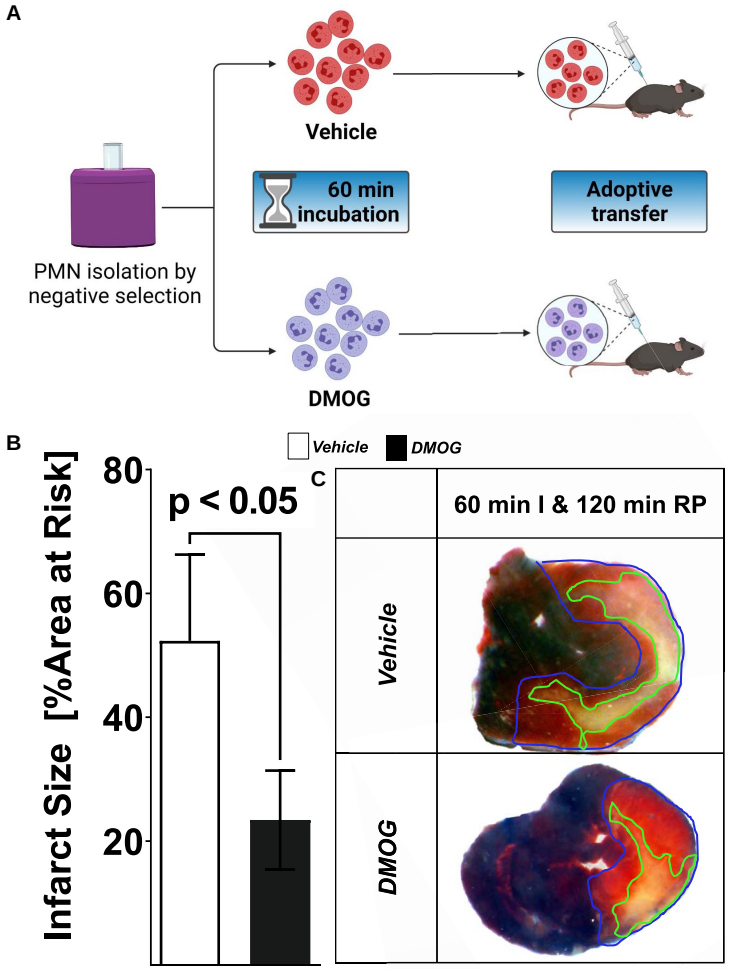

FIGURE 4
Effect of HIF stabilization in PMN on myocardial injury. **(A)** Schematic of the pharmacological stabilization of HIF in PMN. Cells were harvested by negative selection from C57BL6 mice; isolated cells were incubated for 60 min in vehicle or 1 mM DMOG solution. The cells were then adoptively transferred to PMN-depleted C57BL6, treated with 1A8 Ly6G-specific antibody 24 h before the experiment. **(B)** Infarct sizes ± SD in mice receiving vehicle or DMOG treated PMNs presented as percentage to the area-at-risk after 60 min of ischemia, followed by 120 min of reperfusion (vehicle $n = 5$; DMOG $n = 4$; all values represented as mean ± SD; statistical significance assessed by two-sided, unpaired Student's *t*-test). **(C)** Representative infarct staining from neutrophil-depleted mice receiving PMN treated with DMOG or vehicle.

HIF1A in neutrophils implicated PMN-dependent netrin-1 in mediating HIF1A elicited cardioprotection. Together, these studies highlight a functional role of myeloid-dependent HIF1A in attenuating myocardial ischemia and reperfusion, and its transcriptional target netrin-1. Based on these studies, using HIF stabilizers or treatment with recombinant netrin-1 may represent novel approaches to treat or prevent myocardial injury during myocardial ischemia and reperfusion.

Netrin-1 improves the signaling events of the adenosine receptor Adora2b (53), which elicits strong anti-inflammatory effects, as previous studies have shown (47). In recent studies, netrin-1 was shown to require a functional Adora2b receptor on the surface of neutrophils to induce cardio protective effects (12). Likewise, Adora2b was previously identified as the target for hypoxia signaling through HIF1A. Studies of murine models of myocardial infarction and reperfusion injuries demonstrate the strong cardiovascular protection of Adora2b. A specific agonist for Adora2b significantly reduced the size of infarct after myocardial ischemia (5). Studies using the HIF activator DMOG as a treatment approach for experimental myocardial ischemia showed that cardioprotection was eliminated in mice lacking Adora2b (5). This directly links the signaling of HIF1A and ADORA2B during cardioprotection.

Adora2b reduces the size of the infarct due to its strong inhibition of the inflammatory response. This has been demonstrated in studies in which Adora2b deficiency in mice increased the expression of pro-inflammatory and cardiotoxic cytokine tumor necrosis factor alpha (TNF-α) (36). Netrin-1 has similar anti-inflammatory effects in hypoxic inflammation that require the presence of ADORA2B (47) – and both Netrin-1

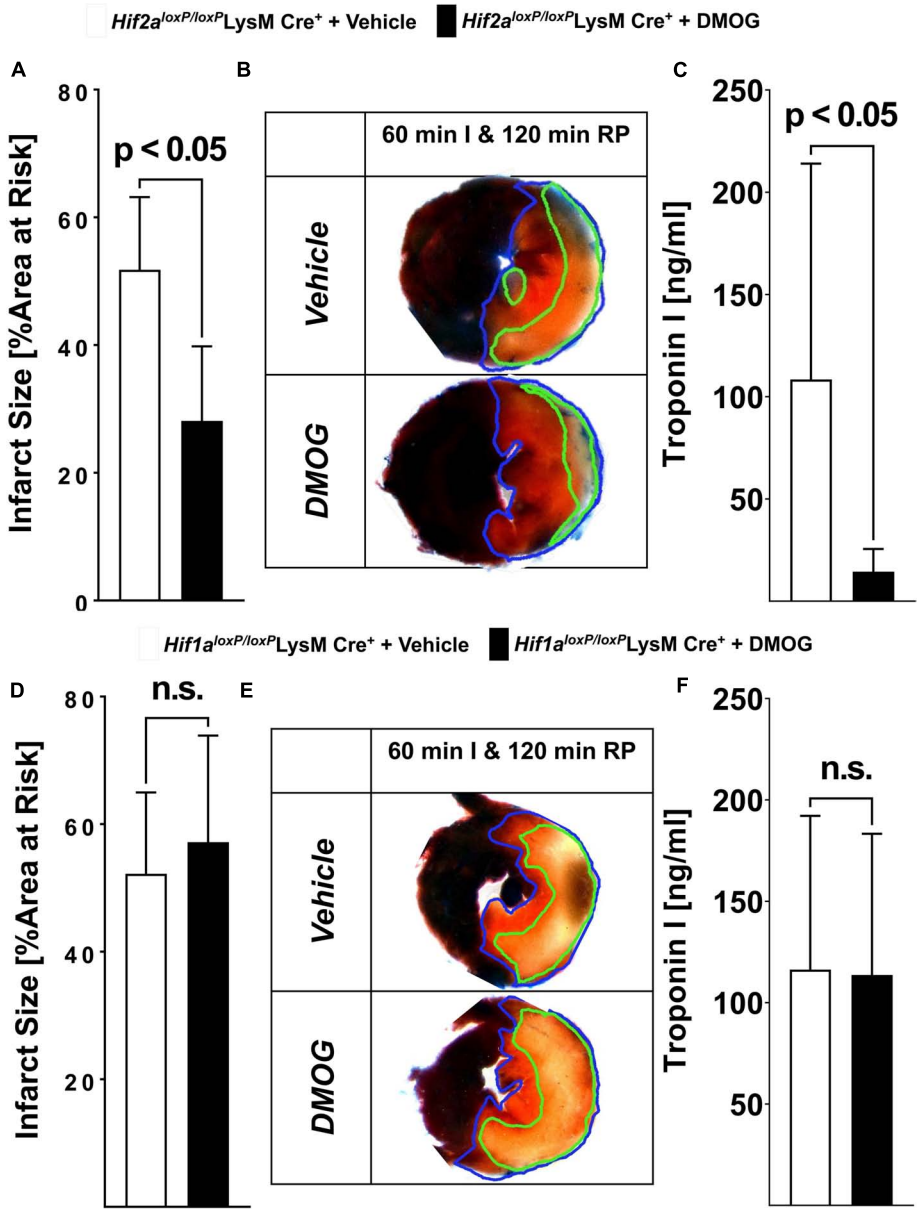

FIGURE 5
Selective HIF-isoform deletion in PMN in myocardial ischemia and reperfusion. **(A–F)** *Hif1a*$^{loxP/loxP}$ or *Hif2a*$^{loxP/loxP}$ were crossed with Cre recombinase expressing mice under the control of the lysozyme 2 promoter (LysM Cre+) to generate animals deficient in myeloids-specific Hif1a or Hif2a. Mice received vehicle or 1 mg of HIF stabilizing DMOG 4 h before ischemia. Mice underwent 60 min of ischemia and 120 min of reperfusion and evaluation of myocardial injury infarct sizes measurement and serum troponin I concentrations. **(A)** Infarct sizes were determined in vehicle or DMOG treated *Hif2a*$^{loxP/loxP}$ LysM Cre+ mice (n = 5 per group). **(B)** Representative infarct staining from vehicle or DMOG treated *Hif2a*$^{loxP/loxP}$ LysM Cre+ mice. **(C)** Serum levels of troponin in vehicle or DMOG treated *Hif2a*$^{loxP/loxP}$ LysM Cre+ mice (n = 5 per group). **(D)** Infarct sizes were determined in vehicle or DMOG treated *Hif1a*$^{loxP/loxP}$ LysM Cre+ mice (*Hif1a*$^{loxP/loxP}$ LysM Cre+ + vehicle n = 5; *Hif1a*$^{loxP/loxP}$ LysM Cre+ + DMOG n = 6). **(E)** Representative infarct staining from vehicle or DMOG treated *Hif1a*$^{loxP/loxP}$ LysM Cre+ mice. **(F)** Serum levels of troponin in vehicle or DMOG treated *Hif1a*$^{loxP/loxP}$ LysM Cre+ mice (*Hif1a*$^{loxP/loxP}$ LysM Cre+ + vehicle n = 5; *Hif1a*$^{loxP/loxP}$ LysM Cre+ + DMOG n = 6) (All data presented as mean ± SD. Statistical significance assessed by two-sided, unpaired Student's t-test).

and ADORA2B are HIF1a-target genes. This suggests that, in response to myocardial infarction and reperfusion, activation of HIF1A coordinates cardioprotective effects by activating the expressions of Netrin-1 and ADORA2B, which both reduce post-ischemic myocardial inflammation.

While the current studies directly implicate HIF1A in attenuating myocardial ischemia and reperfusion injury, other studies have also implicated HIF2A in cardioprotection. HIF2A is an isoform of HIF1A and several studies have identified either complementary or opposing functions to HIF1A (35,

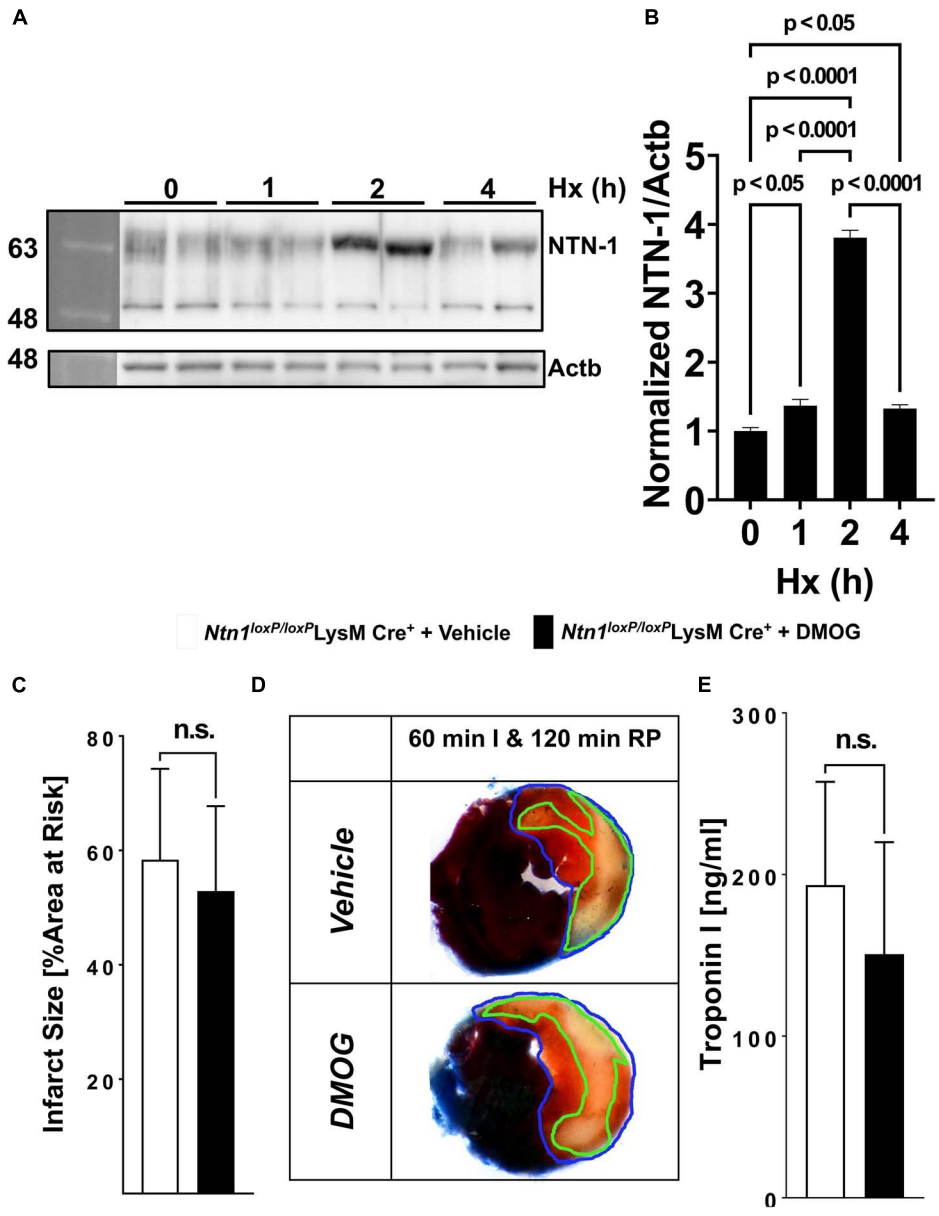

FIGURE 6
Netrin-1 as a PMN-dependent Hif1A target critical for HIF-dependent cardioprotection. **(A,B)** Isolated human PMNs from healthy donors underwent hypoxia for 0, 2 and 4 h followed by cell lysis and total protein harvest. **(A)** Immunoblot for NTN1. b-Actin (Actb) served as the loading control. One representative blot of three experiments is shown. **(B)** Quantitation by densitometry of the NTN1 immunoblot results relative to b-Actin (n = 2 per group; per group mean ± SD; compared by one-way ANOVA followed by Tukey's multiple comparison test). **(C–E)** *Ntn-1*$^{loxP/loxP}$ *mice* were crossed with Cre recombinase-expressing mice under the control of the lysozyme 2 promoter (LysM Cre+) to generate mice deficient in myeloid-specific Ntn-1. Mice received vehicle or 1 mg DMOG 4 h prior to ischemia, then underwent 60 min of ischemia followed by 120 min of reperfusion and assessment of myocardial injury. **(C)** Infarct sizes were determined in vehicle or DMOG treated Ntn-1loxP/loxP LysM Cre+ (*Ntn-1*$^{loxP/loxP}$ LysM Cre+ with vehicle n = 5; *Ntn-1*$^{loxP/loxP}$ LysM Cre+ with DMOG n = 6). **(D)** Representative infarct staining from vehicle or DMOG treated *Ntn-1*$^{loxP/loxP}$ LysM Cre+. **(E)** Troponin serum levels of vehicle or DMOG treated *Ntn-1*$^{loxP/loxP}$ LysM Cre+ mice (*Ntn-1*$^{loxP/loxP}$ LysM Cre+ with vehicle n = 5; *Ntn-1*$^{loxP/loxP}$ LysM Cre+ with DMOG n = 6). All data are presented as mean ± SD. Statistical significance assessed by two-sided, unpaired Student's t-test. DMOG-induced cardioprotection was absent in *Ntn-1*$^{loxP/loxP}$ LysM Cre+.

54–57). As such, it is not surprising that previous studies have also identified a functional role of Hif2A in attenuating myocardial infarct sizes during ischemia and reperfusion injury (23). In contrast to the current studies that implicated myeloid-dependent Hif1A in cardioprotection, those studies demonstrated a functional role of HIF2A expressed in cardiac myocytes. In fact, *Hif2a*$^{loxP/loxP}$ Myosin Cre+ mice exhibited larger infarct sizes during *in situ* myocardial ischemia and

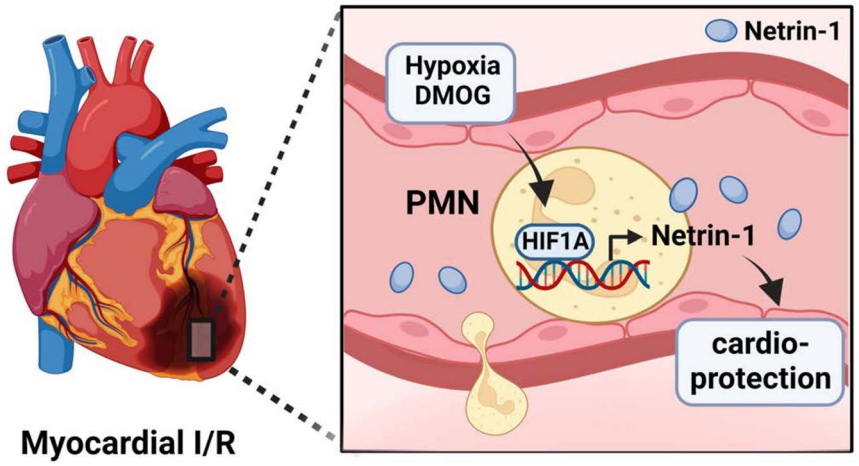

FIGURE 7
Suggested mechanism of HIF1A-induced cardioprotection during myocardial ischemia and reperfusion injury. During myocardial ischemia and reperfusion injury, neutrophils undergo hypoxia, leading to stabilization of HIF1A. HIF1A subsequently induces increased expression and release of neuronal guidance proteins Netrin-1 by PMN. Netrin-1 then reduces a reduction in infarct sizes.

reperfusion injury (23). Subsequent studies on myocyte-dependent HIF2A target genes implicate the epidermal growth factor amphiregulin (AREG) in mediating HIF2A dependent cardioprotection (23). Additional studies in myocardial biopsies of patients with ongoing ischemia revealed elevated levels of AREG (23), of the amphiregulin receptor ERBB1 (35). Mice with global deletion of Areg (*Areg*$^{-/-}$ mice), or with deletion of the *ErbB1* receptor expressed on cardiac myocytes (*ErbB1*$^{loxP/loxP}$ Myosin Cre+) experienced increased susceptibility to myocardial ischemia and reperfusion injury. Together, those studies implicate myocyte-dependent HIF2A in coordinating the induction and signaling events of AREG through the ERBB1 receptor in cardioprotection (23, 35). Together with the current studies, those findings accentuate a cardioprotective role of HIF, by attenuating myocardial ischemic injury through myocyte-dependent HIF2A and myocardial reperfusion injury through myeloid-dependent HIF1A.

While the current studies concentrate on myocardial ischemia and reperfusion injury, previous studies had also implicated HIF in promoting ischemic preconditioning of the heart. Ischemic preconditioning involves short episode of ischemia that confers protection to a subsequent myocardial infarction (58). Several previous studies have shown functional roles of HIF1A in mediating the tissue-protective effects of ischemic preconditioning, including studies to address tissue-specific functions of HIF1A. Initial studies demonstrated that mice with partial deletion of *Hif1a* (*Hif1a*$^{\pm}$ mice) experienced a complete loss of cardioprotection from ischemic preconditioning (26). Similarly, mice with siRNA *in vivo* silencing of Hif1a demonstrated a lack of cardio-protection by ischemic preconditioning, while pre-treatment with the HIF stabilizer DMOG preconditioned the myocardium (5). Subsequent studies to address tissue-specific functions of HIF1A in ischemic preconditioning implicated HIF1A activity in vascular endothelia (50). Other studies found that deletion of *Hif1a* in cardiomyocytes (*Hif1a*$^{loxP/loxP}$ Myosin Cre+) also abolishes the cardio-protective effects of ischemic preconditioning (23). In contrast, mice with cardiomyocyte-specific deletion of *Hif2a* (*Hif2a*$^{loxP/loxP}$ Myosin Cre+) were protected by ischemic preconditioning (23). Interestingly, more recent studies also implicate HIF1A in mediating the cardioprotective effects of remote ischemic preconditioning, where repeated episodes of remote ischemia to a limb can produce protection from myocardial or acute kidney injury (59). These studies indicate that during remote ischemic preconditioning, HIF1A is stabilized, and transcriptionally induces the HIF target gene L-10 with subsequent IL-10 signaling as a mechanism of cardioprotection (49). Taken together, these studies provide evidence from multiple studies that HIF1A – as opposed to HIF2A – mediates the cardioprotective effects of direct or remote ischemic preconditioning (17, 60).

The current studies implicate the HIF1A target netrin-1 in PMNs as critical target for mediating the cardioprotective effects of myeloid HIF1A. Netrin-1 is a neuronal guidance molecule that was initially described as a diffusible axon outgrowth promoting factor in nematodes (61). However, it became apparent that netrin-1 is much more ubiquitously expressed (62). In addition to its function as neuronal guidance molecule during brain development (45), it became apparent that netrin-1 can also function to modulate inflammatory endpoints or ischemia and reperfusion injury (63, 64). For example, netrin-1 released from the vagal nerve has been shown to attenuate excessive inflammation and promote the resolution of injury

(64). Several previous studies have linked netrin-1 signaling in cardioprotection from ischemia and reperfusion injury, for example *via* interaction of netrin-1 with the classic netrin-1 receptor deleted in colorectal cancer DCC expressed on endothelial cells (65, 66). Consistent with current findings, a recent study indicates that PMN-dependent netrin-1 can function to provide cardioprotection during *in situ* ischemia and reperfusion injury by enhancing extracellular adenosine signaling events through the Adora2b adenosine receptor (12, 53, 63, 67, 68). Although extracellular adenosine signaling was initially described to induce a transient slowing of heart rate (69), many subsequent studies have sown functional roles for extracellular adenosine signaling in attenuating myocardial ischemia and reperfusion injury, including studies directly implicating myeloid Adora2b signaling (7, 36, 43) (**Figure 7**). Taken together, these studies provide additional support for the concept that myeloid HIF1A provides cardioprotection through transcriptional induction of its target gene netrin-1, leading to attenuated myocardial ischemia and reperfusion injury.

The current findings have important translational implications. For example, it is possible that patients experiencing myocardial ischemia and reperfusion injury could be treated with recombinant netrin-1 to activate the HIF1A-netrin-1 pathway for cardioprotection. Several other studies have shown that recombinant netrin-1 treatment can function to dampen myocardial injury (12) or other states of inflammatory disease (67). However, an alternative treatment approach would include the use of pharmacological HIF stabilizers. Over the past decade, several pharmaceutical companies have developed pharmacologic HIF activators (17, 18, 70–72). These pharmacological HIF activators function by inhibiting prolylhydroxylases and thus prevent the degradation of HIF1A *via* the proteasomal pathway (3). Pharmacological HIF activators, such as roxadustat or vadadustat, have been successfully tested for the treatment of renal anemia and phase 3 clinical trials and are available as oral medications (19–22). These orally available HIF activators could be used in patients experiencing myocardial ischemia and reperfusion injury. Furthermore, it is possible that these medications could be given to patients at high risk of experiencing myocardial injury, such as patients undergoing cardiac surgery. Treatment with an oral HIF activator would likely cause stabilization of HIF, including neutrophils, and thus dampen myocardial ischemia and reperfusion injury (73). This highlights that HIF1A coordinates the transcriptional response in response to myocardial ischemia.

Data availability statement

The raw data supporting the conclusions of this article will be made available by the authors, without undue reservation.

Ethics statement

This animal study was reviewed and approved by the University of Colorado Denver and the Institutional Animal Care and Use Committee of the University of Texas Health Science Center at Houston.

Author contributions

KH-S, JL, and WR performed the experiments. XY and YW helped with data analysis. MK designed the study, performed the experiments and data analysis, and wrote the manuscript. HE designed the study and wrote the manuscript. All authors contributed to the article and approved the submitted version.

Funding

This study was supported by Deutsche Forschungsgemeinschaft (DFG; KO 3884/5-1) to MK and National Institute of Health Grants R01HL154720, R01DK122796, R01DK109574, and R01HL133900 and the Department of Defense Grant W81XWH2110032 to HE. Natural Science Foundation of Hunan Province Grant 2018JJ3736, Hunan Youth Talents Program 2021RC3034, and 2022 International Anesthesia Research Society Mentored Research Award to WR.

Acknowledgments

All schematics were generated using BioRender.com.

Conflict of interest

The authors declare that the research was conducted in the absence of any commercial or financial relationships that could be construed as a potential conflict of interest.

Publisher's note

References

1. Heusch G. Myocardial ischaemia-reperfusion injury and cardioprotection in perspective. *Nat Rev Cardiol.* (2020) 17:773–89. doi: 10.1038/s41569-020-0403-y

2. Eltzschig HK, Carmeliet P. Hypoxia and inflammation. *N Engl J Med.* (2011) 364:656–65. doi: 10.1056/NEJMra0910283

3. Eltzschig HK, Bratton DL, Colgan SP. Targeting hypoxia signalling for the treatment of ischaemic and inflammatory diseases. *Nat Rev Drug Discov.* (2014) 13:852–69. doi: 10.1038/nrd4422

4. Sitkovsky M, Lukashev D. Regulation of immune cells by local-tissue oxygen tension: HIF1 alpha and adenosine receptors. *Nat Rev Immunol.* (2005) 5:712–21. doi: 10.1038/nri1685

5. Eckle T, Kohler D, Lehmann R, El Kasmi KC, Eltzschig HK. Hypoxia-inducible factor-1 is central to cardioprotection: a new paradigm for ischemic preconditioning. *Circulation.* (2008) 118:166–75. doi: 10.1161/CIRCULATIONAHA.107.758516

6. Koeppen M, Eckle T, Eltzschig HK. The hypoxia-inflammation link and potential drug targets. *Curr Opin Anaesthesiol.* (2011) 24:363–9. doi: 10.1097/ACO.0b013e32834873fd

7. Koeppen M, Eckle T, Eltzschig HK. Interplay of hypoxia and ADORA2B adenosine receptors in tissue protection. *Adv Pharmacol.* (2011) 61:145–86. doi: 10.1016/B978-0-12-385526-8.00006-0

8. Manalo DJ, Rowan A, Lavoie T, Natarajan L, Kelly BD, Ye SQ, et al. Transcriptional regulation of vascular endothelial cell responses to hypoxia by HIF-1. *Blood.* (2005) 105:659–69. doi: 10.1182/blood-2004-07-2958

9. Bonney S, Kominsky D, Brodsky K, Eltzschig H, Walker L, Eckle T. Cardiac per2 functions as novel link between fatty acid metabolism and myocardial inflammation during ischemia and reperfusion injury of the heart. *PLoS One.* (2013) 8:e71493. doi: 10.1371/journal.pone.0071493

10. Shepardson KM, Jhingran A, Caffrey A, Obar JJ, Suratt BT, Berwin BL, et al. Myeloid derived hypoxia inducible factor 1-alpha is required for protection against pulmonary *Aspergillus fumigatus* infection. *PLoS Pathog.* (2014) 10:16. doi: 10.1371/journal.ppat.1004378

11. Alexander LEC, Akong-Moore K, Feldstein S, Johansson P, Nguyen A, McEachern EK, et al. Myeloid cell HIF-1 alpha regulates asthma airway resistance and eosinophil function. *J Mol Med.* (2013) 91:637–44. doi: 10.1007/s00109-012-0986-9

12. Li J, Conrad C, Mills TW, Berg NK, Kim B, Ruan W, et al. PMN-derived netrin-1 attenuates cardiac ischemia-reperfusion injury *via* myeloid ADORADORA2B signaling. *J Exp Med.* (2021) 218:e20210008. doi: 10.1084/jem.20210008

13. Lin N, Simon MC. Hypoxia-inducible factors: key regulators of myeloid cells during inflammation. *J Clin Invest.* (2016) 126:3661–71. doi: 10.1172/JCI84426

14. Walmsley SR, Print C, Farahi N, Peyssonnaux C, Johnson RS, Cramer T, et al. Hypoxia-induced neutrophil survival is mediated by HIF-1alpha-dependent NF-kappaB activity. *J Exp Med.* (2005) 201:105–15. doi: 10.1084/jem.20040624

15. Cramer T, Yamanishi Y, Clausen BE, Forster I, Pawlinski R, Mackman N, et al. HIF-1alpha is essential for myeloid cell-mediated inflammation. *Cell.* (2003) 112:645–57. doi: 10.1016/S0092-8674(03)00154-5

16. Taylor CT, Colgan SP. Regulation of immunity and inflammation by hypoxia in immunological niches. *Nat Rev Immunol.* (2017) 17:774–85. doi: 10.1038/nri.2017.103

17. Yuan X, Lee JW, Bowser JL, Neudecker V, Sridhar S, Eltzschig HK. Targeting hypoxia signaling for perioperative organ injury. *Anesth Analg.* (2017) 126:308–21.

18. Bowser JL, Lee JW, Yuan X, Eltzschig HK. The hypoxia-adenosine link during inflammation. *J Appl Physiol.* (2017) 123:1303–20. doi: 10.1152/japplphysiol.00101.2017

19. Chen N, Hao C, Peng X, Lin H, Yin A, Hao L, et al. Roxadustat for anemia in patients with kidney disease not receiving dialysis. *N Engl J Med.* (2019) 381:1001–10. doi: 10.1056/NEJMoa1813599

20. Chen N, Hao C, Liu BC, Lin H, Wang C, Xing C, et al. Roxadustat treatment for anemia in patients undergoing long-term dialysis. *N Engl J Med.* (2019) 381:1011–22. doi: 10.1056/NEJMoa1901713

21. Eckardt KU, Agarwal R, Aswad A, Awad A, Block GA, Bacci MR, et al. Safety and efficacy of vadadustat for anemia in patients undergoing dialysis. *N Engl J Med.* (2021) 384:1601–12. doi: 10.1056/NEJMoa2025956

22. Chertow GM, Pergola PE, Farag YMK, Agarwal R, Arnold S, Bako G, et al. Vadadustat in patients with anemia and non-dialysis-dependent CKD. *N Engl J Med.* (2021) 384:1589–600. doi: 10.1056/NEJMoa2035938

23. Koeppen M, Lee JW, Seo SW, Brodsky KS, Kreth S, Yang IV, et al. Hypoxia-inducible factor 2-alpha-dependent induction of amphiregulin dampens myocardial ischemia-reperfusion injury. *Nat Commun.* (2018) 9:816. doi: 10.1038/s41467-018-03105-2

24. Eltzschig HK, Bonney SK, Eckle T. Attenuating myocardial ischemia by targeting ADORA2B adenosine receptors. *Trends Mol Med.* (2013) 19:345–54. doi: 10.1016/j.molmed.2013.02.005

25. Adluri RS, Thirunavukkarasu M, Dunna NR, Zhan L, Oriowo B, Takeda K, et al. Disruption of hypoxia-inducible transcription factor-prolyl hydroxylase domain-1 (PHD-1-/-) attenuates ex vivo myocardial ischemia/reperfusion injury through hypoxia-inducible factor-1alpha transcription factor and its target genes in mice. *Antioxid Redox Signal.* (2011) 15:1789–97. doi: 10.1089/ars.2010.3769

26. Cai, Z, Zhong H, Bosch-Marce M, Fox-Talbot K, Wang L, Wei C, et al. Complete loss of ischaemic preconditioning-induced cardioprotection in mice with partialdeficiency of HIF-1{alpha}. *Cardiovasc Res.* (2007) 77:463–70. doi: 10.1093/cvr/cvm035

27. Eckle T, Brodsky K, Bonney M, Packard T, Han J, Borchers CH, et al. HIF1A reduces acute lung injury by optimizing carbohydrate metabolism in the alveolar epithelium. *PLoS Biol.* (2013) 11:e1001665. doi: 10.1371/journal.pbio.1001665

28. Ryan HE, Poloni M, McNulty W, Elson D, Gassmann M, Arbeit JM, et al. Hypoxia-inducible factor-1alpha is a positive factor in solid tumor growth. *Cancer Res.* (2000) 60:4010–5.

29. Ruzankina Y, Pinzon-Guzman C, Asare A, Ong T, Pontano L, Cotsarelis G, et al. Deletion of the developmentally essential gene ATR in adult mice leads to age-related phenotypes and stem cell loss. *Cell Stem Cell.* (2007) 1:113–26. doi: 10.1016/j.stem.2007.03.002

30. Clausen BE, Burkhardt C, Reith W, Renkawitz R, Forster I. Conditional gene targeting in macrophages and granulocytes using LysMcre mice. *Transgenic Res.* (1999) 8:265–77. doi: 10.1023/A:1008942828960

31. Alva JA, Zovein AC, Monvoisin A, Murphy T, Salazar A, Harvey NL, et al. VE-Cadherin-Cre-recombinase transgenic mouse: a tool for lineage analysis and gene deletion in endothelial cells. *Dev Dyn.* (2006) 235:759–67. doi: 10.1002/dvdy.20643

32. Hall ME, Smith G, Hall JE, Stec DE. Systolic dysfunction in cardiac-specific ligand-inducible MerCreMer transgenic mice. *Am J Physiol Heart Circ Physiol.* (2011) 301:H253–60. doi: 10.1152/ajpheart.00786.2010

33. Eckle T, Koeppen M, Eltzschig H. Use of a hanging weight system for coronary artery occlusion in mice. *J Vis Exp.* (2011) 50:2526–2532. doi: 10.3791/2526

34. Eckle T, Grenz A, Kohler D, Redel A, Falk M, Rolauffs B, et al. Systematic evaluation of a novel model for cardiac ischemic preconditioning in mice. *Am J Physiol Heart Circ Physiol.* (2006) 291:H2533–40. doi: 10.1152/ajpheart.00472.2006

35. Lee JW, Koeppen M, Seo SW, Bowser JL, Yuan X, Li J, et al. Transcription-independent induction of ERBB1 through hypoxia-inducible factor 2A provides cardioprotection during ischemia and reperfusion. *Anesthesiology.* (2020) 132:763–80. doi: 10.1097/ALN.0000000000003037

36. Koeppen M, Harter PN, Bonney S, Bonney M, Reithel S, Zachskorn C, et al. AdorAdora2b signaling on bone marrow derived cells dampens myocardial ischemia-reperfusion injury. *Anesthesiology.* (2012) 116:1245–57. doi: 10.1097/ALN.0b013e318255793c

37. Daley JM, Thomay AA, Connolly MD, Reichner JS, Albina JE. Use of Ly6G-specific monoclonal antibody to deplete neutrophils in mice. *J Leukoc Biol.* (2008) 83:64–70. doi: 10.1189/jlb.0407247

38. Eckle T, Hartmann K, Bonney S, Reithel S, Mittelbronn M, Walker LA, et al. AdorAdora2b-elicited Per2 stabilization promotes a HIF-dependent metabolic switch crucial for myocardial adaptation to ischemia. *Nat Med.* (2012) 18:774–82. doi: 10.1038/nm.2728

39. Cai Z, Zhong H, Bosch-Marce M, Fox-Talbot K, Wang L, Wei C, et al. Complete loss of ischaemic preconditioning-induced cardioprotection in mice with partial deficiency of HIF-1 alpha. *Cardiovasc Res.* (2008) 77:463–70.

40. Yu AY, Shimoda LA, Iyer NV, Huso DL, Sun X, McWilliams R, et al. Impaired physiological responses to chronic hypoxia in mice partially deficient for hypoxia-inducible factor 1{alpha}. *J Clin Invest.* (1999) 103:691–6. doi: 10.1172/JCI5912

41. Soro-Arnaiz I, Li QOY, Torres-Capelli M, Melendez-Rodriguez F, Veiga S, Veys K, et al. Role of mitochondrial complex IV in age-dependent obesity. *Cell Rep.* (2016) 16:2991–3002. doi: 10.1016/j.celrep.2016.08.041

42. Berg NK, Li J, Kim B, Mills T, Pei G, Zhao Z, et al. Hypoxia-inducible factor-dependent induction of myeloid-derived netrin-1 attenuates natural killer cell infiltration during endotoxin-induced lung injury. *FASEB J.* (2021) 35:e21334. doi: 10.1096/fj.202002407R

43. Seo SW, Koeppen M, Bonney S, Gobel M, Thayer M, Harter PN, et al. Differential Tissue-specific function of AdorAdora2b in cardioprotection. *J Immunol.* (2015) 195:1732–43. doi: 10.4049/jimmunol.1402288

44. Ong CWM, Fox K, Ettorre A, Elkington PT, Friedland JS. Hypoxia increases neutrophil-driven matrix destruction after exposure to *Mycobacterium tuberculosis*. *Sci Rep.* (2018) 8:11475. doi: 10.1038/s41598-018-29659-1

45. Serafini T, Colamarino SA, Leonardo ED, Wang H, Beddington R, Skarnes WC, et al. Netrin-1 is required for commissural axon guidance in the developing vertebrate nervous system. *Cell.* (1996) 87:1001–14. doi: 10.1016/S0092-8674(00)81795-X

46. Keller M, Mirakaj V, Koeppen M, Rosenberger P. Neuronal guidance proteins in cardiovascular inflammation. *Basic Res Cardiol.* (2021) 116:6. doi: 10.1007/s00395-021-00847-x

47. Rosenberger P, Schwab JM, Mirakaj V, Masekowsky E, Mager A, Morote-Garcia JC, et al. Hypoxia-inducible factor-dependent induction of netrin-1 dampens inflammation caused by hypoxia. *Nat Immunol.* (2009) 10:195–202. doi: 10.1038/ni.1683

48. Eckle T, Kewley EM, Brodsky KS, Tak E, Bonney S, Gobel M, et al. Identification of hypoxia-inducible factor HIF-1A as transcriptional regulator of the ADORA2B adenosine receptor during acute lung injury. *J Immunol.* (2014) 192:1249–56. doi: 10.4049/jimmunol.1100593

49. Cai Z, Luo W, Zhan H, Semenza GL. Hypoxia-inducible factor 1 is required for remote ischemic preconditioning of the heart. *Proc Natl Acad Sci U.S.A.* (2013) 110:17462–7. doi: 10.1073/pnas.1317158110

50. Sarkar K, Cai Z, Gupta R, Parajuli N, Fox-Talbot K, Darshan MS, et al. Hypoxia-inducible factor 1 transcriptional activity in endothelial cells is required for acute phase cardioprotection induced by ischemic preconditioning. *Proc Natl Acad Sci U.S.A.* (2012) 109:10504–9. doi: 10.1073/pnas.1208314109

51. Yellon DM, Hausenloy DJ. Myocardial reperfusion injury. *N Engl J Med.* (2007) 357:1121–35. doi: 10.1056/NEJMra071667

52. Koeppen M, McNamee EN, Brodsky KS, Aherne CM, Faigle M, Downey GP, et al. Detrimental role of the airway mucin Muc5ac during ventilator-induced lung injury. *Mucosal Immunol.* (2013) 6:762–75. doi: 10.1038/mi.2012.114

53. Corset V, Nguyen-Ba-Charvet KT, Forcet C, Moyse E, Chedotal A, Mehlen P. Netrin-1-mediated axon outgrowth and cAMP production requires interaction with adenosine Adora2b receptor. *Nature.* (2000) 407:747–50. doi: 10.1038/35037600

54. Keith B, Johnson RS, Simon MC. HIF1alpha and HIF2alpha: sibling rivalry in hypoxic tumour growth and progression. *Nat Rev Cancer.* (2012) 12:9–22. doi: 10.1038/nrc3183

55. Takeda N, O'Dea EL, Doedens A, Kim JW, Weidemann A, Stockmann C, et al. Differential activation and antagonistic function of HIF-{alpha} isoforms in macrophages are essential for NO homeostasis. *Genes Dev.* (2010) 24:491–501. doi: 10.1101/gad.1881410

56. Ju C, Wang M, Tak E, Kim B, Emontzpohl C, Yang Y, et al. Hypoxia-inducible factor-1alpha-dependent induction of miR122 enhances hepatic ischemia tolerance. *J Clin Invest.* (2021) 131:e140300. doi: 10.1172/JCI140300

57. Gao RY, Wang M, Liu Q, Feng D, Wen Y, Xia Y, et al. Hypoxia-inducible factor-2alpha reprograms liver macrophages to protect against acute liver injury through the production of interleukin-6. *Hepatology.* (2020) 71:2105–17. doi: 10.1002/hep.30954

58. Murry CE, Jennings RB, Reimer KA. Preconditioning with ischemia: a delay of lethal cell injury in ischemic myocardium. *Circulation.* (1986) 74:1124–36. doi: 10.1161/01.CIR.74.5.1124

59. Gumbert SD, Kork F, Jackson ML, Vanga N, Ghebremichael SJ, Wang CY, et al. Perioperative acute kidney injury. *Anesthesiology.* (2020) 132:180–204. doi: 10.1097/ALN.0000000000002968

60. Lee JW, Ko J, Ju C, Eltzschig HK. Hypoxia signaling in human diseases and therapeutic targets. *Exp Mol Med.* (2019) 51:1–13. doi: 10.1038/s12276-019-0235-1

61. Serafini T, Kennedy TE, Galko MJ, Mirzayan C, Jessell TM, Tessier-Lavigne M. The netrins define a family of axon outgrowth-promoting proteins homologous to C. elegans UNC-6. *Cell.* (1994) 78:409–24. doi: 10.1016/0092-8674(94)90420-0

62. Mirakaj V, Rosenberger P. Immunomodulatory functions of neuronal guidance proteins. *Trends Immunol.* (2017) 38:444–56. doi: 10.1016/j.it.2017.03.007

63. Schlegel M, Kohler D, Korner A, Granja T, Straub A, Giera M, et al. The neuroimmune guidance cue netrin-1 controls resolution programs and promotes liver regeneration. *Hepatology.* (2016) 63:1689–705. doi: 10.1002/hep.28347

64. Mirakaj V, Dalli J, Granja T, Rosenberger P, Serhan CN. Vagus nerve controls resolution and pro-resolving mediators of inflammation. *J Exp Med.* (2014) 211:1037–48. doi: 10.1084/jem.20132103

65. Li Q, Wang P, Ye K, Cai H. Central role of SIAH inhibition in DCC-dependent cardioprotection provoked by netrin-1/NO. *Proc Natl Acad Sci U.S.A.* (2015) 112:899–904. doi: 10.1073/pnas.1420695112

66. Zhang J, Cai H. Netrin-1 prevents ischemia/reperfusion-induced myocardial infarction *via* a DCC/ERK1/2/eNOS s1177/NO/DCC feed-forward mechanism. *J Mol Cell Cardiol.* (2010) 48:1060–70. doi: 10.1016/j.yjmcc.2009.11.020

67. Aherne CM, Collins CB, Masterson JC, Tizzano M, Boyle TA, Westrich JA, et al. Neuronal guidance molecule netrin-1 attenuates inflammatory cell trafficking during acute experimental colitis. *Gut.* (2012) 61:695–705. doi: 10.1136/gutjnl-2011-300012

68. Ohta A, Sitkovsky M. Role of G-protein-coupled adenosine receptors in downregulation of inflammation and protection from tissue damage. *Nature.* (2001) 414:916–20. doi: 10.1038/414916a

69. Koeppen M, Eckle T, Eltzschig HK. Selective deletion of the A1 adenosine receptor abolishes heart-rate slowing effects of intravascular adenosine *in vivo*. *PLoS One.* (2009) 4:e6784. doi: 10.1371/journal.pone.0006784

70. Li X, Berg NK, Mills T, Zhang K, Eltzschig HK, Yuan X. Adenosine at the interphase of hypoxia and inflammation in lung injury. *Front Immunol.* (2020) 11:604944. doi: 10.3389/fimmu.2020.604944

71. Bowser JL, Phan LH, Eltzschig HK. The hypoxia-adenosine link during intestinal inflammation. *J Immunol.* (2018) 200:897–907. doi: 10.4049/jimmunol.1701414

72. Yuan X, Lee JW, Bowser JL, Neudecker V, Sridhar S, Eltzschig HK. Targeting hypoxia signaling for perioperative organ injury. *Anesth Analg.* (2018) 126:308–21. doi: 10.1213/ANE.0000000000002288

73. Vafadarnejad E, Rizzo G, Krampert L, Arampatzi P, Arias-Loza AP, Nazzal Y, et al. Dynamics of cardiac neutrophil diversity in murine myocardial infarction. *Circ Res.* (2020) 127:e232–49. doi: 10.1161/CIRCRESAHA.120.317200

frontiers | Frontiers in Cardiovascular Medicine

TYPE Original Research
PUBLISHED 06 October 2022
DOI 10.3389/fcvm.2022.1019917

OPEN ACCESS

EDITED BY
Turgay Celik,
VM Medical Park Ankara (Kecioren), Turkey

REVIEWED BY
MacRae Fort Linton,
Vanderbilt University Medical Center, United States
Federico Vancheri,
S. Elia Hospital, Italy

*CORRESPONDENCE
Luis Cardoso
cardoso@ccny.cuny.edu

†These authors have contributed equally to this work

SPECIALTY SECTION
This article was submitted to Coronary Artery Disease, a section of the journal Frontiers in Cardiovascular Medicine

RECEIVED 15 August 2022
ACCEPTED 20 September 2022
PUBLISHED 06 October 2022

CITATION
Corti A, De Paolis A, Grossman P, Dinh PA, Aikawa E, Weinbaum S and Cardoso L (2022) The effect of plaque morphology, material composition and microcalcifications on the risk of cap rupture: A structural analysis of vulnerable atherosclerotic plaques. *Front. Cardiovasc. Med.* 9:1019917. doi: 10.3389/fcvm.2022.1019917

The effect of plaque morphology, material composition and microcalcifications on the risk of cap rupture: A structural analysis of vulnerable atherosclerotic plaques

Andrea Corti[1], Annalisa De Paolis[1], Pnina Grossman[1], Phuc A. Dinh[1], Elena Aikawa[2†], Sheldon Weinbaum[1†] and Luis Cardoso[1*†]

[1]Department of Biomedical Engineering, City College, City University of New York, New York, NY, United States, [2]Department of Medicine, Brigham and Women's Hospital, Harvard Medical School, Boston, MA, United States

Background: The mechanical rupture of an atheroma cap may initiate a thrombus formation, followed by an acute coronary event and death. Several morphology and tissue composition factors have been identified to play a role on the mechanical stability of an atheroma, including cap thickness, lipid core stiffness, remodeling index, and blood pressure. More recently, the presence of microcalcifications (μCalcs) in the atheroma cap has been demonstrated, but their combined effect with other vulnerability factors has not been fully investigated.

Materials and methods: We performed numerical simulations on 3D idealized lesions and a microCT-derived human coronary atheroma, to quantitatively analyze the atheroma cap rupture. From the predicted cap stresses, we defined a biomechanics-based vulnerability index (VI) to classify the impact of each risk factor on plaque stability, and developed a predictive model based on their synergistic effect.

Results: Plaques with low remodeling index and soft lipid cores exhibit higher VI and can shift the location of maximal wall stresses. The VI exponentially rises as the cap becomes thinner, while the presence of a μCalc causes an additional 2.5-fold increase in vulnerability for a spherical inclusion. The human coronary atheroma model had a stable phenotype, but it was transformed into a vulnerable plaque after introducing a single spherical μCalc in its cap. Overall, cap thickness and μCalcs are the two most influential factors of mechanical rupture risk.

Conclusions: Our findings provide supporting evidence that high risk lesions are non-obstructive plaques with softer (lipid-rich) cores and a thin cap with μCalcs. However, stable plaques may still rupture in the presence of μ Calcs.

KEYWORDS

plaque rupture, microcalcifications, acute coronary events, cap thickness, remodeling index, numerical modeling, vulnerable plaque

Introduction

The vulnerable patient concept (1, 2) refers to individuals at increased risk of suffering an acute coronary event, i.e., patients with high atherosclerotic burden, presence of one or several vulnerable plaques, endothelial injury or dysfunction due to clinical risk factors (3). Plaque rupture, plaque erosion and calcified nodules (4–6) are the three most important vulnerable plaque phenotypes that are linked to coronary thrombosis and acute coronary events (3). The plaque rupture (7) is characterized by a thin fibrous cap measuring < 65 μm thickness over a lipid-rich or necrotic core; where the cap is infiltrated by macrophages and other inflammatory cells, apoptotic cells, lipids, neovessels and intraplaque hemorrhage (8–12). In some cases, the ruptured atheroma may heal and contribute to the increase of atheroma volume, stenosis, and subsequent rupture(s) that may be responsible for acute coronary events. In turn, plaque erosion is characterized by denudation of the coronary artery endothelium (5, 13) and the plaque calcified nodules consist of mineralized tissue present at the neointima layer of the vessel, that comes in contact with the arterial blood flow (5). Patients that develop acute coronary events also exhibit vulnerable blood and vulnerable myocardium. Vulnerable blood has an increased thrombotic potential, which could lead to thrombosis in fibrotic and severely stenotic plaques (3). Vulnerable myocardium refers to functional coronary alterations and hemodynamic changes (2) such as stasis, non-laminar blood flow, endothelial injury or dysfunction (3). It is now accepted that the pathophysiology of an acute coronary event involve patients with vulnerable blood, myocardium and plaque rupture/erosion, and that their respective contributions in isolation are inadequate to predict coronary events. Nonetheless, the underlying biomechanics of atheroma cap rupture, a major component of acute coronary events, has not been fully elucidated.

The biomechanics of plaque rupture depends on several tissue composition and morphological factors, including the fibrous cap (FC) thickness (14, 15), the lipid core material properties and thickness (16), vessel wall tissue properties (17), and the morphology of the lesion (16, 18). The combination of these intrinsic factors, together with the blood pressure (e.g., hypertension), determines the mechanical background stress levels on the cap. When the developed stresses exceed the ultimate tensile strength (UTS) in the circumferential direction of the cap tissue, the cap ruptures and initiates a thrombogenic response that may restrict the blood flow to downstream tissues. Importantly, the role of calcified tissue in vulnerable plaque rupture is not fully understood. On one hand, large calcifications potentially lead to mechanical stabilization of the atheroma. On the other hand, calcified nodules have been shown to initiate a thrombogenic response following a coronary event. While calcium scoring is an indicator of atherosclerotic burden (19–23), in this longstanding cap rupture paradigm, the culprit plaque of an acute coronary event is believed to have a low amount of calcification, when compared with non-ruptured advanced lesions, which show much larger calcium scores (19–23). This paradigm has been challenged since Vengrenyuk et al. first showed in 2006 that there were small cellular size microcalcifications (μCalcs) in thin fibrous caps, and that these inclusions could at least double the local tissue stresses (15–17, 19–21, 24–30). Indeed, it has been shown using high-resolution micro-CT (HR-μCT) that μCalcs in fibrous caps are not rare but numerous (27, 30, 31), and that the overall effect of μCalcs in plaque vulnerability can be summarized as an intensifier of the background circumferential stress in the cap, resulting in increased vulnerability (25, 29). μCalcs are formed by aggregation of calcifying extracellular vesicles (32) and have been reported at the site of rupture (27). The key concept in the role of μCalcs as a risk factor for vulnerability is that they have to reside in the fibrous cap tissue, where they amplify the background stress and increase the likelihood of rupture. Otherwise, if μCalcs are located in the lipid/necrotic core, they won't affect the biomechanics of the plaque, as they would behave as floating debris.

The purpose of this study was to provide a quantitative analysis of atheroma cap rupture risk using three-dimensional (3D) idealized atherosclerotic coronary plaques under the combined effect of μCalcs with several other known risk factors (i.e., cap thickness, lipid core stiffness, remodeling index, blood pressure). To investigate the individual and synergistic effect of these risk factors to the biomechanics of plaque rupture, a vulnerability index was defined and a non-linear model was proposed to predict the vulnerability index based on the combined effect of each risk factor. Finally, a stable,

non-ruptured human atherosclerotic coronary artery was used to create a model derived from high-resolution microCT images, and tested under normal and hypertensive blood pressure, as well as with and without 1 μCalc in its cap, to determine the effect of blood pressure and presence of 1 μCalc on the vulnerability of such atheroma.

Materials and methods

To examine the influence of different biomechanical risk factors on cap stability, we performed numerical simulations on 3D idealized geometries of atherosclerotic arteries with various morphological features, including lipid core material properties and μCalcs in their cap under normal and hypertensive blood pressures. First, we studied the effect of different remodeling indices and lipid core Young's moduli on the cap background stress and the location of highest stresses in the artery. This way, we were able to determine the combinations of plaque morphology traits and material properties that represent the upper and lower limit of cap rupture risk. The most unstable condition was then considered for studying the impact of cap thickness, μCalcs inclusion and blood pressure regime. Finally, the predictive property of our results was tested on the case of a human atherosclerotic coronary artery in the presence and absence of 1 μCalc and under varying blood pressure levels and lipid core stiffnesses.

Anatomical features of arterial models

Idealized atherosclerotic plaque models were conceived to present thickening of the intima layer (33) and an eccentric plaque with remodeling index (RI), degree of stenosis and lumen reduction in agreement with Glagov's morphological and mathematical description of lesion growth (16, 18) (see **Supplementary Appendix Section 1A**, Equations I, II, III). The values of each anatomical feature for all models are reported in **Table 1**. In this study, we covered RI values of 1.25 (asymptomatic plaque with minimal lumen occlusion), 1.4 (moderate stenosis) and 1.6 (symptomatic critical stenosis) (**Figure 1A**). The fibrous cap (FC) thickness values that we considered were of 50, 100, 150 and 200 μm (**Figure 1B**), and were obtained by increasing the core thickness toward the cap proper.

The human model (**Figure 1C**) represents a segment of the left anterior descending coronary artery dissected from a fresh heart obtained from The National Disease Research Interchange (recovered < 6 h post mortem) with myocardial infarction, and it was part of the data set studied in 30. The sample was scanned with 6.7 μm high-resolution microcomputed tomography (HR-μCT) as described in the **Supplementary Appendix Section 1A**. The plaque consists of an 8.45 mm-long lipid core with a minimum fibrous cap thickness of 125 μm. The sample presents a remodeling index of 1.29 with a degree of stenosis of 61% that causes a 31% luminal occlusion. This atheroma exhibits the typical morphological traits of a vulnerable plaque, except for the thickness of its cap. Compared to the idealized models with RI of 1.25 and 1.4, the human sample contains a thicker core of 1.1 mm. However, the relative core thickness with respect to the whole plaque is 66%, which is similar to the 72% and 65% in the idealized geometries with 100 μm- and 150 μm-thick caps and 1.25 remodeling index. The μCalc was designed to represent a single solid calcified particle of spherical profile with a diameter of 15 μm and was placed at the center of the FC.

Material properties

The arterial wall vessel layers were considered as anisotropic and homogeneous. Their material properties were defined by the Holzapfel-Gasser-Ogden (HGO) hyperelastic constitutive model (34, 35) which takes into consideration the collagenous fiber orientation in the tissue. To reproduce the tissue rupture mechanism, we coupled the hyperelastic failure description proposed by Volokh et al. (36) to the HGO model of the intimal layer. The damage model was fit to not alter the stress-strain response of the intima from that reported by Holzapfel et al. and to trigger tissue rupture at an average Principal Stress of 545 kPa (14). A detailed description of the model definition and layer-specific material properties are provided in the **Supplementary Appendix Section 1**. The lipid core was considered as an isotropic, almost incompressible, elastic material with Young's modulus (E_{core}) of 5, 25 and 50 kPa and Poisson's ratio (ν) of 0.49 (15). The μCalcs were modeled with properties similar to calcified bone tissue, with E_{calc} = 18 GPa and ν = 0.3 (32).

Boundary conditions and loadings

Two blood flow regimes were considered in this study (**Figure 2A**). The first one represents a normal pressure wave of 120/60 mmHg extracted from patient-based coronary measurement (24). The second case resembles a stage 2 hypertensive condition with a blood pressure of 160/90 mmHg and was obtained by amplifying the normal pressure wave. The two axial ends of the artery were free to move in the radial

TABLE 1 List of the remodeling indices considered in this study with their respective degrees of stenosis, luminal occlusion and lipid core length.

RI	Stenosis (lumen reduction)	Core length (mm)
1.25	50% (10%)	7.4
1.4	62% (23%)	7.8
1.6	80% (50%)	8.2

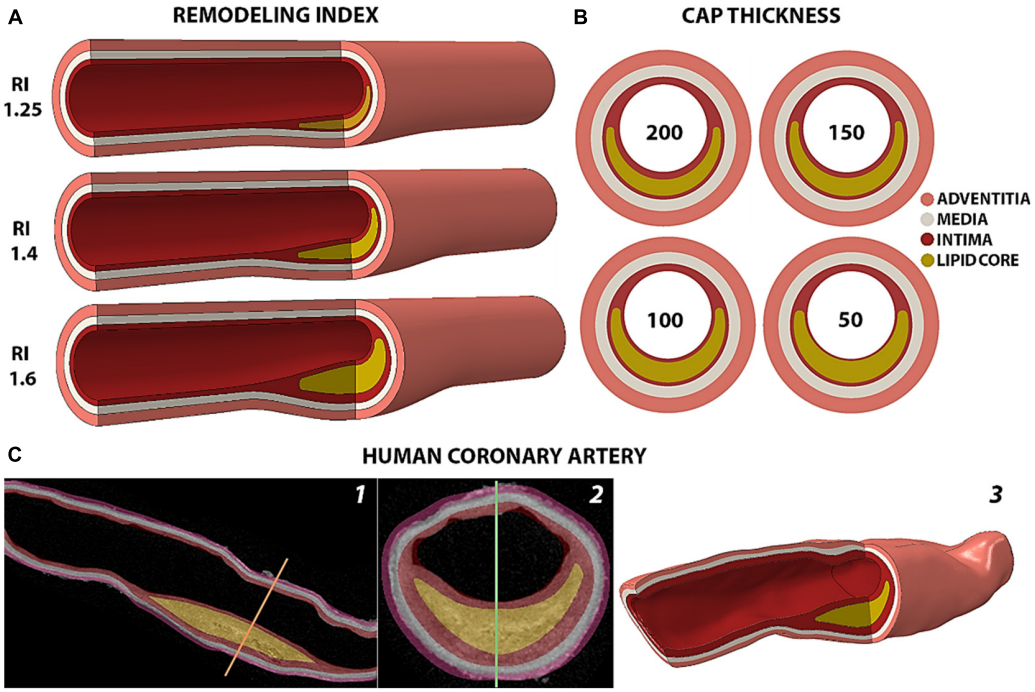

FIGURE 1
Representation of the arterial models analyzed. **(A)** Isometric view of the idealized geometries of human coronary arteries with different remodeling indices and a 200 μm-thick fibrous cap. **(B)** Cross section of fibroatheromas with different cap thicknesses of 200, 150, 100 and 50 μm for the case of RI = 1.25. **(C)** Rendering of the human coronary artery from 2D HR-μCT images in sagittal (1) and coronal (2) views to the 3D geometry reconstruction (3).

direction only, reflecting the constraint from the artery to tissue tethering. To maximize the accuracy of the cap stress calculation we implemented a sub-modeling approach (**Figures 2B,C**) described in detail in the **Supplementary Appendix Section 1C**. A total of 57 finite element simulations were performed in Abaqus (Abaqus/CAE, Dassault Systèmes, v.2019).

Results

The goal of this parametric analysis was to determine the relative effect of morphological and tissue composition risk factors on the atheroma cap rupture. In this section, we first present a qualitative overview of the location of maximal wall stresses as a function of plaque morphology and material properties. Then, we provide a quantitative description of peak cap stresses (PCS) and cap rupture by simulating tissue failure and deriving a biomechanical vulnerability index (VI) for each risk factor. This non-dimensional coefficient was defined as:

$$VI = \frac{PCS\ [MPa]}{Ultimate\ tensile\ stresss\ [MPa]} \quad (1)$$

where the PCS is the average cap stress obtained considering 30 mesh elements in the region of highest principal stresses in the cap, and the ultimate tensile stress is the threshold stress for rupture (545 kPa) reported in the literature (14, 15). The structure-function relationship between each risk factor and the vulnerability index was analyzed by obtaining the Spearman's correlation coefficient (ρ) followed by two-tailed t-test to quantify the strength of correlation (MatLab, Mathworks, v.R2022a). To describe the combined effect of all the risk factors on plaque vulnerability, we derived a multi-variable predictive model based on a stepwise non-linear regression analysis. The null hypothesis was rejected if p-value < 0.05.

Role of remodeling index, lipid core material properties and cap thickness on atheroma background stresses

In order to investigate the relative importance of the different predictor variables on the atheroma background stresses and vulnerability index, we studied 3 remodeling indices, 3 lipid core Young's moduli and 3 cap thicknesses. The effect of the remodeling index was analyzed while keeping a constant E_{core} of 5 kPa. On the other hand, varying E_{core} values were examined in the case of RI = 1.25. Every case was further combined with 3 different cap thicknesses of 200, 100 and 50 μm under normal blood pressure (120/60 mmHg). In addition, we included in the analysis the phenotype with RI = 1.6

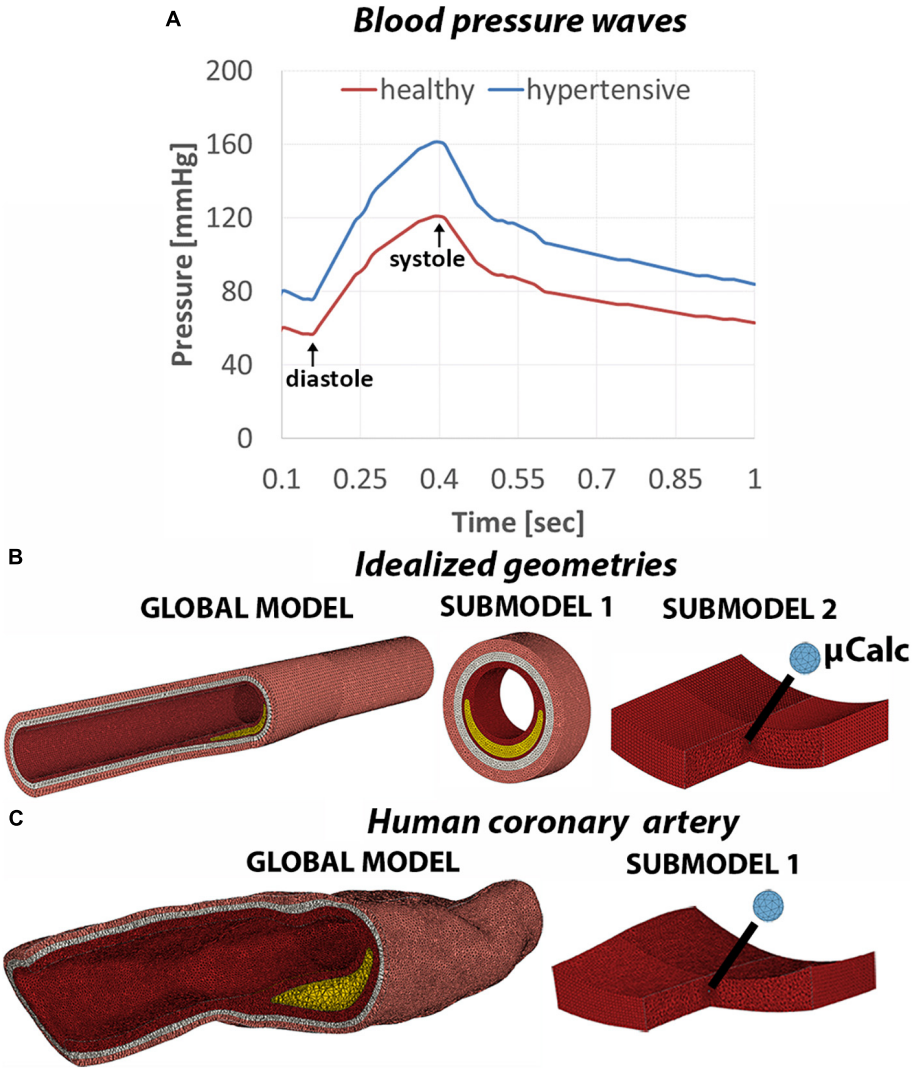

FIGURE 2
(A) Normal and hypertensive pressure waves applied to the lumen of the artery to replicate blood flow on 1-second time span. Mesh view of the global model and subsequent submodels of the idealized geometries **(B)** and human coronary sample **(C)**.

and E_{core} = 50 kPa, for all three cap thicknesses, as it represents the most stable condition, for a total of 18 cases investigated (Figure 3).

Our results show that greater remodeling indices and stiffer lipid cores correspond to lower cap stresses and thus more stable plaques. Conversely, atheroma with low remodeling index and soft lipid core result in higher cap stresses. Also, it was observed that both the remodeling index and lipid core properties can shift the location of highest stresses from the atheroma cap region to outside the atheroma, at the proximal and distal sides of the artery. Thus, the maximal principal stress does not occur at the atheroma when the remodeling index is high and the lipid core is stiff. This phenomenon is especially evident when the cap is 200 or 100 μm thick, in which case a higher degree of stenosis or core stiffness yields to atheroma cap stresses that are lower than the stresses in healthy regions of the blood vessel. Interestingly, if the background stress in the atheroma is low, such as the case when RI = 1.6 and E_{core} = 50 kPa, even a 50 μm-thick cap appears to experience PCS levels that are far below the threshold for rupture and the cap stresses are lower than those at proximal/distal luminal areas of the vessel. Thus, atheroma characterized by soft lipid core (i.e., E_{core} = 5 kPa) and low remodeling index values (i.e., RI = 1.25), which are typical of early stage plaques, induce the highest stresses in the cap proper, while more advanced plaques, exhibiting greater remodeling index (RI > 1.6), become mostly stable.

These observations are supported by the biomechanical vulnerability index obtained for each phenotype (Figure 4). Plaques with 50 μm-thick FC reach threshold for rupture except when E_{core} = 50 kPa or RI = 1.6, suggesting that the stability of

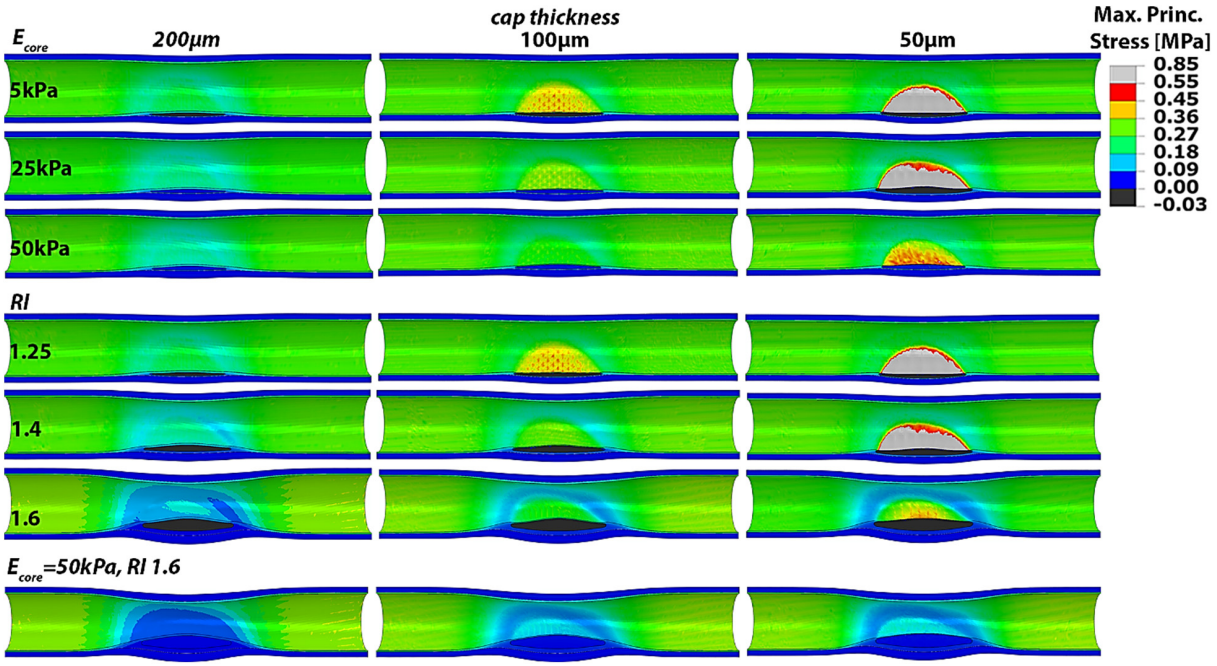

FIGURE 3
Longitudinal cut of idealized models with varying RI, Ecore and cap thickness showing the Max Principal Stress distributions. Higher remodeling indices and stiffer lipid cores clearly influence the PCS and the location of highest wall stress.

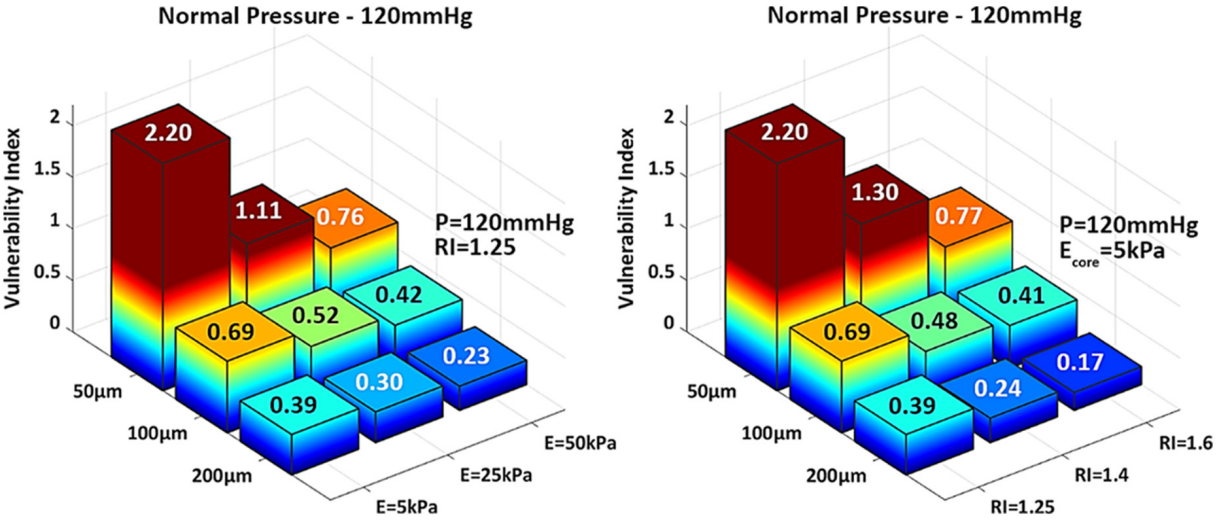

FIGURE 4
3D-barplots of the change of the vulnerability index based on cap thickness, lipid core Young's Modulus **(Left)** and remodeling index **(Right)**. The exact VI value is reported on top of every bar.

very thin caps can increase under certain plaque morphologies and lipid core stiffness. All other cases exhibit VI < 1, indicating that tissue failure would not occur in these circumstances. Figure 4 also shows the significant impact of cap thickness on plaque vulnerability, with an exponential increase in stresses as the cap becomes thinner. For the same RI and E_{core}, a 50 μm-cap experiences more than fivefold increase in PCS levels compared to a 200 μm-thick cap. Statistical analysis of Spearman's correlation coefficient among remodeling index, lipid core stiffness, cap thickness and vulnerability index indicates that the strongest relationship exist between the cap thickness and the vulnerability index, $\rho_{CT\text{-}VI} = -0.62$ with $p_{CT\text{-}VI} = 4.85E\text{-}04$.

A weaker effect of RI and Ecore on the vulnerability index was observed, $\rho_{RI\text{-}VI}$ = −0.38 and $\rho_{Ecore\text{-}VI}$ = −0.35, respectively, with p-values $p_{RI\text{-}VI}$ = 0.049 and $p_{Ecore\text{-}VI}$ = 0.0697. Thus, cap thickness is the most influential factor on the behavior of the vulnerability index among the analyzed parameters.

Role of cap thickness, blood pressure and μCalcs in caps on atheroma vulnerability index

The impact of cap thickness analyzed in the previous section was further investigated under the action of normal and hypertensive pressures and for the case of one spherical μCalc embedded in the cap tissue, using a tissue failure algorithm. The effect of these factors was studied in arteries with RI = 1.25 and E_{core} = 5 kPa, which were shown to lead to the highest atheroma background stress in the previous section.

The tissue failure mechanism and rupture propagation due to the presence of a spherical micro-calcification is exemplified in Figure 5. The μCalc amplifies the tissue background stresses by a factor of about 2.5 at its tensile poles. In the presence of a μCalc, the rupture mechanism is driven by stress concentrations at the tensile poles of the calcification (Figure 5) while the background stresses in the cap tissue (e.g., 216 kPa in Figure 5) is way below the ultimate tensile stress threshold for rupture (545 kPa). When the stresses at the μCalc poles exceed the ultimate tensile stress threshold for rupture, tissue rupture initiates as small voids around the μCalc, which then explosively grows through the thickness of the cap, ultimately exposing the underlying core to the flowing blood. Comparison of the stress-strain response of a 100 μm cap with and without one spherical μCalc, under the same systolic pressure is shown in the right hand side panel in Figure 5.

The results of this analysis confirm the substantial influence of cap thinning on PCS levels and vulnerability index. In the absence of a μCalc, the 50 μm thick cap is the only phenotype that ruptures under normal pressure levels, where the vulnerability index exceeds more than two times the threshold for failure (Figure 6 left). In the case of hypertension however, the 100 μm cap also undergoes rupture, with a vulnerability index that is 30% higher than under healthy systolic pressure (Figure 6 right). However, a significant increase in vulnerability index is observed in all cases after a μCalc was introduced in the atheroma cap. Each phenotype that was considered mechanically stable (i.e., thick caps under normal or hypertensive blood pressure), became vulnerable and reached rupture when a μCalc was introduced in the cap (Figure 6).

Statistical analysis of these results indicates that the cap thickness ($\rho_{CT\text{-}VI}$ = −0.62 with $p_{CT\text{-}VI}$ = 4.85E-04) and the presence of a μCalc in the cap ($\rho_{\mu Calc\text{-}VI}$ = 0.61 and $p_{\mu Calc\text{-}VI}$ = 6.17E-04) have equally strong impact on cap stability. Indeed, one μCalc in the fibrous cap causes a 2.5-fold increase in the vulnerability index, regardless of cap thickness or peak systolic pressure. The blood pressure also exhibits a significant influence on the vulnerability index, with $\rho_{BP\text{-}VI}$ = 0.43 and $p_{BP\text{-}VI}$ = 0.02. A model capable of predicting the vulnerability index as a function of all the risk factors considered in this study was designed using regression analysis (MatLab, Mathworks, v.R2022a). The non-linear model was obtained by first considering the intrinsic components that determine the cap background stress (i.e., cap thickness, remodeling index and core stiffness) and deriving a generalized stepwise quadratic model. Then, this model is multiplied by a factor that depends on the blood pressure and the μCalc binary variable:

$$VI = f(CT, RI, Ecore, BP, uCalc) = (b_1 + b_2 CT + b_3 RI + b_4 Ecore + b_5 CT * RI + b_6 CT * Ecore + b_7 CT^2) * (b_8 BP) * (1 + b_9 uCalc) \quad (2)$$

with coefficients: b_1 = 7.863, b_2 = −0.052, b_3 = −3.688, b_4 = −0.031, b_5 = 0.017, b_6 = 1.537e-4, b_7 = 7.830e-5, b_8 = 9.972e-3, b_9 = 1.5. The model shows a strong Spearman correlation coefficient ρ = 0.967 (p = 5.359e-8) with the VIs measured from the FEM simulations. This analysis was

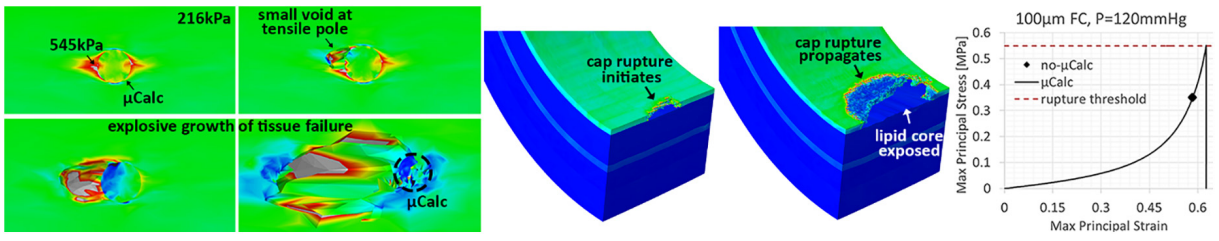

FIGURE 5
Illustration of the tissue failure mechanism and rupture propagation due to the presence of a spherical micro-calcification. **(Left)** The μCalc amplifies the tissue background stresses by a factor of about 2.5 at its tensile poles. When these stresses exceed the threshold for rupture, small voids start forming in these regions. If the tissue continues to stretch, the voids grow explosively through the tissue. **(Center)** Cap rupture initiates as a small fissuring at the luminal side and then propagates as the tissue is more exerted, until exposing the underlying lipid core. **(Right)** Comparison of the stress-strain response of a 100 μm cap with and without one spherical μCalc, under the same systolic pressure.

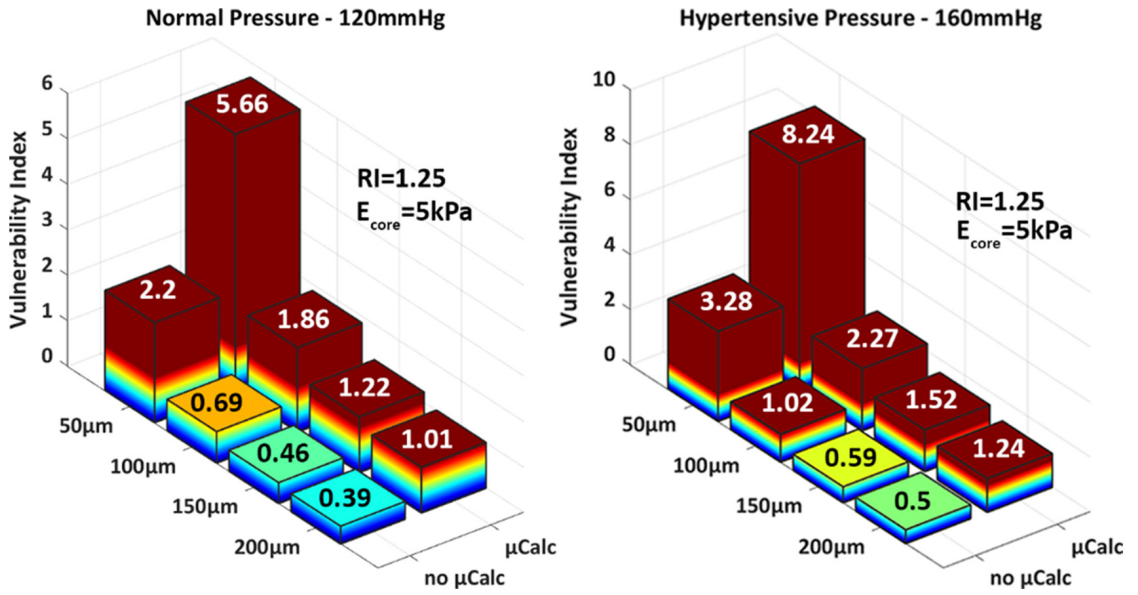

FIGURE 6
3D-barplots of the change of the vulnerability index based on cap thickness, the presence of a spherical µCalcs at the center of the cap and blood pressure.

preferred to a linear Pearson analysis as the model's residuals are not normality distributed, based on a Kolmogorov–Smirnov test.

Human coronary artery

A microCT-derived patient-specific model of a human coronary artery was analyzed under normal and hypertensive blood pressures, with and without one spherical µCalc embedded in its cap. Wall stress distributions show higher stresses in the cap but also in other luminal regions (Figure 7A). The latter case is likely the result of the original shape of the sample, which presented a non-circular lumen profile. Peak cap stresses at systolic pressures are close to values measured in the idealized case with 150 µm cap and RI = 1.25. Our results show that the fibrous cap does not rupture under normal nor hypertensive pressure in the absence of the µCalc. Conversely, the presence of the µCalc amplifies the local stresses in the cap, causing the plaque to reach failure under both regimes of pressure, with rupture of the cap tissue occurring around 80 mmHg and quickly propagating through the tissue, as shown in Figure 7B.

The predictive power of our statistical model was tested against the vulnerability indices computed in numerical simulations of the human coronary at 5 different blood pressures (80, 100, 120, 140, 160 mmHg) and 5 lipid core Young's Moduli (5, 15, 25, 35, 50 kPa) (Figure 7C). Our results indicate that the model is capable of accurately predicting the VI for 9 out of 10 conditions considered. The only phenotype where the vulnerability index was significantly under-predicted is the plaque with Ecore = 50 kPa. Nonetheless, the model showed a 100% accuracy at distinguishing vulnerable from stable atheromas (i.e., VI < 1 or VI > 1).

Discussion

In the present study, we investigated the contribution of several major biomechanical factors (i.e., cap thickness, lipid core stiffness, remodeling index, blood pressure, and the presence of a µCalc in the cap tissue) to plaque vulnerability using 3D finite element models. A vulnerability index was defined based on the ratio of maximal stresses and the ultimate tensile stress in the cap tissue. The two most significant factors were identified and a non-linear model combining these factors was obtained. The approach was also used to analyze a human atherosclerotic coronary artery model derived from high-resolution microCT images, under normal and hypertensive blood pressure, as well as with and without 1 µCalc in its cap.

Overall, the presence of a µCalc in the FC and a thin cap compromise the plaque mechanical stability to the greatest extent. We demonstrated that one spherical µCalc amplifies the background stress in the tissue by a factor of 2.5. These findings agree with previous observations from analytical and numerical analyses that reported twofold increase in interfacial stresses at the µCalc poles (25, 26). Although one spherical

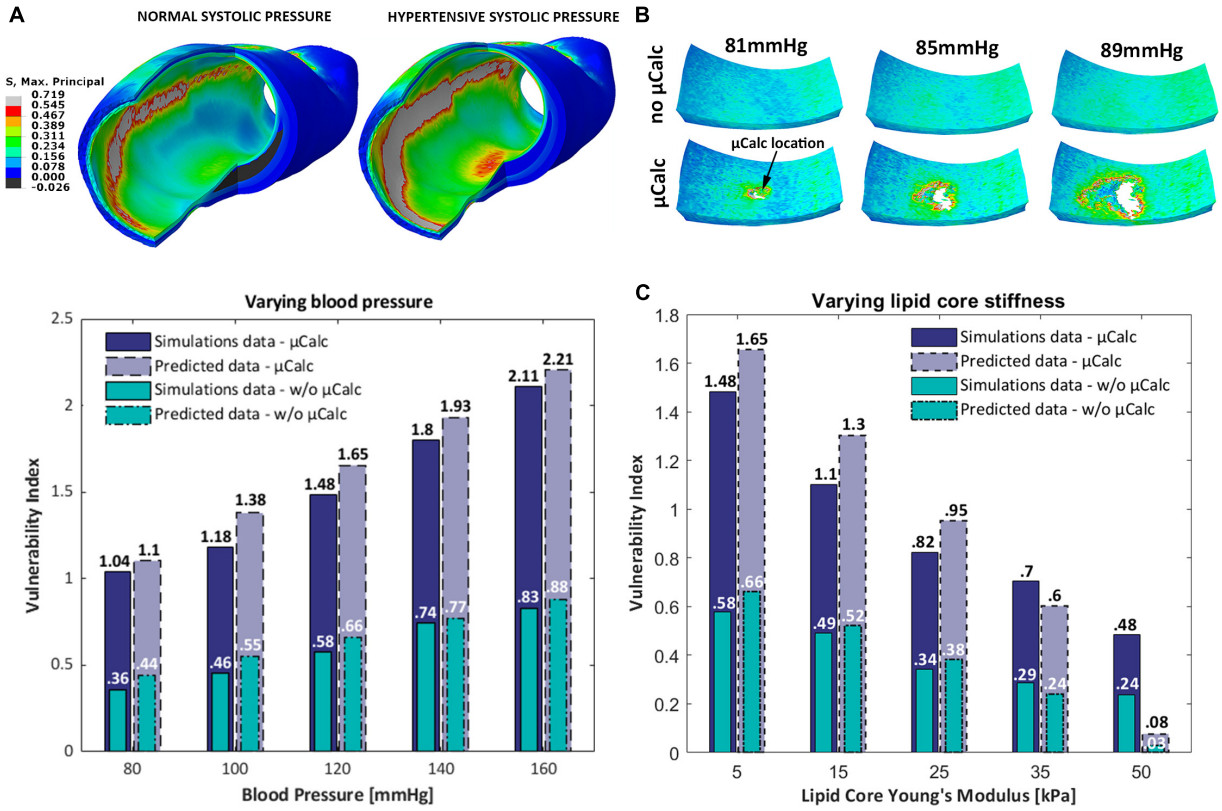

FIGURE 7
(A) Isometric view of the Maximal Principal Stress distributions on the human coronary under normal and hypertensive blood pressure; **(B)** sequence of the cap segment submodel with and without the μCalc. In the presence of the μCalc, the cap rupture extensively, starting at the location of the μCalc; **(C)** 3D-barplot of the change of the vulnerability index for different blood pressures, lipid core stiffness and the presence of one spherical μCalc from FEM analyses and predicted by the statistical model.

μCalc already exhibits a severe effect on plaque vulnerability, other studies have shown that μCalcs can cause up to a sevenfold increase in local tissue stresses, depending on their shape and proximity. Vengrenyuk et al. (37) found that μCalcs with a prolate ellipsoidal configuration could lead to more than a fourfold increase in stress at their poles, when aligned along the tensile axis. Additionally, Kelly-Arnold et al. (27) calculated the stress concentration factor between closely spaced μCalcs and reported a sevenfold increase in stresses when the ratio of the gap between 2 μCalcs and their diameter is lower than 0.4, if the particles are aligned with the tensile axis. In this study, we demonstrated that one spherical μCalcs is the strongest predictor of cap rupture among other major risk factors. However, μCalcs clusters or ellipsoidal particles could have even more drastic consequences (19, 25, 27, 29).

A fundamental difference between the present study and Kelly-Arnold et al. (27) is that in the former study nearly 35,000 μCalcs were examined in 22 caps of 66 atheroma that had not ruptured. With an average of more than 1,500 μCalcs in each cap how was it possible that so many μCalcs could exist in a cap and still not cause an acute coronary event. The answer to this is that the background stress in all these caps was far below the 545 kPa threshold. Indeed, 193 μCalc pairs were observed with a spacing that was less than 1 μCalc diameter and a few were as close 0.5 diameters where the local increase in stress could be fivefold or higher in the intervening space. Analysis of all these μCalc pairs showed that in no case was the 545 kPa threshold exceeded. While μCalcs greatly increase the risk of rupture, most fortunately, they must also reside at a location where the background tissue stress is high enough to promote plaque rupture.

The other most significant contributor to plaque vulnerability is the cap thickness. Our results show an exponential increase in peak cap stress as the cap becomes thinner, with 50 μm-thick caps that are significantly more vulnerable than thicker caps of 100–200 μm. These observations correlate well with previous data of 2D and 3D numerical studies (15, 38). Finet el al. (15) demonstrated that fibrous caps thinner than 62 μm induced a peak circumferential stress greater than 300 kPa, supporting previous histological observations that reported a critical thickness for rupture of 65 μm (39). Thin caps have been a widely accepted indicator of plaque instability

(40) as they exhibit higher local stresses and have been observed in pathological studies of ruptured plaques (5, 39). However, there is also evidence of non-ruptured plaques with thin caps (5) as well as caps thicker than 100 μm that ruptured under exertion (41).

Our results capture well the influence of the core material properties and plaque remodeling on the cap stress levels. We showed that softer cores and a low remodeling index correlate with higher peak cap stresses and plaque vulnerability, in agreement with published data on 2D atherosclerotic arterial models (15–17). Ohayon et al. (16) performed finite element analyses on 5,500 2D idealized atherosclerotic arteries and showed that plaques are more vulnerable at a low remodeling index, with minimal lumen narrowing. As described by Glagov et al. (18), the early stages of plaque development are characterized by a predominant positive (expansive) remodeling of the artery, with a nearly constant lumen area until a remodeling index of 1.23. Thus, young asymptomatic plaques emerge as the type of lesions at highest risk of rupture. This seems to be supported by *in vivo* observations in Maehara et al. (42), where the authors examined 300 ruptured coronary plaques detected by intravascular ultrasound. Here, ruptured plaques presented an average remodeling index of 1.15 ± 0.28, with positive remodeling accounting for 73% of the plaque area. In this study, we also showed that the combination of a high remodeling index with a stiff core can shift the location of maximal stresses from the cap proper to the proximal and distal sides of the artery, outside the atheroma, even when the cap is thinner than the rest of the intima layer. Similar wall stress distributions have been previously reported in numerical simulations on 3D arterial models with high remodeling indices or elevated lumen narrowing (38, 41).

Our findings on the effect of plaque morphology and cap thickness are consistent with the parametric analysis performed by Cilla et al. on 3D numerical models (38). Here the authors also studied the significance of varying core length ($1 \leq L \leq 8$ mm) and lipid core angle ($40 \leq \alpha \leq 88$) on the cap stresses. They showed that PCS are not significantly influenced by the core angle and the lipid core length, when the core is longer than 4 mm. Based on this knowledge, we believe our idealized 3D models are a comprehensive representation of the most impactful morphological features of the atheroma. Another distinctive driver of wall stresses is high blood pressure. Hypertension leads to increased stretch and vulnerability index even in thicker caps when μCalcs are present, as our results show for the case of a 200 μm cap. Additionally, phenotypes without μCalcs and a thick cap (100 μm) could still reach rupture, as shown in our analysis and observed in *in vivo* studies (41).

Finally, the results obtained from the human coronary artery simulations compares well with parametric analyses on idealized models. In particular, the human geometry compares closely to the idealized case of a 150 μm cap with RI = 1.25. These models experience similar PCS levels under normal and hypertensive blood pressure (PCS_{human} = 236–375 kPa, PCS_{ideal} = 252–322 kPa) and don't undergo rupture in the absence of μCalcs. Conversely, when the μCalc is introduced in the cap tissue, plaque rupture occurs under both pressure regimes. These findings confirm the fact that the human plaque sample was intact, as we didn't notice any calcified particle in the HR-μCT images. As opposed to the idealized case, the human model experiences the maximal wall stresses on non-stenotic regions at the location of high lumen curvature. This condition has been observed previously by Akyildiz et al. in 2D models of atherosclerotic coronary arteries (17).

Our extensive structural analysis was used to derive a multi-variable non-linear predictive model that takes into account the individual and combined effect of each risk factor. This model has proved capable of predicting the vulnerability risk of the human atheroma under varying conditions, with full precision in determining whether the cap would rupture or be stable.

This study also presents some limitations that should be acknowledged. First, our models don't include circumferential or axial residual stresses. Ohayon et al. (43) demonstrated that neglecting residual stresses leads to overestimated peak stresses. However, the location of maximal stresses does not seem to shift. Additionally, we did not introduce the effect of the lumen radius in our analysis, which shows a certain degree of influence on plaque vulnerability (38). Lastly, we simulated the presence of blood flow by applying a uniform radial pressure, neglecting the contribution of luminal shear stresses. However, since tensional wall stresses are 10^3–10^5 (3–5 orders of magnitude) greater than wall shear stresses, we believe our analysis properly reproduces the vascular stress distributions that reflect the plaque mechanical stability.

In conclusion, the present study provides an analysis of several major morphology and tissue composition factors that play an important role in the background stresses in the atheroma cap, and its combined effect with the presence of a μCalc in the cap tissue. We showed that μCalcs and cap thickness are the two most alarming biomechanical traits that govern the risk of mechanical rupture. Our findings provide supporting evidence that the combination of these risk factors have a synergistic effect on the vulnerability of the atheroma. Certainly, the vulnerability index of caps is greatly enhanced by the presence of even one μCalc, an effect that was not observed when the cap thickness and the μCalc were analyzed in isolation. A μCalc has the potential to transform relatively thick caps into vulnerable ones. The phenotype of biomechanically vulnerable lesions can be described as non-obstructive plaques with softer (lipid-rich) cores and a thin cap with μCalcs. Indeed, the appearance of a μCalc in the cap of an otherwise stable plaque is able to transform it into a vulnerable one.

Data availability statement

The original contributions presented in this study are included in the article/**Supplementary material**, further inquiries can be directed to the corresponding author.

Author contributions

AC: conceptualization, methodology, data curation, validation, and writing-original draft. AD: methodology, data curation, and validation. PG and PD: methodology and data curation. EA and SW: supervision, writing-review and editing, and funding acquisition. LC: conceptualization, methodology, supervision, writing-review and editing, and funding acquisition. All authors contributed to the article and approved the submitted version.

Funding

This work was supported by NIH grant 1R01HL136431 and 1R16GM145474, NSF grants CMMI-1662970, MRI-2018485, PSC-CUNY 64696-00 52, and CUNY 2021-IRG program.

Conflict of interest

The authors declare that the research was conducted in the absence of any commercial or financial relationships that could be construed as a potential conflict of interest.

Publisher's note

Supplementary material

The Supplementary Material for this article can be found online at: https://www.frontiersin.org/articles/10.3389/fcvm.2022.1019917/full#supplementary-material

References

1. Arbab-Zadeh A, Fuster V. From detecting the vulnerable plaque to managing the vulnerable patient: JACC state-of-the-art review. *J Am Coll Cardiol.* (2019) 74:1582–93. doi: 10.1016/j.jacc.2019.07.062

2. Tomaniak M, Katagiri Y, Modolo R, de Silva R, Khamis RY, Bourantas CV, et al. Vulnerable plaques and patients: State-of-the-art. *Eur Heart J.* (2020) 41:2997–3004. doi: 10.1093/eurheartj/ehaa227

3. Arbab-Zadeh A, Nakano M, Virmani R, Fuster V. Acute coronary events. *Circulation.* (2012) 125:1147–56. doi: 10.1161/CIRCULATIONAHA.111.047431

4. Virmani R, Burke AP, Farb A, Kolodgie FD. Pathology of the vulnerable plaque. *J Am Coll Cardiol.* (2006) 47(Suppl. 8):C13–8. doi: 10.1016/j.jacc.2005.10.065

5. Virmani R, Kolodgie FD, Burke AP, Farb A, Schwartz SM. Lessons from sudden coronary death. *Arterioscler Thromb Vasc Biol.* (2000) 20:1262–75. doi: 10.1161/01.ATV.20.5.1262

6. Kramer MCA, Rittersma SZH, de Winter RJ, Ladich ER, Fowler DR, Liang YH, et al. Relationship of thrombus healing to underlying plaque morphology in sudden coronary death. *J Am Coll Cardiol.* (2010) 55:122–32. doi: 10.1016/j.jacc.2009.09.007

7. Fuster V, Moreno PR, Fayad ZA, Corti R, Badimon JJ. Atherothrombosis and high-risk plaque: Part I: Evolving concepts. *J Am Coll Cardiol.* (2005) 46:937–54. doi: 10.1016/j.jacc.2005.03.074

8. Varnava AM, Mills PG, Davies MJ. Relationship between coronary artery remodeling and plaque vulnerability. *Circulation.* (2002) 105:939–43. doi: 10.1161/hc0802.104327

9. Lendon CL, Davies MJ, Born GVR, Richardson PD. Atherosclerotic plaque caps are locally weakened when macrophages density is increased. *Atherosclerosis.* (1991) 87:87–90. doi: 10.1016/0021-9150(91)90235-u

10. Underhill HR, Hatsukami TS, Fayad ZA, Fuster V, Yuan C. MRI of carotid atherosclerosis: Clinical implications and future directions. *Nat Rev Cardiol.* (2010) 7:165–73. doi: 10.1038/nrcardio.2009.246

11. Virmani R, Narula J, Leon MB, Willerson JT. *The vulnerable atherosclerotic plaque*. Hoboken, NJ: Wiley-Blackwell (2008). 384 p.

12. Virmani R, Kolodgie FD, Burke AP, Finn AV, Gold HK, Tulenko TN, et al. Atherosclerotic plaque progression and vulnerability to rupture: Angiogenesis as a source of intraplaque hemorrhage. *Arterioscler Thromb Vasc Biol.* (2005) 25:2054–61. doi: 10.1161/01.ATV.0000178991.71605.18

13. Partida RA, Libby P, Crea F, Jang IK. Plaque erosion: A new *in vivo* diagnosis and a potential major shift in the management of patients with acute coronary syndromes. *Eur Heart J.* (2018) 39:2070–6. doi: 10.1093/eurheartj/ehx786

14. Cheng GC, Loree HM, Kamm RD, Fishbein MC, Lee RT. Distribution of circumferential stress in ruptured and stable atherosclerotic lesions: A structural analysis with histopathological correlation. *Circulation.* (1993) 87:1179–87. doi: 10.1161/01.cir.87.4.1179

15. Finet G, Ohayon J, Rioufol G. Biomechanical interaction between cap thickness, lipid core composition and blood pressure in vulnerable coronary plaque: Impact on stability or instability. *Coron Artery Dis.* (2004) 15:13–20. doi: 10.1097/00019501-200402000-00003

16. Ohayon J, Finet G, Gharib AM, Herzka DA, Tracqui P, Heroux J, et al. Necrotic core thickness and positive arterial remodeling index: Emergent biomechanical factors for evaluating the risk of plaque rupture. *Am J Physiol Hear Circ Physiol.* (2008) 295:717–27. doi: 10.1152/ajpheart.00005.2008

17. Akyildiz AC, Speelman L, Nieuwstadt HA, van Brummelen H, Virmani R, van der Lugt A, et al. Effects of plaque morphology and material properties on peak cap stress in human coronary arteries. *Comput Methods Biomech Biomed Engin.* (2016) 19:771–9. doi: 10.1080/10255842.2015.1062091

18. Glagov S. Remodeling 1987 Compensatory enlargement of human atherosclerotic coronary arteries. *N Engl J Med.* (1971) 18:1182–6.

19. Cardoso L, Weinbaum S. Changing views of the biomechanics of vulnerable plaque rupture: A review. *Ann Biomed Eng.* (2014) 42:415–31. doi: 10.1007/s10439-013-0855-x

20. Fu BM, Wright NT. *Molecular, cellular, and tissue engineering of the vascular system*. (Vol. 1097). Cham: springer (2018). 335 p. doi: 10.1007/978-3-319-96445-4

21. Ohayon J, Finet G, Pettigrew R. *Biomechanics of coronary atherosclerotic plaque from model to patient*. Cambridge, MA: Academic Press (2020). p. 633–53.

22. Criqui MH, Denenberg JO, Ix JH, McClelland RL, Wassel CL, Rifkin DE, et al. Calcium density of coronary artery plaque and risk of incident cardiovascular events. *JAMA J Am Med Assoc.* (2014) 311:271–8. doi: 10.1001/jama.2013.282535

23. Criqui MH, Knox JB, Denenberg JO, Forbang NI, McClelland RL, Novotny TE, et al. Coronary artery calcium volume and density: Potential interactions and overall predictive value: The multi-ethnic study of atherosclerosis. *JACC Cardiovasc Imaging.* (2017) 10:845–54. doi: 10.1016/j.jcmg.2017.04.018

24. Rambhia SH, Liang X, Xenos M, Alemu Y, Maldonado N, Kelly A, et al. Microcalcifications increase coronary vulnerable plaque rupture potential: A patient-based micro-ct fluid-structure interaction study. *Ann Biomed Eng.* (2012) 40:1443–54. doi: 10.1007/s10439-012-0511-x

25. Cardoso L, Kelly-Arnold A, Maldonado N, Laudier D, Weinbaum S. Effect of tissue properties, shape and orientation of microcalcifications on vulnerable cap stability using different hyperelastic constitutive models. *J Biomech.* (2014) 47:870–7. doi: 10.1016/j.jbiomech.2014.01.010

26. Vengrenyuk Y, Carlier S, Xanthos S, Cardoso L, Ganatos P, Virmnani R, et al. A hypothesis for vulnerable plaque rupture due to stress-induced debonding around cellular microcalcifications in thin fibrous caps. *Proc Natl Acad Sci U.S.A.* (2006) 103:14678–83. doi: 10.1073/pnas.0606310103

27. Kelly-Arnold A, Maldonado N, Laudier D, Aikawa E, Cardoso L, Weinbaum S. Revised microcalcification hypothesis for fibrous cap rupture in human coronary arteries. *Proc Natl Acad Sci U.S.A.* (2013) 110:10741–6. doi: 10.1073/pnas.1308814110

28. Loree HM, Tobias BJ, Gibson LJ, Kamm RD, Small DM, Lee RT. Mechanical properties of model atherosclerotic lesion lipid pools. *Arterioscler Thromb.* (1994) 14:230–4. doi: 10.1161/01.ATV.14.2.230

29. Maldonado N, Kelly-Arnold A, Cardoso L, Weinbaum S. The explosive growth of small voids in vulnerable cap rupture; cavitation and interfacial debonding. *J Biomech.* (2013) 46:396–401. doi: 10.1016/j.jbiomech.2012.10.040

30. Maldonado N, Kelly-Arnold A, Vengrenyuk Y, Laudier D, Fallon JT, Virmani R, et al. A mechanistic analysis of the role of microcalcifications in atherosclerotic plaque stability: Potential implications for plaque rupture. *Am J Physiol Circ Physiol.* (2012) 303:H619–28. doi: 10.1152/ajpheart.00036.2012

31. Maldonado N, Kelly-Arnold A, Laudier D, Weinbaum S, Cardoso L. Imaging and analysis of microcalcifications and lipid/necrotic core calcification in fibrous cap atheroma. *Int J Cardiovasc Imaging.* (2015) 31:1079–87. doi: 10.1007/s10554-015-0650-x

32. Hutcheson JD, Goettsch C, Bertazzo S, Maldonado N, Ruiz JL, Goh W, et al. Genesis and growth of extracellular-vesicle-derived microcalcification in atherosclerotic plaques. *Nat Mater.* (2016) 15:335–43. doi: 10.1038/nmat4519

33. Holzapfel GA, Sommer G, Gasser CT, Regitnig P. Determination of layer-specific mechanical properties of human coronary arteries with nonatherosclerotic intimal thickening and related constitutive modeling. *Am J Physiol Circ Physiol.* (2005) 289:H2048–58. doi: 10.1152/ajpheart.00934.2004

34. Gasser TC, Ogden RW, Holzapfel GA. Hyperelastic modelling of arterial layers with distributed collagen fibre orientations. *J R Soc Interface.* (2006) 3:15–35. doi: 10.1098/rsif.2005.0073

35. Corti A, De Paolis A, Tarbell J, Cardoso L. Stenting-induced Vasa Vasorum compression and subsequent flow resistance: A finite element study. *Biomech Model Mechanobiol.* (2021) 20:121–33. doi: 10.1007/s10237-020-01372-x

36. Volokh KY. Modeling failure of soft anisotropic materials with application to arteries. *J Mech Behav Biomed Mater.* (2011) 4:1582–94. doi: 10.1016/j.jmbbm.2011.01.002

37. Vengrenyuk Y, Cardoso L, Weinbaum S. Micro-CT based analysis of a new paradigm for vulnerable plaque rupture: Cellular microcalcifications in fibrous caps. *MCB Mol Cell Biomech.* (2008) 5:37–47.

38. Cilla M, Peña E, Martínez MA. 3D computational parametric analysis of eccentric atheroma plaque: Influence of axial and circumferential residual stresses. *Biomech Model Mechanobiol.* (2012) 11:1001–13. doi: 10.1007/s10237-011-0369-0

39. Burke AP, Farb A, Malcom GT, Liang YH, Smialek J, Virmani R. Coronary risk factors and plaque morphology in men with coronary disease who died suddenly. *N Engl J Med.* (1997) 336:1276–82. doi: 10.1056/NEJM199705013361802

40. Virmani R, Burke AP, Kolodgie FD, Farb A. Pathology of the thin-cap fibroatheroma: A type of vulnerable plaque. *J Interv Cardiol.* (2003) 16:267–72. doi: 10.1034/j.1600-0854.2003.8042.x

41. Tanaka A, Imanishi T, Kitabata H, Kubo T, Takarada S, Tanimoto T, et al. Morphology of exertion-triggered plaque rupture in patients with acute coronary syndrome: An optical coherence tomography study. *Circulation.* (2008) 118:2368–73. doi: 10.1161/CIRCULATIONAHA.108.782540

42. Maehara A, Mintz GS, Bui AB, Walter OR, Castagna MT, Canos D, et al. Morphologic and angiographic features of coronary plaque rupture detected by intravascular ultrasound. *J Am Coll Cardiol.* (2002) 40:904–10. doi: 10.1016/S0735-1097(02)02047-8

43. Ohayon J, Dubreuil O, Tracqui P, Le Floc'h S, Rioufol G, Chalabreysse L, et al. Influence of residual stress/strain on the biomechanical stability of vulnerable coronary plaques: Potential impact for evaluating the risk of plaque rupture. *Am J Physiol Hear Circ Physiol.* (2007) 293:H1987–96. doi: 10.1152/ajpheart.00018.2007

frontiers | Frontiers in Cardiovascular Medicine

TYPE Review
PUBLISHED 08 November 2022
DOI 10.3389/fcvm.2022.970422

OPEN ACCESS

EDITED BY
Srdjan Aleksandric,
Clinical Center of Serbia, University of Belgrade, Serbia

REVIEWED BY
Giulio Russo,
Policlinico Tor Vergata, Italy
Eugenio Picano,
National Research Council (CNR), Italy

*CORRESPONDENCE
Domenico D'Amario
domenico.damario@gmail.com

†These authors have contributed equally to this work and share first authorship

SPECIALTY SECTION
This article was submitted to Coronary Artery Disease, a section of the journal Frontiers in Cardiovascular Medicine

RECEIVED 15 June 2022
ACCEPTED 21 October 2022
PUBLISHED 08 November 2022

CITATION
Ciliberti G, Laborante R, Di Francesco M, Restivo A, Rizzo G, Galli M, Canonico F, Zito A, Princi G, Vergallo R, Leone AM, Burzotta F, Trani C, Palmieri V, Zeppilli P, Crea F and D'Amario D (2022) Comprehensive functional and anatomic assessment of myocardial bridging: Unlocking the Gordian Knot. *Front. Cardiovasc. Med.* 9:970422. doi: 10.3389/fcvm.2022.970422

Comprehensive functional and anatomic assessment of myocardial bridging: Unlocking the Gordian Knot

Giuseppe Ciliberti[1†], Renzo Laborante[1†], Marco Di Francesco[1], Attilio Restivo[1], Gaetano Rizzo[1], Mattia Galli[1,2], Francesco Canonico[1], Andrea Zito[1], Giuseppe Princi[1], Rocco Vergallo[1,3], Antonio Maria Leone[1,3], Francesco Burzotta[1,3], Carlo Trani[1,3], Vincenzo Palmieri[1,4], Paolo Zeppilli[1,4], Filippo Crea[1,3] and Domenico D'Amario[1,3]*

[1]Department of Cardiovascular and Thoracic Sciences, Catholic University of the Sacred Heart, Rome, Italy, [2]Maria Cecilia Hospital, Gruppo Villa Maria (GVM) Care and Research, Cotignola, Italy, [3]Department of Cardiovascular and Thoracic Sciences, Fondazione Policlinico Universitario Agostino Gemelli Istituto di Ricovero e Cura a Carattere Scientifico (IRCCS), Rome, Italy, [4]Sports Medicine Unit, Fondazione Policlinico Universitario Agostino Gemelli Istituto di Ricovero e Cura a Carattere Scientifico (IRCCS), Rome, Italy

Myocardial bridging (MB) is the most frequent congenital coronary anomaly in which a segment of an epicardial coronary artery takes a tunneled course under a bridge of the myocardium. This segment is compressed during systole, resulting in the so-called "milking effect" at coronary angiography. As coronary blood flow occurs primarily during diastole, the clinical relevance of MB is heterogeneous, being usually considered an asymptomatic bystander. However, many studies have suggested its association with myocardial ischemia, anginal symptoms, and adverse cardiac events. The advent of contemporary non-invasive and invasive imaging modalities and the standardization of intracoronary functional assessment tools have remarkably improved our understanding of MB-related ischemia, suggesting the role of atherosclerotic lesions proximal to MB, vasomotor disorders and microvascular dysfunction as possible pathophysiological substrates. The aim of this review is to provide a contemporary overview of the pathophysiology and of the non-invasive and invasive assessment of MB, in the attempt to implement a case-by-case therapeutic approach according to the specific endotype of MB-related ischemia.

KEYWORDS

myocardial bridging, myocardial ischemia, invasive intracoronary assessment, intracoronary physiology, intracoronary imaging, non-invasive tests, tailored therapy

Introduction

Myocardial Bridging (MB) is the most common inborn coronary artery variant in which a segment of an epicardial coronary artery, most frequently (70–98%) the left anterior descending (LAD) coronary artery, takes an intramural course under a bridge of myocardium (1).

Coronary angiography (CA) has been typically considered the gold standard for the diagnosis of MB, detecting the "milking effect" induced by the systolic compression of the intramural artery in addition to its delayed diastolic relaxation (2–4). Nevertheless, CA may underestimate the presence of MB, whose incidence depends on the modality used to identify the tunneled segment. Indeed, MB has been documented from 5 to 8% of invasive angiographic series, but from 18 to 25% or 30 to 55% when using coronary computed tomography angiography (CCTA) or autopsy reports, respectively (5).

As coronary blood flow occurs primarily during diastole, the clinical relevance of MB is still a matter of debate, being typically considered as an innocent bystander (6). However, several studies documented that patients with MB experienced a high burden of anginal symptoms, angina-equivalents (i.e., dyspnea) and, less frequently, palpitations and/or ventricular arrhythmias (7). Although this anomaly is present at birth, the onset of symptoms usually does not occur before the third decade of age. Several factors, such as concomitant coronary artery disease (CAD), tachycardia, and the rise in left ventricular (LV) pressures, usually associated with aging, diastolic dysfunction and LV hypertrophy, may worsen the supply-demand mismatch imposed by MB and unmask or exacerbate the hemodynamic impact of MB (8, 9).

Interestingly, MB patients may also present with acute coronary syndrome (ACS), as a result of coronary artery spasm (CAS), coronary artery dissection, or coronary artery thrombosis (10).

Nowadays, a growing body of evidence suggests a direct association between MB and myocardial ischemia. Moreover, MB has been recently recognized as a cause of ischemia with non-obstructive coronary artery disease (INOCA) (11), and several mechanisms have been described as possible pathophysiological substrates of MB-related ischemia (8, 10, 12, 13; **Figure 1**).

Nevertheless, these multiple mechanisms cannot be unmasked by a single diagnostic modality (**Table 1**).

The aim of our review is to show the role of different diagnostic strategies (both non-invasive and invasive) in the anatomical and functional assessment of MB. A comprehensive approach might play a key role in implementing personalized medical or invasive therapeutic strategies, ultimately yielding a benefit on symptoms and reducing the occurrence of adverse cardiac events (13, 14).

Mechanisms of myocardial ischemia and clinical relevance in patients with myocardial bridging

The systolic phase of the myocardial cycle is only marginally involved in the myocardial perfusion (∼15%) (1). Nonetheless, an increasing body of evidence supports the involvement of different mechanisms of ischemia in patients with MB: delayed early diastolic artery relaxation, development of atherosclerotic stenosis proximal to MB, functional disorders of the coronary circulation (i.e., impaired endothelium-dependent vasodilatation and microvascular dysfunction) and the "branch steal" phenomenon.

The assumption that MB affects coronary blood flow during systole has been overcome since the diastolic lumen gain may be late and incomplete once the systolic compression of the tunneled artery ends (15–18). In 1993, Erbel et al. were the first to describe the delayed early diastolic artery relaxation within the tunneled segment through angiography and IVUS (19). Subsequently, other IVUS studies confirmed the same phenomenon, showing the concordance between delayed diastolic relaxation, increased intracoronary Doppler flow velocity, and ischemic symptoms and signs (20). Furthermore, stress-echocardiography (SE) studies also suggested that slow and incomplete MB decompression may underlie stress-induced ischemia in MB patients (18).

Myocardial bridging-related ischemia is not to be exclusively sought in the systo-diastolic hemodynamic modifications imposed by MB, but also in the anatomical and/or functional anomalies of the coronary circulation that may coexist or be favored by the MB itself. In this regard, an association between MB and CAD has long been described (8, 13). A local systolic retrograde flow phenomenon proximal to MB has been detected, predisposing to the development of atherosclerosis (21). Furthermore, the compression-relaxation of the intramural segment induces changes in wall shear stress (WSS), producing an area of low WSS proximal to MB (21). Low WSS induces the release of inflammatory mediators and endothelial vasoactive agents, whose levels were found to be significantly higher in the proximal segment compared with the intramural segment (2, 22). Using a parametric finite element model, Nikoliæ et al. found a correlation between the position of plaque near MB with WSS and oscillatory shear index. This finding reinforces the notion that plaque progression may be favored by hemodynamic disturbances provoked by MB (23).

On the contrary, the intramural tract is typically spared from atherosclerosis, probably because of the "separation" of the tunneled segment from epicardial adipose tissue and its pro-inflammatory signals (i.e., cytokines and adipokines) (24–26) as shown in preclinical models by the lack of foam cells and modified smooth muscle cells in the intramural artery (27).

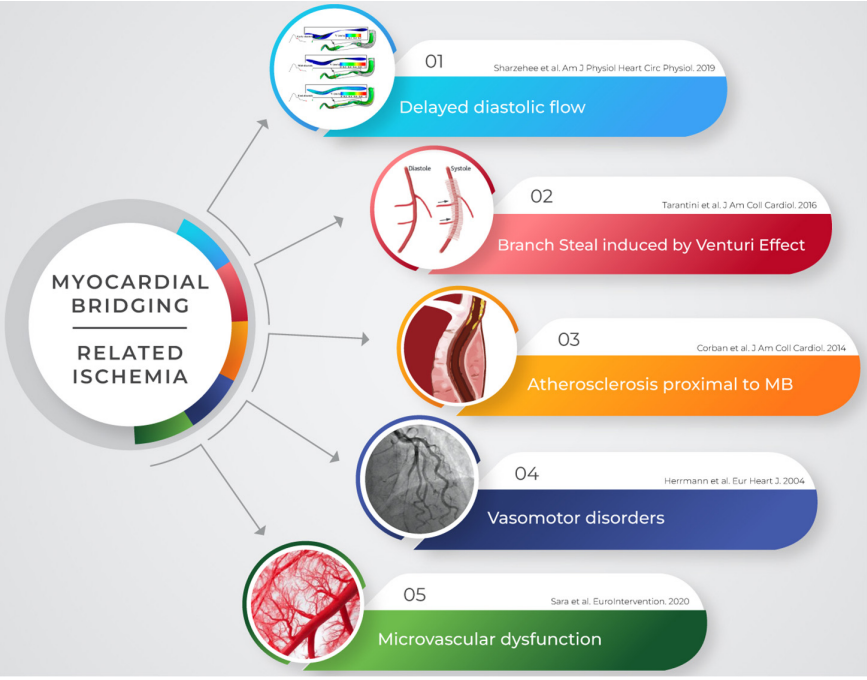

FIGURE 1
Myocardial ischemia is not purely related to vessel systolic compression in patients with MB. Several mechanisms may account for the occurrence of symptoms and may be detected though invasive and non-invasive modalities. MB, myocardial bridging.

The presence of atherosclerotic plaques proximal to MB is a potential cause of chronic coronary syndrome (CCS) (10, 15–17), as well as ACS due to plaque erosion/rupture or vasospasm and coronary dissection (10, 28–31).

Myocardial bridging has also been associated with impaired endothelium-dependent vasodilatation (32–36). Endothelial dysfunction, together with the hyper-reactivity of vascular smooth muscle cells, represent the two pathophysiological mechanisms implicated in the occurrence of CAS (37). Previous studies, using a provocative test with incremental acetylcholine (ACH) dose infusion, demonstrated that CAS is more common in patients with MB (32–36). Furthermore, anatomical properties of MB, such as length and percentage of systolic compression, were demonstrated to predict the occurrence of provoked LAD spasm (32, 34).

It has been proposed that the turbulent flow and changes in WSS, due to MB, may promote direct injury to the endothelium and endothelial cell apoptosis (33, 35). Moreover, the expression of endothelial nitric oxide synthase (eNOS), a marker of preserved endothelial function, is significantly lower in the MB segment than in proximal and distal segments (36). These mechanisms ultimately converge to a paradoxical response to ACH and an increased risk of CAS (36). The occurrence of CAS in MB patients may have significant clinical relevance: Nam et al. reported that patients with MB and CAS experienced a higher rate of recurrent angina and a more frequent prescription of anti-anginal medication (32). Furthermore, according to the correlation between MB and myocardial infarction risk (38), CAS may also represent a mechanism underlying the development of ACS (39).

Endothelial dysfunction is, however, not confined to the epicardial coronary artery but may extend to the coronary microcirculation (11). Indeed, it is not unlikely that impaired endothelium-dependent vasodilatation affects also distal arterioles, resulting in microvascular spasm as well as spasm of the epicardial tract strictly close to MB (40).

Nowadays, little data is available on the link between MB and coronary microvascular dysfunction (CMD). CMD is prevalent across several cardiovascular conditions, emerging as an increasing cause of INOCA (41, 42). Two different endotypes of microvascular dysfunction currently exists: structural microvascular remodeling and functional arteriolar dysregulation (11). The former is caused by an increase in wall to lumen ratio and a loss of myocardial capillary density, and it is characterized by an impaired endothelium-independent vasodilatation, represented by a reduced coronary flow reserve (CFR) and an increased index of microcirculatory resistance (IMR) (11). The latter is caused by endothelial dysfunction of medium and large size arterioles, with a pathological response to ACH test (impaired endothelium-dependent vasodilatation) (11).

Only two studies investigated the presence of CMD in patients with MB (40, 43). Among patients with chest pain and non-obstructive CAD, Sara et al. showed that those with

angiographic evidence of MB had a higher frequency of microvascular endothelial dysfunction compared to patients without MB (57.7 vs. 51.0%, $p = 0.075$). However, this reached statistical significance among patients aged ≤ 50 years (57.3 vs. 44.2%, $p = 0.010$) (40). The second study showed a high rate of CMD (22.1%) among patients with persistent angina, non-obstructive CAD and angiographic evidence of MB (43). On the basis of these results, CMD may represent an additional mechanism of ischemia in patients with MB. Therefore, a comprehensive invasive assessment of MB patients that includes the evaluation of coronary microcirculation (i.e., IMR and CFR) might provide additional information. However, further data are needed to suspect a more marked involvement of microvascular dysfunction in these patients.

Lastly, the "branch steal effect" is an additional ischemic mechanism in MB patients: the crossing of blood through the constrict segment in the end systole/early diastole leads to an increase in diastolic flow velocity ("Venturi effect") that results in a depressurization at the ostium of side branches within the MB (44, 45). This phenomenon is more evident in the case of septal perforator arteries of the LAD coronary artery (7). Interestingly, Lin et al. proposed this mechanism to explain the echocardiographic finding of "septal wall motion abnormality" during dobutamine stress test as sign of focal ischemia. Conversely, the recovery of perfusion pressure distal to the LAD was not associated with ischemic signs (i.e., echocardiographic finding of "apical sparing") (44).

In summary, several mechanisms suggest the ischemic relevance of MB: exertion-induced angina may occur for a delay in early diastolic artery relaxation, "branch steal," hemodynamically significant proximal CAD and CMD. On the other hand, epicardial spasm, coronary artery dissection, and coronary artery thrombosis may underlie the development of ACS.

Non-invasive anatomical and functional assessment

Although CA may detect the presence of MB, there are specific patient-dependent and procedure-related complications that are inherent to the invasive procedure (46). Some non-invasive imaging modalities may be useful to detect MB and to investigate myocardial ischemia in MB patients, since this cohort of patients is typically younger, has a lower rate of cardiovascular risk factors and, therefore, a low pre-test probability of CAD (47).

Among non-invasive imaging tests, CCTA plays a prominent role. Its strength is represented by a high spatial resolution, accounting for a higher detection of MB compared with CA (48). CCTA enables an accurate evaluation of the vessel wall and lumen, as well as the surrounding myocardium, allowing to classify MB of the LAD coronary artery in terms of depth and length, suitable only for MB located in the LAD coronary artery (49). In this regard, MB is classifiable into superficial (<2 mm), deep (≥2 mm), and very deep (≥5 mm) according to the depth; and into short (<25 mm) or long (≥25 mm) according to the length of the tunneled segment (49, 50). Kim et al. proposed an alternative classification of LAD MB into three types: the type I, characterized by a partial muscular encasement; the type II, characterized by a full encasement of the vessel by myocardium but without measurable overlying myocardium; the type III, characterized by a measurable overlying myocardium > 0.7 mm (48).

These anatomical evaluations have relevant clinical, prognostic and therapeutical implications: indeed, the deeper variant is more commonly associated with symptoms and adverse cardiac events; moreover, CCTA may be helpful to guide the choice of surgical treatment (myotomy vs. CABG) (13, 51).

The pivotal limitation of CCTA is the low temporal resolution, making difficult to assess the hemodynamic significance of MB. Moreover, the use of a "cocktail" of drugs before scanning, such as beta-blockers and nitroglycerin that prolong diastolic time and induce vasodilation, respectively, results in an underestimation of the impairment in blood flow imposed by MB (13).

Among non-invasive tests, echocardiogram plays a role in the functional assessment of MB patients. Lin et al. described an echocardiographic finding characterized by a focal abnormality in the end-systolic to early-diastolic septal wall motion with apical sparing (44). Eighteen patients with angina and this sign were prospectively enrolled for invasive assessment (CA, IVUS, and intracoronary pressure measurements): all these patients were found to have MB of the LAD coronary artery and an abnormal diastolic-fractional flow reserve (dFFR ≤ 0.75) (44). In addition, patients with hemodynamically significant LAD MB present lower septal longitudinal strain compared to controls during stress echocardiographic strain imaging (52). "Septal buckling with apical sparing" has a diagnostic accuracy similar to SE in identifying significant CAD through a new wall motion abnormality (52). However, even though SE is a well-established diagnostic tool in detecting myocardial ischemia, its key limitation is related to the impossibility to understand if the wall motion abnormalities are attributable to MB, CAD or other pathological conditions, if an anatomical assessment is not performed.

The evaluation of coronary flow velocity reserve (CFVR) measured by transthoracic Doppler echocardiography (TTDE) has been found to represent another modality to hemodynamically assess LAD MB. In this regard, Aleksandric et al. showed that non-invasive CFVR-TTDE during dobutamine infusion was a predictor of functional significant MB, found to be more accurate than CFVR during adenosine infusion (18, 53). A cut-off value of ≤2.1 was found to have the best accuracy for identifying MB associated with

TABLE 1 Invasive and non-invasive diagnostic modalities for the detection, anatomic and functional assessment of MB.

Imaging modality	Diagnostic sign	Prevalence of MB (%)	Limitations	Strong points
CA	Milking effect	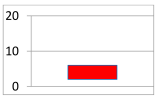	- Invasive - No functional assessment - Contrast agent - Radiation	- Anatomic assessment - Relatively fast and simple procedure
FFR	Pressure drop (<0.75 or 0.8)	N/A	- Invasive - Contrast agent - Radiation Longer procedural time - Pharmacotherapy side effects (adenosine)	- Functional gold standard for CAD - Hemodynamic assessment of MB
Intracoronary Doppler	Fingertip phenomenon	N/A	- Invasive - Value in guiding treatment no standardized - Contrast agent - Radiation - Longer procedural time - Pharmacotherapy side effects (adenosine, dobutamine)	- Lesion-specific sign - Functional assessment of coronary lesions - Assessment of microvascular disease or endothelial dysfunction
iFR	Pressure drop (≤0.85)	N/A	- Invasive - Contrast agent Radiation - Longer procedural time	- Diastolic specific-index - Functional assessment of CAD - Hemodynamic assessment of MB
IVUS	Half-moon sign	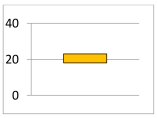	- Invasive - No functional assessment - Contrast agent - Radiation - Longer procedural time - Operator-dependent variability in pullback velocity may influence detection and morphological assessment of MB	- Lesion specific sign - Morphological assessment of proximal plaque - Quantification of persistence of arterial compression during diastole Guide to PCI
OCT	Heterogeneous fusiform band with intermediate-intensity signal surrounding the vessel adventitia	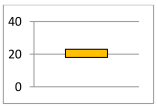	- Invasive - No functional assessment - Contrast agent - Radiation - Longer procedural time - Operator-dependent variability in pullback velocity influencing detection and morphological assessment of MB	- Lesion specific sign - Morphological assessment of proximal plaque - Guide to PCI
CCTA	Intramural coronary artery	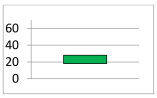	- Radiation - Contrast agent - Pharmacotherapy side effects (nitrates, BBs) - No functional assessment	- High-sensitivity - Non-invasive - High spatial resolution - Well-standardized - Concomitant detection of CAD
FFR-CCTA	Intramural coronary artery	N/A	- Radiation - Contrast agent - Pharmacotherapy side effects (nitrates, beta-blockers) - Longer procedural time - Value in guiding treatment no standardized	- Functional assessment - High-sensitivity - Non-invasive - High spatial resolution - Concomitant detection of CAD
Echocardiogram	Septal buckling with apical sparing or lower septal longitudinal strain with exercise	N/A	- Inability to distinguish between CAD and MB - No anatomic assessment - Operator-dependent variability - Value in guiding diagnosis and treatment not standardized	- Non-invasive - No radiation - No contrast exposure - Wall motion assessment - Fast and rapidly available
CMRI	Intramural coronary artery	N/A	- Contrast agent - Value in guiding diagnosis and treatment not standardized	- Non-invasive - No radiation - Anatomic assessment - Functional assessment - Wall motion assessment

BBs, beta-blockers; CA, coronary angiography; CAD, coronary artery disease; CCTA, coronary computed tomography; CMRI, cardiac magnetic resonance imaging; FFR, fractional flow reserve; iFR, instantaneous wave-free ratio; IVUS, intravascular ultrasound; MB, myocardial bridging; OCT, optical coherence tomography; N/A, not applicable; PCI, percutaneous coronary intervention.

stress-induced myocardial ischemia with a sensitivity (Sn), specificity (Sp), positive (PPV), and negative predictive value (NPV) of 96, 95, 88, and 98%, respectively (area under curve AUC 0.986) (53). Inotropic stimulation with dobutamine, compared to vasodilatation with adenosine, provides better significance of MB in relation to stress-induced myocardial ischemia in the invasive setting too (4). Interestingly, the cut-off value of ≤2.1 is similar to the cut-off value for TTDE-CFVR during adenosine as well as during dobutamine provocation in the functional assessment of fixed coronary stenosis (Sn 92 vs. 92%; Sp 90 vs. 86%; PPV 85 vs. 73%; NPV 95 vs. 96%) (54, 55).

Among non-invasive diagnostic modalities, cardiovascular magnetic resonance imaging (CMRI), single-photon emission computed tomography (SPECT), and positron emission tomography (PET) provide the quantification of myocardial blood flow at rest and during induced-hyperemia, representing possible tools in the assessment of inducible-ischemia and CMD in MB patients (41).

However, little data supported the role of these modalities in detecting ischemia in patients with MB and anginal symptoms, and there are no standardized diagnostic criteria for functional evaluation of MB with non-invasive stress testing or myocardial perfusion imaging because previous studies were based on small number of patients (56). Further studies are needed to better validate these tools.

Invasive anatomical and functional assessment

Intracoronary imaging

If we consider the gap in incidence rate between CA and other imaging modalities, routine CA is not completely sensitive for the detection of MB (5). The use of intracoronary vasodilators (i.e., nitrates) can increase, through a reflex rise of the adrenergic drive, the systolic narrowing of the tunneled artery and the angiographic sensitivity in diagnosing MB (57). Nevertheless, in patients with thin MB, the "milking effect" may be missed and invasive intracoronary imaging techniques may be required to limit the underdiagnose of MB.

Intravascular ultrasound (IVUS) has been used throughout a multitude of studies for the morphological assessment of MB. It allows for accurate measurement of the lumen diameter and evaluation of vessel wall morphology (58). IVUS is able to detect the systolic compression of the bridged segment, but the peculiar finding is an echolucent area between the tunneled artery and the epicardial tissue, persisting throughout the cardiac cycle. This phenomenon is called "half-moon" sign and represents a muscle band overlying the tunneled segment (1). This sign is highly specific because it is detectable only in the segment with systolic compression (59). Moreover, IVUS confirms that vessel compression within MB is not exclusively a systolic event but it extends to early diastole (59). Additionally, IVUS is a useful tool for the quantitative and qualitative assessment of atherosclerosis proximal to MB. In this regard, Yamada et al. found that the percentage of arterial compression was directly related to the atherosclerotic burden located proximally to MB (60).

Similarly, optical coherence tomography (OCT) may represent an adjuvant tool in the diagnosis of MB, detecting angiographically undetectable MB (61). OCT is a light-based technique that provides *in vivo* high-resolution (~10 μm) imaging of coronary artery (62). Although its resolution is higher than IVUS, the role of OCT in detecting MB has not been completely elucidated. Some studies proposed the main OCT features of MB, describing a heterogeneous fusiform band with sharp borders and low/intermediate-intensity signal, similar to tunica media, surrounding the vessel adventitia. Obviously, the fusiform band detected by OCT, corresponds to the "half-moon" sign using IVUS (63–67). OCT provides the detection and anatomic characterization of atherosclerotic lesions proximal to MB too (64). Furthermore, in cases of ACS and concomitant presence of MB, OCT helps in differentiating between different pathophysiological subtypes, such as plaque rupture/erosion, thrombosis or spontaneous coronary artery dissection (SCAD) (30). Finally, despite weak evidence, the use of OCT might help in guiding percutaneous revascularization, with the aim of minimizing peri- and post-procedural complications during stent implantation in a MB segment (63).

The key limitation of IVUS and OCT in the assessment of MB is related to the lack of functional and hemodynamic information on both MB and proximal atherosclerotic lesions. Furthermore, they increased procedural cost and the risk of underestimating the length of MB when rapid pullback is performed (**Table 1**).

In conclusion, the use of invasive anatomical assessment with imaging tools such as IVUS and OCT allows to maximize the diagnosis of MB, quantify arterial compression, characterize the coexisting proximal CAD, and identify the mechanism underlying the occurrence of ACS.

Physiological assessment of myocardial bridging

Functional assessment tools should be considered complementary to imaging tests. In this regard, the Doppler flow wire and pressure wire methods represent useful modalities to define the hemodynamic impact of MB (13; **Figure 2**).

Fractional flow reserve (FFR) is a pressure wire-based index that, through the measurement of the trans-stenotic pressure gradient during maximal hyperemia (achieved by adenosine administration), is recommended to assess the hemodynamic relevance of intermediate-grade stenosis when evidence of ischemia is not available (68, 69). To date, 0.80 is the accepted

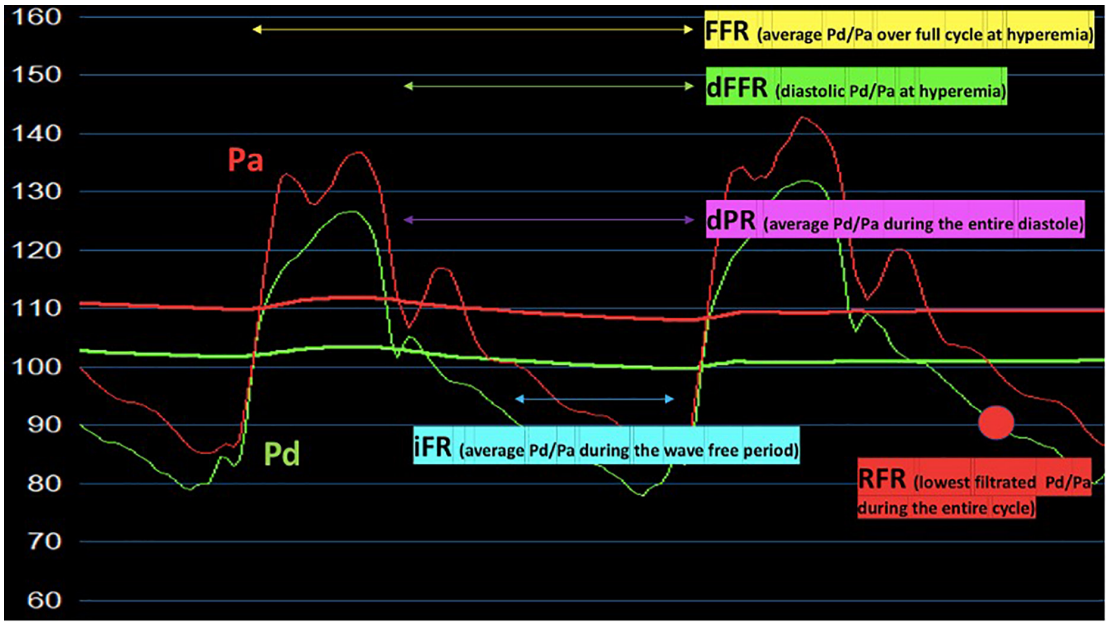

FIGURE 2
Hyperemic and non-hyperemic pressure ratios (FFR, dFFR, iFR, RFR, dPR) proposed for the invasive functional assessment of patients with myocardial bridging. Pa, aortic pressure; Pd, distal pressure; FFR, fractional flow reserve; dFFR, diastolic-fractional flow reserve; iFR, instantaneous wave-free pressure ratio; RFR, resting full-cycle ratio dPR, diastolic pressure ratio.

FFR threshold for defining hemodynamically relevant fixed stenosis (68, 69).

Although FFR is generally considered the gold standard for the physiological invasive assessment of atherosclerotic plaque, it may fail to identify the hemodynamic impact of dynamic coronary obstructions such as MB (14). FFR is based on the assumption that the difference between mean and diastolic pressure gradient values across the lesion is not significant: this is true for fixed stenosis, but it might not be valid for dynamic flow obstruction (7, 14). MB reduces systolic pressure gradients, as a consequence of distal pressure overshooting during myocardial contraction. This leads to an overestimation of the mean pressure (evaluated by FFR) and to an underestimation of the hemodynamic significance of MB (7). Therefore, specific diastolic functional indices have been developed to overcome the limits of FFR (13), such as dFFR which has proven to be more sensitive than conventional FFR for functional assessment of MB (70).

Moreover, as MB is a dynamic stenosis deeply influenced by the degree of extravascular compression and intra-myocardial tension, the assessment during rest may underestimate the hemodynamic relevance of a significant proportion of MBs. Dobutamine represents the drug of choice for inotropic stimulation in MB patients (18). In this regard, Escaned et al. evaluated the usefulness and safety of combining dobutamine challenge with FFR and dFFR in the presence of MB. This investigation revealed that dobutamine challenge enhanced diagnostic sensitivity of both FFR and dFFR. Interestingly, dobutamine challenge increased the discrepancy between FFR and dFFR (70). This may be explained by the decreased and negativization of systolic pressure gradient across MB segment during dobutamine provocation, leading to an artificial and paradoxical elevation in the mean pressure gradient used by traditional FFR.

The diagnostic superiority of dFFR during dobutamine provocation, compared to conventional FFR during adenosine provocation, has been recently confirmed by Aleksandric et al. using exercise-induced myocardial ischemia (4). They proposed the cut-off value of $\leq$0.76 for dFFR during dobutamine provocation to identify stress-induced myocardial ischemia in MB patients with a Sn, Sp, PPV and NPV of 95, 95, 90, and 98%, respectively (AUC 0.927). Curiously, this value is the same as the cut-off value used for dFFR during adenosine provocation in the functional assessment of fixed coronary stenosis (Sn 96%; Sp 100%) (71).

However, despite the promising diagnostic value, dFFR is not routinely performed in clinical practice, due to the difficulty of execution and time-consuming.

Other non-hyperemic pressure indices, including instantaneous wave-free ratio (iFR), diastolic pressure ratio (dPR), and resting full-cycle ratio (RFR) have been developed. They are obtained without the administration of vasodilators, resulting easier to perform than dFFR.

Instantaneous wave-free ratio is a pressure-derived index, recently validated for the assessment of coronary artery stenosis. It is a specific-diastolic index, calculated during a portion of

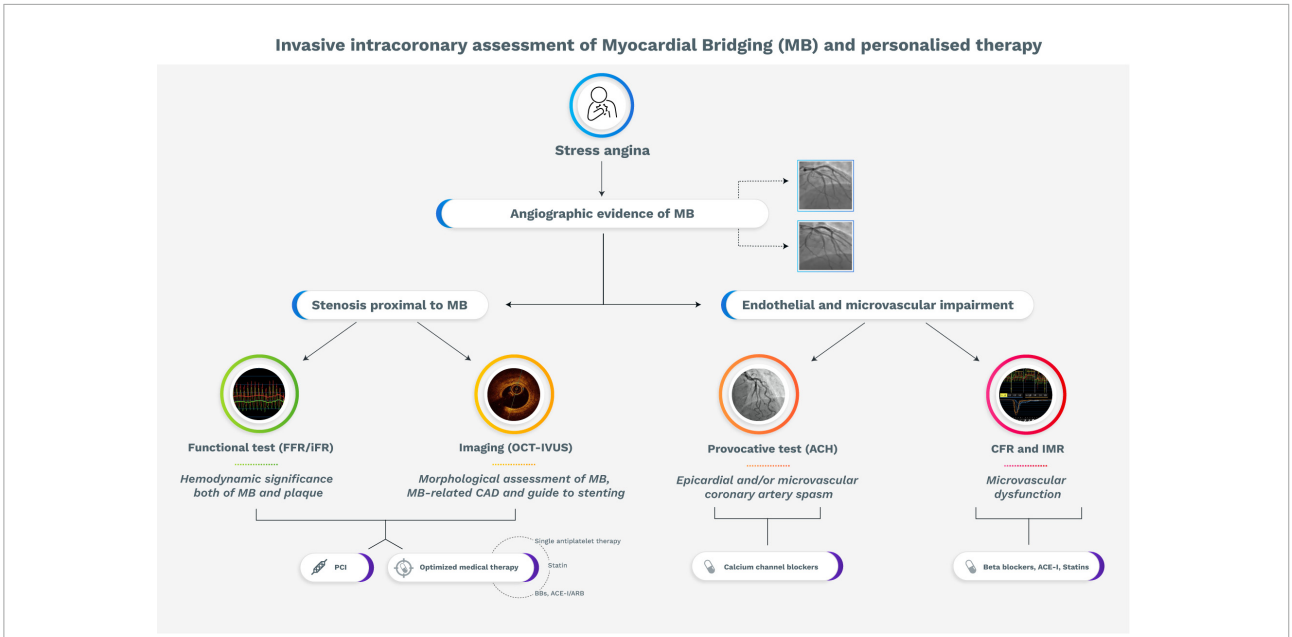

FIGURE 3
Flow diagram with proposed strategy for the management of symptomatic patients with myocardial bridging. ACE-I, Angiotensin-converting enzyme-inhibitors; Ach, acetylcholine; ARB, Angiotensin receptor blocker; BBs, beta-blockers; CAD, coronary artery disease; CFR, coronary flow reserve; FFR, fractional flow reserve; iFR, instantaneous wave-free ratio; IMR, index of microvascular resistance IVUS, intravascular ultrasound; MB, myocardial bridging; OCT, optical coherence tomography; PCI, percutaneous coronary intervention.

diastole when vascular resistance is low and stable, the so-called "wave-free period" (72). In a prospective study by Tarantini et al., among 20 patients with angina and/or positive non-invasive stress test, absence of CAD and angiographic evidence of MB, iFR was found to be more consistent with angina and/or inducible ischemia compared with FFR. Indeed, iFR at rest was abnormal (≤0.89) in 7 patients, while no MB was hemodynamically significant according to FFR. During inotropic challenge, median FFR did not change significantly, whereas dobutamine-induced iFR resulted to be remarkable lower compared to iFR at rest (73).

Collectively, diastolic indices may identify a proportion of hemodynamically relevant MBs that are not unmasked by conventional FFR. The superiority of diastolic indices over systo-diastolic indices (i.e., FFR) in the evaluation of ischemic burden related to MB reflects the fundamental involvement of diastole in the pathophysiology of MB-related ischemia (70, 74).

Nevertheless, the evaluation of iFR depends on the assumption that maximal flow and minimal microcirculatory resistance occur during a period within diastole (the "wave-free period"), while the hemodynamic modifications imposed by MB and concomitant CAD may be not completely predictable. In this regard, two alternative non-hyperaemic pressure indices might be proposed: dPR and RFR.

Diastolic pressure ratio is the ratio between mean distal coronary pressure averaged over the entire diastolic period and the mean aortic pressure (75). Instead, RFR is calculated from the lowest value of distal pressure (Pd) and aortic pressure (Pa) over the entire cardiac cycle (76). These indices may potentially unmask significant or multiple occlusions that would be missed by an assessment dedicated only to specific periods of the cardiac cycle (75, 76).

Unfortunately, ischemic cut-off values for the above-discussed indices, at rest and during inotropic provocation, are not available for MB patients. Further studies are needed for the validation of these tools and for the definition of reliable cut-off values.

The Doppler guide wire, through selective catheterization and measuring phasic flow velocity of MB segment, reveals a typical velocity pattern termed "fingertip" phenomenon, characterized by an abrupt early-diastolic acceleration, a rapid mid-diastolic deceleration and a mid-to-late diastolic plateau (10, 13). However, the absence of the "fingertip" was found in 13% of MB patients, probably because the systolic compression sometimes is not strong enough to induce the hemodynamic changes that lead to this sign (10). Further studies are needed to confirm these results and to determine whether this phenomenon, as a marker of MB severity, predicts adverse cardiovascular events.

Provocative test

It is well-known that endothelial dysfunction is a pathophysiological hallmark of MB-related ischemia,

promoting the development of vasomotor disorders such as epicardial and microvascular CAS. In order to unmask endothelial dysfunction and CAS, three provocative tests (with ACH, ergonovine and hyperventilation) can be performed in the catheterization laboratory (77). ACH test is preferred over ergonovine and hyperventilation, because it is associated with a lower rate of complications compared to ergonovine, and it is more standardized and reproducible than hyperventilation (78). On the other hand, non-invasive provocative tests (i.e., ergonovine and hyperventilation) have been associated with significant adverse events including death, because detection and alleviation of the induced spasm may be delayed (79).

The 2019 ESC CCS guidelines support the use of intracoronary ACH test in patients with normal findings or non-obstructive lesions on coronary arteriography and clinical suspicion of CAS for the assessment of epicardial spasm (IIa recommendation) and/or microvascular spasm (IIb recommendation) (80–82). Therefore, interventional cardiologists should not refrain from performing provocative test in patients with MB and clinical picture of vasospastic angina.

Several studies investigated the relationship between CAS and MB, demonstrating that MB patients present a high rate of CAS. Furthermore, MB patients with a positive response to ACH test have a worse prognosis compared with those without spasm (10, 32–36, 83–88). However, the location of provoked spasm was not always the same: most of studies found epicardial spasm of the intramural segment. On the contrary, Saito et al. found that epicardial CAS was more frequently provoked in the proximal segment of MB (34). Moreover, heterogeneity in dose-response relationship has been noted in patients with MB and ACH-induced spasm. MB patients who responded to lower ACH doses (20 μg) have higher incidence of severe, diffuse and long (>30 mm) spasm. This results in a higher occurrence of adverse events at 12-month follow-up, compared to MB patients reacting to higher ACH doses (50 and 100 μ g) (88).

Therefore, the use of ACH provocative test may be useful in the identification and quantification of a pathophysiological mechanism (impaired endothelium-dependent vasodilatation) of MB-related ischemia, with relevant prognostic and therapeutic implications.

Therapeutic management of patients with myocardial bridging

The therapeutic management of MB patients remains a relevant challenge. Treatment options should be considered according to clinical presentation, evidence and degree of inducible ischemia, coronary and cardiac anatomy, comorbidities and patient preference (13). Nevertheless, no guidelines or expert consensus are currently available.

As discussed, the ischemic burden related to MB is supported by various pathophysiological mechanisms. In this regard, invasive and non-invasive physiological assessment, intracoronary imaging, and provocative test may unmask the dominant mechanism of myocardial ischemia, allowing to guide the treatment according to specific pathophysiological endotypes of myocardial ischemia (**Figure 3**).

Pharmacologic therapy is considered the first strategy for most of symptomatic MB patients (8). Beta-blockers (BBs) represent the mainstay of treatment in patients with MB and ischemic symptoms or signs of inducible ischemia. Due to their negative chronotropic effect, BBs allow to increase diastolic perfusion and diastolic filling time. In addition, they reduce compression of the tunneled vessel by their negative inotropic effect (7). Similarly, non-dihydropyridine calcium channel blockers (CCBs) may satisfy the same target, and they should be preferred in patients with contraindications to betablockers (89).

However, BBs, especially non-selective ones, may be detrimental in MB patients with concomitant CAS. In fact, blockade of the beta-2 receptors, which mediate vasodilation, increases the risk of CAS and, supposedly, adverse cardiac events (90). On the contrary, CCBs, by combining their negative ino-chronotropic effect and vasodilatory effect, may represent the treatment of choice in MB patients with concomitant vasomotor disorders unmasked by a positive ACH test (13, 91). Conversely, nitrates, although powerful vasodilators, should be avoided since they worsen systolic narrowing and symptoms through a reflex rise of the adrenergic drive.

Since MB has been associated with an increased prevalence of CAD proximal to the bridged segment, optimized medical therapy of cardiovascular risk factors should be considered once atherosclerosis is detected (13).

If symptoms persist despite maximally tolerated medical therapy, a "revascularization" strategy should be considered. The choice among percutaneous coronary intervention (PCI), coronary artery bypass graft (CABG) or supra-arterial myotomy should be guided by anatomical features of MB (i.e., length and depth), age, concomitant CAD, and patient preference.

Randomized data are lacking for the use of PCI in the treatment of MB, and this approach was historically reserved to patients with anginal symptoms refractory to maximal medical therapy (92). Any rationale for PCI in this setting would be to treat stenosis proximal to MB as well as the dynamic obstruction within the tunneled segment, aiming at protecting it from systolic compression (8). However, PCI with stenting in MB patients may lead to a high rate of complications such as in-stent restenosis (ISR), very late stent thrombosis, and coronary perforation, due to the sustained stress over time within the intramural tract. These complications were described mainly in studies using bare-metal stent (BMS) and first-generation drug eluting stent (DES) (8, 63, 93–96). Probably, the use of second-generation DES or future bioabsorbable scaffolds

may potentially limit these complications (13). Furthermore, the use of intracoronary imaging tools may provide accurate information about MB sizing, guiding the percutaneous treatment. In this regard, a recent retrospective study showed that the guidance of OCT limited the incidence of perforation and ISR in the MB segment covered with DES (63).

Given the MB stenting-related complications, surgery is an effective therapeutic alternative for symptomatic MB refractory to maximally tolerated medical therapy. Myotomy is the treatment of choice for MB with favorable anatomy (i.e., non-tortuous artery, short and superficial intra-myocardial course), especially in pediatric population (97). Conversely, myotomy presents a high rate of failure in adult patients, probably because abnormal flow related to MB causes damage to coronary circulation (i.e., endothelial dysfunction), persisting and impairing coronary flow after surgical intervention (5). CABG is superior to myotomy in case of complex anatomy (i.e., deep and/or long MB) and adult patients (51).

Unfortunately, studies assessing short- and long-term effect of antianginal drugs vs. PCI or surgical treatment in MB patients are lacking. Large and prospective randomized clinical trials are needed in this regard.

Conclusion

Myocardial bridging has long been considered an accidental finding. However, a growing body of evidence suggested that it is associated with impaired quality of life and might lead to adverse cardiac events.

Invasive intracoronary assessment, *via* imaging techniques (i.e., OCT and IVUS), or full invasive physiological evaluation (i.e., FFR, iFR, CFR, IMR), together with the utilization of provocative test (i.e., ACH test), improved the ability to evaluate the hemodynamic relevance of MB, to understand the underlying pathophysiological mechanisms, leading to an optimization of the therapy according to each specific endotypes.

Nevertheless, the uncertainties we are currently facing in the diagnosis, characterization, and treatment of patients presenting with MB and evidence of ischemia are remarkable, and related, at least in part, to the skepticism and the paucity of evidence that support the clinical and prognostic relevance of MB in the setting of CCS and ACS. Therefore, there is an unmet need in defining unequivocally the diagnostic tools and the related cut-offs to be used, guiding the therapeutic management of patients with MB. The present review, systematically addressing the current shreds of evidence in the field, set the stage for considering MB as a novel and interesting therapeutic target, aiming to launch in the near future reliable and compelling efficacy endpoints to be utilized in proof-of-concept clinical trials.

Author contributions

RL and GC had a leading role in writing the manuscript. DD'A had a leading role in manuscript revision. FCr, PZ, AR, GR, MD, MG, AZ, FCa, RV, GP, AL, FB, CT, and VP had a supporting role in manuscript revision. All authors have read and agreed to the content of the manuscript.

Conflict of interest

Author MG declares that he has received consulting fees or honoraria from Terumo, outside the present work.

The remaining authors declare that the research was conducted in the absence of any commercial or financial relationships that could be construed as a potential conflict of interest.

Publisher's note

References

1. Alegria JR, Herrmann J, Holmes DR Jr, Lerman A, Rihal CS. Myocardial bridging. *Eur Heart J.* (2005) 26:1159–68. doi: 10.1093/eurheartj/ehi203

2. Möhlenkamp S, Hort W, Ge J, Erbel R. Update on myocardial bridging. *Circulation.* (2002) 106:2616–22. doi: 10.1161/01.CIR.0000038420.14867.7A

3. Sharzehee M, Chang Y, Song JP, Han HC. Hemodynamic effects of myocardial bridging in patients with hypertrophic cardiomyopathy. *Am J Physiol Heart Circ Physiol.* (2019) 317:H1282–91. doi: 10.1152/ajpheart.00466.2019

4. Aleksandric SB, Djordjevic-Dikic AD, Dobric MR, Giga VL, Soldatovic IA, Vukcevic V, et al. Functional assessment of myocardial bridging with conventional and diastolic fractional flow reserve: vasodilator versus inotropic provocation. *J Am Heart Assoc.* (2021) 10:e020597. doi: 10.1161/JAHA.120.020597

5. Hostiuc S, Negoi I, Rusu MC, Hostiuc M. Myocardial bridging: a meta-analysis of prevalence. *J Forensic Sci.* (2018) 63:1176–85. doi: 10.1111/1556-4029.13665

6. Hayashi T, Ishikawa K. Myocardial bridge: harmless or harmful. *Intern Med.* (2004) 43:1097–8. doi: 10.2169/internalmedicine.43.1097

7. Tarantini G, Migliore F, Cademartiri F, Fraccaro C, Iliceto S. Left anterior descending artery myocardial bridging: a clinical approach. *J Am Coll Cardiol.* (2016) 68:2887–99. doi: 10.1016/j.jacc.2016.09.973

8. Corban MT, Hung OY, Eshtehardi P, Rasoul-Arzrumly E, McDaniel M, Mekonnen G, et al. Myocardial bridging: contemporary understanding of pathophysiology with implications for diagnostic and therapeutic strategies. *J Am Coll Cardiol.* (2014) 63:2346–55. doi: 10.1016/j.jacc.2014.01.049

9. Cappannoli L, Ciliberti G, Restivo A, Palumbo P, D'Alò F, Sanna T, et al. 'Here comes the story of the Hurricane': a case report of AL cardiac amyloidosis and myocardial bridging. *Eur Heart J Case Rep.* (2022) 6:ytac225. doi: 10.1093/ehjcr/ytac225

10. Teragawa H, Oshita C, Ueda T. The myocardial bridge: potential influences on the coronary artery vasculature. *Clin Med Insights Cardiol.* (2019) 1:1179546819846493. doi: 10.1177/1179546819846493

11. Kunadian V, Chieffo A, Camici PG, Berry C, Escaned J, Maas AHEM, et al. An EAPCI expert consensus document on ischaemia with non-obstructive coronary arteries in collaboration with european society of cardiology working group on coronary pathophysiology & microcirculation endorsed by coronary vasomotor disorders international study group. *Eur Heart J.* (2020) 41:3504–20. doi: 10.1093/eurheartj/ehaa503

12. Yuan SM. Myocardial bridging. *Braz J Cardiovasc Surg.* (2016) 31:60–2. doi: 10.5935/1678-9741.20150082

13. Sternheim D, Power DA, Samtani R, Kini A, Fuster V, Sharma S, et al. Myocardial bridging: diagnosis, functional assessment, and management: JACC state-of-the-art review. *J Am Coll Cardiol.* (2021) 78:2196–212. doi: 10.1016/j.jacc.2021.09.859

14. Gould KL, Johnson NP. Myocardial bridges: lessons in clinical coronary pathophysiology. *JACC Cardiovasc Imaging.* (2015) 8:705–9. doi: 10.1016/j.jcmg.2015.02.013

15. Ge J, Erbel R, Rupprecht HJ, Koch L, Kearney P, Görge G, et al. Comparison of intravascular ultrasound and angiography in the assessment of myocardial bridging. *Circulation.* (1994) 89:1725–32. doi: 10.1161/01.CIR.89.4.1725

16. Schwarz ER, Klues HG, vom Dahl J, Klein I, Krebs W, Hanrath P. Functional characteristics of myocardial bridging. a combined angiographic and intracoronary Doppler flow study. *Eur Heart J.* (1997) 18:434–42. doi: 10.1093/oxfordjournals.eurheartj.a015263

17. Ge J, Jeremias A, Rupp A, Abels M, Baumgart D, Liu F, et al. New signs characteristic of myocardial bridging demonstrated by intracoronary ultrasound and Doppler. *Eur Heart J.* (1999) 20:1707–16. doi: 10.1053/euhj.1999.1661

18. Aleksandric S, Djordjevic-Dikic A, Beleslin B, Parapid B, Teofilovski-Parapid G, Stepanovic J, et al. Noninvasive assessment of myocardial bridging by coronary flow velocity reserve with transthoracic Doppler echocardiography: vasodilator vs. inotropic stimulation. *Int J Cardiol.* (2016) 225:37–45. doi: 10.1016/j.ijcard.2016.09.101

19. Erbel R, Rupprecht HJ, Ge J, Gerber T, Gunter G, Meyer J. Coronary artery shape and flow changes induced by myocardial bridging. *Echocardiography.* (1993) 10:71–7. doi: 10.1111/j.1540-8175.1993.tb00013.x

20. Schwarz ER, Gupta R, Haager PK, vom Dahl J, Klues HG, Minartz J, et al. Myocardial bridging in absence of coronary artery disease: proposal of a new classification based on clinical-angiographic data and long-term follow-up. *Cardiology.* (2009) 112:13–21. doi: 10.1159/000137693

21. Corban MT, Hung OY, Timmins LH, Rasoul-Arzrumly E, McDaniel M, Mekonnen G, et al. Myocardial bridging. *J Am Coll Cardiol.* (2014) 64:2179–81.

22. Malek AM, Alper SL, Izumo S. Hemodynamic shear stress and its role in atherosclerosis. *JAMA.* (1999) 282:2035–42. doi: 10.1001/jama.282.21.2035

23. Nikoliæ D, Radoviæ M, Aleksandriæ S, Tomaševiæ M, Filipoviæ N. Prediction of coronary plaque location on arteries having myocardial bridge, using finite element models. *Comput Methods Programs Biomed.* (2014) 117:137–44. doi: 10.1016/j.cmpb.2014.07.012

24. Chatzizisis YS, Giannoglou GD. Myocardial bridges spared from atherosclerosis: overview of the underlying mechanisms. *Can J Cardiol.* (2009) 25:219–22. doi: 10.1016/S0828-282X(09)70065-0

25. Verhagen SN, Rutten A, Meijs MF, Isgum I, Cramer MJ, van der Graaf Y, et al. Relationship between myocardial bridges and reduced coronary atherosclerosis in patients with angina pectoris. *Int J Cardiol.* (2013) 167:883–8. doi: 10.1016/j.ijcard.2012.01.091

26. Ishii T, Asuwa N, Masuda S. The effects of a myocardial bridge on coronary atherosclerosis and ischaemia. *J Pathol.* (1998) 185:4–9. doi: 10.1002/(SICI)1096-9896(199805)185:1<4::AID-PATH50>3.0.CO;2-3

27. Ishikawa Y, Ishii T, Asuwa N. Absence of atherosclerosis evolution in the coronary arterial segment covered by myocardial tissue in cholesterol-fed rabbits. *Virchows Arch.* (1997) 430:163–71. doi: 10.1007/BF01008038

28. Ishikawa Y, Akasaka Y, Suzuki K, Fujiwara M, Ogawa T, Yamazaki K, et al. Anatomic properties of myocardial bridge predisposing to myocardial infarction. *Circulation.* (2009) 120:376–83. doi: 10.1161/CIRCULATIONAHA.108.820720

29. Ishikawa Y, Akasaka Y, Akishima-Fukasawa Y, Iuchi A, Suzuki K, Uno M, et al. Histopathologic profiles of coronary atherosclerosis by myocardial bridge underlying myocardial infarction. *Atherosclerosis.* (2013) 226:118–23. doi: 10.1016/j.atherosclerosis.2012.10.037

30. Wu S, Liu W, Zhou Y. Spontaneous coronary artery dissection in the presence of myocardial bridge causing myocardial infarction: an insight into mechanism. *Int J Cardiol.* (2016) 206:77–8. doi: 10.1016/j.ijcard.2016.01.085

31. Fujibayashi D, Morino Y, Ikari Y. A case of acute myocardial infarction due to coronary spasm in the myocardial bridge. *J Invasive Cardiol.* (2008) 20:E217–9.

32. Nam P, Choi BG, Choi SY, Byun JK, Mashaly A, Park Y, et al. The impact of myocardial bridge on coronary artery spasm and long-term clinical outcomes in patients without significant atherosclerotic stenosis. *Atherosclerosis.* (2018) 270:8–12. doi: 10.1016/j.atherosclerosis.2018.01.026

33. Kim JW, Park CG, Suh SY, Choi CU, Kim EJ, Rha SW, et al. Comparison of frequency of coronary spasm in Korean patients with versus without myocardial bridging. *Am J Cardiol.* (2007) 100:1083–6. doi: 10.1016/j.amjcard.2007.05.030

34. Saito Y, Kitahara H, Shoji T, Tokimasa S, Nakayama T, Sugimoto K, et al. Relation between severity of myocardial bridge and vasospasm. *Int J Cardiol.* (2017) 248:34–8. doi: 10.1016/j.ijcard.2017.07.002

35. Teragawa H, Fukuda Y, Matsuda K, Hirao H, Higashi Y, Yamagata T, et al. Myocardial bridging increases the risk of coronary spasm. *Clin Cardiol.* (2003) 26:377–83. doi: 10.1002/clc.4950260806

36. Masuda T, Ishikawa Y, Akasaka Y, Itoh K, Kiguchi H, Ishii T, et al. The effect of myocardial bridging of the coronary artery on vasoactive agents and atherosclerosis localization. *J Pathol.* (2001) 193:408–14. doi: 10.1002/1096-9896(2000)9999:9999<::AID-PATH792>3.0.CO;2-R

37. Lanza GA, Careri G, Crea F. Mechanisms of coronary artery spasm. *Circulation.* (2011) 124:1774–82. doi: 10.1161/CIRCULATIONAHA.111.037283

38. Thygesen K, Alpert JS, Jaffe AS, Chaitman BR, Bax JJ, Morrow DA, et al. Executive Group on behalf of the Joint European Society of Cardiology (ESC)/American College of Cardiology (ACC)/American Heart Association (AHA)/World Heart Federation (WHF) Task Force for the Universal Definition of Myocardial Infarction. Fourth Universal Definition of Myocardial Infarction (2018). *J Am Coll Cardiol.* (2018) 72:2231–64. doi: 10.1161/CIR.0000000000000617

39. Hong L, Liu J, Luo S, Li J. Relation of myocardial bridge to myocardial infarction: a meta-analysis. *Chin Med J.* (2014) 127:945–50.

40. Sara JDS, Corban MT, Prasad M, Prasad A, Gulati R, Lerman LO, et al. Prevalence of myocardial bridging associated with coronary endothelial dysfunction in patients with chest pain and non-obstructive coronary artery disease. *EuroIntervention.* (2020) 15:1262–8. doi: 10.4244/EIJ-D-18-00920

41. D'Amario D, Borovac JA, Crea F. Coronary microvascular dysfunction in heart failure with preserved ejection fraction: not the end but the end of the beginning. *Eur J Heart Fail.* (2021) 23:773–5. doi: 10.1002/ejhf.2069

42. D'Amario D, Migliaro S, Borovac JA, Restivo A, Vergallo R, Galli M, et al. Microvascular dysfunction in heart failure with preserved ejection fraction. *Front Physiol.* (2019) 10:1347. doi: 10.3389/fphys.2019.01347

43. Pargaonkar VS, Kimura T, Kameda R, Tanaka S, Yamada R, Schwartz JG, et al. Invasive assessment of myocardial bridging in patients with angina and no obstructive coronary artery disease. *EuroIntervention.* (2021) 16:1070–8. doi: 10.4244/EIJ-D-20-00779

44. Lin S, Tremmel JA, Yamada R, Rogers IS, Yong CM, Turcott R, et al. A novel stress echocardiography pattern for myocardial bridge with invasive structural and hemodynamic correlation. *J Am Heart Assoc.* (2013) 2:e000097. doi: 10.1161/JAHA.113.000097

45. Gould KL, Kirkeeide R, Johnson NP. Coronary branch steal: experimental validation and clinical implications of interacting stenosis in branching coronary arteries. *Circ Cardiovasc Imaging.* (2010) 3:701–9. doi: 10.1161/CIRCIMAGING.110.937656

46. Tavakol M, Ashraf S, Brener SJ. Risks and complications of coronary angiography: a comprehensive review. *Glob J Health Sci.* (2012) 4:65–93. doi: 10.5539/gjhs.v4n1p65

47. Podolec J, Wiewiórka Ł, Siudak Z, Malinowski K, Dudek D, Gackowski A. Prevalence and clinical presentation of myocardial bridge on the basis of the National Polish Percutaneous Interventions Registry and the Classification of Rare Cardiovascular Diseases. *Kardiol Pol.* (2018) 77:465–70. doi: 10.5603/KP.a2019.0041

48. Kim PJ, Hur G, Kim SY, Namgung J, Hong SW, Kim YH, et al. Frequency of myocardial bridges and dynamic compression of epicardial coronary arteries: a comparison between computed tomography and invasive coronary angiography. *Circulation.* (2009) 119:1408–16. doi: 10.1161/CIRCULATIONAHA.108.788901

49. Konen E, Goitein O, Sternik L, Eshet Y, Shemesh J, Di Segni E. The prevalence and anatomical patterns of intramuscular coronary arteries: a coronary computed tomography angiographic study. *J Am Coll Cardiol.* (2007) 49:587–93. doi: 10.1016/j.jacc.2006.09.039

50. Forsdahl SH, Rogers IS, Schnittger I, Tanaka S, Kimura T, Pargaonkar VS, et al. Myocardial bridges on coronary computed tomography angiography – correlation with intravascular ultrasound and fractional flow reserve. *Circ J.* (2017) 81:1894–900. doi: 10.1253/circj.CJ-17-0284

51. Zhang JZ, Zhu GY, Zhang Y, Bai LJ, Wang Z. Myocardial bridge bypass graft: a novel surgical procedure for extensive myocardial bridges. *Ann Thorac Surg.* (2021) 112:e115–7. doi: 10.1016/j.athoracsur.2020.11.055

52. Pargaonkar VS, Rogers IS, Su J, Forsdahl SH, Kameda R, Schreiber D, et al. Accuracy of a novel stress echocardiography pattern for myocardial bridging in patients with angina and no obstructive coronary artery disease - A retrospective and prospective cohort study. *Int J Cardiol.* (2020) 311:107–13. doi: 10.1016/j.ijcard.2020.02.006

53. Aleksandric SB, Djordjevic-Dikic AD, Giga VL, Tesic MB, Soldatovic IA, Banovic MD, et al. Coronary flow velocity reserve using dobutamine test for noninvasive functional assessment of myocardial bridging. *J Clin Med.* (2021) 11:204. doi: 10.3390/jcm11010204

54. Daimon M, Watanabe H, Yamagishi H, Muro T, Akioka K, Hirata K, et al. Physiologic assessment of coronary artery stenosis by coronary flow reserve measurements with transthoracic Doppler echocardiography: comparison with exercise thallium-201 single piston emission computed tomography. *J Am Coll Cardiol.* (2001) 37:1310–5. doi: 10.1016/S0735-1097(01)01167-6

55. Takeuchi M, Miyazaki C, Yoshitani H, Otani S, Sakamoto K, Yoshikawa J. Assessment of coronary flow velocity with transthoracic Doppler echocardiography during dobutamine stress echocardiography. *J Am Coll Cardiol.* (2001) 38:117–23. doi: 10.1016/S0735-1097(01)01322-5

56. Abadie B, Jaber W. Dobutamine stress PET/CT for assessment of hemodynamic significance of coronary myocardial bridges. *J Nucl Cardiol.* (2021) doi: 10.1007/s12350-021-02759-8 [Epub ahead of print].

57. Hongo Y, Tada H, Ito K, Yasumura Y, Miyatake K, Yamagishi M. Augmentation of vessel squeezing at coronary-myocardial bridge by nitroglycerin: study by quantitative coronary angiography and intravascular ultrasound. *Am Heart J.* (1999) 138:345–50. doi: 10.1016/S0002-8703(99)70123-7

58. Bangalore S, Bhatt DL. Coronary intravascular ultrasound. *Circulation.* (2013) 127:e868–74. doi: 10.1161/CIRCULATIONAHA.113.003534

59. Ge J, Jeremias A, Rupp A, Abels M, Abels M, Baumgart D, et al. New signs characteristic of myocardial bridging demonstrated by intracoronary ultrasound and Doppler. *Eur Heart J.* (1999) 20:1707–16. doi: 10.1053/euhj.1999.1661

60. Yamada R, Tremmel JA, Tanaka S, Lin S, Kobayashi Y, Hollak MB, et al. Functional versus anatomic assessment of myocardial bridging by intravascular ultrasound: impact of arterial compression on proximal atherosclerotic plaque. *J Am Heart Assoc.* (2016) 5:e001735. doi: 10.1161/JAHA.114.001735

61. Shimamura K, Kubo T, Akasaka T. Evaluation of coronary plaques and atherosclerosis using optical coherence tomography. *Expert Rev Cardiovasc Ther.* (2021) 19:379–86. doi: 10.1080/14779072.2021.1914588

62. Triantafyllis AS, de Ridder S, Teeuwen K, Otterspoor LC. Myocardial bridging, a trigger for Takotsubo syndrome. *Neth Heart J.* (2018) 26:573–4. doi: 10.1007/s12471-018-1142-0

63. Xu T, You W, Wu Z, Meng P, Ye F, Wu X, et al. Retrospective analysis of OCT on MB characteristics and 1-year follow-up of the ISR incidence after the DES implantation in patients with MB. *Sci Rep.* (2022) 12:534. doi: 10.1038/s41598-021-04579-9

64. Cao HM, Jiang JF, Deng B, Xu JH, Xu WJ. Evaluation of myocardial bridges with optical coherence tomography. *J Int Med Res.* (2010) 38:681–5. doi: 10.1177/147323001003800232

65. Ye Z, Lai Y, Mintz GS, Yao Y, Tang J, Luo Y, et al. Fusiform appearance of myocardial bridging detected by OCT. *JACC Cardiovasc Imaging.* (2016) 9:892–4. doi: 10.1016/j.jcmg.2015.05.006

66. Okamura A, Okura H, Iwai S, Kyodo A, Kamon D, Hashimoto Y, et al. Detection of myocardial bridge by optical coherence tomography. *Int J Cardiovasc Imaging.* (2022) doi: 10.1007/s10554-021-02497-5 [Epub ahead of print].

67. Ye Z, Lai Y, Yao Y, Mintz GS, Liu X. Optical coherence tomography and intravascular ultrasound assessment of the anatomic size and wall thickness of a muscle bridge segment. *Catheter Cardiovasc Interv.* (2019) 93:772–8. doi: 10.1002/ccd.28094

68. Elgendy IY, Conti CR, Bavry AA. Fractional flow reserve: an updated review. *Clin Cardiol.* (2014) 37:371–80. doi: 10.1002/clc.22273

69. Neumann FJ, Sousa-Uva M, Ahlsson A, Alfonso F, Banning AP, Benedetto U, et al. ESC Scientific Document Group. 2018 ESC/EACTS Guidelines on myocardial revascularization. *Eur Heart J.* (2019) 40:87–165. doi: 10.1093/eurheartj/ehy855

70. Escaned J, Cortés J, Flores A, Goicolea J, Alfonso F, Hernández R, et al. Importance of diastolic fractional flow reserve and dobutamine challenge in physiologic assessment of myocardial bridging. *J Am Coll Cardiol.* (2003) 42:226–33. doi: 10.1016/S0735-1097(03)00588-6

71. Abe M, Tomiyama H, Yoshida H, Doba N. Diastolic fractional flow reserve to assess the functional severity of moderate coronary artery stenoses: comparison with fractional flow reserve and coronary flow velocity reserve. *Circulation.* (2000) 102:2365–70. doi: 10.1161/01.CIR.102.19.2365

72. Davies JE, Sen S, Dehbi HM, Al-Lamee R, Petraco R, Nijjer SS, et al. Use of the instantaneous wave-free ratio or fractional flow reserve in PCI. *N Engl J Med.* (2017) 376:1824–34.

73. Tarantini G, Barioli A, Nai Fovino L, Fraccaro C, Masiero G, Iliceto S, et al. Unmasking myocardial bridge-related ischemia by intracoronary functional evaluation. *Circ Cardiovasc Interv.* (2018) 11:e006247. doi: 10.1161/CIRCINTERVENTIONS.117.006247

74. Kumar G, Desai R, Gore A, Rahim H, Maehara A, Matsumura M, et al. Real world validation of the nonhyperemic index of coronary artery stenosis severity-Resting full-cycle ratio-RE-VALIDATE. *Catheter Cardiovasc Interv.* (2020) 96:E53–8. doi: 10.1002/ccd.28523

75. Kern MJ, Seto AH. dPR, Another diastolic resting pressure ratio. *Circ Cardiovasc Interv.* (2018) 11:e007540. doi: 10.1161/CIRCINTERVENTIONS.118.007540

76. Svanerud J, Ahn JM, Jeremias A, van 't Veer M, Gore A, Maehara A, et al. Validation of a novel non-hyperaemic index of coronary artery stenosis severity: the Resting Full-cycle Ratio (VALIDATE RFR) study. *EuroIntervention.* (2018) 14:806–14. doi: 10.4244/EIJ-D-18-00342

77. Previtali M, Ardissino D, Barberis P, Panciroli C, Chimienti M, Salerno JA, et al. Hyperventilation and ergonovine tests in Prinzmetal's variant angina pectoris in men. *Am J Cardiol.* (1989) 63:17–20. doi: 10.1016/0002-9149(89)91068-0

78. Ong P, Athanasiadis A, Borgulya G, Vokshi I, Bastiaenen R, Kubik S, et al. Clinical usefulness, angiographic characteristics, and safety evaluation of intracoronary acetylcholine provocation testing among 921 consecutive white patients with unobstructed coronary arteries. *Circulation.* (2014) 129:1723–30. doi: 10.1161/CIRCULATIONAHA.113.004096

79. Buxton A, Goldberg S, Hirshfeld JW, Wilson J, Mann T, Williams DO, et al. Refractory ergonovine-induced coronary vasospasm: importance of intracoronary nitroglycerin. *Am J Cardiol.* (1980) 46:329–34. doi: 10.1016/0002-9149(80)90080-6

80. Knuuti J, Wijns W, Saraste A, Capodanno D, Barbato E, Funck-Brentano C, et al. 2019 ESC Guidelines for the diagnosis and management of chronic coronary syndromes. *Eur Heart J.* (2020) 41:407–77.

81. Beltrame JF, Crea F, Kaski JC, Ogawa H, Ong P, Sechtem U, et al. International standardization of diagnostic criteria for vasospastic angina. *Eur Heart J.* (2017) 38:2565–8.

82. Ong P, Camici PG, Beltrame JF, Crea F, Shimokawa H, Sechtem U, et al. International standardization of diagnostic criteria for microvascular angina. *Int J Cardiol.* (2018) 250:16–20. doi: 10.1016/j.ijcard.2017.08.068

83. Shiode N, Kato M, Teragawa H, Yamada T, Hirao H, Nomura K, et al. Vasomotility and nitric oxide bioactivity of the bridging segments of the left anterior descending coronary artery. *Am J Cardiol.* (1998) 81:341–3. doi: 10.1016/S0002-9149(97)00912-0

84. Herrmann J, Higano ST, Lenon RJ, Rihal CS, Lerman A. Myocardial bridging is associated with alteration in coronary vasoreactivity. *Eur Heart J.* (2004) 25:2134–42. doi: 10.1016/j.ehj.2004.08.015

85. Montone RA, Gurgoglione FL, Del Buono MG, Rinaldi R, Meucci MC, Iannaccone G, et al. Interplay between myocardial bridging and coronary spasm in patients with myocardial ischemia and non-obstructive coronary arteries: pathogenic and prognostic implications. *J Am Heart Assoc.* (2021) 10:e020535. doi: 10.1093/ehjacc/zuab020.139

86. Kim JW, Seo HS, Na JO, Na JO, Suh SY, Choi CU, et al. Myocardial bridging is related to endothelial dysfunction but not to plaque as assessed by intracoronary ultrasound. *Heart.* (2008) 94:765–9. doi: 10.1136/hrt.2007.115980

87. Arai R, Kano H, Suzuki S, Semba H, Arita T, Yagi N, et al. Myocardial bridging is an independent predictor of positive spasm provocation testing by intracoronary ergonovine injections: a retrospective observational study. *Heart Vessels.* (2020) 35:474–86. doi: 10.1007/s00380-019-01518-7

88. Im SI, Rha SW, Choi BG, Choi SY, Kim SW, Na JO, et al. Angiographic and clinical characteristics according to intracoronary acetylcholine dose in patients with myocardial bridge. *Cardiology.* (2013) 125:250–7. doi: 10.1159/000351181

89. Lee MS, Chen CH. Myocardial bridging: an up-to-date review. *J Invasive Cardiol.* (2015) 27:521–8.

90. Kern MJ, Ganz P, Horowitz JD, Gaspar J, Barry WH, Lorell BH, et al. Potentiation of coronary vasoconstriction by beta-adrenergic blockade in patients with coronary artery disease. *Circulation.* (1983) 67:1178–85. doi: 10.1161/01.CIR.67.6.1178

91. Beltrame JF, Crea F, Kaski JC, Ogawa H, Ong P, Sechtem U, et al. The Who, What, Why, When, How and Where of Vasospastic Angina. *Circ J.* (2016) 80:289–98. doi: 10.1253/circj.CJ-15-1202

92. Klues HG, Schwarz ER, vom Dahl J, Reffelmann T, Reul H, Potthast K, et al. Disturbed intracoronary hemodynamics in myocardial bridging: early normalization by intracoronary stent placement. *Circulation.* (1997) 96:2905. doi: 10.1161/01.CIR.96.9.2905

93. Pourhoseini S, Bakhtiari M, Babaee A, Ostovan MA, Eftekhar-Vaghefi SH, Ostovan N, et al. Increased risk of coronary perforation durings percutaneous intervention of myocardial bridge: What histopathology says. *J Cardiovasc Thorac Res.* (2017) 9:108–12. doi: 10.15171/jcvtr.2017.18

94. Li W, Li Y, Sheng L, Gong Y. Myocardial bridge: is the risk of perforation increased? *Can J Cardiol.* (2008) 24:e80–1. doi: 10.1016/S0828-282X(08)70198-3

95. Borovac JA, D'Amario D, Vergallo R, Porto I, Bisignani A, Galli M, et al. Neoatherosclerosis after drug-eluting stent implantation: a novel clinical and therapeutic challenge. *Eur Heart J Cardiovasc Pharmacother.* (2019) 5:105–16. doi: 10.1093/ehjcvp/pvy036

96. Jiang Q, Liang C, Wu Z. Myocardial bridging is a potential risk factor of very late stent thrombosis of drug eluting stent. *Med Sci Monit.* (2012) 18:HY9–12. doi: 10.12659/MSM.882717

97. Ji Q, Shen J, Xia L, Ding W, Wang C. Surgical treatment of symptomatic left anterior descending myocardial bridges: myotomy vs. bypass surgery. *Surg Today.* (2020) 50:685–92. doi: 10.1007/s00595-019-01935-1

frontiers | Frontiers in Cardiovascular Medicine

TYPE Systematic Review
PUBLISHED 14 November 2022
DOI 10.3389/fcvm.2022.1017833

OPEN ACCESS

EDITED BY
Antonio Maria Leone,
Agostino Gemelli University Polyclinic (IRCCS), Italy

REVIEWED BY
Angelo Silverio,
University of Salerno, Italy
ELisabetta Ricottini,
Campus Bio-Medico University of Rome, Italy

*CORRESPONDENCE
Yao-Jun Zhang
13770668667@139.com

†These authors have contributed equally to this work

SPECIALTY SECTION
This article was submitted to Coronary Artery Disease, a section of the journal Frontiers in Cardiovascular Medicine

RECEIVED 12 August 2022
ACCEPTED 31 October 2022
PUBLISHED 14 November 2022

CITATION
Ma W-R, Chandrasekharan KH, Nai C-S, Zhu Y-X, Iqbal J, Chang S, Cheng Y-W, Wang X-Y, Bourantas CV and Zhang Y-J (2022) Clinical outcomes of percutaneous coronary intervention for *de novo* lesions in small coronary arteries: A systematic review and network meta-analysis.
Front. Cardiovasc. Med. 9:1017833.
doi: 10.3389/fcvm.2022.1017833

Clinical outcomes of percutaneous coronary intervention for *de novo* lesions in small coronary arteries: A systematic review and network meta-analysis

Wen-Rui Ma[1†], Karthik H. Chandrasekharan[2†], Chang-Sheng Nai[1†], Yong-Xiang Zhu[1], Javaid Iqbal[3], Shang Chang[1], You-Wei Cheng[1], Xin-Yu Wang[1], Christos V. Bourantas[2] and Yao-Jun Zhang[1*]

[1]Department of Cardiology, Xuzhou Third People's Hospital, Xuzhou Medical University, Xuzhou, China, [2]Department of Cardiology, Barts Heart Centre, Barts Health NHS Trust, London, United Kingdom, [3]Department of Cardiology, Sheffield Teaching Hospitals NHS Foundation Trust, Sheffield, United Kingdom

Background: Percutaneous coronary intervention (PCI) has a well-established role in revascularization for coronary artery disease. We performed network meta-analysis to provide evidence on optimal intervention strategies for *de novo* lesions in small coronary arteries.

Materials and methods: Enrolled studies were randomized clinical trials that compared different intervention strategies [balloon angioplasty (BA), biolimus-coated balloon (BCB), bare-metal stent (BMS), new-generation drug-eluting stent (New-DES), older generation sirolimus-eluting stent (Old-SES), paclitaxel-coated balloon (PCB), and paclitaxel-eluting stent (PES)] for *de novo* lesions in small coronary arteries. The primary outcome was major adverse cardiac events (MACE).

Results: A total of 23 randomized clinical trials comparing seven intervention devices were analyzed. In terms of the primary outcome, New-DES was the intervention device with the best efficacy [surface under the cumulative ranking curve (SUCRA), 89.1%; mean rank, 1.7], and the Old-SES [risk ratio (RR), 1.09; 95% confidence interval (CI), 0.45–2.64] and PCB (RR, 1.40; 95% CI, 0.72–2.74) secondary to New-DES, but there was no statistically significant difference between these three intervention devices. All DES and PCB were superior to BMS and BA for MACE in both primary and sensitivity analysis. For secondary outcomes, there was no association between all-cause mortality and myocardial infarction (MI) with any intervention strategy, and additionally, the findings of target lesion revascularization (TLR) were similar to the primary outcomes.

Conclusion: Paclitaxel-coated balloon yielded similar outcomes to New-DES for *de novo* lesions in small coronary arteries. Therefore, this network meta-analysis may provide potential support for PCB as a feasible, effective, and safe alternative intervention strategy for the revascularization of small coronary arteries.

Systematic review registration: [https://www.crd.york.ac.uk/PROSPERO/#recordDetails], identifier [CRD42022338433].

KEYWORDS

clinical outcome, *de novo* lesions, drug-coated balloon, new-generation drug-eluting stent, small coronary arteries

Introduction

Small vessel lesions are commonly observed in patients with coronary stenoses on coronary angiography (1). However, there are no currently available guidelines for the optimal and appropriate intervention strategies for percutaneous revascularization for patients with *de novo* small-vessel coronary disease (2, 3). When compared with treatment with bare-metal stents (BMS), the contemporary intervention strategy with drug-eluting stents (DES), reduces the rates of stent thrombosis from neointimal hyperplasia, but there is some evidence that there is an increased risk of late and very late stent thrombosis (4–6). Furthermore, late complications include in-stent restenosis, and subsequently, the introduction of the drug-coated balloon (DCB) has addressed this (7–9). Despite these advances in treating coronary artery disease, there remains controversy in defining the most appropriate treatment strategy for small-vessel coronary disease.

Paclitaxel and sirolimus and its derivatives are mainly used in coating DES and DCB, and with improving technology and techniques, clinical outcomes varied between the older generation and new-generation DES (New-DES), and between different types of antiproliferative drugs (10, 11). Previous network meta-analysis has suggested that older generation sirolimus-eluting stent (Old-SES) is superior to paclitaxel-eluting stent (PES) and even DCB for target lesion revascularization (TLR) in small-vessel coronary disease (12). However, several recent studies have established that DCB was associated with comparable outcomes for the treatment of *de novo* small-vessel disease when compared with DES (13–15).

Despite the promising outcomes demonstrated by DCB and DES, the most appropriate intervention strategy in terms of clinical outcome remains inconclusive. Therefore, we performed a network meta-analysis comparing the clinical outcomes of the different intervention strategies, with the aim of establishing whether there is one strategy that may be optimal, based on current evidence.

Materials and methods

This network meta-analysis followed the PRISMA Statement (16) and was registered with PROSPERO (CRD42022338433).

Data sources and search

PubMed, Embase, and Cochrane databases were systematically searched to collect all eligible randomized clinical trials that assessed different intervention strategies for the treatment of small vessel coronary stenoses up to July 2022. The detailed search strategy is presented in **Supplementary Table 1**. All citations were imported into Endnote X9 for manual screening according to the inclusion criteria.

Intervention strategies

The intervention strategies were divided into seven classifications for comparison: balloon angioplasty (BA), biolimus-coated balloon (BCB), BMS, New-DES, Old-SES, paclitaxel-coated balloon (PCB), and PES. Classification of DCB and DES based on the type of antiproliferative drug is included in **Supplementary Table 2**.

Study selection

All eligible randomized clinical studies compared intervention devices in *de novo* lesions of native small coronary vessels (vessel diameter $\leq$2.75 or $\leq$3.0 mm) and reported one or more clinical outcomes of interest. The primary outcome was major adverse cardiac events (MACE), and secondary outcomes were all-cause mortality, myocardial infarction (MI), and TLR. The definitions of MACE are similar in most studies and are summarized in **Supplementary Table 3**.

Additionally, studies comparing a combination of intervention devices were excluded. Meanwhile, we screened studies from published meta-analyses to compensate for the limitation of the search algorithm.

Data extraction and quality assessment

Two investigators (WRM, CSN) independently assessed the terms to avoid bias in the data search and abstraction process. The opinion of a third investigator was sought in case of disagreement. Extracted data included study and patient characteristics, the diameter of reference vessels, the longest time of clinical follow-up, and relevant clinical outcomes. The trials were subsequently divided into low risk, unclear risk, and high risk followed by the Cochrane risk of bias assessment tool (17).

Statistical analysis

We compared different intervention strategies for treating *de novo* lesions in small vessel coronary arteries with a network meta-analysis using a random-effects model in a frequentist framework. All data were analyzed by *network* and *mvmeta* packages using STATA version 13.0 (StataCorp, college station, TX, USA). The risk ratio (RR) and 95% confidence intervals (CIs) were used to evaluate clinical outcomes. We used network plots to visualize the connections between studies in each clinical outcome. The league tables were employed to illustrate the result of direct and indirect comparisons in different clinical outcomes and 95% CI of 1 indicated no statistical significance. The surface under the cumulative ranking curve (SUCRA) was used to rank intervention strategies in clinical outcomes, with larger values ranked relatively higher. The radar plot was used to summarize the ranking of pre-defined clinical outcomes. The heterogeneity was assessed by I^2 and τ^2 statistics. The node split method was used to detect local inconsistency, and P-value > 0.05 indicated no inconsistency. Funnel plots were used to detect the existence of publication bias by visual inspection. Sensitivity analysis was performed on clinical outcomes of MACE and TLR, excluding the PICCOLETO study (18) with a sample size of <100, and was terminated early due to the higher incidence of MACE suffered by the DCB group.

Results

Study selection and characteristics

The flowchart of study selection is presented in **Figure 1**. Twenty-three eligible randomized clinical trials were screened

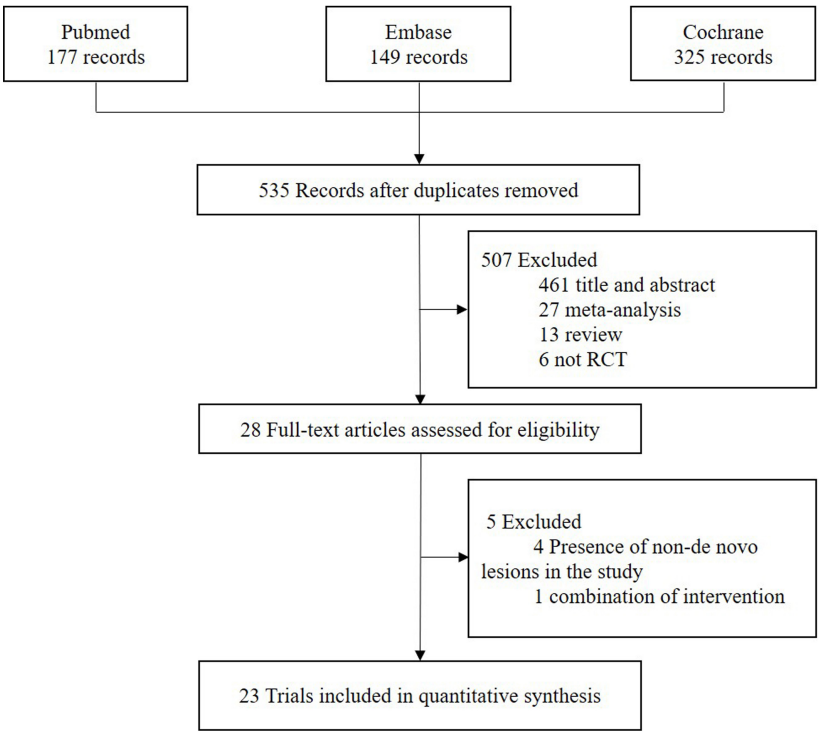

FIGURE 1
Flowchart of study selection.

TABLE 1 Basic characteristics of included studies.

Trial	Year	Reference vessel, mm	Interventions	Sample size	Mean age	Males, (%)	Diabetes, (%)	Prior MI, (%)	Unstable angina (%)	Follow up, months
Ardissino et al. (20)	2004	≤2.75	SES/BMS	129	63.6 ± 11.27	76.7	19.4	29.5	NA	8
				128	63.7 ± 10.9	66.4	29.7	28.1		
BELLO	2015	<2.8	PCB/PES	90	64.8 ± 8.5	80.0	43.3	51.1	24.4	24
				92	66.4 ± 9.0	77.2	38.0	35.9	21.7	
BESMART	2001	<3.0	BMS/BA	176	62 ± 10	73.4	22	31.7	50.0	6
				166	61 ± 10	79.3	12	43.3	42.8	
BIO-RISE CHINA	2022	2.0–2.75	BCB/BA	105	61.3 ± 8.8	72.4	34.3	20.0	60.0	12
				103	61.6 ± 8.1	66.3	34.7	26.7	61.4	
COAST	2015	2.0–2.6	BMS/BA	393	61 ± 10	72.3	19.6	48.3	17.5	8
				195	61 ± 10	75.1	17	46.0	15	
C-SIRIUS	2003	2.5–3.0	SES/BMS	50	60.3 ± 10.6	70	24	48	48	9
				50	60.7 ± 9.1	68	24	42	54	
De luca et al. (22)	2006	≤3.0	BMS/BA	387	61 ± 12	74.2	12.1	10.6	NA	12
				411	61 ± 12	74.2	11.7	8.3		
E-SIRIUS	2003	2.5–3.0	SES/BMS	175	62.0 ± 11.4	70	19	41	30	9
				177	62.6 ± 10.3	71	27	43	36	
Funatsu et al. (24)	2017	2.0–2.75	PCB/BA	92	68 ± 10	78	48	NA	NA	6
				41	69 ± 11	68	32			
Hanekamp et al. (25)	2004	<3.0	BMS/BA	250	61 ± 9	64	32	17	NA	12
				246	61 ± 10	71	32	16		
ISAR-SMART 3	2006	<2.8	SES/PES	180	65.7 ± 10.4	75	NA	31/29	27	12
				180	67.4 ± 10.9	69			35	
Kinsara et al. (39)	2003	≤2.5	BMS/BA	96	54 ± 11	70	61	64	15	6
				106	56 ± 11	86	50	59	16	
LASMAL I	2005	<2.9	BMS/BA	124	NA	82	25	NA	65	9
				122		73	28		59	
LASMAL II	2005	2.0–2.9	BMS/BA	111	NA	73	NA	NA	64.5	12
				109		77			69	
Park et al. (40)	2000	<3.0	BMS/BA	60	60.2 ± 7.5	62	13.3	15	18.3	6
				60	61.5 ± 8.4	65	11.6	10	20	
PICCOLETO	2015	≤2.75	PCB/PES	28	68 ± 9	78.6	37.9	17.9	NA	9
				29	67 ± 10	75.9	46.4	20.7		
PICCOLETO II	2020	2.0–2.75	PCB/EES	118	64 ± 23.7	70.3	38.0	38	14.4	12
				114	66 ± 23.7	76.9	35.4	30	18	
RESTORE	2018	2.25–2.75	PCB/ZES	116	60.1 ± 10.5	66.4	39.7	22.4	69.0	24
				114	60.5 ± 10.8	77.2	42.1	24.6	71.1	

(Continued)

10.3389/fcvm.2022.1017833

TABLE 1 (Continued)

Trial	Year	Reference vessel, mm	Interventions	Sample size	Mean age	Males, (%)	Diabetes, (%)	Prior MI, (%)	Unstable angina (%)	Follow up, months
SISA	2001	2.3–2.9	BMS/BA	182	60.6 ± 10.3	66.3	17.8	31.9	34.3	6
				169	59.9 ± 10.5	67.0	20.9	35.1	29.1	
SISCA	2001	2.1–3.0	BMS/BA	74	63.1 ± 11.2	56.8	12.2	41.9	25.7	5
				71	62.7 ± 10.1	73.3	14.1	45.1	21.1	
SPIRIT III	2009	2.5	EES/PES	160	63.84 ± 10.71	60.6	34.4	23.7	23.7	9
				59	63.62 ± 10.31	47.5	39.0	17.2	31.0	
STRESS	1998	<3.0	BMS/BA	163	59 ± 10	74	17	19	56	12
				168	61 ± 11	68	16	15	48	
TAXUS V subgroup	2005	2.25	PES/BMS	106	NA	NA	NA	NA	31.5	9
				93					29.9	

BA, balloon angioplasty; BMS, bare-metal stent; DCB, drug-coated balloon; EES, everolimus-generation drug-eluting stent; PES, paclitaxel-eluting stent; SES, sirolimus-eluting stent; ZES, zotarolimus-eluting stent.

for this network meta-analysis. The characteristics of these included studies are summarized in **Table 1**. The longest clinical follow-up period was 24 months. The network plot of direct comparisons in seven intervention strategies (BA, BCB, BMS, New-DES, Old-SES, PCB, and PES) was shown in **Figure 2**. The BCB is the latest intervention device available, leading to limited comparisons with other devices. A large-scale trial, BASKET SMALL 2, was excluded due to a combination of PES and New-DES in the DES group (19).

Risk of bias assessment

The risk of bias assessment of the 23 included trials is presented in **Supplementary Figure 1**. Furthermore funnel plots for each clinical outcome to visually show publication bias are presented in **Supplementary Figure 2**. Loop inconsistency was low for all-cause mortality in the primary analysis, and MACE and TLR in the sensitivity analysis (**Supplementary Figure 3**). In contrast, loop-specific heterogeneity was relatively higher for other clinical outcomes in the primary analysis (**Supplementary Figure 4**).

Primary outcome

The network of intervention device comparisons for MACE was available in 20 studies (18, 20–37). All intervention devices

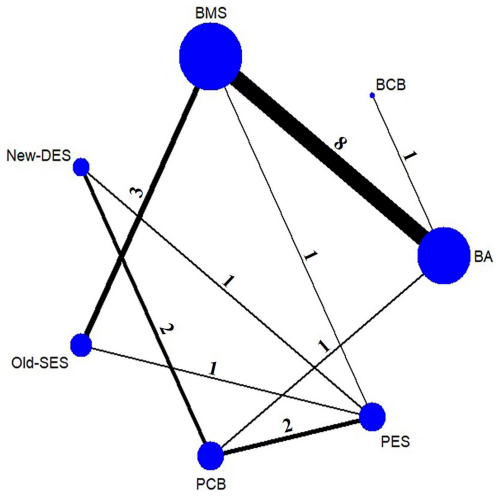

FIGURE 2
Network plot of intervention strategies for MACE. The nodes indicate intervention strategies. The size of the nodes represents the sample size of the study. The line between nodes is the number of studies for direct comparison. BA, balloon angioplasty; BCB, biolimus-coated balloon; BMS, bare-metal stent; New-DES, new-generation drug-eluting stent; Old-SES, older generation sirolimus-eluting stent; PCB, paclitaxel-coated balloon; PES, paclitaxel-eluting stent.

TABLE 2 The primary network meta-analysis estimates of MACE and TLR.

A

MACE

New-DES	1.09 (0.45, 2.64)	1.40 (0.72, 2.74)	1.90 (0.92, 3.92)	2.87 (0.99, 8.27)	3.18 (1.37, 7.38)	4.37 (1.86, 10.28)
0.92 (0.38, 2.24)	Old-SES	1.29 (0.64, 2.58)	1.74 (1.02, 2.98)	2.64 (1.24, 5.62)	2.93 (1.98,4.33)	4.02 (2.63, 6.16)
0.71 (0.36, 1.40)	0.78 (0.39, 1.56)	PCB	1.35 (0.83, 2.20)	2.05 (0.83, 5.03)	2.27 (1.21, 4.27)	3.12 (1.63, 5.96)
0.53 (0.26, 1.09)	0.57 (0.34, 0.98)	0.74 (0.45, 1.20)	PES	1.51 (0.68, 3.35)	1.68 (1.06, 2.66)	2.31 (1.41, 3.78)
0.35 (0.12, 1.01)	0.38 (0.18, 0.81)	0.49 (0.20, 1.20)	0.66 (0.30, 1.46)	BCB	1.11 (0.58, 2.12)	1.52 (0.82, 2.85)
0.31 (0.14, 0.73)	0.34 (0.23, 0.50)	0.44 (0.23, 0.83)	0.60 (0.38, 0.94)	0.90 (0.47, 1.72)	BMS	1.37 (1.16, 1.63)
0.23 (0.10, 0.54)	0.25 (0.16, 0.38)	0.32 (0.17, 0.61)	0.43 (0.26, 0.71)	0.66 (0.35, 1.22)	0.73 (0.61, 0.86)	BA

B

TLR

New-DES	1.20 (0.43, 3.36)	1.96 (0.90, 4.28)	2.55 (1.03, 6.35)	3.92 (0.94, 16.42)	4.97 (1.79, 13.82)	7.48 (2.65, 21.10)
0.83 (0.30, 2.34)	Old-SES	1.64 (0.73, 3.67)	2.13 (1.26, 3.60)	3.28 (1.09, 9.89)	4.15 (2.63, 6.55)	6.24 (3.80, 10.25)
0.51 (0.23, 1.11)	0.61 (0.27, 1.37)	PCB	1.30 (0.68, 2.50)	2.00 (0.56, 7.13)	2.53 (1.15, 5.57)	3.81 (1.70, 8.50)
0.39 (0.16, 0.97)	0.47 (0.28, 0.79)	0.77 (0.40, 1.48)	PES	1.54 (0.49, 4.77)	1.95 (1.15, 3.29)	2.93 (1.68, 5.12)
0.25 (0.06, 1.07)	0.31 (0.10, 0.92)	0.50 (0.14, 1.79)	0.65 (0.21, 2.02)	BCB	1.27 (0.46, 3.47)	1.91 (0.71, 5.11)
0.20 (0.07, 0.56)	0.24 (0.15, 0.38)	0.39 (0.18, 0.87)	0.51 (0.30, 0.87)	0.79 (0.29, 2.16)	BMS	1.50 (1.23, 1.84)
0.13 (0.05, 0.38)	0.16 (0.10, 0.26)	0.26 (0.12, 0.59)	0.34 (0.20, 0.60)	0.52 (0.20, 1.41)	0.67 (0.54, 0.81)	BA

BA, balloon angioplasty; BCB, biolimus-coated balloon; BMS, bare-metal stent; MACE, major adverse cardiac events; New-DES, new-generation drug-eluting stent; Old-SES, older generation sirolimus-eluting stent; PCB, paclitaxel-coated balloon; PES, paclitaxel-eluting stent; TLR, target lesion revascularization. Each area represents the value of RR and 95% CI. The blue area represents different intervention strategies; the brown area represents statistically significant.

except BCB were superior to BMS and with regards to MACE, while BMS was more effective than BA (Table 2A). New-DES was ranked as the most appropriate intervention strategies for MACE (Figure 3), with a non-significant RR of 0.92 (0.38–2.24) compared with Old-SES, 0.71 (0.36–1.40) compared with PCB, 0.53 (0.26–1.09) compared with PES, 0.35 (0.12–1.01) compared with BCB (Table 2A). In addition, Old-SES ranked second to New-DES, with a significant difference RR of 0.57 (0.34–0.98) compared with PES, and 0.38 (0.18–0.81) compared with BCB (Table 2A). For the primary outcome, PCB is more effective than BMS and BA whilst not being inferior to other intervention devices.

Secondary outcomes

Twenty-three trials yielded data for direct and indirect comparisons of all-cause mortality and MI (18, 20–40). BCB was ranked the highest, followed by PCB (Figure 2), but no statistically significant differences were found among all intervention strategies (Supplementary Table 4).

The results of TLR were similar to those of MACE. New-DES, Old-SES, PCB, and PES had a significantly lower risk of TLR than BMS and BA, whereas BMS was superior to BA (Table 2B). New-DES was the optimal intervention device and Old-SES second best with RR of 0.83 (0.30–2.34) for New-DES vs. Old-SES (Figure 2, Table 2B); followed by PCB with RR of 0.51 (0.23–1.11) for New-DES vs. PCB; by PES with RR of 0.39 (0.16–0.97) for New-DES vs. PES; by BCB with RR of 0.25 (0.06–1.07) for New-DES vs. BCB. Moreover, Old-SES was superior to PES (RR 0.47, 95% CI 0.28–0.79) and BCB (RR 0.31, 95% CI 0.10–0.92) (Table 2B). With regards to TLR, there was no significant difference in the effectiveness of percutaneous coronary intervention (PCI) with PCB device for *de novo* lesions in small coronary vessels vs. DES.

Sensitivity analysis

A sensitivity analysis was performed for MACE and TLR by excluding PICCOLETO trial due to the potential risk of bias. With regards to MACE, the efficacy of New-DES was superior to both PES (RR 0.42, 95% CI 0.20–0.88) and BCB (RR 0.29, 95% CI 0.10–0.84). Furthermore, PCB was superior to PES (RR 0.53, 95% CI 0.31–0.90) and BCB (RR 0.37, 95% CI 0.15–0.91) for primary outcomes (Table 3A). With regards to TLR, New-DES was superior to BCB (RR of 0.18 95% CI 0.04–0.75); additionally, PCB was superior to BCB (RR 0.44, 95% CI 0.21–0.94) (Table 3B). Similar to the primary analysis, PCB was not inferior to New-DES and Old-SES.

Discussion

To our knowledge, this is the first network meta-analysis to compare the efficacy and safety of older generation and

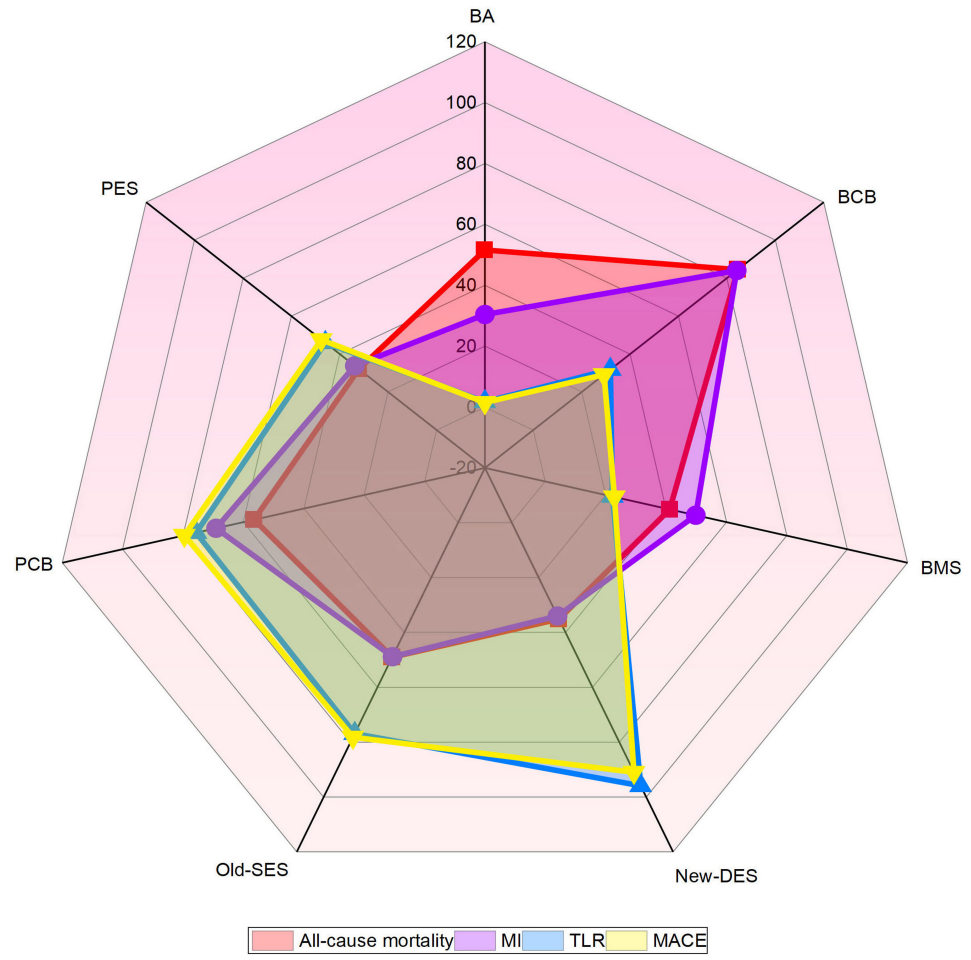

FIGURE 3
Radar map of ranked intervention strategies in all clinical outcomes. The different colored labeled points represent the SUCRA of each intervention strategy for different clinical outcomes. BA, balloon angioplasty; BCB, biolimus-coated balloon; BMS, bare-metal stent; MACE, major adverse cardiac events; MI, myocardial infarction; New-DES, new-generation drug-eluting stent; Old-SES, older generation sirolimus-eluting stent; PCB, paclitaxel-coated balloon; PES, paclitaxel-eluting stent; TLR, target lesion revascularization.

new generation PCI devices in the context of small coronary artery stenosis. The major findings are as follows: (1) PCB is not inferior to New-DES and Old-SES in all clinical outcomes of interest and can be considered as an effective alternative intervention device for *de novo* lesions in small coronary arteries; (2) New-DES ranked first but was not statistically different from the Old-SES and PCB either in the primary or sensitivity analysis; (3) There was no significant difference in the risk of all-cause mortality and MI across all included intervention strategies.

A complication of stent implantation is vessel restenosis which can be angiographically quantified measured by late lumen loss, and the absolute value of late lumen loss does not vary by vessel diameter, therefore smaller vessels are more affected by and are more prone to restenosis (41–43). Devices used for PCI are rapidly evolving, with the advent of new-generation devices as described. For instance, DES have been shown to be effective in the treatment of small vessel lesions in multiple studies (26, 34, 35). However, more recently the use of DCB in the treatment of small vessel coronary disease has been highlighted, delivering the highly lipophilic drug directly and rapidly to the vessel wall (43). Specific DCB such as PCB are already established in treating in-stent restenosis (9), and furthermore, DCB are now suggested in guidelines for the treatment of in-stent restenosis, to improve quality of life (44). This study provides further evidence that PCB is as effective as DES for all clinical outcomes of interest in *de novo* lesions of small coronary arteries. Therefore, DCB can be an alternative interventional strategy to DES without implantation.

While this study found that BA without antiproliferative drugs was the least effective intervention device for the treatment of coronary stenoses, PCB combines properties of both BA and DES, i.e., intervening without implantation while delivering antiproliferative drugs to the vessel wall. An

10.3389/fcvm.2022.1017833

TABLE 3 The sensitivity network meta-analysis estimates of MACE and TLR.

A

MACE

New-DES	1.25 (0.64, 2.44)	1.32 (0.54, 3.20)	2.37 (1.13, 4.94)	3.41 (1.20, 9.70)	3.84 (1.66, 8.88)	5.20 (2.21, 12.20)
0.80 (0.41, 1.56)	PCB	1.05 (0.51, 2.16)	1.89 (1.11, 3.22)	2.73 (1.10, 6.73)	3.07 (1.59, 5.91)	4.16 (2.13, 8.13)
0.76 (0.31, 1.84)	0.95 (0.46, 1.94)	Old-SES	1.80 (1.07, 3.03)	2.59 (1.24, 5.39)	2.91 (1.99, 4.26)	3.95 (2.61, 5.96)
0.42 (0.20, 0.88)	0.53 (0.31, 0.90)	0.56 (0.33, 0.94)	PES	1.44 (0.67, 3.11)	1.62 (1.04, 2.53)	2.20 (1.37, 3.52)
0.29 (0.10, 0.84)	0.37 (0.15, 0.91)	0.39 (0.19, 0.80)	0.69 (0.32, 1.50)	BCB	1.13 (0.60, 2.11)	1.52 (0.83, 2.79)
0.26 (0.11, 0.60)	0.33 (0.17, 0.63)	0.34 (0.23, 0.50)	0.62 (0.39, 0.96)	0.89 (0.47, 1.66)	BMS	1.35 (1.15, 1.59)
0.19 (0.08, 0.45)	0.24 (0.12, 0.47)	0.25 (0.17, 0.38)	0.46 (0.28, 0.73)	0.66 (0.36, 1.20)	0.74 (0.63, 0.87)	BA

B

TLR

New-DES	1.77 (0.62, 5.09)	1.71 (0.79, 3.73)	3.90 (1.50, 10.11)	5.59 (1.34, 23.44)	7.21 (2.54, 20.45)	10.66 (3.72, 30.60)
0.56 (0.20, 1.62)	Old-SES	0.97 (0.40, 2.33)	2.20 (1.33, 3.65)	3.16 (1.07, 9.32)	4.07 (2.61, 6.34)	6.02 (3.73, 9.72)
0.58 (0.27, 1.27)	1.03 (0.43, 2.49)	PCB	2.27 (1.06, 4.88)	3.26 (0.89, 12.00)	4.20 (1.78, 9.92)	6.22 (2.61, 14.82)
0.26 (0.10, 0.67)	0.45 (0.27, 0.75)	0.44 (0.21, 0.94)	PES	1.44 (0.47, 4.35)	1.85 (1.11, 3.08)	2.74 (1.60, 4.69)
0.18 (0.04, 0.75)	0.32 (0.11, 0.93)	0.31 (0.08, 1.13)	0.70 (0.23, 2.11)	BCB	1.29 (0.48, 3.46)	1.91 (0.72, 5.03)
0.14 (0.05, 0.39)	0.25 (0.16, 0.38)	0.24 (0.10, 0.56)	0.54 (0.32, 0.90)	0.78 (0.29, 2.09)	BMS	1.48 (1.23, 1.78)
0.09 (0.03, 0.27)	0.17 (0.10, 0.27)	0.16 (0.07, 0.38)	0.37 (0.21, 0.63)	0.52 (0.20, 1.38)	0.68 (0.56, 0.81)	BA

BA, balloon angioplasty; BCB, biolimus-coated balloon; BMS, bare-metal stent; MACE, major adverse cardiac events; New-DES, new-generation drug-eluting stent; Old-SES, older generation sirolimus-eluting stent; PCB, paclitaxel-coated balloon; PES, paclitaxel-eluting stent; TLR, target lesion revascularization. Each area represents the value of RR and 95% CI. The blue area represents different intervention strategies; the brown area represents statistically significant.

additional benefit of PCB compared with DES is the shortened duration of dual antiplatelet therapy, which may be especially valuable in patients with high bleeding risk (45, 46). Moreover, PCB could reduce thrombosis and MI without altering the anatomical morphology of the vessels (47, 48). In addition, consistent with previous studies (37, 49) our additional analysis further provides evidence that DCB was not inferior to DES in terms of TLR and MACE (**Supplementary Table 5**). Thus, PCB provides effective treatment of *de novo* lesions in small coronary arteries while allowing repeatability of the procedure. In this network meta-analysis, the composite endpoint of MACE mostly consisted of revascularization (**Supplementary Table 3**), which may drive similar clinical outcomes of MACE and TLR in the treatment of small vessels in *de novo* lesions by different intervention strategies. Alternatively, the pre-determined angiographic follow-up of the included studies may contribute to an increased incidence of TLR, which directly correlates to a higher MACE. Conversely, an observational study reported that the risk of restenosis was twice as high in the DCB group as in the New-DES group. Therefore, the efficacy and safety of DCB still require longer clinical follow-up to be determined (50, 51). In previous studies, the risk of clinical events did not increase significantly over time, and DCB may be an intervention strategy that will benefit patients undergoing PCI in the long term (30, 49). However, the efficacy and safety of DCB still require longer clinical follow-up to be determined. Sirolimus and its derivatives have also been used in DCB in recent years (52, 53), but in this analysis, we could not draw similar conclusions to PCB since only one study included sirolimus-coated balloon was eligible. Similarly, the effect of different brands of DCB varies. The DIOR DCB in the PICCOLETO study was terminated early due to its lower paclitaxel drug concentration resulting in a higher incidence of MACE. However, Venetsanos et al. (54) showed that no significant differences were found among the SeQuent Please, IN.PACT Falcon, and Pantera Lux DCB in clinical outcomes. More studies are needed in the future to demonstrate the availability of sirolimus-coated balloons in small coronary arteries. Compared to older generation DES, the New-DES has improved the technology and technique of stents, contributing to more effective clinical outcomes (55, 56). Recent studies have shown that New-DES could be effective in treating lesions in small coronary arteries (57, 58). New-DES with thinner stent struts may improve the feasibility of the treatment of small coronary arteries. A previous network meta-analysis including 89 trials comparing different contemporary intervention devices reported that new generation bioabsorbable polymers biolimus-eluting stents demonstrated superior clinical outcomes when compared with older generation DES (59). In addition, a pooled analysis yielded similar conclusions (60). Unfortunately, our findings failed to validate the superiority of New-DES for

Old-SES in *de novo* lesions of small arteries despite the New-DES ranking highest but do so for PES specifically. It is also important to note that the comparison between the Old-SES and New-DES was derived only from an indirect comparison, and there was no direct comparison of the results to prove the inferiority or superiority of both, and this limited statistical power may be the reason for the lack of statistical difference between them. Therefore, head-to-head studies are needed in the future to investigate whether differences are available between Old-SES and New-DES.

Another finding is that there is no association with the risk of all-cause mortality and MI, regardless of the intervention device used. It has been demonstrated that the type of intervention devices was independent of the incidence of MI in the long-term follow-up (61). Indeed, in our network meta-analysis, although PCB and DES without PES significantly reduced the risk of MACE and TLR, this benefit did not extend to all-cause mortality and MI, which requires additional trials to explore the contributing factors affecting them.

Limitations

Firstly, the inconsistency of the patient population in the included studies may lead to instability of the results. Secondly, varying follow-up times may result in the benefits of different intervention strategies for certain clinical outcomes not being apparent, but for our study, the longest follow-up time was selected. Thirdly, the definition of the primary outcome was not uniform across the included trials, but this limitation is frequently encountered in all meta-analyses. In addition, small coronary arteries were defined as $\leq$3 mm in diameter in this network meta-analysis, but the cut-offs used to define small vessels varied among the included studies, and so there is a need for further studies to compare the effectiveness of different intervention strategies in "truly" small vessels. Finally, despite the inclusion of sensitivity analyses, with the exception of BMS vs. BA, there are limited studies directly comparing intervention devices.

Conclusion

This network meta-analysis provides evidence that when compared with new-generation DES, DCB is associated with comparable outcomes in treating *de novo* lesions of small coronary arteries, suggesting that DCB may be a favorable alternative intervention strategy for small vessels.

Data availability statement

The original contributions presented in this study are included in the article/**Supplementary material**, further inquiries can be directed to the corresponding author.

Author contributions

Y-JZ conceptualized and designed the study. W-RM, KC, and C-SN collected the data, conducted the analyses, and drafted the manuscript. Y-JZ, JI, and CB revised the manuscript. Y-XZ, SC, Y-WC, and X-YW performed the data extraction. All authors read and approved the final manuscript.

Conflict of interest

The authors declare that the research was conducted in the absence of any commercial or financial relationships that could be construed as a potential conflict of interest.

Publisher's note

All claims expressed in this article are solely those of the authors and do not necessarily represent those of their affiliated organizations, or those of the publisher, the editors and the reviewers. Any product that may be evaluated in this article, or claim that may be made by its manufacturer, is not guaranteed or endorsed by the publisher.

Supplementary material

The Supplementary Material for this article can be found online at: https://www.frontiersin.org/articles/10.3389/fcvm.2022.1017833/full#supplementary-material

References

1. Kastrati A, Schühlen H, Schömig A. Stenting for small coronary vessels: a contestable winner. *J Am Coll Cardiol.* (2001) 38:1604–7. doi: 10.1016/s0735-1097(01)01589-3

2. Jeger RV, Eccleshall S, Wan Ahmad WA, Ge J, Poerner TC, Shin ES, et al. Drug-coated balloons for coronary artery disease: third report of the International DCB Consensus Group. *JACC Cardiovasc Interv.* (2020) 13:1391–402. doi: 10.1016/j.jcin.2020.02.043

3. Neumann FJ, Sousa-Uva M, Ahlsson A, Alfonso F, Banning AP, Benedetto U, et al. 2018 ESC/EACTS guidelines on myocardial revascularization. *Eur Heart J.* (2019) 40:87–165. doi: 10.1093/eurheartj/ehy394

4. Kalesan B, Pilgrim T, Heinimann K, Räber L, Stefanini GG, Valgimigli M, et al. Comparison of drug-eluting stents with bare metal stents in patients with ST-segment elevation myocardial infarction. *Eur Heart J.* (2012) 33:977–87. doi: 10.1093/eurheartj/ehs036

5. Palmerini T, Biondi-Zoccai G, Della Riva D, Stettler C, Sangiorgi D, D'Ascenzo F, et al. Stent thrombosis with drug-eluting and bare-metal stents: evidence from a comprehensive network meta-analysis. *Lancet.* (2012) 379:1393–402. doi: 10.1016/s0140-6736(12)60324-9

6. Palmerini T, Kirtane AJ, Serruys PW, Smits PC, Kedhi E, Kereiakes D, et al. Stent thrombosis with everolimus-eluting stents: meta-analysis of comparative randomized controlled trials. *Circ Cardiovasc Interv.* (2012) 5:357–64. doi: 10.1161/circinterventions.111.967083

7. Giacoppo D, Alfonso F, Xu B, Claessen B, Adriaenssens T, Jensen C, et al. Paclitaxel-coated balloon angioplasty vs. drug-eluting stenting for the treatment of coronary in-stent restenosis: a comprehensive, collaborative, individual patient data meta-analysis of 10 randomized clinical trials (DAEDALUS study). *Eur Heart J.* (2020) 41:3715–28. doi: 10.1093/eurheartj/ehz594

8. Navarese EP, Austin D, Gurbel PA, Andreotti F, Tantry U, James S, et al. Drug-coated balloons in treatment of in-stent restenosis: a meta-analysis of randomised controlled trials. *Clin Res Cardiol.* (2013) 102:279–87. doi: 10.1007/s00392-012-0532-3

9. Unverdorben M, Vallbracht C, Cremers B, Heuer H, Hengstenberg C, Maikowski C, et al. Paclitaxel-coated balloon catheter versus paclitaxel-coated stent for the treatment of coronary in-stent restenosis. *Circulation.* (2009) 119:2986–94. doi: 10.1161/circulationaha.108.839282

10. Kang SH, Chae IH, Park JJ, Lee HS, Kang DY, Hwang SS, et al. Stent thrombosis with drug-eluting stents and bioresorbable scaffolds: evidence from a network meta-analysis of 147 trials. *JACC Cardiovasc Interv.* (2016) 9:1203–12. doi: 10.1016/j.jcin.2016.03.038

11. Schömig A, Dibra A, Windecker S, Mehilli J, Suárez de Lezo J, Kaiser C, et al. A meta-analysis of 16 randomized trials of sirolimus-eluting stents versus paclitaxel-eluting stents in patients with coronary artery disease. *J Am Coll Cardiol.* (2007) 50:1373–80. doi: 10.1016/j.jacc.2007.06.047

12. Siontis GC, Piccolo R, Praz F, Valgimigli M, Räber L, Mavridis D, et al. Percutaneous coronary interventions for the treatment of stenoses in small coronary arteries: a network meta-analysis. *JACC Cardiovasc Interv.* (2016) 9:1324–34. doi: 10.1016/j.jcin.2016.03.025

13. Li M, Guo C, Lv YH, Zhang MB, Wang ZL. Drug-coated balloon versus drug-eluting stent in de novo small coronary vessel disease: a systematic review and meta-analysis. *Medicine.* (2019) 98:e15622. doi: 10.1097/md.0000000000015622

14. Megaly M, Buda K, Saad M, Tawadros M, Elbadawi A, Basir M, et al. Outcomes with drug-coated balloons vs. drug-eluting stents in small-vessel coronary artery disease. *Cardiovasc Revasc Med.* (2022) 35:76–82. doi: 10.1016/j.carrev.2021.03.008

15. Megaly M, Rofael M, Saad M, Rezq A, Kohl LP, Kalra A, et al. Outcomes with drug-coated balloons in small-vessel coronary artery disease. *Catheter Cardiovasc Interv.* (2019) 93:e277–86. doi: 10.1002/ccd.27996

16. Moher D, Liberati A, Tetzlaff J, Altman DG. Preferred reporting items for systematic reviews and meta-analyses: the PRISMA statement. *BMJ.* (2009) 339:b2535. doi: 10.1136/bmj.b2535

17. Higgins JP, Altman DG, Gøtzsche PC, Jüni P, Moher D, Oxman AD, et al. The Cochrane Collaboration's tool for assessing risk of bias in randomised trials. *BMJ.* (2011) 343:d5928. doi: 10.1136/bmj.d5928

18. Cortese B, Micheli A, Picchi A, Coppolaro A, Bandinelli L, Severi S, et al. Paclitaxel-coated balloon versus drug-eluting stent during PCI of small coronary vessels, a prospective randomised clinical trial. The PICCOLETO study. *Heart.* (2010) 96:1291–6. doi: 10.1136/hrt.2010.195057

19. Jeger RV, Farah A, Ohlow MA, Mangner N, Möbius-Winkler S, Leibundgut G, et al. Drug-coated balloons for small coronary artery disease (BASKET-SMALL 2): an open-label randomised non-inferiority trial. *Lancet.* (2018) 392:849–56. doi: 10.1016/s0140-6736(18)31719-7

20. Ardissino D, Cavallini C, Bramucci E, Indolfi C, Marzocchi A, Manari A, et al. Sirolimus-eluting vs uncoated stents for prevention of restenosis in small coronary arteries: a randomized trial. *JAMA.* (2004) 292:2727–34. doi: 10.1001/jama.292.22.2727

21. Cortese B, Di Palma G, Guimaraes MG, Piraino D, Orrego PS, Buccheri D, et al. Drug-coated balloon versus drug-eluting stent for small coronary vessel disease: PICCOLETO II randomized clinical trial. *JACC Cardiovasc Interv.* (2020) 13:2840–9. doi: 10.1016/j.jcin.2020.08.035

22. De Luca G, Suryapranata H, van 't Hof AW, Ottervanger JP, Hoorntje JC, Dambrink JH, et al. Comparison between stenting and balloon angioplasty in patients undergoing primary angioplasty of small coronary vessels. *Am Heart J.* (2006) 152:915–20. doi: 10.1016/j.ahj.2006.05.023

23. Doucet S, Schalij MJ, Vrolix MC, Hilton D, Chenu P, de Bruyne B, et al. Stent placement to prevent restenosis after angioplasty in small coronary arteries. *Circulation.* (2001) 104:2029–33.

24. Funatsu A, Nakamura S, Inoue N, Nanto S, Nakamura M, Iwabuchi M, et al. A multicenter randomized comparison of paclitaxel-coated balloon with plain balloon angioplasty in patients with small vessel disease. *Clin Res Cardiol.* (2017) 106:824–32. doi: 10.1007/s00392-017-1126-x

25. Hanekamp C, Koolen J, Bonnier H, Oldroyd K, de Boer MJ, Heublein B, et al. Randomized comparison of balloon angioplasty versus silicon carbon-coated stent implantation for de novo lesions in small coronary arteries. *Am J Cardiol.* (2004) 93:1233–7. doi: 10.1016/j.amjcard.2004.01.066

26. Hermiller JB, Fergus T, Pierson W, Su X, Sood P, Sudhir K, et al. Clinical and angiographic comparison of everolimus-eluting and paclitaxel-eluting stents in small coronary arteries: a post hoc analysis of the SPIRIT III randomized trial. *Am Heart J.* (2009) 158:1005–10. doi: 10.1016/j.ahj.2009.09.018

27. Koning R, Eltchaninoff H, Commeau P, Khalife K, Gilard M, Lipiecki J, et al. Stent placement compared with balloon angioplasty for small coronary arteries: in-hospital and 6-month clinical and angiographic results. *Circulation.* (2001) 104:1604–8. doi: 10.1161/hc3901.096695

28. Mehilli J, Dibra A, Kastrati A, Pache J, Dirschinger J, Schömig A. Randomized trial of paclitaxel- and sirolimus-eluting stents in small coronary vessels. *Eur Heart J.* (2006) 27:260–6. doi: 10.1093/eurheartj/ehi721

29. Moer R, Myreng Y, Mølstad P, Albertsson P, Gunnes P, Lindvall B, et al. Stenting in small coronary arteries (SISCA) trial. A randomized comparison between balloon angioplasty and the heparin-coated beStent. *J Am Coll Cardiol.* (2001) 38:1598–603. doi: 10.1016/s0735-1097(01)01602-3

30. Naganuma T, Latib A, Sgueglia GA, Menozzi A, Castriota F, Micari A, et al. A 2-year follow-up of a randomized multicenter study comparing a paclitaxel drug-eluting balloon with a paclitaxel-eluting stent in small coronary vessels the BELLO study. *Int J Cardiol.* (2015) 184:17–21. doi: 10.1016/j.ijcard.2015.01.080

31. Rodriguez A, Rodríguez Alemparte M, Fernández Pereira C, Sampaolesi A, da Rocha Loures Bueno R, Vigo F, et al. Latin American randomized trial of balloon angioplasty vs coronary stenting for small vessels (LASMAL): immediate and long-term results. *Am J Med.* (2005) 118:743–51. doi: 10.1016/j.amjmed.2005.03.030

32. Rodriguez AE, Rodriguez Alemparte M, Fernandez Pereira C, Vigo CF, Sampaolesi A, Bernardi V, et al. Latin American randomized trial of balloon angioplasty versus coronary stenting in diabetic patients with small vessel reference size (Latin American Small Vessel [LASMAL II] trial): immediate and long-term results. *Am Heart J.* (2005) 150:188. doi: 10.1016/j.ahj.2005.05.013

33. Savage MP, Fischman DL, Rake R, Leon MB, Schatz RA, Penn I, et al. Efficacy of coronary stenting versus balloon angioplasty in small coronary arteries. Stent Restenosis Study (STRESS) investigators. *J Am Coll Cardiol.* (1998) 31:307–11. doi: 10.1016/s0735-1097(97)00511-1

34. Schampaert E, Cohen EA, Schlüter M, Reeves F, Traboulsi M, Title LM, et al. The Canadian study of the sirolimus-eluting stent in the treatment of patients with long de novo lesions in small native coronary arteries (C-SIRIUS). *J Am Coll Cardiol.* (2004) 43:1110–5. doi: 10.1016/j.jacc.2004.01.024

35. Schofer J, Schlüter M, Gershlick AH, Wijns W, Garcia E, Schampaert E, et al. Sirolimus-eluting stents for treatment of patients with long atherosclerotic lesions in small coronary arteries: double-blind, randomised controlled trial (E-SIRIUS). *Lancet.* (2003) 362:1093–9. doi: 10.1016/s0140-6736(03)14462-5

36. Stone GW, Ellis SG, Cannon L, Mann JT, Greenberg JD, Spriggs D, et al. Comparison of a polymer-based paclitaxel-eluting stent with a bare metal stent in patients with complex coronary artery disease: a randomized controlled trial. *JAMA.* (2005) 294:1215–23. doi: 10.1001/jama.294.10.1215

37. Tian J, Tang YD, Qiao S, Su X, Chen Y, Jin Z, et al. Two-year follow-up of a randomized multicenter study comparing a drug-coated balloon with a drug-eluting stent in native small coronary vessels: the RESTORE small vessel disease China trial. *Catheter Cardiovasc Interv.* (2020) 95(Suppl. 1):587–97. doi: 10.1002/ccd.28705

38. Haude M, Konorza TF, Kalnins U, Erglis A, Saunamäki K, Glogar HD, et al. Heparin-coated stent placement for the treatment of stenoses in small coronary arteries of symptomatic patients. *Circulation.* (2003) 107:1265–70. doi: 10.1161/01.cir.0000053442.64637.34

39. Kinsara AJ, Niazi K, Patel I, Amoudi O. Effectiveness of stents in small coronary arteries. *Am J Cardiol.* (2003) 92:584–7. doi: 10.1016/s0002-9149(03)00727-6

40. Park SW, Lee CW, Hong MK, Kim JJ, Cho GY, Nah DY, et al. Randomized comparison of coronary stenting with optimal balloon angioplasty for treatment of lesions in small coronary arteries. *Eur Heart J.* (2000) 21:1785–9. doi: 10.1053/euhj.1999.1947

41. Kuntz RE, Safian RD, Levine MJ, Reis GJ, Diver DJ, Baim DS. Novel approach to the analysis of restenosis after the use of three new coronary devices. *J Am Coll Cardiol.* (1992) 19:1493–9. doi: 10.1016/0735-1097(92)90609-q

42. Mauri L, Orav EJ, Kuntz RE. Late loss in lumen diameter and binary restenosis for drug-eluting stent comparison. *Circulation.* (2005) 111:3435–42. doi: 10.1161/circulationaha.104.513952

43. Nestelberger T, Jeger R. Drug-coated balloons for small coronary vessel interventions: a literature review. *Interv Cardiol.* (2019) 14:131–6. doi: 10.15420/icr.2019.06.R3

44. Windecker S, Kolh P, Alfonso F, Collet JP, Cremer J, Falk V, et al. 2014 ESC/EACTS guidelines on myocardial revascularization: the task force on myocardial revascularization of the European Society of Cardiology (ESC) and the European Association for Cardio-Thoracic Surgery (EACTS)developed with the special contribution of the European Association of Percutaneous Cardiovascular Interventions (EAPCI). *Eur Heart J.* (2014) 35:2541–619. doi: 10.1093/eurheartj/ehu278

45. Scheller B, Rissanen TT, Farah A, Ohlow MA, Mangner N, Wöhrle J, et al. Drug-coated balloon for small coronary artery disease in patients with and without high-bleeding risk in the BASKET-SMALL 2 trial. *Circ Cardiovasc Interv.* (2022) 15:e011569. doi: 10.1161/circinterventions.121.011569

46. Corballis NH, Wickramarachchi U, Vassiliou VS, Eccleshall SC. Duration of dual antiplatelet therapy in elective drug-coated balloon angioplasty. *Catheter Cardiovasc Interv.* (2020) 96:1016–20. doi: 10.1002/ccd.28632

47. Sinaga DA, Ho HH, Watson TJ, Sim A, Nyein TT, Jafary FH, et al. Drug-coated balloons: a safe and effective alternative to drug-eluting stents in small vessel coronary artery disease. *J Interv Cardiol.* (2016) 29:454–60. doi: 10.1111/joic.12333

48. Venetsanos D, Lawesson SS, Panayi G, Tödt T, Berglund U, Swahn E, et al. Long-term efficacy of drug coated balloons compared with new generation drug-eluting stents for the treatment of de novo coronary artery lesions. *Catheter Cardiovasc Interv.* (2018) 92:e317–26. doi: 10.1002/ccd.27548

49. Jeger RV, Farah A, Ohlow MA, Mangner N, Möbius-Winkler S, Weilenmann D, et al. Long-term efficacy and safety of drug-coated balloons versus drug-eluting stents for small coronary artery disease (BASKET-SMALL 2): 3-year follow-up of a randomised, non-inferiority trial. *Lancet.* (2020) 396:1504–10. doi: 10.1016/s0140-6736(20)32173-5

50. Silverio A, Buccheri S, Venetsanos D, Alfredsson J, Lagerqvist B, Persson J, et al. Percutaneous treatment and outcomes of small coronary vessels: a SCAAR report. *JACC Cardiovasc Interv.* (2020) 13:793–804. doi: 10.1016/j.jcin.2019.10.062

51. Silverio A, James S, Sarno G. Reply: Swedish coronary angiography and angioplasty registry scare on drug-coated balloons: is it really scary? *JACC Cardiovasc Interv.* (2020) 13:1380–1. doi: 10.1016/j.jcin.2020.04.009

52. Jim MH, Fung RC, Yiu KH. Angiographic result of sirolimus-eluting balloon in de novo small coronary artery lesion (ARSENAL). *Int J Cardiol.* (2016) 222:992–4. doi: 10.1016/j.ijcard.2016.08.133

53. Cortese B, Pellegrini D, Latini RA, Di Palma G, Perotto A, Orrego PS. Angiographic performance of a novel sirolimus-coated balloon in native coronary lesions: the FAtebenefratelli SIrolimus COated NATIVES prospective registry. *J Cardiovasc Med.* (2019) 20:471–6. doi: 10.2459/jcm.0000000000000806

54. Venetsanos D, Omerovic E, Sarno G, Pagonis C, Witt N, Calais F, et al. Long term outcome after treatment of de novo coronary artery lesions using three different drug coated balloons. *Int J Cardiol.* (2021) 325:30–6. doi: 10.1016/j.ijcard.2020.09.054

55. Yoshizaki T, Naganuma T, Kobayashi T, Horikoshi T, Onishi H, Kawamoto H, et al. Long-term follow-up of first generation versus new-generation drug-eluting stents in three-vessel coronary artery disease. *Cardiovasc Revasc Med.* (2017) 18:492–6. doi: 10.1016/j.carrev.2017.04.006

56. Jensen LO, Thayssen P, Christiansen EH, Maeng M, Ravkilde J, Hansen KN, et al. Safety and efficacy of everolimus- versus sirolimus-eluting stents: 5-year results from SORT OUT IV. *J Am Coll Cardiol.* (2016) 67:751–62. doi: 10.1016/j.jacc.2015.11.051

57. Wöhrle J, Markovic S, Rottbauer W, Muramatsu T, Kadota K, Vázquez-González N, et al. Bioresorbable polymer sirolimus-eluting coronary stent compared with permanent polymer everolimus-eluting coronary stent implantation for treatment of small vessel coronary artery disease: CENTURY II trial. *Eurointervention.* (2016) 12:e167–74. doi: 10.4244/eijv12i2a30

58. Buiten RA, Ploumen EH, Zocca P, Doggen CJM, van der Heijden LC, Kok MM, et al. Outcomes in patients treated with thin-strut, very thin-strut, or ultrathin-strut drug-eluting stents in small coronary vessels: a prespecified analysis of the randomized BIO-RESORT trial. *JAMA Cardiol.* (2019) 4:659–69. doi: 10.1001/jamacardio.2019.1776

59. Palmerini T, Biondi-Zoccai G, Della Riva D, Mariani A, Sabaté M, Smits PC, et al. Clinical outcomes with bioabsorbable polymer- versus durable polymer-based drug-eluting and bare-metal stents: evidence from a comprehensive network meta-analysis. *J Am Coll Cardiol.* (2014) 63:299–307. doi: 10.1016/j.jacc.2013.09.061

60. Stefanini GG, Byrne RA, Serruys PW, de Waha A, Meier B, Massberg S, et al. Biodegradable polymer drug-eluting stents reduce the risk of stent thrombosis at 4 years in patients undergoing percutaneous coronary intervention: a pooled analysis of individual patient data from the ISAR-TEST 3, ISAR-TEST 4, and LEADERS randomized trials. *Eur Heart J.* (2012) 33:1214–22. doi: 10.1093/eurheartj/ehs086

61. Palmerini T, Biondi-Zoccai G, Della Riva D, Mariani A, Sabaté M, Valgimigli M, et al. Clinical outcomes with drug-eluting and bare-metal stents in patients with ST-segment elevation myocardial infarction: evidence from a comprehensive network meta-analysis. *J Am Coll Cardiol.* (2013) 62:496–504. doi: 10.1016/j.jacc.2013.05.022

frontiers | Frontiers in Cardiovascular Medicine

TYPE Original Research
PUBLISHED 14 November 2022
DOI 10.3389/fcvm.2022.1051995

OPEN ACCESS

EDITED BY
István Ferenc Édes,
Semmelweis University, Hungary

REVIEWED BY
Attila Oláh,
Semmelweis University, Hungary
Yufeng Jiang,
Suzhou Dushu Lake Hospital, China

*CORRESPONDENCE
Peter Wohlfahrt
wohlfp@gmail.com

SPECIALTY SECTION
This article was submitted to Coronary Artery Disease, a section of the journal Frontiers in Cardiovascular Medicine

RECEIVED 23 September 2022
ACCEPTED 27 October 2022
PUBLISHED 14 November 2022

CITATION
Wohlfahrt P, Jenča D, Melenovský V, Šramko M, Kotrč M, Želízko M, Mrázková J, Adámková V, Pitha J and Kautzner J (2022) Trajectories and determinants of left ventricular ejection fraction after the first myocardial infarction in the current era of primary coronary interventions. *Front. Cardiovasc. Med.* 9:1051995. doi: 10.3389/fcvm.2022.1051995

Trajectories and determinants of left ventricular ejection fraction after the first myocardial infarction in the current era of primary coronary interventions

Peter Wohlfahrt[1,2]*, Dominik Jenča[3,4], Vojtěch Melenovský[3], Marek Šramko[3], Martin Kotrč[3], Michael Želízko[3], Jolana Mrázková[3], Věra Adámková[1], Jan Pitha[3] and Josef Kautzner[3,5]

[1]Department of Preventive Cardiology, Institute for Clinical and Experimental Medicine (IKEM), Prague, Czechia, [2]First Medical School, Charles University, Prague, Czechia, [3]Department of Cardiology, Institute for Clinical and Experimental Medicine (IKEM), Prague, Czechia, [4]Third Medical School, Charles University, Prague, Czechia, [5]Medical and Dentistry School, Palacký University, Olomouc, Czechia

Background: Left ventricular ejection fraction (EF) is an independent predictor of adverse outcomes after myocardial infarction (MI). However, current data on trajectories and determinants of EF are scarce. The present study aimed to describe the epidemiology of EF after MI.

Methods: Data from a single-center prospectively-designed registry of consecutive patients hospitalized at a large tertiary cardiology center were utilized.

Results: Out of 1,593 patients in the registry, 1,065 were hospitalized for MI type I (65.4% STEMI) and had no previous history of heart failure or MI. At discharge, EF < 40% was present in 238 (22.3%), EF 40–50% in 326 (30.6%) and EF >50% in 501 (47.0%). Patients with EF < 40% were often those who suffered subacute and anterior STEMI, had higher heart rate at admission and higher maximal troponin level, and had more often HF signs requiring intravenous diuretics. Among subjects with EF < 40%, the follow-up EF was available in 166 (80% of eligible). Systolic function recovered to EF > 50% in 39 (23.1%), slightly improved to EF 40–50% in 44 (26.0%) and remained below 40% in 86 (50.9%). Systolic function improvement to EF > 40% was predicted by lower severity of coronary atherosclerosis, lower leukocyte count, and the absence of atrial fibrillation.

Conclusions: Despite recent improvements in in-hospital MI care, one in five patients has systolic dysfunction at hospital discharge. Out of these, EF improves in 51%, and full recovery is observed in 23%. The severity of coronary atherosclerosis, inflammatory response to MI, and atrial fibrillation may affect EF recovery.

KEYWORDS

myocardial infarction, ejection fraction (EF%), systolic dysfunction, inflammation, atrial fibrillation, epidemiology

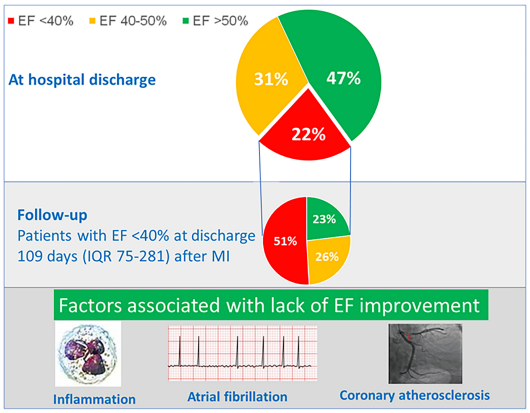

GRAPHICAL ABSTRACT
Trajectories and determinants of EF after the first MI.

Introduction

Left ventricular ejection fraction (EF) is a guideline-recommended tool for risk stratification of patients with acute myocardial infarction (MI) (1). Numerous studies have shown that low EF after MI is associated with an increased risk of cardiovascular and total mortality, heart failure, and sudden cardiac death (2–5). Several studies have also shown that EF may improve after hospital discharge, and such EF recovery is associated with a lower risk of cardiovascular events (6–9) and improved quality of life (10). The phenotype of heart failure with improved ejection fraction has been recently recognized by the guidelines and refers to patients with previous heart failure with reduced ejection fraction who have an LVEF >40% (11, 12).

In the last 20 years, the implementation of evidence-based therapy as primary percutaneous coronary intervention (PCI), dual antiplatelet therapy, and statin therapy have significantly improved MI mortality (13, 14). This may have also influenced systolic dysfunction prevalence and trajectories after MI. However, epidemiologic studies evaluating systolic dysfunction prevalence and trajectories coming from the contemporary era of MI therapy are scarce. Therefore, we sought to evaluate the incidence, trajectories, and determinants of left ventricular ejection fraction among consecutive patients hospitalized for their first MI.

Methods

Population

This study utilized data from the prospective AMBITION registry (Institute for Clinical and Experimental Medicine Acute Myocardial Infarction Registry), which collects clinical data and biospecimens from all consecutive patients hospitalized for acute coronary syndrome at a tertiary heart center since June 2017. During the hospital stay, all patients underwent detailed interviews, and additional information was obtained through manual chart abstraction and laboratory studies. For this analysis, data from individuals without previous history of heart failure and coronary artery disease, hospitalized for type I MI between June 2017 and November 2021 were used. The institutional review board of the Institute for Clinical and Experimental Medicine approved the study, and all participants signed informed consent.

Left ventricular ejection fraction

Left ventricular EF was measured using transthoracic echocardiography. In patients with several in-hospital EF measurements, the last one before hospital discharge was used as the baseline value. According to baseline EF, patients were categorized as having systolic dysfunction (EF < 40%), mid-range EF (EF 40–50%), or preserved systolic function (EF > 50%). In patients with systolic dysfunction at the time of MI hospitalization, optimal medical therapy with angiotensin converting enzyme inhibitor, beta-blocker and spironolactone was initiated. However, in patients with contraindications as hypotension or bradycardia/bradyarrhythmia this was not initiated. The patient was discharged with the recommendation for OMT therapy up-titration by an outpatient cardiologist. In patients with EF <40% at hospital discharge, follow-up EF beyond 6 weeks from the index hospitalization was recorded. By the follow-up EF, patients with systolic dysfunction at hospital discharge were categorized as having full EF recovery (follow-up EF > 50%), slightly improved EF (follow-up EF 40–50%), or persistent systolic dysfunction (follow-up EF < 40%).

Definition of comorbidities

History of diabetes was defined by the use of oral antidiabetic drugs or insulin at the time of hospital admission or by glycated hemoglobin ≥48 mmol/L at the time of hospitalization. Arterial hypertension was defined as self-reported use of antihypertensive drugs at admission. Self-reported history of smoking was used. A person was considered a current smoker if smoking at least one cigarette per day during the last 12 months. Positive family history of CVD was defined by MI or stroke in the first-degree relatives before 55 years in males and before 60 years in females, respectively.

Coronary artery stenosis degree was based on percent diameter stenosis by visual estimation done by an experienced invasive cardiologist. Culprit lesion intervention was performed during the index hospitalization. In patients with multiple vessel disease, additional interventions of non-culprit lesions were done during the index-hospitalization or patients were

invited for additional elective procedure, aiming for complete revascularization. During the follow-up, in none of the studied patient additional intervention was required due to restenosis, in-stent thrombosis or recurrent MI.

Gensini score was used to quantify the overall severity of coronary artery atherosclerosis, while accounting for lesion location, as previously described (15, 16). Mortality data were provided by the Institute of Health Information and Statistics, keeping a list of all deceased by law.

Statistical methods

Data are presented as mean ± standard deviation, median (interquartile range–IQR), or frequency (percent). Analysis of variance (ANOVA), Kruskal-Wallis or chi-square tests were used to compare differences across the three EF groups, as appropriate. Multivariate logistic and linear regression were used to assess factors associated with systolic dysfunction at baseline and EF recovery at follow-up. Factors with a significant association ($p<0.05$) in the univariate analysis (Table 1; Supplementary Table 1) were used as inputs for the multivariate model. Log-rank test was used to compare survival by EF categories. Cox proportional hazard model was used to assess the prognostic value of EF.

Results

Of 1,593 patients in the AMBITION registry, 1,347 had type I MI. Of these, 268 had a previous history of coronary artery disease, and another 14 had chronic heart failure history. Of the 1,065 eligible patients (65.4% STEMI), all had available EF at the time of MI hospitalization.

Systolic dysfunction at the time of MI hospitalization

Baseline echocardiography was performed on the median 1 day (IQR 0–2) after MI. Systolic dysfunction with EF below 40% was present in 238 (22.3%), mid-range systolic function with EF 40–50% in 326 (30.6%) and EF above 50% in 501 (47.0%), respectively. Population demographics by EF categories are shown in Table 1. In the multivariate analysis (Table 2), patients with systolic dysfunction at the time of hospitalization (EF < 40%) were more likely to experience subacute and anterior STEMI, had higher heart rate at admission and higher maximal troponin level, more often clinical signs of heart failure requiring intravenous diuretic therapy and more often pericarditis. After adjustment for age and gender, we found a non-linear association between discharge EF and mortality risk, with increased mortality in subjects with EF < 40% (Figure 1).

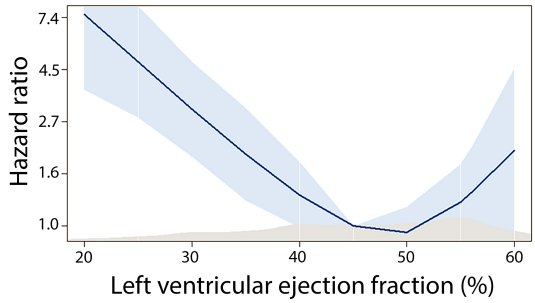

FIGURE 1
Association between discharge ejection fraction and mortality risk.

In the multivariate model, discharge EF was an independent predictor of total mortality risk after MI (Table 3).

Recovery of systolic function

Of the 238 patients with EF < 40% at the time of hospitalization, follow-up EF was not available in 26 due to in-hospital death or death within 6 months since the hospital discharge. Of the 212 eligible patients, follow-up EF was collected in 169 (80% of eligible). The follow-up systolic function evaluation was done on a median of 109 days (IQR 75–281) after MI. During this period, systolic function recovered to EF > 50% in 39 (23.1%), slightly improved to EF 40–50% in 44 (26.0%) and remained below 40% in 86 (50.9%).

Characteristics of patients by EF improvement at follow-up are shown in the Supplementary Table 1. In the multivariate analysis, improvement in systolic function to EF > 40% was predicted by lower severity of coronary artery atherosclerosis (lower GENSINI score), a higher discharge EF, lower leukocyte count and the absence of atrial fibrillation (AF) during MI hospitalization (Table 4). These factors were confirmed in the sensitivity analysis with the absolute change in EF as a dependent variable, with the addition of female gender associated with EF improvement (Supplementary Table 2). Recovery of systolic function was associated with lower mortality risk (log-rank $p = 0.012$) (Figure 2).

Discussion

The present study shows that in the current era of MI therapy, one in five patients after the first MI has reduced EF. In the months following the MI, one in four patients will fully recover EF, with severity of coronary atherosclerosis, inflammatory response, and AF being associated with lack of EF improvement.

10.3389/fcvm.2022.1051995

TABLE 1 Population demographics by left ventricular ejection fraction at the time of hospitalization.

Variable	EF < 40 *N* = 238	EF 40–50 *N* = 326	EF > 50 *N* = 501	*p* for linear trend
Age, years	66.2 ± 12.6	62.8 ± 12.2	63.4 ± 11.7	0.012
Male gender, *n* (%)	177 (74.4)	249 (76.4)	368 (73.5)	0.654
Risk factors				
Arterial hypertension, *n* (%)	106 (44.7)	145 (44.5)	193 (38.6)	0.074
Diabetes, *n* (%)	65 (27.3)	84 (25.8)	122 (24.4)	0.380
Current smoking, *n* (%)	101 (42.4)	168 (51.5)	218 (43.5)	0.801
Statin use before admission, *n* (%)	35 (14.7)	46 (14.1)	112 (22.4)	0.003
Family history of CVD, *n* (%)	68 (28.6)	75 (23.0)	151 (30.1)	0.371
COPD, *n* (%)	15 (6.3)	22 (6.7)	26 (5.2)	0.457
AF history, *n* (%)	11 (4.6)	15 (4.6)	24 (4.8)	0.905
Index event				
CPR before admission, *n* (%)	19 (8.0)	14 (4.3)	20 (4.0)	0.032
STEMI, *n* (%)	202 (84.9)	252 (77.3)	242 (48.5)	0.0001
Subacute MI, *n* (%)	63 (26.5)	51 (15.6)	35 (7.0)	0.0001
Killip class >1, *n* (%)	114 (47.9)	59 (18.1)	47 (9.4)	0.0001
Selective coronarography, *n* (%)	233 (97.9)	323 (99.1)	500 (99.8)	0.009
PCI, *n* (%)	196 (82.4)	277 (85.0)	434 (86.6)	0.129
CABG, *n* (%)	17 (7.1)	35 (10.7)	43 (8.6)	0.732
In-hospital AF, *n* (%)	44 (18.5)	46 (14.1)	40 (8.0)	0.0001
Pericarditis, *n* (%)	14 (5.9)	7 (2.1)	6 (1.2)	0.0001
Intravenous diuretics, *n* (%)	135 (56.7)	64 (19.6)	53 (10.6)	0.0001
Anterior MI, *n* (%)	186 (78.2)	134 (41.1)	142 (28.3)	0.0001
Admission SBP, mmHg	138.2 ± 25.4	140.4 ± 26.3	147.5 ± 26.8	0.0001
Admission DBP, mmHg	79.9 ± 15.9	78.5 ± 14.1	79.6 ± 12.5	0.958
Admission heart rate, min^{-1}	85.2 ± 20.2	76.8 ± 16.8	73.9 ± 16.4	0.0001
Max Troponin natural log, ng/L	7.58 ± 1.56	7.47 ± 1.30	6.4 ± 1.4	0.0001
CKD EPI, ml/min/1.73 m^2	73.9 ± 23.2	78.5 ± 22.1	78.6 ± 21.3	0.014
BMI, kg/m^2	28.3 ± 4.8	28.6 ± 4.9	28.9 ± 4.9	0.135
HbA1c, mmol/L/mol	45.9 ± 13.3	45.7 ± 13.9	44.5 ± 12.4	0.145
Fasting glycemia, mmol/L	9.4 ± 4.6	8.4 ± 3.9	7.8 ± 3.2	0.0001
Total cholesterol, mmol/L	4.9 ± 1.3	4.9 ± 1.2	4.8 ± 1.2	0.829
Triglycerides, mmol/L	1.7 ± 1.7	1.6 ± 1.0	1.9 ± 1.3	0.048
HDL cholesterol, mmol/L	1.2 ± 0.3	1.2 ± 0.3	1.1 ± 0.3	0.002
LDL cholesterol, mmol/L	3.2 ± 1.1	3.3 ± 1.1	3.2 ± 1.1	0.998
Leukocytes, 10^9/L	12.4 ± 4.3	12.0 ± 4.0	11.3 ± 20.7	0.309
Erythrocytes, 10^{12}/L	4.7 ± 0.6	4.7 ± 0.5	4.6 ± 0.5	0.683
Hemoglobin, g/L	141.9 ± 16.8	142.8 ± 16.7	142.2 ± 14.6	0.939
Discharge medication				
ACEi/ARB, *n* (%)	163 (72.4)	258 (79.4)	377 (75.9)	0.538
Beta-blocker, *n* (%)	187 (83.1)	279 (85.8)	384 (77.3)	0.017
Statin, *n* (%)	209 (92.9)	314 (96.6)	485 (97.6)	0.003
Furosemide, *n* (%)	143 (63.6)	56 (17.2)	30 (6.0)	<0.001
Spironolactone, *n* (%)	157 (69.8)	45 (13.8)	16 (3.2)	<0.001
Acetylsalicylic acid, *n* (%)	208 (92.4)	306 (94.2)	481 (96.8)	0.009
Clopidogrel, *n* (%)	87 (38.7)	83 (25.5)	132 (26.6)	0.004
Prasugrel, *n* (%)	5 (2.2)	5 (1.5)	16 (3.2)	0.285
Ticagrelor, *n* (%)	119 (52.9)	222 (68.3)	335 (67.4)	0.001
Warfarin, *n* (%)	24 (10.7)	29 (8.9)	17 (3.4)	<0.001
Apixaban, *n* (%)	4 (1.8)	3 (0.9)	3 (0.6)	0.147
Dabigatran, *n* (%)	6 (2.7)	6 (1.8)	4 (0.8)	0.049
Rivaroxaban, *n* (%)	5 (2.2)	5 (1.5)	8 (1.6)	0.614
Outcome				
Death, *n* (%)	39 (16.4)	18 (5.5)	32 (6.4)	0.0001

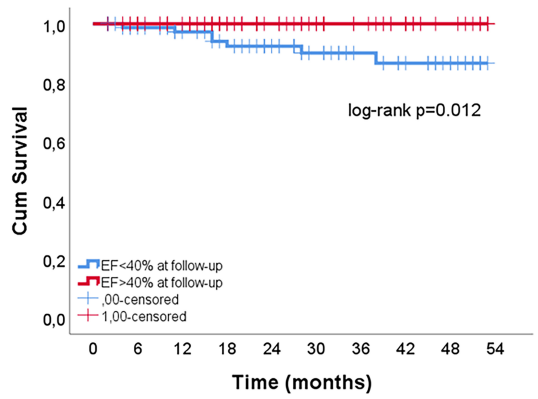

FIGURE 2
The influence of EF improvement on mortality risk in patients with EF<40% at hospital discharge.

TABLE 2 Multivariate logistic regression of factors associated with EF < 40% at the time of hospitalization.

Variable	OR (95% CI)	*p*
Anterior MI	8.39 (5.57–12.65)	0.001
Admission heart rate	1.01 (1.00–10.2)	0.01
STEMI	2.57 (1.60–4.14)	0.001
Subacute MI	1.95 (1.20–3.20)	0.01
Pericarditis	3.13 (1.12–8.74)	0.029
Intravenous diuretics	3.64 (2.16–6.13)	0.001
Maximal troponin level	1.22 (1.07–1.40)	0.003
Killip class above I	2.00 (1.15–3.45)	0.013

TABLE 3 Cox regression of factors associated with mortality after myocardial infarction.

Variable	HR (95% CI)	*p*
Age	1.047 (1.021–1.74)	0.001
CKD EPI	0.978 (0.968–0.989)	0.001
Current smoking	1.875 (1.153–3.048)	0.011
LV EF		0.004
EF < 40% vs. EF > 50%	1.841 (1.065–3.184)	0.029
EF 40–50% vs. EF > 50%	0.669 (0.357–1.251)	0.208
AF during hospitalization	1.688 (1.024–2.785)	0.040
Glycemia	1.063 (1.019–1.110)	0.005
Killip class >I	2.339 (1.402–3.900)	0.001
STEMI	0.510 (0.322–0.809)	0.004

TABLE 4 Multivariate logistic regression of factors associated with systolic function improvement to EF to >40% during follow-up.

Variable	OR (95% CI)	*p*
Coronary atherosclerosis severity (GENSINI score)	0.983 (0.969–0.997)	0.017
Leukocyte count	0.827 (0.735–0.931)	0.002
AF during hospitalization	0.359 (0.130–0.995)	0.049
Left ventricular ejection fraction	1.212 (1.100–1.337)	0.001

There is a lack of historical data on left ventricular systolic function after MI, because EF was not routinely measured in the past. In the Euro Heart Survey analyzing MI management in the year 2000 in 25 European countries, only 73% of STEMI and 61% of non-STEMI patients had EF measured (17). Thus, reported data may be a subject of a selection bias. This may bias direct comparison of historical data coming from the thrombolysis era with data observed in our study.

In the present study, 53% of patients at hospital discharge had EF < 50%. This is very similar to the 46–60% prevalence observed in the thrombolysis era (18–20). Similarly, the 22% prevalence of EF < 40% in our study is close to the 27–36% range observed at the turn of the century (21–24). Thus, despite significant improvements in MI management, systolic dysfunction immediately after MI is still common, with a prevalence similar to that observed in the thrombolysis era. There are several explanations for this finding. First, recent improvements in pre-hospital care led to a decrease in out of hospital mortality (25, 26). Second, introduction of PCI has decreased in-hospital mortality (27, 28). Thus, more patients that would previous die pre- or in-hospital are discharged with systolic dysfunction. Third, the landscape of MI patients is changing, (29) with risk factors as obesity and obesity-related comorbidities increasing especially in young patients with MI (30). Therefore, the higher burden of metabolic risk factors may have influenced systolic dysfunction prevalence.

Among patients with EF < 40% at the hospital discharge, we have observed full EF recovery in 23%. This is much lower than the 42% EF recovery rate observed in a retrospective cohort study of consecutive young patients aged ≤50 hospitalized for their first MI (9). While we did not find any direct effect of age on EF recovery in the present study, the different burden of comorbidities affecting EF recovery in younger subjects may explain this difference. On the other hand, the observed 51% proportion of patients with systolic function improvement to EF ≥ 40 in the present study is higher than the 24% proportion observed at the turn of the century (24). In other recent studies, the proportion of patients with systolic function improvement varies around 50% (8, 31, 32). This suggests that implementation of evidence-based therapy may have increased the proportion of patients with EF recovery. Recent recommendation to use Sodium-glucose

Cotransporter-2 (SGLT2) inhibitors and angiotensin receptor-neprilysin inhibitor (ARNI) in patients with heart failure with reduced ejection fraction may further increase the proportion of patients with EF improvement after MI (11). However, the PARADISE-MI study in patients with acute MI did not show superiority of ARNI on cardiovascular mortality and incident heart failure as compared to ramipril (33).

In the present study, we have identified several factors that may influence the course of EF recovery. Increased leukocytes count as a proxy of excess innate immunity activation was associated with a lower likelihood of EF improvement at follow-up. Lately, the importance of inflammation in patients after MI has been increasingly recognized (34). Due to excessive and prolonged inflammatory response to MI leukocytes infiltrate viable border zone of the infarction, thereby extending ischemic injury beyond the original MI zone (35). Prolonged inflammation also triggers adverse left ventricular remodeling. In the CANTOS study among patients after MI, monoclonal antibody targeting IL-1β significantly reduced recurrent major adverse cardiovascular events (36). Similarly, a low-dose colchicine, a potent anti-inflammatory drug affecting inflammasome, has decreased risk of ischemic cardiovascular events in patients after recent MI (37). Our results suggest that targeting of the inflammatory resolution pathways may influence EF recovery in patients with systolic dysfunction and increased inflammatory response to MI.

Another factor identified in the present study, that increased mortality risk by 69% and decreased EF improvement odds by 64%, was the new onset of AF during the MI hospitalization. On the other hand, pre-existing AF was not associated with mortality risk or EF recovery. This is in line with a previous study, in which mortality risk associated with a new onset AF during MI was 87% higher as compared to pre-existing AF (38). Several mechanisms such as atrial ischemia, volume overload, inflammation, and pericarditis have been described to trigger AF during MI (39). Thus new onset AF may be a marker of risk factors, which are known to affect EF recovery and increase heart failure risk. However direct hemodynamic effects of AF caused by the loss of atrial contraction, heart rate irregularity and increased heart rate may negatively influence EF recovery (40). Whether targeting patients with new onset AF can decrease mortality risk and improve EF after MI needs to be further evaluated.

In our sensitivity analysis, female gender was associated with a higher increase in EF during follow-up. This is in line with a meta-analysis of 18 studies, in which females had a higher odds of EF recovery (41). The gender difference may be explained by a higher level of signaling molecules with anti-inflammatory effects and more reparative immune cells in females (42).

Our study evaluating EF trajectories after MI is limited by the echocardiographic method of EF measurement. A large intra- and inter-individual variability in echocardiographic EF measurement has been reported (43). Despite this limitation, our and other studies have shown the prognostic value of this parameter. Because follow-up EF was available in 80% of eligible patients, our results may be influenced by the selection bias. The major strength of our study is the use of prospective registry which collects data of all consecutive patients hospitalized for MI at a high-volume center. This precludes several sources of bias. Furthermore, all patient records were adjudicated by the study physicians, which is more accurate that data derived from billing codes.

In summary, systolic dysfunction after the first MI is still common, with 1 in 5 patients having EF $< 40\%$. Severity of coronary atherosclerosis, inflammatory response to MI, and AF may all affect EF recovery. These observations provide novel therapeutic targets for EF recovery.

Data availability statement

The raw data supporting the conclusions of this article will be made available by the authors, upon reasonable request.

Ethics statement

The studies involving human participants were reviewed and approved by IKEM Ethics Committee. The patients/participants provided their written informed consent to participate in this study.

Author contributions

All authors have contributed in full extent to the conception and design of the work, to the acquisition of data and/or their analysis, interpretation, have participated in drafting the manuscript, revising it critically for its intellectual content, and have given their approval of the final version to be published.

Funding

Supported by Ministry of Health of the Czech Republic, Grant nr. NV 19-09-00125 and by the project National Institute for Research of Metabolic and Cardiovascular Diseases (Programme EXCELES, Project No. LX22NPO5104)—Funded by the European Union—Next Generation EU.

Conflict of interest

PW has received consulting fees or honoraria from Servier. JK reports grants and personal fees from Biosense Webster, Biotronik, Boston Scientific, Medtronic, grants and personal fees

from Abbott (SJM), personal fees from Merit Medical, Daiichi Sankyo, Boehringer Ingelheim, BMS, Bayer, Merck, MSD, Pfizer, all outside the submitted work.

The remaining authors declare that the research was conducted in the absence of any commercial or financial relationships that could be construed as a potential conflict of interest.

Publisher's note

All claims expressed in this article are solely those of the authors and do not necessarily represent those of their affiliated organizations, or those of the publisher, the editors and the reviewers. Any product that may be evaluated in this article, or claim that may be made by its manufacturer, is not guaranteed or endorsed by the publisher.

Supplementary material

The Supplementary Material for this article can be found online at: https://www.frontiersin.org/articles/10.3389/fcvm.2022.1051995/full#supplementary-material

References

1. Ibanez B, James S, Agewall S, Antunes MJ, Bucciarelli-Ducci C, Bueno H, et al. 2017 ESC Guidelines for the management of acute myocardial infarction in patients presenting with ST-segment elevation: The Task Force for the management of acute myocardial infarction in patients presenting with ST-segment elevation of the European Society of Cardiology (ESC). *Eur Heart J.* (2017) 39:119–77. doi: 10.1093/eurheartj/ehx393

2. Ng VG, Lansky AJ, Meller S, Witzenbichler B, Guagliumi G, Peruga JZ, et al. The prognostic importance of left ventricular function in patients with ST-segment elevation myocardial infarction: the HORIZONS-AMI trial. *Eur Heart J Acute ular Care.* (2014) 3:67–77. doi: 10.1177/2048872613507149

3. Multicenter Postinfarction Research Group. Risk stratification and survival after myocardial infarction. *N Engl J Med.* (1983) 309:331–6. doi: 10.1056/NEJM198308113090602

4. Rouleau JL, Talajic M, Sussex B, Potvin L, Warnica W, Davies RF, et al. Myocardial infarction patients in the 1990s–their risk factors, stratification and survival in Canada: the Canadian Assessment of Myocardial Infarction (CAMI) Study. *J Am Coll Cardiol.* (1996) 27:1119–27. doi: 10.1016/0735-1097(95)00599-4

5. Exner DV, Kavanagh KM, Slawnych MP, Mitchell LB, Ramadan D, Aggarwal SG, et al. Noninvasive risk assessment early after a myocardial infarction the REFINE study. *J Am Coll Cardiol.* (2007) 50:2275–84. doi: 10.1016/j.jacc.2007.08.042

6. Chew DS, Heikki H, Schmidt G, Kavanagh KM, Dommasch M, Bloch Thomsen PE, et al. Change in Left Ventricular Ejection Fraction Following First Myocardial Infarction and Outcome. *JACC Clin Electrophysiol.* (2018) 4:672–82. doi: 10.1016/j.jacep.2017.12.015

7. Chew DS, Wilton SB, Kavanagh K, Southern DA, Tan-Mesiatowsky LE, Exner DV. Left ventricular ejection fraction reassessment post–myocardial infarction: Current clinical practice and determinants of adverse remodeling. *Am Heart J.* (2018) 198:91–6. doi: 10.1016/j.ahj.2017.11.014

8. Parodi G, Memisha G, Carrabba N, Signorini U, Migliorini A, Cerisano G, et al. Prevalence, predictors, time course, and long-term clinical implications of left ventricular functional recovery after mechanical reperfusion for acute myocardial infarction. *Am J Cardiol.* (2007) 100:1718–22. doi: 10.1016/j.amjcard.2007.07.022

9. Wu WY, Biery DW, Singh A, Divakaran S, Berman AN, Ayuba G, et al. Recovery of left ventricular systolic function and clinical outcomes in young adults with myocardial infarction. *J Am Coll Cardiol.* (2020) 75:2804–15. doi: 10.1016/j.jacc.2020.03.074

10. Wohlfahrt P, Nativi-Nicolau J, Zhang M, Selzman CH, Greene T, Conte J, et al. Quality of life in patients with heart failure with recovered ejection fraction. *JAMA Cardiol.* (2021) 6:957–62. doi: 10.1001/jamacardio.2021.0939

11. McDonagh TA, Metra M, Adamo M, Gardner RS, Baumbach A, Böhm M, et al. 2021 ESC Guidelines for the diagnosis treatment of acute chronic heart failure: Developed by the Task Force for the diagnosis treatment of acute chronic heart failure of the European Society of Cardiology (ESC) With the special contribution of the Heart Failure Association (HFA) of the ESC. Eur Heart J. (2021) 42:3599–726. doi: 10.1093/eurheartj/ehab368

12. Heidenreich PA, Bozkurt B, Aguilar D, Allen LA, Byun JJ, Colvin MM, et al. 2022 AHA/ACC/HFSA guideline for the management of heart failure: a report of the American College of Cardiology/American Heart Association Joint Committee on clinical practice guidelines. *Circulation.* (2022) 145:e895–e1032. doi: 10.1161/CIR.0000000000001073

13. Szummer K, Wallentin L, Lindhagen L, Alfredsson J, Erlinge D, Held C, et al. Improved outcomes in patients with ST-elevation myocardial infarction during the last 20 years are related to implementation of evidence-based treatments: experiences from the SWEDEHEART registry 1995-2014. *Eur Heart J.* (2017) 38:3056–65. doi: 10.1093/eurheartj/ehx515

14. Szummer K, Wallentin L, Lindhagen L, Alfredsson J, Erlinge D, Held C, et al. Relations between implementation of new treatments and improved outcomes in patients with non-ST-elevation myocardial infarction during the last 20 years: experiences from SWEDEHEART registry 1995 to 2014. *Eur Heart J.* (2018) 39:3766–76. doi: 10.1093/eurheartj/ehy554

15. Gensini GG, A. more meaningful scoring system for determining the severity of coronary heart disease. *Am J Cardiol.* (1983) 51:606. doi: 10.1016/S0002-9149(83)80105-2

16. Rampidis GP, Benetos G, Benz DC, Giannopoulos AA, Buechel RR. A guide for Gensini Score calculation. *Atherosclerosis.* (2019) 287:181–3. doi: 10.1016/j.atherosclerosis.2019.05.012

17. Hasdai D, Behar S, Wallentin L, Danchin N, Gitt AK, Boersma E, et al. A prospective survey of the characteristics, treatments and outcomes of patients with acute coronary syndromes in Europe and the Mediterranean basin; the Euro Heart Survey of Acute Coronary Syndromes (Euro Heart Survey ACS). *Eur Heart J.* (2002) 23:1190–201. doi: 10.1053/euhj.2002.3193

18. Danchin N, Vaur L, Genès N, Renault M, Ferrières J, Etienne S, et al. Management of acute myocardial infarction in intensive care units in 1995: a nationwide French survey of practice and early hospital results. *J Am Coll Cardiol.* (1997) 30:1598–605. doi: 10.1016/S0735-1097(97)00371-9

19. Hanania G, Cambou JP, Guéret P, Vaur L, Blanchard D, Lablanche JM, et al. Management and in-hospital outcome of patients with acute myocardial infarction admitted to intensive care units at the turn of the century: results from the French nationwide USIC 2000 registry. *Heart.* (2004) 90:1404–10. doi: 10.1136/hrt.2003.025460

20. Magnesium in Coronaries (MAGIC) Trial Investigators. Early administration of intravenous magnesium to high-risk patients with acute myocardial infarction in the Magnesium in Coronaries (MAGIC) Trial: a randomised controlled trial. *Lancet.* (2002) 360:1189–96. doi: 10.1016/S0140-6736(02)11278-5

21. Shlipak MG, Browner WS, Noguchi H, Massie B, Frances CD, McClellan M. Comparison of the effects of angiotensin converting-enzyme inhibitors and beta blockers on survival in elderly patients with reduced left ventricular function after myocardial infarction. *Am J Med.* (2001) 110:425–33. doi: 10.1016/S0002-9343(01)00652-0

22. Møller JE, Brendorp B, Ottesen M, Køber L, Egstrup K, Poulsen SH, et al. Congestive heart failure with preserved left ventricular systolic function after acute myocardial infarction: clinical and prognostic implications. *Eur J Heart Fail.* (2003) 5:811–9. doi: 10.1016/S1388-9842(03)00159-4

23. Rott D, Behar S, Hod H, Feinberg MS, Boyko V, Mandelzweig L, et al. Improved survival of patients with acute myocardial infarction with significant left ventricular dysfunction undergoing invasive coronary procedures. *Am Heart J.* (2001) 141:267–76. doi: 10.1067/mhj.2001.111545

24. Ottervanger JP, Van't Hof AWJ, Reiffers S, Hoorntje JCA, Suryapranata H, de Boer MJ, et al. Long-term recovery of left ventricular function after primary angioplasty for acute myocardial infarction. *Eur Heart J.* (2001) 22:785–90. doi: 10.1053/euhj.2000.2316

25. Salomaa V, Ketonen M, Koukkunen H, Immonen-Räihä P, Jerkkola T, Kärjä-Koskenkari P, et al. Decline in out-of-hospital coronary heart disease deaths has contributed the main part to the overall decline in Coronary Heart Disease mortality rates among persons 35 to 64 years of age in Finland. *Circulation.* (2003) 108:691–6. doi: 10.1161/01.CIR.0000083720.35869.CA

26. Dudas K, Lappas G, Stewart S, Rosengren A. Trends in out-of-hospital deaths due to coronary heart disease in Sweden (1991 to 2006). *Circulation.* (2011) 123:46–52. doi: 10.1161/CIRCULATIONAHA.110.964999

27. Movahed MR, Hashemzadeh M, Jamal MM, Ramaraj R. Decreasing in-hospital mortality of patients undergoing percutaneous coronary intervention with persistent higher mortality rates in women and minorities in the United States. *J Invasive Cardiol.* (2010) 22:58–60.

28. Chacko L, Howard JP, Rajkumar C, Nowbar AN, Kane C, Mahdi D, et al. Effects of percutaneous coronary intervention on death and myocardial infarction stratified by stable and unstable coronary artery disease: a meta-analysis of randomized controlled trials. *Circ Cardiovasc Qual Outcomes.* (2020) 13:e006363. doi: 10.1161/CIRCOUTCOMES.119.006363

29. Puymirat E, Simon T, Cayla G, Cottin Y, Elbaz M, Coste P, et al. Acute myocardial infarction: changes in patient characteristics, management, and 6-month outcomes over a period of 20 years in the FAST-MI program (French Registry of Acute ST-Elevation or Non-ST-Elevation Myocardial Infarction) 1995 to 2015. *Circulation.* (2017) 136:1908–19. doi: 10.1161/CIRCULATIONAHA.117.030798

30. Rogers WJ, Frederick PD, Stoehr E, Canto JG, Ornato JP, Gibson CM, et al. Trends in presenting characteristics and hospital mortality among patients with ST elevation and non-ST elevation myocardial infarction in the National Registry of Myocardial Infarction from 1990 to 2006. *Am Heart J.* (2008) 156:1026–34. doi: 10.1016/j.ahj.2008.07.030

31. Oh PC, Choi IS, Ahn T, Moon J, Park Y, Seo JG, et al. Predictors of recovery of left ventricular systolic dysfunction after acute myocardial infarction: from the korean acute myocardial infarction registry and korean myocardial infarction registry. *Korean Circ J.* (2013) 43:527–33. doi: 10.4070/kcj.2013.43.8.527

32. Sjöblom J, Muhrbeck J, Witt N, Alam M, Frykman-Kull V. Evolution of left ventricular ejection fraction after acute myocardial infarction: implications for implantable cardioverter-defibrillator eligibility. *Circulation.* (2014) 130:743–8. doi: 10.1161/CIRCULATIONAHA.114.009924

33. Pfeffer MA, Claggett B, Lewis EF, Granger CB, Køber L, Maggioni AP, et al. Angiotensin Receptor-Neprilysin Inhibition in Acute Myocardial Infarction. *N Engl J Med.* (2021) 385:1845–55. doi: 10.1056/NEJMx210024

34. Halade GV, Lee DH. Inflammation and resolution signaling in cardiac repair and heart failure. *EBioMedicine.* (2022) 79:103992. doi: 10.1016/j.ebiom.2022.103992

35. Ong SB, Hernández-Reséndiz S, Crespo-Avilan GE, Mukhametshina RT, Kwek XY, Cabrera-Fuentes HA, et al. Inflammation following acute myocardial infarction: Multiple players, dynamic roles, and novel therapeutic opportunities. *Pharmacol Ther.* (2018) 186:73–87. doi: 10.1016/j.pharmthera.2018.01.001

36. Ridker PM, Everett BM, Thuren T, MacFadyen JG, Chang WH, Ballantyne C, et al. Antiinflammatory therapy with canakinumab for atherosclerotic disease. *N Engl J Med.* (2017) 377:1119–31. doi: 10.1056/NEJMoa1707914

37. Tardif JC, Kouz S, Waters DD, Bertrand OF, Diaz R, Maggioni AP, et al. Efficacy and safety of low-dose colchicine after myocardial infarction. *N Engl J Med.* (2019) 381:2497–505. doi: 10.1056/NEJMoa1912388

38. Angeli F, Reboldi G, Garofoli M, Ramundo E, Poltronieri C, Mazzotta G, et al. Atrial fibrillation and mortality in patients with acute myocardial infarction: a systematic overview and meta-analysis. *Curr Cardiol Rep.* (2012) 14:601–10. doi: 10.1007/s11886-012-0289-3

39. Börschel CS, Schnabel RB. The imminent epidemic of atrial fibrillation and its concomitant diseases - myocardial infarction and heart failure - a cause for concern. *Int J Cardiol.* (2019) 287:162–73. doi: 10.1016/j.ijcard.2018.11.123

40. Stojadinović P, Deshraju A, Wichterle D, Fukunaga M, Peichl P, Kautzner J, et al. The hemodynamic effect of simulated atrial fibrillation on left ventricular function. *J Cardiovasc Electrophysiol.* (2022). doi: 10.1111/jce.15669 [Epub ahead of print].

41. Kewcharoen J, Trongtorsak A, Thangjui S, Kanitsoraphan C, Prasitlumkum N. Female gender is associated with an increased left ventricular ejection fraction recovery in patients with heart failure with reduced ejection fraction. *Med Sci.* (2022) 10:21. doi: 10.3390/medsci10020021

42. Pullen AB, Kain V, Serhan CN, Halade GV. Molecular and cellular differences in cardiac repair of male and female mice. *J Am Heart Assoc.* (2020) 9:e015672. doi: 10.1161/JAHA.119.015672

43. McGowan JH, Cleland JG. Reliability of reporting left ventricular systolic function by echocardiography: a systematic review of 3 methods. *Am Heart J.* (2003) 146:388–97. doi: 10.1016/S0002-8703(03)00248-5

frontiers | Frontiers in Cardiovascular Medicine

TYPE Original Research
PUBLISHED 02 December 2022
DOI 10.3389/fcvm.2022.1051174

OPEN ACCESS

EDITED BY
Antonio Maria Leone,
Agostino Gemelli University Polyclinic (IRCCS), Italy

REVIEWED BY
Roberto Scarsini,
Integrated University Hospital Verona, Italy
Alexandru Scafa Udriste,
Carol Davila University of Medicine and Pharmacy, Romania

*CORRESPONDENCE
Giuseppe Tarantini
giuseppe.tarantini.1@gmail.com

SPECIALTY SECTION
This article was submitted to Coronary Artery Disease, a section of the journal Frontiers in Cardiovascular Medicine

RECEIVED 22 September 2022
ACCEPTED 21 November 2022
PUBLISHED 02 December 2022

CITATION
Fineschi M, Verna E, Barioli A, Mezzapelle G, Bartolini D, Turiano G, Guiducci V, Manari A, Lucarelli K, Uguccioni L, Repetto A and Tarantini G (2022) One-year results from the Assessing MICRO-vascular resistances *via* IMR to predict outcome in ST-elevation myocardial infarction patients with multivessel disease undergoing primary PCI (AMICRO) trial.
Front. Cardiovasc. Med. 9:1051174.
doi: 10.3389/fcvm.2022.1051174

One-year results from the Assessing MICRO-vascular resistances *via* IMR to predict outcome in ST-elevation myocardial infarction patients with multivessel disease undergoing primary PCI (AMICRO) trial

Massimo Fineschi[1], Edoardo Verna[2], Alberto Barioli[3,4], Giuseppe Mezzapelle[5], Davide Bartolini[6], Giovanni Turiano[7], Vincenzo Guiducci[8], Antonio Manari[8], Katya Lucarelli[9], Lucia Uguccioni[10], Alessandra Repetto[11] and Giuseppe Tarantini[4]*

[1]Policlinico Santa Maria alle Scotte, Siena, SI, Italy, [2]Ospedale di Circolo e Fondazione Macchi, Università dell'Insubria, Varese, VA, Italy, [3]Ospedale Ca' Foncello, Treviso, TV, Italy, [4]Azienda Ospedaliera Universitaria, Padova, PD, Italy, [5]Ospedale Giovanni Paolo II, Sciacca, AG, Italy, [6]Azienda Ospedaliera Villa Scassi, Genoa, Italy, [7]Ospedale di Conegliano, Conegliano, TV, Italy, [8]Azienda USL-IRCCS, Reggio Emilia, RE, Italy, [9]Ospedale Generale Regionale F. Miulli, Acquaviva delle Fonti, BA, Italy, [10]Ospedali Riuniti Marche Nord, Pesaro, PU, Italy, [11]Fondazione IRCCS Policlinico S. Matteo, Pavia, PV, Italy

Background: In ST-elevation myocardial infarction (STEMI) patients undergoing primary percutaneous coronary angioplasty (PPCI) the index of microcirculatory resistance (IMR) correlates to the extent of myocardial damage and left ventricular (LV) function recovery. Data on the IMR time-course and impact on clinical outcome in STEMI patients with multi-vessel disease (MVD) are scarce.

Aims: We designed a prospective, multicenter clinical trial to assess the infarct-related artery (IRA)-IMR in STEMI patients with MVD undergoing PPCI and to explore its potential in relationship with outcome and LV remodeling.

Methods: The study enrolled 242 STEMI patients with MVD. Both fractional flow reserve (FFR) and IMR of the IRA were assessed after successful PPCI. Then, FFR/IMR measurements were repeated in the IRA at a staged angiography, and FFR-guided angioplasty was performed in non-IRA lesions. The primary endpoint was the composite of cardiovascular death, re-infarction, re-hospitalization for heart failure, resuscitation or appropriate ICD shock at 1-year follow-up.

Results: A significant improvement of IRA-IMR values (from 47.9 to 34.2, $p < 0.0001$) was observed early after PPCI. Staged FFR-guided angioplasty was performed in 102 non-IRA lesions. We failed to find a correlation between IRA-IMR, clinical events and LV remodeling. Notwithstanding, in patients with anterior STEMI an inverse correlation between initial IMR values and LV function at follow-up was observed.

Conclusion: After successful PPCI, a significant proportion of patients with STEMI and MVD had coronary microvascular dysfunction as assessed by IMR that recovered early after reperfusion. Higher IMR values predicted lack of improvement of LV function only in anterior STEMI.

Clinical trial registration: [https://clinicaltrials.gov/], identifier [NCT 0232 5973].

KEYWORDS

STEMI, multivessel disease (MVD), microvascular resistance, índex of microvascular resistance (IMR), fractional flow reserve (FFR)

Introduction

Although primary percutaneous coronary intervention (PPCI), in comparison with thrombolysis, may guarantee a higher rate of recanalization in ST-elevation myocardial infarction (STEMI) patients, it cannot fully prevent tissue and microvascular damage, which are commonly seen and strongly related to the delay of reperfusion (1–3). Interestingly, although infarct size is a major determinant of microvascular obstruction at any given delay in treatment, both experimental and clinical studies suggest that microvascular obstruction *per se* is a stronger predictor of worse outcome and left ventricular function compared with infarct size (4–6). Myocardial reperfusion has been previously assessed by means of ST-segment resolution (7), myocardial blush grade (8), thrombolysis in myocardial infarction (TIMI) perfusion grade (9), myocardial contrast echocardiography and magnetic resonance (CMR) imaging (10, 11). In the last few decades, a method based on a pressure sensor/thermistor-tipped guidewire, that allows for measurement of hyperemic distal coronary pressure and blood flow by thermodilution technique and that permit calculation of an index of microcirculatory coronary resistance (IMR) (12–16), has been introduced. The IMR appears promising in the assessment of the extent of microvascular damage. However, the extent, the time-course and the role of IMR after PPCI is less well defined. Only few studies addressed this point in patients with predominantly single-vessel disease (17–20). Nevertheless, patients with multivessel disease (MVD) may have worse prognosis after PPCI for STEMI compared to patients with single vessel disease (21, 22).

The impact of IMR on clinical outcome in PPCI patients with MVD remains unsettled. We designed a prospective, multicenter clinical trial to assess the infarct-related artery (IRA) IMR time-course in STEMI patients with MVD undergoing PPCI and to explore its relationship with outcome and LV remodeling.

Abbreviations: CABG, coronary artery bypass graft; CFR, coronary flow reserve; CHF, congestive heart failure; CMR, cardiac magnetic resonance; CR, complete revascularization; EF, ejection fraction; FFR, fractional flow reserve; FSS, functional syntax score; HF, heart failure; ICD, implantable cardioverter defibrillator; IMR, index of microvascular resistance; IRA, infarct-related artery; LAD, left anterior descending artery; LV, left ventricle; MI, myocardial infarction; MVD, multivessel disease; PCI, percutaneous coronary intervention; PPCI, primary percutaneous coronary intervention; SS, syntax score; STEMI, ST-elevation myocardial infarction; TIMI, thrombolysis in myocardial infarction; WMSI, wall motion score index.

Materials and methods

Study design

The AMICRO ("Assessing MICRO-vascular resistances *via* IMR to predict outcome in STEMI patients with multivessel disease undergoing primary PCI") trial was a prospective, multicenter clinical study that included patients with MVD undergoing PPCI for STEMI in 11 hospitals in Italy. The study design and statistical plan has been described previously in detail (23). The study complies with the Declaration of Helsinki concerning medical research and with local legal and regulatory requirements. The trial was a St. Jude Medical (now Abbott Medical) sponsored study, and all study analyses were conducted with the assistance of Abbott. The AMICRO trial is registered with the National Institutes of Health sponsored ClinicalTrials.gov (www.clinicaltrials.gov) as study number NCT 02325973.

Patients

Patient enrollment started on June 2013. Key eligibility criteria were as follows: (1) diagnosis of STEMI with typical chest pain and ST-segment elevation of >0.1 mV in ≥2 consecutive leads on surface ECG or left bundle-branch block; (2) hospital admission either within 12 h of symptom onset or between 12 and 24 h after onset with evidence of continuing ischemia; (3) clearly defined infarct-related culprit lesion on index angiography and evidence of MVD defined as the presence of at least one angiographically significant (>50% by visual estimation) non-culprit lesion in a non-infarct-related artery; (4) successful drug-eluting stent PPCI of the culprit lesion. Key exclusion criteria included life expectancy of less than 1-year, prior myocardial infarction on the same area, hemodynamic instability not controllable with medical therapy and/or intra-aortic balloon pumping, prior coronary artery bypass grafting (CABG), and left main coronary artery disease or indication for CABG. All patients provided written informed consent.

Procedures

Patients were enrolled if they met all eligibility criteria. At index coronary angiogram the severity of all coronary artery lesions and the angiographic SYNTAX Score™ (SS) were reported. Percutaneous coronary intervention was performed according to the current standard of care. Deployment of a second-generation drug-eluting stent with proper stent post-dilatation was required to fix the culprit lesion. After angiographically successful PPCI, both FFR and IMR were measured in the IRA. Measurements of FFR and IMR were repeated in the IRA and performed in the non-culprit vessels at pre-discharge staged coronary angiography. After functional evaluation of all coronary artery stenoses, the "functional" SYNTAX Score™ (FSS) was calculated, and functionally significant (FFR < 0.75) non-culprit artery lesions were treated by PCI accordingly.

Twelve-lead ECG and cardiac enzyme level were recorded at the time of hospital admission. Blood samples were taken to measure in-hospital peak of cardiac enzymes [creatine-phosphokinase (CK), myocardial CK (MB-CK) and/or Troponin-I (Tn-I)] as per hospital clinical practice. Medical treatment during hospitalization and on hospital discharge was left to clinical practice of the enrolling site, guidelines and standard of care recommendations. To assess clinical status, medication and adverse events, patients were followed by hospital visit at 1 and 12 months after hospital discharge; additional 6 months visit has been done by phone. Echocardiographic evaluation of changes in LV volumes and ejection fraction (EF) from hospital discharge to 1-year follow-up visit was also performed.

Outcomes

The primary endpoint was the composite of cardiovascular death, re-myocardial infarction, re-hospitalization for heart failure, resuscitation or appropriate ICD shock at 1 year. Secondary endpoints were the evaluation of IMR index better cut-off based on primary endpoint events, new congestive heart failure (CHF) during index hospitalization and LV remodeling, new revascularization and stent thrombosis at 1 year follow-up, and additional possible event predictors.

Statistical analysis

Statistical analyses were performed as previously outlined in the study design publication (23). To calculate the sample size, a cut-off IMR value of 32 was assumed, as previously reported (16, 24). An incidence of events/year of 7% in the group of patients with lower IMR values and of 21% in the group with higher IMR values has been hypothesized. With an alpha error = 0.05 and a power of 85%, and on applying the 2-tailed $\chi 2$ test, the final estimated sample size was of 242 patients assuming a dropout rate of 10%. Categorical variables are reported as frequencies and relative percentages, whereas continuous variables are described by means of position indexes (mean, median) and indexes of dispersion (standard deviation, range). For any given parameter estimate, a 95% confidence interval (CI) was provided. Composite endpoints were evaluated as time to first event, whichever individual component occurred first. The Fisher's exact test was used to evaluate the existence of associations between IMR values (above and below the median or the cut-off value of 32) and outcome. In addition, the correlation between the delta IMR, expressed as the absolute average variation [Δ = IMR(T0) – IMR(T1)] or the average percent change [Δ% = [IMR(T0) – IMR(T1)]/ IMR(T0)%] of the index from time 0 (T0) to time 1 (T1), and outcomes was investigated. Continuous variables were compared using the Wilcoxon–Mann–Whitney test. A discriminant model (ROC curve) was used to determine whether there were IMR threshold values (cut-off) that allowed patients to be classified as being at increased or decreased risk of future events. For all comparisons, differences were considered statistically significant when $p < 0.05$.

Results

As per protocol, 242 subjects were enrolled in the AMICRO study between June 13, 2013 and February 14, 2017 in 11 Italian centers. Last 12 months follow-up examination was completed on March 22, 2018. 221 subjects (91.3%) completed the study participation; the remaining patients were withdrawn (16) or lost to 12M follow up (5) (**Figure 1**). Baseline clinical and

angiographic characteristics of the enrolled patients are shown in Table 1. The mean age was 63.5 years, and more than three quarters of participants were male. Hypertension was present in 47.9% of the total population, 43.4% had dyslipidemia, and 15.3% diabetes. A small percentage of patients had previous MI (2.9%) or prior PCI (5.3%). At admission, 95% of patients were in Killip class I and 5% in Killip class II. All patients underwent successful PPCI of the IRA within a mean of 6 h of symptoms onset (median time = 3 h). All patients had multivessel coronary artery disease (2.7 lesions per patient), and three-vessel disease

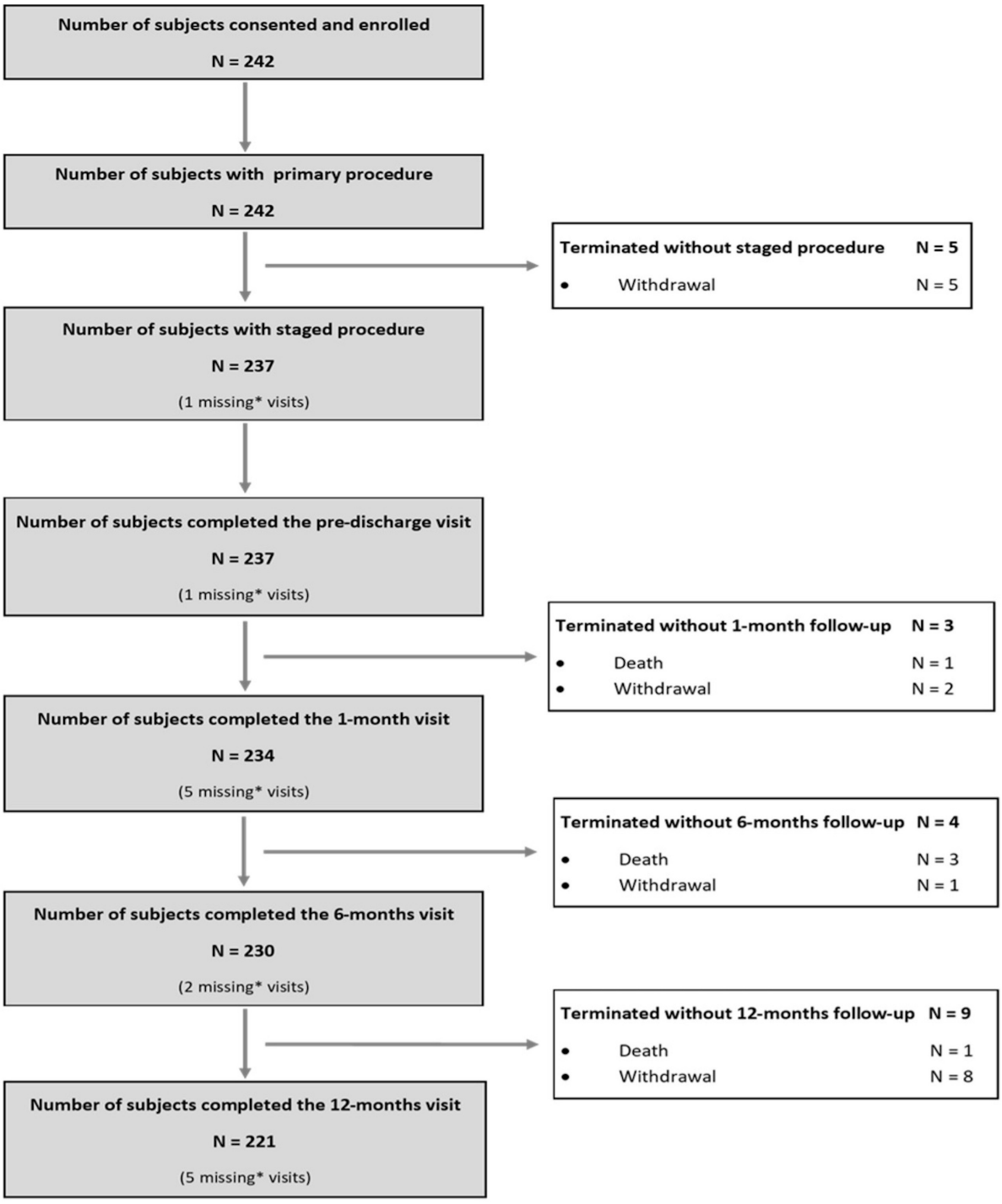

FIGURE 1
Flow chart of enrolled patients.

was present in 86 patients (35.5%). Mean baseline angiographic SS was 16.3 ± 5.8. LAD was the IRA in 43% of total cases.

Index of microcirculatory resistance measurements

After successful PPCI, IMR was measured in 236 (97.5%) IRA lesions with a mean value of 47.9 ± 42.7. IMR was found to be higher than the pre-defined cut-off of 32 in 127 patients (53.8% of the total population). Staged angiography and physiologic evaluation were performed in 236 subjects (97.5%) within 5.2 ± 3.7 days from index procedure. Infarct-related artery IMR values significantly decreased (from 47.9 ± 42.7 to 34.2 ± 28.5, $p < 0.0001$) from index to staged procedure.

Fractional flow reserve measurements

Fractional flow reserve (FFR) evaluation was performed in 238 (98.3%) IRA lesions after PPCI. Mean FFR was 0.92 ± 0.06 and did not change when measured at staged procedure (FFR at staged procedure 0.92 ± 0.06, p = NS). Physiologic evaluation of non-culprit lesions was also performed at staged procedure. Among 430 non-IRA lesions (angiographically >50% by visual estimation, mean angiographic stenosis 73.2% ± 14.5), 309 were tested with FFR and only 113 (36.6%) were significant (FFR was lower than 0.75 in 78 patients and between 0.75 and 0.80 in 35 patients). Of these, 102 (90%) underwent staged FFR-guided PCI. Functional assessment of non-IRA lesions was not performed in the remaining 121 lesions because of technical issues (i.e., vessel anatomy, lesion distality, patient non-compliance; **Supplementary Figure 1** in **Supplementary material**). Mean syntax score after functional stenosis evaluation (FSS) was significantly lower than the baseline angiographic SS (FSS 11.9 ± 6.1 vs. SS 16.3 ± 5.8; $p < 0.001$).

Primary endpoint results and correlation between index of microcirculatory resistance and outcomes

Twenty patients experienced cardiac events during the follow-up period: there were 4 cardiac deaths (1.7%), 2 re-hospitalizations for CHF, 2 resuscitations by ICD appropriate shock, 12 new coronary revascularizations (4 IRA re-do angioplasty for restenosis or subacute stent thrombosis and 8 non-IRA new PCI for restenosis or *de novo* lesions). Only 8 (3.3%) patients reported pre-defined primary endpoint events.

IMR measured in the culprit coronary artery (both post-PPCI and at staged procedure) was not associated with the pre-defined clinical endpoint, regardless of the IMR cut-off value used for the analysis (median cut-off: IMR post-PPCI $p = 0.281$, IMR at staged procedure $p = 0.446$; cut-off value of 32: IMR post-PPCI $p = 0.072$, IMR at staged procedure $p = 0.251$). The results were unchanged even by adopting an IMR cut-off of 40 (IMR

TABLE 1 Baseline patient characteristics and lesions.

Baseline demographics		***n* = 242**
Age, years		63.5 ± 9.9
Male, *n* (%)		207 (85.5)
Medical history		
None, *n* (%)		23 (9.5%)
Hypertension, *n* (%)		116 (47.9%)
Diabetes, *n* (%)		37 (15.3%)
	Diet	*5 (2.1%)*
	Insulin	*7 (2.9%)*
	Oral treatment	*25 (10.3%)*
Hyperlipidemia, dyslipidemia, *n* (%)		105 (43.4%)
Renal dysfunction*, *n* (%)	*With dialysis*	*0 (0%)*
	Without dialysis	*3 (1.2%)*
Significant alcohol intake, *n* (%)		3 (1.2%)
Smoker, *n* (%)		131 (54%)
	Current	*100 (41.3%)*
	Ex	*31 (12.8%)*
Other, *n* (%)		17 (7%)
Cardiovascular history		
None, *n* (%)		148 (61.2%)
Stroke, *n* (%)		3 (1.2%)
TIA, *n* (%)		5 (2.1%)
Myocardial infarction, *n* (%)		7 (2.9%)
Prior PCI, *n* (%)		13 (5.3%)
Family history of heart disease, *n* (%)		67 (27.7%)
Story of heart failure, *n* (%)		3 (1.2%)
Other, *n* (%)		12 (4.9%)
Coronary lesions characteristics		
SS (*n* = 242)		16.3 ± 5.8
FSS (*n* = 234)		11.9 ± 6.1
Three-vessel disease		86 (35.5%)
IRA, *n* (%) (*n* = 242)	*LAD*	*104 (43%)*
	RCA	*100 (41.3%)*
	LCX	*38 (15.7%)*
Non-IRA stenosis (>50%), *n* (%) (*n* = 430)	*LAD*	*171 (39.7%)*
	RCA	*103 (23.9%)*
	LCX	*156 (36.2%)*

Values are % (*n*) or mean ± SD.
*Defined as an estimated glomerular filtration rate (eGFR) of less than 60 ml/min/1.73 m^2. TIA, transient ischemic attach; PCI, percutaneous coronary angioplasty; SS, syntax score; FSS, functional syntax score; IRA, infarct related artery; LAD, left anterior descending artery; RCA, right coronary artery; LCX, left circumflex artery.

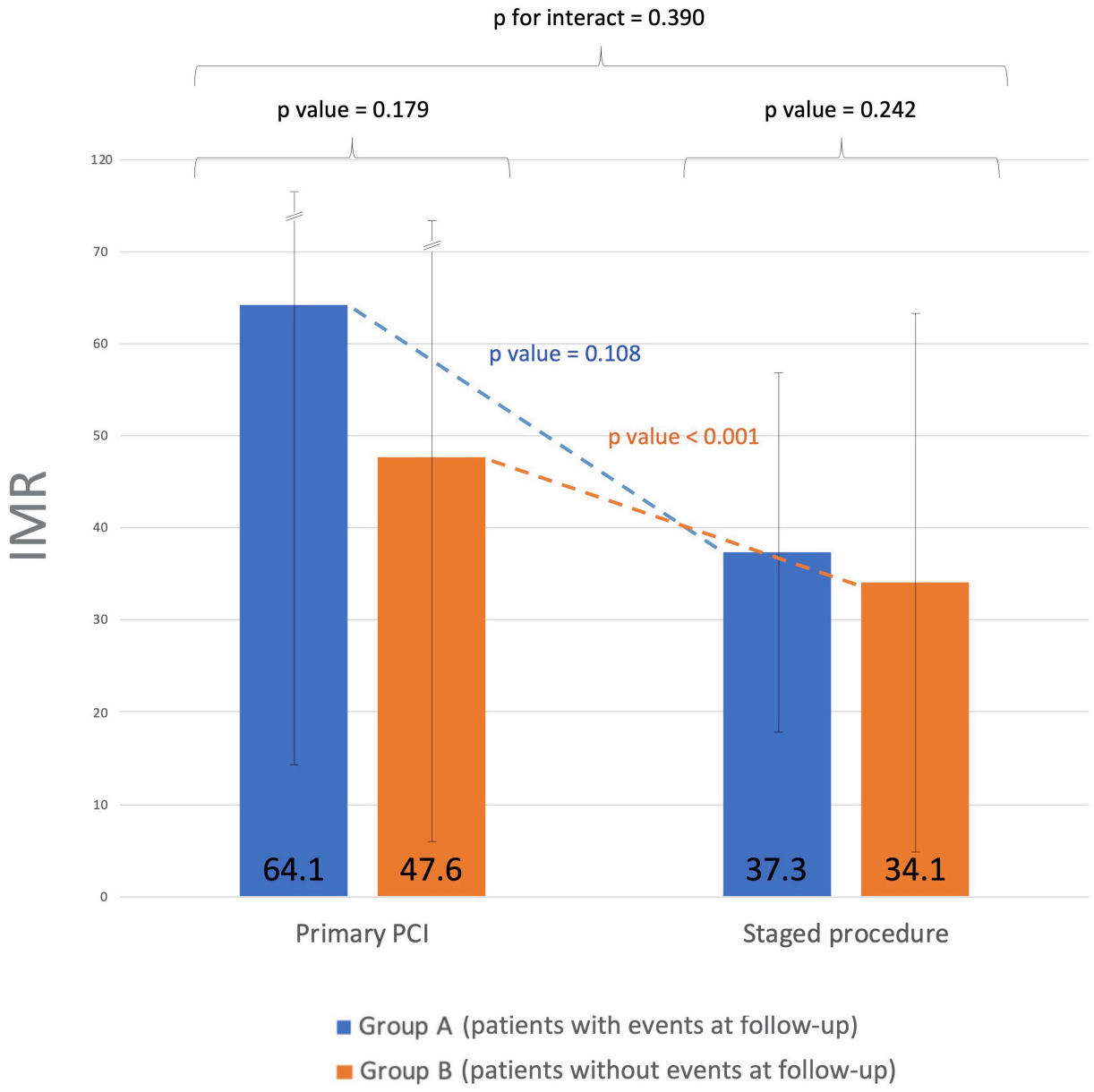

FIGURE 2
Index of microvascular resistance (IMR) time course from primary to staged procedure. Group A: patients who experienced primary endpoints. Group B: primary endpoints event-free patients. No significant differences in IMR values were observed between the two groups after successful PPCI of the culprit lesion. The IRA IMR significantly improved in event-free patients between PPCI and staged procedure. IMR, index of microvascular resistance; PPCI, primary percutaneous coronary intervention; IRA, infarct-related artery.

post-PPCI $p = 0.279$, IMR at staged procedure $p = 0.99$). Hence, we were not able to identify an IMR cut-off value to best predict primary endpoint events.

IMR variation between patients who experienced primary endpoints (Group A) and primary endpoints event-free patients (Group B) was also analyzed (**Figure 2**). No significant differences in IRA IMR after PPCI were observed between the 2 groups (64.1 ± 49.9 vs. 47.6 ± 42.8; $p = 0.18$), although a trend toward higher IMR values in the first group was noted, suggesting a likely worse outcome in patients with greater microcirculatory dysfunction at presentation. While IMR did not significantly change between PPCI and staged procedure (from 64.1 ± 49.9 to 37.3 ± 19.3; $p = 0.11$) in group A, in event-free patients the IRA IMR significantly improved (from 47.6 ± 42.8 to 34.1 ± 28.8; $p < 0.001$). However, considering the "delta" IMR (i.e., the variation of the index over time) from PCI to staged procedure in both groups, no statistically significant differences were observed ($p = 0.39$).

TABLE 2 Echocardiographic measurements.

	Overall			IMR ≤32			IMR >32		
	Discharge	12 months	*P*-value (discharge vs. 12 months)	Discharge	12 months	*P*-value (discharge vs. 12 months)	Discharge	12 months	*P*-value (discharge vs. 12 months)
Ejection fraction (%)	53.3 ± 8.6	56.2 ± 7.9	<0.0001	54.5 ± 8.1	56.9 ± 8.2	0.0017	52.2 ± 8.9	55.6 ± 7.6	<0.0001
LVESV (ml)	50.6 ± 21.8	47.4 ± 20.3	0.0810	50.4 ± 19.8	46.8 ± 20.6	0.1514	50.8 ± 23.4	48.0 ± 20.1	0.2974
LVEDV (ml)	101.7 ± 28.5	102.3 ± 32.4	0.7884	103.5 ± 29.7	103.2 ± 33.8	0.4079	100.3 ± 27.5	101.6 ± 31.4	0.7251
LVESD (mm)	35.5 ± 8.5	33.9 ± 6.6	0.0038	34.4 ± 9.0	33.6 ± 6.4	0.2530	36.5 ± 7.9	34.3 ± 6.7	0.0023
LVEDD (mm)	51.4 ± 29.7	50.2 ± 7.5	0.3250	53.5 ± 41.6	50.6 ± 8.8	0.4079	49.3 ± 7.2	49.7 ± 6.0	0.5296
16 segment WMSI	1.8 ± 2.9	1.9 ± 3.9	<0.0001	1.9 ± 3.4	2.3 ± 5.1	0.0005	1.7 ± 2.4	1.5 ± 2.4	<0.0001

Values are mean ± SD (*n*). LVESV, left ventricular end systolic volume; LVEDV, left ventricular end diastolic volume; LVESD, left ventricular end systolic diameter; LVEDD, left ventricular end diastolic diameter; WMSI, wall motion score index.

Echocardiographic findings

Echocardiography evaluation of LV function was performed in all subjects before discharge and at 1-year follow-up. A significant improvement in LVEF (from 53.3 ± 8.6 to 56.2 ± 7.9%; $p < 0.001$) and a slight deterioration in LV wall motion score index (WMSI) (from 1.8 ± 2.9 to 1.9 ± 3.9; $p < 0.001$) were observed in the overall population. While LVEF improved from discharge to 1-year follow-up both in patients with high and low IMR, an improvement in WMSI (from 1.7 ± 2.4 to 1.5 ± 2.4, $p < 0.0001$) was observed only in patients with higher IMR values at presentation (**Table 2**). No relationship was found between the delta IMR (staged-primary) and changes in LV volumes and function in the whole study population. Notwithstanding, a correlation between median value of IMR and changes in LV function has been found in the subgroup of patients with anterior STEMI. Patients with an IMR >31.5 after PPCI of the LAD artery showed a lower LVEF value than those with a IMR < 31.5 both at hospital discharge and at 12 months follow-up (47.3 ± 8.4 vs. 53.6 ± 7.6; $p = 0.0004$ and 52.7 ± 7.7 vs. 56.5 ± 8.4; $p = 0.0298$; **Figure 3**).

Discussion

The main findings of this prospective, multicenter, clinical study enrolling MVD patients undergoing PPCI for STEMI can be summarized as follows: (1) Coronary microvascular dysfunction, as assessed by IMR, is common in the infarct related territory and tends to recover early after revascularization; (2) The overall incidence rate of adverse events was unexpectedly low in our population at one-year follow-up; (3) No relationship between IRA-IMR, clinical events and LV remodeling was observed over the one-year follow-up period; (4) A correlation between IMR values and changes in LV function was found only in patients with anterior STEMI.

Despite PPCI in acute myocardial infarction can provide high epicardial coronary patency rates, insufficient myocardial reperfusion may occur as a result of microvascular obstruction and myocardial hemorrhage. Failure of reperfusion may have negative impact on outcome, being associated with LV adverse remodeling and dysfunction, re-hospitalization for heart failure and increased mortality (3). The IMR is a direct intravascular guidewire–based method for assessing coronary microvascular function on regional basis, which is quantitative in nature, and independent of the epicardial vessels size (14, 16).

In acute STEMI patients, coronary microvascular resistance as measured by IMR is usually increased. Conversely, coronary flow reserve (CFR), which reflects the vasodilatory potential of the coronary circulation, is significantly reduced. However, a progressive improvement of CFR and a reduction of IMR has been reported at 24 h and at 6 months after MI, indicating early and sustained recovery of microvascular function over time (25, 26). Our study confirms this finding, both in event-free patients and, to a lesser extent, in patients who experienced events at follow-up.

There is a large body of evidence showing that IMR measured immediately after PPCI is correlated with final infarct size as assessed by biomarker elevation, positron emission tomography, and CMR and predicts LV function at 3 and 6 months after STEMI (16, 24, 27–31). On the other hand, only few studies have focused on the value of IMR in predicting patient clinical outcome. Fearon et al. (17) assessed the incidence of death or re-hospitalization for HF in 253 single vessel disease patients undergoing PPCI for STEMI. During a median follow-up period of 2.8 years, 13.8% of the enrolled patients experienced the primary endpoint and 4.3% died. Patients with an IMR >40 had a higher risk of death or re-hospitalization for HF (hazard ratio [HR] 2.1; $p = 0.034$) and of death alone (HR 3.95; $p = 0.028$) at 1 year than patients with an IMR ≤40, while other indices of microvascular damage such as CFR were not predictive of clinical events. An IMR >40 was the only

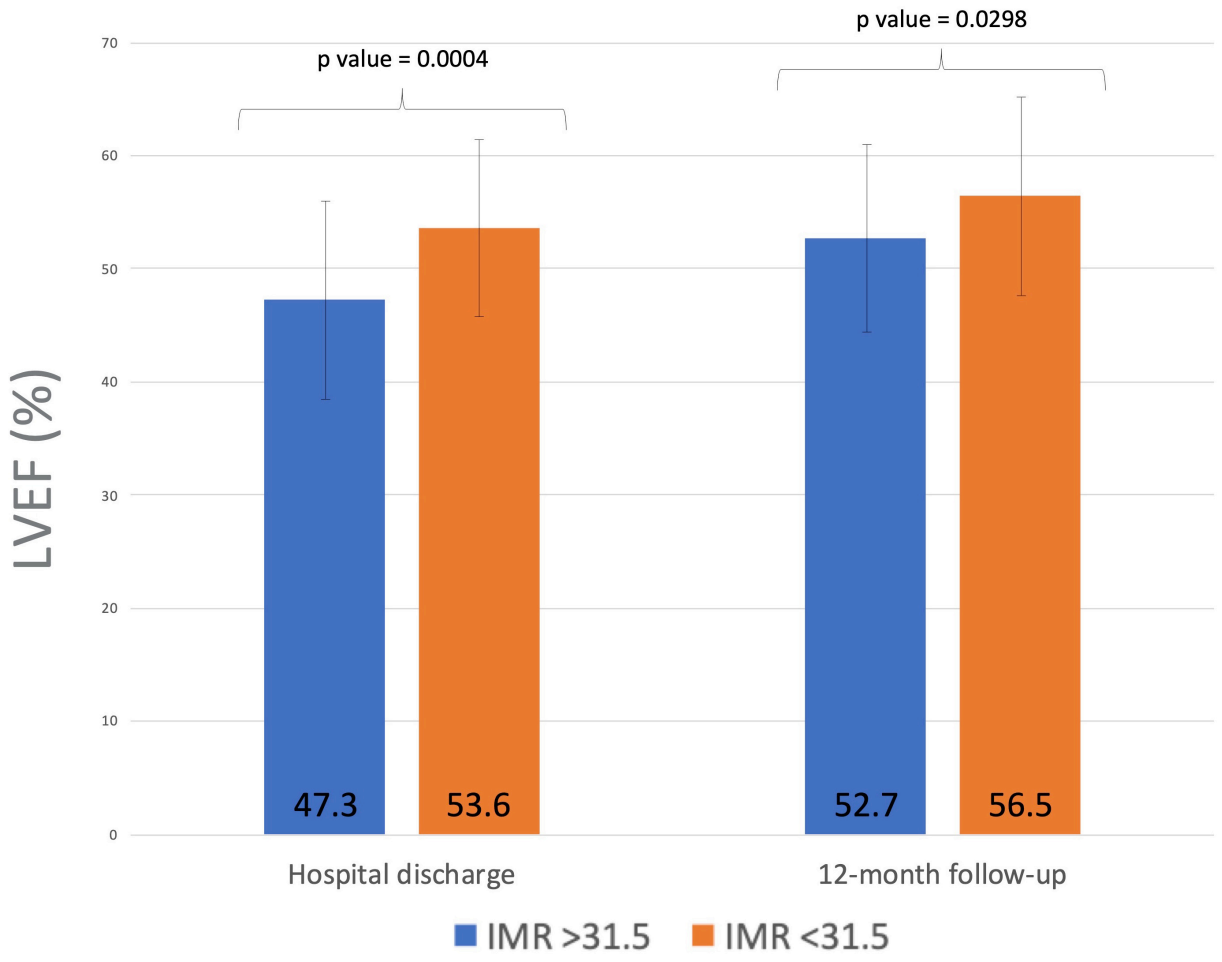

FIGURE 3
Index of microvascular resistance (IMR) after PPCI of the left anterior descending artery and left ventricular EF at hospital discharge and 12 months follow-up. Higher IMR measurements after PPCI predicted lack of improvement of LV function at follow-up in patients with anterior myocardial infarction. IMR, index of microvascular resistance; PPCI, primary percutaneous coronary intervention; EF, ejection fraction; LV, left ventricle.

independent predictor of death alone (HR 4.3; $p = 0.02$) or re-hospitalization for HF at multivariable analysis. Similarly, in the study by Carrick et al. (18), 283 patients with STEMI were prospectively enrolled after PPCI and categorized according to IMR ($\leq$40 or $>$40) and CFR ($\leq$2.0 or $>$2) values. The primary endpoint of death or first CHF hospitalization occurred in 11% of patients during the index hospitalization or after discharge. An IMR $>$40 was associated with microvascular obstruction and negative changes in LVEF and LV end-diastolic volumes. Also, higher IMR values were associated with a 4-fold increase in all-cause death or heart failure at a median follow-up of 2.3 years. The combination of IMR with CFR did not have superior prognostic value. Scarsini et al. (19) reported comparable results in a group of 198 patients with STEMI undergoing PPCI. At long-term follow-up (mean follow-up of 40.1 months), patients with an IMR $>$40 and/or microvascular obstruction assessed by CMR reported worse clinical outcomes compared with those with lower IMR values and no microvascular obstruction.

Compared with these studies, our trial enrolled only patients with MVD at baseline angiography that were expected to be at higher risk of clinical adverse events at follow-up. However, we observed an unexpected low rate of adverse clinical events in our population and were not able to find a significant association between IMR and the pre-defined clinical outcome endpoints. As a matter of fact, the primary endpoint was met in only 3.3% of patients, and this may have led to a power issue in assessing differences in clinical outcome between patients according to the value of IMR. Possible explanations for the low event rate observed in the AMICRO trial may be a potential selection bias, the relatively short follow-up period and the strategy of revascularization, which included a staged evaluation of non-IRA lesions followed by FFR-guided complete revascularization (CR). Indeed, over the last few years,

several studies have shown that in STEMI patients with MVD undergoing PPCI, a strategy of CR before hospital discharge may result in significant reduction of event rate at short term follow-up (32–37). In the current study, among 309 non-IRA lesions tested, appropriate revascularization was performed in the majority (90%) of lesions whose measured FFR was lower than 0.80. We can then speculate that in the present trial the observed event rate at follow-up may have been partially reduced by the effect of an FFR-guided CR strategy before hospital discharge.

In contrast to what we observed in the whole population, a correlation between IMR and changes in LV function was found in the subgroup of patients with anterior STEMI. Higher IMR measurements post-PPCI of the LAD artery were significantly associated with lower LVEF values both at hospital discharge and at 12-month follow-up. These results provide further support for the hypothesis that IMR value in predicting LVEF is most likely to be discriminative in patients with higher myocardium at risk such as those with large anterior infarction (29).

Limitations

The low event rate observed at follow-up get the study unpowered to end-point. As already discussed, follow-up duration [shorter than the >2-year follow-up of other studies exploring the potential value of IMR in predicting patient clinical outcome (17–19)] and the strategy of revascularization may have contributed in part to the low event rate observed in the study. In addition, the short time frame from symptoms onset to revascularization, the low Killip class at admission, the relatively low rate of diabetes and the extensive use of radial approach may have further influenced to the low number of events observed. The absence of a screening log of the study population also does not allow for exclusion and definition of potential selection biases underneath. The low primary endpoint event rate may also explain the inability to identify an IMR cut-off value to best predict adverse events at follow-up, which was among the pre-specified secondary endpoints.

Non-homogeneous laboratory tests for myocardial damage were used (e.g., CK, Tn, and HsTn), making them difficult to use for clinical correlations. Also, it should be considered that the definition of STEMI has suffered numerous changes from 2013, when enrollment began.

The IMR measured after the PPCI was found to be predictive of lower EF values both at discharge and at 12 months follow-up only when the median IMR cut-off of 31.5 was adopted. Conversely, when using the pre-specified cut-off of 32, higher IMR values were associated with worse LVEF at discharge (53.5 ± 7.5 vs. 47.2 ± 8.5, p = 0.0004) but not at 12 months follow-up (56.2 ± 8.4 vs. 52.9 ± 7.7, p = 0.0586), although a trend was noted. In addition, we must recognize that more accurate echocardiographic parameters to determine subclinical LV dysfunction, such as speckle tracking, were not used in this study.

Furthermore, the study is limited by the lack of information on CFR even though, in patients with STEMI, IMR and not CFR demonstrated a significant association with clinical outcomes (18, 38). Data about Pd/Pa and hyperemic transit time were also not collected.

Lastly, although a close monitoring was performed during the entire follow-up to minimize the loss of patients, a total of 16 patients (6.6%) were lost to follow-up/withdrawn.

Conclusion

Despite the routine success of PPCI in STEMI, impaired coronary microvascular function is commonly detected by IMR evaluation in the infarct territory and shows a slow recovery early over the time after reperfusion. Post-angioplasty IMR values negatively correlated with LVEF only in patients with anterior acute MI. Further work is required to establish the validity of IMR in predicting clinical outcomes in specific subgroups of patients.

Data availability statement

The raw data supporting the conclusions of this article will be made available by the authors, without undue reservation.

Ethics statement

The studies involving human participants were reviewed and approved by Comitato Etico Area Vasta Sud-Est (SI) Comitato Etico Provinciale dell'Insubria (VR) CESC province di Treviso e Belluno (TV) CESC della provincia di Padova (PD) Comitato Etico Palermo 2 (PA) Comitato Etico Regionale Liguria (GE) Comitato Etico dell'Area Vasta Emilia Nord (RE) Comitato Etico Interregionale (BA) Comitato Etico Regionale delle Marche (AN) Comitato Etico referente per l'Area di Pavia (PV). The patients/participants provided their written informed consent to participate in this study.

Author contributions

MF, EV, GTa, AM, KL, and LU contributed to the study design. All authors contributed to patient

enrolment/management and/or data analysis/article writing, and all have approved the final manuscript.

Funding

This study was sponsored by Abbott Italia.

Conflict of interest

Authors MF, EV, and GM report speaker honoraria from St. Jude Medical Italia (now Abbott). Authors MF and EV also report consulting fees for St. Jude Medical Italia (now Abbott).

The remaining authors declare that the research was conducted in the absence of any commercial or financial relationships that could be construed as a potential conflict of interest.

Publisher's note

Supplementary material

The Supplementary Material for this article can be found online at: https://www.frontiersin.org/articles/10.3389/fcvm.2022.1051174/full#supplementary-material

SUPPLEMENTARY FIGURE 1
Treatment of infarct related vessel (IRA) lesions and non-infarct related vessel (non-IRA) lesions.

References

1. Kawamoto T, Yoshida K, Akasaka T, Hozumi T, Takagi T, Kaji S, et al. Can coronary blood flow velocity pattern after primary percutaneous transluminal coronary angioplasty [correction of angiography] predict recovery of regional left ventricular function in patients with acute myocardial infarction? *Circulation.* (1999) 100:339–45. doi: 10.1161/01.cir.100.4.339

2. Gibson C, Cannon C, Murphy S, Ryan K, Mesley R, Marble S, et al. Relationship of TIMI myocardial perfusion grade to mortality after administration of thrombolytic drugs. *Circulation.* (2000) 101:125–30. doi: 10.1161/01.cir.101.2.125

3. Niccoli G, Burzotta F, Galiuto L, Crea F. Myocardial no-reflow in humans. *J Am Coll Cardiol.* (2009) 54:281–92. doi: 10.1016/j.jacc.2009.03.054

4. Nijveldt R, Beek A, Hirsch A, Stoel M, Hofman M, Umans V, et al. Functional recovery after acute myocardial infarction: comparison between angiography, electrocardiography, and cardiovascular magnetic resonance measures of microvascular injury. *J Am Coll Cardiol.* (2008) 52:181–9. doi: 10.1016/j.jacc.2008.04.006

5. Ndrepepa G, Tiroch K, Fusaro M, Keta D, Seyfarth M, Byrne R, et al. 5-year prognostic value of no-reflow phenomenon after percutaneous coronary intervention in patients with acute myocardial infarction. *J Am Coll Cardiol.* (2010) 55:2383–9. doi: 10.1016/j.jacc.2009.12.054

6. de Waha S, Patel M, Granger C, Ohman E, Maehara A, Eitel I, et al. Relationship between microvascular obstruction and adverse events following primary percutaneous coronary intervention for ST-segment elevation myocardial infarction: an individual patient data pooled analysis from seven randomized trials. *Eur Heart J.* (2017) 38:3502–10. doi: 10.1093/eurheartj/ehx414

7. Schröder R, Dissmann R, Brüggemann T, Wegscheider K, Linderer T, Tebbe U, et al. Extent of early ST segment elevation resolution: a simple but strong predictor of outcome in patients with acute myocardial infarction. *J Am Coll Cardiol.* (1994) 24:384–91. doi: 10.1016/0735-1097(94)90292-5

8. van 't Hof A, Liem A, Suryapranata H, Hoorntje J, de Boer M, Zijlstra F. Angiographic assessment of myocardial reperfusion in patients treated with primary angioplasty for acute myocardial infarction: myocardial blush grade. Zwolle myocardial infarction study group. *Circulation.* (1998) 97:2302–6. doi: 10.1161/01.cir.97.23.2302

9. Gibson C, Cannon C, Murphy S, Marble S, Barron H, Braunwald E. Relationship of the TIMI myocardial perfusion grades, flow grades, frame count, and percutaneous coronary intervention to long-term outcomes after thrombolytic administration in acute myocardial infarction. *Circulation.* (2002) 105:1909–13. doi: 10.1161/01.cir.0000014683.52177.b5

10. Bolognese L, Antoniucci D, Rovai D, Buonamici P, Cerisano G, Santoro G, et al. Myocardial contrast echocardiography versus dobutamine echocardiography for predicting functional recovery after acute myocardial infarction treated with primary coronary angioplasty. *J Am Coll Cardiol.* (1996) 28:1677–83. doi: 10.1016/S0735-1097(96)00400-7

11. Nijveldt R, Hofman M, Hirsch A, Beek A, Umans V, Algra P, et al. Assessment of microvascular obstruction and prediction of short-term remodeling after acute myocardial infarction: cardiac MR imaging study. *Radiology.* (2009) 250:363–70. doi: 10.1148/radiol.2502080739

12. Fearon W, Balsam L, Farouque H, Caffarelli A, Robbins R, Fitzgerald P, et al. Novel index for invasively assessing the coronary microcirculation. *Circulation.* (2003) 107:3129–32. doi: 10.1161/01.CIR.0000080700.98607.D1

13. Fearon W, Aarnoudse W, Pijls N, De Bruyne B, Balsam L, Cooke D, et al. Microvascular resistance is not influenced by epicardial coronary artery stenosis severity: experimental validation. *Circulation.* (2004) 109:2269–72. doi: 10.1161/01.CIR.0000128669.99355.CB

14. Aarnoudse W, Fearon W, Manoharan G, Geven M, van de Vosse F, Rutten M, et al. Epicardial stenosis severity does not affect minimal microcirculatory resistance. *Circulation.* (2004) 110:2137–42. doi: 10.1161/01.CIR.0000143893.18451.0E

15. Ng M, Yeung A, Fearon W. Invasive assessment of the coronary microcirculation: superior reproducibility and less hemodynamic dependence of index of microcirculatory resistance compared with coronary flow reserve. *Circulation.* (2006) 113:2054–61. doi: 10.1161/CIRCULATIONAHA.105.603522

16. Sezer M, Umman B, Okcular I, Nisanci Y, Umman S. Relationship between microvascular resistance and perfusion in patients with reperfused acute myocardial infarction. *J Interv Cardiol.* (2007) 20:340–50. doi: 10.1111/j.1540-8183.2007.00274.x

17. Fearon W, Low A, Yong A, McGeoch R, Berry C, Shah M, et al. Prognostic value of the index of microcirculatory resistance measured after primary percutaneous coronary intervention. *Circulation.* (2013) 127:2436–41. doi: 10.1161/CIRCULATIONAHA.112.000298

18. Carrick D, Haig C, Ahmed N, Carberry J, Yue May V, McEntegart M, et al. Comparative prognostic utility of indexes of microvascular function alone or in combination in patients with an acute st-segment-elevation myocardial infarction. *Circulation.* (2016) 134:1833–47. doi: 10.1161/CIRCULATIONAHA.116.022603

19. Scarsini R, Shanmuganathan M, De Maria G, Borlotti A, Kotronias R, Burrage M, et al. Coronary microvascular dysfunction assessed by pressure wire and CMR after STEMI predicts long-term outcomes. *JACC Cardiovasc Imaging.* (2021) 14:1948–59. doi: 10.1016/j.jcmg.2021.02.023

20. De Maria G, Cuculi F, Patel N, Dawkins S, Fahrni G, Kassimis G, et al. How does coronary stent implantation impact on the status of the microcirculation

during primary percutaneous coronary intervention in patients with ST-elevation myocardial infarction? *Eur Heart J.* (2015) 36:3165–77. doi: 10.1093/eurheartj/ehv353

21. Dziewierz A, Siudak Z, Rakowski T, Zasada W, Dubiel J, Dudek D. Impact of multivessel coronary artery disease and noninfarct-related artery revascularization on outcome of patients with ST-elevation myocardial infarction transferred for primary percutaneous coronary intervention (from the EUROTRANSFER Registry). *Am J Cardiol.* (2010) 106:342–7. doi: 10.1016/j.amjcard.2010.03.029

22. Sorajja P, Gersh B, Cox D, McLaughlin M, Zimetbaum P, Costantini C, et al. Impact of multivessel disease on reperfusion success and clinical outcomes in patients undergoing primary percutaneous coronary intervention for acute myocardial infarction. *Eur Heart J.* (2007) 28:1709–16. doi: 10.1093/eurheartj/ehm184

23. Fineschi M, Verna E, Mezzapelle G, Bartolini D, Turiano G, Manari A, et al. Assessing MICRO-vascular resistances *via* IMR to predict outcome in STEMI patients with multivessel disease undergoing primary PCI (AMICRO): rationale and design of a prospective multicenter clinical trial. *Am Heart J.* (2017) 187:37–44. doi: 10.1016/j.ahj.2017.02.019

24. McGeoch R, Watkins S, Berry C, Steedman T, Davie A, Byrne J, et al. The index of microcirculatory resistance measured acutely predicts the extent and severity of myocardial infarction in patients with ST-segment elevation myocardial infarction. *JACC Cardiovasc Interv.* (2010) 3:715–22. doi: 10.1016/j.jcin.2010.04.009

25. Bax M, de Winter R, Koch K, Schotborgh C, Tijssen J, Piek J. Time course of microvascular resistance of the infarct and noninfarct coronary artery following an anterior wall acute myocardial infarction. *Am J Cardiol.* (2006) 97:1131–6. doi: 10.1016/j.amjcard.2005.11.026

26. Cuculi F, Dall'Armellina E, Manlhiot C, De Caterina A, Colyer S, Ferreira V, et al. Early change in invasive measures of microvascular function can predict myocardial recovery following PCI for ST-elevation myocardial infarction. *Eur Heart J.* (2014) 35:1971–80. doi: 10.1093/eurheartj/eht434

27. Fearon W, Shah M, Ng M, Brinton T, Wilson A, Tremmel J, et al. Predictive value of the index of microcirculatory resistance in patients with ST-segment elevation myocardial infarction. *J Am Coll Cardiol.* (2008) 51:560–5. doi: 10.1016/j.jacc.2007.08.062

28. Lim H, Yoon M, Tahk S, Yang H, Choi B, Choi S, et al. Usefulness of the index of microcirculatory resistance for invasively assessing myocardial viability immediately after primary angioplasty for anterior myocardial infarction. *Eur Heart J.* (2009) 30:2854–60. doi: 10.1093/eurheartj/ehp313

29. Payne A, Berry C, Doolin O, McEntegart M, Petrie M, Lindsay M, et al. Microvascular resistance predicts myocardial salvage and infarct characteristics in ST-elevation myocardial infarction. *J Am Heart Assoc.* (2012) 1:e002246. doi: 10.1161/JAHA.112.002246

30. Qi Y, Gu R, Xu J, Kang L, Liu Y, Wang L, et al. Index of microcirculatory resistance predicts long term cardiac systolic function in patients with STEMI undergoing primary PCI. *BMC Cardiovasc Disord.* (2021) 21:66. doi: 10.1186/s12872-021-01887-w

31. De Maria G, Alkhalil M, Wolfrum M, Fahrni G, Borlotti A, Gaughran L, et al. Index of microcirculatory resistance as a tool to characterize microvascular obstruction and to predict infarct size regression in patients with STEMI undergoing primary PCI. *JACC Cardiovasc Imaging.* (2019) 12:837–48. doi: 10.1016/j.jcmg.2018.02.018

32. Wald D, Morris J, Wald N, Chase A, Edwards R, Hughes L, et al. Randomized trial of preventive angioplasty in myocardial infarction. *N Engl J Med.* (2013) 369:1115–23. doi: 10.1056/NEJMoa1305520

33. Gershlick A, Khan J, Kelly D, Greenwood J, Sasikaran T, Curzen N, et al. Randomized trial of complete versus lesion-only revascularization in patients undergoing primary percutaneous coronary intervention for STEMI and multivessel disease: the CvLPRIT trial. *J Am Coll Cardiol.* (2015) 65:963–72. doi: 10.1016/j.jacc.2014.12.038

34. Engstrøm T, Kelbæk H, Helqvist S, Høfsten D, Kløvgaard L, Holmvang L, et al. Complete revascularisation versus treatment of the culprit lesion only in patients with ST-segment elevation myocardial infarction and multivessel disease (DANAMI-3—PRIMULTI): an open-label, randomised controlled trial. *Lancet.* (2015) 386:665–71. doi: 10.1016/s0140-6736(15)60648-1

35. Smits P, Abdel-Wahab M, Neumann F, Boxma-de Klerk B, Lunde K, Schotborgh C, et al. Fractional flow reserve-guided multivessel angioplasty in myocardial infarction. *N Engl J Med.* (2017) 376:1234–44. doi: 10.1056/NEJMoa1701067

36. Mehta S, Wood D, Storey R, Mehran R, Bainey K, Nguyen H, et al. Complete revascularization with multivessel PCI for myocardial infarction. *N Engl J Med.* (2019) 381:1411–21. doi: 10.1056/NEJMoa1907775

37. Bainey K, Engstrøm T, Smits P, Gershlick A, James S, Storey R, et al. Complete vs culprit-lesion-only revascularization for ST-segment elevation myocardial infarction: a systematic review and meta-analysis. *JAMA Cardiol.* (2020) 5:881–8. doi: 10.1001/jamacardio.2020.1251

38. Maznyczka A, Oldroyd K, Greenwood J, McCartney P, Cotton J, Lindsay M, et al. Comparative significance of invasive measures of microvascular injury in acute myocardial infarction. *Circ Cardiovasc Interv.* (2020) 13:e008505. doi: 10.1161/CIRCINTERVENTIONS.119.008505

frontiers | Frontiers in Cardiovascular Medicine

TYPE Original Research
PUBLISHED 09 January 2023
DOI 10.3389/fcvm.2022.1014664

OPEN ACCESS

EDITED BY
Sabato Sorrentino,
University of Magna Graecia, Italy

REVIEWED BY
Manel Sabate,
Hospital Clinic of Barcelona, Spain
Bimmer Claessen,
Amsterdam University Medical Center,
Netherlands

*CORRESPONDENCE
Sinisa M. Stojkovic
✉ sstojkovi@mts.rs

SPECIALTY SECTION
This article was submitted to
Coronary Artery Disease,
a section of the journal
Frontiers in Cardiovascular Medicine

RECEIVED 08 August 2022
ACCEPTED 20 December 2022
PUBLISHED 09 January 2023

CITATION
Juricic SA, Stojkovic SM, Galassi AR, Stankovic GR, Orlic DN, Vukcevic VD, Milasinovic DG, Aleksandric SB, Tomasevic MV, Dobric MR, Nedeljkovic MA, Beleslin BD, Dikic MP, Banovic MD, Ostojic MC and Tesic MB (2023) Long-term follow-up of patients with chronic total coronary artery occlusion previously randomized to treatment with optimal drug therapy or percutaneous revascularization of chronic total occlusion (COMET-CTO). *Front. Cardiovasc. Med.* 9:1014664. doi: 10.3389/fcvm.2022.1014664

Long-term follow-up of patients with chronic total coronary artery occlusion previously randomized to treatment with optimal drug therapy or percutaneous revascularization of chronic total occlusion (COMET-CTO)

Stefan A. Juricic[1], Sinisa M. Stojkovic[1,2]*, Alfredo R. Galassi[3,4], Goran R. Stankovic[1,2,5], Dejan N. Orlic[1,2], Vladan D. Vukcevic[1,2], Dejan G. Milasinovic[1,2], Srdjan B. Aleksandric[1,2], Miloje V. Tomasevic[1,6], Milan R. Dobric[2,7], Milan A. Nedeljkovic[1,2], Branko D. Beleslin[1,2], Miodrag P. Dikic[1], Marko D. Banovic[1,2], Miodrag C. Ostojic[2,5] and Milorad B. Tesic[1,2]

[1]Clinic for Cardiology, University Clinical Center of Serbia, Belgrade, Serbia, [2]School of Medicine, University of Belgrade, Belgrade, Serbia, [3]Department of Health Promotion, Mother and Child Care, Internal Medicine and Medical Specialties (ProMISE), University of Palermo, Palermo, Italy, [4]Royal Brompton & Harefield NHS Foundation Trust, London, United Kingdom, [5]Serbian Academy of Sciences and Arts, Belgrade, Serbia, [6]Department of Internal Medicine, Faculty of Medical Sciences, University of Kragujevac, Kragujevac, Serbia, [7]Dedinje Cardiovascular Institute, Belgrade, Serbia

Background: The COMET-CTO trial was a randomized prospective study that assessed long-term follow-up in patients with chronic total occlusion (CTO) in coronary arteries treated with percutaneous coronary intervention (PCI) or with optimal medical therapy (OMT). During the 9-month follow-up, the incidence of major adverse cardiac events (MACE) did not differ between the two groups; no death or myocardial infarction (MI) was observed. There was a significant difference in quality of life (QoL), assessed by the Seattle Angina Questionnaire (SAQ), in favor of the PCI group. Here we report long-term follow-up results (56 ± 12 months).

Methods: Between October 2015 and May 2017, a total of 100 patients with CTO were randomized into two groups of 50 patients: PCI CTO or OMT group. The primary endpoint of the current study was the incidence of MACE defined as cardiac death, MI, and revascularization [PCI or coronary artery bypass graft (CABG)]. As the secondary exploratory outcome, we analyzed all the cause-mortality rate.

Results: Out of 100 randomized patients, 92 were available for long-term follow-up (44 in the PCI group and 48 in the OMT group). The incidence of MACE did not differ significantly between the two groups (p = 0.363). Individual components of MACE were distributed, respectively: cardiac death (OMT vs. PCI group, 6 vs. 3, p = 0.489), MI (OMT vs. PCI group, 1 vs. 0, p = 1), and revascularization (PCI: OMT vs. PCI group, 2 vs. 2, p = 1; CABG: OMT vs. PCI group, 1 vs. 1, p = 1). There was no significant difference between the two groups regarding the individual component of MACE. Six patients died from non-cardiac causes [five deaths were reported in the OMT group and one death in the PCI group (p = 0.206)]. Kaplan-Meier survival curves for MACE did not differ significantly between the study groups (log-rank 0.804, p = 0.370). Regarding the secondary exploratory outcome, a total of 15 patients died at 56 ± 12 months (11 in the OMT and 4 in the PCI group) (p = 0.093). The Kaplan-Meier survival curves for all-cause mortality rates did not differ significantly between the two groups (log rank 3.404, p = 0.065). There were no statistically significant differences between OMT and PCI groups in all five SAQ domains. There was a significant improvement in three SAQ domains in the PCI group: PL ($p < 0.001$), AF (p = 0.007), and QoL (p = 0.001).

Conclusion: After 56 ± 12 months of follow-up, the incidence of MACE, as well as QoL measured by SAQ, did not differ significantly between the PCI and OMT groups.

KEYWORDS

percutaneous coronary intervention, chronic total occlusion, optimal medical therapy, outcomes, long-term follow-up

Introduction

Recanalization of chronic total occlusions (CTO) of the coronary arteries is certainly one of the most technically demanding procedures in interventional cardiology. Furthermore, between 15 and 20% of patients who have an indication for coronary angiography have a CTO of at least one blood vessel (1–3). However, a significantly lower percentage of these patients are candidates for percutaneous coronary intervention (4, 5). Over the years observational studies have proven that successful recanalization of CTO is associated with improved patient symptoms, quality of life, and long-term survival compared with failed recanalization (6–8). According to the observational, non-randomized data, under elective circumstances, long-term benefits of successful percutaneous coronary intervention (PCI) of CTO have been suggested: improved survival, reduced need for coronary artery bypass grafting (CABG), and a better survival of future myocardial infarctions (MI) related to non-CTO arteries (9, 10). Several randomized studies also assessed the long-term treatment outcomes of patients with CTO; however, their initial results were slightly controversial including major adverse cardiovascular events (MACE) (11–13).

COMET–CTO was one of the first randomized studies that assessed the quality of life (QoL) in patients with CTO allocated to PCI of CTO or to optimal medical therapy (OMT). The primary endpoint of the study was the QoL assessed by the Seattle Angina Questionnaire (SAQ). The results showed that there was a significant improvement in QoL in patients with one CTO on the main coronary blood vessel in patients treated with percutaneous recanalization of CTO when compared to patients randomized to OMT only (14). However, during the 9-month follow-up, the incidence of MACE was very low, with no cardiac death or MI. Therefore, the aim of this study was to determine the long-term treatment outcome (>4 years) of patients with chronic total coronary artery occlusion previously randomized to PCI of the CTO plus OMT or just to OMT. This would be one of the first research papers on this topic in elective patients.

Materials and methods

The study design, methods (including the sample size calculation), and results were described previously (14). The study was registered on ClinicalTrials.gov (NCT02964975). Shortly, the study was designed as an open-label, randomized,

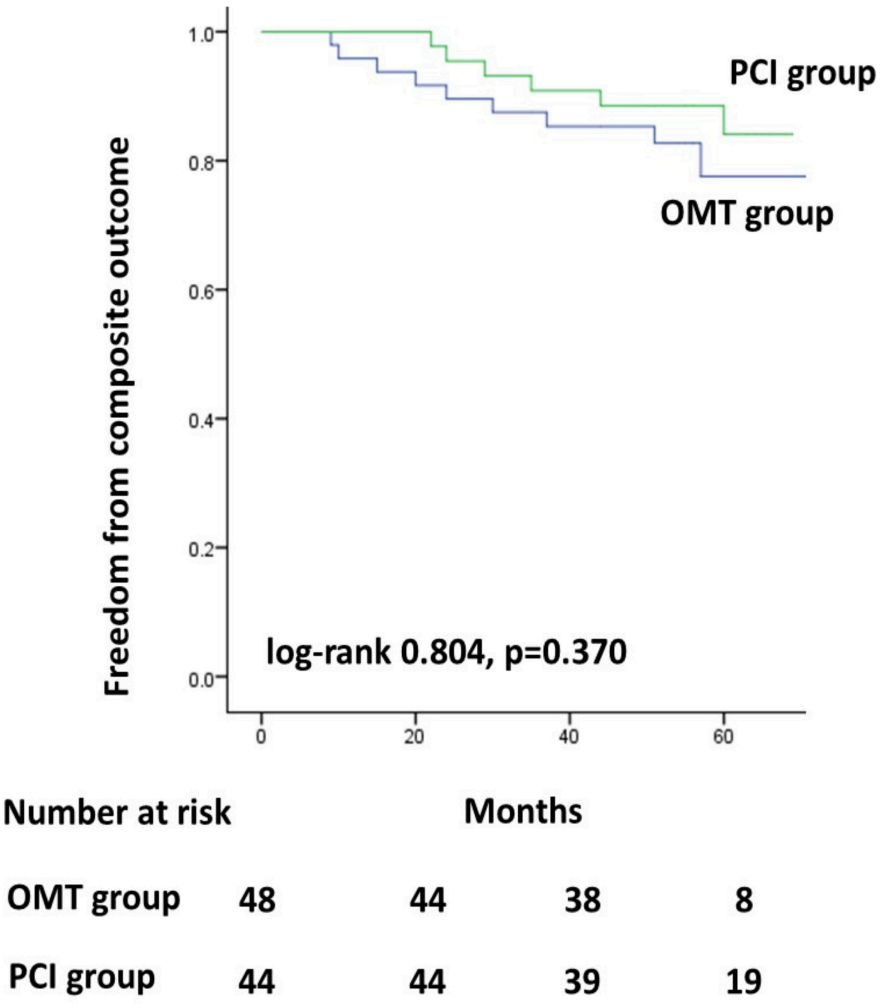

FIGURE 1
Kaplan–Meier survival curves for the MACE. PCI, percutaneous coronary intervention; OMT, optimal medical therapy.

prospective study which included patients with a single chronically occluded epicardial coronary artery. Between October 2015 and May 2017, 100 patients were randomized into two groups (50 pts in each group) after signing the informed consent. They participated in the study and completed the SAQ at baseline and after the 9-month follow-up. The first group was randomized to PCI of CTO with OMT and the second group of patients was randomized to OMT only.

During the long-term follow-up, patients were contacted to assess their clinical status and their adverse events. All events were recorded in the appropriate database. For the patients we were unable to reach, information was obtained from their cardiologists, general practitioners, or hospital records. The mean follow-up time was 56 ± 12 months. The primary clinical composite endpoint was the incidence of MACE, defined as cardiovascular death, nonfatal MI, and coronary revascularization (PCI or CABG). For the secondary exploratory outcomes, we analyzed the all cause-mortality rate (15). Cardiac death was defined according to the Academic Research Consortium (ARC) criteria. MI was defined with symptoms of cardiac ischemia and a troponin level of at least one value above the 99th percentile upper reference limit according to the recent guidelines (16).

Statistical analysis

All the data were analyzed with the statistical program SPSS version 21 (SPSS, Chicago, IL). Continuous variables are presented as the mean ± SD. Categorical variables are presented as frequencies and proportions. Differences in continuous variables were assessed with Student's *t*-test or the Mann–Whitney *U* test, following the Kolmogorov–Smirnov test. Differences in categorical variables were compared using the chi-squared test when appropriate (expected frequencies > 5;

10.3389/fcvm.2022.1014664

TABLE 1 Baseline patient and lesion characteristics.

Variable	OMT $n = 50$	PCI $n = 50$	P OMT vs. PCI	Total $n = 100$
Age (years)	63 ± 5	61 ± 7	0.107	62 ± 6
Follow-up (days)	267 ± 93	284 ± 84	0.354	275 ± 88
BMI	27.41 ± 3.46	28.40 ± 3.86	0.176	27.91 ± 3.68
Baseline creatinine (mmol/L)	84.44 ± 17.46	81.64 ± 15.27	0.395	83.04 ± 16.38
LVEF	51.34 ± 11.28	54.90 ± 9.420	0.090	53.12 ± 10.49
Male	44 (88)	38 (76)	0.118	82 (82)
Family history of CAD	23 (46)	24 (48)	0.841	47 (4)
Hypertension	43 (86)	43 (86)	1.0	86 (86)
Hypercholesterolemia	35 (70)	36 (72)	0.826	71 (71)
NIDDM	12 (24)	10 (20)	0.664	22 (22)
IDDM	6 (12)	4 (8)	0.370	10 (10)
Non-smoker	13 (26)	20 (40)	0.149	30 (30)
Ex-smoker	23 (46)	14 (28)	0.147	37 (37)
Current smoker	14 (28)	16 (32)	0.531	33 (33)
PAD	2 (4)	2 (4)	1.0	4 (4)
Previous stroke	4 (8)	1 (2)	0.169	5 (5)
Previous MI	35 (70)	29 (58)	0.211	64 (64)
In-stent CTO	3 (6)	5 (10)	0.461	8 (8)
Angina			0.769	
CCS I	11 (22)	12 (24)		23 (23)
CCS II	26 (52)	21 (42)		47 (47)
CCS III	11 (22)	14 (28)		25 (25)
CCS IV	2 (4)	3 (6)		5 (5)
Reversible ischemia	29 (58)	26 (52)	0.814	55 (55)
demonstrated	44 (88)	47 (94)	0.295	91 (91)
Presence of viability				
CTO artery			0.060	
LAD	5 (10)	12 (24)		17 (17)
Cx	6 (12)	10 (20)		16 (16)
RCA	39 (78)	28 (56)		67 (67)
Visual reference VD	3.03 ± 0.38	2.90 ± 0.30	0.60	2.96 ± 0.34
Visual length of occlusion	20.06 ± 6.40	20.46 ± 11.47	0.830	20.26 ± 9.24
Calcification			0.585	
Mild	28 (56)	33 (66)		61 (61)
Moderate	16 (32)	12 (24)		28 (28)
Severe	6 (12)	5 (10)		11 (11)
Proximal cap tapered	26 (52)	32 (64)	0.224	58 (58)
Moderate/severe tortuosity	2 (4)	4 (8)	0.513	6 (12)
"Interventional" collateral present	26 (52)	22 (44)	0.423	48 (48)
J-CTO score	1.72 ± 1.09	1.48 ± 1.27	0.219	1.60 ± 1.18
Syntax score I	9.87 ± 3.41	10.79 ± 4.89	0.822	10.33 ± 4.22
EuroSCORE II	0.87 ± 0.34	0.80 ± 0.31	0.133	0.84 ± 0.32

Data are expressed as the mean ± SD or as the number (percentage). BMI, body mass index; LVEF, left ventricular ejection fraction; NIDDM, non-insulin-dependent diabetes mellitus; IDDM, insulin-dependent diabetes mellitus; PAD, peripheral artery disease; MI, myocardial infarction; CTO, chronic total occlusion; LAD, left anterior descending; Cx, circumflex; RCA, right coronary artery; VD, vessel diameter. Presence of viability: LV normokinesis or segmental LV hypokinesis or documented viability in CTO territory.

10.3389/fcvm.2022.1014664

TABLE 2 Clinical outcomes: long-term follow-up.

Long-term follow-up (mean 56 ± 12 months)			
	OMT	PCI	*p*
Cardiac death	6	3	0.489
MI	1	0	1
PCI–TVR	2	2	1
CABG	1	1	1
All-cause mortality	11	4	0.093

The data is numerical. PCI, percutaneous coronary intervention; OMT, optimal medical therapy; MI, myocardial infarction; CABG, coronary artery bypass graft; TVR, target vessel revascularization.

otherwise, Fisher's exact test was used). Changes in all five components of the SAQ were tested using repeated-measures analysis of variance for each factor. SAQ domains at the baseline and after the FUP were entered as within-subject variables, whereas the study group was entered as the between-subject variable.

Results

Nine-month results

In terms of baseline characteristics, the compared groups were similar (14). Patient and lesion characteristics did not differ significantly between the groups at baseline (**Table 1**). The mean follow-up was 275 ± 88 days. In the PCI CTO group, 94% of patients had a successful recanalization of the occlusion. The mean number of implanted drug-eluting stents per lesion was 1.78 ± 1.02, while the mean stent diameter was 2.98 ± 0.35 mm. The mean length of implanted stents was 46.84 ± 26.80 mm. This study observed a significant improvement in QoL (in all five domains of the SAQ) in patients treated with PCI of CTO plus OMT when compared with patients treated with OMT only.

Long-term outcomes

Out of 100 randomized patients, 92 were available for long-term follow-up (44 in PCI and 48 in OMT group). During the long-term follow-up, a total of 15 patients died (11 in the OMT group and 4 in the PCI group) ($p = 0.093$) (**Table 2**).

The incidence of MACE did not differ significantly between the two groups ($p = 0.363$). There was no statistically significant difference between the two groups regarding cardiac death, MI, or revascularization (**Table 2**). From the non-cardiac causes of death in the OMT group, there were five deaths, and in the PCI group, there was one death ($p = 0.206$). The causes of death along with some of the baseline characteristics are shown in **Table 3**.

The Kaplan–Meier survival curves for the MACE did not differ significantly between the two groups (**Figure 1**, $p = 0.370$).

TABLE 3 Deceased patients and their characteristics.

	CTO location	LVEF at baseline (%)	Randomization group	CTO-PCI successful	Time to death (months)	Cause of death
1.	LAD	55	OMT	/	72	CV
2.	RCA	50	OMT	/	61	COVID
3.	LAD	43	PCI	Yes	44	CV
4.	Cx	53	OMT	/	37	Traffic acc.
5.	LAD	57	OMT	/	30	CV
6.	RCA	55	OMT	/	51	Malignancy
7.	RCA	40	OMT	/	15	CV
8.	RCA	45	PCI	Yes	60	CV
9.	RCA	60	OMT	/	9	CV
10.	RCA	55	OMT	/	54	Dementia
11.	RCA	40	OMT	/	10	CV
12.	RCA	49	PCI	Yes	34	Malignancy
13.	LAD	50	PCI	Yes	24	CV
14.	Cx	30	OMT	/	37	CV
15.	RCA	55	OMT	/	45	COVID

Data are numerical. LAD, left anterior descending artery; Cx, left circumflex artery; RCA, right coronary artery; PCI, percutaneous coronary intervention; OMT, optimal medical therapy; LVEF, left ventricular function; CTO, chronic total occlusion; CV, cardiovascular; Acc, accident.

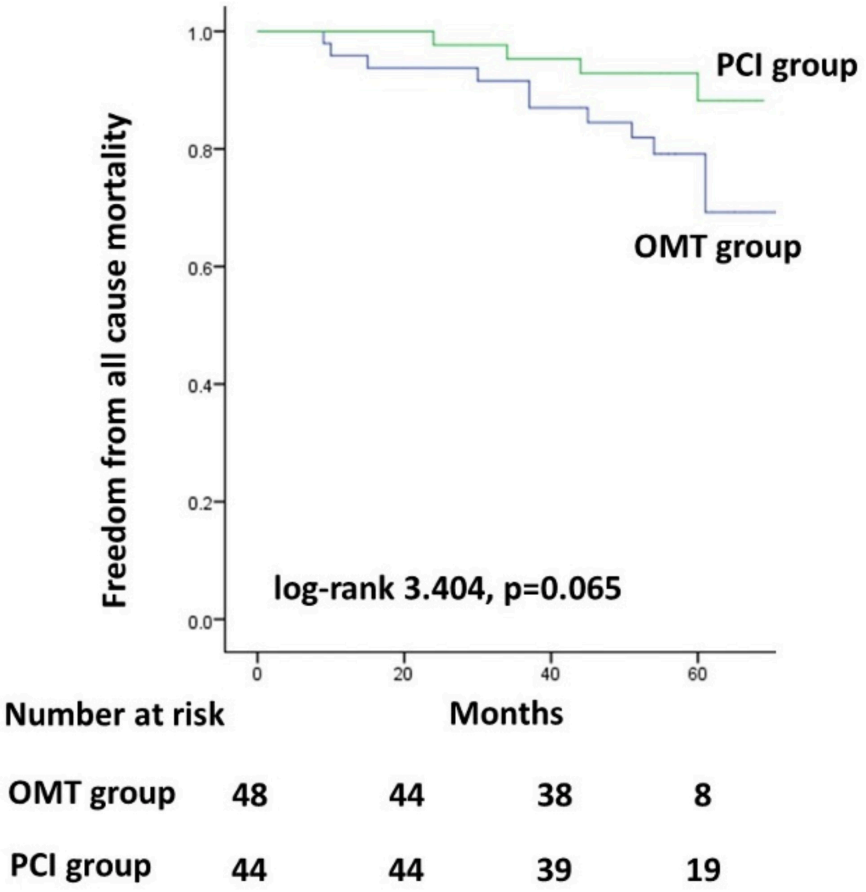

FIGURE 2
Kaplan–Meier survival curves for all-cause mortality. PCI, percutaneous coronary intervention; OMT, optimal medical therapy.

In addition, the Kaplan–Meier survival curves for all-cause mortality also did not differ significantly between the two groups (Figure 2, $p = 0.065$).

After the initial FUP where we had a total of three events (one CABG in the PCI group and two cross-overs in the OMT group due to anginal complaints), during the long-term FUP, there was no statistically significant difference in revascularization between the two groups (PCI: OMT vs. PCI group, 2 vs. 2, $p = 1$; CABG: OMT vs. PCI group, 1 vs. 1, $p = 1$).

A total of 40 patients were analyzed for the SAQ in the PCI group and 37 patients in the OMT group. The scores for the five angina symptom domains at the FUP and their changes from the pre-procedural scores are reported in Figure 3. Baseline scores for a total of 77 patients were not different between the two groups, except for PL (PCI group 49.6 ± 22.4 vs. OMT group 61.9 ± 24.7, $p = 0.024$) (Table 4). During the FUP, there were no statistically significant differences between groups in all five SAQ domains (Figure 3). There was a significant improvement in three SAQ domains in the PCI group: PL ($p < 0.001$), AF ($p = 0.007$), and I-QoL ($p = 0.001$) (Figure 3).

Discussion

To the best of our knowledge, COMET-CTO is a randomized study in elective CTO patients with the longest follow-up. The study has demonstrated that there was a trend to significantly lower all-cause mortality in the PCI group ($p = 0.065$). MACE and all the individual components of MACE did not differ significantly during the average 4.7 years of follow-up.

This study showed that QoL improved significantly in the PCI group of patients compared to the patients assigned to OMT alone. During the short-term follow-up, we observed no deaths, MIs, stent thrombosis, or strokes. However, we observed low rates of revascularization in both groups of patients. The present study extended the previous clinical outcomes from the COMET-CTO trial.

The EURO-CTO trial included 407 patients with CTO (randomization 2:1—OMT with CTO PCI or OMT, respectively) (11). In the group of patients who underwent PCI CTO, they had a significant improvement in the frequency of

TABLE 4 Seattle angina questionnaire health status at baseline.

	OMT $n = 37$	PCI $n = 40$	P OMT vs. PCI
Baseline			
PL	61.9 ± 24.7	49.6 ± 22.4	0.024
AS	48.6 ± 25.0	40.0 ± 22.5	0.114
AF	78.9 ± 20.1	70.5 ± 20.2	0.071
TS	79.2 ± 18.1	81.7 ± 18.3	0.550
QoL	62.8 ± 23.3	54.2 ± 26.6	0.133

Data are expressed as the mean ± SD. PL, physical limitation; AS, angina stability; AF, angina frequency; TS, treatment satisfaction; QoL, quality of life; OMT, optimal medical therapy; PCI, percutaneous coronary intervention.

angina and QoL ($p = 0.003$ and $p = 0.007$), while in our study, we had a statistically significant improvement in all five domains of the SAQ. Also, the MACE rate was very similar in the EURO CTO and COMET-CTO trial during the initial follow-up.

EXPLORE (13) and DECISION-CTO (12) are two randomized studies published on this topic that did not confirm a significant reduction in MACE in the revascularized CTO group compared to the OMT group. Several things need to be addressed in both studies. Out of the 1,284 patients originally planned, only 65% (834) of the patients were included in the DECISION-CTO study. There were difficulties observed in recruiting patients which led to the main reason for the premature termination of the study. Furthermore, the significant cross-over between the two study groups (approximately one in five patients) was probably caused by the fact that PCI of non-CTO lesion was left on operator discretion before PCI of CTO. Hence, the majority of PCI of non-CTO lesions were performed after the PCI of CTO (77% of patients had multi-vessel disease).

However, overall mortality in the PCI group was lower than in the OMT group (3.0 vs. 4.4% at the 3-year follow-up and 4.5 vs. 7.9% at the 5-year follow-up). These figures did not reach statistical significance which is similar to our results.

Furthermore, in the DECISION-CTO trial, the number of patients at risk was significantly lower at the 5-year than at the 3-year follow-up (12). This could mean that the follow-up was incomplete or that a large number of patients were lost during the follow-up period. Otherwise, it is very possible that the difference would have been significant. Precisely, due to all the above-mentioned facts, the opinion of many experts in the field of CTO is that the DECISION-CTO study should not be considered as definitely negative for the primary endpoint.

In the EXPLORE trial, the MACE (composite of cardiac death, myocardial infarction, and CABG) rate did not differ significantly between the groups (13.5 vs. 12.3%, $p = 0.93$), during the median follow-up of 3.9 years. This finding is

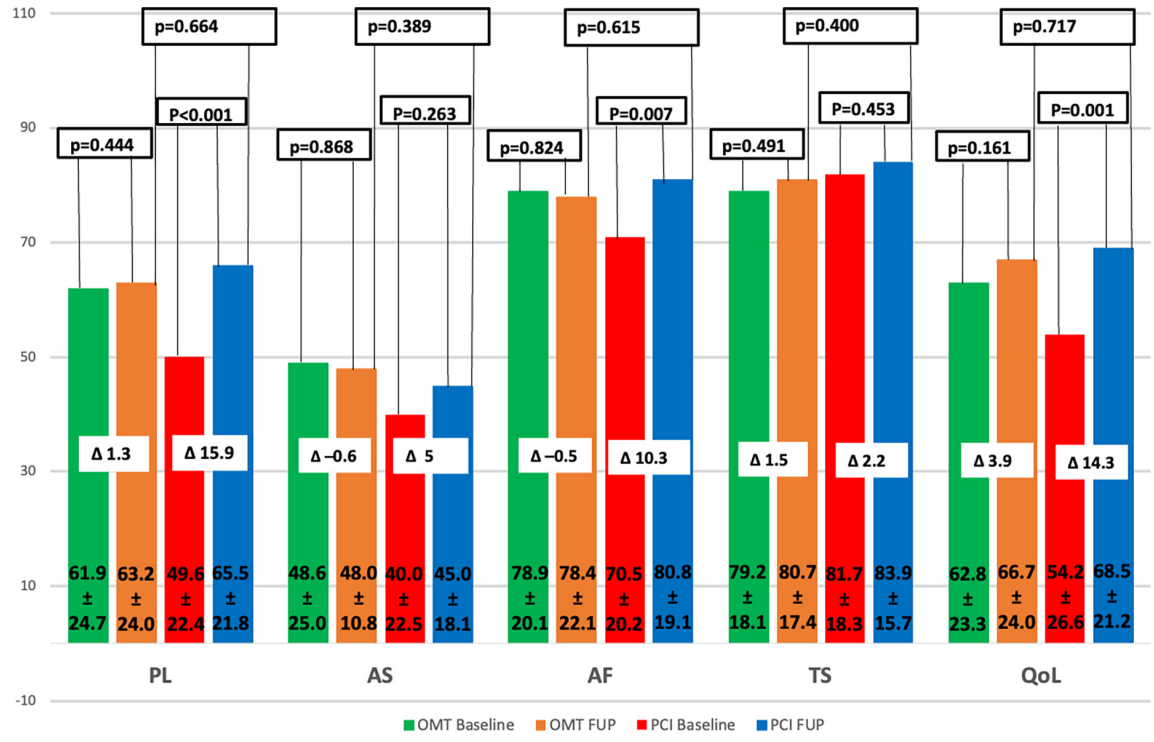

FIGURE 3
SAQ subscale changes. QoL, quality of life; PL, physical limitation; AS, angina stability; AF, angina frequency; TS, treatment satisfaction; PCI, percutaneous coronary intervention; OMT, optimal medical therapy; FUP, follow-up. Δ: difference between f-up and baseline mean values.

consistent with our results. An increasing trend without statistical significance was observed in the overall mortality of the CTO PCI group (12.9 vs. 6.9%, $P = 0.11$). These results should be interpreted with caution due to the small absolute number of events. Also, we cannot rule out a possibly harmful effect of PCI CTO within 7 days of an acute myocardial infarction.

Two large prospective registers, Canadian (17) and Korean (18) registers, were published in the recent years which evaluated CTO revascularization using a long-term follow-up. In the Canadian Multicenter Chronic Total Occlusion Registry 1,624 patients were assigned either to the CTO revascularized group or to the group where no revascularization of the CTO artery was performed. In the group where CTO was revascularized, there was a significantly lower mortality rate at 10 years (22.7 vs. 36.6%), lower revascularization rates (14.0 vs. 22.8%), and a shorter acute coronary syndrome hospitalizations (10.0 vs. 16.6%).

The Korean registry is a single center register with patients with CTO classified into two groups, PCI CTO ($n = 883$) or OMT group ($n = 664$), depending on the initial treatment strategy. Patients were enrolled during the period from 2003 to 2012 with typical angina or a positive functional test. At the end of the 3-year follow-up, there was no significant difference between the groups in terms of mortality due to a cardiac cause. However, between 3 and 10 years of follow-up, there was a significantly lower mortality in the revascularized group (8.3 vs. 16.6%; HR, 0.43 [95% CI, 0.27–0.71]; $P < 0.001$).

Furthermore, it is observed that the results of randomized studies and prospective registries are more similar for MACE when it comes to long-term follow-up.

In COMET CTO initial result of significant difference in QoL in favor of the PCI group after 9 months of F-up for all five SAQ domains, vanished during the next 4 years. In contrast, ISCHEMIA trial showed that QoL assessed by SAQ was significantly improved after 36 months of FUP (19). This discrepancy could be in a part explained by the fact that the number of patients available for QoL assessment decreased to 77 by time [numerically more patients died in the OMT group (11 pts) than in PCI group (4 pts)]. Bearing this in mind, it is not insignificant to emphasize that, in our trial, SAQ scores were numerically higher in four domains at the end of long-term FUP.

Limitations

This is a prospective randomized study conducted in a single center. This study does not have statistical power to detect differences in the incidence of major adverse cardiovascular events between the examined groups (which was considered as a secondary endpoint).

Conclusion

In patients with a single CTO treated by percutaneous coronary intervention with OMT (study group) in comparison with a group of patients only treated with OMT (control group), there was no difference observed in long-term MACE or other clinical events between the two groups. Similarly, SAQ data showed that QoL did not differ significantly between OMT and PCI groups. Further research is needed to clarify and evaluate this important area.

Data availability statement

The raw data supporting the conclusions of this article will be made available by the authors, without undue reservation.

Ethics statement

The studies involving human participants were reviewed and approved by the Medical Ethical Committee of the University Clinical Center of Serbia. The patients/participants provided their written informed consent to participate in this study.

Author contributions

SJ, SS, and MBT contributed to drafting of the manuscript, analysis and interpretation of data, and discussions on the results. SJ, DM, MRD, MB, SA, and MPD collected the data. SS, SJ, AG, VV, GS, MVT, BB, MO, DO, and MN revised the final revision and final approval of the manuscript. All authors provided critical feedback and contributed to the manuscript.

Conflict of interest

The authors declare that the research was conducted in the absence of any commercial or financial relationships that could be construed as a potential conflict of interest.

Publisher's note

References

1. Fefer P, Knudtson M, Cheema A, Galbraith P, Osherov A, Yalonetsky S, et al. Current perspectives on coronary chronic total occlusions: the Canadian multicenter chronic total occlusions registry. *J Am Coll Cardiol.* (2012) 59:991–7. doi: 10.1016/j.jacc.2011.12.007

2. Gössl M, Faxon D, Bell M, Holmes D, Gersh B. Complete versus incomplete revascularization with coronary artery bypass graft or percutaneous intervention in stable coronary artery disease. *Circ Cardiovasc Interv.* (2012) 5:597–604. doi: 10.1161/CIRCINTERVENTIONS.111.965509

3. Kahn J. Angiographic suitability for catheter revascularization of total coronary occlusions in patients from a community hospital setting. *Am Heart J.* (1993) 126:561–4. doi: 10.1016/0002-8703(93)90404-W

4. Azzalini L, Jolicoeur E, Pighi M, Millán X, Picard F, Tadros V, et al. Epidemiology, management strategies, and outcomes of patients with chronic total coronary occlusion. *Am J Cardiol.* (2016) 118:1128–35. doi: 10.1016/j.amjcard.2016.07.023

5. Brilakis E, Banerjee S, Karmpaliotis D, Lombardi W, Tsai T, Shunk K, et al. Procedural outcomes of chronic total occlusion percutaneous coronary intervention: a report from the NCDR (National Cardiovascular Data Registry). *JACC Cardiovasc Interv.* (2015) 8:245–53. doi: 10.1016/j.jcin.2014.08.014

6. Galassi A, Werner G, Boukhris M, Azzalini L, Mashayekhi K, Carlino M, et al. Percutaneous recanalisation of chronic total occlusions: 2019 consensus document from the EuroCTO club. *Eurointervention.* (2019) 15:198–208. doi: 10.4244/EIJ-D-18-00826

7. Teramoto T, Tsuchikane E, Yamamoto M, Matsuo H, Kawase Y, Suzuki Y, et al. Successful revascularization improves long-term clinical outcome in patients with chronic coronary total occlusion. *Int J Cardiol Heart Vasc.* (2017) 14:28–32. doi: 10.1016/j.ijcha.2016.11.001

8. Stojkovic S, Juricic S, Dobric M, Nedeljkovic M, Vukcevic V, Orlic D, et al. Improved propensity-score matched long-term clinical outcomes in patients with successful percutaneous coronary interventions of coronary chronic total occlusion. *Int Heart J.* (2018) 59:719–26. doi: 10.1536/ihj.17-360

9. Christakopoulos G, Christopoulos G, Carlino M, Jeroudi O, Roesle M, Rangan BV, et al. Meta-analysis of clinical outcomes of patients who underwent percutaneous coronary interventions for chronic total occlusions. *Am J Cardiol.* (2015) 115:1367–75. doi: 10.1016/j.amjcard.2015.02.038

10. Hoebers L, Claessen B, Elias J, Dangas G, Mehran R, Henriques J. Meta-analysis on the impact of percutaneous coronary intervention of chronic total occlusions on left ventricular function and clinical outcome. *Int J Cardiol.* (2015) 187:90–6. doi: 10.1016/j.ijcard.2015.03.164

11. Werner G, Martin-Yuste V, Hildick-Smith D, Boudou N, Sianos G, Gelev V, et al. A randomized multicentre trial to compare revascularization with optimal medical therapy for the treatment of chronic total coronary occlusions. *Eur Heart J.* (2018) 39:2484–93. doi: 10.1093/eurheartj/ehy220

12. Lee S, Lee P, Ahn J, Park D, Yun S, Han S, et al. Randomized trial evaluating percutaneous coronary intervention for the treatment of chronic total occlusion: the DECISION-CTO trial. *Circulation.* (2019) 139:1674–83. doi: 10.1161/CIRCULATIONAHA.118.031313

13. Henriques J, Hoebers L, Råmunddal T, Laanmets P, Eriksen E, Bax M, et al. Percutaneous intervention for concurrent chronic total occlusions in patients with STEMI: the EXPLORE trial. *J Am Coll Cardiol.* (2016) 68:1622–32. doi: 10.1016/j.jacc.2016.07.744

14. Juricic S, Tesic M, Galassi A, Petrovic O, Dobric M, Orlic D, et al. Randomized controlled comparison of optimal medical therapy with percutaneous recanalization of chronic total occlusion (COMET-CTO). *Int Heart J.* (2021) 62:16–22. doi: 10.1536/ihj.20-427

15. Ybarra L, Rinfret S, Brilakis E, Karmpaliotis D, Azzalini L, Grantham J, et al. Definitions and clinical trial design principles for coronary artery chronic total occlusion therapies: CTO-ARC consensus recommendations. *Circulation.* (2021) 143:479–500. doi: 10.1161/CIRCULATIONAHA.120.046754

16. Thygesen K, Alpert J, Jaffe A, Chaitman B, Bax J, Morrow D, et al. Fourth universal definition of myocardial infarction (2018). *Eur Heart J.* (2019) 40:237–69. doi: 10.1093/eurheartj/ehy856

17. Strauss B, Knudtson M, Cheema A, Galbraith P, Elbaz-Greener G, Abuzeid W, et al. Canadian multicenter chronic total occlusion registry: ten-year follow-up results of chronic total occlusion revascularization. *Circ Cardiovasc Interv.* (2021) 14:e010546. doi: 10.1161/CIRCINTERVENTIONS.121.010546

18. Park T, Lee S, Choi K, Lee J, Yang J, Song Y, et al. Late survival benefit of percutaneous coronary intervention compared with medical therapy in patients with coronary chronic total occlusion: a 10-year follow-up study. *J Am Heart Assoc.* (2021) 10:e019022. doi: 10.1161/JAHA.120.019022

19. Spertus J, Jones P, Maron D, O'Brien S, Reynolds H, Rosenberg Y, et al. Health-status outcomes with invasive or conservative care in coronary disease. *New Engl J Med.* (2020) 382:1408–19. doi: 10.1056/NEJMoa1916370

frontiers | Frontiers in Cardiovascular Medicine

TYPE Original Research
PUBLISHED 10 January 2023
DOI 10.3389/fcvm.2022.1062894

OPEN ACCESS

EDITED BY
Tommaso Gori,
Johannes Gutenberg University Mainz, Germany

REVIEWED BY
Sree Kondapally,
St George's University Hospitals NHS Foundation Trust, United Kingdom
Hiroki Teragawa,
JR Hiroshima Hospital, Japan

*CORRESPONDENCE
Hideo Fujita
✉ hideofujita@jichi.ac.jp

SPECIALTY SECTION
This article was submitted to Coronary Artery Disease, a section of the journal Frontiers in Cardiovascular Medicine

RECEIVED 06 October 2022
ACCEPTED 27 December 2022
PUBLISHED 10 January 2023

CITATION
Akashi N, Kuwabara M, Matoba T, Kohro T, Oba Y, Kabutoya T, Imai Y, Kario K, Kiyosue A, Mizuno Y, Nochioka K, Nakayama M, Iwai T, Nakao Y, Iwanaga Y, Miyamoto Y, Ishii M, Nakamura T, Tsujita K, Sato H, Fujita H and Nagai R (2023) Hyperuricemia predicts increased cardiovascular events in patients with chronic coronary syndrome after percutaneous coronary intervention: A nationwide cohort study from Japan. *Front. Cardiovasc. Med.* 9:1062894. doi: 10.3389/fcvm.2022.1062894

Hyperuricemia predicts increased cardiovascular events in patients with chronic coronary syndrome after percutaneous coronary intervention: A nationwide cohort study from Japan

Naoyuki Akashi[1], Masanari Kuwabara[2], Tetsuya Matoba[3], Takahide Kohro[4], Yusuke Oba[5], Tomoyuki Kabutoya[5], Yasushi Imai[6], Kazuomi Kario[5], Arihiro Kiyosue[7], Yoshiko Mizuno[7], Kotaro Nochioka[8], Masaharu Nakayama[9], Takamasa Iwai[10], Yoko Nakao[11], Yoshitaka Iwanaga[11], Yoshihiro Miyamoto[11], Masanobu Ishii[12], Taishi Nakamura[12], Kenichi Tsujita[12], Hisahiko Sato[13], Hideo Fujita[1]* and Ryozo Nagai[14]

[1]Division of Cardiovascular Medicine, Jichi Medical University Saitama Medical Center, Saitama, Japan, [2]Department of Cardiology, Toranomon Hospital, Tokyo, Japan, [3]Department of Cardiovascular Medicine, Kyushu University Graduate School of Medical Sciences, Fukuoka, Japan, [4]Department of Clinical Informatics, Jichi Medical University School of Medicine, Tochigi, Japan, [5]Division of Cardiovascular Medicine, Department of Medicine, Jichi Medical University School of Medicine, Tochigi, Japan, [6]Division of Clinical Pharmacology, Department of Pharmacology, Jichi Medical University, Tochigi, Japan, [7]Department of Cardiovascular Medicine, The University of Tokyo Hospital, Tokyo, Japan, [8]Department of Cardiovascular Medicine, Tohoku University Graduate School of Medicine, Clinical Research, Innovation and Education Center, Tohoku University Hospital, Sendai, Japan, [9]Department of Medical Informatics, Tohoku University Graduate School of Medicine, Sendai, Japan, [10]Department of Cardiovascular Medicine, National Cerebral and Cardiovascular Center, Suita, Japan, [11]Open Innovation Center, National Cerebral and Cardiovascular Center, Suita, Japan, [12]Department of Cardiovascular Medicine, Graduate School of Medical Sciences, Kumamoto University, Kumamoto, Japan, [13]Precision Inc., Tokyo, Japan, [14]Jichi Medical University, Tochigi, Japan

Background: The causal relationship between hyperuricemia and cardiovascular diseases is still unknown. We hypothesized that hyperuricemic patients after percutaneous coronary intervention (PCI) had a higher risk of major adverse cardiovascular events (MACE).

Methods: This was a large-scale multicenter cohort study. We enrolled patients with chronic coronary syndrome (CCS) after PCI between April 2013 and March 2019 using the database from the Clinical Deep Data Accumulation System (CLIDAS), and compared the incidence of MACE, defined as a composite of cardiovascular death, myocardial infarction, and hospitalization for heart failure, between hyperuricemia and non-hyperuricemia groups.

Results: In total, 9,936 patients underwent PCI during the study period. Of these, 5,138 patients with CCS after PCI were divided into two group (1,724 and 3,414 in the hyperuricemia and non-hyperuricemia groups, respectively). The hyperuricemia group had a higher prevalence of hypertension, atrial fibrillation, history of previous hospitalization for heart failure, and baseline creatinine, and a lower prevalence of diabetes than the non-hyperuricemia group, but the proportion of men and age were similar between the two groups. The incidence of MACE in the hyperuricemia group was significantly higher than that in the non-hyperuricemia group (13.1 vs. 6.4%, log-rank $P <$ 0.001). Multivariable Cox regression analyses revealed that hyperuricemia was significantly associated with increased MACE [hazard ratio (HR), 1.52; 95% confidential interval (CI), 1.23–1.86] after multiple adjustments for age, sex, body mass index, estimated glomerular filtration rate, left main disease or three-vessel disease, hypertension, diabetes mellitus, dyslipidemia, history of myocardial infarction, and history of hospitalization for heart failure. Moreover, hyperuricemia was independently associated with increased hospitalization for heart failure (HR, 2.19; 95% CI, 1.69–2.83), but not cardiovascular death or myocardial infarction after multiple adjustments. Sensitive analyses by sex and diuretic use, B-type natriuretic peptide level, and left ventricular ejection fraction showed similar results.

Conclusion: CLIDAS revealed that hyperuricemia was associated with increased MACE in patients with CCS after PCI. Further clinical trials are needed whether treating hyperuricemia could reduce cardiovascular events or not.

KEYWORDS

hyperuricemia, serum uric acid, chronic coronary syndrome, percutaneous coronary intervention, real-world database

1. Introduction

Epidemiological studies have shown that elevated serum uric acid (SUA) levels are associated with the increase of cardiovascular events (1–4). Cardiovascular risk factors such as hypertension, diabetes mellitus (DM), and chronic kidney disease may also coexist with hyperuricemia (5–7). Hyperuricemia and cardiovascular diseases are known to be associated with both, but it is unclear whether the relationship is causal or not (8). Some studies showed the positive relationship between hyperuricemia and cardiovascular disease (9, 10), but several studies did not show the relationship (11, 12). We hypothesized that this discrepancy could be mainly from the study subjects and study design because SUA is confounded with many cardiovascular risk factors, such as diet, obesity, hypertension, DM, chronic kidney disease, and so on (13). Therefore, we conducted a large-scale, cohort study to evaluate the relationship between hyperuricemia and cardiovascular events in patients after percutaneous coronary intervention (PCI) with multiple cardiovascular risk factor adjustments.

The study was conducted to test our hypothesis that hyperuricemic patients with chronic coronary syndrome (CCS) after PCI is associated with increased risk of major adverse cardiovascular events (MACE).

2. Materials and methods

2.1. Clinical Deep Data Accumulation System (CLIDAS)

The CLIDAS, which involves seven hospitals (six university hospitals and the National Cerebral and Cardiovascular Center Hospital in Japan), obtains clinical data including patient background, laboratory data, prescriptions, echocardiographic parameters, electrocardiogram, cardiac catheterization reports, and long-term prognosis. The Standardized Structured Medical Information eXchange version 2 (SS-MIX2) standard storage is used to collect basic patient information, prescriptions, and laboratory data from electronic medical records, whereas the SS-MIX2 extended storage is used to collect the data with non-standardized formats such as physiological tests, cardiac catheterization, and cardiac catheter intervention reports (14). The development of the CLIDAS started as the Japan Ischemic

heart disease Multimodal Prospective Data Acquisition for Precision Treatment project launched in 2015, aimed at creating a hospital information system (HIS)-based system that electronically collected both medical records and other clinical data in standardized data formats for clinical studies (15). In brief, HIS data, picture archiving and communication system data, and physiology data server were linked to multi-purpose clinical data repository system (MCDRS) then to the SS-MIX2 standard storage system through the firewalls (15). Each institution output data was linked from its own MCDRS server to the CLIDAS server after anonymization. Patient background information and follow-up data were collected by data managers and researchers at each site. After all data collected from each facility was aggregated into a central database, researchers retrieved the information necessary for the study and combined it based on the patient's unique anonymized ID for an integrated analysis of the data. In other fields, such as diabetes and renal disease, there are storage systems using the SS-MIX2 as well as the CLIDAS (16, 17). The collection of detailed longitudinal data on cardiovascular outcomes using SS-MIX is a unique feature of the CLIDAS.

2.2. Study design and population

This was a retrospective, multicenter, observational cohort study. We registered coronary artery disease (CAD) patients who had undergone PCI at seven hospitals between April 2013 and March 2019. This study period was determined as the period from the time when available data could be consistently obtained from each facility to the end of the ethics committee's accreditation. This study was approved by the Institutional Review Board of Jichi Medical University Saitama Medical Center (S21-163), and was conducted in accordance with the Declaration of Helsinki. The requirement for written informed consent was waived due to the retrospective study design. Patients with acute coronary syndrome and those with no event data were excluded. The final study population was categorized into two groups according to baseline SUA levels and/or prescribed urate-lowering drugs; the hyperuricemia group: patients with hyperuricemia at baseline, and the non-hyperuricemia group: patients without hyperuricemia at baseline.

The primary outcome was MACE, defined as a composite of cardiovascular death, myocardial infarction, or hospitalization for heart failure. The secondary outcomes were all-cause death and each component of MACE. The event-free time was calculated from the index PCI to the event date or the last follow-up date. Event confirmation was done at each facility using record information about patient visits, phone calls, and letters.

2.3. Definitions

In the CLIDAS database, index PCI was defined as the first PCI procedure within the study period if multiple vessels were treated in a staged manner. To increase the acquisition rate of laboratory data values, all baseline laboratory data were calculated as the average values from 60 days before the index PCI to 30 days after the procedure. In this study, hyperuricemia was defined as a SUA level $\geq$7.0 mg/dL for men or $\geq$6.0 mg/dL for women and/or taking urate-lowering drugs according to the previous studies (18–21). CCS was defined as cases of PCI other than acute coronary syndrome (22). Hypertension was defined as a systolic blood pressure $\geq$140 mmHg, diastolic blood pressure $\geq$90 mmHg, or a medical treatment for hypertension at index PCI. DM was defined as a hemoglobin A1C level $\geq$6.5%, casual blood glucose level $\geq$200 mg/dL, fasting blood glucose level $\geq$126 mg/dL, or medical treatment for DM at index PCI. Dyslipidemia was defined as a medical treatment for dyslipidemia at the index PCI or description of dyslipidemia on electronic medical records. We calculated the estimated glomerular filtration rate (eGFR) from the serum creatinine level, age, weight, and sex, using the following formula: eGFR $= 194 \times \mathrm{Cr}^{-1.094} \times \mathrm{age}^{-0.287}$ (man); eGFR $= 194 \times \mathrm{Cr}^{-1.094} \times \mathrm{age}^{-0.287} \times 0.739$ (woman) (23). We used echocardiographic findings closest to the index PCI, performed between −100 and 0 days before index PCI. Left ventricular ejection fraction (LVEF) was calculated using the modified Simpson's rule; however, the Teichholz method was used for LVEF measurement if the data of the modified Simpson's rule were missing.

The number of diseased vessels was defined as the number of coronary arteries with severe stenosis ($\geq$75%) in the major epicardial coronary segments of the right coronary artery, left anterior descending artery, and left circumflex artery and their branch lesions that underwent PCI. The diseased left main trunk (LMT), defined as $\geq$75% stenosis, was counted separately. The patients were categorized according to the combination of the number of diseased vessels and LMT disease.

2.4. Statistical analysis

Categorical variables were presented as counts and percentages, and continuous variables were presented as mean $\pm$ standard deviation for normally distributed continuous variables or median [interquartile range (IQR)] for non-normally distributed continuous variables. Categorical variables were compared using the chi-square test or Fisher's exact test for small samples. Normally distributed continuous variables were compared between the groups using an unpaired Student's *t*-test. The Shapiro-Wilk test was performed to determine whether the continuous variables were normally distributed. Conversely, non-normally distributed continuous variables were compared using the Mann–Whitney *U* test. Event-free survival rates

were calculated using the Kaplan–Meier method, and the statistical differences between the groups were calculated using the log-rank test. The patients were censored when they were lost to follow-up. Cox regression analyses were performed to clarify the determinants of MACE, all-cause death, and each component of MACE. For missing values, a complete case analysis was performed. Age, sex, body mass index, eGFR, left main (LM) disease or three-vessel disease (3VD), hypertension, DM, dyslipidemia, history of myocardial infarction, and history of hospitalization for heart failure were used as covariates in Model 1. Model 2 was performed using the covariates in Model 1 and diuretic use at baseline. Model 3 was used as a covariate in Model 2, B-type natriuretic peptide (BNP) levels, and LVEF at baseline. The missing numbers of BNP levels and LVEF were not small; thus, interpretation of Model 3 must be done carefully. Hazard ratios (HR) and 95% confidence intervals (CI) were calculated. All presented *P*-values were determined by two-sided analysis, and a *P*-value of <0.05 was considered statistically significant. *P*-values were presented without adjustment for multiple comparisons in an exploratory manner. All data were analyzed using SPSS ver. 28 for Windows (SPSS Inc., Chicago, Illinois, USA).

3. Results

A total of 9,936 consecutive patients who underwent PCI between April 2013 and March 2019 were enrolled in the CLIDAS database. Of them, 5,138 patients with CCS after PCI were analyzed. They were divided into a hyperuricemia group ($N = 1{,}724$) and a non-hyperuricemia group ($N = 3{,}414$) (Figure 1).

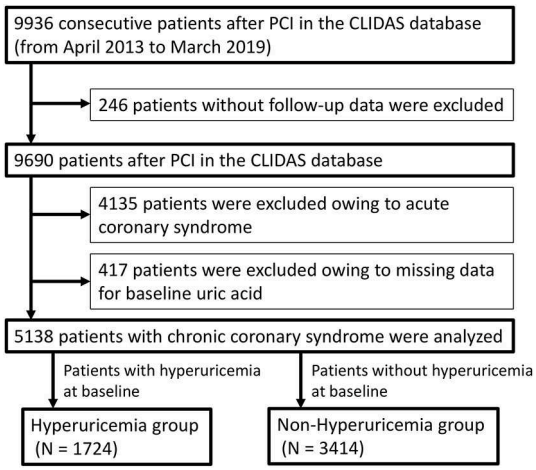

FIGURE 1
Study flow chart. PCI, percutaneous coronary intervention; CLIDAS, Clinical Deep Data Accumulation System.

Table 1 shows the baseline characteristics and comparisons of the hyperuricemia and non-hyperuricemia groups. For the entire cohort, the median (IQR) age was 72 (65–78) years, and 78.4% of the participants were men. Patient age and sex were well-balanced between the two groups. The prevalence of hypertension (87.0 vs. 81.7%), atrial fibrillation (9.0 vs. 4.5%), history of coronary artery bypass grafting (8.0 vs. 6.1%), history of hospitalization for heart failure (14.7 vs. 5.6%), and baseline creatinine value [median (IQR), 1.06 (0.88–1.39) mg/dL vs. 0.85 (0.72–1.02) mg/dL] were significantly higher in the hyperuricemia group than in the non-hyperuricemia group. Conversely, the prevalence of DM (43 vs. 48%) was significantly lower in the hyperuricemia group than that in the non-hyperuricemia group. The median BNP level in the hyperuricemia group [89 (35–282) pg/mL] was higher than that in the non-hyperuricemia group [45 (21–122) pg/mL]. The LVEF was lower in the hyperuricemia group than in the non-hyperuricemia group [60.0 (44.0–67.3)% vs. 62.6 (53.4–69.0)%]. LM disease or 3VD were more frequently observed in the hyperuricemia group than in the non-hyperuricemia group (20.1 vs. 17.0%). Prescription of beta-blockers, angiotensin-converting enzyme inhibitors or angiotensin receptor blockers, diuretics, and statins was significantly higher in the hyperuricemia group than in the non-hyperuricemia group. The number of prescriptions of febuxostat and allopurinol in the hyperuricemia group was 532 (30.9%) and 326 (18.9%), respectively.

The median follow-up duration was 910 days (307–1,479 days). During the follow-up period, there were 445 MACE, 381 all-cause deaths, 133 cardiovascular deaths, 85 myocardial infarctions, and 295 hospitalizations for heart failure (Table 2). The Kaplan–Meier curves for MACE are shown in Figure 2. The incidence of MACE was significantly higher in the hyperuricemia group than in the non-hyperuricemia group (log-rank test; $P < 0.001$). The Kaplan–Meier curves for all-cause death and each component of MACE are shown in Figure 3. The incidence of all-cause death, cardiovascular death and hospitalization for heart failure was significantly higher in the hyperuricemia group than in the non-hyperuricemia group (log-rank test; $P < 0.001$ for all of each). There was no significant difference in the prevalence of myocardial infarction between the two groups.

SUA levels were significantly different between men and women. Therefore, we conducted additional sensitivity analyses based on sex. The results of survival time analyses performed separately for men and women were generally consistent, except for cardiovascular death in women, which did not reach significance (log-rank test; $P = 0.211$).

The Cox regression analysis results are presented in Table 3. The hyperuricemia group was significantly associated with increased MACE in Models 1, 2, and 3 (Model 1: HR, 1.52, 95% CI, 1.23–1.86, $P < 0.001$; Model 2: HR, 1.31, 95% CI, 1.06–1.62, $P = 0.012$; Model 3: HR, 1.33, 95% CI, 1.01–1.77,

10.3389/fcvm.2022.1062894

TABLE 1 Baseline characteristics between the hyperuricemia and non-hyperuricemia groups.

	All ($n = 5,138$)	Missing data	Hyperuricemia ($n = 1,724$)	Non-hyperuricemia ($n = 3,414$)	*P*-value
Patient characteristics					
Age, year, median (IQR)	72 (65–78)	0	72 (65–78)	71 (65–78)	0.42
Men, *n* (%)	4,029 (78.4)	0	1,351 (78.4)	2,678 (78.4)	0.95
Body mass index, kg/m^2, median (IQR)	23.8 (21.8–26.3)	54 (1.1)	24.4 (22.0–27.0)	23.6 (21.6–25.9)	<0.001
Hypertension, *n* (%)	4,276 (83.5)	17 (0.3)	1,495 (87.0)	2,781 (81.7)	<0.001
Dyslipidemia, *n* (%)	4,043 (79.0)	22 (0.4)	1,371 (79.8)	2,672 (78.6)	0.33
Diabetes mellitus, *n* (%)	2,379 (46.6)	31 (0.6)	744 (43.4)	1,635 (48.2)	0.001
Atrial fibrillation, *n* (%)	308 (6.0)	17 (0.3)	154 (9.0)	154 (4.5)	0.001
Chronic kidney disease, *n* (%)	2,518 (50.0)	104 (2.0)	1,188 (70.5)	1,330 (39.7)	<0.001
Hemodialysis, *n* (%)	385 (7.5)	27 (0.5)	122 (7.1)	263 (7.7)	0.42
History of CABG, *n* (%)	345 (6.7)	20 (0.4)	138 (8.0)	207 (6.1)	0.009
History of PCI, *n* (%)	1,300 (25.4)	24 (0.5)	451 (26.3)	849 (25.0)	0.32
History of MI, *n* (%)	857 (16.8)	30 (0.6)	300 (17.5)	557 (16.4)	0.34
History of hospitalization for HF, *n* (%)	442 (8.6)	20 (0.4)	252 (14.7)	190 (5.6)	<0.001
History of stroke, *n* (%)	626 (12.2)	25 (0.5)	228 (13.3)	398 (11.7)	0.10
Systolic blood pressure on admission, mmHg, median (IQR)	127 (115–139)	86 (1.7)	126 (114–140)	127 (115–139)	0.47
Diastolic blood pressure on admission, mmHg, median (IQR)	69 (61–78)	88 (1.7)	70 (60–78)	69 (61–78)	0.29
Laboratory data					
Hemoglobin, g/dL, median (IQR)	12.8 (11.5–13.9)	0	12.5 (11.1–13.8)	12.9 (11.7–13.9)	<0.001
Hemoglobin A1C, %, median (IQR)	6.2 (5.8–6.8)	233 (4.5)	6.1 (5.7–6.7)	6.2 (5.8–6.9)	<0.001
Total cholesterol, mg/dL, median (IQR)	165.0 (144.0–186.0)	110 (2.1)	164.5 (143.0–185.5)	165.0 (144.5–186.3)	0.63
LDL cholesterol, mg/dL, median (IQR)	88.4 (71.8–107.2)	58 (1.1)	87.6 (71.1–106.7)	88.8 (71.9–107.5)	0.37
HDL cholesterol, mg/dL, median (IQR)	46.5 (39.0–55.7)	85 (1.7)	44.0 (37.5–53.0)	47.9 (40.0–57.0)	<0.001
Triglyceride, mg/dL, median (IQR)	120.5 (88.0–169.0)	50 (1.0)	133.3 (94.3–188.0)	114.5 (85.2–160.0)	<0.001
Creatinine, mg/dL, median (IQR)	0.91 (0.76–1.15)	107 (2.1)	1.06 (0.88–1.39)	0.85 (0.72–1.02)	<0.001
eGFR, ml/min/1.73 m^2, median (IQR)	60.1 (45.9–72.2)	107 (2.1)	49.7 (36.6–62.6)	64.5 (53.2–75.5)	<0.001
Uric acid, mg/dL, median (IQR)	5.7 (4.8–6.6)	0	7.0 (5.8–7.7)	5.3 (4.6–6.0)	<0.001
BNP, pg/mL, median (IQR)	55 (24–170)	323 (6.3)	89 (35–282)	45 (21–122)	<0.001
Echocardiographic finding (index −100 to 0 day)					
LVEF, %, median (IQR)	61.9 (50.0–68.5)	2,451 (47.7)	60.0 (44.0–67.3)	62.6 (53.4–69.0)	<0.001
Angiographic finding					
LM disease or 3VD, *n* (%)	927 (18.0)	405 (7.9)	346 (20.1)	581 (17.0)	0.021
Prescription (index −10 to 10 day)					
Beta-blockers, *n* (%)	2,868 (55.8)	0	1,099 (63.7)	1,769 (51.8)	<0.001
ACE-inhibitors or ARBs, *n* (%)	2,997 (58.3)	0	1,189 (69.0)	1,808 (53.0)	<0.001
Diuretics, *n* (%)	1,174 (22.8)	0	700 (40.6)	474 (13.9)	<0.001
Statins, *n* (%)	3,955 (77.0)	0	1,395 (80.9)	2,560 (75.0)	<0.001

(Continued)

TABLE 1 (Continued)

	All ($n = 5,138$)	Missing data	Hyperuricemia ($n = 1,724$)	Non-hyperuricemia ($n = 3,414$)	*P*-value
Febuxostat, *n* (%)	532 (10.4)	0	532 (30.9)		
Allopurinol, *n* (%)	326 (6.3)	0	326 (18.9)		
Benzbromarone, *n* (%)	65 (1.3)	0	65 (3.8)		
Probenecid, *n* (%)	3 (0.05)	0	3 (0.1)		

CABG, coronary artery bypass grafting; PCI, percutaneous coronary intervention; MI, myocardial infarction; HF, heart failure; LDL, low-density lipoprotein; HDL, high-density lipoprotein; eGFR, estimated glomerular filtration rate; BNP, B-type natriuretic peptide; LVEF, left ventricular ejection fraction; LM, left main; VD, vessel disease; ACE, angiotensin-converting enzyme; ARB, angiotensin II receptor blocker; IQR, interquartile range.

TABLE 2 Clinical outcomes between the hyperuricemia and non-hyperuricemia groups.

	All ($n = 5,138$)	Hyperuricemia ($n = 1,724$)	Non-hyperuricemia ($n = 3,414$)
MACE, *n* (%)	445 (8.7)	226 (13.1)	219 (6.4)
All-cause death, *n* (%)	381 (7.4)	171 (9.9)	210 (6.2)
Cardiovascular death, *n* (%)	133 (2.6)	64 (3.7)	69 (2.0)
Myocardial infarction, *n* (%)	85 (1.7)	31 (1.8)	54 (1.6)
Hospitalization for heart failure, *n* (%)	295 (5.7)	173 (11.3)	122 (3.6)

MACE, major adverse cardiovascular events.

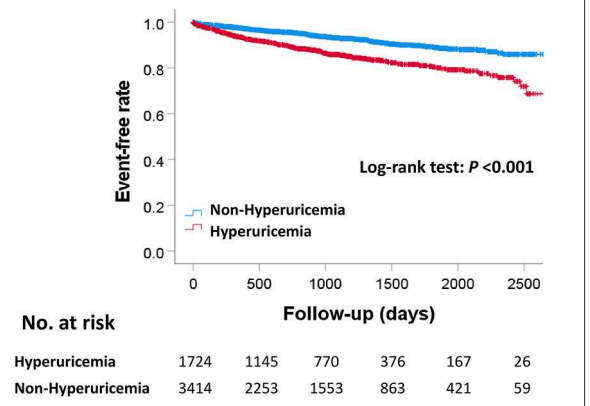

FIGURE 2
Kaplan–Meier curves for MACE between the hyperuricemia and non-hyperuricemia groups. *P*-value were calculated using the log-rank test. MACE, major adverse cardiac events.

$P = 0.046$). The hyperuricemia group was also significantly associated with increased hospitalization for heart failure in Models 1, 2, and 3 (Model 1: HR, 2.19, 95% CI, 1.69–2.83, $P < 0.001$; Model 2: HR, 1.76, 95% CI, 1.35–2.29, $P < 0.001$; Model 3: HR, 1.71, 95% CI, 1.21–2.41, $P = 0.003$). All-cause death was significantly associated with hyperuricemia only in model 1. Neither cardiovascular death nor myocardial infarction were significantly associated with hyperuricemia between the two groups after multiple adjustments for covariates.

Since our results showed that hospitalization for heart failure events have the greatest impact on MACE, we performed additional sensitivity analyses in patients without a history of heart failure ($n = 4676$). The incidence of hospitalization for heart failure was significantly higher in the hyperuricemia group than in the non-hyperuricemia group after multiple adjustments (Model 1: HR, 2.14, 95% CI, 1.58–2.90, $P < 0.001$; Model 2: HR, 1.68, 95% CI, 1.23–2.30, $P = 0.001$; Model 3: HR, 1.61, 95% CI, 1.06–2.44, $P = 0.026$) (Supplementary Figure 1 and Supplementary Table 1).

4. Discussion

This large-scale, multicenter, observational cohort study revealed that the hyperuricemic patients with CCS after PCI had two times higher incidence of MACE than those without hyperuricemia during a median follow-up of 910 days. Even after multiple adjustments, hyperuricemia was independently associated with higher risk for MACE (Model 1: HR, 1.52; Model 2: HR, 1.31; Model 3: HR, 1.33). The sensitivity analyses after multiple adjustments showed that hyperuricemia was independently associated with increased hospitalization for heart failure (Model 1: HR, 2.19; Model 2: HR, 1.76; Model 3: HR, 1.71), but not cardiovascular death and myocardial infarction. These results suggest that hyperuricemia in patients with CCS after PCI could be a risk predictor for MACE, especially for heart failure.

The strengths of the study are that we adjusted many confounding factors of SUA by multiple models. SUA is

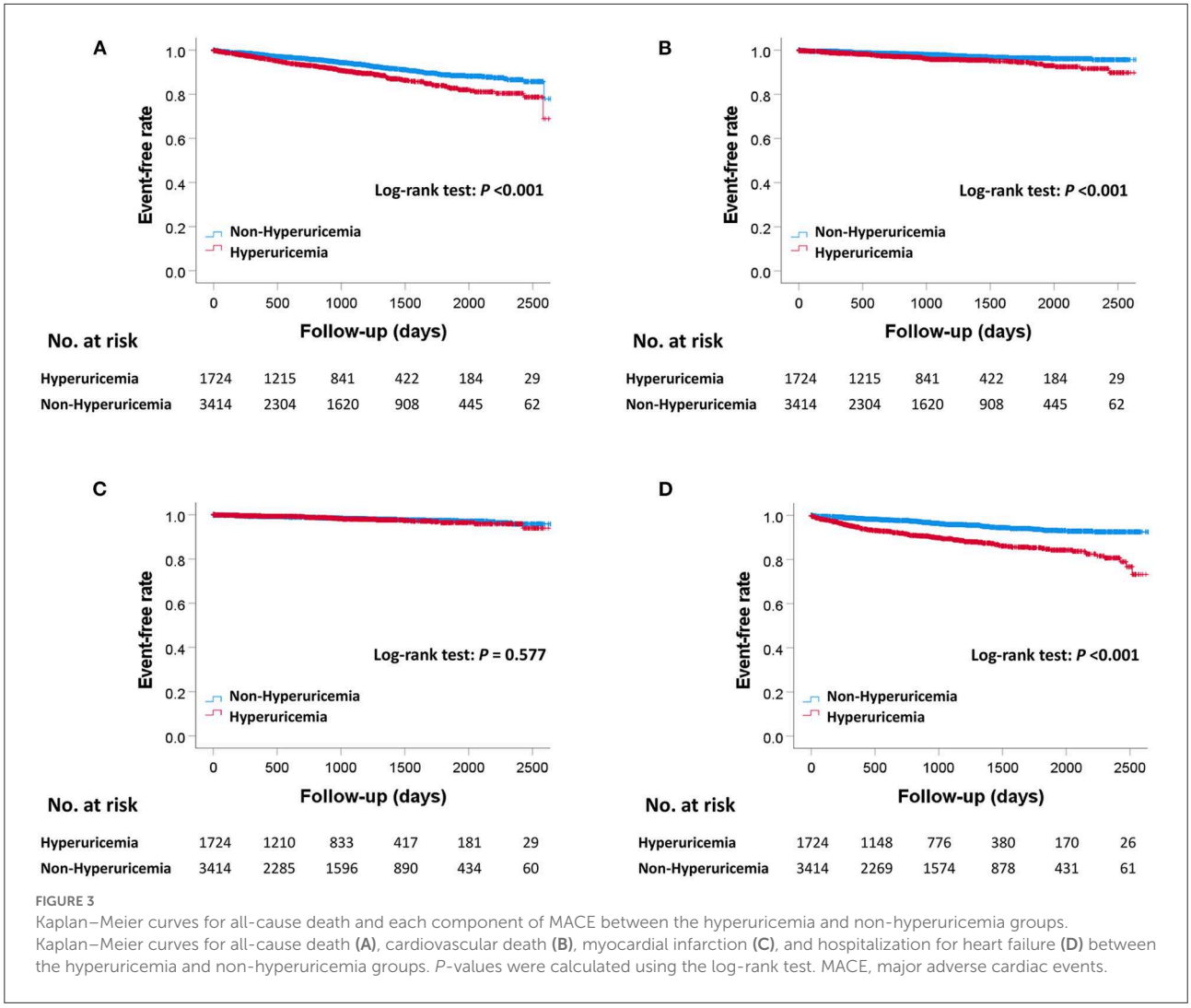

FIGURE 3
Kaplan–Meier curves for all-cause death and each component of MACE between the hyperuricemia and non-hyperuricemia groups. Kaplan–Meier curves for all-cause death **(A)**, cardiovascular death **(B)**, myocardial infarction **(C)**, and hospitalization for heart failure **(D)** between the hyperuricemia and non-hyperuricemia groups. *P*-values were calculated using the log-rank test. MACE, major adverse cardiac events.

associated with many cardiovascular risk factors, including age, sex, body mass index, eGFR, hypertension, DM, and dyslipidemia, and we carefully adjusted these components. Furthermore, diuretics, like thiazide and loop diuretics, increase SUA by reducing urine urate excretion, and we adjusted diuretic use in Model 2. The HR of MACE in Model 2 was less than that in Model 1 (1.31 vs. 1.52), which showed that conducting analyses by multiple models is important to remove the confounding factors associated with SUA. Even after adjustments with diuretics use, every model showed that hyperuricemia was independently associated with increased MACE. Moreover, the HR of hospitalization for heart failure in Model 2 was also lower than that in Model 1 (1.76 vs. 2.19), which suggests that SUA and diuretics are associated with each other during hospitalization for heart failure. Diuretic use is recommended for managing heart failure based on guidelines (24, 25). Our results suggests that we should take care of SUA levels in use of diuretics for heart failure as a competing risk for hospitalization for heart failure.

SUA levels were largely different between men and women, and we conducted every analysis stratified by sex. The results of survival time analyses showed that hyperuricemia was independently associated with increased cardiovascular death in men, but not in women. However, the HR in women were similar with that in men, and both HRs were more than 1. Therefore, the difference could be due to the differences in the number of patients. In fact, there were significant differences both men and women in all-cause death, which has a higher number of events than cardiovascular disease. The number of women patients was less than one-third of that of men patients. Previous studies reported that hyperuricemia in women is more risk than that in men (13, 26). We consider that the difference could be mainly due to less statistical power in women.

TABLE 3 Cox regression analysis predicting MACE, all-cause death, and components of MACE.

Composite endpoint	Hazard ratio	95% confidence interval	*P*-value
MACE			
Non-hyperuricemia	Reference		
Unadjusted hyperuricemia	2.10	1.74–2.52	<0.001
Adjusted hyperuricemia (model 1)	1.52	1.23–1.86	<0.001
Adjusted hyperuricemia (model 2)	1.31	1.06–1.62	0.012
Adjusted hyperuricemia (model 3)	1.33	1.01–1.77	0.046
Component endpoints	**Hazard ratio**	**95% confidence interval**	***P*-value**
All-cause death			
Non-hyperuricemia	Reference		
Unadjusted hyperuricemia	1.60	1.31–1.96	<0.001
Adjusted hyperuricemia (model 1)	1.26	1.01–1.57	0.044
Adjusted hyperuricemia (model 2)	1.15	0.92–1.45	0.23
Adjusted hyperuricemia (model 3)	1.13	0.82–1.56	0.47
Cardiovascular death			
Non-hyperuricemia	Reference		
Unadjusted hyperuricemia	1.83	1.30–2.57	<0.001
Adjusted hyperuricemia (model 1)	1.20	0.82–1.74	0.35
Adjusted hyperuricemia (model 2)	1.05	0.72–1.55	0.80
Adjusted hyperuricemia (model 3)	1.00	0.59–1.71	0.99
Myocardial infarction			
Non-hyperuricemia	Reference		
Unadjusted hyperuricemia	1.13	0.73–1.76	0.58
Adjusted hyperuricemia (model 1)	0.83	0.51–1.33	0.44
Adjusted hyperuricemia (model 2)	0.87	0.53–1.41	0.56
Adjusted hyperuricemia (model 3)	0.89	0.45–1.76	0.74
Hospitalization for heart failure			
Non-hyperuricemia	Reference		
Unadjusted hyperuricemia	2.89	2.29–3.65	<0.001
Adjusted hyperuricemia (model 1)	2.19	1.69–2.83	<0.001
Adjusted hyperuricemia (model 2)	1.76	1.35–2.29	<0.001
Adjusted hyperuricemia (model 3)	1.71	1.21–2.41	0.003

The Cox regression analysis was performed using the following covariates: Model 1 including age, sex, body mass index, eGFR, left main disease or three-vessel disease, hypertension, diabetes mellitus, dyslipidemia, history of myocardial infarction, history of hospitalization for heart failure. Model 2 including covariates in Model 1 and diuretics use at baseline. Model 3 including covariates in Model 2, BNP levels and LVEF at baseline. BNP and LVEF were entered as the categorical variables (BNP ≥100 pg/mL or not, LVEF ≥50% or not, respectively). MACE, major adverse cardiovascular events.

As several studies demonstrated, higher SUA levels were associated with the incidence of cardiovascular events in patients with CAD (9, 27–29). One multicenter, prospective observational study reported that elevated SUA level was an independent predictor of cardiovascular events and all-cause mortality in patients who had coronary artery stenosis ≥75% by coronary angiography in at least one branch of the coronary arteries (9). During the 3-years follow-up, the HR for all events, defined as cardiovascular events and all-cause mortality, was 1.25 (95% CI, 1.07–1.45) in the highest SUA quartile (SUA ≥6.8 mg/dL) after adjusting for covariates. Although these components of the composite endpoint were

slightly different from those in our study, elevated SUA levels were consistently associated with increased adverse events. However, some previous studies demonstrated that increased SUA levels were not significantly associated with a higher rate of cardiovascular mortality in patients with CAD (30, 31). One prospective observational study from the Stable Coronary Artery Diseases Registry (START) registry in Italy reported that high SUA levels did not significantly influence 1-year cardiovascular events in patients with CCS with or without PCI (30). Contrary to our findings, the START registry showed no relationship between SUA levels and cardiovascular events. The above discordance may be due to the fact that the follow-up period in the START registry (1 year) was shorter than our follow-up period (median 910 days). In fact, the highest SUA tertile group (SUA $\geq$6.23 mg/dL) tended to have an increased incidence of MACE, including cardiovascular death and hospitalization for myocardial infarction, heart failure, angina, or revascularization, suggesting that a longer follow-up period might have revealed a significant relationship between increased SUA levels and MACE in the START registry (30).

We should discuss why MACE, especially hospitalization for heart failure, increased in the hyperuricemia group compared with the non-hyperuricemia group. Our results revealed that the presence of hyperuricemia during PCI procedures in patients with CCS after PCI was an independent predictor of hospitalization for heart failure, whereas there was no independent relationship between hyperuricemia and cardiovascular events, including cardiovascular death and myocardial infarction. Additionally, we performed sensitivity analyses to determine whether hyperuricemia affects hospitalization for heart failure in patients without a history of heart failure ($n = 4676$), and the results showed that hyperuricemia was still associated with hospitalization for heart failure after multiple adjustments (Supplementary Table 1). It has been reported that uric acid metabolism plays an important role in the development of cardiovascular disease, especially in the early stages of cardiovascular disease (32). In the CARDIA study, a cohort of young subjects showed that the elevation of SUA levels might be a biomarker for early atherosclerosis, as assessed by coronary artery calcified plaque and carotid intima-media thickness (33). A recent study using dual-energy computed tomography detected coronary monosodium uric acid crystal deposition in gout patients (34). However, some studies showed that higher SUA levels were not significantly linked to a higher rate of cardiovascular mortality in CAD patients. These findings suggest that hyperuricemia may contribute to CAD progression in the early stages of atherosclerosis. Despite these findings, our results showed no statistically significant difference in myocardial infarction between the two groups, suggesting that hyperuricemia may contribute to heart failure events more than atherosclerotic disease progression in patients with CCS after PCI. Even after adding covariates such as diuretic use at baseline, BNP level, and LVEF at baseline, hyperuricemia was consistently associated with MACE and hospitalization for heart failure. One meta-analysis reported that every 1 mg/dL increase in SUA increases the risk of developing heart failure by 19% (HR 1.19, 95% CI 1.17–1.21) (35). Moreover, some retrospective observational studies have shown that elevated SUA levels are associated with a higher risk of heart failure in patients with CAD (36, 37). The mechanism by which uric acid influences the development of heart failure is thought to be the result of oxidative stress caused by xanthine oxidase-derived elevated uric acid and reactive oxygen species (38). Other factors, such as the renin-angiotensin-aldosterone system and the use of diuretics (39), have not been fully elucidated.

The clinical implications of this study are as follows. We revealed that the presence of hyperuricemia in patients with CCS after PCI was associated with increased MACE, especially hospitalization for heart failure. Some recent clinical guidelines have shown that urate-lowering drugs may be associated with a reduction in the risk of cardiovascular events in patients with hyperuricemia and gout (40); however, it remains unclear whether urate-lowering drugs could prevent the subsequent development of cardiovascular disease among CCS patients. The results of two randomized controlled trials on the effects of the urate-lowering drugs oxypurinol (41) and allopurinol (42) on cardiovascular events in patients with symptomatic heart failure and reduced LVEF did not show improved clinical status. Although not significant, taking allopurinol tended to reduce hospitalization for heart failure in the EXACT-HF study (42). Considering these results and our results, future studies are warranted to determine whether urate-lowering therapy in patients with CCS after PCI can reduce cardiovascular events, including hospitalization for heart failure.

4.1. Limitations

This study had some limitations that need to be addressed. First, because this was a retrospective observation study, we could not show the causal relationship between hyperuricemia and MACE. Further clinical trials are needed whether urate lowering treatment for hyperuricemia could reduce MACE or not. Moreover, this study has a possibility of selection bias. To reduce the selection bias, this study included all patients over the study period from seven hospitals. Second, due to the missing echocardiographic data and BNP values, these were analyzed separately in the multivariable analysis, which might lead to biased results. To address this problem, we created several models using a multivariable analysis. The results of the three models showed the same direction, and we believe that the results were reliable. Additionally, our results in Table 3 showed that hyperuricemia was significantly associated with hospitalization for heart failure, and not any other components of MACE. It is crucial to take into account echocardiographic

results, such as LVEF. We performed sensitivity analyses of only those evaluated for LVEF (n = 2,687), and the trend of the results did not differ from that of the overall population (log-rank test for MACE, $P < 0.001$; that for cardiovascular death, $P = 0.005$; that for myocardial infarction, $P = 0.489$; that for heart failure, $P < 0.001$). Third, our database does not contain information about the history of gout; therefore, we have a mix of symptomatic and asymptomatic hyperuricemia patients. Although patients taking urate-lowering drugs may have a history of gout, survival time analysis of MACE in the hyperuricemia group according to the presence or absence of urate-lowering drugs showed no significant difference (log-rank test; $P = 0.232$). Fourth, in this study, all baseline laboratory data were calculated as the average values from 60 days before the index PCI to 30 days after the procedure, and it had time gap between the sample collection and the index PCI procedure. Therefore, the time gap could cause the associations significantly impacted. However, it is also important to increase the acquisition rate of laboratory data values, and this study adopted this methodology. Fifth, the definition of LM disease generally used a significant stenosis as ≥50% for LM. In our study, we used the definition of LM disease as ≥75% for LM when making the study protocol following the previous study (43). We have to take account for the difference of the definition of LM disease between our study and most international studies. Sixth, this study could not get the information of food, alcohol and fructose intake. SUA levels are affected by alcohol and fructose consumption. It is a limitation in a nature of this retrospective study.

5. Conclusion

The CLIDAS study showed that hyperuricemia was associated with an increased risk of MACE, especially increased hospitalization for heart failure, in patients with CCS after PCI. Further intervention studies are needed to determine whether urate-lowering treatment could prevent MACE in patients with CCS.

Data availability statement

The raw data supporting the conclusions of this article will be made available by the authors, without undue reservation.

Ethics statement

The studies involving human participants were reviewed and approved by the Institutional Review Board of Jichi Medical University Saitama Medical Center (S21-163). Written informed consent for participation was not required for this study in accordance with the national legislation and the institutional requirements.

Author contributions

NA and HF contributed to conception and design of the study. NA, TM, TKo, TKa, MI, TN, and HS collected data and organized the database. NA performed the statistical analysis. NA, MK, and HF contributed to interpretation of the data and writing. All authors contributed to the critical revision and final approval of the manuscript.

Funding

CLIDAS was developed with funding from Kowa Company Limited.

Acknowledgments

The authors thank the Kowa Company for funding the development of CLIDAS. The authors appreciate the contributions of all CLIDAS research group members. We thank Yuri Matoba (Precision Inc., Tokyo, Japan) for helping us integrate the data.

Conflict of interest

HS was employed by Precision, Inc. TM has received research grants from Amgen; and honoraria from Abbott Medical and Bayer. TKa has received scholarship funds from Abbott Medical. YIm has received honoraria from Daiichi Sankyo and Toa Eiyo. KK has received research grants and honoraria from Sanwa Kagaku Kenkyusho. AK has received honoraria from AstraZeneca, Eli Lilly, and Sumitomo Pharma. YN has received research grants and consulting fees from Bayer. KT has received research grants from PPD-Shin Nippon Biomedical Laboratories and Alexion Pharmaceuticals; and scholarship funds from Abbott Medical, Bayer, Boehringer Ingelheim, Daiichi Sankyo, ITI, Ono Pharmaceutical, Otsuka Pharmaceutical, and Takeda Pharmaceutical; affiliation with endowed department from Abbott Medical, Boston Scientific, Cardinal Health, Fides-ONE, Fukuda Denshi, GM Medical, ITI, Japan Lifeline, Kaneka Medix, Medical Appliance, Medtronic, Nipro, and Terumo; and honoraria from Abbott Medical, Amgen, AstraZeneca, Bayer, Daiichi Sankyo, Medtronic, Kowa, Novartis Pharma, Otsuka Pharmaceutical, Pfizer, and Janssen Pharmaceutical. HS reports stock or stock options in Precision. HF has received consulting fees from Mehergen

Group Holdings; and honoraria from Novartis Pharma and Otsuka Pharmaceutical. RN has received from honoraria from Kowa, Takeda Pharmaceutical, Tanabe-Mitsubishi Pharmaceutical, Boehringer-Ingelheim.

The remaining authors declare that the research was conducted in the absence of any commercial or financial relationships that could be construed as a potential conflict of interest.

Publisher's note

All claims expressed in this article are solely those of the authors and do not necessarily represent those of their affiliated organizations, or those of the publisher, the editors and the reviewers. Any product that may be evaluated in this article, or claim that may be made by its manufacturer, is not guaranteed or endorsed by the publisher.

Supplementary material

The Supplementary Material for this article can be found online at: https://www.frontiersin.org/articles/10.3389/fcvm.2022.1062894/full#supplementary-material

SUPPLEMENTARY FIGURE 1
Kaplan–Meier curves for hospitalization for heart failure in patients without a history of heart failure.

SUPPLEMENTARY TABLE 1
Cox regression analysis predicting hospitalization for heart failure in patients without a history of heart failure.

References

1. Fang J, Alderman MH. Serum uric acid and cardiovascular mortality the NHANES I epidemiologic follow-up study, 1971–1992. National health and nutrition examination survey. *JAMA*. (2000) 283:2404–10. doi: 10.1001/jama.283.18.2404

2. Bos MJ, Koudstaal PJ, Hofman A, Witteman JC, Breteler MM. Uric acid is a risk factor for myocardial infarction and stroke: the Rotterdam study. *Stroke*. (2006) 37:1503–7. doi: 10.1161/01.STR.0000221716.55088.d4

3. Lopez-Pineda A, Cordero A, Carratala-Munuera C, Orozco-Beltran D, Quesada JA, Bertomeu-Gonzalez V, et al. Hyperuricemia as a prognostic factor after acute coronary syndrome. *Atherosclerosis*. (2018) 269:229–35. doi: 10.1016/j.atherosclerosis.2018.01.017

4. Seki H, Kaneko H, Morita H, Itoh H, Morita K, Matsuoka S, et al. Relation of serum uric acid and cardiovascular events in young adults aged 20–49 years. *Am J Cardiol*. (2021) 152:150–57. doi: 10.1016/j.amjcard.2021.05.007

5. Wang J, Qin T, Chen J, Li Y, Wang L, Huang H, et al. Hyperuricemia and risk of incident hypertension: a systematic review and meta-analysis of observational studies. *PLoS ONE*. (2014) 9:e114259. doi: 10.1371/journal.pone.0114259

6. Lv Q, Meng XF, He FF, Chen S, Su H, Xiong J, et al. High serum uric acid and increased risk of type 2 diabetes: a systemic review and meta-analysis of prospective cohort studies. *PLoS ONE*. (2013) 8:e56864. doi: 10.1371/journal.pone.0056864

7. Bonino B, Leoncini G, Russo E, Pontremoli R, Viazzi F. Uric acid in CKD: has the jury come to the verdict? *J Nephrol*. (2020) 33:715–24. doi: 10.1007/s40620-020-00702-7

8. Johnson RJ, Bakris GL, Borghi C, Chonchol MB, Feldman D, Lanaspa MA, et al. Hyperuricemia, acute and chronic kidney disease, hypertension, and cardiovascular disease: report of a scientific workshop organized by the national kidney foundation. *Am J Kidney Dis*. (2018) 71:851–65. doi: 10.1053/j.ajkd.2017.12.009

9. Okura T, Higaki J, Kurata M, Irita J, Miyoshi K, Yamazaki T, et al. Elevated serum uric acid is an independent predictor for cardiovascular events in patients with severe coronary artery stenosis: subanalysis of the Japanese Coronary Artery Disease (JCAD) study. *Circ J*. (2009) 73:885–91. doi: 10.1253/circj.CJ-08-0828

10. Braga F, Pasqualetti S, Ferraro S, Panteghini M. Hyperuricemia as risk factor for coronary heart disease incidence and mortality in the general population: a systematic review and meta-analysis. *Clin Chem Lab Med*. (2016) 54:7–15. doi: 10.1515/cclm-2015-0523

11. Culleton BF, Larson MG, Kannel WB, Levy D. Serum uric acid and risk for cardiovascular disease and death: the Framingham Heart Study. *Ann Intern Med*. (1999) 131:7–13. doi: 10.7326/0003-4819-131-1-199907060-00003

12. Moriarity JT, Folsom AR, Iribarren C, Nieto FJ, Rosamond WD. Serum uric acid and risk of coronary heart disease: atherosclerosis risk in communities (ARIC) study. *Ann Epidemiol*. (2000) 10:136–43. doi: 10.1016/S1047-2797(99)00037-X

13. Kuwabara M. Hyperuricemia, Cardiovascular Disease, and Hypertension. *Pulse (Basel)*. (2016) 3:242–52. doi: 10.1159/000443769

14. Kimura M, Nakayasu K, Ohshima Y, Fujita N, Nakashima N, Jozaki H, et al. SS-MIX: a ministry project to promote standardized healthcare information exchange. *Methods Inf Med*. (2011) 50:131–9. doi: 10.3414/ME10-01-0015

15. Matoba T, Kohro T, Fujita H, Nakayama M, Kiyosue A, Miyamoto Y, et al. Architecture of the Japan ischemic heart disease multimodal prospective data acquisition for precision treatment (J-IMPACT) System. *Int Heart J*. (2019) 60:264–70. doi: 10.1536/ihj.18-113

16. Ishii M, Miyo K, Sugiyama T, Ohsugi M, Ueki K. Development of patient state model to overview clinical registry database. *Stud Health Technol Inform*. (2019) 264:1492–93. doi: 10.3233/SHTI190500

17. Nakagawa N, Sofue T, Kanda E, Nagasu H, Matsushita K, Nangaku M, et al. J-CKD-DB: a nationwide multicentre electronic health record-based chronic kidney disease database in Japan. *Sci Rep*. (2020) 10:7351. doi: 10.1038/s41598-020-64123-z

18. Suwazono Y, Kobayashi E, Uetani M, Miura K, Morikawa Y, Ishizaki M, et al. G-protein beta3 subunit gene variant is unlikely to have a significant influence on serum uric acid level in Japanese workers. *Tohoku J Exp Med*. (2006) 209:149–57. doi: 10.1620/tjem.209.149

19. Han M, Lee JP, Park S, Kim Y, Kim YC, Ahn C, et al. Early onset hyperuricemia is a prognostic marker for kidney graft failure: propensity score matching analysis in a Korean multicenter cohort. *PLoS ONE*. (2017) 12:e0176786. doi: 10.1371/journal.pone.0176786

20. Tanaka K, Hara S, Kushiyama A, Ubara Y, Yoshida Y, Mizuiri S, et al. Risk of macrovascular disease stratified by stage of chronic kidney disease in type 2 diabetic patients: critical level of the estimated glomerular filtration rate and the significance of hyperuricemia. *Clin Exp Nephrol*. (2011) 15:391–97. doi: 10.1007/s10157-011-0420-6

21. Tanaka K, Hara S, Hattori M, Sakai K, Onishi Y, Yoshida Y, et al. Role of elevated serum uric acid levels at the onset of overt nephropathy in the risk for renal function decline in patients with type 2 diabetes. *J Diabetes Investig*. (2015) 6:98–104. doi: 10.1111/jdi.12243

22. Oba Y, Kabutoya T, Kohro T, Imai Y, Kario K, Sato H, et al. Relationships among heart rate, β-blocker dosage, and prognosis in patients with coronary artery disease in a real-world database using a multimodal data acquisition system. *Circ J*. (2022). doi: 10.1253/circj.CJ-22-0314. [Epub ahead of print].

23. Matsuo S, Imai E, Horio M, Yasuda Y, Tomita K, Nitta K, et al. Revised equations for estimated GFR from serum creatinine in Japan. *Am J Kidney Dis*. (2009) 53:982–92. doi: 10.1053/j.ajkd.2008.12.034

24. Heidenreich PA, Bozkurt B, Aguilar D, Allen LA, Byun JJ, Colvin MM, et al. 2022 AHA/ACC/HFSA guideline for the management of heart failure: a report of the American college of cardiology/American heart association joint committee on clinical practice guidelines. *J Am Coll Cardiol*. (2022) 79:e263–421. doi: 10.1016/j.jacc.2021.12.012

25. McDonagh TA, Metra M, Adamo M, Gardner RS, Baumbach A, Böhm M, et al. 2021 ESC Guidelines for the diagnosis and treatment of acute and

chronic heart failure. *Eur Heart J*. (2021) 42:3599–726. doi: 10.1093/eurheartj/ehab368

26. Barbieri L, Verdoia M, Schaffer A, Marino P, Suryapranata H, De Luca G. Impact of sex on uric acid levels and its relationship with the extent of coronary artery disease: a single-centre study. *Atherosclerosis*. (2015) 241:241–8. doi: 10.1016/j.atherosclerosis.2015.03.030

27. Lin GM, Li YH, Zheng NC, Lai CP, Lin CL, Wang JH, et al. Serum uric acid as an independent predictor of mortality in high-risk patients with obstructive coronary artery disease: a prospective observational cohort study from the ET-CHD registry, 1997–2003. *J Cardiol*. (2013) 61:122–7. doi: 10.1016/j.jjcc.2012.09.004

28. Chen C, Dong J, Lv Q, Liu X, Zhang Q, Du X. Effect of asymptomatic hyperuricemia on mortality of elderly patients after elective percutaneous coronary intervention. *Front Cardiovasc Med*. (2022) 9:800414. doi: 10.3389/fcvm.2022.800414

29. Zhang C, Jiang L, Xu L, Tian J, Liu J, Zhao X, et al. Implications of hyperuricemia in severe coronary artery disease. *Am J Cardiol*. (2019) 123:558–64. doi: 10.1016/j.amjcard.2018.11.027

30. De Luca L, Gulizia MM, Gabrielli D, Meessen J, Mattei L, D'Urbano M, et al. Impact of serum uric acid levels on cardiovascular events and quality of life in patients with chronic coronary syndromes: insights from a contemporary, prospective, nationwide registry. *Nutr Metab Cardiovasc Dis*. (2022) 32:393–401. doi: 10.1016/j.numecd.2021.09.034

31. Tsai TH, Chen YL, Chen SM, Yang CH, Fang CY, Hsieh YK, et al. Uric Acid is not an independent predictor of cardiovascular death in patients with angiographically proven coronary artery disease. *Chang Gung Med J*. (2009) 32:605–13.

32. Feig DI, Kang DH, Johnson RJ. Uric acid and cardiovascular risk. *N Engl J Med*. (2008) 359:1811–21. doi: 10.1056/NEJMra0800885

33. Wang H, Jacobs DR, Jr., Gaffo AL, Gross MD, Goff DC, Jr., Carr JJ. Longitudinal association between serum urate and subclinical atherosclerosis: the Coronary Artery Risk Development in Young Adults (CARDIA) study. *J Intern Med*. (2013) 274:594–609. doi: 10.1111/joim.12120

34. Feuchtner GM, Plank F, Beyer C, Schwabl C, Held J, Bellmann-Weiler R, et al. Monosodium urate crystal deposition in coronary artery plaque by 128-slice dual-energy computed tomography: an *ex vivo* phantom and *in vivo* study. *J Comput Assist Tomogr*. (2021) 45:856–62. doi: 10.1097/RCT.0000000000001222

35. Huang H, Huang B, Li Y, Huang Y, Li J, Yao H, et al. Uric acid and risk of heart failure: a systematic review and meta-analysis. *Eur J Heart Fail*. (2014) 16:15–24. doi: 10.1093/eurjhf/hft132

36. Eisen A, Benderly M, Goldbourt U, Haim M. Is serum uric acid level an independent predictor of heart failure among patients with coronary artery disease? *Clin Cardiol*. (2013) 36:110–6. doi: 10.1002/clc.22083

37. Lim SS, Yang YL, Chen SC, Wu CH, Huang SS, Chan WL, et al. Association of variability in uric acid and future clinical outcomes of patient with coronary artery disease undergoing percutaneous coronary intervention. *Atherosclerosis*. (2020) 297:40–6. doi: 10.1016/j.atherosclerosis.2020.01.025

38. Hare JM, Johnson RJ. Uric acid predicts clinical outcomes in heart failure: insights regarding the role of xanthine oxidase and uric acid in disease pathophysiology. *Circulation*. (2003) 107:1951–3. doi: 10.1161/01.CIR.0000066420.36123.35

39. Saito Y, Tanaka A, Node K, Kobayashi Y. Uric acid and cardiovascular disease: a clinical review. *J Cardiol*. (2021) 78:51–7. doi: 10.1016/j.jjcc.2020.12.013

40. Li Q, Li X, Wang J, Liu H, Kwong JS, Chen H, et al. Diagnosis and treatment for hyperuricemia and gout: a systematic review of clinical practice guidelines and consensus statements. *BMJ Open*. (2019) 9:e026677. doi: 10.1136/bmjopen-2018-026677

41. Hare JM, Mangal B, Brown J, Fisher C, Jr., Freudenberger R, Colucci WS, et al. Impact of oxypurinol in patients with symptomatic heart failure. Results of the OPT-CHF study. *J Am Coll Cardiol*. (2008) 51:2301–9. doi: 10.1016/j.jacc.2008.01.068

42. Givertz MM, Anstrom KJ, Redfield MM, Deswal A, Haddad H, Butler J, et al. Effects of xanthine oxidase inhibition in hyperuricemic heart failure patients: the xanthine oxidase inhibition for hyperuricemic heart failure patients (EXACT-HF) Study. *Circulation*. (2015) 131:1763–71. doi: 10.1161/CIRCULATIONAHA.114.014536

43. Wood FO, Saylors EK, Schneider JE, Jobe RL, Mann JT III. Unprotected left main disease managed with drug-eluting stents: long-term outcome of 100 patients with increased surgical risk. *Catheter Cardiovasc Interv*. (2008) 71:533–8. doi: 10.1002/ccd.21447

frontiers | Frontiers in Cardiovascular Medicine

TYPE Systematic Review
PUBLISHED 05 June 2023
DOI 10.3389/fcvm.2023.1062130

OPEN ACCESS

EDITED BY
Turgay Celik,
Wake Forest University, United States

REVIEWED BY
Li Liang,
Xuzhou Medical University, China
Fabrizio D'Ascenzo,
University of Turin, Italy

*CORRESPONDENCE
István Ferenc Édes
✉ edes789@gmail.com

RECEIVED 05 October 2022
ACCEPTED 02 May 2023
PUBLISHED 05 June 2023

CITATION
Kulyassa P, Engh MA, Vámosi P, Fehérvári P, Hegyi P, Merkely B and Édes IF (2023) Drug-coated balloon therapy is more effective in treating late drug-eluting stent in-stent restenosis than the early occurring one—a systematic review and meta-analysis. Front. Cardiovasc. Med. 10:1062130. doi: 10.3389/fcvm.2023.1062130

Drug-coated balloon therapy is more effective in treating late drug-eluting stent in-stent restenosis than the early occurring one—a systematic review and meta-analysis

Péter Kulyassa[1,2], Marie Anne Engh[2], Péter Vámosi[1,2], Péter Fehérvári[1,2,3], Péter Hegyi[2], Béla Merkely[1] and István Ferenc Édes[1]*

[1]Heart and Vascular Center, Department of Cardiology, Semmelweis University, Budapest, Hungary, [2]Centre for Translational Medicine, Semmelweis University, Budapest, Hungary, [3]Department of Biomathematics and Informatics, University of Veterinary Medicine, Budapest, Hungary

Drug-eluting stent in-stent restenosis (DES-ISR) remains one of the important assignments to be resolved in interventional cardiology, as it is present in 5%–10% of total percutaneous coronary intervention cases. Drug-coated balloon (DCB) utilization is promising, as it comes with long-term protection from recurrent restenosis in optimal conditions without the hazard of higher risk for stent thrombosis and in-stent restenosis. We aim to reduce the need for recurrent revascularization in DES-ISR, specifying the population in which the DCB therapy should be used. In this meta-analysis, the results of studies containing data on the time frame between drug-eluting stent implantation and the clinical presentation of in-stent restenosis and concomitant drug-coated balloon treatment were summarized. A systematic search was performed in Medline, Central, Web of Science, Scopus and Embase databases on November 11th, 2021. The QUIPS tool was used to assess the risk of bias in the included studies. The occurrence of a major cardiac adverse events (MACE) composite endpoint, containing target lesion revascularization (TLR), myocardial infarction, and cardiac death, and each of these separately, was assessed at 12 months after the balloon treatment. Random effects meta-analysis models were used for statistical analysis. Data of 882 patients from four studies were analyzed. Across the included studies, a 1.68 OR (CI 1.57–1.80, $p < 0.01$) for MACE and a 1.69 OR (CI 1.18–2.42 $p < 0.01$) for TLR were observed, both in favor of late DES-ISR. The main limitation of the study is the relatively low patient number. Nevertheless, this analysis shows the first statistically significant results for the effect of DCB treatment in the early or late presentation of DES-ISR. As to date, intravascular imaging (IVI) remains limitedly accessible, other landmarks as the time frame of in-stent restenosis development are to be pursued to advance therapeutic outcomes. In consideration of other biological, technical and mechanical factors, time frame of occurrence as a prognostic factor could reduce the burden of recurrent revascularization in patients at an already high risk.
Systematic Review Registration: identifier [CRD42021286262].

KEYWORDS

in-stent restenois, drug coated balloon, drug eluting stent, recurrent revascularization, neointima proliferation, neoatherosclerosis

1. Introduction

Coronary heart disease affects approximately 126 million people worldwide (1). Alongside the preventive approach and medication-based treatment, in the event of hemodynamically significant stenosis of the epicardial vessels, percutaneous coronary intervention (PCI) is performed with drug-eluting stent (DES) implantation. The applied invasive proceedings are intended to reduce symptoms and/or improve prognosis. Although the eluted drug inhibiting cell proliferation is added on purpose to prevent in-stent restenosis from developing (ISR), DES-ISR is still observed in 5%–10% of total procedures based on implanted stent characteristics (2).

A variety of underlying pathophysiological processes can contribute to the development of ISR. Mechanical and technical factors include stent underexpansion prone to vessel calcification or multiple stent layers, stent fracture, stent undersizing, and geographic miss. Biological mechanisms of ISR mainly include neointimal hyperplasia and neoatherosclerosis (3–5). These may coexist; therefore, all possible factors should be identified and addressed properly. Neointimal hyperplasia is the intimal accumulation of smooth muscle cells and extracellular matrix. Neoatherosclerosis is characterized by an accumulation of lipid-laden foamy macrophages, with possible but not mandatory necrotic core formation, and neointima calcification (6, 7). Neoatherosclerosis with calcified parts can be challenging to manage, and this finding may rightly influence decisions regarding percutaneous intervention (8, 9).

Different types of DES-ISR (focal in-stent, focal peri-stent, and diffuse) may require a peculiar palette of treatment devices to attain optimal results. Some severely calcified lesions require thorough lesion preparation by cutting or scoring balloons, by rotational atherectomy or by intravascular lithotripsy. Two main treatment strategies emerged with favorable long-term outcomes in previous studies. Currently, the implantation of a new layer of DES appears to be a mildly superior option, yet it yields an elevated risk of acute stent closure, and stent thrombosis (10). Drug-coated balloon (DCB) therapy is a relatively novel modality, which, in addition to having about the same results as DES treatment, does not come with an elevated risk of such serious events. A recent publication suggests that tailored antiplatelet therapy is reducing the burden of recurrent revascularization after DES implantation. Besides the proven, there is a supposed additional clinical benefit of stronger agents when low bleeding risk is paired with low ischaemic risk (11).

The time course of DES-ISR after the index procedure appears to be dependent on the underlying stent type, and this may have relevance when patient follow-up is planned after coronary stent implantation. While bare metal stent (BMS) ISR was recognized to peak within the first six months after stent implantation, the incidence of DES-ISR appears to continue to increase steadily as a result of different mechanisms, including accelerated neoatherosclerosis, for several years (7, 12–14).

The changes of stent technologies led over the years to substantial changes in ISR pathomorphosis in comparison to the BMS era. The qualitative and quantitative representation of the three main components of ISR (neoatherosclerosis, VSMC, extracellular matrix) has changed since newer-generation DES ISR is often hypocellular and proteoglycan-rich, while in BMS-ISR VSMCs are predominantly present with a moderate proteoglycan content. Neoatherosclerosis is accelerated with first-generation DES, rare with BMS, and habitually develop over the long term with newer-generation DES, more often observed after one year. Late lumen loss with BMS often reaches a peak 6 to 8 months after implantation and then declines. Concerning DES, there is a slow and progressive neointimal buildup through 5 years following implantation.

One year from the index procedure is considered as a defining point to differentiate between early and late DES-ISR (15–17). It is based on OCT studies, where morphological findings differed between early and late (>1 year) second-generation DES ISR. Early ISR is more often associated with stent underexpansion and neointimal hyperplasia, while neoatherosclerosis prevails in late ISR (18). In a recently published study, neoatherosclerosis was the prevalent mechanism of ISR, with incidence ranging from 20% at 1 to 3 years and reaching above 70% at 7 years (19).

There are limited data showing that treatment with DCB might not be as effective in early DES-ISR (developing in <12 months) as in late DES-ISR (developing in >12 months) (20). As the current available literature takes the effect of time needed to develop in-stent restenosis only partially into consideration, there is a knowledge gap regarding this matter. The clinical relevance of measuring the time rather than performing IVI based revascularization is a question still waiting to be addressed. However, currently these additional proceedings of plaque visualization are more than doubling the costs of a PCI and are not accessible in most countries. The use of the target stent age could be an important measure determining the modality chosen in recurrent revascularization, and it could lead to a reduced burden of adverse events and possible accompanying complications. The timing of DES-ISR presentation could foreshadow a more aggressive nature of the vascular disease; nevertheless, it is not known whether early or late plaques would have better outcomes after DCB treatment. In late DES-ISR cases where neoatherosclerosis is commonly observed, progressively developing calcification is more prone to be present. It could lead to the attenuation of long-term lumen patency after recurrent revascularization (15, 17, 21).

Our hypothesis was that DCB is more effective in late DES-ISR than in the early one. The question to answer in this meta-analysis is whether or not the timing of DES-ISR (early vs. late) affects the outcomes of DCB treatment. We aim to reduce the need for recurrent revascularization in DES-ISR, specifying the population in which the DCB therapy should be used. We assessed the available literature and summarized quantified results.

2. Methods

2.1. Search strategy and selection criteria

This systematic review is being reported in accordance with the PRISMA (Preferred Reporting Items for Systematic Review and Meta-Analyses) 2020 guideline (22). A systematic search was performed in five databases on November 11th, 2021, and altogether 832 articles were found. The databases included Medline (181), Central (117), Web of Science (214), and Scopus (192), with the search key: (early OR late) AND (in-stent restenosis OR ISR) AND (drug coated balloon OR DCB OR paclitaxel coated balloon OR PCB OR sirolimus coated balloon OR SCB) and Embase (128) with the search key: (early OR late) AND ("in-stent restenosis" OR ISR) AND ("drug coated balloon" OR DCB OR "paclitaxel coated balloon" OR PCB OR "sirolimus coated balloon" OR SCB). Studies examining cases of DES-ISR and DCB as treatment modality were eligible for the analysis. The time frame between DES implantation and DCB treatment was needed to determine DES-ISR presentation timing. In the absence of the latter, requests were sent to the authors for patient level data. Data pools containing the treatment of lesions with modalities other than DCB were not excluded when separate group analysis and detailed patient characteristics were disclosed. Two independent reviewers assessed the available articles. The citations were managed in Endnote ×9 by Clarivate Analytics. After automatic and consecutive manual duplicate removal, the selection was done in a two-stage process (Title-abstract, Full-text). Cohen's kappa coefficient (κ) was calculated after each selection step for inter-reviewer reliability measurement (23). Disagreements were resolved by a third author. The data were collected from the full-text articles and conference abstracts by two independent reviewers systematically with the use of pre-planned data extraction tables. These were constructed under the surveillance of our statistical team and with the consent of all authors of this article.

2.2. Outcomes and extraction

Primary and secondary outcomes were defined. All outcomes were searched for in all published articles conformant with our selection criteria. Insufficient or compromised data were not included in the analysis. The primary outcome was the major adverse cardiac event (MACE), which includes three subcomponents: target lesion revascularization (TLR), cardiac death (CD), and myocardial infarction (MI). These outcomes were also examined separately. The secondary endpoints were target lesion thrombosis, target vessel revascularization, and late lumen loss, which were not found in any of the articles. General patient characteristics like age, sex, smoking status, and medical comorbidities like hypertension, diabetes mellitus, dyslipidemia, chronic kidney disease, and earlier cardiovascular events were registered if available. There were no assumptions made for missing values from accessible data. Subgroup analysis was planned to be performed if at least three studies are present in a given subgroup.

2.3. Risk of bias assessment

Two independent authors assessed the risk of bias of the included trials separately. The QUIPS tool was used as an assessment guide for prognostic studies. It investigates six domains: study participation, study attrition, prognostic factor measurement, outcome measurement, study confounding, and statistical analysis and reporting (24). The disagreements in assessment grades between the studies were resolved by consensus of the two authors. There was no automation used in the process.

2.4. Statistical analyses

The odds ratio with 95% CI was used for the effect measure; to calculate the odds ratio, the total number of patients in each group, and those with the event of interest were extracted from each study. Raw data from the selected studies were pooled using a random effects model with the Mantel-Haenszel method and the Hartung-Knapp adjustment (25, 26). To estimate $\tau 2$ the Paule-Mandel method was utilized together with the Q profile method to calculate the confidence interval of $\tau 2$ (27, 28). For publication bias evaluation, a funnel plot of the logarithm of effect size and comparison with the standard error for each trial was used. Statistical heterogeneity across trials was assessed by means of Cochrane Q test, and the I2 values (29). Outlier and influence analyses were carried out in light of the recommendations of Harrer et al. (28) and Viechtbauer and Cheung (30). Publication bias was visually assessed with a funnel plot, as the number of studies was low for all outcomes.

3. Results

3.1. Selection of articles

There were 832 studies in the initial search, four of which were selected for full-text review. All four articles were included in further inquiries. The PRISMA flow diagram of the systematic search and the selection process can be seen in **Figure 1** (31).

3.2. Major cardiovascular adverse events

In the meta-analysis, the MACE OR was 1.68 (CI 1.57–1.80, $p < 0.01$) in the early vs. late DES-ISR group. This outcome was identified in two studies (20, 32). In connection with MACE, one study (20) compared early DES-ISR patients with late DES-ISR patients and found that the former group showed a significantly higher risk (25.9% vs. 17.0%; $p = 0.04$) 12 months after DCB treatment, OR was 1.68 (CI 0.99–2.86). According to one study (32) the incidence of MACE in the early DES-ISR group 12 months after DCB treatment was 5 and in the late DES-ISR group 16 (23.8% vs. 15.8%; $P < 0.01$), the OR was 1.66 (CI 0.53–5.18) 12 months after DCB treatment. The summary of the results can be seen in **Figure 2**.

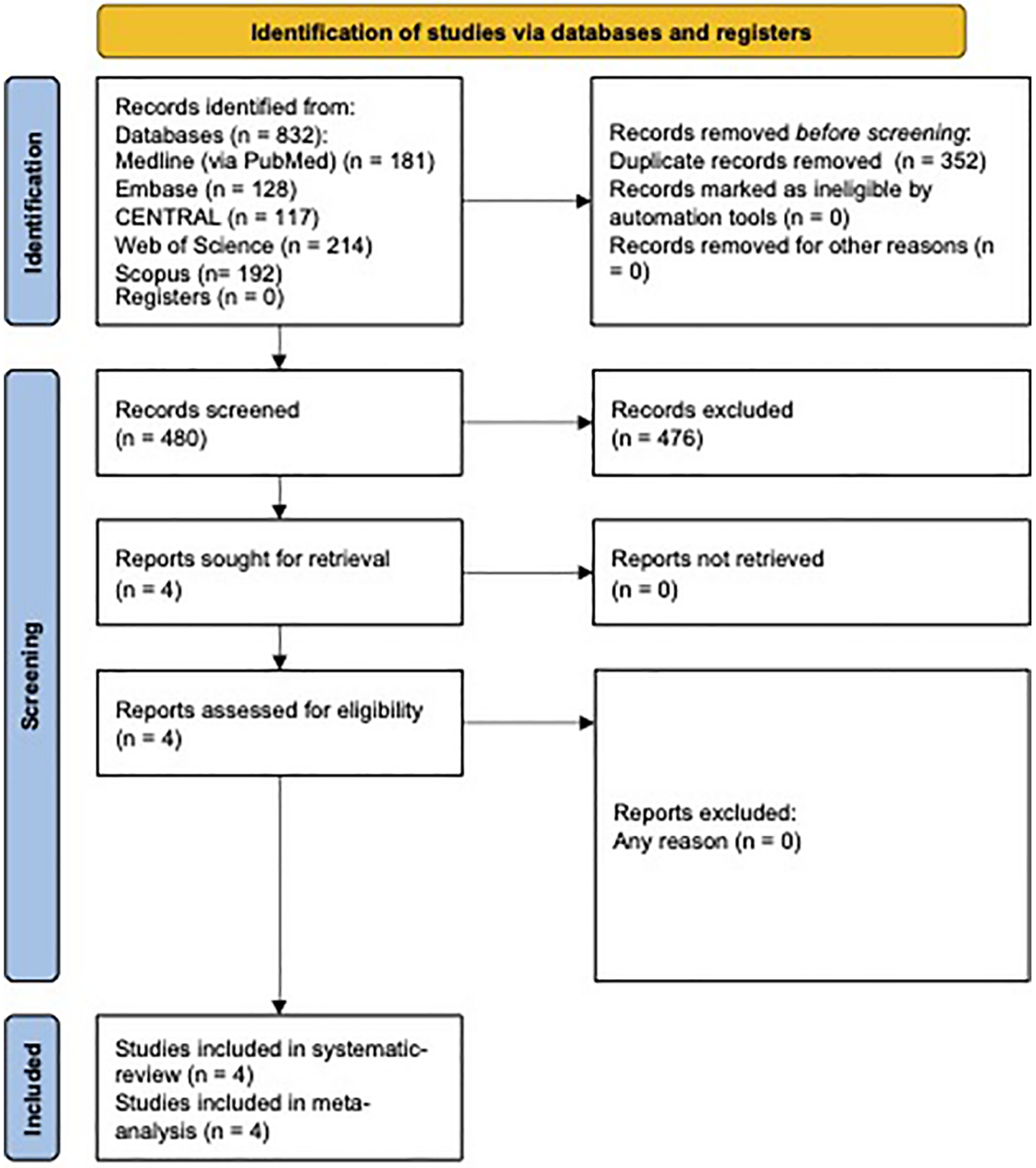

FIGURE 1
Flow diagram of systematic search and article selection.

3.3. Target lesion revascularization

When TLR was assessed across the included studies, a 1.69 OR (CI 1.18–2.42, $p < 0.01$) was observed. TLR was found in three studies. In one (20), TLR was 47 (24.0) in the early DES-ISR group and 24 (15.7) in the late DES-ISR group 12 months after DCB treatment, giving an OR of 1.66 (CI 0.96–2.78). In 187 ISR cases in the study by Sato et al. (33), the overall TLR rate was 0.33 (128), which distributed as 0.40 (88) in the early and 0.16 (30) in the late DES-ISR group at a median of 12 months after DCB treatment, the OR was 1.77 (CI 0.94–3.36). Kuramitsu et al. (34) found that the TLR rate was significantly higher in the early ISR group than in the late ISR group (30.0% vs. 18.3%, $p = 0.035$) 12 months after DCB treatment, which resulted in an OR of 1.63 (CI 0.78–3.37). The one-year outcomes from the Kuramitsu study were extracted from the figure "cumulative incidence of TLR after DCB" in the abstract with the use of Web Plot Digitizer (35). The TLR endpoint in one study (32) was not fit for data extraction using this method, as the figure and the numbers showed ambiguity. Based on this, the author group decided not to include this study in the statistical analysis. The summary of the results can be seen in **Figure 3**.

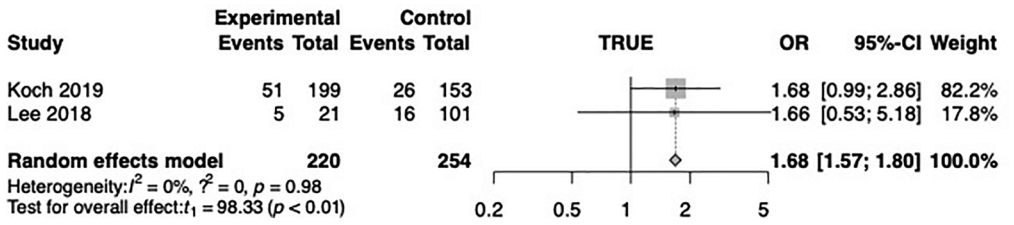

FIGURE 2
Forest plot of major cardiac adverse events (MACE).

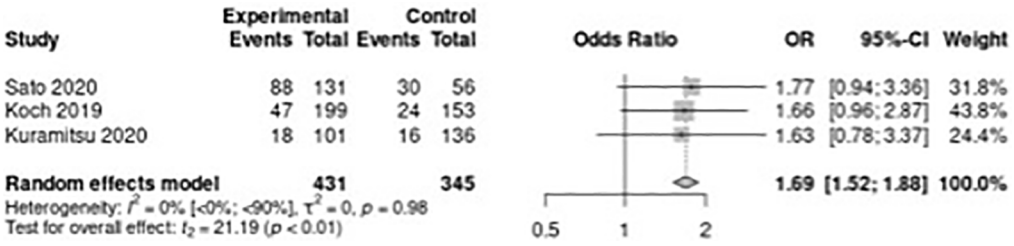

FIGURE 3
Forest plot of target lesion revascularization (TLR).

3.4. Cardiac death

One paper reported (20) three (1.5%) cardiac deaths in the early DES-ISR group and none in the late ($p = 0.82$). In another (32) there were no cardiac deaths in either of the groups. In the studies by Sato et al. and Kuramitsu et al. there was no information disclosed on the matter.

3.5. Myocardial infarction

In one study there were six (3.0%) myocardial infarctions in the early and two (1.3%) in the late DES-ISR group ($p = 0.29$). In one other (32), data were not extractable for one year. In the studies by Sato et al. and Kuramitsu et al. there were no data published for this outcome.

3.6. Target lesion thrombosis

In Koch et al. (20), the rate of target lesion thrombosis was low. There was one event in the early DES-ISR group (0.5%) and no events in the late DES-ISR group (0.0%, $p = 0.90$). In the studies by Lee et al. (32) and Sato et al. (33) there were no data published about the outcome. Kuramitsu et al. (34) had low event numbers (3.3% in early DES-ISR vs. 0.8% in late DES-ISR group, $p = 0.20$) in two years; however, the one-year data were not extractable from the text, and no graphs were available on this outcome either.

3.7. Target vessel revascularization

There were no data disclosed in the included studies about this outcome. No further data were provided on this subject by the contacted authors.

3.8. Late lumen loss

There were no data disclosed in the included studies about this outcome. No further data were provided by the contacted authors on this subject.

3.9. Subgroup analysis

There were not enough number of studies as planned in the protocol for subgroup analysis, therefore it was not performed.

3.10. Summary of included articles

Sato et al. included 187 patients who encountered ISR after the implantation of second-generation DES. Their patients received target lesion revascularization (TLR) with DCB angioplasty. They received coronary angiography after a median of one-year of follow-up or symptomatic reasons. Some of the patients encountered recurrent ISR and received further TLR. As the primary endpoint, the recurrent TLR was assessed. The cutoff

10.3389/fcvm.2023.1062130

between early and late ISR was determined by Receiver Operating Characteristic curve ($n = 131$). The early ISR group had ISR within 1.6 years, the late ISR group ($n = 56$) had the occurrence at more than 1.6 years after the index procedure.

Lee et al. included 122 patients (122 ISR lesions), treated with DCB under optical coherence tomography (OCT) examination before and after DCB, and categorized ISR (<12 months; E-ISR; $n = 21$) and late ISR (≥12 months; L-ISR; $n = 101$). Associations between OCT-based neointima characteristics and the period of ISR and also clinical outcomes after DCB were evaluated. Major adverse cardiac events (MACE) were a composite of cardiac death, non-fatal myocardial infarction, or target lesion revascularization (TLR). Although the data for MACE could be seen in the graphical interpretation for one year of follow-up, the presented numbers and the figure could not be definitively determined; therefore, it was not included in that outcome.

Koch et al. published a pooled analysis including patients with DES-ISR assigned to treatment with DCB in the setting of the ISAR DESIRE 3 and 4 trials. According to the time of ISR occurrence after DES implantation clinical outcomes were evaluated, in patients presenting with early (≤12 months) vs. late DES-ISR (>12 months) undergoing treatment with DCB. The primary endpoint of this analysis was major adverse cardiac event (MACE), defined as the combined incidence of death, myocardial infarction and target lesion revascularization (TLR) 12 months after DCB treatment. Secondary endpoints included the incidence of death, myocardial infarction, TLR and target lesion thrombosis 12 months after DCB treatment. The analysis included 352 patients, 199 patients presented with early-ISR, 153 patients with late-ISR.

Kuramitsu et al. disclosed the results of a total of 239 consecutive patients with 291 ISR lesions after newer-generation DES were treated with DCB. According to the timing of ISR, patients were divided into the two groups: early ISR group (<1 year after the index procedure, $n = 103$) and late ISR group (≥1 year after the index procedure, $n = 136$). The cumulative incidence of TLR and stent thrombosis (ST) within the first two years after DES implantation were assessed. No significant differences in baseline patient and lesion characteristics were found in the early and late ISR groups except for a higher prevalence of hemodialysis in the early ISR group (33.0% vs. 15.4%, $p = 0.002$). Patient, intervention and outcome characteristics are summarized in **Table 1**.

TABLE 1 Patient, intervention and outcome characteristics of included studies.

Study	Early/late definition	Exposed group (early DES-ISR) population	Comparison group (late DES-ISR) population	Outcome assessment time	MACE intervention arm	MACE control arm	TLR intervention arm	TLR control arm	Inclusion criteria
Sato	Average 19 months	131	56	Median 1 year or based on symptom occurrence	Not published	Not published	88	30	DCB treatment of the lesion
Koch	12 months	199	153	1 year based on symptom occurrence	51	26	47	24	DCB treatment of the lesion
Lee	12 months	21	101	5 years based on symptom occurrence	5	16	Not published	Not published	DCB treatment of the lesion
Kuramitsu	12 months	101	136	2 years based on symptom occurrence	Not published	Not published	18	16	DCB treatment of the lesion

3.11. Risk of bias and heterogeneity assessment

The overall risk of bias was low in two studies and moderate in the other two. The assessment is summarized in **Figure 4**. The included full-text articles discussed patient characteristics. As patient and publication numbers were limited, no further heterogeneity assessment was performed.

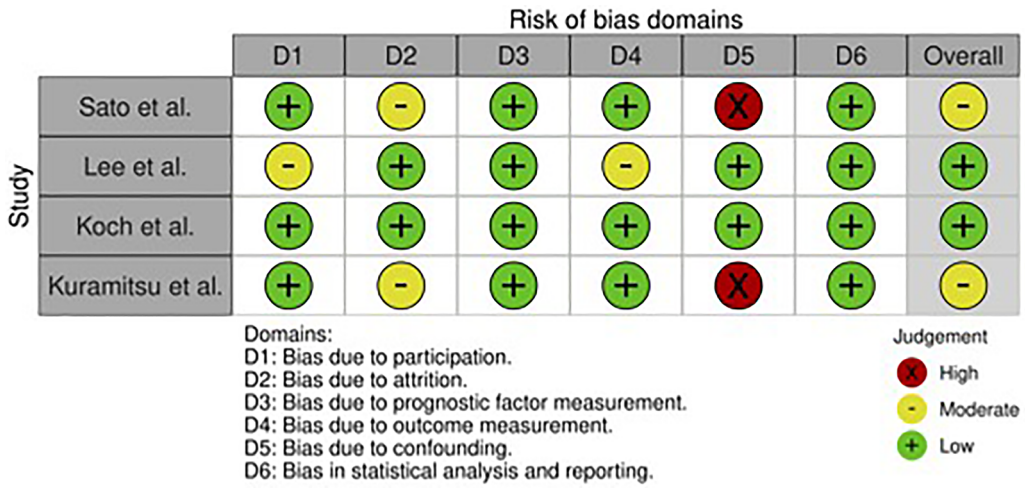

FIGURE 4
Risk of bias assessment across included studies.

4. Discussion

4.1. Main findings

This meta-analysis is the first of its kind to assess the effect of the early or late presentation of DES-ISR, done here on the basis of four trials. In the early DES-ISR population treated with DCB, the risk of having repeated revascularization on the given artery segment is 69% higher than in late DES-ISR. Patients presenting with early DES-ISR had 68% higher chance of suffering myocardial infarction, cardiac death or having repeated revascularization compared to patients presenting with late DES-ISR for DCB treatment.

For the TLR outcome, the events were assessed differently in the trials. In the study by Sato et al., at median one year, a repeated coronary angiography was performed. The authors did not disclose any further details on the timing of the coronary patency reassessment. In the study by Koch et al. a one-year follow-up was allowed, and if symptoms occurred, repeated coronary angiography and revascularization were performed based on the current guidelines of ISR revascularization. Lee et al. and Kuramitsu et al. followed the same process based on the available data, but with extended follow-up time. However, the precise event count at one year follow-up could be extracted only from the article by Kuramitsu et al. but not from that by Lee et al. as discussed earlier. Further patient characteristics assessment was not possible based on the low number of included trials. This enhances the possibility of confounding bias present in the outcomes. The reporting bias was medium to low in the included studies. The certainty of proper outcome measurement is high as the nature of the observed outcomes is principally clinically driven. There are no earlier data on this subject, as DES-ISR is observed to have a relatively low frequency after initial revascularization.

It is worth mentioning that Sato et al. found on the basis of a multi-variable analysis that late ISR (Hazard ratio: HR 0.44, 95% CI 0.29–0.67, $p < 0.001$), and restenosis type of Mehran Ic (focal restenosis) (HR 0.57, 95% CI 0.34–0.97, $p = 0.04$) were the independent factors related to the recurrent TLR. According to Kuramitsu et al., hemodialysis (hazard ratio [HR] 3.03, 95% confidence intervals [CI]: 1.68–5.38, $p < 0.001$) and diffuse ISR pattern (HR 2.39, 95% CI: 1.34–4.19, $p = 0.004$) were predictors of TLR. In a multivariate analysis by Koch et al. including diabetic status, clinical presentation, previous coronary bypass graft, and diameter stenosis after DCB-treatment, the adjusted hazard ratio showed significantly higher risk for MACE of early DES-ISR as compared to late DES-ISR (HRadj = 1.8, [95% CI = 1.1–3.0], $p = .02$). These observations are parallel with the theory that the simpler and the later presenting subtypes of ISR by patients with less cardiovascular risk are prone to appear with better outcomes after recurrent revascularization whereas stent thrombosis rate did not significantly differ between groups (3.3% vs. 0.8%, $p = 0.20$) (36).

4.2. In-stent restenosis characteristics

ISR develops in two distinct, but often mixed histopathological forms. Neointimal hyperplasia is characterized by the migration and proliferation of vascular smooth muscle cells (37). The forming of a novel fibroatheroma within the stent struts, also called neoatherosclerosis, is a longer-term process, promoting late DES-ISR and very late stent thrombosis (38). It is characterised by an accumulation of lipid-laden foamy macrophages, potential calcification within the neointima with or without necrotic core formation (6). Neoatherosclerotic ISR appears to develop in tandem with native atherosclerotic disease progression. Is suggests similar underlying pathomechanisms, but in comparison, neoatherosclerosis demonstrates an accelerated course to *de novo* atherosclerotic CAD (39).

The ISR IVI appearance is most likely representative of the underlying histopathology. A homogenous tissue appearance on

OCT has been shown to correspond to neointima and fibrous connective tissue as a result of smooth muscle cell proliferation. Conversely, heterogenous tissue patterns are associated with increased display of fibrin depositions and loose connective tissue (40). In DES ISR, different types of heterogenous patterns are observed, which seem to gradually change in time. In an observational OCT study thin cap fibroatheroma-like pattern image and intra-intima microvessels were increasing from the early to the late phase, the speckled pattern image rarefacted from the early to the late phase (16).

BMS-ISR and different generations of DES-ISR shows different histopathological and IVI characteristics. BMS-ISR is characterized by homogeneous tissue rich in smooth muscle cells, whereas DES restenosis is more often hypocellular and proteoglycan-rich. A key determining factor in the difference in OCT findings observed between BMS-ISR and DES-ISR appears to be the timing of the ISR progression. As studies pointed out, neoatherosclerosis is more likely to be present in the setting of DES implantation, where the released anti-proliferative agents delay vascular healing, promoting the formation of atheromas (36). In a human pathological study which examined first generation DES, neoatherosclerosis occured more frequent and earlier in DES compared to BMS (38).

Studies also suggest a different time course and different morphological characteristics in first and second generation DES. A human autopsy study found that second generation DES demonstrated greater strut coverage with less inflammation, less fibrin deposition compared to first generation DES. Nevertheless, the observed frequencies of neoatherosclerosis in the two groups were comparable (41). An OCT-driven observational study found that in second generation DES a heterogeneous pattern was prevalent both before and after 1 year. Neoatherosclerosis was more common in the early period in first generation DES, but after one year, was more prevalent in second generation DES (17). It has been also demonstrated that OCT findings suggestive of neoatherosclerosis seem less common in early DES-ISR than in late DES-ISR (15, 17, 42).

4.3. Clinical implications

According to Lee et al. the incidence of MACE was significantly higher for lesions with a heterogeneous than with a non-heterogeneous neointima (43.7% vs. 19.6%; $P = 0.018$), but it was not significantly associated with neoatherosclerosis (33.4% vs. 18.4%; $P = 0.168$). This parallels the findings of this meta-analysis that early presenting DES-ISR tends to display heterogenous tissue characteristics on IVI and is more resistant to recurrent revascularization with DCB (32). Expert consensus and guidelines recommend (Class IIa, Level B) the use of IVI to assess ISR (43, 44). However, it is still not accessible for all-case utilization based mainly on financial reasons. If IVI is not available in the decision making, after consideration of the earlier described mechanisms of DES-ISR, all gathered information should be used to tailor the chosen therapeutic approach.

The presence of a metal scaffold brings some additional considerations compared with *de novo* disease, and persistent issues leading to the original stent failure may need to be identified and addressed to avoid recurrence. It is important to note that in the setting of ISR, the following need of repeated revascularization will be impacted by not only the choice of treatment modality but also by extrinsic mechanical factors. A significant proportion of ISR lesions is associated with stent underexpansion, which may itself be secondary to vessel calcification. In addition, calcified neoatherosclerotic ISR can also result in specific challenges with respect to achieving a maximal acute gain.

4.4. Strengths and limitations

The results show the first statistically significant evidence that the early presentation of DES-ISR may predict worse outcomes after DCB revascularization. The results show a marked difference between the two groups despite the relatively low study and patient number. A significant proportion of aligned patient data is missing. This is a considerable limitation for the implementation of the results of this analysis, also shedding light on the need for further research on this subject. With the currently used generation of DES, there is limited evidence of long-term results. It is important to consider that the incidence of ISR may also be dependent on the nature of the follow-up, with increased identification of "silent" ISR in patients who have undergone a stent implantation and are reassessed without the presence of recurring symptoms. The different time frames used to determine early and late DES-ISR are considered a minor limitation of the meta-analysis, given the tendency for worse outcomes by developing DES-ISR earlier. There are no data on the different types of the second-generation DES involved in the study.

4.5. Conclusion

The age of the implanted stent could be an important prognostic factor in the case of DES-ISR. If other biological, technical, and mechanical factors are taken into consideration, it may assist the optimal choice of a treatment device in this patient population at high risk for more repeated revascularization. In order to verify this hypothesis, more clinical trials in randomized fashion are needed to be carried out on this subject. If IVI is available and the clinical scenario allows its use, then that is the preferable method for guiding therapy of ISR lesions. However, it remains limited in accessibility, and other relevant information regarding lesion characteristics seems worth pursuing. Therefore, further data collection on DES-ISR presentation timing and its effects on outcomes is also required.

Data availability statement

The original contributions presented in the study are included in the article, further inquiries can be directed to the corresponding author.

Author contributions

IFÉ, PK, ME and PH contributed to the ideation, conception, approval, and design of the study. PF provided all statistical analysis. PK wrote the initial draft. All authors contributed to the article and approved the submitted version.

Conflict of interest

The authors declare that the research was conducted in the absence of any commercial or financial relationships that could be construed as a potential conflict of interest.

Publisher's note

All claims expressed in this article are solely those of the authors and do not necessarily represent those of their affiliated organizations, or those of the publisher, the editors and the reviewers. Any product that may be evaluated in this article, or claim that may be made by its manufacturer, is not guaranteed or endorsed by the publisher.

References

1. Khan MA, Hashim MJ, Mustafa H, Baniyas MY, al Suwaidi SKBM, AlKatheeri R, et al. Global epidemiology of ischemic heart disease: results from the global burden of disease study. *Cureus*. (2020) 12:9349. doi: 10.7759/cureus.9349

2. Alfonso F, Kastrati A. Clinical burden and implications of coronary interventions for in-stent restenosis. *EuroIntervention*. (2021) 17:E355–7. doi: 10.4244/EIJV17I5A60

3. Fujii K, Mintz GS, Kobayashi Y, Carlier SG, Takebayashi H, Yasuda T, et al. Contribution of stent underexpansion to recurrence after sirolimus-eluting stent implantation for in-stent restenosis. *Circulation*. (2004) 109:1085–8. doi: 10.1161/01.CIR.0000121327.67756.19

4. Yin D, Mintz GS, Song L, Chen Z, Lee T, Kirtane AJ, et al. In-stent restenosis characteristics and repeat stenting underexpansion: insights from optical coherence tomography. *EuroIntervention*. (2021) 16:E335–43. doi: 10.4244/eij-d-18-01191

5. Alfonso F, Coughlan JJ, Giacoppo D. State of the Art Management of in-stent restenosis. (2022) doi: 10.4244/EIJ-D-21-01034

6. Otsuka F, Byrne RA, Yahagi K, Mori H, Ladich E, Fowler DR, et al. Neoatherosclerosis: overview of histopathologic findings and implications for intravascular imaging assessment. *Eur Heart J*. (2015) 36:2147–59. doi: 10.1093/eurheartj/ehv205

7. Pylayeva-Gupta Y, Martin KC, Ho J-AL MV. 基因的改变NIH public access. *Bone*. (2012) 23:1–7. doi: 10.1016/j.jacc.2011.01.011.The

8. Ruzsa Z, Lux Á, Édes IF, Molnár L, Merkely B. Successful removal of entrapped burr with sheathless guiding during stent rotablation. *Anatol J Cardiol*. (2017) 17:156–7. doi: 10.14744/AnatolJCardiol.2017.7519

9. Garcia-Guimaraes M, Antuña P, Maruri-Sanchez R, Vera A, Cuesta J, Bastante T, et al. Calcified neoatherosclerosis causing in-stent restenosis: prevalence, predictors, and implications. *Coron Artery Dis*. (2019) 30:1–8. doi: 10.1097/MCA.0000000000000669

10. Kheiri B, Simpson T, Osman M, Kumar K, Radaideh Q, Golwala H, et al. Drug-Coated balloons in the treatment of De-Novo coronary artery disease: a network meta-analysis of all randomized controlled trials. *J Am Coll Cardiol*. (2020) 75:1330. doi: 10.1016/S0735-1097(20)31957-4

11. Patti G, D'Ascenzo F, De Filippo O, Bruno F, Leonardi S, Chieffo A, et al. Safety and efficacy of different P2Y12 inhibitors in patients with acute coronary syndromes stratified by the PRAISE risk score: a multicentre study. *Eur Heart J Qual Care Clin Outcomes*. (2022) 8:881–91. doi: 10.1093/ehjqcco/qcac002

12. Giacoppo D, Alfonso F, Xu B, Claessen BEPM, Adriaenssens T, Jensen C, et al. Paclitaxel-coated balloon angioplasty vs. drug-eluting stenting for the treatment of coronary in-stent restenosis: a comprehensive, collaborative, individual patient data meta-analysis of 10 randomized clinical trials (DAEDALUS study). doi: 10.1093/eurheartj/ehz731

13. Byrne RA, Iijima R, Mehilli J, Pinieck S, Bruskina O, Schömig A, et al. Durability of antirestenotic efficacy in drug-eluting stents with and without permanent polymer. *JACC Cardiovasc Interv*. (2009) 2:291–9. doi: 10.1016/j.jcin.2008.11.015

14. Räber L, Wohlwend L, Wigger M, Togni M, Wandel S, Wenaweser P, et al. Five-year clinical and angiographic outcomes of a randomized comparison of sirolimus-eluting and paclitaxel-eluting stents: results of the sirolimus-eluting versus paclitaxel-eluting stents for coronary revascularization LATE trial. *Circulation*. (2011) 123:2819–28. doi: 10.1161/CIRCULATIONAHA.110.004762

15. Kang SJ, Mintz GS, Akasaka T, Park DW, Lee JY, Kim WJ, et al. Optical coherence tomographic analysis of in-stent neoatherosclerosis after drug-eluting stent implantation. *Circulation*. (2011) 123:2954–63. doi: 10.1161/CIRCULATIONAHA.110.988436

16. Habara M, Terashima M, Nasu K, Kaneda H, Yokota D, Ito T, et al. Morphological differences of tissue characteristics between early, late, and very late restenosis lesions after first generation drug-eluting stent implantation: an optical coherence tomography study. *Eur Heart J Cardiovasc Imaging*. (2013) 14:276–84. doi: 10.1093/ehjci/jes183

17. Kilickesmez K, Dall'Ara G, Rama-Merchan JC, Ghione M, Mattesini A, Vinues CM, et al. Optical coherence tomography characteristics of in-stent restenosis are different between first and second generation drug eluting stents. *IJC Heart and Vessels*. (2014) 3:68–74. doi: 10.1016/j.ijchv.2014.03.003

18. Song L, Mintz GS, Yin D, Yamamoto MH, Chin CY, Matsumura M, et al. Characteristics of early versus late in-stent restenosis in second-generation drug-eluting stents: an optical coherence tomography study. *EuroIntervention*. (2017) 13:294–302. doi: 10.4244/EIJ-D-16-00787

19. Chen Z, Matsumura M, Mintz GS, Noguchi M, Fujimura T, Usui E, et al. Prevalence and impact of neoatherosclerosis on clinical outcomes after percutaneous treatment of second-generation drug-eluting stent restenosis. *Circ Cardiovasc Interv*. (2022) 15:E011693. doi: 10.1161/CIRCINTERVENTIONS.121.011693

20. Koch T, Cassese S, Xhepa E, Mayer K, Tölg R, Hoppmann P, et al. Efficacy of drug-coated balloon angioplasty in early versus late occurring drug-eluting stent restenosis: a pooled analysis from the randomized ISAR DESIRE 3 and DESIRE 4 trials. *Catheter Cardiovasc Interv*. (2020) 96:1008–15. doi: 10.1002/ccd.28638

21. Habara S, Kadota K, Hasegawa D, Tada T, Tanaka H, Fuku Y, et al. Late restenosis following paclitaxel-coated balloon angioplasty occurs in patients with drug-eluting stent restenosis. *EuroIntervention*. (2015) 66(1):14–22. doi: 10.1016/j.jacc.2015.05.002 https://www.embase.com/search/results?subaction=viewrecord&id=L71979876&from=export

22. Page MJ, McKenzie JE, Bossuyt PM, Boutron I, Hoffmann TC, Mulrow CD, et al. The PRISMA 2020 statement: an updated guideline for reporting systematic reviews. *The BMJ*. (2021) 372:71. doi: 10.1136/bmj.n71

23. McHugh ML. Interrater reliability: the kappa statistic. *Biochem Med (Zagreb)*. (2012) 22:276–82. doi: 10.11613/BM.2012.031

24. Hayden JA, Windt Dvd, Cartwright JL, Co P. Assessing bias in studies of prognostic factors. *Ann Intern Med*. (2006) 158:280–6. doi: 10.7326/0003-4819-158-4-201302190-00009

25. Mantel N, Haenszel W. Statistical Aspects of the Analysis of Data From Retrospective Studies of Disease 1. http://jnci.oxfordjournals.org/

26. Knapp G, Hartung J. Improved tests for a random effects meta-regression with a single covariate. *Stat Med*. (2003) 22:2693–710. doi: 10.1002/sim.1482

27. Paule RC, Mandel J. Consensus Values and Weighting Factors.

28. Harrer M, Cuijpers P, Furukawa TA, Ebert DD. *Doing meta-analysis with R*. New York: Chapman and Hall/CRC (2021). doi: 10.1201/9781003107347

29. Higgins JPT, Thompson SG. Quantifying heterogeneity in a meta-analysis. *Stat Med*. (2002) 21:1539–58. doi: 10.1002/sim.1186

30. Viechtbauer W, Cheung MW-L. Outlier and influence diagnostics for meta-analysis. *Res Synth Methods*. (2010) 1:112–25. doi: 10.1002/jrsm.11

31. Haddaway NR, Page MJ, Pritchard CC, McGuinness LA. PRISMA2020: an R package and shiny app for producing PRISMA 2020-compliant flow diagrams, with

interactivity for optimised digital transparency and open synthesis. *Campbell Systematic Reviews*. (2022) 18:e1230. doi: 10.1002/cl2.1230

32. Lee J-H, Jung HW, Kim J-S, Hong S-J, Ahn C-M, Kim B-K, et al. Different neointimal pattern in early vs. Late in-stent restenosis and clinical outcomes after drug-coated balloon angioplasty: an optical coherence tomography study. *Circ J*. (2018) 82:2745–52. doi: 10.1253/circj.CJ-18-0619

33. Sato T. Shorter duration from the Index pci correlates with higher recurrent target lesion revascularization rate after the drug coated balloon angioplasty. *J Am Coll Cardiol*. (2020) 75:1236. doi: 10.1016/s0735-1097(20)31863-5

34. Kuramitsu S, Masuda H, Domei T, Hyodo M, Shirai KAndoKM S. Difference in clinical outcomes of drug-coated balloon between patients with early and late drug-eluting stent restenosis. *Coronary Artery Dis—Diagnosis, Pharmacotherapy and Revascularisation*. (2016) 6449:2674–81. doi: 10.1093/eurheartj/ehy566

35. Rohatgi A. Web Plot Digitizer. (2020).

36. Nusca A, Viscusi MM, Piccirillo F, de Filippis A, Nenna A, Spadaccio C, et al. In stent neo-atherosclerosis: pathophysiology, clinical implications, prevention, and therapeutic approaches. *Life*. (2022) 12:393. doi: 10.3390/life12030393

37. Komatsu R, Ueda M, Naruko T, Kojima A, Becker AE. Neointimal Tissue Response at Sites of Coronary Stenting in Humans Macroscopic, Histological, and Immunohistochemical Analyses. (1998).

38. Nakazawa G, Otsuka F, Nakano M, Vorpahl M, Yazdani SK, Ladich E, et al. The pathology of neoatherosclerosis in human coronary implants: bare-metal and drug-eluting stents. *J Am Coll Cardiol*. (2011) 57:1314–22. doi: 10.1016/j.jacc.2011.01.011

39. Taniwaki M, Windecker S, Zaugg S, Stefanini GG, Baumgartner S, Zanchin T, et al. The association between in-stent neoatherosclerosis and native coronary artery disease progression: a long-term angiographic and optical coherence tomography cohort study. *Eur Heart J*. (2015) 36:2167–76. doi: 10.1093/eurheartj/ehv227

40. Kim JS, Afari ME, Ha J, Tellez A, Milewski K, Conditt G, et al. Neointimal patterns obtained by optical coherence tomography correlate with specific histological components and neointimal proliferation in a swine model of restenosis. *Eur Heart J Cardiovasc Imaging*. (2014) 15:292–8. doi: 10.1093/ehjci/jet162

41. Otsuka F, Vorpahl M, Nakano M, Foerst J, Newell JB, Sakakura K, et al. Pathology of second-generation everolimus-eluting stents versus first-generation sirolimus-and paclitaxel-eluting stents in humans. *Circulation*. (2014) 129:211–23. doi: 10.1161/CIRCULATIONAHA.113.001790

42. Habara S, Kadota K, Tanaka H, Fuku Y, Goto T, Mitsudo K. Predictors of recurrent restenosis after treatment of in stent restenosis with paclitaxel-coated balloon. *J Am Coll Cardiol*. (2014) 64:B81. https://www.embase.com/search/results?subaction=viewrecord&id=L71633196&from=export doi: 10.1016/j.jacc.2014.07.322

43. Räber L, Mintz GS, Koskinas KC, Johnson TW, Holm NR, Onuma Y, et al. Clinical use of intracoronary imaging. Part 1: guidance and optimization of coronary interventions. An expert consensus document of the European association of percutaneous cardiovascular interventions. *EuroIntervention*. (2018) 14:656–77. doi: 10.4244/eijy18m06_01

44. Neumann FJ, Sousa-Uva M, Ahlsson A, Alfonso F, Banning AP, Benedetto U, et al. 2018 ESC/EACTS guidelines on myocardial revascularization. *Eur Heart J*. (2019) 40:87–165. doi: 10.1093/eurheartj/ehy394

Frontiers in
Cardiovascular Medicine

Innovations and improvements in cardiovascular treatment and practice

Focuses on research that challenges the status quo of cardiovascular care, or facilitates the translation of advances into new therapies and diagnostic tools.

Discover the latest Research Topics

See more →

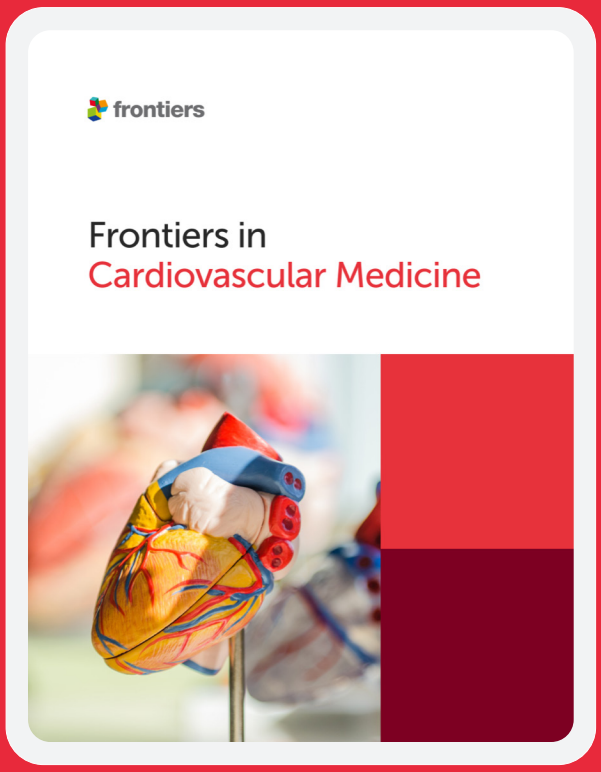

Frontiers

Avenue du Tribunal-Fédéral 34
1005 Lausanne, Switzerland
frontiersin.org

Contact us

+41 (0)21 510 17 00
frontiersin.org/about/contact